RADICAL FLUORINATION METHODS FOR THE SYNTHESIS OF ARYL MONO-, DI-, AND TRI- FLUOROMETHYL ETHERS.

by

Joe Cho Tak Leung

B.Sc., University of Toronto, 2007

A THESIS SUBMITTED IN PARTIAL FULFILLMENT OF

THE REQUIREMENTS FOR THE DEGREE OF

DOCTOR OF PHILOSOPHY

in

THE FACULTY OF GRADUATE AND POSTDOCTORAL STUDIES

(Chemistry)

THE UNIVERSITY OF BRITISH COLUMBIA

(Vancouver)

December 2013

Abstract

New reagents for selective radical fluorine transfer have been identified and utilized to develop two novel photochemical reactions to access fluorinated methoxy arenes. I have discovered that Selectfluor™ can be employed as a radical fluorinating agent, leading to the development of a photochemical methodology (in aqueous alkaline Selectfluor™ solutions containing 2-aryloxyacetic acids) for the synthesis of aryl fluoromethyl, difluoromethyl, and trifluoromethyl ethers. In the second reaction developed, acetone *N*-fluorobenzensulfonimide solutions containing 2-aryloxyacetic acids will promote a different, milder, photosensitized decarboxylative fluorination reaction capable of delivering more electron rich aryl fluoromethyl ethers, and aryl difluoromethyl ethers. Density Functional Theory calculations support the assertion that radical intermediates are involved in fluorination.

Alkoxyl radical reactions have also been investigated. I have found that the rate of alkoxyl 5-*exo* cyclization onto a silyl enol ether is only marginally faster than cyclization onto a trisubstituted alkene. The assumption that secondary and primary alkoxyl radicals display similar cyclization behaviour was proven unsound, and primary alkoxyl 5-*exo* cyclization onto a simple terminal alkene is likely faster than published rates. Alkoxyl radical 1, 5-hydrogen atom transfer was studied in the context of a radical relay cyclization methodology. I have demonstrated that primary, secondary and tertiary alkoxyl radicals may be successfully employed in the relay cyclization of 5 (5-*exo*), and 6 (6-*endo*) membered carbocyclic rings.

Preface

The discovery of *N*-fluorobenzensulfonimide and Selectfluor™ as radical fluorinating agents (Chapter 2) was accomplished in collaboration with M. Rueda-Becerril, C. Chatalova-Sazepin, T. Okbinoglu, P. Kennepohl (professor), Paquin, J.-F. (professor) and published in 2012: Rueda-Becerril, M.; Chatalova-Sazepin, C.; Leung, J. C. T.; Okbinoglu, T.; Kennepohl, P.; Paquin, J.-F.; Sammis, G. M. *J. Am. Chem. Soc.* **2012**, *134*, 4026 (summarized in Scheme 2.14). The work of M. Rueda-Becerril is depicted in Scheme 2.5, and the work of C. Chatalova-Sazepin will be clearly demarcated. Computational studies performed by T. Okbinoglu and P. Kennepohl are presented in Table 2.3. I performed all other synthesis, characterizations, and experimental work.

The studies on photodecarboxylative fluorination (Chapter 3) was accomplished in collaboration with M. Rueda-Becerril, C. Chatalova-Sazepin, J. West, P. Kennepohl (professor), G. Sammis (professor) and produced one published: Leung, J. C. T.; Chatalova-Sazepin, C.; West, J. G.; Rueda-Becerril, M.; Paquin, J.; Sammis, G. M. *Angew. Chem. Int. Ed.* **2012**, *51*, 10804. The work of C. Chatalova-Sazepin appears in Scheme 3.25, and 3.33. The work of J. West appears in Scheme 3.25, and 3.33. I performed all other synthesis, characterizations, and experimental work. DFT calculations were performed under the guidance of P. Kennephol.

Alkoxyl radical competition kinetic studies (Chapter 4) were performed in collaboration with M. Rueda-Becerril. Her work will be clearly demarcated and appears in Scheme 4.27. Some of these studies were published in 2011: Rueda-Becerril, M.; Leung, J. C. T.; Dunbar, C. R.; Sammis, G. M. *J. Org. Chem.* **2011**, *76*, 7720. I performed all other synthesis, characterizations, and experimental work.

Alkoxyl radical 1, 5-hydrogen atom transfer relay cyclization studies (Chapter 4) were performed in collaboration with H. Zhu, K. Johnson, J. Wickenden, N. Campbell and were published in 2009: Zhu, H.; Wickenden, J. G.; Campbell, N. E.; Leung, J. C. T.; Johnson, K. M.; Sammis, G. M. *Org. Lett.* **2009**, *11*, 2019 (summarized in Scheme 4.36). The work of H. Zhu appears in Scheme 4.35 and will be clearly demarcated. The work of K. Johnson appears in Scheme 4.35 and will be clearly demarcated. I performed all other synthesis, characterizations, and experimental work.

Table of Contents

List of Tables

List of Figures

List of Schemes

List of Abbreviations and Symbols

δ	chemical shift
µl	microlitre
1, 5-HAT	1, 5-hydrogen atom transfer
Ac	acetyl
AIBN	azoisobutyronitrile
Ar	aryl
Boc	*tert*-butylcarbonyl
Bn	benzyl
bpy	bipyridine
Bu	butyl
Bz	benzoyl
°C	degrees Celsius
calcd	calculated
CDI	carbonyldiimidazole
cm^{-1}	reciprocal centimetres
COSY	correlated spectroscopy
d	doublet
DBU	1, 8-diazabicycloundec-7-ene
DCC	dicyclohexylcarbodiimide
DIAD	diisopropyl azodicarboxylate
DIB	diacetoxyiodobenzene
DIBAL	diisobutylaluminium hydride
DMAP	4-dimethylaminopyridine
DMF	dimethylformamide
DMSO	dimethylsulfoxide
dr	diastereomeric ratio
DtBuPy	2, 6-di-*tert*-butyl pyridine
DtBuMPy	2, 6-di-*tert*-butyl 4-methyl pyridine
E	entgegen
EA	electron affinity
eV	electron volt
EI	electron impact ionization
eqn.	equation
equiv.	equivalents
ESI	electrospray ionization
Et	ethyl
F-TEDA	1-chloromethyl-4-fluoro-1,4-diazoniabicyclo[2.2.2]octane
h	hour
HRMS	high resolution mass spectrum
HSQC	Heteronuclear Single Quantum Correlation
hν	light
IP	ionisation potential

IR	infrared
J	coupling constant
k	rate constant
kcal	kilocalories
LUMO	lowest unoccupied molecular orbital
m	multiplet
M	molarity or parent mass
mg	milligram
MHz	megahertz
min	minute
ml	millilitre
mmol	millimole
mol	mole
m.p.	melting point
NFPY	*N*-fluoropyridinium
NFSI	*N*-fluorobenzenesulfonimide
nOe	nuclear Overhauser effect
nm	nanometer
NMR	nuclear magnetic resonance
Nuc	nucleophile
OTf	trifluoromethanesulfonate
p	para
PDC	photodecarboxylation
PDC-F	photodecarboxylative fluorination
PET	photoinduced electron transfer
pet. ether	light petrolium ethers
Pg	protecting group
Ph	phenyl
Phth	phthalimide
PIFA	phenyliododitrifluoroacetate
pm	picometre
ppm	parts per million
Prof.	professor
q	quartet
quin	quintet
R	undefined portion of a molecule
R	rectus
Rf	retention factor
s	second or singlet
S	sinister
SCE	saturated calomel electrode
Sel-F	Selectfluor™ 1-chloromethyl-4-fluoro-1,4-diazoniabicyclo[2.2.2]octane bis(tetrafluoroborate)
SET	single electron transfer
S_H2	substitution, homolytic, bimolecular

S_N1	substitution, nucleophilic, unimolecular
S_N2	substitution, nucleophilic, bimolecular
SOMO	singly occupied molecular orbital
t	triplet
TBDMS	*tert*-butyldimethylsilyl
TES	triethylsilyl
THF	tetrahydrofuran
TIPS	triisopropylsilyl
TMS	trimethylsilyl
Ts	*para*-toluenesulfonyl
UV	ultraviolet
UV-Vis	ultraviolet-visible
wt	weight
Z	zusammen

Acknowledgements

A thousand thanks to my supervisor, Prof. Glenn Sammis, for his guidance, instruction, and encouragement these last 6 years. He has given me resources and freedom to explore many of my own ideas, and I am forever grateful for this trust. I also thank Prof. Pierre Kennepohl for teaching me how to perform DFT calculations.

Thank you to my thesis committee members: Prof. Stephen Withers, Prof. Lawrence McIntosh and especially Prof. Marco Ciufolini for his assistance in editing my thesis.

I am grateful for the support and friendship of my group (past and present): Hai Zhu, Jason Wickenden, Maria Zlotorzynska, Robby Zhai, Natalie Campbell, Claire Chatalova-Sazepin, Kayli Johnson, Julian West, and Jason Hudlicky. I am especially thankful to Montserrat Rueda-Becerril who I have worked most closely with and has been co-author with me on three publications.

My graduate work would not have been possible without the support staff of the Chemistry Department at UBC. I wish to thank the NMR lab, the Mass Spec. lab, Chem stores, the Mech. shop, and the main office for all their work over the years. I also thank the Natural Sciences and Engineering Research Council (NSERC) for funding my graduate degree and UBC for tuition relief.

Finally, endless thanks to my family, especially my wife for joining me in Vancouver, for their enduring love and support throughout my education.

Chapter 1: Introduction to radical fluorination

1.1 Motivation and history of radical fluorination

In 1886 Henri Moissan isolated elemental fluorine.[1] As the most electronegative element, and the most reactive of all the known elements, the preparation of fluorine gas was a monumental achievement. Although fluorine is the 13th most abundant element in the earth's crust,[2] only 18 natural products are known which possess a carbon-fluorine bond.[3] The rarity of naturally occuring fluorinated organics may be partially explained by the unique properties associated with a carbon-fluorine bond.

Incorporation of fluorine into bioactive small molecules can produce many positive physicochemical and conformational properties.[4,5] As the most electronegative element on the periodic table, inductive effects by fluorine can greatly alter the pKa of nearby functional groups.[6] The electronegativity of fluorine can manifest in the appearance of hydrogen bonding and other electrostatic interactions leading to conformational changes in molecules. Modulation of lipophilicity may be achieved as the addition of fluorine to organic molecules will increase solubility in non-polar media.

Substitution of carbon-hydrogen bonds for carbon-fluorine bonds can dramatically increase the metabolic stability of bioactive small molecules. The change in homolytic bond strength from a C-H bond (96-99 kcal/mol)[7] to a C-F bond (109 kcal/mol)[8] renders the carbon immune to oxidative degradation by Cytochrome P450 monooxygenases.[9] Substitution of a potentially acidic hydrogen atom for a fluorine atom can block racemisation pathways preserving the bioactive enantiomer longer *in-vivo*. Compounds resistant to enzymatic degredation are active longer and lower drug dosages can be employed to achieve the same levels of effectiveness.

The desire for fluorine incorporation into bioactive small molecules has led to ever-increasing methods for ionic fluorination;[5, 6, 10] however, the development of radical methods for fluorination has been lacking. A significant reason for the dearth of radical methods has been the hazards associated with employing atomic fluorine. Organic compounds react rapidly with atomic fluorine at rates near diffusion[11] and such reactions are almost always exothermic.[6, 12] Many scientists who studied the reagents capable of atomic fluorine generation made efforts to channel reactivity towards ionic pathways.[13]

Until very recently, the only known sources of atomic fluorine (elemental fluorine, trifluoromethyl hypofluorite, xenon difluoride) were prone to spontaneous generation of atomic fluorine and virtually no reagents were known where an atom of fluorine could be transferred to an alkyl radical without the simultaneous generation of a second highly reactive radical species. Radical abstraction of fluorine from fluorine gas leads to the liberation of a fluorine radical. Likewise, abstraction of fluorine from trifluoromethyl hypofluorite leads to the generation of a highly reactive trifluoromethoxyl radical.

A breakthrough in the field of radical fluorination came following our discovery that Selectfluor™ (Sel-F) and *N*-fluorobenzenesulfonimide (NFSI) can be used to fluorinate carbon radicals.[14] Transfer of a fluorine atom to an alkyl radical by Sel-F or NFSI would not result in the formation of a second highly reactive radical. Following our disclosure, other sources of radical fluorine (resistant to spontaneous generation of atomic fluorine) were discovered and the field of radical fluorination is currently experiencing a surge in popularity.

This thesis details my contributions to the field of radical fluorination. Chapter 1 presents an overview of selective alkyl radical fluorination and is divided into two sections which detail work before and after our discovery that Sel-F and NFSI are radical fluorination agents. Chapter 2 details the discovery of Sel-F and NFSI as radical fluorinating agents, and presents studies towards radical aryl fluoride synthesis. Chapter 3 covers my discovery of two novel photochemical fluorination reactions. Chapter 4 is a summary of my work on alkoxyl radicals prior to radical fluorination studies and Chapter 5 will conclude this thesis with some ideas for future directions.

1.2 Radical fluorination prior to 2011

Prior to our landmark discovery, the most commonly employed reagents for selective radical fluorination were fluorine gas (**1.1**), trifluoromethyl hypofluorite (**1.2**) and xenon difluoride (**1.3**). Although other reagents are known to fluorinate organic compounds through radical intermediates, these three compounds have been implicated in S_H2 reactions and rate constants have been measured for the alkyl radical abstraction of fluorine from **1.1**, **1.2** and **1.3**. High-valency metal reagents such as CoF_3, MnF_3, CeF_4, and $CsSO_4F$, operate exclusively by single electron transfer processes.[15] Fluorination reactions with these reagents are directly related to electrochemical fluorination,[16] and are outside the scope of this coverage.

1.2.1 Radical fluorination with fluorine gas

Early studies with fluorine gas and organic compounds were beset with many difficulties with most reactions yielding the products of combustion − often explosively.[17] After isolating fluorine, Moissan brought various sources of carbon into contact with the gas, but uncontrolled reactions, combustion, and even detonation occurred. For example, solid methane (**1.4**) reacted with liquid

fluorine (**1.1)** at -187 °C, but even at this low temperature an explosion took place.[18] Approximately 40 years after Moissan's discovery, some of the first successfully studied reactions with elemental fluorine (reactions that did not lead to only combustion products of carbontetrafluoride and hydrofluoric acid) were gas-phase and liquid-gas interphase reactions with hydrocarbons and hydrochlorocarbons.

Bigelow devoted much study to the fluorination of the simplest hydrocarbons: ethane (**1.5**) (Scheme 1.1)[19] and methane (**1.4**) (Scheme 1.2).[20] Gas phase fluorination of ethane at ambient temperatures lead predominately to the perfluorination products **1.6** and **1.7**, indicating that thermal cracking of the C-C bond takes place.[19] In the gas phase fluorination of methane (**1.4**), the expected products of sequential radical fluorination (**1.9**, **1.10**, **1.8**, **1.6**) were obtained with higher proportions favouring **1.10** and **1.8**.[20] Henne also observed the fluorination of fluoroform (**1.8**) to tetrafluoromethane (**1.6**).[21] In addition to the complete set of one carbon hydrofluorides, telomerisation products perfluoroethane (**1.7**) and perfluoropropane (**1.11**) could be isolated allowing for positive identification.[20] Perfluoroethane (**1.7**) can be produced by the dimerisation of trifluoromethyl radicals. The mechanism for chain elongation to perfluoropropane (**1.11**) involves termination of the trifluoromethyl radical with the difluoromethyl radical (Scheme 1.2).

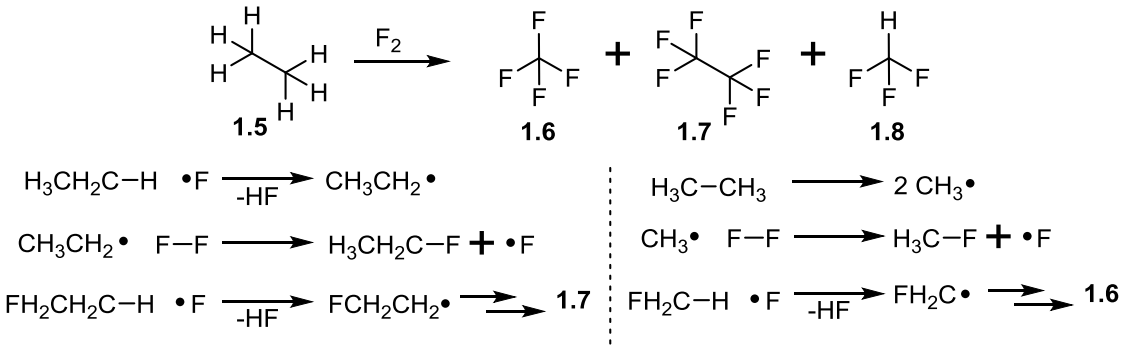

Scheme 1.1. Gas phase fluorination of ethane

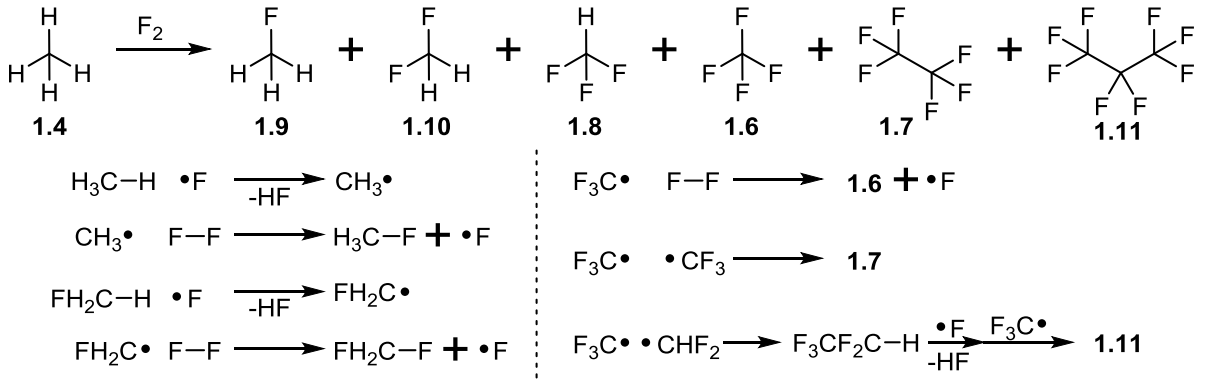

Scheme 1.2. Gas phase fluorination of methane

Increasing the chemical complexity of gas phase fluorination, chlorohydrocarbons were exposed to elemental fluorine (Scheme 1.3). Fluorination of chloroform (**1.12**) lead to the expected product of hydrogen substitution (**1.13**) along with large amounts of trichloromethyl dimerization product **1.14**. Fluorination of chloroethane (**1.15**) (Scheme 1.3, middle reaction) produced a mixture of products both expected (**1.17**, **1.6**, **1.18**, **11.9**) and unexpected (**1.16**, **1.20**). This list is by no means exhaustive as many other unidentifiable compounds were observed. Methane derivatives **1.17** and **1.6** can be produced from thermal cracking of chloroethane and **1.18** is the expected perfluorination product. An important discovery was that the carbon chlorine bond was not inert under these conditions, thus explaining the presence of difluorodichloromethane (**1.16**). This is further highlighted by the fluorination of pentachloroethane (**1.21**) (Scheme 1.3, bottom reaction), demonstrating that chlorine radicals can be easily generated with the production of tetrachloroethene (**1.23**). Under these conditions, dimerization of **1.14** yields **1.25**, and the fluorination of **1.23** leads to **1.24**. Even hexachloroethane (**1.14**) can be fluorinated with a 20% isolated yield of **1.24** indicating that fluorine radicals may abstract chlorine, leading to intermediate **1.23**.[22]

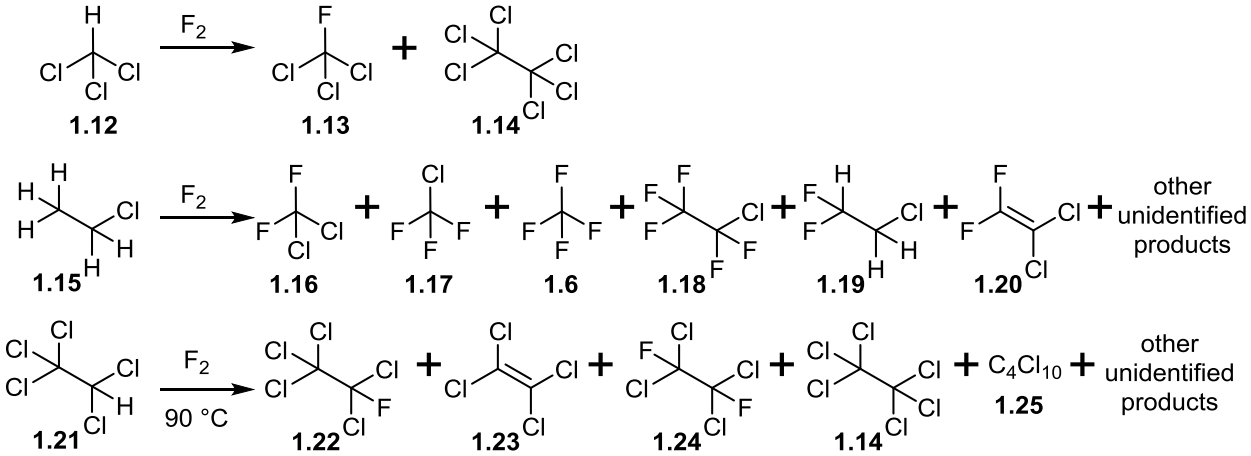

Scheme 1.3. Fluorination of selected chlorohydrocarbons

The reaction of fluorine gas (**1.1**) with tetrachloroethylene (**1.23**) lead to the isolation of the desired 1,2-difluoro adduct **1.24** along with significant amounts of the dimer **1.26** and the monofluorinated **1.22** (Scheme 1.4).[22, 23] Addition of a fluorine radical generates the common intermediate radical **1.27** which can be fluorinated to yield **1.24** as anticipated. Chain elongation by addition of **1.27** to a second molecule of **1.23** prior to fluorination yields **1.28**, and the trapping of **1.27** with a source of chlorine radical yields the monofluorinated product **1.22**. Radical sources of chlorine include fluorochloride obtained by fluorine radical abstraction of chlorine and elimination of chlorine radical from **1.27**.

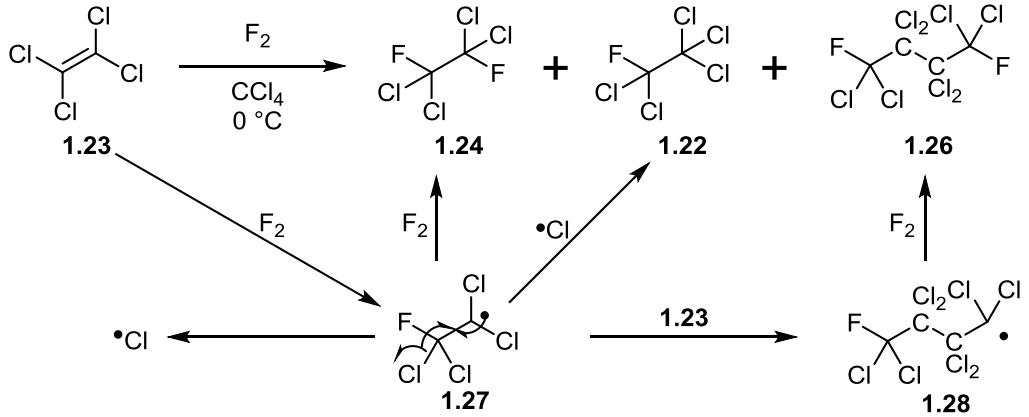

Scheme 1.4. Radical fluorination of tetrachloroethylene

Combining the processes in Schemes 1.3 and 1.4, Miller[24] has synthesized chlorofluoro-carbons **1.30** and **1.34** (Scheme 1.5). Coupling of the trichloromethyl radical derived from **1.12** with the fluoro radical adduct **1.32** yields 10% of **1.30**. The synthesis of **1.34** in 47% yield from coupling of fluoro radical adducts **1.32** and **1.33** is more synthetically useful.

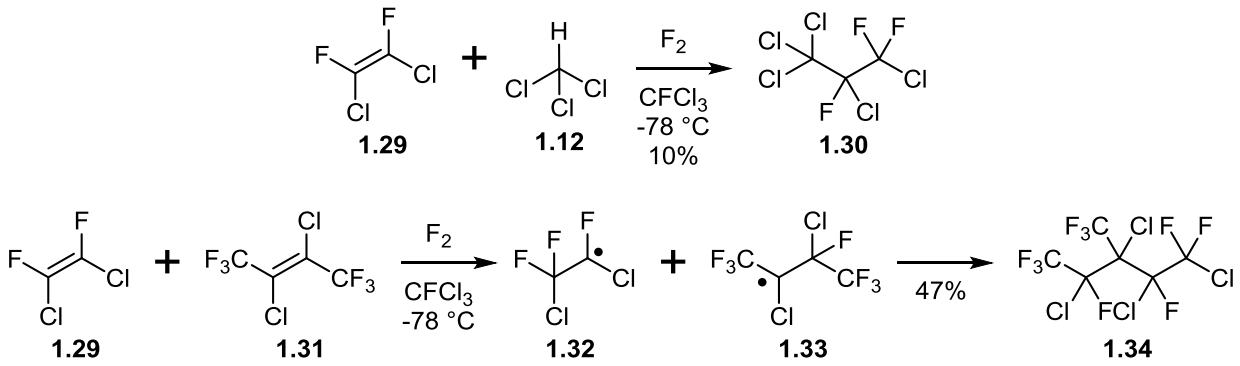

Scheme 1.5. Synthesis of chlorofluorocarbons 1.30 and 1.34

The action of elemental fluorine on aromatic compounds such as benzene leads the loss of aromaticity and the accumulation of polymeric by-products[23a,25] or the opposite problem of radical fragmentation to CF_4, C_2F_6, C_3F_8, C_4F_{10}, and C_5F_{10}.[26] Atomic fluorine (F•) generated from the homolysis of fluorine gas (**1.1**) undergoes an addition reaction into the aromatic ring leading to intermediate radical **1.36** which may add to another alkene or aryl ring leading to **1.38** and ultimately to polymerisation products (Scheme 1.6).[23a,25] Alternatively, **1.36** may be fluorinated to **1.37**, with the resulting diene more susceptible to radical addition and ultimately perfluorination to **1.39**. Fragmentation by homolytic cleavage of C-C bonds from excess thermal energy produced, leads to products related to combustion with fluorine. Fluorination of hexachlorobenzene also provided complex mixtures of non-aromatic chlorofluorocarbons.[27]

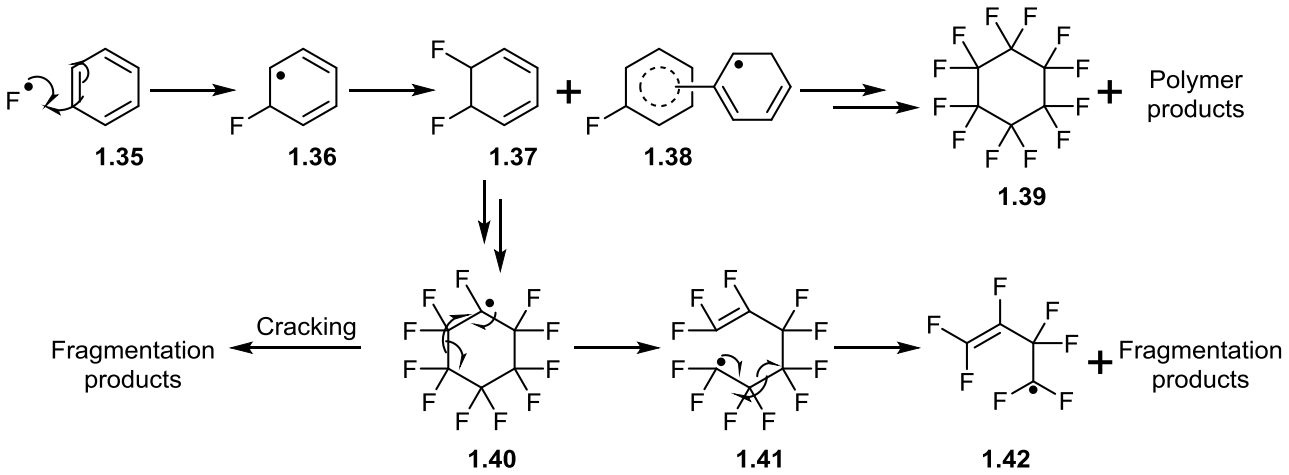

Scheme 1.6. Perfluorination of benzene by fluorine radicals

The problem of introducing fluorine into organic molecules can be understood by examining the thermochemistry of radical fluorination with elemental fluorine (Scheme 1.7).[12] Radical initiation can occur by the homolytic cleavage of the F-F bond (eqn. 1.1), but in the presence of an organic compound, two additional initiation pathways are possible. Unique to fluorine is a low energy pathway (eqn. 1.2) whereby a C-H bond reacts with F_2 to generate hydrofluoric acid, an alkyl radical and atomic fluorine. In the presence of unsaturation, even with a highly electron deficient alkene such as tetrafluoroethylene, radical initiation is an exothermic process (eqn. 1.3). The presence of these low-energy initiation pathways allows for reactions between fluorine gas and organic compounds to occur immediately on contact. Propagation of the radical chain (eqn. 1.4-1.7) is also exothermic; furthermore, the radical recombination of atomic fluorine with an alkyl radical (termination step) releases enough energy to dissociate C-C bonds. C-F bond formation releases 106.8 kcal/mol of energy (eqn. 1.8) for the first fluorination reaction with formation of perfluoroC-F bonds releasing as much as -163.7 kcal/mol of energy (eqn. 1.9). Overall, the reactions are highly exothermic with enough energy released to cause extensive fragmentation of organic molecules to carbon tetrafluoride (**1.6**) and hydrofluoric acid: a process analogus to combustion.

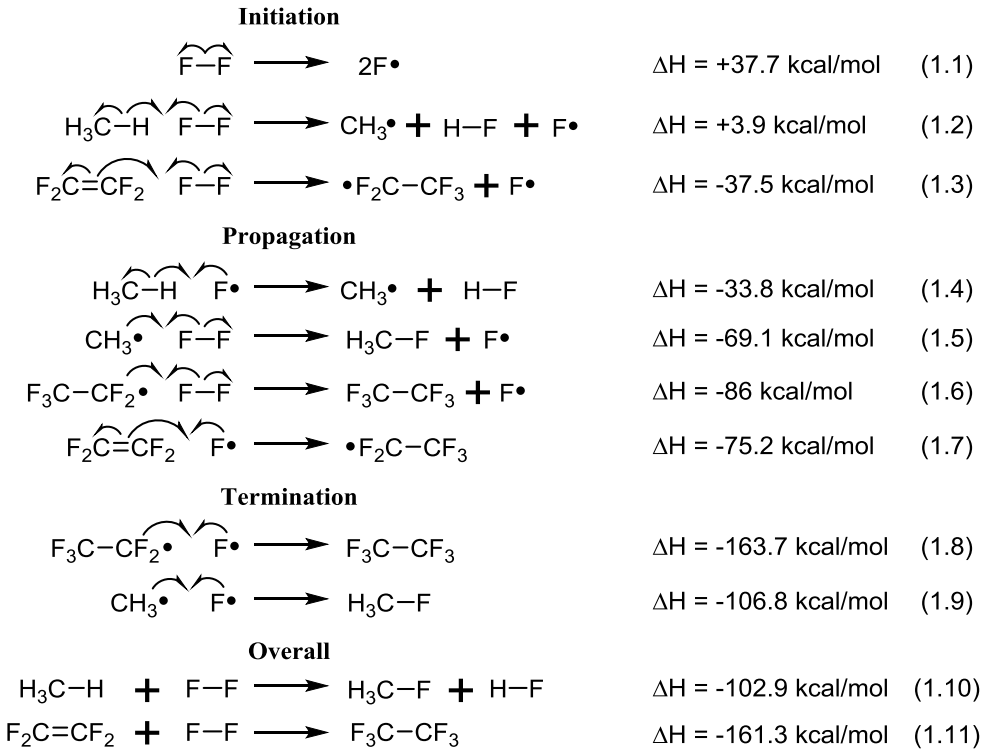

Scheme 1.7. Thermochemistry of radical fluorination with elemental fluorine

Any successful fluorination process must be able to control the vast amounts of energy released in carbon fluorine bond formation. A kinetic control method was introduced by Lagow and Margrave which revolutionized hydrocarbon fluorination chemistry.[28] By gradually introducing fluorine gas as a diluted mixture with nitrogen gas, energy could be sufficiently dissipated in molecular relaxation processes. Again, through dilution control, the probability of simultaneous fluorination and collision with a C-C bond was kept at a minimum, thus reducing C-C bond homolysis. As the hydrocarbon substrate accumulates more C-F bonds, a steric shielding affect is produced, which protects against C-C bond homolysis. Perfluorination can be achieved with higher concentrations of elemental fluorine and heating. The LaMar process[12] for perfluorination and other perfluorination methodologies employing elemental fluorine in a microreactor,[29] are an important class of radical fluorination reactions. Perfluorination can also be achieved by metal fluorides such as CoF_3,[30] although such a mechanism is

less radical and more electrochemical in nature.[15a] This thesis is primarily concerned with selective radical mono-fluorination, thus the topic of perfluorination will not be covered further.[31]

In the above mentioned work, elemental fluorine adds rapidly to sites of unsaturation. However, McEwan and Wolf have shown that it is possible to control addition to some extent (Scheme 1.8).[32] For instance, addition of fluorine to aromatic systems can be suppressed when the fluorination of tolanes (**1.43**) is carried out at -78 °C in solution phase. Tetrafluorination product **1.45** is the terminal product of fluorine addition, but the intermediate difluoroalkene **1.44** can also be obtained.

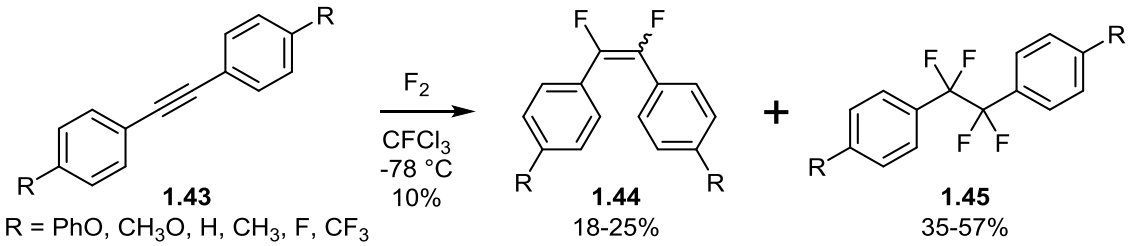

Scheme 1.8. Fluorination of tolanes

Some of the first selective organic transformations involving radical fluorination were performed on carboxylic acids in the solution phase. Bockemuller isolated 3-fluorobutyric acid (**1.47**) and 4-fluorobutyric acid (**1.48**) from the fluorination of butyric acid **1.46** in CCl_4 (Scheme 1.9).[23a] It is likely that this reaction occurs by a radical fluorination mechanism involving steps similar to eqn. 1.2.1, eqn. 1.2.2, eqn 1.2.4, and eqn 1.2.5, as analogous radical chlorination products (predominately the 3- and 4- chlorobutyric acids) have been obtained by Kharasch and Brown from the reaction of butyric acid **1.46** with sulfuryl chloride and a radical initatior.[33] This is in contrast to the known ability of elemental fluorine (**1.1**) to undergo ionic C-H substitution as demonstrated by Barton.[34] Fluorine inserts into the C-H bond and fluorination is achieved with retention of C-H configuartion.[10d,35]

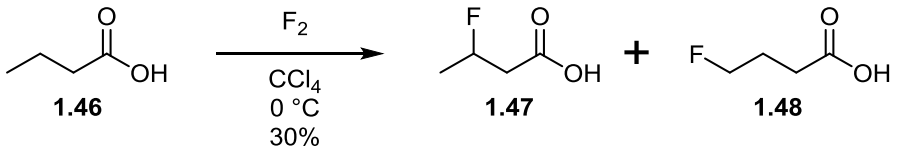

Scheme 1.9. Radical fluorination of butyric acid

Fluorodecarboxylation of alkanoic and perfluoroalkanoic acids have also been observed with elemental fluorine (**1.1**) (Scheme 1.10). Grakauskas has reported the fluorodecarboxylation of dicarboxylic acid salts **1.49** in water with elemental fluorine.[36] Yields up to 40% were obtained for terminal fluoroalkanoic acids (**1.50**). Although he claimed an ionic mechanism based on the known ionic reactivity of elemental fluorine in polar solvents, later work by Rozen and Hebel with aqueous fluorine solutions demonstrates otherwise.[37] A fluorodecarboxylation mechanism involving hypofluorite (**1.55**) decomposition (analogous to a Hunsdieker reaction)[38] and solvent-cage radical recombination is likely responsible for the observed mono-fluorodecarboxylation **1.50** and di-fluorodecarboxylation **1.51** products (Scheme 1.10, lower section).

In a similar manner, Marchionni and coworkers have obtained fluorodecarboxylation products from perfluoroether diacids.[39] Photochemical treatment of polymeric perfluoroether diacids (**1.52**) with elemental fluorine in perfluoroheptane provides quantitative conversion to the fully fluorinated products **1.53** (Scheme 1.10). The Hundiecker-like mechanism may be active, but the highly oxidizing conditions present in photochemical atomic fluorine generation allow for alternative decarboxylation pathways.

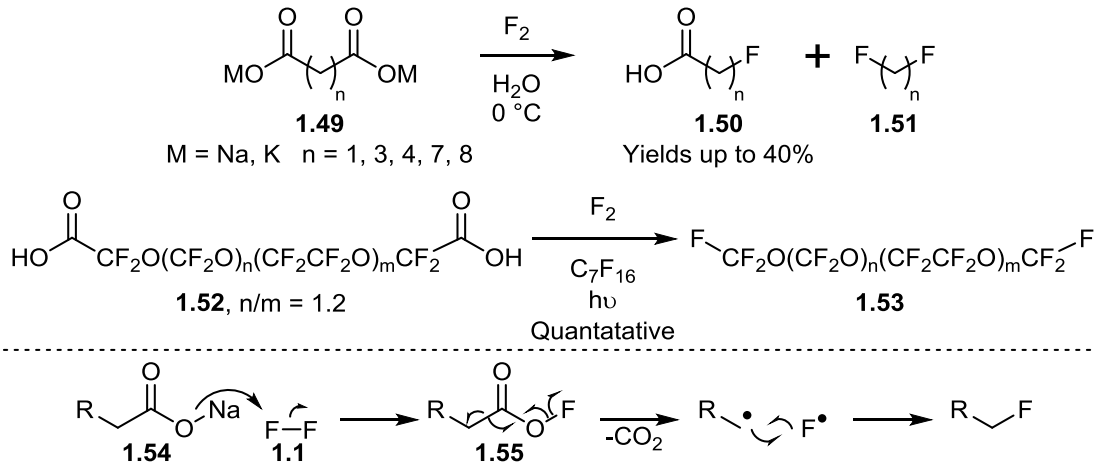

Scheme 1.10. Fluorodecarboxylation with elemental fluorine

Recently, microreactors[29] have been employed for direct fluorination of organic compounds as the small volumes and high surface areas in microchannels allow for easy dissipation of thermal energy. Early studies in gas phase fluorination of acetone (**1.56**) lead to complex reaction mixtures containing fluoroacetone (**1.57**), perfluoroacetone (**1.58**), as well as a host of products deriving from degradation and radical recombination (Scheme 1.11).[41] Chambers has studied the selective fluorination of 1, 3-dicarbonyl compounds in solutions of acetonitrile and formic acid (Scheme 1.12, top reactions).[41,42] High yields of the mono-fluoro products (**1.63**, **1.65**) can be obtained with ketoester **1.62** and diketone **1.64**. Although the reaction is carried out in a polar reaction medium, which favours electrophilic reactivity of elemental fluorine, radical processes may still be active.[43] Only a radical mechanism can adequately explain the 46% yield of fluoroethyl ester **1.67** (Scheme 1.12, bottom reaction).[42]

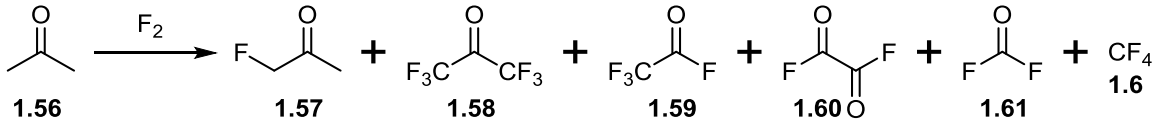

Scheme 1.11. Direct fluorination of acetone

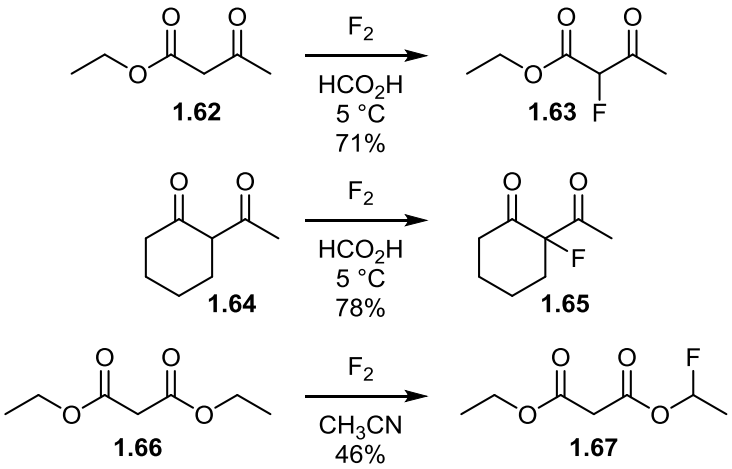

Scheme 1.12. Fluorination of 1, 3- dicarbonyl compounds in a microreactor

The fluorination of toluene (**1.68**)[44,45] and nitrotoluenes[41] with elemental fluorine has been achieved with selectivity for the monofluorinated arene **1.69** as high as those obtainable by the industrial Schiemann process (Scheme 1.13).[44] Electrophilic aromatic substitution with elemental fluorine is the dominant reaction mechanism for solution phase chemistry;[46] however, since these reactions are occurring at the liquid-gas interphase, radical mechanisms are likely also active and can explain the presence of undesired benzyl fluoride (**1.70**) and polymer products.

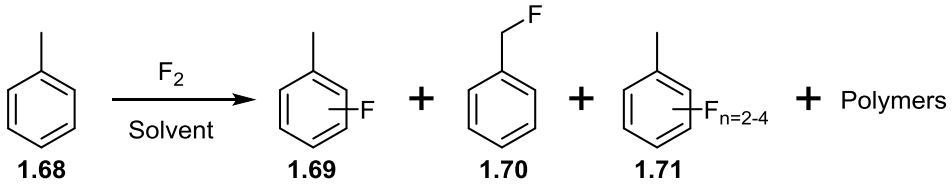

Scheme 1.13. Direct fluorination of toluene

1.2.2 Radical fluorination with trifluoromethyl hypofluorite

Trifluoromethyl hypofluorite (**1.2**) can be prepared by the action of elemental fluorine on methanol or carbon monoxide in the presence of a silver difluoride catalyst.[47] Under conditions similar to those which promote electrophilic behaviour in elemental fluorine, electrophilic reactivity can also be favoured with **1.2**.[48] The majority of selective fluorinations involving CF_3OF fall under the category of electrophilic fluorination as excellent yields can be obtained in the presence of radical inhibitors. After trifluoromethyl hypofluorite (**1.2**) became commercially available, the popularity of this reagent increased greatly as a 'safer' alternative to fluorine gas (**1.1**).[49]

Under reaction conditions that favour the generation of radicals, such as gas phase reactions or photochemically promoted reactions,[50] trifluoromethyl hypofluorite (**1.2**) is an excellent source of atomic fluorine. Rate constants have been measured for fluorine radical abstraction from **1.2** by the trifluoromethyl radical,[51] ethyl radical,[52] and radical intermediates derived from the polymerization assorted olefins.[53] The fast rates of fluorine abstraction from **1.2** by alkyl radicals prompted Roland to declare CF_3OF a "fluorine-donating radical scavenger."[52]

Addition of CF_3OF to alkenes has been the most studied of all reactions involving radical fluorination with **1.2** (Table 1.1).[54-61] Fluorine and trifluoromethoxyl radicals add to simple alkenes (entries 1-3) with no polymer formation reported. More complex alkenes (entries 4-6) do not lead to a productive reaction. An enol trifluoroacetate (entry 8) is a better substrate than an enol acetate (entry 7). In both cases, the selectivity is indicative of trifluoromethyoxy radical addition to the terminal carbon, followed by radical abstraction from the resulting heteratom-stabilized radical. Haloalkeness

(entries 9-20) containing fluorine, chlorine, or bromine are good substrates for addition reactions, with the exception of trichloroethane, which leads to minor amounts of polymerisation products (entry 18).

Perfluoroalkenes (Table 1.1, entries 21-26) were some of the first alkenes to be studied as substrates for the addition of trifluoromethyl hypofluorite (**1.2**). Tetrafluoroethylene lead to combustion or polymerisation products (entry 21), while perfluorocyclopentene provided quantitative yield of the addition product (entry 24). The addition of **1.2** to various perfluoroalkenes has been studied by EPR spectroscopy, which has produced evidence in support of the now widely accepted radical addition mechanism (Scheme 1.14).[53c,53e] Some haloalkenes (entries 27-30) participate in the reaection with formation of some interesting byproducts (entries 27, 29). With 1,1-difluoro, 2,2-dibromoethene, the double fluorine addition product CF_3CBr_2F is favoured (entry 29).

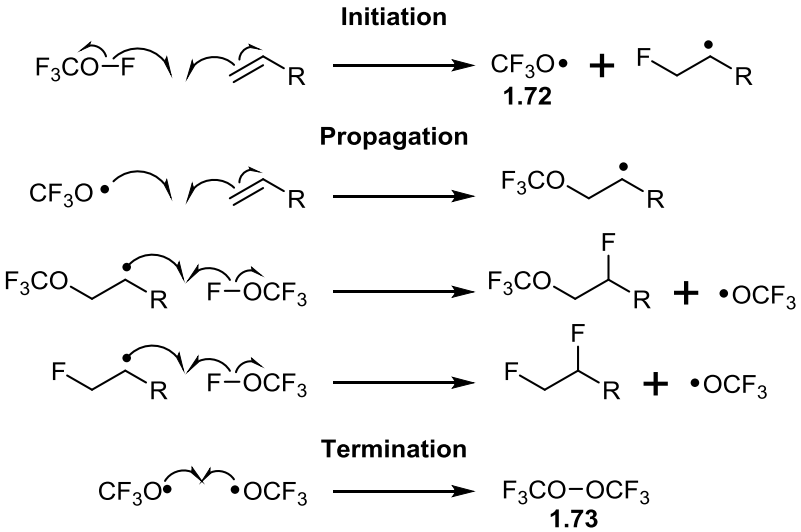

Scheme 1.14. Radical chain mechanism for addition of trifluoromethyl hypofluorite to alkenes

Table 1.1. Addition of trifluoromethyl hypofluorite to various alkenes

entry	alkene[a]-[h]	conditions	[%]products (%)[i]
1	$CH_2=CH_2$[c]	N_2 (hv)	[100] $CF_3OCH_2CH_2F$
2	$CH_2=CH_2$[e]	neat (-111 to 20 °C)	[83] $CF_3OCH_2CH_2F$
3	$CH_2=CHCH_3$[a]	CF_2Cl_2 (-155 to 22 °C)	$CF_3OCH_2CHFCH_3$(80), $CF_3OCH(CH_3)CH_2F$ (20)
4	c*is*- or *trans*-2-butene[a]	$CFCl_3$ (-155 to 22 °C)	charring
5	cyclohexene[a]	$CFCl_3$ (-160 to 22 °C)	charring
6	norbornylene[a]	$CFCl_3$ (-160 to 22 °C)	charring
7	$CH_2=CHOAc$[a]	$CFCl_3$ (-155 to 22 °C)	[33] $CF_3OCH_2CHFOCOCH_3$ (61), $CF_3OCH(OCOCH_3)CH_2F$ (39), $CH_3COOCHFCH_2F$ (trace)
8	$CH_2=CHOCOCF_3$[a]	CF_2Cl_2+$CFCl_3$ (-155 to 22 °C)	[83] $CF_3OCH_2CHFOCOCF_3$ (77), $CF_3OCH(OCOCF_3)CH_2F$ (23)
9	$CH_2=CHF$[a]	CF_2Cl_2 (-155 to 22 °C)	$CF_3OCH_2CHF_2$(87), $CF_3OCHFCH_2F$ (13)
10	$CH_2=CHF$[e]	neat (-111 to 20 °C)	[84]$CF_3OCH_2CHF_2$(90), $CF_3OCHFCH_2F$ (10)
11	*cis*-CHF=CHF[a]	neat (-150 to 22 °C)	$CF_3OCHFCHF_2$(100)
12	$CH_2=CF_2$[a]	$CFCl_3$ (-160 to 22 °C)	[76] $CF_3OCH_2CF_3$ (97.5), $CF_3OCF_2CH_2F$ (2), CF,CH,F (trace)
13	$CH_2=CF_2$[e]	neat (-111 to 20 °C)	[83] $CF_3OCH_2CF_3$
14	$CH_2=CHCH_2Cl$[a]	CF_2Cl_2+$CFCl_3$ (-165 to -30 °C)	[50] $CF_3OCH_2CHFCH_2Cl$ (84), $CF_3OCH(CH_2Cl)CH_2F$ (16)
15	*trans*-HClC=CHCl[a]	$CFCl_3$ (-50 °C)	[50] *threo*-$CF_3OCHCHClF$ (50), *erythro*-$CF_3OCHClCHClF$(50)
16	$CH_2=CCl_2$[a]	$CFCl_3$ (-150 to 22 °C)	[75] $CF_3OCH_2CCl_2F$
17	*cis*-$ClCH_2CH=CHCH_2Cl$[a]	$CFCl_3$ (-155 to 22 °C)	[90] *threo*-$CF_3OCH(CH_2Cl)CHFCH_2Cl$ (35), *erythro*-$CF_3OCH(CH_2Cl)CHFCH_2Cl$ (65)
18	CCl2=CHCl[f]	neat (31 °C)	CF3OCHClCCl2F (major) + polymer (minor)
19	$CH_2=CHBr$[a]	$CFCl_3$ (-140 to 22 °C)	[43] CF_3OCH_2CHBrF
20	$CF_2=CHF$[e]	neat (-111 to 20 °C)	[75] $CF_3OCHFCF_3$ (66), $CF_3OCF_2CF_2H$(33)
21	$CF_2=CF_2$[b]	neat (25 °C)	combustion or polymerisation
22	$CF_3CF=CF_2$[a]	neat (-155 to 22 °C)	[34] $CH_3OCF_2CH_2CH_3$ (67), $CF_3OCF(CF_3)_2$ (33)
23	$CF_3CF=CF_2$[d]	neat (various temp)	$CH_3OCF_2CH_2CH_3$ (68), $CF_3OCF(CF_3)_2$ (32)
24	perfluorocyclopentene[b]	neat (80 °C)	[100] perfluoromethoxycyclopentane

entry	alkene[a]-[h]	conditions	[%]products (%)[i]
25	*trans-i*$C_3F_7CF=CFCF_3$[g]	$CFCl_3$ (45 °C)	$(CF_3)_2CFCF_2CF(CF_3)OCF_3$ (96), $(CF_3)_2CFCF(OCF_3)CF_2CF_3$ (4)
26	$(CF_3)_2C=CFCF_2CF_3$[g]	$CFCl_3$ (45 °C)	$(CF_3)_2CFCF_2CF(CF_3)OCF_3$ (70), $CF_3CF_2CF_2C(CF_3)_2OCF_3$ (30)
27	$CF_2=CCl_2$[a]	neat (-150 to 22 °C)	$CF_3OCF_2CCl_2F$ (63), CF_3CCl_2F (25), $CF_3OCCl_2CF_3$(12)
28	$CF_2=CHBr$[a]	neat (-140 to 22 °C)	CF_3OCF_2CHBrF (70), $CF_3OCHBrCF_3$(24)
29	$CF_2=CBr_2$[a]	neat (-160 to 22 °C)	$CF_3OCBr_2CF_3$(20), CF_3CBr_2F(50), $CF_3OCF_2CBr_2F$(21)
30	$CF_2=CFBr$[a]	neat (-150 to 22 °C)	$CF_3OCF_2CF_2Br$ (80). $CF_3OCFBrCF_3$(20)
31	$C_6H_5CH=CH_2$[h]	$CFCl_3$ (-78 °C)	$C_6H_5CH(CF_3O)CH_2F$ (31), $C_6H_5CHFCH_2F$ (31), Other[j] (38)
32	*p*$(CH_3)C_6H_4CH=CH_2$[h]	$CFCl_3$ (-78 °C)	*p*$(CH_3)C_6H_4CH(CF_3O)CH_2F$ (43), *p*$(CH_3)C_6H_4CHFCH_2F$ (26), Other[j] (31)
33	*p*$(CH_3O)C_6H_4CH=CH_2$[h]	$CFCl_3$ (-78 °C)	Other[j] (100)
34	*p*$(Cl)C_6H_4CH=CH_2$[h]	$CFCl_3$ (-78 °C)	*p*$(Cl)C_6H_4CH(CF_3O)CH_2F$ (30), *p*$(Cl)C_6H_4CHFCH_2F$ (30), Other[j] (41)
35	*m*$(Cl)C_6H_4CH=CH_2$[h]	$CFCl_3$ (-78 °C)	*m*$(Cl)C_6H_4CH(CF_3O)CH_2F$ (24), *m*$(Cl)C_6H_4CHFCH_2F$ (32), Other[j] (44)
36	*m*$(NO_2)C_6H_4CH=CH_2$[h]	$CFCl_3$ (-78 °C)	*m*$(NO_2)C_6H_4CH(CF_3O)CH_2F$ (37), *m*$(NO_2)C_6H_4CHFCH_2F$ (11), Other[j] (53)

[a]Data from reference 54. [b]Data from reference 55. [c]Data from reference 56. [d]Data from reference 57. [e]Data from reference 58. [f]Data from reference 59. [g]Data from reference 60. [h]Data from reference 61. [i][combined isolated yield] product (percent composition) [j]Other = $Ar(CF_3O)CHCF_2H$ (**1.78**) + $ArCHFCF_2H$ (**1.79**) + ArCH=CHF (**1.80**).

Addition of **1.2** to styrenes (Table 1.1, entries 31-36) provides a different regioselectivity than expected by the radical chain mechanism in Scheme 1.14. The trifluoromethoxyl moiety attaches in the internal alkene position and, as similarly observed with 1, 1-difluoro, 2,2-dibromoethene (entry 29), the difluorinated compounds become increasingly noticeable. Additionally, new fluorinated compounds related to β-fluorostyrene **1.80** are present and even dominate with electron-rich styrenes (entry 33). To explain the observed reactivity, Levy has postulated a mechanism involving oxidation of intermediate radical **1.75** to the ion pair **1.76** and **1.77**, followed by cage-recombination to yield **1.78**, or deprotonation of **1.76** to β-fluorostyrene **1.80** products (Scheme 1.15).[61] Radicals **1.75** that escape oxidation can be fluorinated leading to the difluorinated products **1.79**.

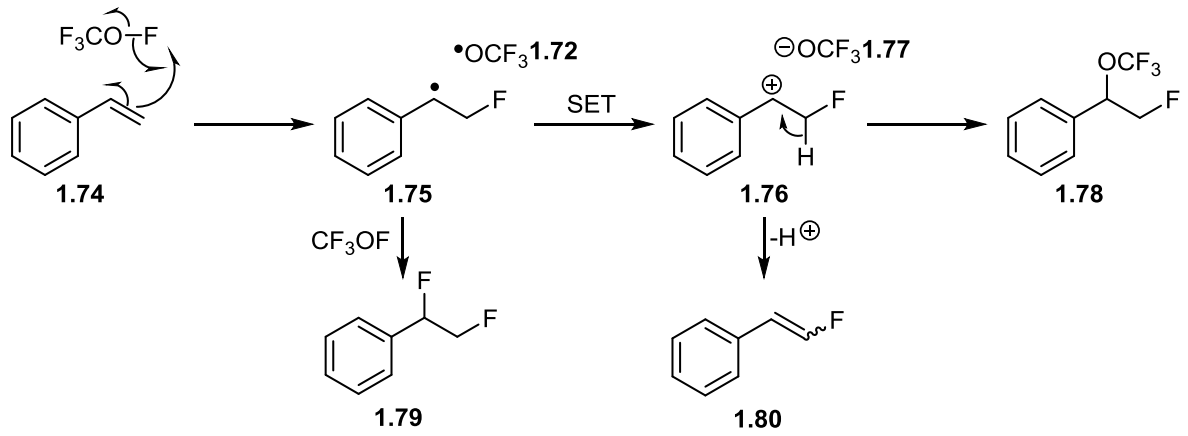

Scheme 1.15. Mechanism of trifluoromethyl hypofluorite addition to styrene

Despite the established efficient radical fluorinating ability of CF_3OF, few have employed it for radical fluorination. Early work by Allison and Cady on the radical fluorination of benzene (**1.35**) by trifluoromethyl hypofluorite in the gas phase reported a 5% yield of fluorobenzene (**1.82**) and an equivalent amount of trifluoromethoxybenzene (**1.83**).[56] It was postulated that radical addition into

benzene provides intermediate **1.81**, which eliminates either trifluoromethanol or hydrofluoric acid with equivalent selectivity to **1.82** and **1.83** (Scheme 1.16).

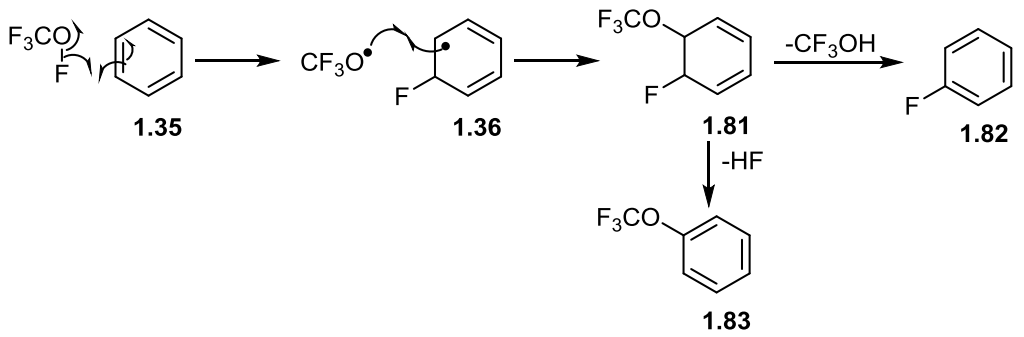

Scheme 1.16. Trifluoromethoxyl radical addition to benzene

An improved procedure described by Kollonitsch and co-workers entails the ultraviolet irradiation of a solution of trifluoromethyl hypofluorite (**1.2**) and an arene at low temperatures (Scheme 1.17).[62] By this method, fluorobenzene (**1.82**) was synthesized in 65% yield from benzene along with 10% yield of trifluoromethoxybenzene (**1.83**). The photochemical fluorination of toluene (**1.68**) lead to high selectivity for *ortho*-fluorotoluene (*o*-**1.69**) along with 25% yield of **1.70**.

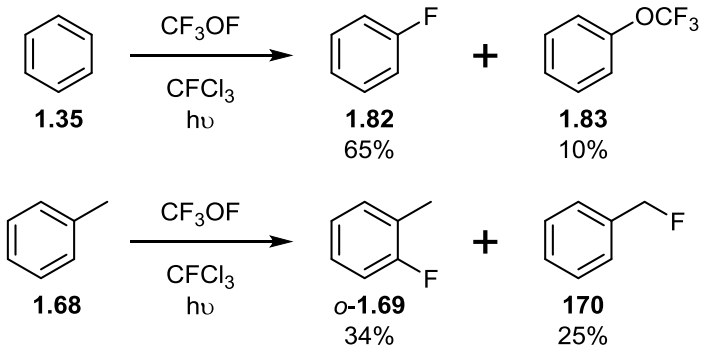

Scheme 1.17. Photochemical fluorination of arenes with trifluoromethyl hypofluorite

Kollonitsch and co-workers at Merck's research laboratories contributed greatly to the field of radical fluorination with CF_3OF.[63] Direct photochemical fluorination of various organic compounds (Scheme 1.18),[62] including amino acids (Scheme 1.19),[64] were performed with reasonable selectivity and yields on multi-gram scales. Under photochemical irradiation, the O-F bond of trifluoromethyl hypofluorite (**1.2**) is homolyzed (eqn. 1.12)[50] to generate the reactive fluorine (F•) and trifluoromethoxyl radicals (**1.72**). Abstraction of susceptible C-H bonds by the electron deficient **1.72** generates an alkyl radical (eqn. 1.13), which is fluorinated rapidly by **1.2** (eqn. 1.14). In this manner, cyclohexylfluoride (**1.85**) can be obtained in 44% yield and isobutyric acid (**1.86**) can be monofluorinated to **1.87** and **1.88** in a combined 70% yield (Scheme 1.2.18, upper section).[62]

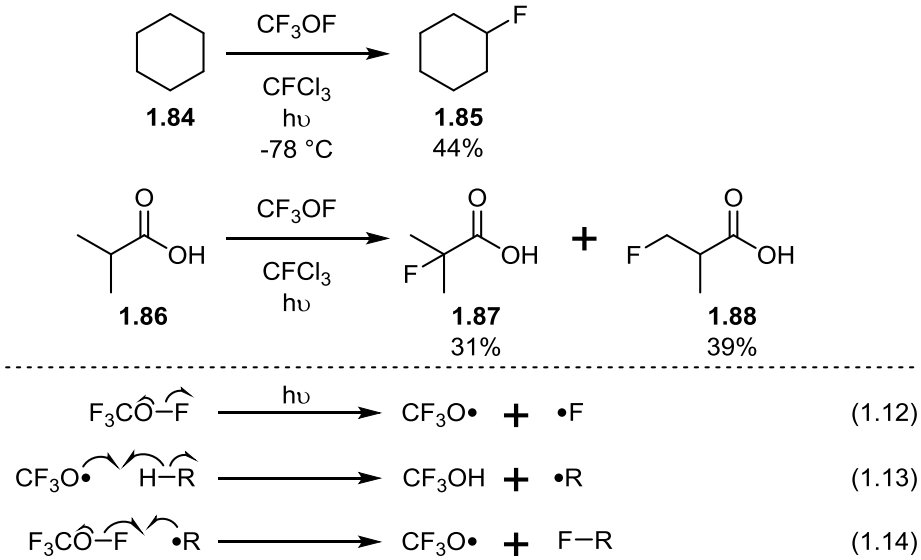

Scheme 1.18. Photofluorination with trifluoromethyl hypofluorite

A powerful application of this methodology is the selective fluorination of bioactive compounds such as amino acids employing hydrofluoric acid as the solvent (Scheme 1.19).[64] Not only does hydrofluoric acid act as a protecting group to prevent oxidation of the nitrogen, it also reduces the

susceptibility of the α-amino proton to radical abstraction.[63] Both enantiomers of alanine can thus be selectively fluorinated on the terminal methyl carbon in synthetically useful yields. The resultant fluoroaminoacids have been studied for their antibiotic properties.[64] Fluorinated products of *S*-azetidine-2-carboxylic acid (**1.91**) and *S*-isoleucine (**1.94**) can also be isolated in reasonable yields.

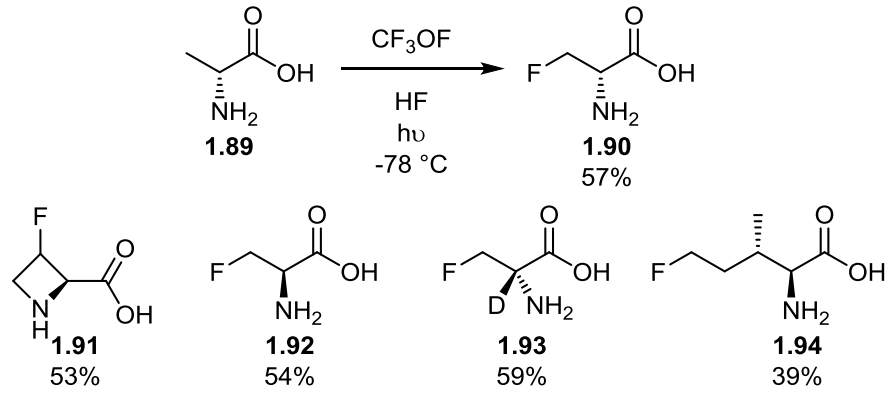

Scheme 1.19. Photofluorination of amino acids with trifluoromethyl hypofluorite

1.2.3 Hypofluorites other than trifluoromethyl hypofluorite

While trifluoromethyl hypofluorite is the most studied member of the hypofluorite family (Figure 1.1) for radical fluorination, a plethora of other hypofluorites have been investigated.[49,65] The reactivity of compounds such as $CF_2(OF)_2$, CF_3CF_2OF, and $CF_3(CF_2)_nOF$, is analogous to that of trifluoromethyl hypofluorite (**1.2**),[65] and thus present no significatn advantage over it. Indeed, these hypofluorites are not commercially available, and substances like $CF_2(OF)_2$, are more hazardous than **1.2**.[66] Trifluoromethyl hypofluorite thus remains the reagent of choice for radical fluorionation. However, the foregoing perfluorohypofluorites find important applications in industrial synthesis of fluoro-monomers and perfluoropolymers.[49]

Perfluoroacyl hypofluorites (**1.95**, **1.96**) are very important compounds in regards to industrial applications towards fluoropolymers. The O-F bond is highly susceptible to homolytic breakage with formation of a fluorine radical, carbon dioxide, and a perfluoroalkyl radical.[67] Perfluoroacyl hypofluorites (**1.96**) are effective radical initiators for perfluoroalkene polymerization.[68] The application of perfluoroacyl hypofluorites has been limited to polymer chemistry and selective radical fluorination has not been studied with this class of compounds.

Acetyl hypofluorite (**1.97**) is another source of radical fluorine.[69] Early studies on the synthesis,[70] isolation, and characterization[71] of this compound in pure form have demonstrated the O-F bond is susceptible to homolytic breakage with formation of a fluorine radical, carbon dioxide and the methyl radical, which ultimately leads to the formation of methyl fluoride.[72] This is analogous to the decomposition of trifluoroacetyl hypofluorite (**1.95**) into carbon dioxide and tetrafluoromethane (**1.6**).[67b] However, in an aqueous solution, acetyl hypofluorite (**1.97**) is remarkably stable, unlike other members of the acyl hypofluorite family (**1.55**) that rapidly decompose through radical pathways.[37] In polar media, radical pathways for acetyl hypofluorite (**1.97**) are almost entirely suppressed and this reagent has found widespread application as an electrophilic fluorinating agent.[73] Although acetyl hypofluorite may be considered a radical fluorination agent, it has not been studied as such. A qualification of this statement must be made as Visser[74] treats **1.97** as a radical fluorinating agent invoking radical cation intermediates (much like the chemistry of xenon difluoride).[15] However, the vast majority of literature supports non-radical pathways for fluorination with **1.97**.

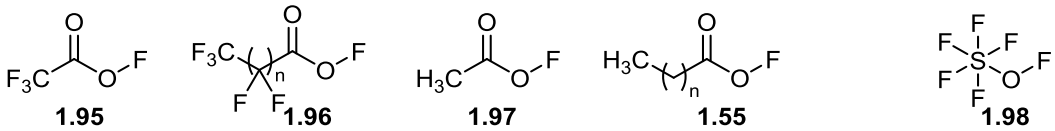

Figure 1.1. Members of the acyl hypofluorite family of compounds and pentafluorosulfur hypofluorite

Pentafluorosulfur hypofluorite (**1.98**) has been studied as a radical fluorinating agent.[75-77] Addition of **1.98** to alkenes display evidence of radical reactivity as polymeric materials can be obtained if the reaction conditions are not carefully controlled. The addition of pentafluorosulfur hypofluorite (**1.98**) to various alkenes is summarized in Table 1.2. The reported fluorination regioselectivity of **1.98** additions (entries 2, 3, 6, 7) resemble the addition of **1.2** to styrenes[61] in that a C-F bond is formed with the most electron poor alkene carbon.[77] This suggests that the mechanism of addition begins with fluorination followed by O-C bond formation. Another similarity between **1.98** and **1.2** is the poor yields and increased side-products resulting from addition to brominated alkenes (entry 10).

Table 1.2. Addition of pentafluorosulphur hypofluorite to various alkenes

entry	alkene	product (%)
1	$CH_2=CH_2$[b]	$F_5SOCH_2CH_2F$
2	$CH_2=CHF$[c]	$F_5SOCH_2CHF_2$ (100)
3	$CH_2=CF_2$[c]	$F_5SOCH_2CF_3$ (100)
4	$CF_2=CF_2$[b]	$F_5SOCF_2CF_3$
5	perfluorocylopentene[b]	F_5SO-*cyclo*C_5F_9
6	$CH_2=CHCl$[b]	F_5SOCH_2CHClF
7	$CH_2=CCl_2$[d]	$F_5SOCH_2CCl_2F$ (71)
8	*cis*- or *trans*- CHCl=CHCl[d]	$F_5SOCHClCHClF$ (81)
9	$CCl_2=CCl_2$[b]	$F_5SOCCl_2CCl_2F$
10	CHBr=CHBr[d]	$F_5SOCHBrCHBrF$ (15)

[a]Reactions performed in the gas phase at ambient temperatures. [b]Data from reference 75. [c]Data from reference 76. [d]Data from reference 77. [e]product (reported yield in percent)

1.2.4 Radical fluorination with xenon difluoride

Xenon difluoride (**1.3**) can be prepared by the action of elemental fluorine (**1.1**) on xenon gas under ultraviolet irraditation.[78] The ease of synthesis is exemplified by the procedure of exposing a pyrex glass bulb containing a 1: 1 mixture of the two gases to sunlight and observing the condensation of solid XeF_2 to the glass walls.[78b] The reagent is commercially-available, and it is a solid, stable in air at room-temperature. As a consequence, it is a very popular fluorinating reagent (Figure 1.2).[79]

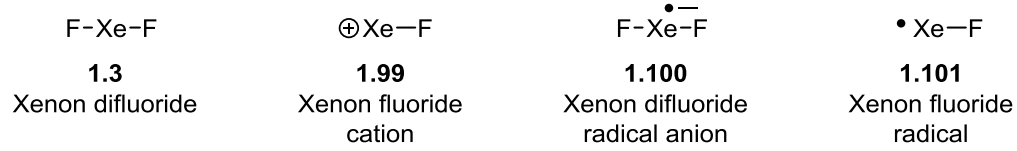

Figure 1.2. Xenon fluorides

The fluorination chemistry of XeF_2 cannot be easily classified as nucleophilic, electrophilic, radical, or electrochemical. Fluorine ligands on xenon can be exchanged for oxygen-containing ligands, in a manner reminiscent of the nucleophilic fluorination chemistry of fluoro-sulfur reagents. Electrophilic fluorination with **1.3** can be catalyzed by the addition of Bronsted or Lewis acids, and are likely to proceed through intermediate **1.99**. The majority of fluorination reactions mediated by **1.3** belong in this category. Even the surface of Pyrex glass can behave as a heterogeneous Lewis acid catalyst. [80]

The reaction of XeF_2 with unsaturated compounds such as alkenes, alkynes, arenes, and enol ethers is believed to occur through SET chemistry. However, radical recombination leading to the ultimate fluorination product occurs rapidly so that it is difficult to distinguish this sequence from

electrophilic fluorination (Scheme 1.20). Activation of XeF_2 by an acid catalyst is typically required for effective fluorination, and although coordination complex **1.102** may be formed, *in-situ* conversion of XeF_2 to **1.99** is equally likely. Both SET to coordination complex 1.102 (radical reactivity) and electrophilic addition to cationic **1.99** (ionic reactivity) are invoked to explain XeF_2 addition to unsaturation. Nevertheless, cationic intermediates **1.104** and carbocation rearrangements appear to best explain the observed reactivity of XeF_2-mediated fluorination of alkenes, alkynes, arenes, and enol ethers (electrophilic fluorination mechanism).[81] In the follow section, I will limit the overview of XeF_2 mediated fluorination to examples where direct evidence for radical intermediates can be found, namely: fluorination of halocarbons, fluorodecarboxylation, fluorodesilylation, and nitronate anion fluorination.

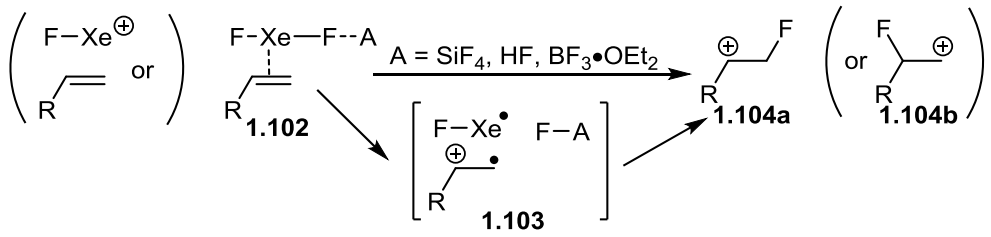

Scheme 1.20. Electrophilic addition of XeF_2 to alkenes

Similar to elemental fluorine (**1.1**)[12,17] and trifluormethoxy hypofluorite (**1.2**),[50] xenon difluoride (**1.3**) may be utilized directly as a source of fluorine radicals[11] and will react with many hydro-halocarbons (Scheme 1.21).[82] Bucher and Scaiano have used laser flash photolysis of XeF_2 to study fluorine radicals.[11] Holloway and co-workers have found that XeF_2 in dichloromethane (**1.105**) will decompose in 2 days, yielding primarily chlorofluoromethane (**1.106**), dichlorofluoromethane (**1.107**) and hydrofluoric acid. In dibromomethane (**1.109**), XeF_2 decomposition occurs within minutes

yielding bromofluoromethane (**1.110**) and difluoromethane (**1.10**).[82] Trace amounts of water from improperly purified solvents are believed to induce formation of hydrofluoric acid, which activates XeF_2 by polarizing the Xe-F bond. The mechanism of degradation is anticipated to be complex as activated xenon difluoride can be utilized in both electrophilic and single electron oxidation pathways.

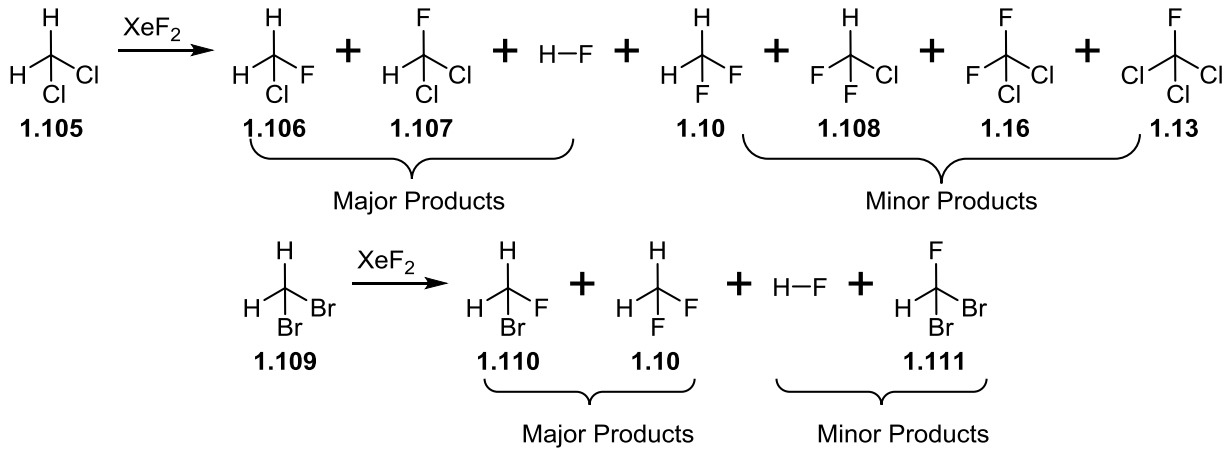

Scheme 1.21. Reaction of XeF_2 with hydrohalocarbon solvents

Patrick and co-workers studied the fluorodecarboxylation of alkyl carboxylic acids with xenon difluoride (Scheme 1.22).[83,84] A variety of primary, tertiary, α-aryloxy and benzylic alkyl fluorides can be obtained in moderate to good yields from decarboxylation of the corresponding carboxylic acid. Compounds **1.112** and **1.113** represent the first aryl fluoromethyl ethers to be synthesized through direct radical fluorination (64% and 84% yield, respectively). Double fluorodecarboxylation of **1.117** to difluoroalkene **1.118** can also be performed in good yields.

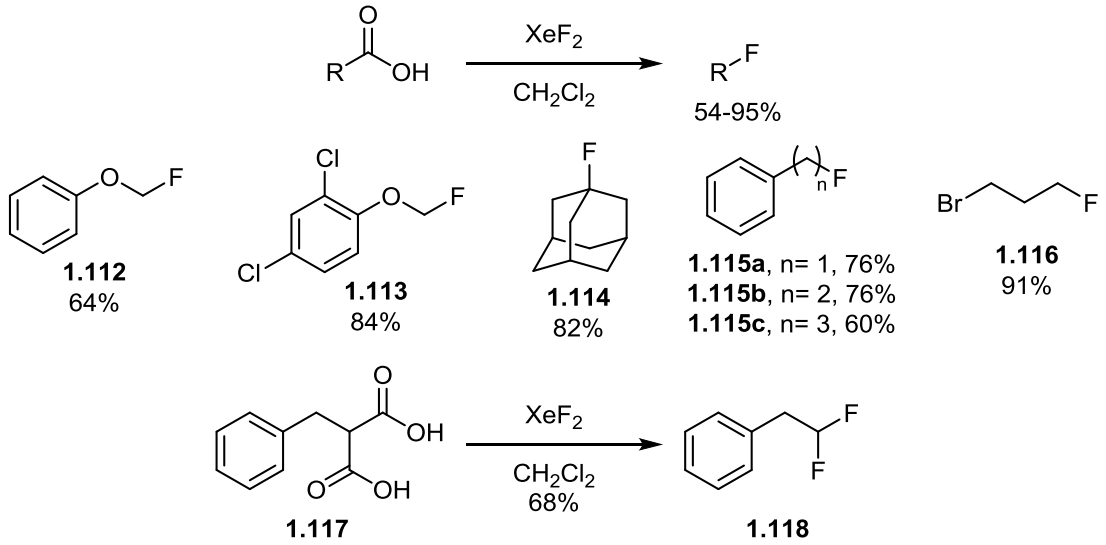

Scheme 1.22. Fluorodecarboxylation with xenon difluoride

Investigations into the mechanism of fluorodecarboxylation revealed that both radical and ionic pathways to fluorodecarboxylation are possible. These studies provide insight as to why secondary alkyl fluoride synthesis by this method is scarce (*vide infra*).[84] Optically active Mosher's acid (**1.119**) can be fluorodecarboxylated in excellent yields; however, product **1.120** is obtained as the racemate, which indicates that a planar radical or carbocation intermediate is involved. Fluorodecarboxylation of 6-heptenoic acid (**1.121**) yields the cyclization product **1.122** (obtained through cyclization of an intermediate 5-hexenyl radical) along with the linear alkylfluoride **1.123** in a 1: 3 ratio. Treating the cyclization of **1.122** as a kinetic competition experiment, fluorination of the alkyl radical occurs at an estimated rate of 1.1 x 10^6 M^{-1} s^{-1}.[84] Fluorodecarboxylation of primary alkyl carboxylic acids with XeF_2 in solutions saturated with [^{18}F] fluoride yields the radioactive fluorination product [^{18}F]**1.116** in 78% radiochemical yield.[83b] Ligand exchange to generate a mixed ^{19}F-Xe-^{18}F reagent would provide a 50%

radiochemical yield at best and is not likely occurring.[a] Thus alkyl carboxylic acids may be fluorinated through a nucleophilic mechanism involving fluoride in some instances.

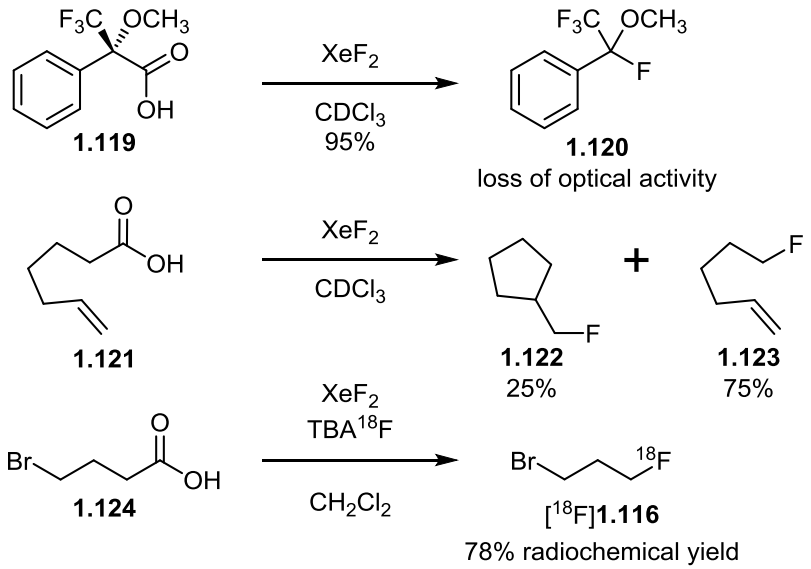

Scheme 1.23. Mechanistic investigations of fluorodecarboxylation with XeF_2

From the experiments in Scheme 1.23, Patrick and co-workers have postulated that both a radical fluorination mechanism and a nucleophilic displacement mechanism are active (Scheme 1.24). The presence of cyclopentylmethyl fluoride (**1.122**) strongly supports the radical nature of this reaction as cyclization of the 5-hexenyl radical is a well-established radical clock.[86] Single electron transfer oxidation of the carboxylic acid followed by the loss of hydrofluoric acid and decarboxylation yields an alkyl radical, which can undergo cyclization. Fluorination of the resulting radical may occur directly by an S_H2 reaction with XeF_2 or the **1.101**. Alternatively, the radical may be first oxidized to the cation followed by recombination with fluoride.

---

[a] The formation of [^{18}F]XeF_2 requires specific conditions not likely obtained by Patrick and coworkers. See reference 85 and references within on the controversy surrounding the synthesis of this reagent.

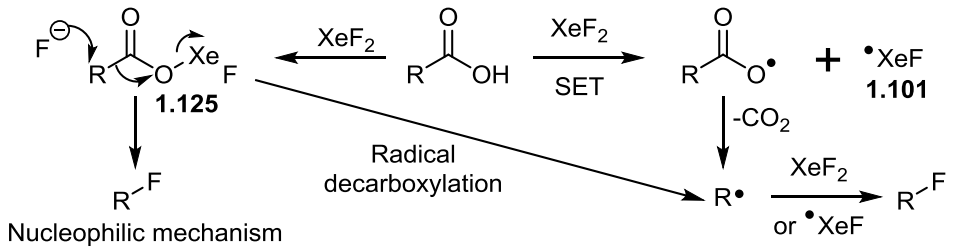

Scheme 1.24. Proposed mechanisms for fluorodecarboxylation with XeF_2

In the presence of acid, ligand exchange of fluoride from **1.3** generates a mixed fluoroxenon ester **1.125** which can be susceptible to nucleophilic attack by fluoride. Such a mechanism adequately explains the formation of [^{18}F]**1.116** whereas cage-recombination products would dominate a decarboxylation-oxidation mechanism leading to less radioactive product. Radical decarboxylation through a Hunsdiecker-like mechanism from the xenoester **1.125** to an alkyl radical is also know to occur and is an excellent method for the generation of perfluoroalkyl radicals.[87] Gregorcic and Zupan have combined these two reactions for the tandem radical addition of fluorine and trifluoromethyl to styrenes (Scheme 1.25).[88] While the combined products from electrophilic addition of fluorine (**1.79** and **1.127**) account for a greater percentage of reaction products, addition of trifluoromethyl radical to **1.129** followed by fluorine trapping (**1.126**) was observed in 26% relative yield.

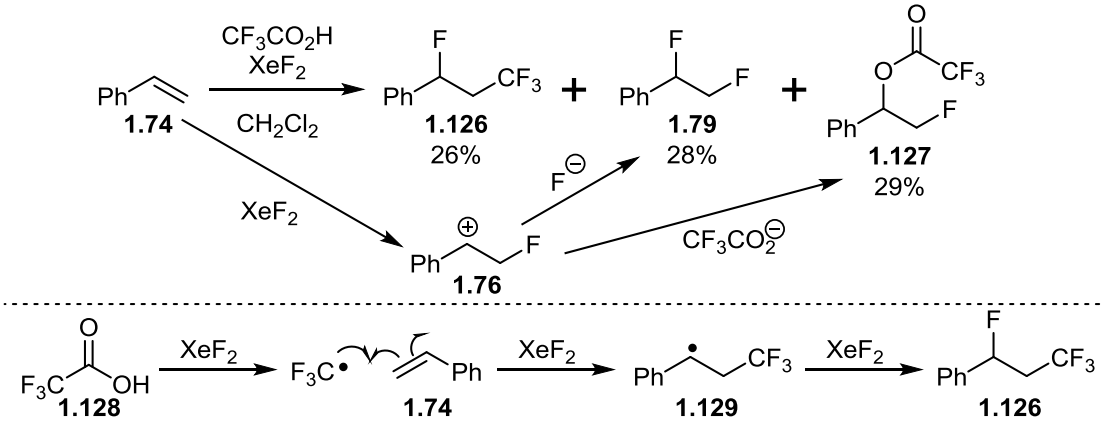

Scheme 1.25. Radical addition of trifluoromethyl and fluorine to styrene

Lothian and Ramsden have reported the fluorodesilylation of trimethylsilylbenzenes in good yields through an aryl radical intermediate (Scheme 1.26).[89] Essential to the success of this reaction was the use of hexafluorobenzene as an inert solvent. When the reaction was carried out in chloroform, significantly decreased yields of the desired fluorobenzene **1.131c** were obtained along with **1.132-1.134** in a combined yield of 48%. The presence of **1.132** and **1.133** strongly implicates an aryl radical intermediate. The mechanism for fluorodesilylation, as proposed by Lothian and Ramsden, commences with the SET oxidation of trimethylsilylbenzene to the radical cation **1.135** with the concurrent reduction of **1.3** to **1.101** and fluoride (Scheme 1.26, lower section). The authors state that it is unclear whether the fluoroxenon radical recombines to **1.136** prior to fluoride-assisted desilylation. The ultimate aryl radical **1.138** is then fluorinated by xenon difluoride.

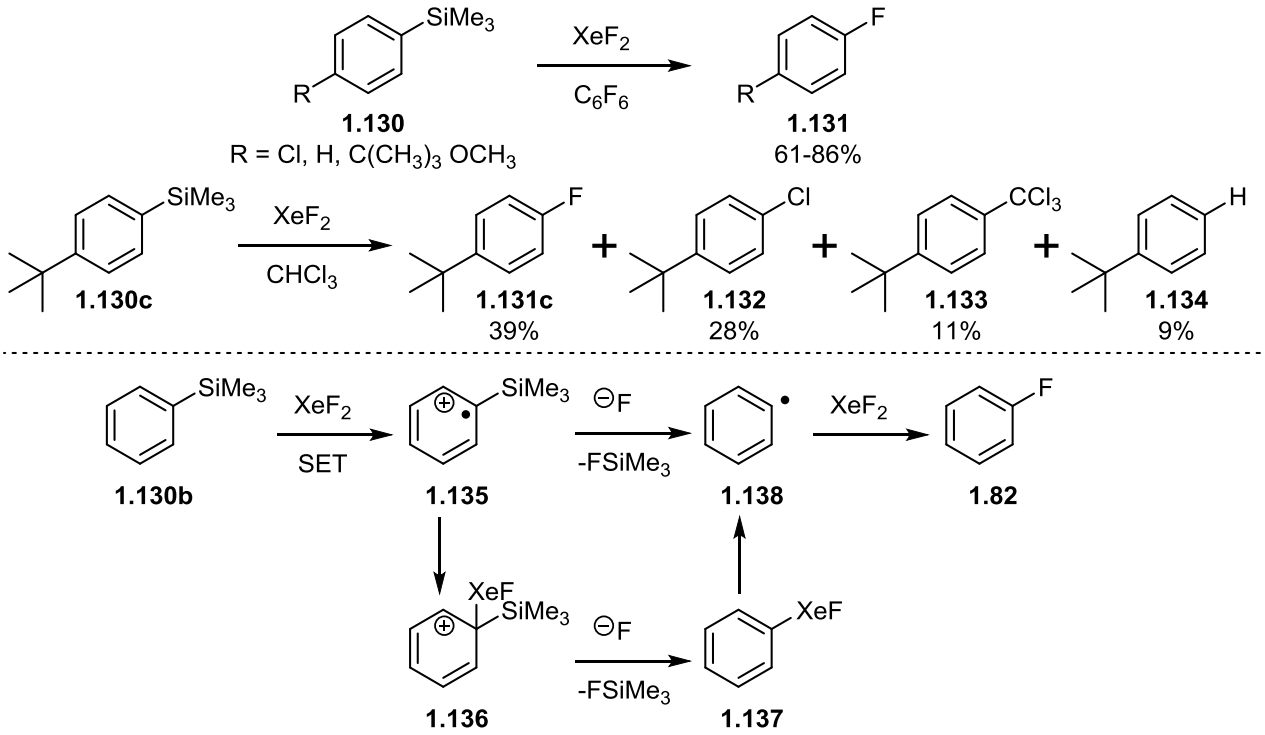

Scheme 1.26. Fluorodesilylation of trimethylsilylbenzenes with XeF_2

It is important to note that fluorodesilylation only occurs with electron-rich substrates. Bardin and Frohn have shown that the reaction manifold of electron-poor trimethylsilylarenes with XeF_2 in the presence of Lewis acids occurs through alternative pathways (Scheme 1.27).[90] To illustrate, trimethylsilylbenzene **1.139** is fluorinated to diene **1.140** when exposed to XeF_2 activated by boron trifluoride, which encourages electrophilic behaviour. When Ramsden tried to extend the fluorodesilylation reaction to aryl trimethylsilyl ester **1.141**, the rearranged fluoroformate **1.142** was obtained as the major product.[91] Further studies showed that trace amounts of acid were promoting an ionic rearrangement mechanism and that aryl radicals generated through decarboxylation did not lead to fluorination products.[80a] Recently, Ramsden has revised his mechanistic hypothesis for the fluorodesilylation of trimethylsilylbenzenes (Scheme 1.26) to include an electrophilic fluorination mechanism involving the XeF cation (**1.99**).[92]

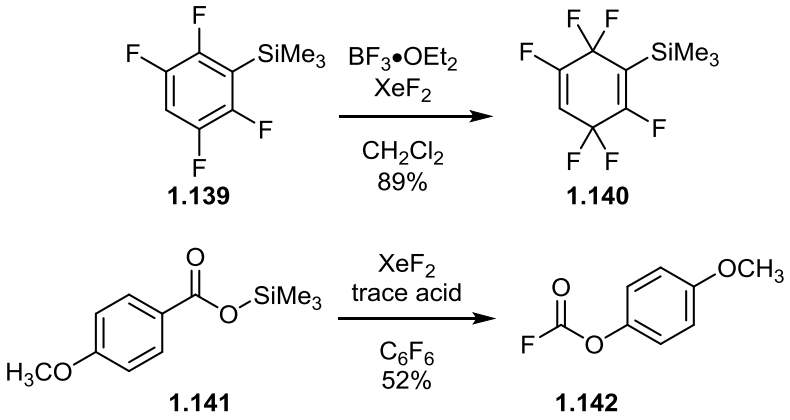

Scheme 1.27. Acid catalyzed XeF_2 reactions of silylated compounds

The fluorination of silyl enol ethers by xenon difluoride is generally believed to occur through an electrophilic pathway,[93] similar to electrophilic fluorination of vinyl ethers, enol esters,[94] silyl ketene acetals,[95] and 1, 3- dicarbonyls.[94,96] However, recent studies by Ramsden and Smith provide compelling evidence to support an SET pathway for silyl enol ether fluorination under select reaction

conditions (Scheme 1.28, lower section).[97] Carbocyclic silyl enol ether **1.143** is fluorodesilylated quantitatively to α-fluoroketone **1.144** with XeF_2 in acetonitrile as the solvent and in a reaction vessel made of Pyrex glass. The specific combination of acetonitrile in a Pyrex glass reaction vessel was chosen to prevent polarization of the Xe-F bond and prevent the formation of the formation of XeF cation (**1.99**).[80a,97] Under identical reaction conditions, acyclic silyl enol ether **1.145** produced fluoroketone **1.146** in 38% yield with the major reaction product being acetophenone (**1.147**: 53% yield). When the reaction was carried out in deuteroacetonitrile, no deuterium incorporation was detected in **1.147**.

The following rationale was advanced to account for these observations. An initial SET of **1.145** with XeF_2 delivers the radical cation intermediate **1.148**, which may be fluorinated by the XeF_2 radical anion (**1.100**) and desilylated by fluoride. Alternatively, radical intermediate **1.148** can undergo a 1, 5- hydrogen atom transfer from the trimethylsilyl moiety to generate **1.149**, thus explaining the lack of deuterium incorporation into **1.147** when the reaction was performed in deuterated solvent.

Ramsden proposes that all silyl enol ether fluorinations employing XeF_2 follow a similar course, despite the reported use of acid activation in some instances and analogous results to reactions employing known electrophilic fluorinating conditions.[98] The fluorodesilylation of a peptomimetic fragment **1.151** to fluoro product **1.152** (71% yield; 1:1 mixture of diasteromers) was performed under conditions that could not have generated XeF cation (**1.99**) (Scheme 1.29).[98c]

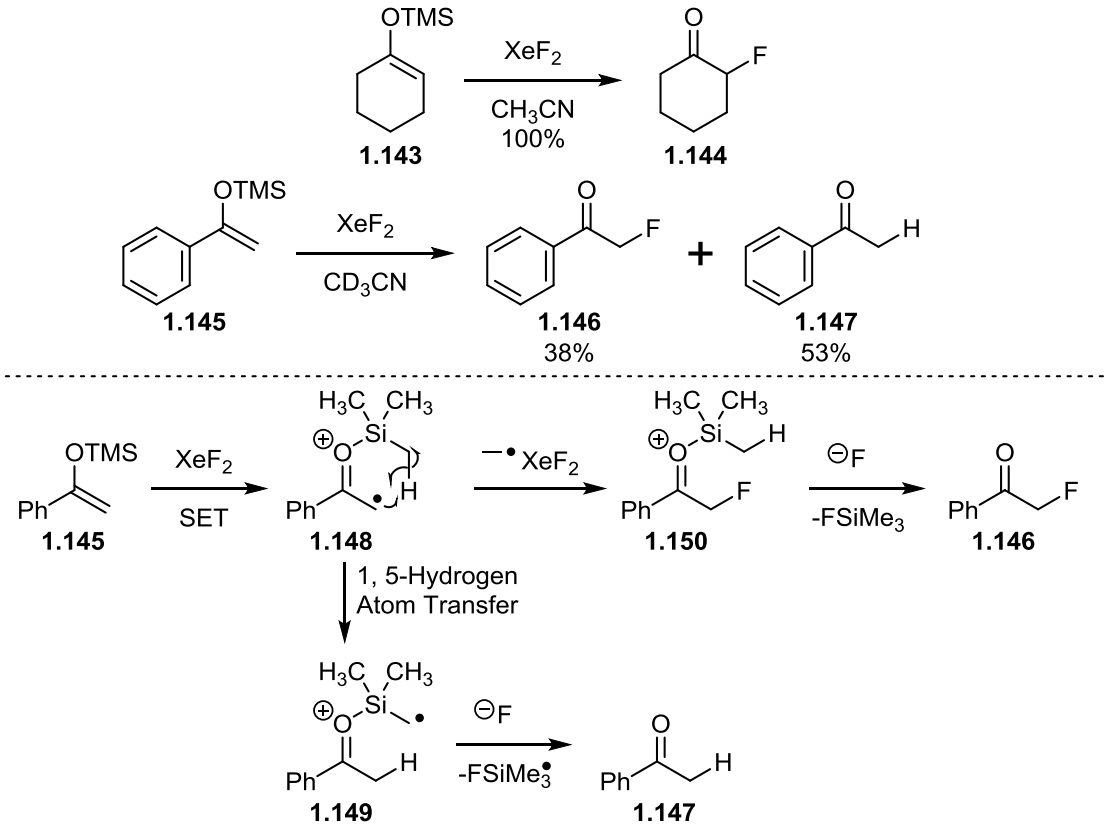

Scheme 1.28. Fluorodesilylation of silyl enol ethers with XeF_2

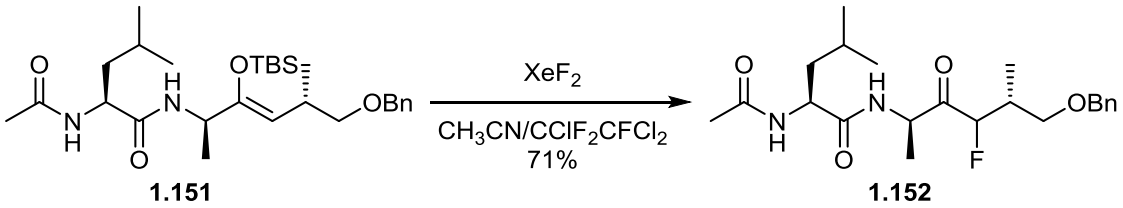

Scheme 1.29. Possible misinterpretation of electrophilic fluorination by XeF_2

The fluorination of aliphatic nitro compounds with XeF_2 has also been demonstrated to occur through discrete radical species (Scheme 1.30).[99] Dinitroethane anion **1.153** reacts with XeF_2 to produce dinitrofluoroethane **1.154** as the main product, along with **1.155** (likely produced by chlorine abstraction from dichloromethane), **1.156** and **1.157**. The addition of nitrogen oxides to the reaction mixture increases the yield of **1.156**, suggesting that it can be produced by radical abstraction of NO_2

from any of the dinitroalkyl compounds. The study of dinitromethane, trinitromethane and phenyldinitromethane in various solvents showed that radical intermediates will abstract atoms (H or Cl) from solvents, although acetonitrile was found to be resistant.[99b,99c]

Further evidence for radical intermediates can be found when the fluorination reaction is carried out in a mixed solvent system. In the study of nitroform salts, addition of benzene or THF to acetonitrile caused radical coupling products with the co-solvent to appear (**1.161** and **1.164**). The reaction mechanism commences with SET oxidation of the nitroalkyl anion to radical **1.166** by XeF_2 (Scheme 1.30, lower section).[99] Fluorination of the radical by **1.3** or **1.100** produces the desired fluorination product **1.159**. However, **1.166** may also participate in radical reactions such as abstraction of the weak THF hydrogen, followed by radical coupling to produce **1.164**.

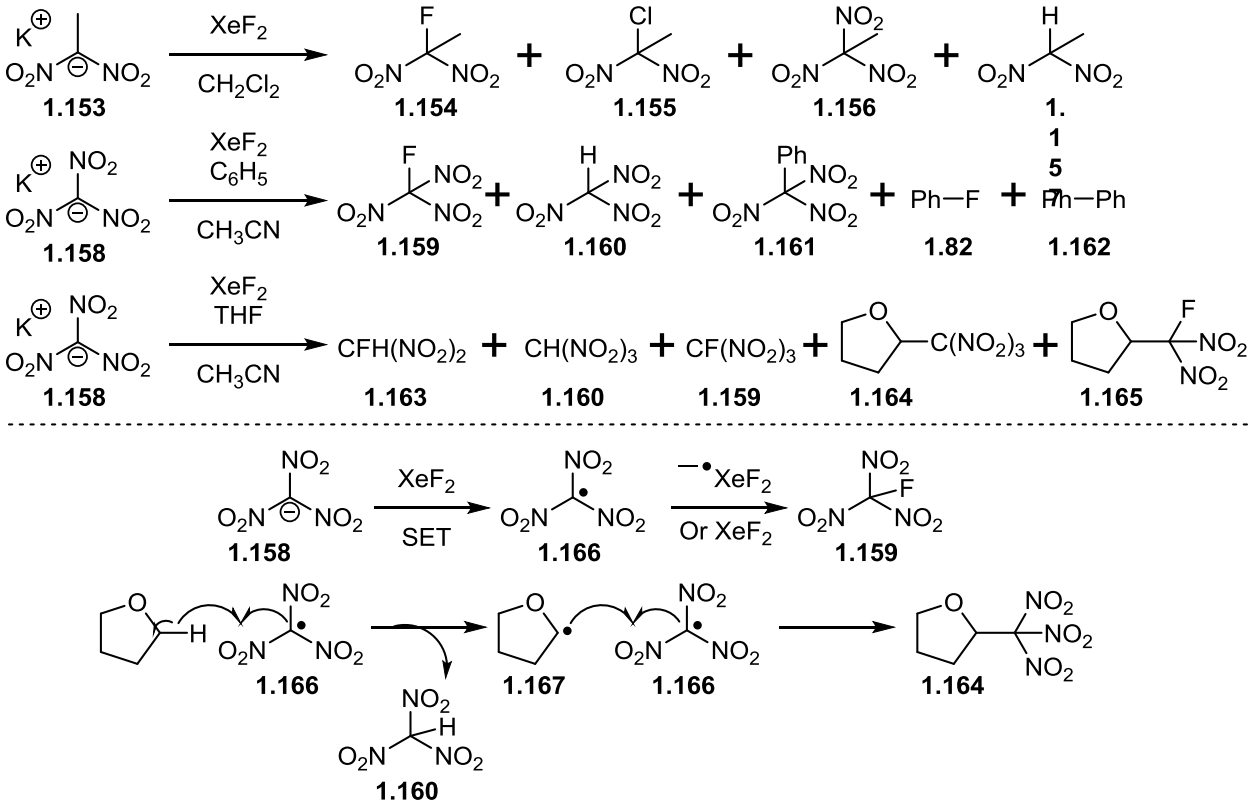

Scheme 1.30. Reactions of nitroalkyl compounds with XeF_2

1.3 Selective radical fluorination of organic small molecules after 2011

In December 2011, we submitted a communication to the Journal of the American Chemical Society detailing the discovery that two electrophilic N-F fluorinating agents could transfer fluorine to alkyl radicals.[14] We found that alkyl radicals generated by the decarboxylation of peresters could be fluorinated by N-fluorobenzenesulfonimide (NFSI, **1.168**) or Selectfluor (Sel-F, **1.169**), thus expanding the field of radical fluorination to include N-F reagents. Chapter 2 details my contributions to this discovery and a summary of the paper can be found in Scheme 2.14. Following this landmark publication, a series of manuscripts appeared in the literature concerning the use of Sel-F and other metal fluoride complexes as sources of atomic fluorine.[100-106]

1.3.1 Radical fluorination with Sel-F

Radical hydrofluorination of alkenes has been achieved by Barker and Boger (Scheme 1.31).[100] While the reaction mechanism is not entirely clear, it is believed that the Fe(III)/$NaBH_4$ complex activates a hydrogen to be susceptible to radical abstraction by an alkene. The resulting alkyl radical is fluorinated by Sel-F providing secondary and tertiary fluorides in moderate to good yields. Strong evidence of radical formation is found in the cyclization of **1.172** to **1.175** delivering the fluorination product in 40% isolated yield. Employing NFSI in aqueous THF provides fluorinated alcohol **1.171** in 23% yield. With the exception of studies within the Sammis group, this work by Barker and Boger is the only example, to date, to the use of NFSI as a radical fluorinating agent.

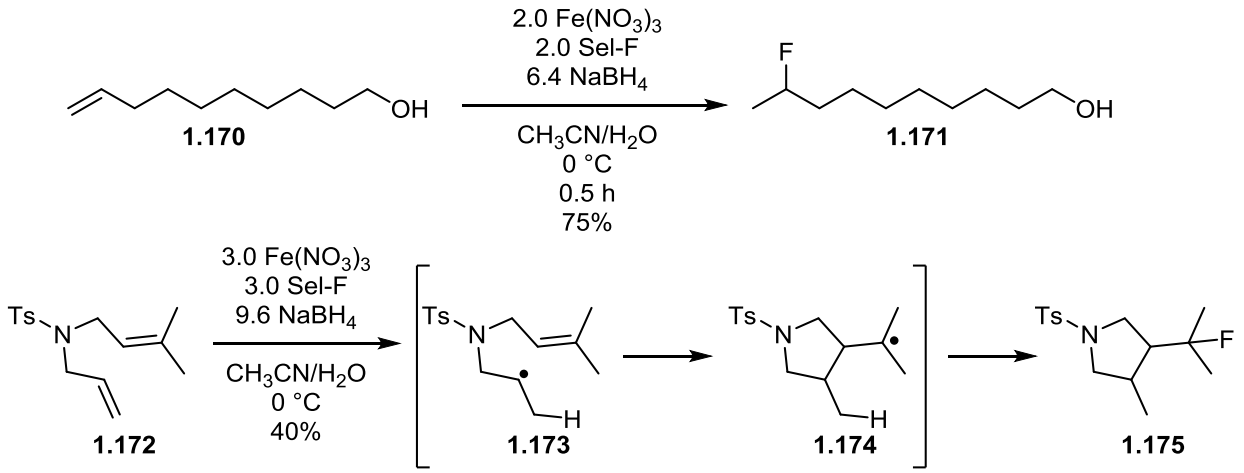

Scheme 1.31. Hydrofluorination of alkenes

Sel-F has served as an effective source of radical fluorine in three additional C-H to C-F bond transformations. Lectka and co-workers have disclosed two metal-mediated methods (Scheme 1.32),[101] while Inoue and co-workers have developed a metal-free system (Scheme 1.33).[102] In the first methodology, a multi-component catalytic system employing BDMEDCuI (**1.178**) and *N*-hydroxypthalimide effected the fluorination of aliphatic, allylic, and benzylic C-H bonds.[101a] In the second methodology, the inexpensive iron(II) acetylacetonate salt is employed for the selective radical abstraction and fluorination of benzylic C-H bonds (**1.178**).[101b] For both systems, yields range from ~30 to 75%, but the iron (II) system displays higher selectivity as fluorination with the copper system appears to be somewhat uncontrolled.

The metal-free system developed by Inoue and coworkers relies on hydrogen atom transfer from weaker C-H bonds to an *N*-oxyl radical. The yields obtained, in general, are slightly lower than the systems developed by Lectka, but C-H bond selectivity is quite high. This methodology is an excellent application of the electron-deficient nature of the oxyl radical **1.185** for radical hydrogen atom transfer. While the mechanism of fluorination is not explicitly detailed by Lectka, the mechanism

proposed by Inoue may be applied to all three methodologies (Scheme 1.33). The alkyl radical **1.183** (generated from abstraction of a C-H bond or possibly by SET-oxidation in the Fe(II) system) is fluorinated by Sel-F. The resulting aminium radical **1.187** propagates the catalytic cycle by SET oxidation and deprotonation.

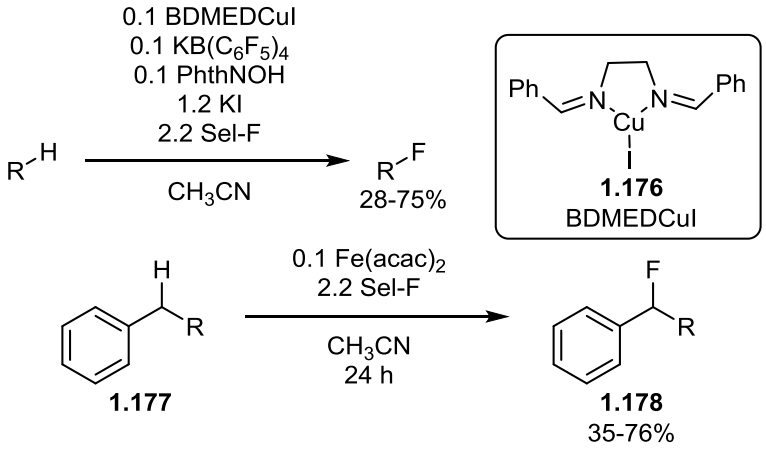

Scheme 1.32. Radical fluorination of C-H bonds with Sel-F by metal-mediated systems

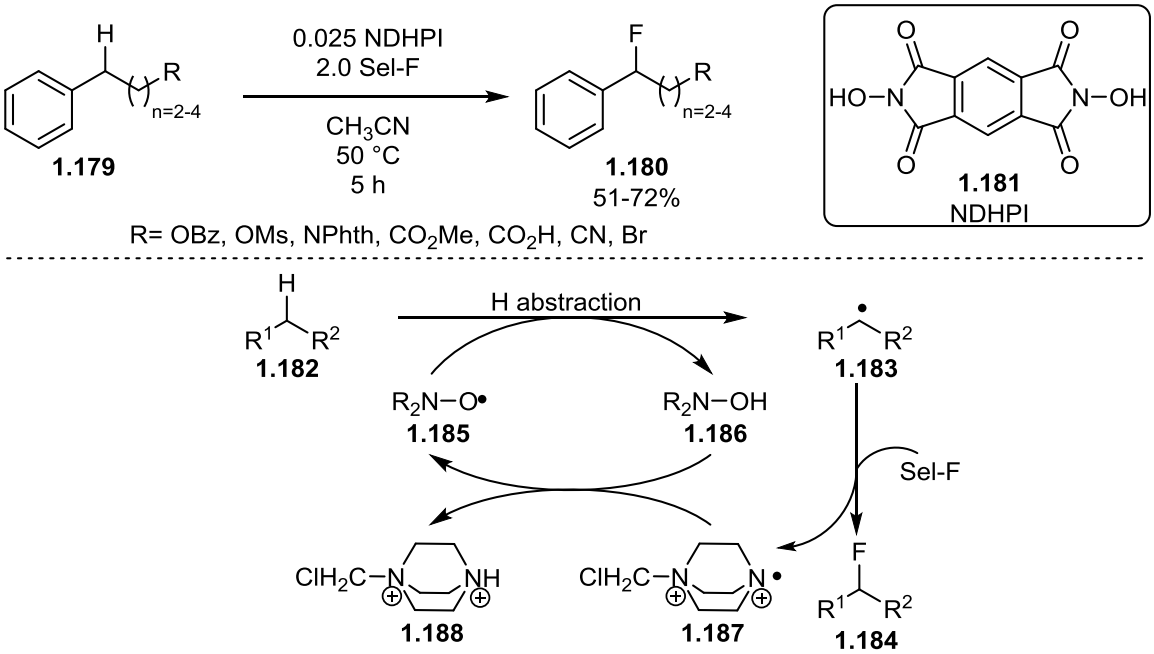

Scheme 1.33. Metal-free radical fluorination of C-H bonds with Sel-F

1.3.2 Radical fluorination with metal fluoride complexes

High-valence silver fluoride has been employed as a radical perfluorination agent in a manner similar to cobalt (III) fluoride. However, selective fluorination reactions have been demonstrated only recently. Kellogg and Cady described the synthesis of trifluoromethyl hypofluorite by the use of AgF_2 and AgF_3, which were presumed to form when a silver coated copper ribbon was exposed to fluorine gas.[47]

Li and co-workers have demonstrated the silver-catalyzed decarboxylative fluorination of aliphatic carboxylic acids in aqueous acetone solutions (Scheme 1.34).[103] A variety of primary, secondary, tertiary, and α-heteroatom activated carboxylic acids may be fluorodecarboxylated in high yields. The substrate scope appears to be very broad and alkyl fluorides that are prone to elimination such as **1.189** and **1.190** can be isolated intact. This methodology may be applied to the synthesis of aryl fluoromethyl ethers; compound **1.192** was thus obtained in 87% yield.

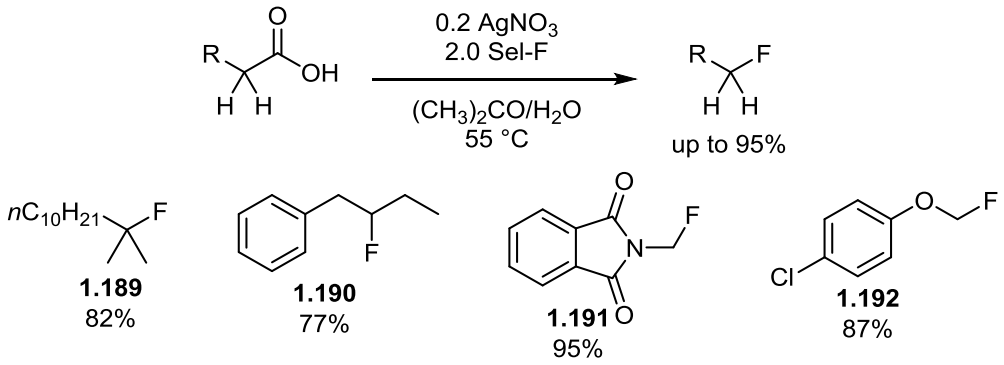

Scheme 1.34. Silver catalyzed fluorodecarboxylation of alkanoic acids by Li

Gouverneur and co-workers have expanded on this methodology to synthesize difluoromethyl and trifluoromethyl arenes from the corresponding mono- and di- fluoro phenylacetic acids (Scheme 1.35).[104] The substrate scope appears to be very broad and excellent yields of difluoromethyl and trifluoromethyl arenes can be obtained using conditions identical to those reported by Li.[103] Unique to this paper is the synthesis of radioactive fluoromethyl arenes **1.194**-**1.197** containing ^{18}F. Radiolabeling was accomplished using ^{18}F-TEDA-2OTf (**1.193**) in lieu of Sel-F affording ^{18}F tri- and ^{18}F di-fluoromethyl arenes (unobtainable with ^{18}F fluorine gas).[104]

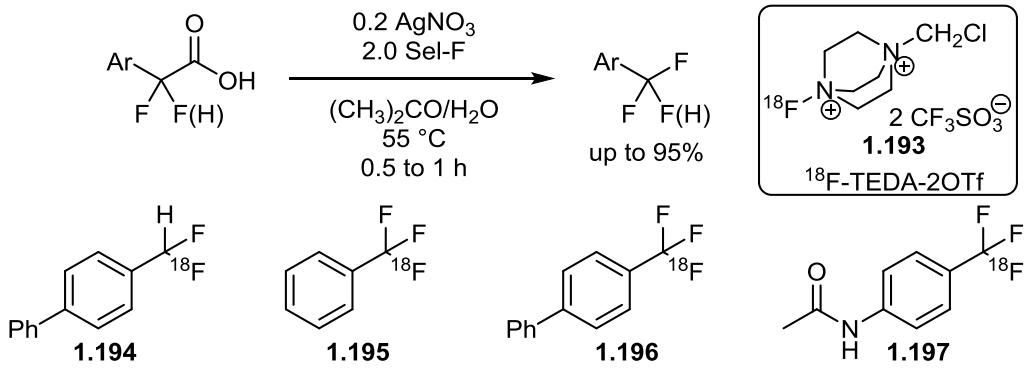

Scheme 1.35. Silver catalyzed fluorodecarboxylation of fluoro phenyl acetic acids by Gouverneur

The mechanism of silver-catalyzed carboxylic acid fluorodecarboxylation, as postulated by Li and coworkers, is presented in Scheme 1.36. Silver (I) is oxidized by Sel-F to a high-valence silver (III) intermediate which acts as a very strong single electron acceptor. Both Li and Gouverneur have examined NFSI as a substitute for Sel-F; however, no fluorodecarboxylation was effected.[103,104] Interestingly, substitution of Sel-F with XeF_2 or F_2 will restore fluorodecarboxylation although the yields are significantly lower than can be obtained with Sel-F.[104] Oxidation and deprotonation of carboxylic acid **1.200** affords the short-lived radical intermediate **1.201** that decarboxylates to alkyl

radical **1.183**. Fluorination of radical **1.183** by a silver (II) fluoride species regenerates silver (I) and restores the catalytic silver cycle. Both Li and Gouverneur have applied this methodology towards aryl fluoride synthesis with no success, an observation relevant to Chapter 2.[103,104]

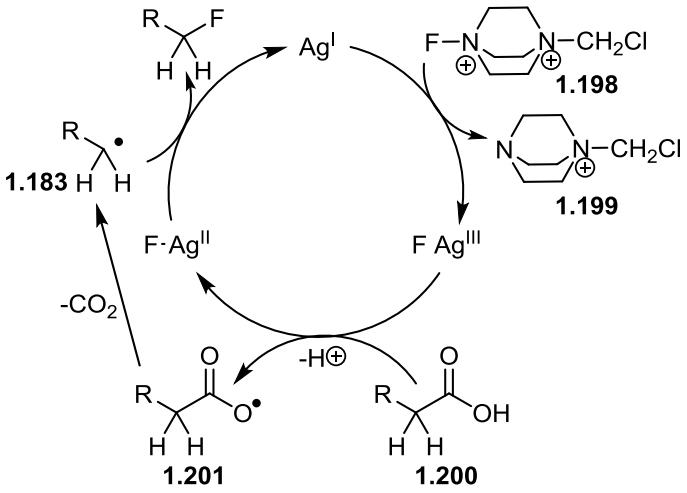

Scheme 1.36. Mechanism of silver catalysed fluorodecarboxylation

Li and co-workers have also developed an alkene amidofluorination methodology with *N*-arylamides (Scheme 1.37).[105] Yields for fluorolactamization (**1.203**) range from moderate to good with a wide variety of electron-poor aniline derivatives. A catalytic cycle for silver similar to that of fluorodecarboxylation is proposed for the amidofluorination reaction. Single electron oxidation of the aryl ring occurs (**1.204**) in lieu of the carboxylic acid and 5-*exo* cyclization of amidyl **1.205** occurs prior to fluorination. An important observation relevant to Chapter 3 is the failure of *N*-(4-methoxyphenyl)pent-4-enamide (**1.202n**, R = OCH_3) to undergo aminofluorination.[105] Whereas ring fluorination occurs to electron-rich phenoxyacetic acids, electron-rich anilines are ring-oxidized to the benzoquinone.

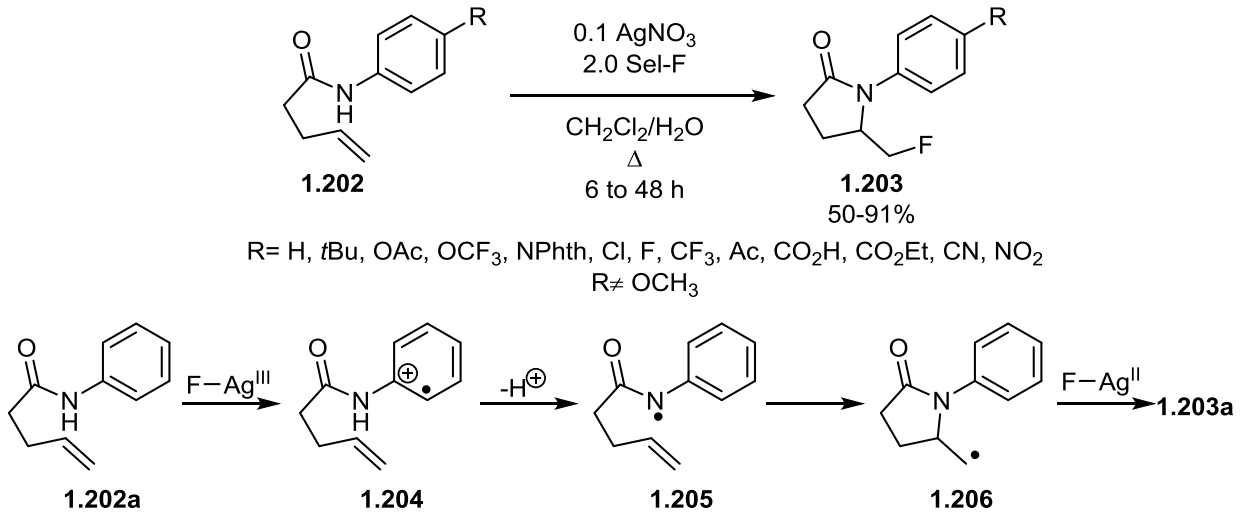

Scheme 1.37. Silver-catalyzed aminofluorination of 4-pentenamides

Groves and co-workers have developed two high-valence manganese catalysts to convert fluoride ions into sources of radical fluorine (Scheme 1.38).[106] In the first system, manganese (III) porphyrin **1.207** is employed in a catalytic cycle for the fluorination of cyclic methylene C-H bonds.[106a] Yields of fluorinated products are moderate (~40 to 60%) but the selectivity of methylene C-H bonds in the presence of weaker tertiary C-H bonds or activated α-heteroatom C-H bonds is notable (although not unexpected with Mn/porphyrin systems).[107] In the second system, manganese (III) salen **1.208** is employed in a catalytic cycle for the fluorination of benzylic C-H bonds.[106b] Yields of fluorinated products are better than the analogous porphyrin system (yields up to 70%) with high selectivity for benzylic bonds.

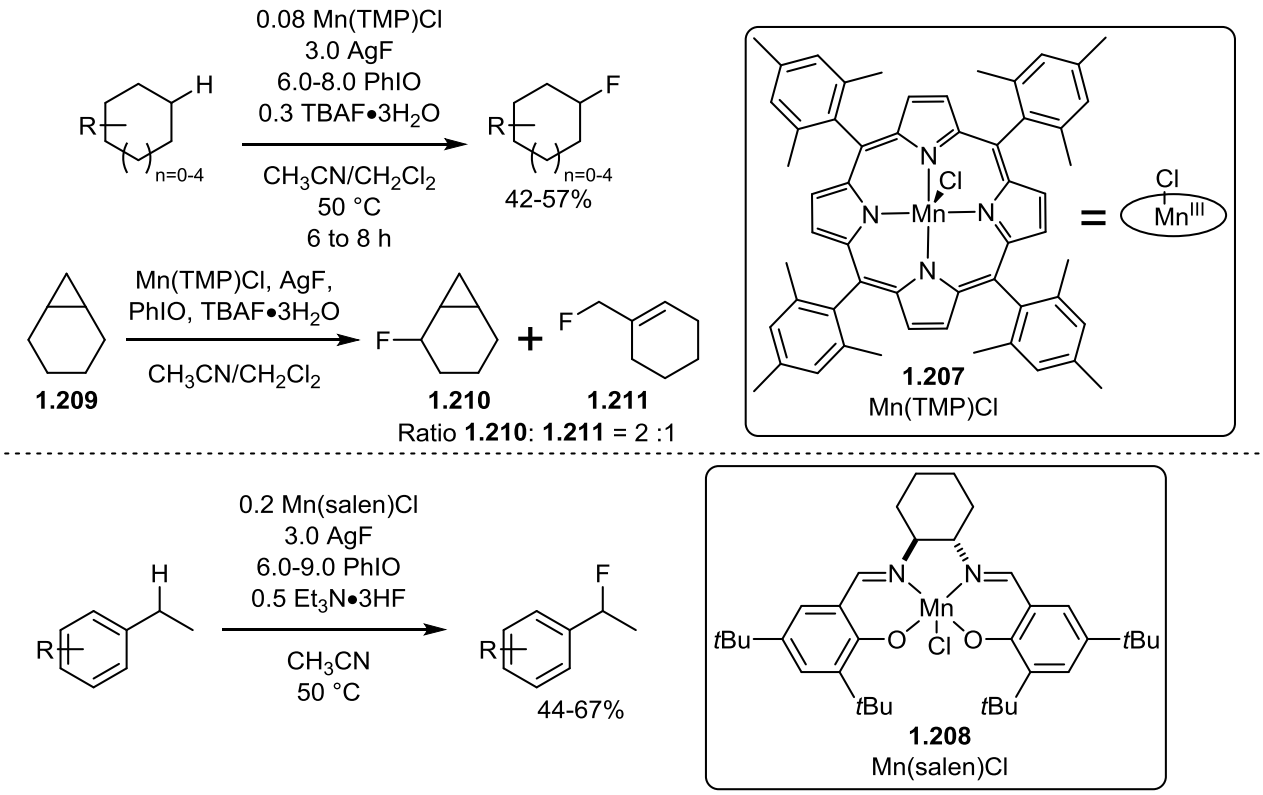

Scheme 1.38. Manganese catalyzed radical fluorination of alkyl and benzylic C-H bonds.

The mechanism for fluorination was investigated in detail through deuterium kinetic isotope effects, isolation of intermediates for crystallography, and Density Functional Theory (DFT) calculations.[106a] Four pieces of evidence strongly suggest a radical mechanism for fluorination: (1) radical quenching in the presence of molecular oxygen was cited to explain the reduced fluorination yields under an air atmosphere; (2) phenethyl radicals generated from thermal decomposition of a diazo precursor are fluorinated in 41% yield by Mn(IV)F_2 (**1.212**, obtained for crystallographic studies); (3) cyclopropane opening was observed during the fluorination of substrate **1.209**; (4) a radical abstraction transition state was found by DFT calculations.

The mechanism for fluorination, as proposed by Groves and co-workers for the Mn(TMP)Cl system, is presented in Scheme 1.39.[106a] Mn(III) is oxizided to the Mn(V)-oxo intermediate which can abstract a hydrogen from the alkyl substrate **1.182** to form a Mn(IV) species. Displacement of hydroxyl, by a source of fluoride, affords the radical fluorinating agent Mn(IV)F_2 (**1.212**). S_H2 radical abstraction of fluorine delivers the alkylfluoride product **1.184**. A similar mechanism is proposed for Mn(salen)-mediated benzylic fluorination.[106b]

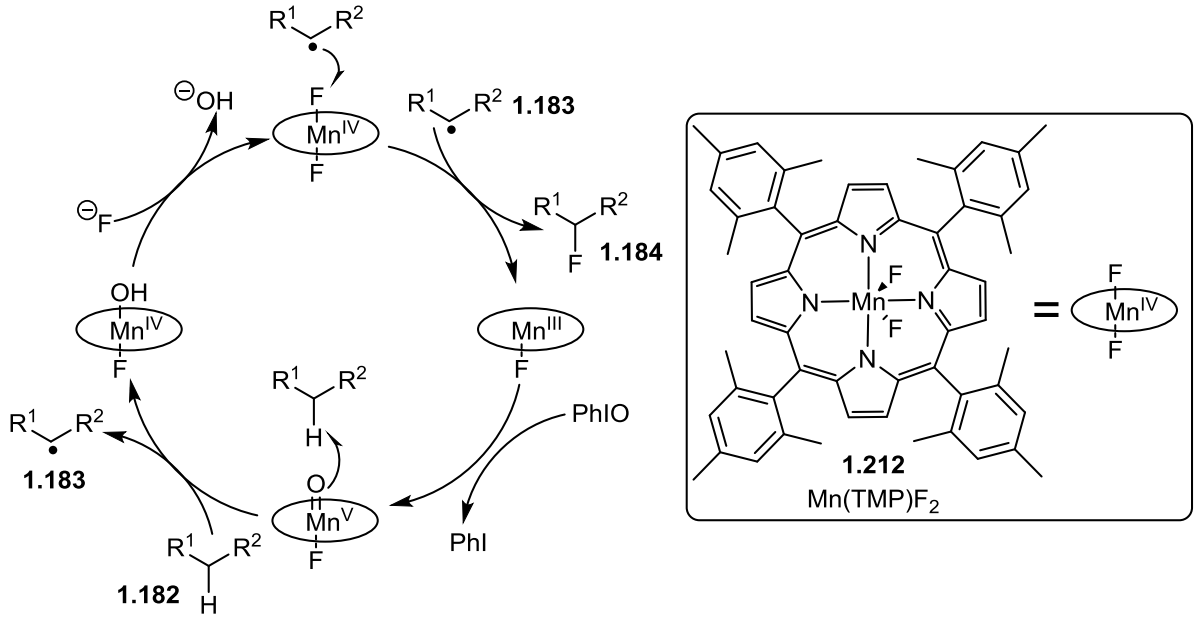

Scheme 1.39. Mechanism for manganese catalyzed radical fluorination

In summary, the list of reagents employed for radical fluorination (F_2, CF_3OF, XeF_2) has been increased to include NFSI, Sel-F, AgF_2, and Mn(IV)F_2. The field of radical fluorination is expanding rapidly and exciting new methodologies for selective fluorination and radio-labeling with ^{18}F are being discovered. The remainder of this thesis will detail my contributions towards this renaissance of research in selective fluorination of alkyl radicals.

Chapter 2: Discovery of NFSI and Sel-F as fluorine atom transfer reagents

Every reagent that has been employed as a radical source of fluorine in Chapter 1 has also been employed as a source of electrophilic fluorine. Indeed, radical pathways are usually avoided because of the non-selective nature of the highly reactive fluorine radical (perfluorination pathways being the notable exception). Current fluorination research employing fluorine gas, hypofluorites, or xenon difluoride deliberately suppresses the radical pathways by employing polar solvents, low reaction temperatures, and in some cases, radical scavengers. In effect, consensus has it that radical fluorinating agents can behave as sources of electrophilic fluorine. Reversing that argument, we arrive at an intriguing hypothesis: *could sources of electrophilic fluorine behave as radical fluorinating agents*?

2.1 Proof of concept

2.1.1 *N*-Fluorobenzenesulfonimide and Selectfluor™ as radical fluorinating agents

A particular group of electrophilic fluorinating agents that has dominated the selective fluorination field in the last two decades is the N-F class of compounds. Privileged members include the Selectfluor™ family of compounds (1-alkyl-4-fluoro-1,4-diazoniabicyclo-[2.2.2]octane salts), *N*-fluoropyridinium (NFPY) salt complexes, and *N*-fluorosulfonimides (Figure 2.1). The popularity of these reagents, all stable and relatively non-hygroscopic solids, can be attributed to their commercial availability and high selectivity in fluorination reactions.

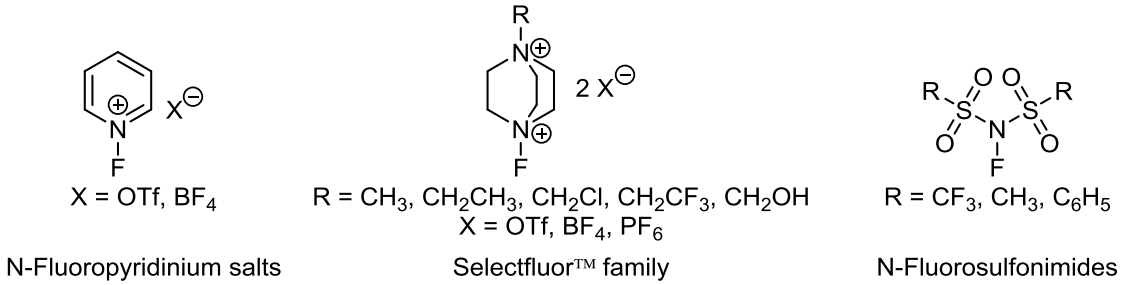

Figure 2.1. Commonly employed electrophilic fluorinating agents

A debate exists on the appropriateness of the term 'electrophilic fluorine,' because this suggets a cationic form of fluorine, which is the most electronegative of the reactive elements. Thus, the exact mechanism of fluorine transfer from these reagents has been researched thoroughly; in particular, to ascertain whether it is more likely to involve a bimolecular nucleophilic substitution (S_N2) at fluorine or a single electron transfer (SET) process involving the N-F bond.[108] While the exact nature of electrophilic fluorine transfer is of passing interest to this thesis, the fact that radicals can be implicated in the fluorine transfer process is of utmost importance.

N-Fluorobenzenesulfonimide (NFSI) is an excellent electrophilic fluorinating reagent because transfer of fluorine to a nucleophile results in a highly delocalized sulfonamide anion (a good leaving group). NFSI (**1.168**) can be prepared by exposing a solution of benzenesulfonimide (**2.1**) in acetonitrile to a dilute mixture of fluorine gas (in nitrogen gas) in an ambient pressure reactor over powdered sodium fluoride (Scheme 2.1).[109] Reviews on the many uses of NFSI demonstrate it to be a versatile reagent for the electrophilic fluorination of aromatic substrates as well as enolates, and other anionic nucleophiles.[6,10]

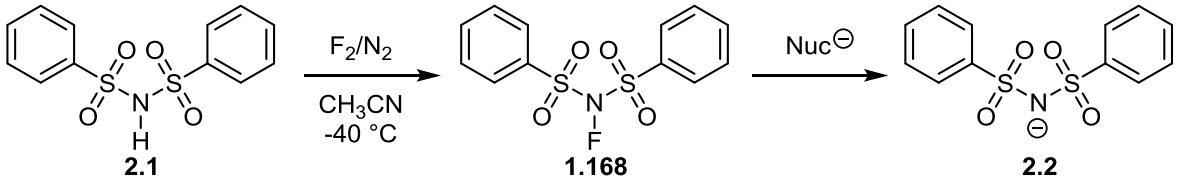

Scheme 2.1. Synthesis and action of NFSI

Interest in NFSI as a radical fluorine transfer agent derives from examining the benzenesulfonimidyl radical (**2.3**). Multiple resonance structures can be drawn to represent delocalization of nitrogen-centered radical **2.3** on all 4 sulfonyl oxygens, which demonstrates the stability of this radical. Radical **2.3** is the known decomposition product from SET reduction of the N-F bond followed by loss of fluoride.[110] Evidence already exists to support a SET mediated fluorination process whereby NFSI first oxidizes the nucleophile followed by rapid radical recombination.[111] Radical **2.3** is also the hypothetical product of S_H2 transfer of fluorine to an alkyl radical (Scheme 2.2). If **2.3** can be stabilized, this may suggest that the homolytic breakage of the N-F bond in NFSI is feasible with an appropriate alkyl radical.

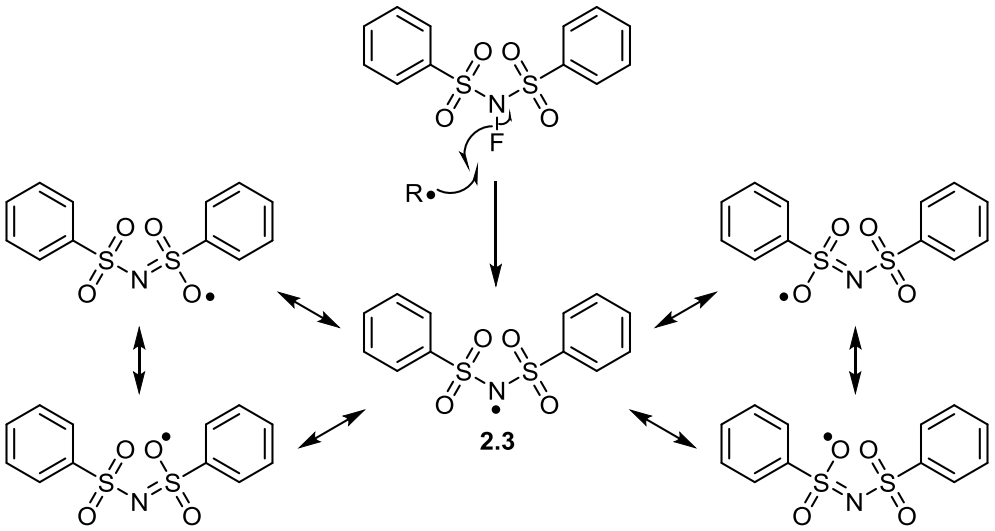

Scheme 2.2. Resonance stabilization of the benzenesulfonyl radical

1-Chloromethyl-4-fluoro-1, 4-diazoniabicyclo-[2.2.2]octane bis(tetrafluoroborate) (**1.169**, F-TEDA-BF_4), is also an excellent source of electrophilic fluorine. Registered trademark by Air products as Selectfluor^{TM} (Sel-F), it can be prepared in a multi-step process starting from the alkylation of 1, 4-diazobicyclo-[2.2.2]octane (**2.4**, TEDA) with dichloromethane, followed by anionic exchange with sodium tetrafluoroborate to **2.6** and finally fluorinated by fluorine gas (Scheme 2.3).[112] The use of Sel-F (or other F-TEDA class compounds) as an electrophilic fluorinating reagent has been reviewed extensively in the literature.[6,10,108]

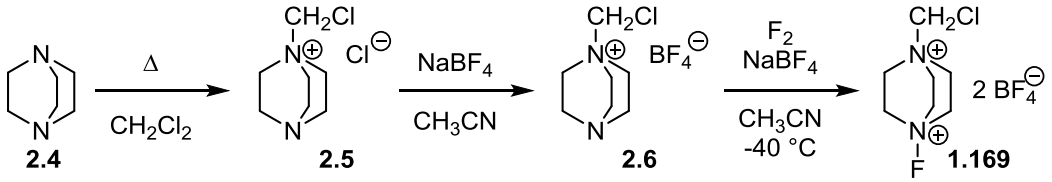

Scheme 2.3. Synthesis of Sel-F

Our interest in Sel-F as a radical fluorine transfer agent derives from the longstanding speculation that the fluorine center has more radical character than fluoronium character.[113] A comparison of the X-ray crystal structures of F-TEDA (**1.198**) and its precursor **1.199** show significant structural changes in the TEDA core and chloromethyl substituent after the nitrogen has been fluorinated (Table 2.1).[113] Fluorination of **1.199** leads to a contraction of the interatomic N-N distance by 8 pm, a contraction of the C-Cl bond by 5 pm and an elongation of the N^2-C bond by 4 pm.

Table 2.1. Comparision of bond lengths between 1.199 and 2.7

bond length or interatomic distance (pm)	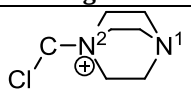 **1.199**	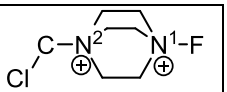 **1.198**
N^1-N^2	256	248
N^2-C	149	153
C-Cl	176	171

Early studies by McKinney and Geske had established that the TEDA radical cation (**2.7**) was remarkably stable, with a lifetime of several seconds.[114] The exceptional stability of **2.7** was attributed to a through-bond interaction in the molecule that was first postulated by Hoffmann[115] and later confirmed experimentally by Wolfe and Brion.[116] Given the known stability of the TEDA radical cation (**2.7**), an interpretation of molecular structure for Sel-F invoking no-bond resonance with a fluorine radical, TEDA radical cation and chloromethyl cation (**2.9**) has been proposed (Scheme 2.4). Radical quenching of structures **2.8** and **2.9** helps to explain why single electron oxidation is the first step towards fluorination of alkenes by Sel-F.[117]

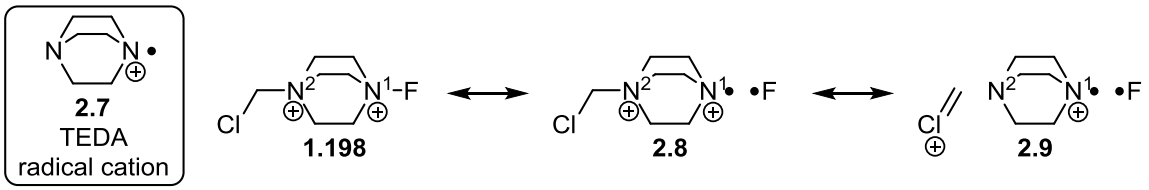

Scheme 2.4. No-bond resonance structures for Sel-F

Common to all known sources of radical fluorine discussed in Chapter 1 is their ability to act as strong oxidants. In this regard, Sel-F performs admirably as an oxidant in single electron transfer processes. A mixture of Sel-F with sodium or potassium salts of iodide, bromide, or even chloride can generate an equivalent electrophilic halogenating agent for electrophilic aromatic substitution.[118] The reagent has even found application in the oxidative removal of certain protecting groups. Examples include the SET cleave of methoxybenzylidine acetals to release 1, 3-diols and of dithanes to release aldehydes.[119] The oxidation of benzyl alcohols to benzaldehydes and the oxidation of benzaldehydes to benzoyl fluorides by Sel-F has been proposed to occur through SET-mediated radical pathways.[120] The versatility of Sel-F as an oxidant further supports the speculation that the fluorine center has significant radical character.

2.1.2 Computational evidence for low N-F bond dissociation energy

Common sources of radical fluorine have low bond dissociation energies. For instance, the experimental bond dissociation energy of fluorine gas is approximately 38 kcal/mol.[121] Similarly, trifluoromethyl hypofluorite has an experimental bond dissociation energy of approximately 44 kcal/mol (Figure 2.2).[122] Both these reagents are able to transfer a fluorine atom to an alkyl radical; however, they are also capable of generating free fluorine radicals through thermal dissociation, which we were eager to avoid. What was required was a reagent exhibiting an X-F bond (X = appropriate atom) weak enough to transfer a fluorine atome to a carbon radical, yet strong enough not to undergo undesired thermal dissociation.

Generic atom transfer reagents that satisfy the above requirement include elemental chlorine and tributyltin hydride, which transfer Cl and H atoms, respectively, to carbon radicals without undergoing unwanted homolysis. The Cl-Cl bond dissociation energy of 58 kcal/mol[121] and that of the Sn-H bond is 74 kcal/mol (Figure 2.1.2).[121] Thus, it seemed that an X-F bond dissociation energy in the neighbourhood of 60-75 kcal/mol would be optimal.

F—F	F_3CO—F	Cl—Cl	Bu_3Sn—H
D_{FF} = 38 kcal/mol	D_{OF} = 44 kcal/mol	D_{ClCl} = 58 kcal/mol	D_{SnH} = 74 kcal/mol

Figure 2.2. Selection of experimental bond dissociation energies of radically active bonds

The search for an appropriate fluorine atom transfer reagent started with a Density Functional Theory (DFT) investigation of N-F bond dissociation energies in various carriers of electrophilic fluorine. These calculations were performed by our collaborators, P. Kennepohl (professor) and T. Okbinoglu using the ORCA 2.8 computational package.[123] The BP86 functional[124] and Alrichs[125] triple zeta valence with single polarization (TZV/P) basis set (for all atoms) were chosen as a satisfactory

combination for accuracy and computational efficiency. BP86 is a long-standing functional, being one of the first generalized gradient approximation functionals, and has a reputation for being well balanced. Small approximation errors across the board ultimately lead to a favourable cancellation of errors, thus the functional performs reasonably well under most circumstances.[b] Molecular geometries were optimized using the COSMO solvation model[126] as implemented in ORCA in four different solvents: hexane, THF, acetonitrile, and water. Numerical frequency calculations for all optimized geometries at the same level of theory indicated that fully optimized geometries were obtained in all cases. Results from calculations with appropriate counterions differed slightly due to ion pairing effects; however, these differences do not affect the overall conclusions from the calculations.[14] The results of these studies are summarized in Table 2.3.

Subsequently, I carried out my own DFT work, which produced the results shown in Table 2.2. My calculations were performed with the ORCA 2.9 computational package,[128] also at the same level of theory, and employed a similar protocol to facilitate comparisons of the predicted values. The data presented in Table 2.2 will help to clarify why the calculated results for NFSI and Sel-F by our collaborators were meaningful.

I performed a series of DFT calculations on two known sources of radical fluorine: trifluoromethyl hypofluorite (**1.2**) and acetyl hypofluorite (**1.97**) (Table 2.1-2). Across a variety of solvents, trifluoromethyl hypofluorite (**1.2**) has a narrow range of bond dissociation energies averaging 50.6 kcal/mol, a Mayer bond order of 0.84, and an O-F bond length of 145.5 pm. Olsen[128] found an O-F bond length of 142.9 pm in his Hartree-Fock calculations (self-consistent field – linear combination

[b] Private communication with P. Kennepohl.

of atomic orbitals – molecular orbitals type [SCF-LCAO-MO]) with a 4-31G basis set (comparable to a double zeta basis set) which is closer to the literature value of 142.1 ± 0.6 pm found by Diodati and Bartelli.[129] The O-F bond strength has been measured (or estimated) to be 44.5 kcal/mol by Levy,[122b] 47 kcal/mol by Cady,[55] 43.5 kcal/mol by Schumacher[130] and revised to 43.1 kcal/mol in 1970.[122a]

The calculations for acetyl hypofluorite (**1.97**) predict a longer O-F bond of 146.8 pm with a similar Mayer bond order of 0.81 but a much weaker bond dissociation energy of 41 kcal/mol. The calculated difference of 1.5 pm in bond length between **1.2** and **1.97** is significant in light of the large 9 kcal/mol difference in bond dissociation energy. A critical analysis of the DFT values show moderate correlation to literature values; however, it should be noted that literature values are reported for the gas phase whereas the calculated DFT values are performed with solvation to facilitate comparisons to NFSI, Sel-F and NFPY (Table 2.1-3).

Table 2.2. DFT calculated properties of trifluoromethyl and acetyl hypofluorite[a]

	trifluoromethyl hypofluorite			acetyl hypofluorite		
	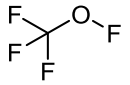 **1.2**			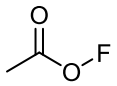 **1.97**		
solvent	r_{OF} (pm)	BO_{OF}	D_{OF} (kcal/mol)	r_{OF} (pm)	BO_{OF}	D_{OF} (kcal/mol)
hexane	145.4	0.843	50.8	146.2	0.822	41.0
THF	145.5	0.841	50.5	146.8	0.812	41.0
CH_3CN	145.5	0.841	50.4	147.1	0.808	41.0
H_2O	145.6	0.841	50.4	147.1	0.807	41.1

[a]DFT calculations were performed using ORCA with the BP86 functional and the TZV/P basis set for all atoms. Molecular geometries were optimized using the COSMO solvation model as implemented in ORCA. For each species, the O−F bond distance (r_{OF} in pm), Mayer bond order (BO_{OF}), and bond dissociation energy (D_{OF} in kcal/mol) are computed.

DFT calculations reveal NFSI to be a very strong candidate as radical fluorine transfer agent (Table 2.3). NFSI has the longest calculated bond length of the 3 electrophilic N-F reagents suggesting

that it possesses the weakest N-F bond. A direct calculation of the N-F bond dissociation energy by this DFT method gives a narrow range of 63.1 kcal/mol in acetonitrile to 63.5 kcal/mol in water indicating the N-F bond is relatively weak. In combination, these factors suggest that a carbon-centered radical could abstract fluorine from NFSI.

Another promising candidate is F-TEDA (as outlined earlier in section 2.1). DFT calculations show the N-F bond length range to be 141.4 pm in hexane to 142.2 pm in water which is approximately 2 pm shorter than the N-F bond length in NFSI. Crystallographic data on Sel-F reveals an N-F bond length of 137.2 pm,[113] which is significantly shorter than calculated. However, this comparison appears to be haphazard as one would expect many deviations between a counterion-paired crystal structure and a solvated dicationic molecule without counterions. The N-F bond dissociation energy (or homolytic bond strength) of Sel-F is lower than the D_{NF} of NFSI, ranging from 60.9 kcal/mol in acetonitrile to 62.2 kcal/mol in water. With the lowest predicted bond dissociation energy of the three electrophilic N-F reagents explored, and the evidence for radical character in the N-F bond, Sel-F has a high probability for success in transferring fluorine to an alkyl radical.

As expected, DFT calculations suggest that NFPY is the least likely to act as a radical fluorine transfer agent of the three N-F electrophilic fluorine sources investigated. Radical transfer of fluorine from NFPY would generate an sp^2 nitrogen radical which we believed to be an unfavourable process. The calculated bond strength ranges from 76.1 kcal/mol to 75.1 kcal/mol and the N-F bond length is notably shorter than in Sel-F or NFSI, ranging between 137.5 pm to 137.9 pm. Crystallographic data on NFPY reveals an N-F bond length of 135.7 pm[131] and theoretical work by Fraenk and co-workers

predicted an N-F bond length of 135.7 pm at the B3LYP level and 137.0 pm at the MP2 level.[132] The experimental (and previously predicted) value is shorter than our calculated value of 138 pm, which suggests the N-F bond in NFPY is even stronger than our calculated value of 76 kcal/mol, confirming our prediction that NFPY would be a poor source of radical fluorine.

Table 2.3. DFT calculated properties of selected electrophilic fluorinating agents

	N-fluorobenzenesulfonimide (NFSI) [a]			Selectfluor™ (Sel-F) [a][b]			*N*-fluoropyridinium (NFPY) [a][b]		
	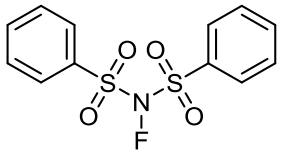 **1.168**			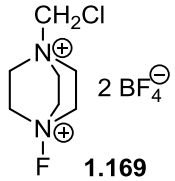 **1.169**			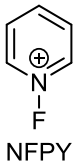 NFPY		
solvent	r_{NF} (pm)	BO_{NF}	D_{NF} (kcal/mol)	r_{NF} (pm)	BO_{NF}	D_{NF} (kcal/mol)	r_{NF} (pm)	BO_{NF}	D_{NF} (kcal/mol)
hexane	143.8	0.839	63.4	141.4	0.986	61.0	137.5	0.933	76.1
THF	143.8	0.837	63.3	141.9	0.966	61.7	137.8	0.922	75.4
CH_3CN	143.7	0.839	63.1	142.1	0.956	60.9	137.8	0.915	75.1
H_2O	143.7	0.831	63.5	142.2	0.956	62.2	137.9	0.914	75.3

[a]DFT calculations were performed by collaborators P. Kennepohl and T. Okbinoglu using ORCA with the VWN/BP86 functional and the available TZV/P basis set for all atoms. Molecular geometries were optimized using the COSMO solvation model as implemented in ORCA in four different solvents: hexane, THF, acetonitrile, and water. For each species, the N−F bond distance (r_{NF} in pm), Mayer bond order (BO_{NF}), and bond dissociation energy (D_{NF} in kcal/mol) are computed. [b]Computational results for the cationic reagents without counterions are shown in this table. Results from calculations with appropriate counterions differ slightly due to ion pairing effects; these differences do not affect the overall conclusions herein.

All three N-F electrophilic fluorine sources were tested for radical fluorine atom transfer capabilities. NFSI was investigated first as the calculations showed it to be the most promising candidate. Additionally, we reasoned that a wider scope of radical precursors could be tested because, relative to the other reagents, NFSI is soluble in a broader range of solvents and is a milder oxidant. Sel-F was investigated second, as the calculations showed it to have the lowest bond dissociation energy and there was good literature precedence for radical character in the N-F bond; however, we

had anticipated solubility issues with Sel-F and did not want to prematurely limit the discovery experiments to only water, acetonitrile and DMF. Evidence for NFSI and Sel-F acting as sources of radical fluorine are presented in the following three chapters of this thesis. In my experiments thus far, no fluorine atom transfer from NFPY salts was ever observed.

2.1.3 Evidence for radical fluorination by Sel-F

When I joined the radical fluorination project, M. Rueda-Becerril had already obtained proof-of-concept for NFSI as suitable reagent for radical fluorine transfer. She found that thermolysis or photolysis of carboxylic acid diacyl peroxide **2.10** in the presence of NFSI lead to the fluorodecarboxylated product **2.11** (Scheme 2.5).

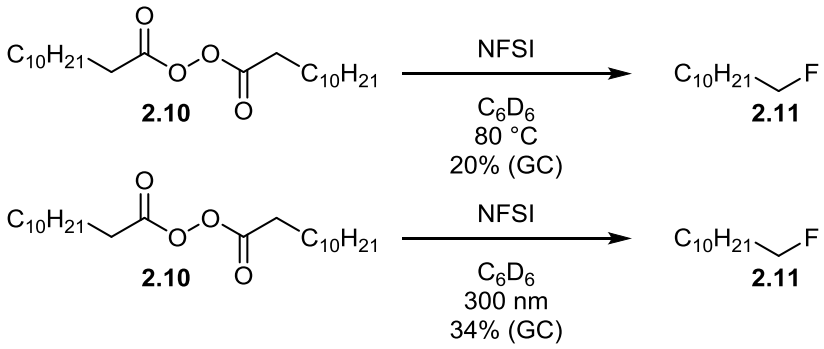

Scheme 2.5. Radical fluorodecarboxylation with NFSI

As the decomposition of symmetrical diacyl peroxides is a well-established method of alkyl radical generation,[133] a radical fluorination mechanism was proposed (Scheme 2.6). Homolysis of the weak O-O bond by thermal or photochemical stimulation generates carboxyl radical intermediate **2.12** which rapidly decarboxylates to radical **2.13**. While it is unclear if **2.13** is first oxidized by NFSI to the carbocation followed by rapid recombination with fluoride or if radical **2.13** abstracts fluorine from

NFSI through an S_H2 mechanism, a fluorine atom is transferred from NFSI to **2.13** for the desired fluorination product **2.11**.

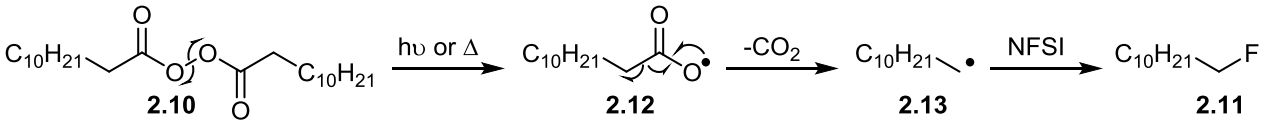

Scheme 2.6. Mechanism of radical fluorodecarboxylation with NFSI

I began studies on radical fluorination with proof of concept experiments utilizing Sel-F as a source of atomic fluorine. According to the DFT calculations in Table 2.3, Sel-F has a lower calculated homolytic bond strength than NFSI, suggesting that Sel-F may also be a candidate radical fluorine transfer agent. Solubility was the first challenge to overcome as Sel-F is a doubly cationic species and most of the diacyl peroxide radical precursors that had been utilized with NFSI were not sufficiently soluble in highly polar solvents suitable for Sel-F. As diazo compound **2.14** is a commonly employed radical initiator for emulsion polymerization, it was selected as a precurser of alkyl radicals. Both Sel-F and the sodium carboxylate salt of **2.14** are water soluble, and the first test experiment yielded a positive result (Scheme 2.7). High resolution mass spectrometry by electrospray ionisation (cationic detection) of the partially purified reaction mixtures showed the presence of a compound with the same charge to mass ratio as **2.15**. Unfortunately, sufficient purification of **2.15** for definitive characterization was not possible.

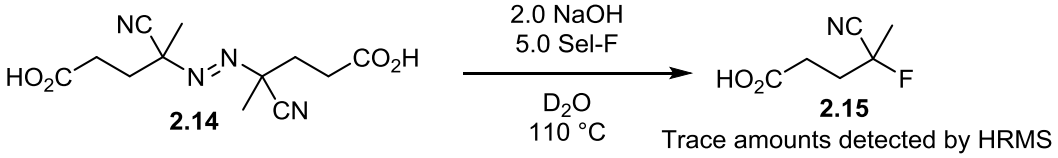

Scheme 2.7. Fluorodediazonation with Sel-F

The radical atom transfer method of radical generation was investigated for testing Sel-F as a radical fluorinating agent (Scheme 2.8). In the radical atom transfer method, stabilized carbon-centered radicals may be generated by the abstraction (or transfer) of halogens (or chalcogens) by alkyl radicals.[134] In the presence of a suitable radical initiator, the iodine atom of iodoacetamide (**2.16**) may be abstracted and the resulting aminocarbonylmethyl radical could then be fluorinated by Sel-F (or NFSI). Since only trace amounts of **2.15** were obtained, it was reasonable to employ **2.14** as an alkyl radical precurser in radical atom transfer because the abstraction of iodine might be the faster than abstraction of fluorine from Sel-F. Fluoroacetamide (**2.17**) was not observed under these radical transfer conditions when either Sel-F or NFSI were employed (Scheme 2.8). Furthermore, no **2.15** was observed, and the initial hit on radical fluorination with Sel-F was re-evaluated.

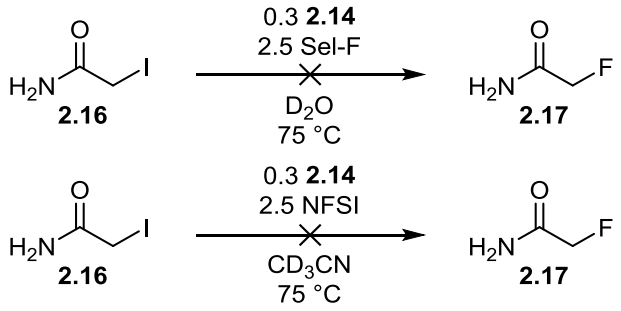

Scheme 2.8. Attempted radical atom transfer synthesis of fluoroacetamide

As only small amounts of **2.15** could be detected from the dediazoniation of **2.14** in Scheme 2.7 and no **2.15** was observed in the radical atom transfer experiments in Scheme 2.8, it is unlikely that Sel-F was transferring fluorine to an alkyl radical. Since the reaction was carried out in alkaline water, fluorination may have occurred through reductive dediazonitization to **2.18** followed by deprotonation to **2.19** and electrophilic fluorination to **2.15** (Scheme 2.9). Nevertheless, this proof of concept study gave me the motivation to continue research into Sel-F as a radical fluorination agent.

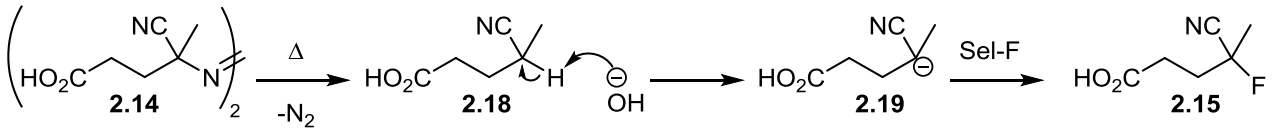

Scheme 2.9. Ionic fluorination mechanism for 2.15 synthesis

NFSI-mediated fluorination of alkyl radicals, generated by the thermolysis of *tert*-butyl peresters, was an effective protocol already employed by coworkers in the lab. Thus, I directed efforts towards a potentially water-soluble perester radical precursor to test Sel-F mediated alkyl radical fluorination. Compound **2.21** was selected as the test substrate as the carboxylic acid could be turned into a salt to increase aqueous solubility, if necessary, and anhydride **2.20** is readily available. Thus, perester **2.21** was obtained in 61% yield by acylation of *tert*-butyl peroxide with anhydride **2.20** (Scheme 2.10).

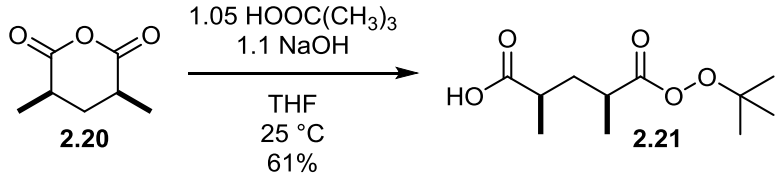

Scheme 2.10. Synthesis of *tert*-butyl perester 2.21

An aqueous solution of **2.21** (and the sodium salt of **2.21**) was heated at 110 °C in a sealed tube. At elevated temperatures, acid **2.21** was water-soluable: therefore, there was no need to convert it into a salt. After 1.5 hours, the reaction mixture was acidified and extracted with deuterochloroform for NMR spectroscopic analysis. ^{19}F NMR spectroscopy provided evidence for the decarboxylative fluorination of **2.21** to **2.22** (Scheme 2.11). Upon proton decoupling, the complex multiplet (Figure 2.3, lower spectrum) resolves into two distinct singlets at -175.3 ppm and -175.5 ppm characteristic of two diastereotopic secondary alkyl fluorides. Unfortunately, I was unable to purify **2.22** for detailed

characterization; however, these experiments provided further supporting evidence for Sel-F as a radical fluorinating agent.

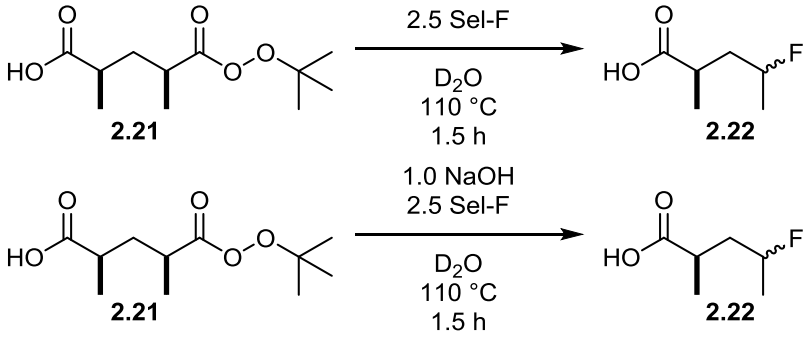

Scheme 2.11. Fluorodecarboxylation of 2.21 with Sel-F

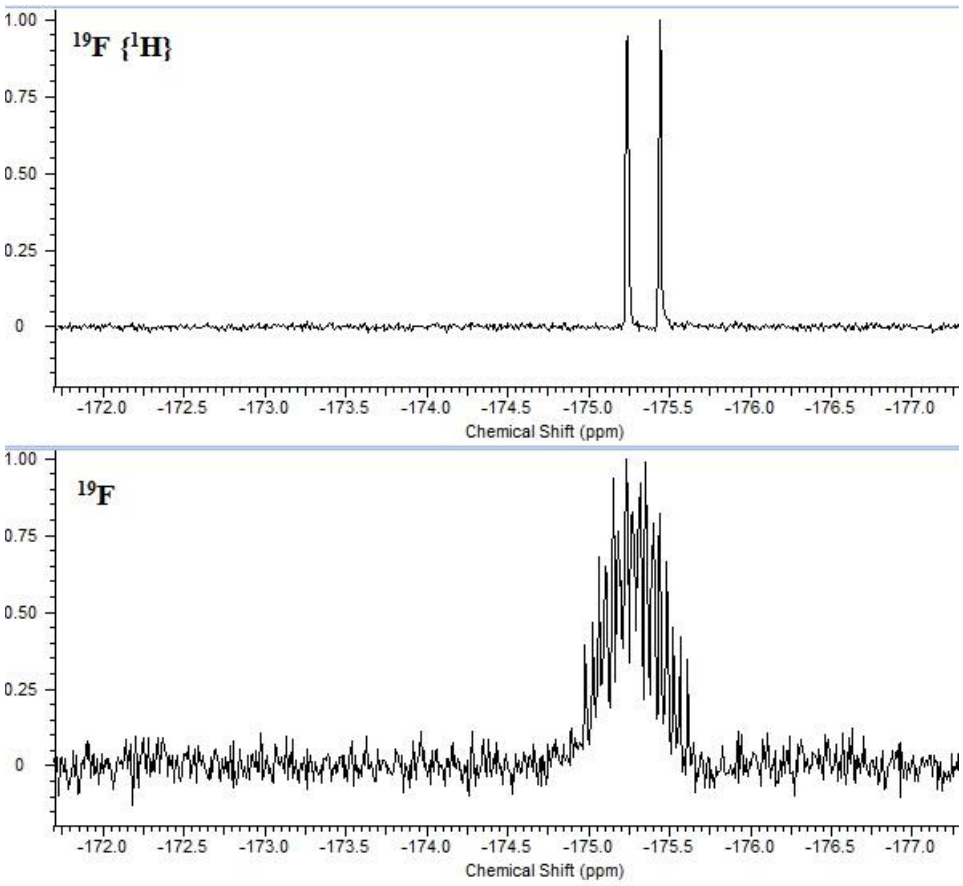

Figure 2.3. ^{19}F NMR spectral analysis of semi-purified products from Scheme 2.11[a]

[a]From top to bottom: Proton-decoupled ^{19}F NMR (282 MHz) of crude reaction mixture. Proton-coupled ^{19}F NMR (282 MHz) of crude reaction mixture.

Colleagues in the group of Prof. Sammis had already established that **2.23** undergoes radical fluoro-decarboxylation in the presence of NFSI in excellent GC yields; therefore, I looked for a solvent that could dissolve both **2.23** and Sel-F. Perfluoroacetone hydrate was examined as an alternative solvent to water for Sel-F studies with perester **2.23** (Scheme 2.12). While both **2.23** and Sel-F dissolved quickly in perfluoroacetone hydrate with heating, no evidence of **2.24** formation was obtained by NMR or mass spectroscopy. Similarly, no evidence for the formation of **2.24** was obtained with NFSI as the fluorinating agent in the perfluoroacetone hydrate solvent.

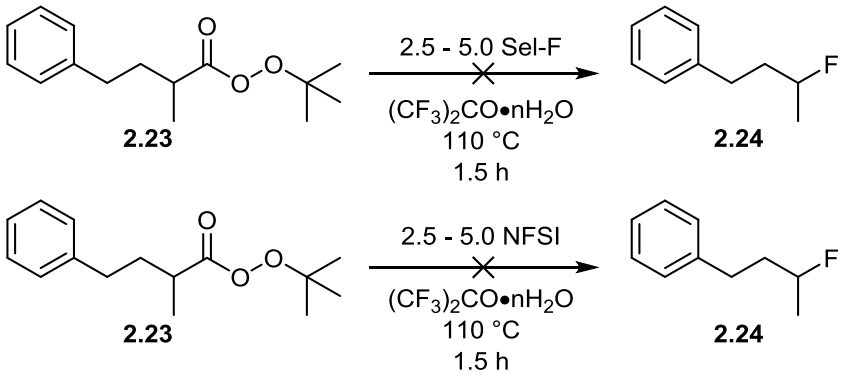

Scheme 2.12. Attempted fluorodecarboxylation of 2.23 in perfluoroacetone hydrate

From the knowledge gained by working with peresters, I can now explain why low yields of fluoroproduct were obtained from these early experiments with Sel-F. The targeted tertiary and secondary alkyl fluorides are prone to degradation at elevated temperatures. Early Sel-F experiments employed conditions, which favour elimination of fluoride from the fluoroalkanes. Water is a very polar solvent and also offers hydrogen bonds to activate fluoride as a leaving group. After loss of fluorine, Sel-F becomes a trialkylamine base, which can facilitate elimination reactions. With the *tert*-butyl perester substrates, hydrolysis competes with homolytic O-O cleavage and the alkaline conditions

inherent to aqueous solutions of Sel-F (water will slowly decompose Sel-F to a TEDA base) can also accelerate the unwanted hydrolysis pathway.

Evidence to suggest that Sel-F is a radical fluorinating agent was uncovered during my subsequent studies on the fluorination of *tert*-butyl perester **2.25** (Scheme 2.13). Thermal decomposition of **2.15** in an acetonitrile solution containing Sel-F at 110 °C in a sealed tube provided fluoromethyl ether **1.112** in 52% yield as observed by ^{1}H NMR spectroscopy (eqn. 2.2). This result provided the strongest evidence in support of the radical fluorinating ability of Sel-F because the same fluoromethyl ether product (**1.112**) could be obtained in 57% NMR yield with NFSI under similar reaction conditions (eqn. 2.1). Because fluorodecarboxylation of **2.25** with NFSI was a radical-mediated fluorination, it was also likely that fluorodecarboxylation of **2.25** with Sel-F was also a radical-mediated fluorination. Studies on the fluorodecarboxylation of **2.25** are presented in greater detail in subsection 2.2.2.

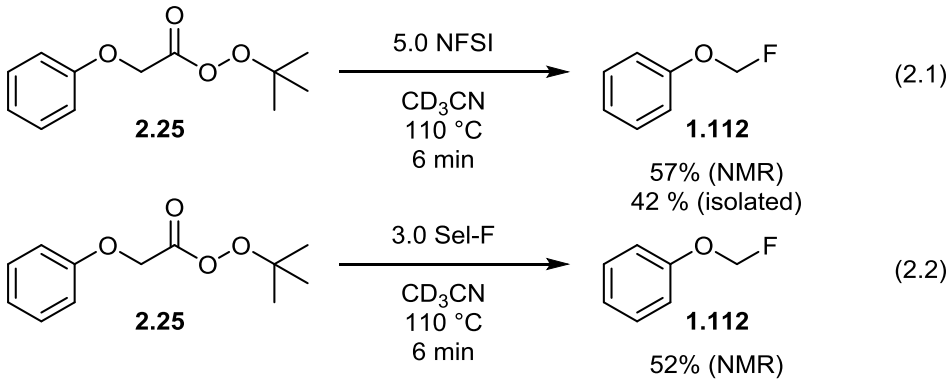

Scheme 2.13. Radical decarboxylative fluorination synthesis of fluoromethoxybenzene

2.2 Radical fluorination of alkyl peresters

Having obtained proof-of-concept for the use of electrophilic fluorination agents Sel-F and NFSI as radical fluorination agents, we continued to investigate the radical decarboxylative fluorination of *tert*-butyl peresters. These substrates were easier to synthesize than diacyl peroxides and their homolysis occurred with formation of reduced amounts of radical cage-recombination products. A summary of our published work is found in Scheme 2.14.[14] The following section will be limited to my contributions, namely: the NMR studies of **1.112** and **2.27** and the isolation of **1.112** and **2.28**.

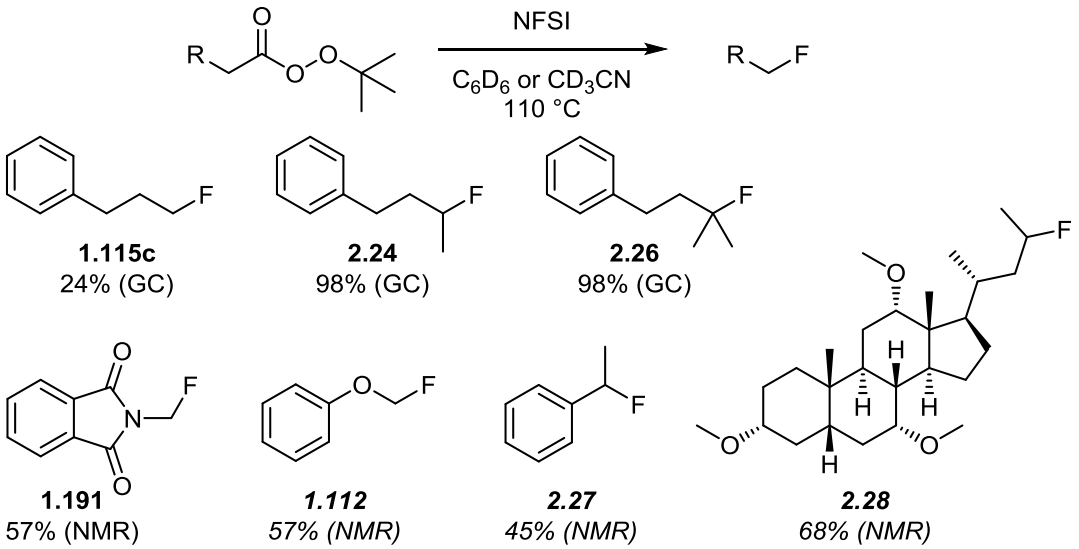

Scheme 2.14. Summary of fluorodecarboxylation of *tert*-butyl peresters[a]

[a]My contributions to the publication are in *italics*.

2.2.1 Fluorodecarboxylation of 2.25

The majority of my studies on radical fluorodecarboxylation focused on phenoxyacetic acid derivative **2.25**. The choice of substrate was motivated by the fact that fluorodecarboxylated product **1.112** would not be liable to undergo elimination of hydrofluoric acid: a side-reaction that complicates the isolation of alkyl fluorides in general. Furthermore, a successful synthesis of fluoromethoxybenzene (**1.112**) might allow an extension of this methodology to the preparation of difluoromethoxybenzenes and trifluoromethoxybenzenes of interest in current medicinal chemistry (see Chapter 3). Perester **2.25** was readily synthesized from phenoxyacetic acid (**2.26**) and *tert*-butyl hydroperoxide through carbonyldiimidazole (CDI) or dicyclohexylcarbodimide (DCC) coupling protocols (Scheme 2.15). Similar to other *tert*-butyl peresters, purified **2.25** was stored in the freezer to prevent decomposition.

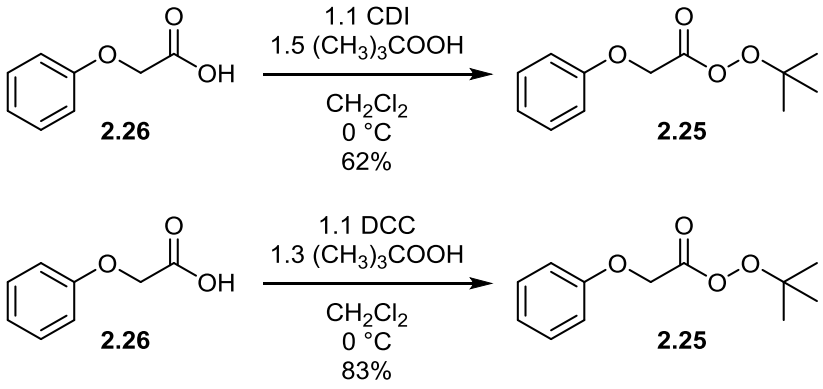

Scheme 2.15. Synthesis of perester 2.25

The fluorodecarboxylation of perester **2.25** was studied in detail (Table 2.4). While **2.25** must be kept at low temperatures to prevent decomposition, thermolysis took place only at temperatures above 80 °C. Thus, no reaction was observed after 15 minutes at 60 °C in benzene (entry 1), but fluorodecarboxylation was observed after 15 minutes at 80 °C (entries 2, 3). As seen in entries 3 to 7, thermolysis of **2.25** at 110 °C is a fast reaction, with 51% conversion after only 1 minute of thermolysis

(entry 4). Optimal yields of **1.112** were obtained in benzene after 3 minutes of immersing a sealed tube containing the reaction mixture in an oil bath maintained at 110 °C (entry 6). Increasing the temperature of the oil bath to 120 °C (entry 8) provided **1.112** in the highest observed yield of 77%; however, this result was not reproducible. A further temperature increase increase to 130 °C (entry 9) induced complete thermolysis within 2 minutes. An oil bath temperature of 110 °C was ultimately selected in order to develop a general reaction protocol for the fluorodecarboxylation of peresters in benzene or acetonitrile, according to Scheme 2.2.1. The thermolysis of **2.25** in acetonitrile produced fluoroether **1.112** in 53% yield after 4 minutes at 110 °C (entry 10), and the best reliable yield of **1.112** was 57% after 6 minutes at 110 °C in acetonitrile (entry 11).

Table 2.4. Fluorodecarboxylation studies of perester 2.25

entry[a][b]	solvent	temperature (°C)	time (min)	yield[c] (%)	conversion[d] (%)
1	C_6D_6	60	15	0	0
2	C_6D_6	80	15	25[e]	68[f]
3	C_6D_6	110	15	23[e]	100[f]
4	C_6D_6	110	1	20[e]	51[f]
5	C_6D_6	110	2	42[e]	90[f]
6	C_6D_6	110	3	46[g]	100
7	C_6D_6	110	5	36[e]	100[f]
8	C_6D_6	120	2	77	93
9	C_6D_6	130	2	50	100
10	CD_3CN	110	4	53[h]	94[h]
11	CD_3CN	110	6	57[h]	100

[a]Reaction conditions: NFSI (5.0 equiv.), **2.25** (1.0 equiv., 0.06 mmol) at 0.2 M in deuterated benzene, sealed reaction vessel immersed in an oil bath (temperature as indicated) for the specified time. [b]Reaction conditions: NFSI (5.0 equiv.), **2.25** (1.0 equiv., 0.06 mmol) at 0.1 M in deuterated acetonitrile, sealed reaction vessel immersed in an oil bath (temperature as indicated) for the specified time. [c]The yields were obtained by ^{1}H NMR spectroscopy using ethyl trifluoracetate as an internal standard. [d]The conversions were obtained by ^{1}H NMR spectroscopy using ethyl trifluoracetate as an internal standard. [e]The yields were obtained by ^{1}H NMR spectroscopy using nitromethane as an internal standard. [f]The conversions were obtained by ^{1}H NMR spectroscopy using nitromethane as an internal standard. [g] Average value of 5 trials. [h]Average value of 3 trials.

Difficulties were encountered upon attempts to isolate fluoromethoxybenzene. Given the low molecular weight of **1.112**, the fluoroether was expected to be suitable for isolation by distillation. For the reactions carried out in benzene, isolation by Kugelrohr distillation produced low yields as decomposition of the fluoroether to phenol was observed (Scheme 2.16). Elimination of fluoride from **1.112** to oxonium **2.29** followed by hydrolysis would produce phenol. Isolation of **1.112** from acetonitrile was more fruitful as hydrolysis was not observed. The main challenge was removal of excess acetonitrile without significant loss of the volatile fluoroether product. After 4 attempts, **1.112** was isolated in 42% yield as an 11.2 M solution in acetonitrile.

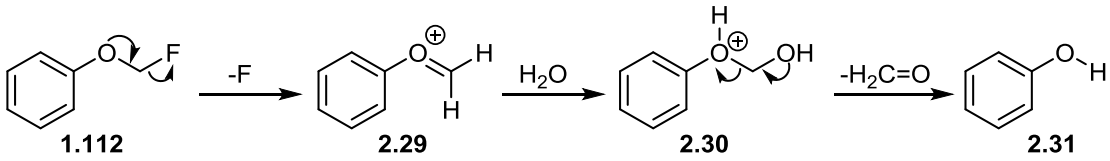

Scheme 2.16. Decomposition pathway for fluoromethoxybenzene

Having successfully demonstrated that fluoromethyl ether **1.112** could be synthesised by radical means employing NFSI in acetonitrile, the radical fluorination ability of Sel-F was investigated (Scheme 2.13). At elevated temperatures, acetonitrile is a suitable solvent for Sel-F, which enables the co-solubilisation of *tert*-butyl peresters and Sel-F without fear of perester hydrolysis. After 6 minutes of heating a solution of **2.25** in the presence of Sel-F, fluoromethyl ether **1.112** was obtained in 52% yield, as determined by ^{1}H NMR spectroscopy (eqn. 2.2). Similarly, thermal decomposition of **2.25** in an acetonitrile solution containing NFSI provided fluoromethyl ether **1.112** in 57% yield (^{1}H NMR, eqn. 2.1). This result provided strong evidence to support the notion that Sel-F is a radical fluorinating agent because an identical radical intermediate presumably involved in fluorination with NFSI was now fluorinated by Sel-F.

A radical fluorination mechanism similar to Scheme 2.6 was proposed for the synthesis of fluoromethyl ether **1.112** with Sel-F (Scheme 2.17). Homolysis of the weak O-O bond by thermal activation generates a carboxyl radical intermediate **2.32**, which rapidly decarboxylates to phenoxymethyl (**2.33**). This stabilized radical is then fluorinated by Sel-F to the desired **1.112**. While it is unclear if radical **2.33** abstracts fluorine from Sel-F through an S_H2 mechanism (Scheme 2.18 A), or if **2.33** is first oxidized to carbocation **2.34** followed by rapid recombination with fluoride (Scheme 2.18 B), a fluorine atom is transferred from Sel-F to radical **2.33** for the desired fluoro product.

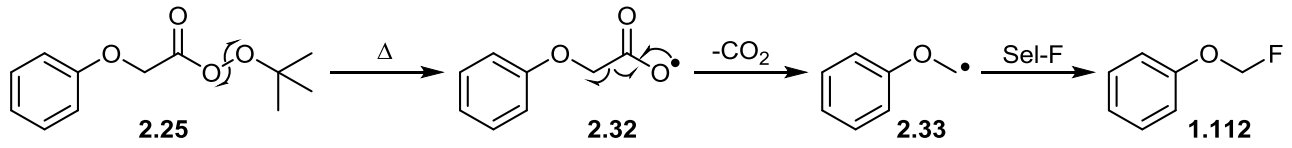

Scheme 2.17. Mechanism for fluorodecarboxylation of 2.25

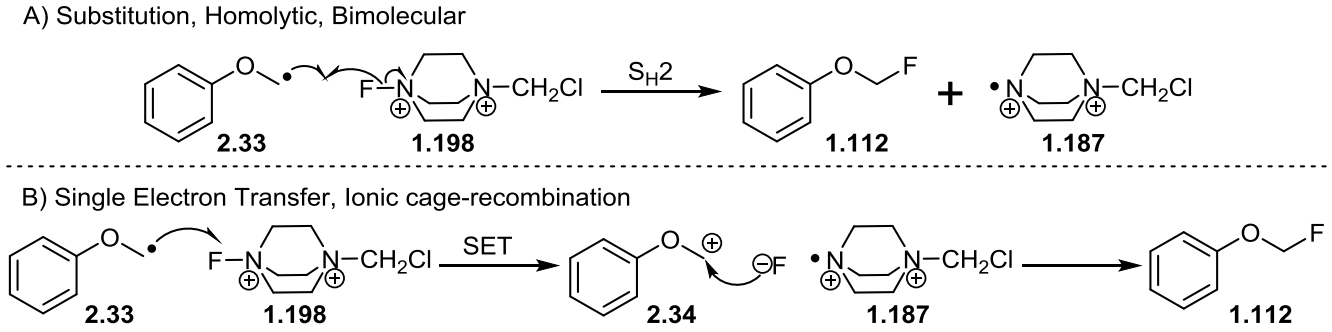

Scheme 2.18. Fluorination pathways for phenoxymethyl

Further support for a radical mechanism can be found in the observation of solvent effects for the decomposition of *tert*-butoxyl radical (**2.35**) to acetone.[135] When **2.25** is thermolyzed in the presence of NFSI, the ratio of acetone to *tert*-butanol is higher (more acetone observed) when the reaction is performed in acetonitrile than in benzene. Similar ratios have been reported for the radical

decomposition of **2.35**,[135] which necessitates the formation of carboxyl radical **2.32** (Scheme 2.19). Rapid decarboxylation of **2.32** to alkyl radical **2.33** then follows.

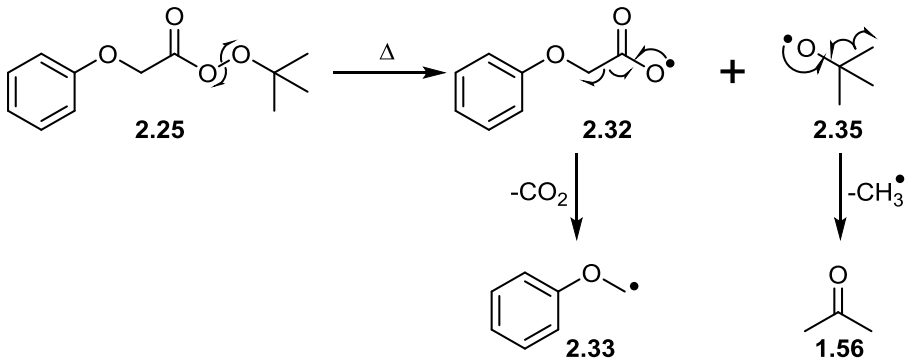

Scheme 2.19. Radical decomposition of *tert*-butoxyl as evidence for alkyl radical formation

A second important set of questions relates to the fate of NFSI: specifically, what happens to NFSI after it transfers fluorine to an alkyl radical and exactly how much NFSI is theoretically required. A radical fluorination mechanism could result in multiple plausible end-products for **2.3** (Scheme 2.20). If radical **2.3** is sufficiently long lived and innocuous, dimerization would yield hydrazide **2.36**. Homolytic cleavage of the perester radical precursor yields an equivalent of *tert*-butyloxyl radical (**2.35**), and as observed earlier, a fraction of which will further fragment to the methyl radical. Both the methyl radical and the *tert*-butyloxyl radical are candidates for radical recombination with **2.3** leading to **2.37** and **2.38**. If **2.3** is sufficiently reactive, it may abstract hydrogen from any number of potential hydrogen atom sources to yield benzenesulfonimide (**2.1**). Although it is hard to envision a mechanism where more than one equivalent of NFSI is theoretically required, it remained to be proven that only one equivalent was necessary.

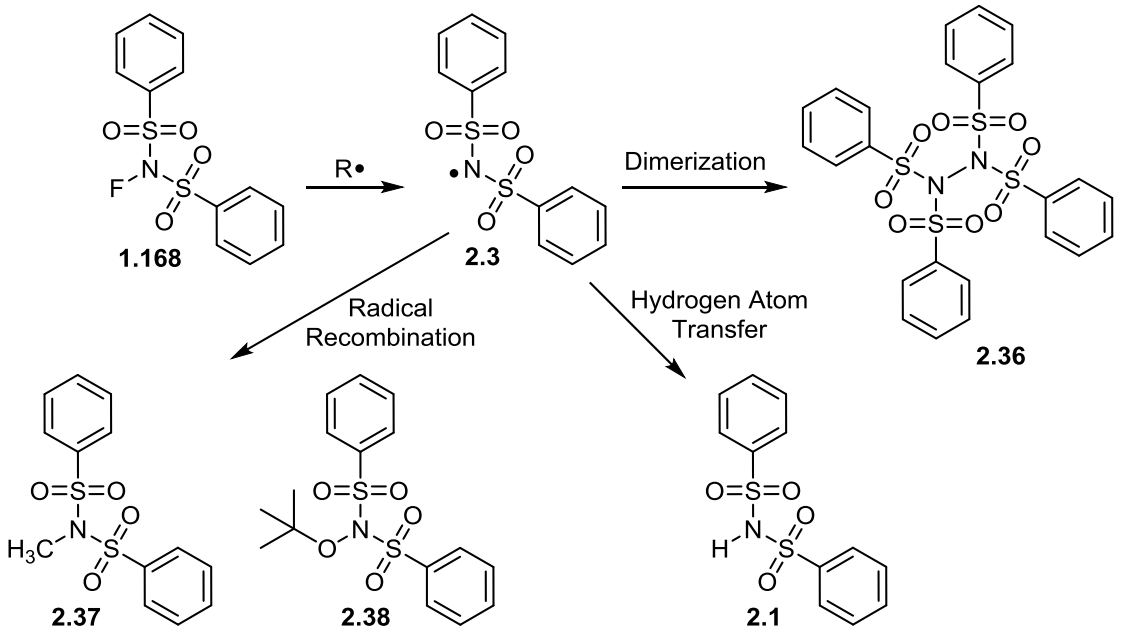

Scheme 2.20. Fate of NFSI after fluorine transfer

To answer these questions, an NMR study was designed, whereby NFSI would be the limiting reagent (Scheme 2.21). Excess **2.25** was thermolyzed in the presence of NFSI to ensure complete consumption of the latter. An examination of the crude reaction mixture by ^{1}H NMR revealed that the theoretical stoichiometry of NFSI required is one equivalent. In Figure 2.4, the top ^{1}H NMR spectrum shows a solution of NFSI in CD_3CN and the lower ^{1}H NMR spectrum is the crude reaction mixture after 10 min of heating at 110 °C. All of the NFSI has been consumed and there is a one to one correlation between the fluoromethyl signal and the NFSI decomposition product. Thus, as expected, only one equivalent of NFSI is theoretically necessary for fluorodecarboxylation.

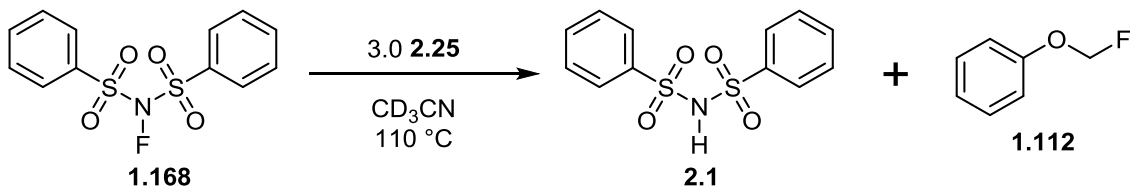

Scheme 2.21. Investigations to elucidate the NFSI decomposition product

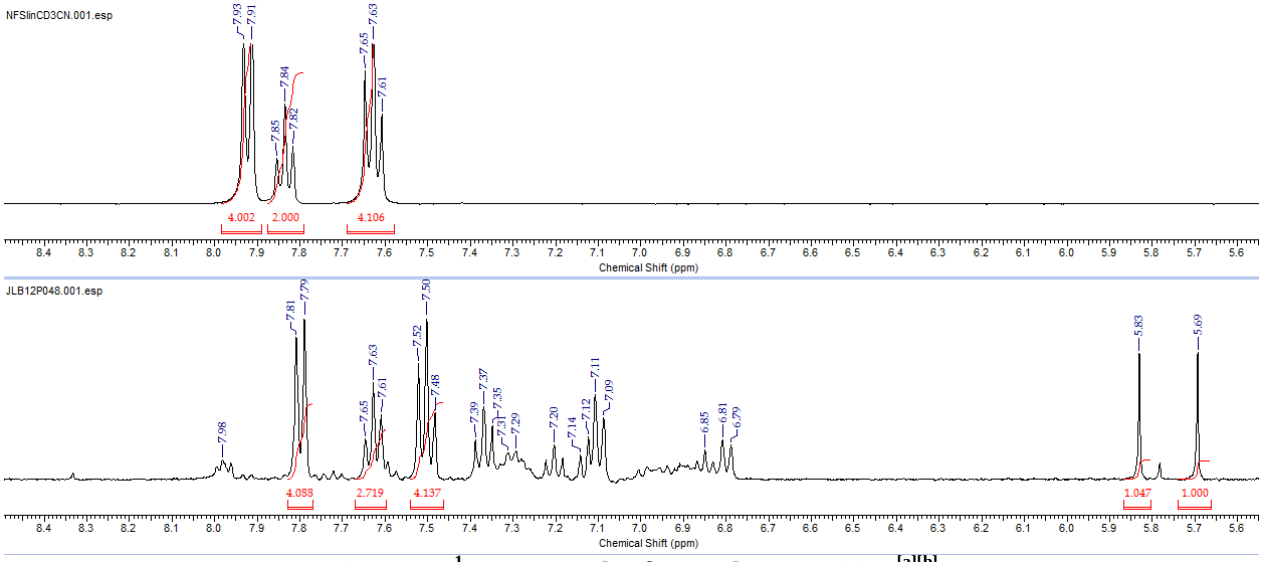

Figure 2.4. ^{1}H NMR study of NFSI decomposition.[a][b]

[a]From top to bottom: ^{1}H NMR of NFSI (400MHz, CD_3CN); ^{1}H NMR (400MHz, CD_3CN) of the crude reaction mixture depicted in Scheme 2.21. [b]Reaction conditions: NFSI (1.0 equiv.), **2.25** (3.0 equiv.) at 0.1 M in deuterated acetonitrile, reaction vessel immersed in an 110 °C oil bath for 10 min.

Having firmly established the theoretical stoichiometry of NFSI, the product arising from the reagent after fluorine transfer was isolated. Spectroscopic analysis identified such a material as benzenesulfonimide (**2.1**). To prove that isolation had not altered the nature of such a product, a separate NMR scale reaction was performed with excess **2.25**, followed by spiking with the previously isolated **2.1**. The top spectrum in Figure 2.5 shows the crude reaction mixture with the methylene signals of **1.112** acting as the internal standard. The following two spectra show slow enrichment with isolated **2.1.** Only the intensitites of the signals at 7.80, 7.63 and 7.50 ppm increase upon addition of **2.1** demonstrating that this substance was not altered during isolation.

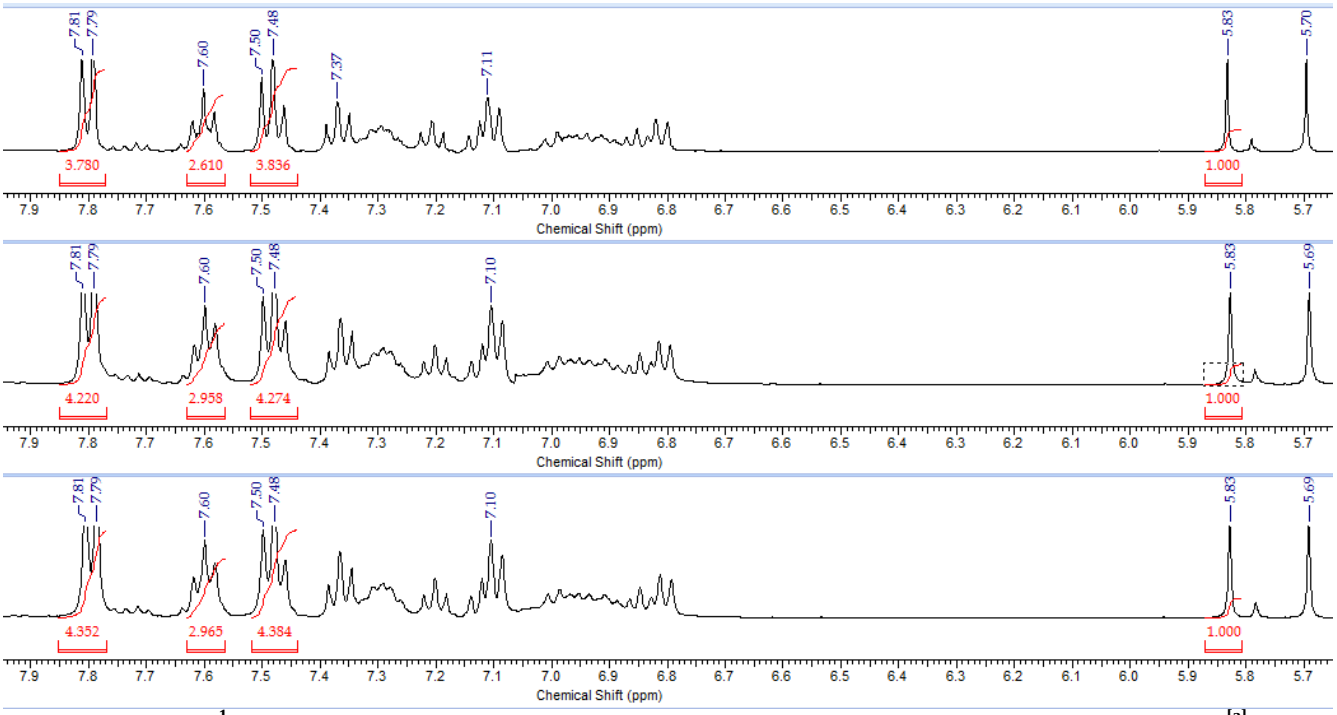

Figure 2.5. ^{1}H NMR study of a crude reaction mixture with increasing enrichment from isolated 2.1.[a]

[a] ^{1}H NMR (400MHz, CD3CN) From top to bottom: crude reaction mixture from Scheme 2.21; enrichment with **2.1** isolated from the experiment in Figure 2.4; increasing enrichment with **2.1**.

The last study performed with this class of aryloxymethyl peresters was the attempted synthesis of aryl difluoromethyl ether **2.40** (Scheme 2.22). As an exploratory reaction, crude perester **2.39** (synthesized from the corresponding α-fluoro acid: see Chapter 3 for details) was thermolyzed in the presence of a radical fluorine transfer agent. Compound **2.39** was completely consumed after 15 min at 110 °C in acetonitrile, but regrettably, no difluoromethyl ether **2.40** was detected by ^{1}H NMR spectroscopy. The failure of perester **2.39** to provide **2.40** highlighted a weakness of the perester methodology and suggested that the method may not be viable for difluoromethoxybenzene synthesis (and by extension, trifluoromethoxybenzene synthesis). In Chapter 3, my discovery of a photochemical transformation that accomplishes the desired synthesis of aryl difluoromethyl ethers will be presented.

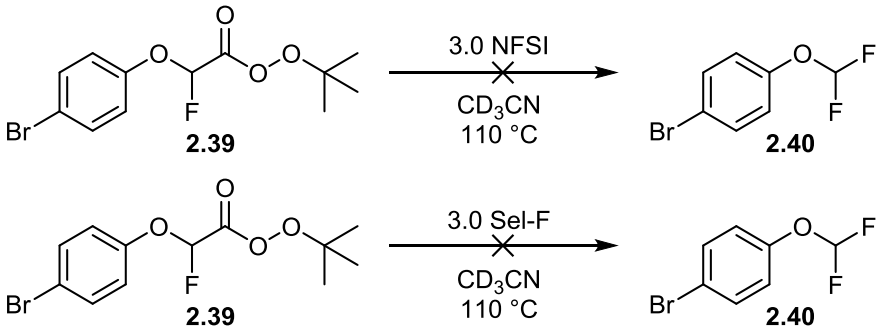

Scheme 2.22. Attempted synthesis of aryl difluoromethyl ethers by perester decomposition

In summary, a wealth of information was gained from studying the fluorodecarboxylation of **2.25**. Radical thermolysis of peresters is faster in benzene than in acetonitrile; however, the decomposition of fluoroproduct **1.112** is also faster in benzene. The isolation of **1.112** from acetonitrile was possible but isolation from benzene was impractical. Only one equivalent of NFSI is theoretically required to fluorinate the alkyl radical, and the NFSI decomposition product is benzenesulfonimide (**2.1**). Both Sel-F and NFSI can be employed as radical fluorine transfer agents for the synthesis of **1.112** from **2.25**. However, extension of perester thermolysis to the synthesis of aryl difluoromethyl and trifluoromethyl ethers was unsuccessful.

2.2.2 Perester fluorodecarboxylation synthesis of 2.27 and 2.28

Early attempts by colleagues in the group of Prof. Sammis suggested that radical decarboxylation of perester **2.41** was not a viable method to synthesize benzyl fluoride **2.27**. This observation was puzzling in light of the success in fluorodecarboxylation to synthesize **2.24** and **2.26** because perester decomposition is a reliable method to generate stabilized radicals. The fluorodecarboxylation of **2.41** was expected to be facile as the resulting secondary alkyl radical was

also benzylic. Further study into alkyl fluorides revealed that elimination of hydrofluoric acid to generate an alkene sometimes complicates isolation of alkyl fluorides. I was charged with re-investigating the fluorodecarboxylation of **2.41** (Table 2.5).

Investigations into the fluorodecarboxylation of **2.41** began with examining early time points of the thermal decomposition in deuterobenzene (Table 2.5, entries 1 to 4). As suspected, formation of **2.27** was possible, but decomposition of **2.27** was also rapid. After 2 minutes at 110 °C, 62% of the perester was consumed with an observed yield of **2.27** in 24% (entry 2). After 4 minutes, all of the starting perester was consumed; however, all of the **2.27** generated was also lost (entry 4). When the solvent was switched to deuterated acetonitrile (entries 5 to 8) the amount of **2.27** decomposition was reduced. After 4 minutes, only 85% of perester **2.41** was consumed (entry 6) with complete consumption of starting material after 6 minutes at 110 °C (entry 8). The optimized NMR yield of **2.27** was 45% after 6 minutes at 110 °C in deuterated acetonitrile.

Table 2.5. Fluorodecarboxylation studies of perester 2.41

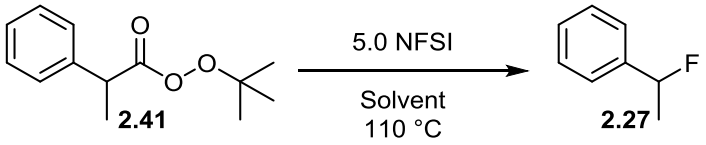

entry[a]	solvent	time (min)	yield[b] (%)	conversion[c] (%)
1	C_6D_6	1	11	23
2	C_6D_6	2	24	62
3	C_6D_6	3	15	89
4	C_6D_6	4	0	100
5	CD_3CN	2	23	53
6	CD_3CN	4	37	85
7	CD_3CN	5	43	95
8	CD_3CN	6	45	100[d]

[a]Reaction conditions: NFSI (5.0 equiv.), **2.41** (1.0 equiv., 0.06 mmol) at 0.2 M in deuterated benzene or at 0.1 M in deuterated acetonitrile, sealed reaction vessel immersed in a 110 °C oil bath for the specified time. [b]The yields were obtained by ^{1}H NMR spectroscopy using ethyl trifluoracetate as an internal standard. [c]The conversions were obtained by ^{1}H NMR spectroscopy using ethyl trifluoracetate as an internal standard. [d] Average value of 3 trials.

Fluorodecarboxylation of perester **2.41** was then tested employing Sel-F as the fluorine transfer agent. Unfortunately, the problem of hydrofluoric acid elimination of **2.27** to styrene was amplified by Sel-F. The loss of fluorine from Sel-F generates the trialkylamine base **1.199** which is a stronger base than disulfonamidyl base **2.2** generated by NFSI after fluorine transfer. Thermal decomposition of **2.41** in acetonitrile in the presence of Sel-F provided a 12% NMR yield of **2.27** (Scheme 2.2.10).

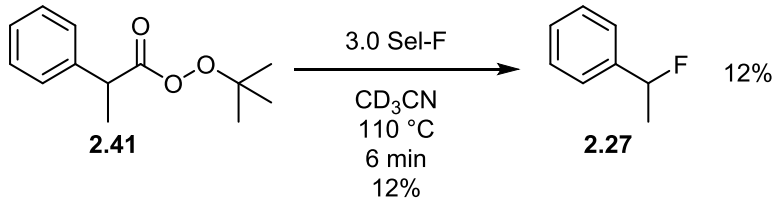

Scheme 2.23. Fluorodecarboxylation of perester 2.41 with Sel-F

To demonstrate the synthetic utility of the fluorodecarboxylation reaction, it was necessary to employ our methodology on a complex molecular target. Our choice fell on cholic acid derivative **2.42,** (Scheme 2.24). This material is an excellent substrate to showcase the selectivity of this radical fluorination method in that it contains multiple C-H bonds that are weak and susceptible to interfere in a poorly selective radical reaction.

The study of **2.42** was truly a team effort as both C. Chatalova-Sazepin and M. Rueda-Becerril performed the synthesis of **2.42** from cholic acid (5 step transformation), Prof. G. Sammis optimized the fluorodecarboxylation conditions, and I performed the isolation of **2.28**. From early isolation attempts of alkyl fluorides, it had been established that silica gel chromatography leads to significant decomposition of the fluorodecarboxylation products. The previous solution was isolation by distillation; however, this was not a viable option for nonvolatile **2.28.** I had made the observation that purified **2.28** (previously isolated in low-yield by M. Rueda-Becerril) could be re-chromatographed on

silica without significant loss of material. I hypothesized that decompositions may have been due to the concerted action of species present in the crude reaction mixture and silica gel. Thus, the problem of material loss during isolation was solved by minimizing exposure of the crude reaction mixture to silica. By running the reaction on a small scale (5 mg, 9.3 μmol) and diluting the reaction mixture with dicholormethane (50% by volume) prior to loading onto pre-treated silica (pre-equilibration with a 75 : 25 : 10 solution of hexanes : EtOAc : triethylamine), **2.28** was isolated in 54% yield.

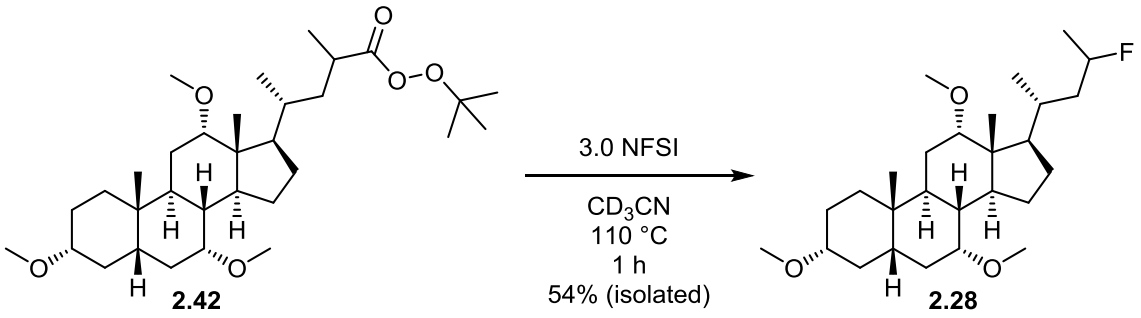

Scheme 2.24. Fluorodecarboxylation of cholic acid derivative 2.42

2.3 Attempted synthesis of aryl fluorides by radical methods

Selective radical-mediated synthesis of aryl fluorides has been, and still remains, a major challenge.[136] Reported methods for radical-mediated fluorination of aryl compounds avoid the generation of an aryl radical. Indeed, the fluorination of an aryl radical with known reagents does not seem possible. All such attepts have led only to aryl radical quenching by the solvent,[92] and no fluorination was ever observed. Instead, the radical avenues to aryl fluorides rely on the generation of atomic fluorine followed by addition thereof to a benzene ring. This is in contrast to methods of radical fluorination for alkyl radicals, which relied on the inherent propensity of hydrogen atom abstraction by

free fluorine. Such a means of aryl radical generation from benzene would be impossible as radical addition into the aryl ring outcompetes hydrogen atom transfer of sp^2 C-H bonds.[23a,25,137]

Thus, my objective became the development of a radical-mediated aryl fluoride synthesis, and to that end, solutions to the following two problems had to be identified: (1) generate an aryl radical without generation of atomic fluorine, and (2) transfer a fluorine atom to the aryl radical.

Both Sel-F and NFSI seemed good candidates as fluorine atom transfer reagents. An advantage of Sel-F and NFSI over F_2 and CF_3OF is that the stabilized radicals generated upon fluorine transfer are unlikely candidates for aryl-addition reactions. Therefore, all non-selective aryl-addition processes that plague the radical synthesis of fluorobenzene would be eliminated.[23a,25] The principal challenge was the selective generation of an aryl radical. Three methods of aryl radical generation[138] were investigated: decarboxylation by carboxylic acid derivatives, decomposition of diazonium salts, and decomposition of boronic acids.

2.3.1 Generation of aryl radicals from decarboxylation of carboxylic acid derivatives

The decomposition of carboxylic acid derivatives to alkyl radicals is a relatively facile process, especially for the generation of stabilized radicals such as secondary and tertiary alkyl radicals. Many variations on the radical decarboxylation theme exist,[38,133,139] all of which converge on the generation of a carboxyl radical. Unlike their alkyl radical counterparts, aryl radicals are higher energy species and are more difficult to generate through decarboxylation. As shown in Figure 2.6 (left portion) the C-H bond dissociation energy of benzene is 112.9 kcal/mol while the C-H bond dissociation energy of the saturated homolog cyclohexane is 95.5 kcal/mol.[140] This is further reflected in the rates of radical

decarboxylation. Thus, the rate of decarboxylation of benzoyloxy radical (**2.43**)[141] is three orders of magnitude slower than that of carboxyl **2.44** (Figure 2.6).[142] Nevertheless, radical decarboxylation may be employed to generate aryl radicals.

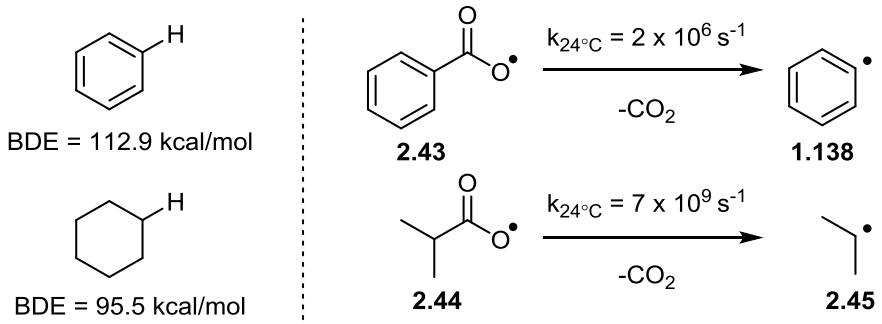

Figure 2.6. Bond dissociation energies and decarboxylation rates for selected compounds

Benzoyl peroxide (**2.46**) is typically employed as a radical initiator or chemical oxidant;[143] however, it has also been used effectively as a reagent for simple atom transfer or aryl radical addition to aromatic systems (Scheme 2.25).[144-146] Thermolysis of benzoyl peroxide (**2.46**) in the presence of iodine leads to high yields of the iododecarboxylation product **2.48**.[144] Thermolysis of benzoyl peroxide in acetic acid solutions containing thiazole (**2.49**) provide 84% yield of 2-phenylthiazole (**2.50**).[145] High yields of the phenyl addition product **2.52** can be obtained from decomposition of benzoyl peroxide in neat difluorobenzene **2.51**.[146]

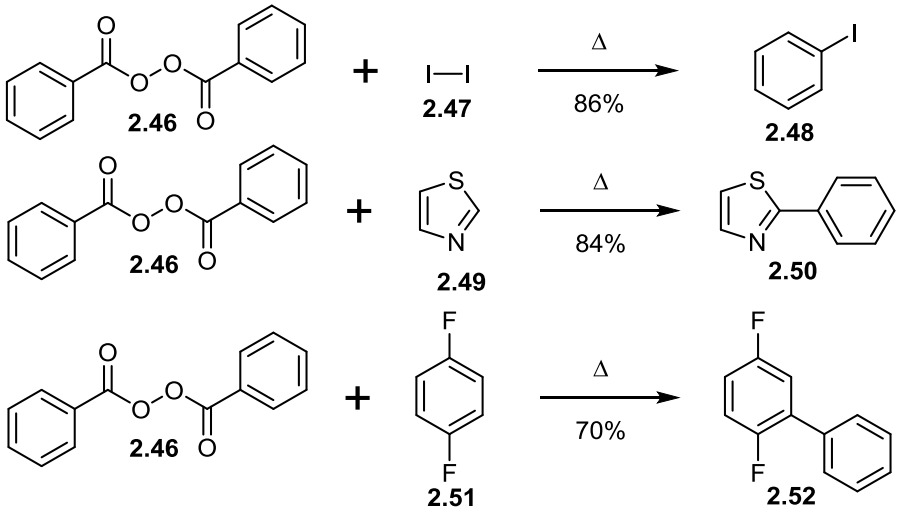

Scheme 2.25. Selected reactions of benzoyl peroxide

Lauroyl peroxide (**2.10**) was successfully employed to discover that decomposition of symmetrical peresters in the presence of NFSI leads to the fluorodecarboxylation product. Extension of that methodology for fluorodecarboxylation of benzoic acid derivatives with benzoyl peroxide (**2.46**) was a logical course of action. Studies toward radical aryl fluoride formation began with simple thermal decomposition experiments in different solvents (Table 2.6). Benzene was not an appropriate solvent choice as aryl radicals readily react with benzene to form biphenyl (**1.162**).[147]

The first experiment was performed in deuterated water with Sel-F in a sealed tube heated to 110°C (entry 1). Water was chosen to ensure complete solubility of the fluorinating agent and reduce the solubility of benzoyl peroxide. This would reduce or suppress electrophilic aryl fluorination of benzoyl peroxide prior to radical decomposition. Unfortunately, no evidence for the formation of fluorobenzene (**1.82**) was ever uncovered by ^{1}H NMR analysis of chloroform extracts of the aqueous reaction mixtures.

Fluorous solvents were investigated next in the hope that both benzoyl peroxide and the fluorinating agent would be soluble (entry 2-4). Unlike reactions run in deuterium oxide, at elevated temperatures, homogeneous solutions were obtained with such fluorous solvents. Fluorobenzene (**1.82**) was not detected by ^{1}H NMR analysis of the organic extracts of reactions executed in either hexafluoroisopropanol or hexafluoroacetone hydrate. Neither was fluorobenzene (**1.82**) observed when NFSI was employed as the fluorinating agent (entry 4).

After 2 hours at 110 °C, significant amounts of benzoyl peroxide were always recovered from the reaction mixtures. Sensing that perhaps the symmetrical peroxide was a poor choice, the aryl radical precorsor was switched to the *tert*-butyl perester **2.53** and the temperature was raised slightly. However, experiments with both NFSI and Sel-F showed no evidence for fluorobenzene formation by ^{19}F NMR analysis. Also, significant amounts of benzoic acid (**2.54**) were observed when the reaction was carried out in perfluoroacetone hydrate, which indicated that the perester hydrolysis outcompetes radical decomposition.

The last solvent screened was acetonitrile, which solubilized benzoyl peroxide, NFSI, and partially solubilized Sel-F. Although preliminary analysis of ^{19}F NMR showed trace signals in the aryl-fluoride region for both Sel-F and NFSI (entries 7 and 8), a spike experiment with authentic fluorobenzene demonstrated that the candidate signal was not fluorobenzene (**1.82**).

Table 2.6. Fluorodecarboxylation studies with aryl peroxides

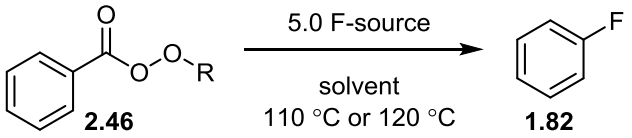

entry	substrate (R)	F-source	solvent	comment
1	C_6H_5 (**2.46**)	Sel-F	D_2O	2 hours in a 110°C bath. No fluorobenzene detected.
2	C_6H_5 (**2.46**)	Sel-F	$(CF_3)_2CHOH$	2 hours in a 110°C bath. No fluorobenzene detected.
3	C_6H_5 (**2.46**)	Sel-F	$(CF_3)_2CO{\bullet}nH_2O$	2 hours in a 110°C bath. No fluorobenzene detected.
4	C_6H_5 (**2.46**)	NFSI	$(CF_3)_2CO{\bullet}nH_2O$	2 hours in a 110°C bath. No fluorobenzene detected.
5	$C(CH_3)_3$ (**2.53**)	Sel-F	$(CF_3)_2CO{\bullet}nH_2O$	1.5 hours in a 120°C bath. No fluorobenzene detected.
6	$C(CH_3)_3$ (**2.53**)	NFSI	$(CF_3)_2CO{\bullet}nH_2O$	1.5 hours in a 120°C bath. No fluorobenzene detected.
7	C_6H_5 (**2.46**)	Sel-F	CD_3CN	2 hours in a 120°C bath. No fluorobenzene detected.
8	C_6H_5 (**2.46**)	NFSI	CD_3CN	2 hours in a 120°C bath. No fluorobenzene detected.

As a final effort, the direct decarboxylation of benzoic acid (**2.54**) was attempted through a Hunsdieker-like process with silver acetate (Scheme 2.26). A suspension of benzoic acid, Sel-F and silver (I) acetate, in a sealed microwave vial, was placed in a 100 °C bath for 24 hours. No fluorobenzene was detected by ^{1}H and ^{19}F NMR spectroscopy. Failed attempts at silver-mediated fluorodecarboxylation of benzoic acid (**2.54**) have also been reported by Li and Gouverneur.[103,104] At this point, another method of aryl radical generation was pursued.

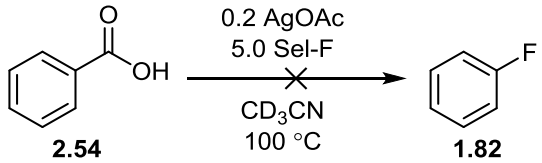

Scheme 2.26. Attempted Hunsdieker-type fluorodecarboxylation

2.3.2 Generation of aryl radicals from dediazoniation of diazo compounds

Another method commonly employed for the generation of aryl radicals is the decomposition of aryl diazoniums (**2.55**).[148] Historically, controversy abounded regarding the mechanism of dediazoniation reactions. The Sandmeyer reaction[149,150] seemed very similar to a host of other related reactions, of which the Balz-Schiemann[151] reaction is most pertinent to this thesis (Figure 2.7). Under Sandmeyer's conditions (treatment of aryl diazoniums with copper (I) halide salts)[149] aryl fluorides cannot be obtained; however, in the absence of solvent and other additives, thermal decomposition of **2.57** (Balz-Schiemann reaction) leads to good yields of fluorobenzene.[152] Eventually, the mechanism of heterolytic dediazoniation through an aryl cation intermediate was shown to be responsible for the Balz-Schiemann reaction.[151] This aryl cation intermediate could be captured by weak nucleophiles such as water to yield phenols[153] or fluoride (from tetrafluoroborate) to yield aryl fluorides.

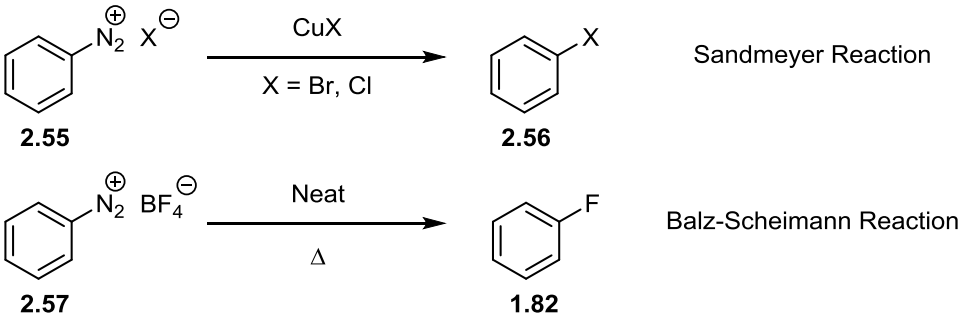

Figure 2.7. Named reactions involving aryldiazoniums

The mechanism of the Sandmeyer reaction[150] can be understood as a homolytic dediazonation (Scheme 2.27, X = Br, Cl) and requires an initial single electron transfer event from copper (I) to the diazonium (eqn. 2.3) prior to radical dediazoniation (eqn. 2.4). The resulting aryl radical then abstracts a halide from a copper (II) species yielding the desired aryl halide (eqn. 2.5). The existence of copper

(I) fluoride is itself questionable as the redox properties of copper and highly electronegative fluorine favour disproportionation to CuF_2 and metallic copper.[154] Thus, the Sandmeyer reaction for aryl fluoride synthesis appears to be –as yet– impossible.

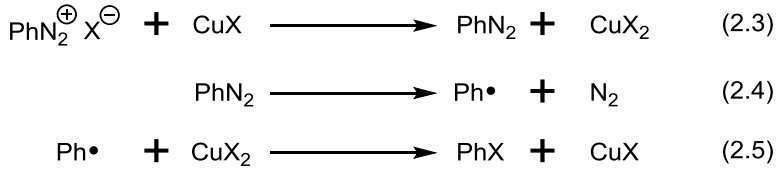

Scheme 2.27. Mechanism of the Sandmeyer reaction

I thought it possible to construct a Sandmeyer-like reaction by assembling the required components separately. Instead of a copper (I) halide, which could act as both SET reducing agent and subsequent radical halide source, two different reagents could be employed. Recent studies by M. Zlotorzynska demonstrated the feasibility of photoinduced electron transfer (PET) by an electron-rich amine into *N*-alkoxypthalimide systems.[155] A similar SET process seem reasonable whereby SET from diisopropylethylamine (DIPEA) would initiate the radical dediazoniation process to generate the necessary aryl radical. Alternatively, pyridine was found by Abramovitch[156] to trigger the radical dediazoniation of aryl diazonium salts, thus a more electron-rich variant, 4-dimethylaminopyridine (DMAP), was selected as a candidate SET reducing agent. For the radical fluorine source, both Sel-F and NFSI would be screened.

To avoid the Balz-Schiemann reaction,[151] studies commenced with 4-bromobenzenediazonium tosylate (**2.58**), which was easily prepared according to literature procedures.[157] To avoid the convential Sandmeyer reaction, no experiments were performed with copper salts. In total, 18

experiments were performed with benezenediazonium salts and the most important results are listed in Table 2.7. Thermal decomposition of **2.58** in water with Sel-F and DMAP (entry 2) provided NMR signals corresponding to 4-bromofluorobenzene (**2.59**). However, in the absence of an amine base (entry 1), which would act as the necessary electron source to trigger radical decomposition of **2.58**, similar amounts of **2.59** was also detected alongside significant amounts of phenol. The combination of these products suggests that a Balz-Schiemann reaction was responsible for fluorination. For this reason, thermal experiments with **2.58** and Sel-F were not pursued further.

Photochemical decomposition of **2.58** was attempted using a broad-spectrum sunlamp (entries 3-5). The photochemical setup was identical to the one used by M. Zlotorzynska for PET from DIPEA to *N*-alkoxyphalimides.[155] Starting with the control experiments, a solution of **2.58** and Sel-F in deutero-DMSO was irradiated by the sunlamp with no detection of aryl fluoride. The second control experiment was designed with an electron source, but no photocatalyst (entry 4). After 2.5 hours of irradiation of a solution of **2.58**, Sel-F, and DIPEA, significant colour changes were observed in the reaction mixture; as expected, no aryl fluoride was detected by ^{1}H and ^{19}F NMR spectroscopy. Finally, a solution of **2.58**, Sel-F, DIPEA, and catalytic amounts of a $Ru(bpy)_3(PF_6)_2$ (**2.60**) were irradiated by a sunlamp for 2.5 hours (entry 5). Significant colour changes were observed in the reaction mixture, but no aryl fluoride was detected. In all experiments, bromobenzene (**2.56a**, X =Br) was the major product resulting from dediazoniation and the diazonium **2.58** was never completely consumed.

Since Sel-F did not yield aryl fluorides by radical means, attention was given to NFSI (entries 6-10). Unlike Sel-F, NFSI does not dissolve in water, thus, acetone was employed. However, thermal treatment of **2.58** with NFSI did not yield any detectable amounts of aryl fluoride **2.59** either without (entry 6) or with (entry 7) an electron source to initiate radical dediazoniation. Again, photochemical

means of radical generation were investigated and a similar series of experiments were performed with NFSI and Ru photocatalyst **2.60**. With no additional electron sources, a solution of **2.58** and NFSI in deutero-DMSO was irradiated by the sunlamp for 2 hours (entry 8). No aryl fluorides were detected by ^{1}H or ^{19}F NMR spectroscopy. Similarly, no aryl fluorides were detected by the second control experiment with DIPEA and no photocatalyst after 2.5 hours of sunlamp irradiation (entry 9). Finally, the experiment of interest contained all the theoretically necessary reagents for PET induced aryl-radical generation, but again, no **2.59** were detected by ^{1}H or ^{19}F NMR spectroscopy (entry 10). Complete consumption of the diazonium **2.58** was observed in all experiments with bromobenzene (**2.56a**, X =Br) as the major product resulting from dediazoniation.

Table 2.7. Fluorodediazonation studies with diazonium salt 2.58

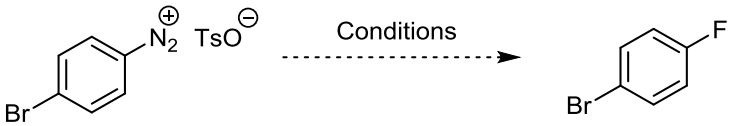

2.58 **2.59**

entry	conditions	comments
1	3.0 Sel-F, D_2O	17 hours @ 60°C. **2.59** detected.
2	3.0 Sel-F, 1.0 DMAP, D_2O	17 hours @ 60°C. **2.59** detected.
3	3.0 Sel-F, $(CD_3)_2SO$	2 hours irradiated with sunlamp. No aryl fluoride detected.
4	3.0 Sel-F, 5.0 DIPEA, $(CD_3)_2SO$	2.5 hours irradiated with sunlamp. No aryl fluoride detected.
5	3.0 Sel-F, 0.05 $Ru(bpy)_3(PF_6)_2$, 5.0 DIPEA, $(CD_3)_2SO$	2.5 hours irradiated with sunlamp. No aryl fluoride detected.
6	3.0 NFSI, $(CD_3)_2CO$	17 hours @ 60°C. **2.59** not detected.
7	3.0 NFSI, 1.0 DMAP, $(CD_3)_2CO$	17 hours @ 60°C. **2.59** not detected.
8	3.0 NFSI, $(CD_3)_2SO$	2 hours irradiated with sunlamp. No aryl fluoride detected.
9	3.0 NFSI, 5.0 DIPEA, $(CD_3)_2SO$	2.5 hours irradiated with sunlamp. No aryl fluoride detected.
10	3.0 NFSI, 0.05 $Ru(bpy)_3(PF_6)_2$, 5.0 DIPEA, $(CD_3)_2SO$	2.5 hours irradiated with sunlamp. No aryl fluoride detected.

The failure of these experiments to generate 4-bromofluorobenzene (**2.59**) can be explained from knowledge gained in subsequent investigations on the mechanism of photodecarboxylative fluorination (Chapter 3). Generation of aryl radicals from diazoinum salts require a single electron reduction of the benzenoid core. However, the two main electron sources tested, DMAP and DIPEA, are both suitable nucleophiles for electrophilic fluorination by Sel-F and NFSI. DMAP can be easily fluorinated by both Sel-F and NFSI through electrophilic aryl substitution, while DIPEA has a nucleophilic nitrogen and is *N*-fluorinated. Furthermore, Sel-F is a strong oxidant and could compete with diazonium **2.58** as the preferred SET acceptor. NFSI is a less powerful oxidant and this difference in oxidizing power might explain why the diazonium **2.58** is mostly recovered in experiments utilizing Sel-F but is consumed in experiments utilizing NFSI. Thus, diazonium salts are very unlikely candidates for radical fluorination.

2.3.3 Generation of aryl radicals from deborylation of arylboronic acids

A recently developed method for aryl radical generation is the oxidation of aryl boronic acids (Scheme 2.28). This transformation can be accomplished by manganese (III) acetate[158,159] or oxyl radicals generated by catalytic amounts of iron.[160] The seminal report by Demir disclosed a method of biaryl synthesis employing arylboronic acids and manganese triacetate (Scheme 2.28. top reaction).[158a] Further reactions of this type promoted by microwave heating have also been reported.[158b,159] Studer has employed this method of aryl radical generation in addition reactions of aryl radicals to alkenes (Scheme 2.28, bottom reaction).[161]

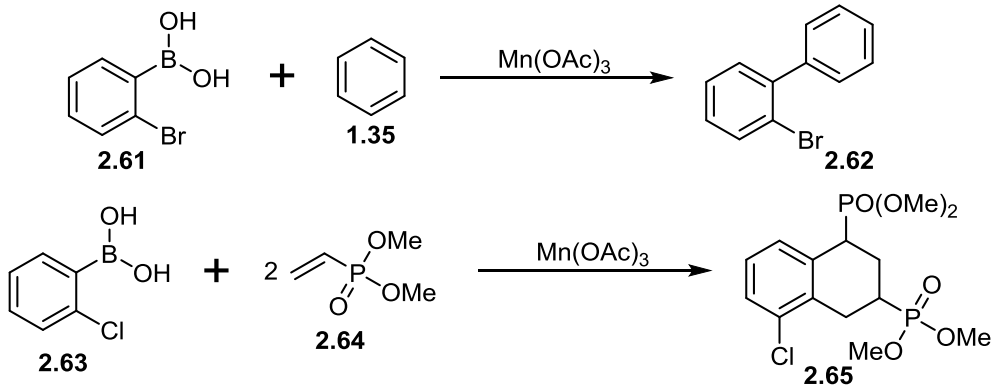

Scheme 2.28. Aryl radical reactions employing boronic acids and Mn(III)

In direct contrast to the methods employed in the previous section, the aryl radical precursor is an arylboronic acid that acts as a SET reducing agent[92] instead of an aryldiazonium that acts as a SET oxidizing agent.[148] This method of aryl radical generation was a promising alternative because it was orthogonal to both the decarboxylation methods in subsection 2.3.1 and dediazontation methods in subsection 2.3.2. The addition of an oxidant such as manganese (III) acetate ($Mn(OAc)_3$) should not affect the electrophilic fluorine sources, which are also oxidants. The catalytic iron systems were avoided as they required more reagents and might complicate the exploratory nature of this work.

Studies of the fluorodeborylation reaction of aryl boronic acids commenced with phenylboronic acid (**2.66)** as the aryl radical source and $Mn(OAc)_3$ as the oxidant. (Table 2.8). The first test reaction of **2.66** with $Mn(OAc)_3$ and Sel-F in water (entry 1) was very exciting as fluorobenzene (**1.82**) was detected by ^1H and ^{19}F NMR spectroscopy. Since Sel-F was known to facilitate electrophilic aromatic substitution, a control experiment with benzene (**1.35**) in place of phenylboronic acid (**2.66**) was necessary (entry 2). ^1H NMR analysis of the reaction mixture showed that no fluorobenzene was formed confirming the necessity of phenylboronic acid. The similar reaction of **2.66** with $Mn(OAc)_3$ and NFSI in hexafluoroacetone hydrate could not be analyzed as paramagnetic compounds were present in the NMR sample (entry 3).

Computational studies in Table 2.3 suggested that the N-F bond of NFPY was stronger than the N-F bonds in Sel-F and NFSI but still somewhat weaker than C-H bonds. Initial tests by alkyl radicals proved unsuccessful in abstracting fluorine from NFPY, but the higher-energy aryl radical might perform differently. Accordingly, both NFPY triflate (Table 2.8, entry 4) and NFPY tetrafluoroborate (entry 5) were tested with phenylboronic acid (**2.66**) and $Mn(OAc)_3$. Unfortunately, fluorobenzene was not formed; furthermore, the majority of phenylboronic acid remained unreacted and suggested that $Mn(OAc)_3$ was not reacting with phenylboronic acid in water. A control experiment was executed with phenylboronic acid (**2.66**) and electrophilic fluorine sources in the absence of $Mn(OAc)_3$ (entries 6-8). NMR analysis of the reactions with **2.66** and the NFPY reagents now showed complete consumption of boronic acid, but no formation of fluorobenzene (entries 6, 7). Interestingly, fluorobenzene was produced from the reaction of boronic acid **2.66** with Sel-F without $Mn(OAc)_3$!

Table 2.8. Fluorodeborylation studies with phenylboronic acid.

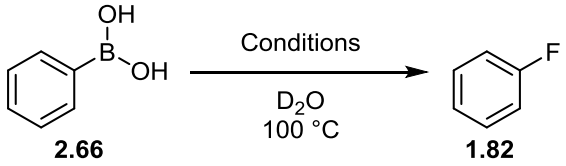

2.66 **1.82**

entry	conditions	comments
1	5.0 Sel-F, 3.0 $Mn(OAc)_3$	2 hours in a 100°C bath. Fluorobenzene detected.
2	5.0 Sel-F, **1.35** tested in place of **2.66**	2 hours in a 100°C bath. No fluorobenzene detected.
3	5.0 NFSI, 3.0 $Mn(OAc)_3$, $(CF_3)_2CO$ hydrate	2 hours in a 100°C bath. NMR analysis failed.
4	5.0 NFPY OTf, 3.0 $Mn(OAc)_3$	2 hours in a 100°C bath. Majority of unreacted **2.66** observed. No fluorobenzene detected.
5	5.0 NFPY BF_4, 3.0 $Mn(OAc)_3$	2 hours in a 100°C bath. Majority of unreacted **2.66** observed. No fluorobenzene detected.
6	5.0 NFPY OTf, no $Mn(OAc)_3$	2 hours in a 100°C bath. No fluorobenzene detected.
7	5.0 NFPY BF_4, no $Mn(OAc)_3$	2 hours in a 100°C bath. No fluorobenzene detected.
8	5.0 Sel-F, no $Mn(OAc)_3$	2 hours in a 100°C bath. Fluorobenzene detected.

With the realization that manganese was unnecessary for deborylative fluorination, optomisation of the reaction between phenylboronic acid (**2.66**) and Sel-F was attempted. The parameters screened included: time, equivalents of Sel-F (as well as sequential versus single addition), additives to encourage borate formation (such as fluoride ion sources, and carbonate bases), and solvents. ^{1}H and ^{19}F NMR analysis were performed on both deuterochloroform and deuterium oxide extracts of the crude reaction mixture.

Experimental yields could not be accurately determined because mass balance was never obtained. No phenylboronic acid (**2.66**) remained in the aqueous layer and ^{1}H NMR signals in the

chloroform layer accounted for approximately 40% of **2.66** added. Therefore, attention was focused on optimising the benzene to fluorobenzene ratio. After 55 trials, the best combination obtained was phenylboronic acid (**2.66**) with 1.5 equivalents of Sel-F (added in one portion) in water heated for 2 hours at 110 °C in a sealed tube, yielding a benzene to fluorobenzene ratio of 1: 43 at 34% yield by ^{19}F NMR analysis (Scheme 2.29).

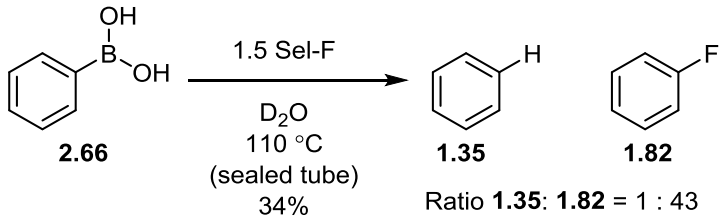

Scheme 2.29 Optimised fluorodeboronation conditions with Sel-F

It is possible that phenylboronic acid (**2.66**) was not a good substrate for fluorodeborylation and better optimisation results could have been obtained with another boronic acid. Since mass balance was never observed, it was reasonable to suspect the low boiling point of fluorobenzene, in combination with the elevated temperatures involved in these reactions, lead to product loss, despite the fact that a 'sealed' microwave vial was employed as the reaction vessel. Concurrent to these studies, the fluorodeborylation of commercially available boronic acids such as 4-boronobenzoic acid **2.67** and dimethylphenylboronic acid **2.70**, as well as the non-aromatic pinacol ester of hexenylboronic acid (**2.71**) were investigated (Scheme 2.30). Fluorodeborylation of **2.67** lead to a mixture of isomeric fluorobenzoic acids consistent with **2.68** and **2.69**. Similarly, fluorodeborylation of **2.70** lead to a mixture of up to 4 fluoroaromatic compounds. In the one alkenyl boronic acid experiment (hydrolysis of the pinacol ester was anticipated for **2.71**), a mixture of geometric isomers **2.72** was detected starting from the *trans*-enriched **2.71**.

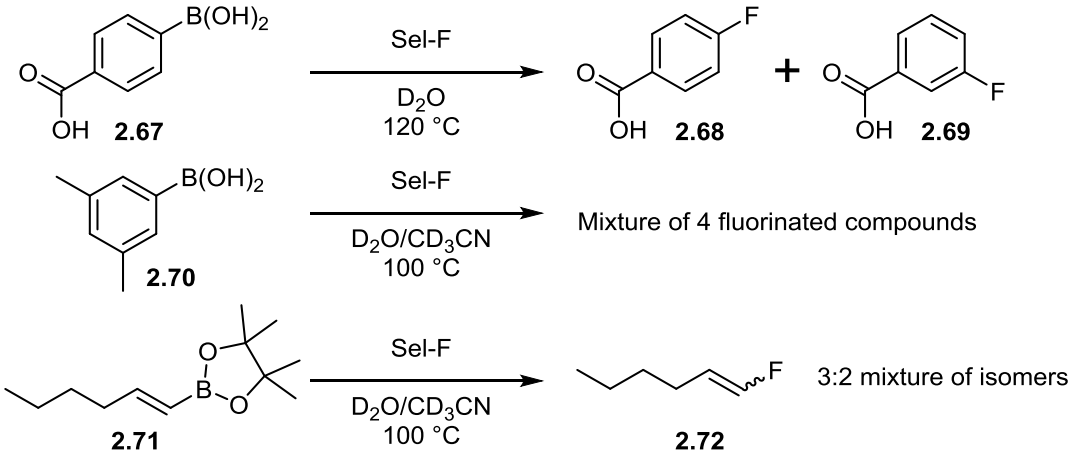

Scheme 2.30. Fluorodeborylation of selected arylboronic acids

At the start of arylboronic acid fluorodeborylation studies, only a cursory scan of the literature was executed. A more diligent exploration revealed that the fluorodeborylation reaction with alkenylboronic acids had already been reported by Petasis and coworkers in 1987,[162] and in 2009, Lemaire and coworkers reported that certain electron-rich arylboronic acids could be fluorinated in anhydrous acetonitrile.[163] I also learned that a colleague in the department (A. Sun) had made the same discovery: that Sel-F reacted with boronic acids and that isomeric aryl fluorides are obtained. In A. Sun's studies on transition-metal mediated cross-coupling reactions, a control experiment in the absence of a metal catalyst revealed the background fluorodeborylation reaction.[164] The studies by Sun employ anhydrous acetonitrile with sodium bicarbonate as an additive to promote boronate formation, thus improving on the fluorodeborylative work of Lemaire in anhydrous acetonitrile with no additives.[164]

Unique to my studies on the fluorodeborylation of arylboronic acids is the role of water. In the fluorodeborylation studies by Petasis and coworkers, after a brief mention of alkenylboronic acids

reacting slowly with Sel-F, they switched to alkenyltrifluoroborates.[162] It is not clear which solvents they investigated with alkenylboronic acids. With alkenyltrifluoroborates in water, they observed that excess Sel-F lead to a subsequent fluoro hydroxylation of the fluoro alkene. In contrast to those studies, my experiments with alkenylboronic acids in water did not yield any detectable amounts of difluoromethyl alcohols. At the time, I did not understand the results of aryl fluorodeborylation and the opportunity to study the fluorination of alkyl radicals by perester thermolysis was presented to me.[c]

There is more to investigate in the fluorodeborylation of arylboronic acids in water. No mechanism for fluorodeborylation was proposed by Lemaire (there has been no follow-up publication and the results described in the paper have yet to be duplicated)[d] and the mechanism of boron-activation by Sun[164] does not adequately explain isomeric formation of vinyl fluorides **2.72**. The fluorodeborylation mechanism postulated by Petasis and coworkers (an addition-elimination pathway via a carbocation intermediate) does not preclude single electron transfer pathways. Chapter 3 will demonstrate that Sel-F is an excellent single electron oxidant and may have effected SET oxidation, in the manner anticipated by $Mn(OAc)_{3,}$ for the generation of aryl radicals from aryl boronic acids. There are also similarities between the thermal reaction of arylboronic acids with Sel-F and the thermal reaction of phenoxyacetic acids with PIFA and NFSI. I will elaborate more on this relationship and reasons why photochemical activation of arylboronic acids may lead to the desired radical fluorination of aryl radicals in Chapter 5.

---

[c] Chronologically speaking, the studies towards arylfluoride formation were performed prior to the work discussed in Chapter 2, section 2.2.
[d] Private communication with G. Sammis.

2.4 Experimental

2.4.1 General experimental

All chemicals were purchased from commercial sources and used as received. Proton nuclear magnetic resonance (^{1}H NMR) spectra were recorded in deuterated solvents using a Bruker AV-400 or AV-300 spectrometer. Fluorine nuclear magnetic resonance (^{19}F NMR) spectra were recorded in deuterated solvents using a Bruker AV-300 spectrometer. Chemical shifts are reported in parts per million (ppm) and are referenced to the centerline of deuterochloroform (7.27 ppm ^{1}H NMR; 77.0 ppm ^{13}C NMR), deuterobenzene (7.16 ppm ^{1}H NMR; 128.4 ppm ^{13}C NMR), acetone-d_6 (2.05 ppm ^{1}H NMR; 29.9 ppm ^{13}C NMR), acetonitrile-d_3 (1.94 ppm ^{1}H NMR; 118.7 ppm ^{13}C NMR).

2.4.2 Experimental procedures related to DFT calculations

Initial structures were obtained from the CambridgeSoft Chem 3D Office program. Geometry optimization was performed using density functional theory (DFT) with the ORCA computational package[127] using the BP86 functional,[124] TZV/P basis set for all the atoms,[125] the split-RI-J approximation,[165] and COSMO dielectric continuum model for solvent effects.[126] Increased integration grids (Grid4) and tight SCF convergence criteria (TightSCF) were also used. Numerical frequency calculations at the same level of theory indicated that the fully optimized geometry was obtained. All figures and diagrams were produced with the Chimera or Mol-Den programs.

2.4.3 Proof-of-concept studies

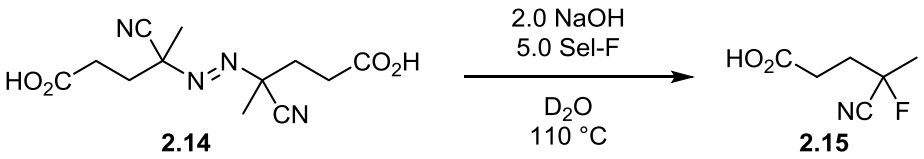

4-cyano-4-fluoropentanoic acid (**2.15**): To an argon filled 0.5-2.5 ml microwave vial was added **2.14** (29 mg, 0.1 mmol), Sel-F (178 mg, 0.5 mmol), NaOH (40 µl, 0.2 mmol, 5.0 M in D_2O), and deuterium oxide (2 ml). The suspension was capped and immersed in a 110 °C oil bath for 1 hour. After cooling to ambient temperature, the crude reaction mixture was poured into Et_2O (30 ml) and extracted with $NaOH_{(aq)}$ (2 x 15 ml). The combined aqueous extracts were acidified with $HCl_{(aq)}$ (10 wt%, 5 ml) and extracted with Et_2O (3 x 10 ml). The combined organic extracts were washed with brine (10 ml), dried over Na_2SO_4, filtered, and concentrated by rotary evaporation to obtain a white solid (13 mg) which was subjected to mass spectrometric analysis.

HRMS-ESI (*m/z*): $[M + Na]^+$ calcd for $C_6H_8NO_2FNa$: 168.0437. Found: 168.0441.

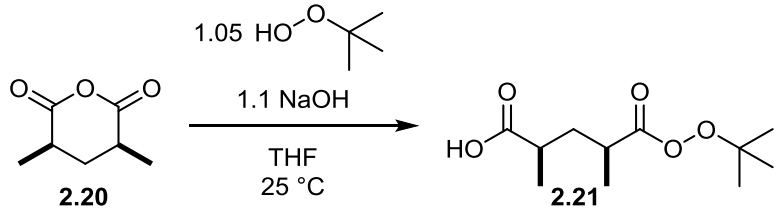

meso-5-(*tert*-butylperoxy)-2,4-dimethyl-5-oxopentanoic acid (**2.21**): To a solution of **2.20** (285 mg, 2.0 mmol, 1.0 equiv.) in tetrahydrofuran (8 ml, 0.25 M) was added sodium hydroxide (88 mg, 2.2 mmol, 1.1 equiv.) then *tert*-butylhydroperoxide (380 µl, 5.5 M solution in decane, 2.1 mmol, 1.05 equiv.). The suspension was stirred at ambient temperature for 21 hours, then quenched with 1.0 M $HCl_{(aq)}$ (3 ml) and poured into Et_2O (50 ml). The organics were washed with 1.0 M $HCl_{(aq)}$ (3 x 10 ml), brine (25 ml),

dried over Na_2SO_4, filtered, and concentrated by rotary evaporation below 45 °C. The crude oil was purified by flash chromatography (2:3 pet. ether: Et_2O, R_f = 0.28, visualization by vanillin stain as a purple spot) and the collected fractions were concentrated by rotary evaporation below 40 °C to obtain **2.21** as a clear colourless oil (280 mg, 61% yield).

^{1}H NMR (400 MHz; C_6D_6): δ = 2.41 (spt, *J* = 6.9 Hz, 2 H), 2.14 (td, *J* = 7.6, 13.8 Hz, 1 H), 1.29 (td, *J* = 6.9, 13.9 Hz, 1 H), 1.15 (s, 9 H), 1.00 - 0.92 (m, 6 H) ppm.

^{13}C NMR (101 MHz; C_6D_6): δ = 182.4, 173.1, 83.2, 37.6, 37.4, 35.5, 26.5, 17.8, 17.1 ppm.

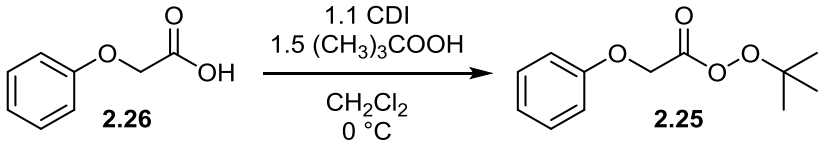

<u>*tert*-butyl 2-phenoxyethaneperoxoate (**2.25**) [employing CDI]:</u> To a solution of carbonyldiimidazole (355 mg, 2.2 mmol, 1.1 equiv.) in dichloromethane (10 ml) was added phenoxyacetic acid (303 mg, 2.0 mmol, 1.0 equiv.) over 1 minute. A steady release for carbon dioxide was observed and the solution remained clear and colourless. After 30 minutes, the reaction was cooled to 0 °C in an ice/water bath and *tert*-butyl hydroperoxide (540 µl, 5.5 M in decane, 3.0 mmol, 1.5 equiv.) was added in one portion. The reaction mixture was stirred in a refrigerator (~ 2 °C) for 15 hours then poured into Et_2O (50 ml). The organics were washed with water (20 ml), 1.0 M $HCl_{(aq)}$ (2 x 20 ml), brine (20 ml), dried over Na_2SO_4, filtered, and concentrated by rotary evaporation below 40 °C. Purification by flash chromatography (8:1 gradient to 7:1 pet. ether: Et_2O, R_f = 0.20 to 0.23, visualization by vanillin stain as a purple spot and UV-light as dark spot) and the collected fractions were concentrated by rotary evaporation below 40 °C to obtain **2.25** as a clear colourless oil (278 mg, 62% yield).

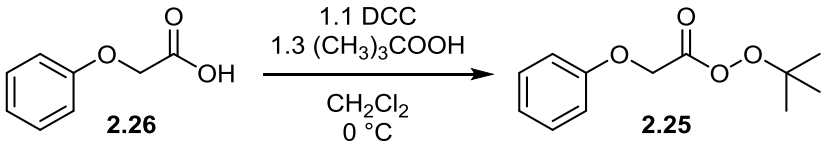

<u>*tert*-butyl 2-phenoxyethaneperoxoate (**2.25**) [employing DCC]:</u> To a solution of phenoxyacetic acid (764 mg, 5.0 mmol, 1.0 equiv.) in dichloromethane (20 ml, 0.25 M) was added *tert*-butyl hydroperoxide (1 ml, 70 wt% in H_2O, 6.5 mmol, 1.3 equiv.) in one portion. The resulting cloudy emulsion was cooled to 0 °C in an ice/water bath. Dicyclohexylcarbodiimide (1.13 g, 5.5 mmol, 1.1 equiv.) was added in two equal portions over 1 hour apart and the emulsion became a white suspension. After stirring an additional 2 hours, the reaction was quenched with Et_2O (40 ml) and placed in a refrigerator (~ 2 °C) for 2 hours to precipitate dicyclohexylurea solids. Solids were removed by suction filtration through a plug of silica and concentrated by rotary evaporation in a cold (15 °C) water bath. Purification by flash chromatography (8:1 pet. ether: Et2O, R_f = 0.20, visualization by vanillin stain as a purple spot and UV-light as dark spot) and the collected fractions were concentrated by rotary evaporation below 40 °C to obtain **2.25** as a clear colourless oil (396 mg). 5 Additional fractions with *tert*-butyl hydroperoxide co-eluting were combined and washed with 3.0 M $NaOH_{(aq)}$ (3x 10 ml), brine (10 ml), dried over Na_2SO_4, filtered, and concentrated by rotary evaporation to obtain and additional 533 mg of **2.25** for a combined yield of 929 mg (83%).

IR (neat): 3065, 3043, 2982, 2936, 1790, 1600, 1495, 1458, 1443, 1391, 1368, 1306, 1232, 1175, 1083, 754, 691 cm^{-1}.

^1H NMR (400MHz; C_6D_6): δ = 7.05 - 6.97 (m, 2 H), 6.81 - 6.73 (m, 3 H), 4.16 (s, 2 H), 1.05 (s, 9 H) ppm.

^{13}C NMR (101MHz; C_6D_6): δ = 166.6, 158.6, 130.1, 122.3, 115.3, 84.0, 64.4, 26.3 ppm.

HRMS-EI (m/z): [M]+ calcd for $C_{12}H_{16}O_4$: 224.10486. Found: 224.10490.

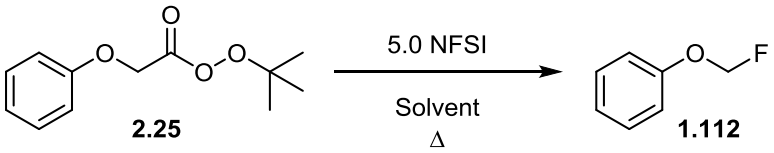

Experimental procedure for Table 2.4 [internal standard = nitromethane]: To a 0.5-2.5 ml microwave vial filled with argon was added perester **2.25** (0.06 mmol, 1.0 equiv.), NFSI (5.0 equiv.), and solvent as appropriate. The vial was then sealed and place into a heated oil bath for the specified time, then immediately removed and placed into an ice/water bath. The crude reaction mixture was transferred to an NMR tube containing nitromethane (0.05 mmol) and subject to ^{1}H NMR analysis.

Experimental procedure for Table 2.4 [internal standard = ethyl trifluoroacetate]:. To a 0.5-2.5 ml microwave vial filled with argon was added perester **2.25** (0.06 mmol, 1.0 equiv.), NFSI (5.0 equiv.), ethyl trifluoroacetate (~1.0 equiv.) and solvent as appropriate. An aliquot was kept for the a t=0 timepoint for 1H NMR analysis. The vial was then sealed and place into a heated oil bath for the specified time, then immediately removed and placed into an ice/water bath. The crude reaction mixture was transferred to an NMR tube and subject to ^{1}H NMR analysis.

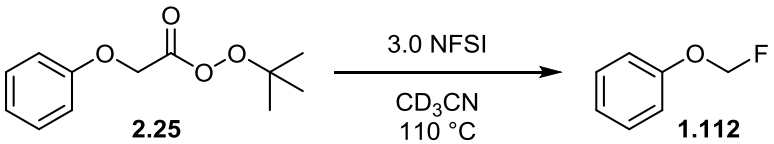

Fluoromethoxybenzene (**1.112**): To an argon filled microwave vial containing **2.25** (112 mg, 0.5 mmol) and NFSI (483 mg, 1.5 mmol, 3.0 equiv) was added acetonitrile (2.5 ml, N_2 sparged) and sealed. The reaction vessel was heated to 110 °C in an oil bath for 10 min then cooled immediately on ice for 5 min. The vial was opened and the crude reaction mixture was transferred to a 50 ml round bottom flask

for kugelrohr distillation. Acetonitrile was removed (20 °C @ 40 torr) then the collection bulb was changed. Phenoxymethyl fluoride (**1.112**) was obtained by kugelrohr distillation (110°C @ 1 torr) as a solution in acetonitrile (26.3 mg, 42% yield, 11.2 M). The compound obtained matched literature characterization data.[264]

^{1}H NMR (300 MHz; $CDCl_3$): δ = 7.35 (t, *J* = 8.0 Hz, 2H), 7.10 (d, *J* = 8.8 Hz, 3H), 5.73 (d, *J* = 54.7 Hz, 2H) ppm.

13C NMR (75 MHz; CD_3CN): δ = 130.8, 124.4, 117.3, 103.3, 100.5 (d, *J* = 139.6 Hz) ppm.

19F NMR (282 MHz; CD_3CN): δ = -151.1 (t, *J* = 54.9 Hz) ppm.

HRMS-EI (*m/z*) [M]+ calcd for C_7H_7OF: 126.04809. Found: 126.04829.

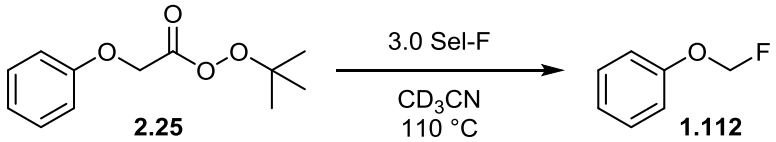

Fluoromethoxybenzene (**1.112**) [NMR experiment with Sel-F]: To an argon filled 0.5-2.5mL microwave vial was added Sel-F (64 mg, 0.18 mmol), **2.25** (600 µl, 0.06 mmol, 1.0 M in CD_3CN), and ethyl trifluoroacetate (as an internal standard). An aliquot was kept for the t=0 timepoint for ^{1}H NMR analysis. The suspension was capped and immersed in a 110 °C oil bath for 6 minutes then immediately cooled on ice. The crude reaction mixture was transferred to an NMR tube and subject to ^{1}H NMR analysis.

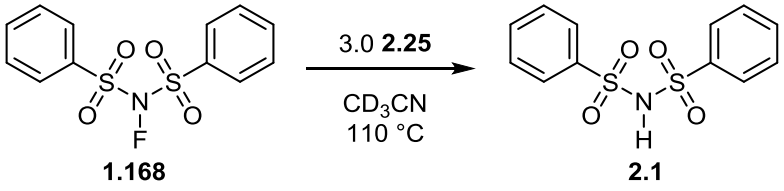

N-(phenylsulfonyl)benzenesulfonamide (**2.1**): To an argon filled microwave vial containing **2.25** (84 mg, 0.375 mmol, 2.5 equiv.) and NFSI (47 mg, 0.15 mmol) was added acetonitrile-d_3 (1.9 mL) and sealed. The reaction vessel was heated to 110 °C for 10 min then cooled immediately on ice for 5 min. An aliquot of the crude reaction mixture was taken for NMR analysis, and subsequently returned to the crude reaction mixture. The solvent was removed by rotary evaporation and purification by flash column chromatography (19:1 EtOAc/MeOH) provided 42 mg of **2.1** (94%) as a yellow-white solid, identical to a commercially obtained sample.

^{1}H NMR (400 MHz; CD_3CN): δ = 7.68 (d, *J* = 7.5 Hz, 4 H), 7.37 (t, *J* = 7.5 Hz, 2 H), 7.26 (t, *J* = 7.7 Hz, 4 H).

^{13}C NMR (75 MHz; CD_3CN): δ = 144.9, 132.3, 129.6, 127.6.

LRMS-ESI (*m/z*): [M+Na]+ calcd for $C_{12}H_{11}NO_4S_2$: 320.01. Found: 320.02.

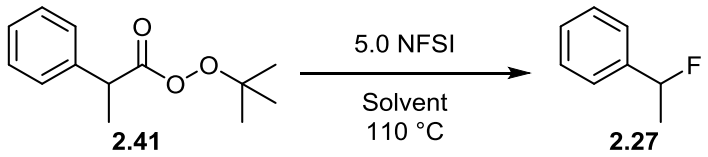

2.41 **2.27**

Experimental procedure for Table 2.5 [internal standard = ethyl trifluoroacetate]:. To a 0.5-2.5 ml microwave vial filled with argon was added perester **2.41** (0.06 mmol, 1.0 equiv.), NFSI (5.0 equiv.), ethyl trifluoroacetate (~1.0 equiv.) and solvent as appropriate. An aliquot was kept for the t=0 timepoint for ^{1}H NMR analysis. The vial was then sealed and place into a heated oil bath for the specified time, then immediately removed and placed into an ice/water bath. The crude reaction mixture was transferred to an NMR tube and subject to ^{1}H NMR analysis.

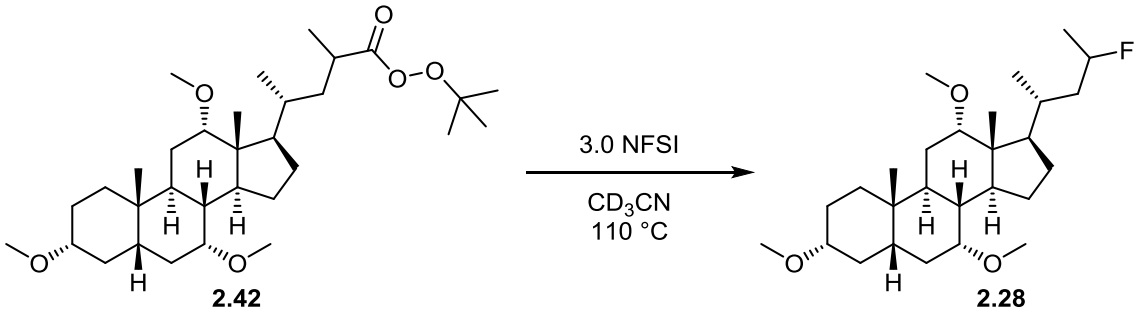

2.42 **2.28**

(3*R*,5*S*,7*R*,8*R*,9*S*,10*S*,12*S*,13*R*,14*S*,17*R*)-17-((2*R*)-4-fluoropentan-2-yl)-3,7,12-trimethoxy-10,13-dimethylhexadecahydro-1*H*cyclopenta[*a*]phenanthrene (**2.28**): To a 500 µl microwave vial was added NFSI (10.0 mg, 0.032 mmol, 3 equiv.) and perester **2.42** (5.0 mg, 0.0093 mmol, 1 equiv.) then sealed, evacuated, and backfilled with N_2. Acetonitrile-d_3 (100 µl) was added and the reaction vessel was placed in an oil bath (maintained at 110 ± 5 °C) such that the solvent line was slightly above the oil line. After 60 min, the reaction vessel was cooled immediately in an ice bath for 3 min. The seal was broken and the crude reaction mixture (diluted with 100 µl dichloromethane) was injected onto an automated flash chromatography loading puck. Purification on a basified biotage SNAP 10 g column (pre-equilibration with 100 ml of a 75 : 25 : 10 solution of hexanes : EtOAc : triethylamine) by gradient flash chromatography (1% EtOAc in hexanes for 1 column volume then 1-12% EtOAc in hexanes over 10 column volumes, then 12% EtOAc in hexanes for 2 column volumes) yielded fluorinated compound **2.28** as a colourless oil after rotary evaporation of fractions at 20 °C (2.2 mg, 54% yield, 1:1 mixture of diastereomers). The compound obtained matched characterization data from M. Rueda-Becerril.[14]

^{1}H NMR (300MHz ,CD_3CN): δ = 4.92 - 4.56 (m, 1 H), 3.41 (td, *J* = 2.7, 5.0 Hz, 1 H), 3.25 (s, 3 H), 3.25 (s, 3 H), 3.21 (s, 3 H), 3.16 (br. d, *J* = 2.5 Hz, 1 H), 3.05 - 2.87 (m, 1 H), 2.02 - 0.82 (m, 28 H), 0.69 (d, *J* = 2.7 Hz, 3 H) ppm.

^{13}C NMR (101 MHz; CD_3CN): δ = 91.2, 90.7, 89.0, 83.3, 81.6, 78.6, 56.5, 56.4, 55.9, 48.6, 48.4, 47.4, 44.8, 44.3, 44.0, 43.1, 40.7, 36.2, 36.0, 33.4, 29.0, 29.0, 28.9, 28.8, 28.7, 28.2, 24.2, 23.5, 23.0, 22.6, 22.4, 21.8, 19.3, 18.6, 13.1, 13.0 ppm.

2.4.4 Experimental procedures for the attempted radical synthesis of arylfluorides

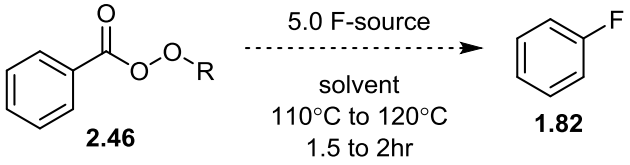

Experimental procedure for reactions reported in Table 2.6: To a 0.5-2.5 ml microwave vial filled with argon was added benzoyl peroxide (1.0 equiv., 75 wt.% wetted with water) or **2.46** (1.0 equiv), electrophilic fluorine source (5.0 equiv.) and solvent as appropriate. The vial was then sealed and place into a heated oil bath or subjected to microwave irradiation for the specified time, then cooled to ambient temperature. For trials run in deuterium oxide, hexafluoroisopropanol or hexafluoroacetone hydrate, the vial was then pierced with a needle for venting as deuterochloroform and deuterium oxide was added to the reaction mixture. All needles were removed and the sealed vial was vigorously agitated for 15 seconds. After phase separation was observed, 0.5 ml sample of the deuterochloroform layer was extracted by syringe from the lower layer for NMR analysis. The deuterium oxide layer could also be analyzed by NMR analysis by careful extraction of a 0.5ml sample from the top layer. For trials run in acetonitrile-d_3, 0.5mL of the crude reaction mixture was filtered through a small plug of cotton prior to NMR analysis.

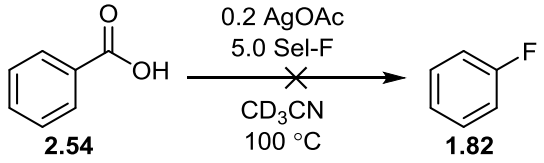

Attempted silver-mediated fluorodecarboxylation of benzoic acid: To a 0.5-2.5 ml microwave vial filled with argon was added benzoic acid (1.0 equiv), Sel-F (5.0 equiv.), silver (I) acetate (0.2 equiv.) and acetonitrile-d_3. The vial was then sealed and place into a 100 °C oil bath for 20 hours. After

cooling the flask to ambient temperature, the vial was opened and 0.5 ml of the crude reaction mixture was filtered through a small plug of cotton, then subject to NMR analysis.

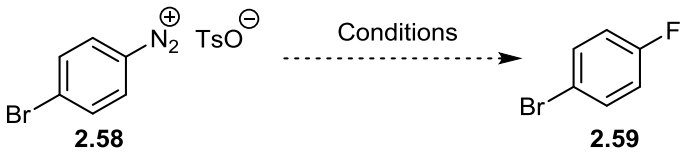

2.58 **2.59**

Experimental procedure for reactions reported in Table 2.7: To a 0.5-2.5 ml microwave vial filled with argon was added diazonium **2.58** (1.0 equiv.), electrophilic fluorine source (3.0 equiv.), amine base (1.0 or 5.0 equiv.), photocatalyst (as appropriate) and solvent as appropriate. The vial was then sealed and place into a heated oil bath or subjected to photochemical irradiation by a broad spectrum sunlamp for the specified time. For trials run in deuterium oxide, the vial was then pierced with a needle for venting as deuterochloroform and deuterium oxide was added to the reaction mixture. All needles were removed and the sealed vial was vigorously agitated for 15 seconds. After phase separation was observed, 0.5 ml sample of the deuterochloroform layer was extracted by syringe from the lower layer for NMR analysis. The deuterium oxide layer could also be analyzed by NMR analysis by careful extraction of a 0.5ml sample from the top layer. For trials run in acetone-d_6 or DMSO-d_6, a homogenous solution was obtained and a 0.5 ml extract was taken for NMR analysis.

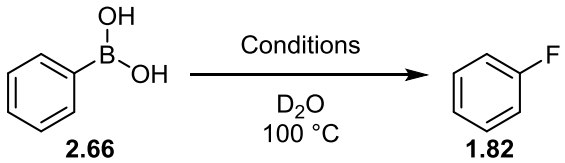

2.66 **1.82**

Experimental procedure for reactions reported in Table 2.8 and Scheme 2.30: To a 0.5-2.5 ml microwave vial filled with argon was added boronic acid or boronic acid pinacol ester (1.0 equiv.), electrophilic fluorine source (as appropriate.), manganese (III) acetate (3.0 equiv.), and solvent as

appropriate. The vial was then sealed and place into a heated oil bath for 2 hours, then cooled to ambient temperatures. For trials run in deuterium oxide, the vial was then pierced with a needle for venting as deuterochloroform and deuterium oxide was added to the reaction mixture. All needles were removed and the sealed vial was vigorously agitated for 15 seconds. The vial was then opened and the reaction mixture was filtered through a plug of celite to remove solids. A 0.5 ml sample of the deuterochloroform layer (lower layer) was extracted by syringe for NMR analysis. The deuterium oxide layer was analyzed by extraction of a 0.5 ml sample from the top layer.

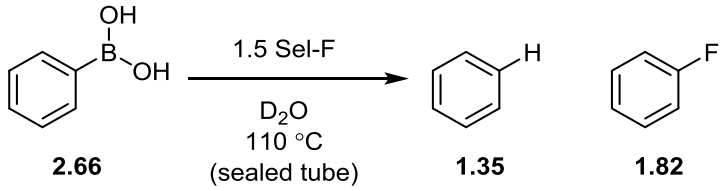

Experimental procedure for optimisation reactions in Scheme 2.29: To a 0.5-2.5 ml microwave vial filled with argon was added phenylboronic acid (1.0 equiv.), Sel-F (as appropriate.), additives as appropriate, and deuterium oxide. The vial was then sealed and place into a heated oil bath or subject to microwave irradiation for the requisite amount of time. After the reaction mixture had cooled to ambient temperature, the vial was then pierced with a needle for venting as deuterochloroform and deuterium oxide was added to the reaction mixture. All needles were removed and the sealed vial was vigorously agitated for 15 seconds. The vial was then opened and the reaction mixture was filtered through a plug of celite to remove solids. A 0.5 ml sample of the deuterochloroform layer was extracted by syringe and combined with 0.1 ml trifluoroacetic acid solution (0.125 M in $CDCl_3$) as an internal standard for NMR analysis. The deuterium oxide layer was analyzed by extraction of a 0.5 ml sample from the top layer.

Chapter 3: Photodecarboxylative fluorination of aryl and aryloxy acetic acids

Aryl fluoromethyl ethers are increasingly pervasive in the agrochemical and pharmaceutical industries as incorporation of fluorinated ethers into bioactive small-molecules leads to many desirable properties. Having demonstrated that radical fluorodecarboxylation of perester **2.25** could deliver the monofluoromethyl ether **1.112**, an extension of this methodology to difluoro- and trifluoromethyl ether synthesis seemed plausible. However, fluorodecarboxylation synthesis of aryl difluoromethyl ethers via *tert*-butyl perester thermolysis proved untenable in Scheme 2.22. By extension, *tert*-butyl perester mediated synthesis of aryl trifluoromethyl ethers would be impossible.

A critical analysis of the radical fluorination method presented in Chapter 2 shows three major deficiencies: (1) the *tert*-butyl perester must be synthesized from the parent carboxylic acid or another activated carboxylic acid derivative, (2) peresters that decarboxylate to highly stabilized radicals (such as tertiary radicals) are difficult to synthesize as decomposition can be observed during purification and isolation processes, and (3) radical decomposition of the peresters requires elevated temperatures that may lead to side-reactions. The failed synthesis of difluoromethyl ether **2.40** in Scheme 2.22 is likely related to the elevated temperatures required for homolysis of the O-O bond. Thus, I sought for alternative methods to promote phenoxymethyl radical formation.

Before presenting my research into the synthesis of aryl mono-, di-, and tri-fluoromethyl ethers through radical fluorodecarboxylation methods, a selection of the most practical methods to synthesize this class of ethers will be reviewed.

3.1 Non-radical methods for the synthesis of aryl fluoromethyl ethers

Comprehensive reviews on the field of fluoromethyl ether synthesis can be found in references 4a, 5a, 10g and 166. Aside from my work, there are only two examples of radical monofluoromethyl ether synthesis[83,103] and no examples of radical difluoromethyl ether synthesis. The radical mediated synthesis of aryl trifluoromethyl ethers will be covered in this section.

The synthesis of monofluoromethyl ethers (**3.3**) is readily accomplished by electrophilic fluoromethylation of phenolate anions (**3.2**) generated in polar solvents from inorganic bases (Scheme 3.1).[10g] Recently, Prakash has developed the air and moisture stable *S*-(monofluoromethyl) diarylsulfonium salt which has distinct synthetic advantages over the gaseous fluoromethylhalide alternatives.[167]

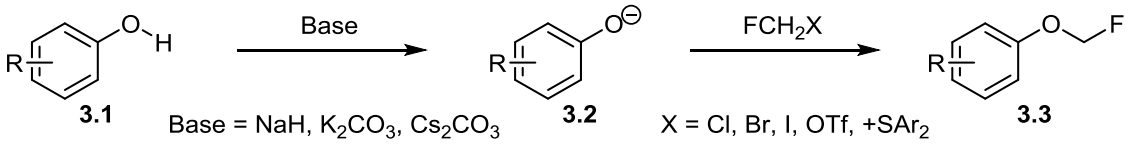

Scheme 3.1. Monofluoromethylation of phenols with electrophilic reagents

The most important application of monofluoromethyl aryl ethers (**3.3**) is in Positron Emission Tomography (PET) imaging. Methods have been developed for the generation of [^{18}F] fluoromethylbromide and [^{18}F] fluoromethyliodide with sufficiently high specific activity to synthesize the monofluoromethyl aryl ether containing PET tracers.[168] Electrophilic fluoromethylation of the corresponding phenol under alkaline conditions with radioactive fluoromethylhalide can be automated.

A selection of monofluoromethyl aryl ether PET tracers, used for *in-vivo* imaging, is presented in Figure 3.1.[169] A variety of enzyme targets exist and binding affinity by PET tracers are very high.

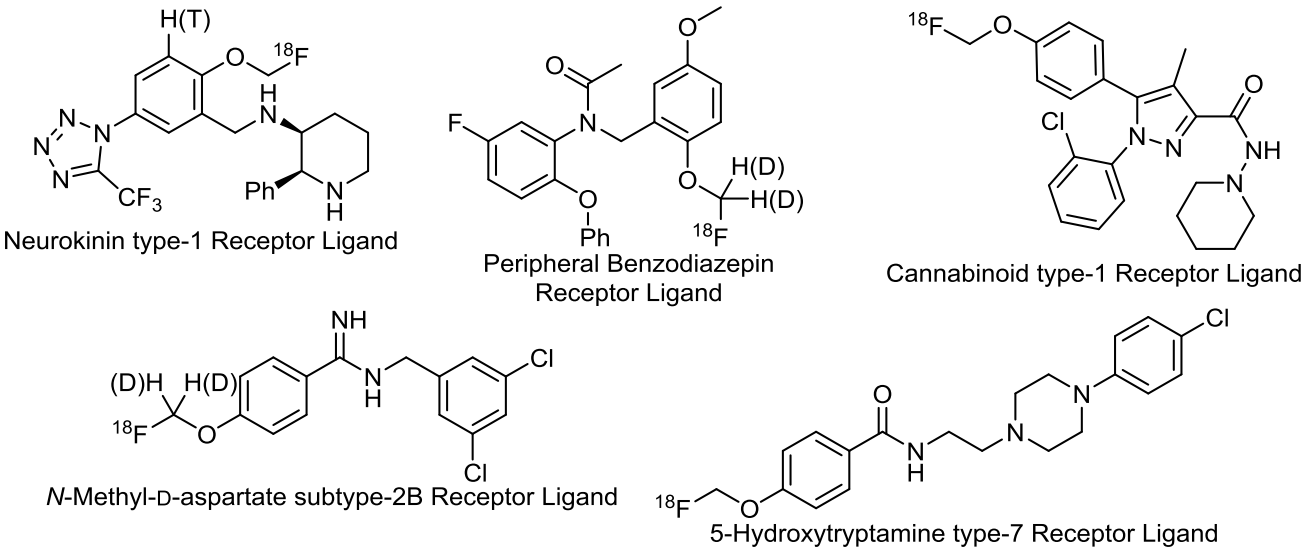

Figure 3.1. Selection of monofluoromethoxyarene containing PET radiotracers

The two most commonly employed synthesis of difluoromethyl ethers on the industrial scale is accomplished by insertion of difluoromethyl carbene (**3.5**) into the phenolic O-H bond (Figure 3.2),[170,171] or by the related alkylation with an alkyl chlorodifluoroacetate (or bromodifluoroacetate) followed by hydrolytic decarboxylation of ester **3.6** (Scheme 3.2).[172] Early work on difluoromethyl aryl ether synthesis employed chlorodifluoromethane (Freon R-22),[170] which is an ozone depleting substance. Current work with difluoromethylcarbene generation focuses on non-ozone depleting sources of carbene precursors, a variety of which are shown in Figure 3.2. While larger scale carbene insertion reactions are possible,[171b] many process chemistry applications rely on the alkylation and decarboxylation sequence depicted in Scheme 3.2.[172]

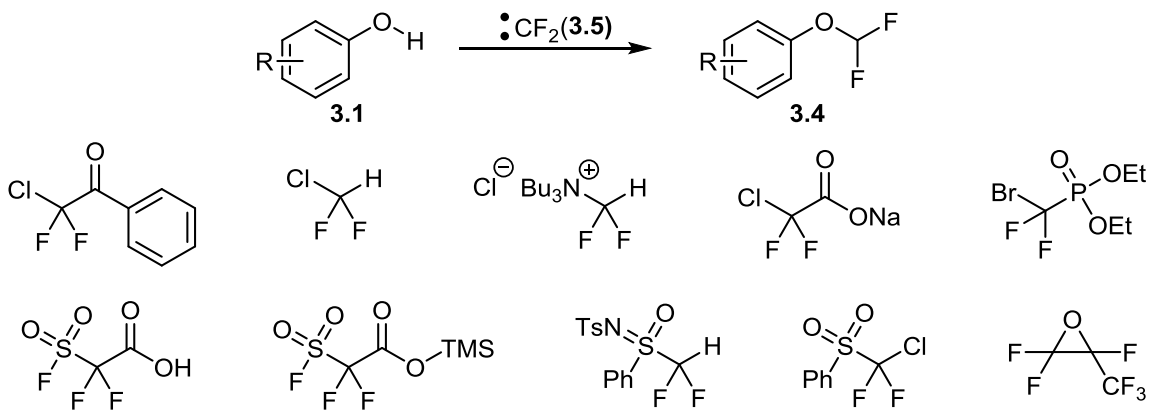

Figure 3.2. Selection of difluoromethylcarbene precursors

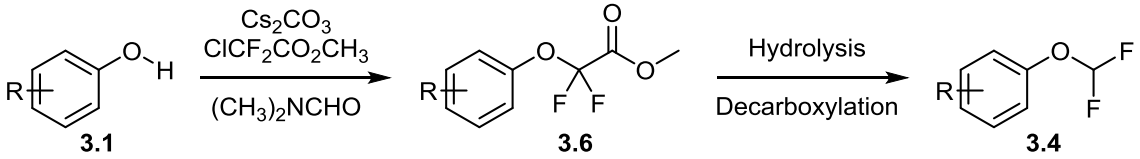

Scheme 3.2. Alkylation and decarboxylation for the synthesis of difluoromethyl aryl ethers

An interesting, although less practical, difluoromethyl aryl ether (**3.4**) synthesis is through the oxidative rearrangement of benzaldehydes (**3.7**) (Scheme 3.3). Oxidation of the carbonyl oxygen (**3.8**) in the presence of fluoride generates fluoro acetal **3.9** which can rearrange to carbocation **3.10**. Trapping by a second equivalent of fluoride delivers the difluoromethoxylation product (**3.4**). Both xenon difluoride[173] and hypervalent bromine **3.11**[174] have been used for this transformation and the isolated yields are moderate to good.

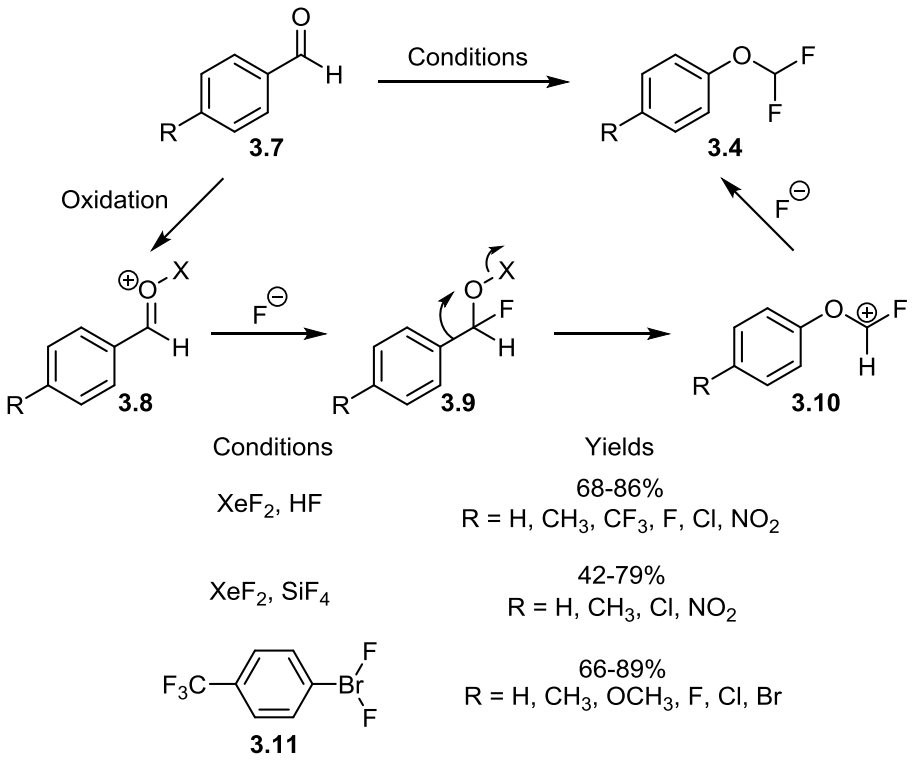

Scheme 3.3. Oxidative rearrangement of benzaldehydes to difluoromethyl ethers

The synthesis of aryl trifluoromethyl ethers (**3.13**) is typically accomplished by nucleophilic displacement of activated anisole derivatives with a source of fluoride.[166b] Early work involved high temperatures and harsh reagent combinations such as antimony trifluoride with antimony pentachloride. A breakthrough was found by Hiyama with the action of dibromohydantoin on phenoxy xanthate esters (**3.12**) and HF/pyridine as the source of fluoride (Scheme 3.4).[175] Sequential sulphur oxidation and displacement with fluoride (**3.14** to **3.15**, repeat x 2) delivers the trifluoromethylated compound **3.13** under relatively mild conditions. Recently, Ritter has disclosed a silver-mediated cross-coupling methodology amenable to late-state conversion of stannanes and boronic acids **3.17** to trifluoromethoxy ethers (**3.13**), which relies on the trifluoromethoxy salt **3.18** (Scheme 3.5).[176]

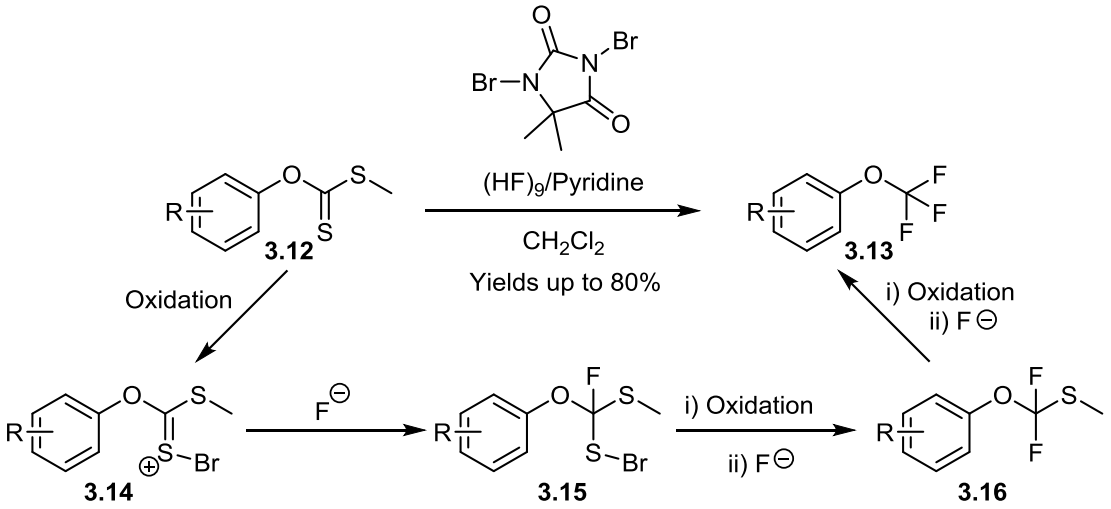

Scheme 3.4. Oxidative transformation of aryloxy xanthates to aryl trifluoromethyl ethers

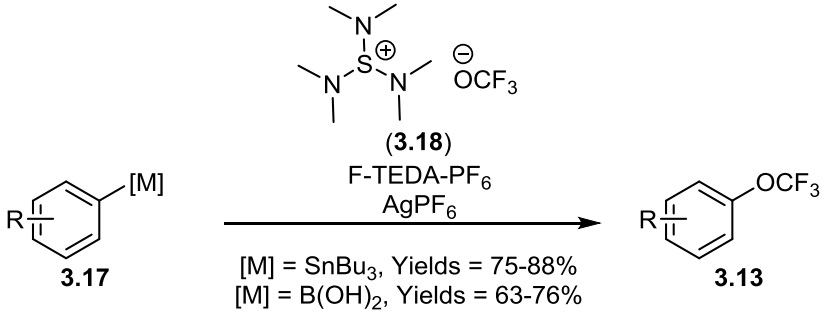

Scheme 3.5. Cross-coupling approach to aryl trifluoromethyl ethers

A radical method for aryl trifluoromethyl ether (**3.13**) synthesis has been recently reported (Scheme 3.6). Trifluoromethoxylation has been investigated by the addition trifluoromethoxyl radical (**1.72**), generated from trifluoromethyl hypofluorite (**1.2**), into arenes (Scheme 3.6).[177] Exploiting the excellent radical fluorinating power of trifluoromethyl hypofluorite, increased concentrations of the trifluoromethoxyl radical (**1.72**) can be obtained with catalytic amounts of perfluoro-enol ether **3.20** (Scheme 3.6, lower section). Addition of trifluoromethoxyl (**1.72**) to the arene followed by oxidation to **3.24** and rearomatization affords the desired aryl trifluoromethyl ether (**3.13**). While the selectivity for

trifluoromethoxy arene is only slightly higher than aryl fluoride formation, this reaction shows promise as electron deficient arenes demonstrate higher selectivity for trifluoromethoxylation.

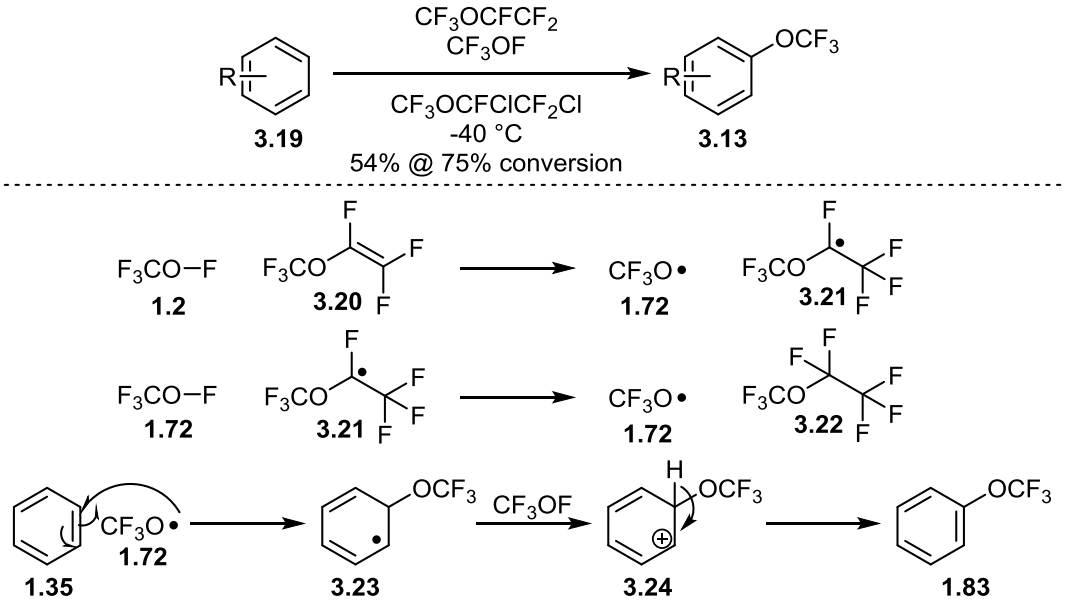

Scheme 3.6. Addition of trifluoromethoxyl to arenes

3.2 Radical generation with hypervalent iodine reagents

3.2.1 Literature precedence for radical decarboxylation initiated by hypervalent iodine

The transformation of an alkyl carboxylic acid to the corresponding decarboxylated alkyl halide is known as the Hunsdieker reaction (Scheme 3.7).[38] Conversion of the carboxylic acid to the metal salt (typically silver, **3.25**), followed by treatment with halogen (bromine is best) forms a hypohalite ester **3.26**. Homolytic fragmentation of the oxygen-halogen bond yields carboxyl radical **1.201**, which rapidly decarboxylates to alkyl radical **1.183**. The corresponding alkyl halide is furnished by trapping with a source of radical halide such as the hypohalite or the diatomic halogen.

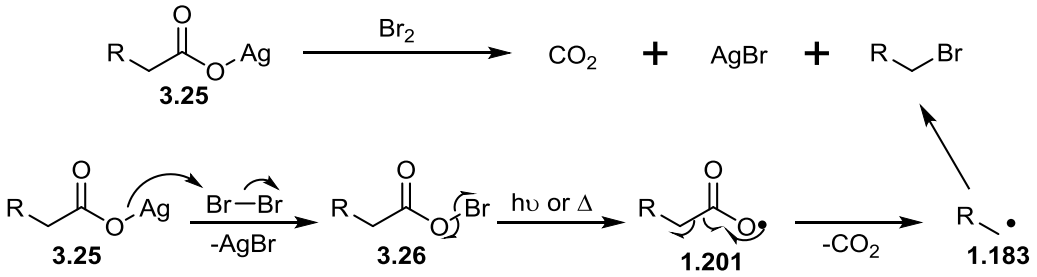

Scheme 3.7. Mechanism of the Hunsdiecker reaction

The fluorodecarboxylation reaction discussed in Chapter 2 is mechanistically similar to the Hunsdieker reaction with difference that the carbonyloxyl radical precursor is a perester and not a hypohalite ester. To address the problems outlined at the beginning of this chapter, a Hunsdieker-like reaction was a potential solution as alkoxyl radicals can be generated at lower temperatures directly from the carboxylic acids (activation *in-situ*). As discussed in Chapter 1, hypofluorite esters **1.55** are carbonyloxyl radical precursors and can be used in a Hunsdieker-like fluorodecarboxylation. However, we were not interested in working with elemental fluorine as it is a strong oxidant and the aryloxyacetic acids are relatively electron rich.

Homolysis of iodine (III) derivatives was suggested[e] as an alternative to *tert*-butyl perester thermolysis.[178] Hypervalent iodine reagents such as diacetoxyiodobenzene (DIB, **3.27**) and phenyliododitrifluoroacetate (PIFA, **3.28**) can be used to effect a Hunsdieker-like transformation (Scheme 3.8). Suarez and coworkers found that treatment of alkyl carboxylic acids such as steroidal derivative **3.29** with DIB and iodine could undergo decarboxylative iodination to **3.31** in high yields via photolysis of hypoiodite intermediate **3.30** (eqn 3.1).[179] Togo and coworkers found that the hypervalent iodine compounds **3.32** formed by ligand exchange from DIB with alkyl carboxylic acids

[e] Private communication with Prof. M. Cuifolini.

could itself be radically decomposed by UV-light (mercury lamp) to generate decarboxylated alkyl radicals.[180] In the presence of a radical acceptor (**3.33**) and a suitable source of radical hydride (**3.34**), the decarboxylated radical addition products **3.35** could be obtained in moderate to excellent yields from a variety of alkyl carboxylic acids and Michael acceptors (eqn. 3.2).[180] Sutherland, and Vederas, in attempts to recreate the Togo conditions,[180] found that thermolysis of the ligand exchanged hypervalent iodine compound **3.36** would also generate decarboxylated alkyl radicals (eqn. 3.3).[181] Thus, we were hopeful that the ligand exchanged hypervalent iodine compound formed *in-situ* (**3.39**) would decompose to the desired alkyl radical and be fluorinated by NFSI or Sel-F.

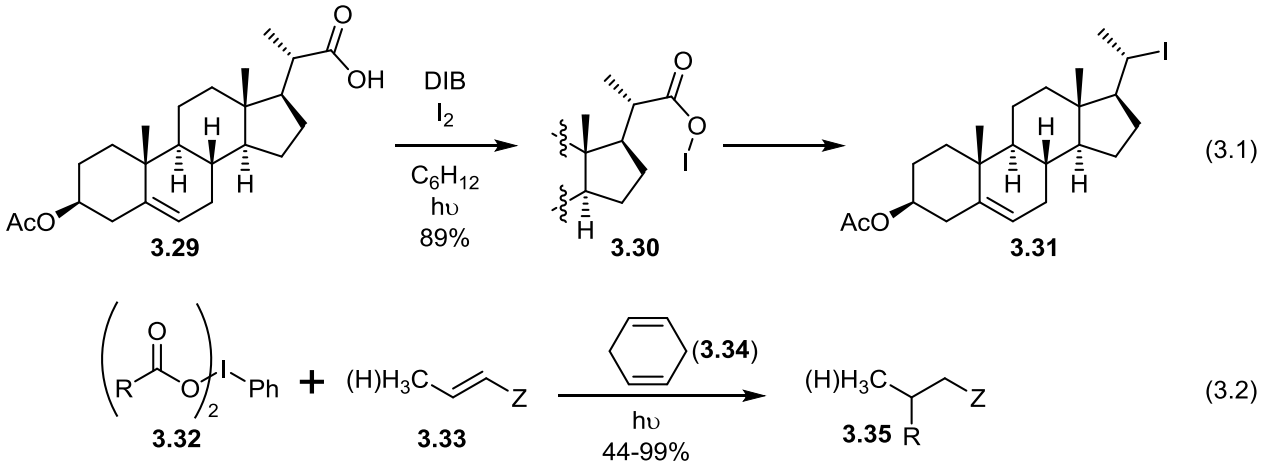

Scheme 3.8. Hunsdieker-like reactions employing hypervalent iodine

3.2.2 Synthesis of aryl monofluoromethyl and difluoromethyl ethers

Investigations employing hypervalent iodine commenced with the simultaneous screen of both DIB and PIFA with phenoxyacetic acid (**2.26**) or phenylacetic acid (**3.40a**) in four thermal experiments (Scheme 3.9). DIB and PIFA were chosen as the starting hypervalent iodine (III) reagents because they were the two most commonly employed commercial sources of iodine (III) and both could access the phenyliodo intermediate **3.3** in eqn. 3.4. Phenoxyacetic acid (**2.26**) and phenylacetic acid (**3.40a**) were selected as both carboxylic acids could generate stabilized radicals upon decarboxylation. One of the four exploratory trials yielded a positive result. Immersion of a sealed microwave vial containing a deuterobenzene solution of PIFA, NFSI, and phenoxyacetic acid, into a 110 °C oil bath for 2 hours yielded 28% of the desired phenyl fluoromethyl ether **1.112**.

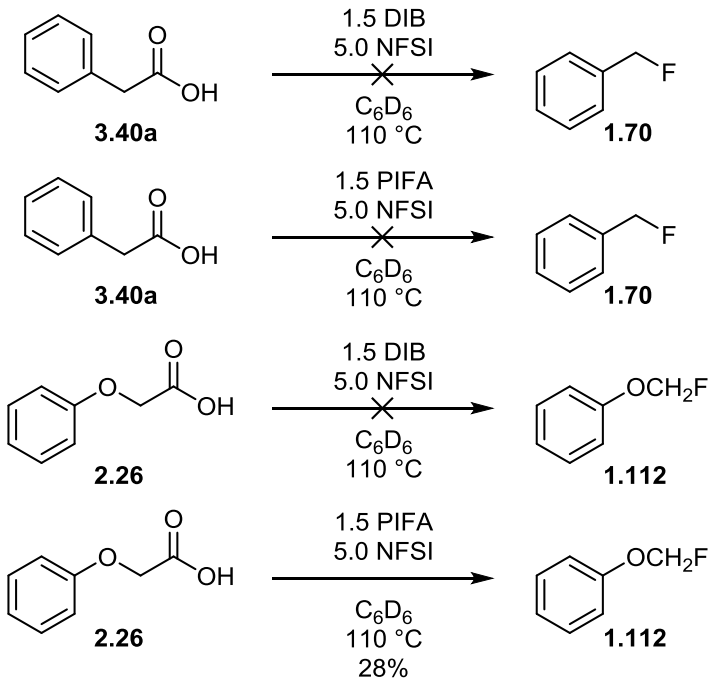

Scheme 3.9. Thermal investigations into fluorodecarboxylation with DIB and PIFA

Attempts to optimise the thermal reaction did not lead to significant improvements in yield; therefore, photochemical stimulation of the reaction was investigated. Based on the mechanism of photodecarboxylation outlined in Scheme 3.10, the I-O bond of iodine (III) intermediate **3.41** could be homolytically cleaved by light. Two acetate ligands on phenyliodobenzene (III) could be exchanged for phenoxyacetate ligands to access intermediate **3.41**. The absorption maximum of intermediate iodine (III) species **3.41** (containing 3 phenyl chromophores) might experience a bathochromic shift and allow absorption of light in the 350 nm region. The subsequent I-O bond cleavage would generate two phenoxymethylcarboxyl radicals (**2.32**), which intercept the radical fluorodecarboxylation pathway established with *tert*-butyl peresters in the previous chapter.

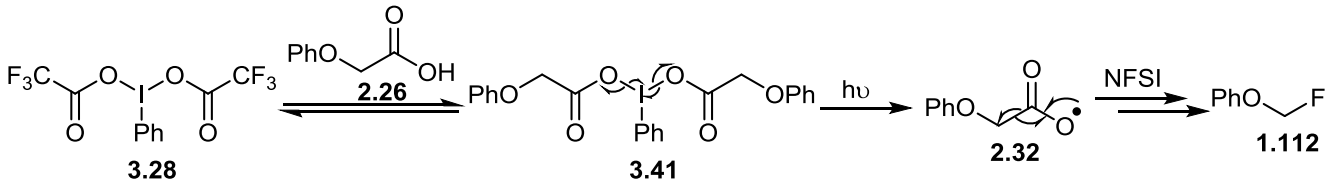

Scheme 3.10. Proposed mechanism for photofluorodecarboxylation with PIFA

Exploratory reactions into photochemically stimulated decarboxylative fluorination with PIFA are summarized in Table 3.1. Photochemical treatment of benzene solutions containing PIFA (1.5 equiv.), NFSI (5.0 equiv.) and phenoxyacetic acid (**2.26**) with 350 nm light in a photoreactor provided 44% yield of fluoromethoxybenzene **1.112** (entry 1). A commercially available broad spectrum sunlamp (used for indoor tanning applications) could be used in lieu of a specialized photochemical setup (entries 2, 6). According to Scheme 3.10, a minimum stoichiometry of 0.5 equivalents of hypervalent iodine reagent would be necessary to access intermediate **3.41**. Excess PIFA could be detrimental to the fluorination step as phenoxymethyl may be oxidized to **2.29** before NFSI can affect

fluorine transfer. Decreasing the amount of PIFA (entries 3 to 5) lead to increased yields of **1.112**, and decreasing the amount of NFSI (entries 7, 8) lead to decreased yields of **1.112**. With the best conditions (PIFA, NFSI and 350 nm light in benzene), fluoromethoxybenzene (**1.112**) could be obtained in 57% yield (entry 5), which is similar to the yields obtained by thermolysis of perester **2.25** in Chapter 2.

Table 3.1.Photodecarboxylative fluorination with PIFA: Exploratory screening

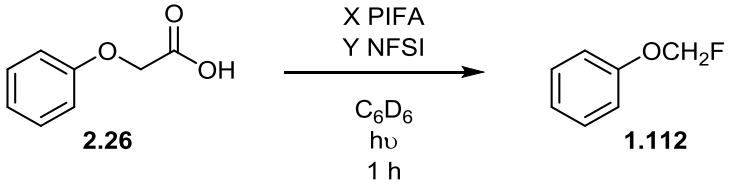

2.26 **1.112**

entry[a]	PIFA (X equiv.)	NFSI (Y equiv.)	light source	yield (%)[b]
1	1.5	5.0	350 nm	44[c]
2	1.5	5.0	Sunlamp	45
3	1.0	5.0	350 nm	55
4	0.75	5.0	350 nm	55
5	0.5	5.0	350 nm	57
6	0.5	5.0	Sunlamp	54
7	0.5	3.0	350 nm	49
8	0.5	1.5	350 nm	26

[a]Reaction conditions: PIFA (as indicated), NFSI (as indicated), **2.26** (1.0 equiv, 0.05 mmol) at 0.1 M in deuterobenzene, irradiated for 1 h with light source as indicated. [b]The yields were obtained by ^{1}H NMR spectroscopy using ethyl trifluoracetate as an internal standard. [c] The yields were obtained by ^{1}H NMR spectroscopy using nitromethane as an internal standard.

During the exploratory reactions detailed above, DIB was also found to be a suitable alternative for PIFA in the iodine (III)-mediated photodecarboxylative fluorination of 2-aryloxy acetic acids with NFSI. DIB has multiple advantages over PIFA: it is lower in molecular weight, it is a less-expensive reagent, and it possesses acetate ligands which can be monitored by ^{1}H NMR spectroscopy. When permissible, DIB was the reagent of choice for the photochemical reactions.

A solvent screen was performed next to investigate the scope of this reaction (Table 3.2). Non-polar solvents were suitable for this DIB-mediated process (entries 1 to 4) while polar solvents inhibited the fluorodecarboxylation (entries 5, 6). It is unclear why such solvent effects are observed for the DIB-mediated photochemical reaction although the results could be duplicated.

Table 3.2. Photodecarboxylative fluorination with DIB: Solvent screen.

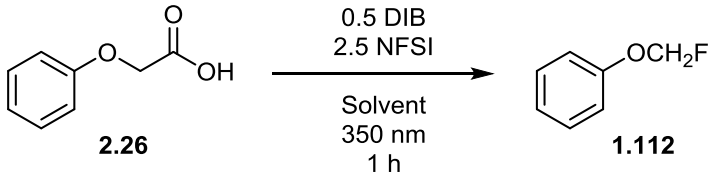

2.26 **1.112**

entry[a]	solvent	**1.112** chemical shift	yield[b]	conversion[c]
1	C_6D_6	5.14 ppm	40	71
2	$C_6D_5CD_3$	5.15 ppm	29	54
3	CD_2Cl_2	5.73 ppm	42	72
4	$CDCl_3$	5.73 ppm	32	66
5	CD_3CN	5.76 ppm[d]	0	6
6	$(CD_3)_2CO$	5.82 ppm[d]	0	0

[a]Reaction conditions: DIB (0.5 equiv), NFSI (2.5 equiv), **2.26** (1.0 equiv, 0.06 mmol) at 0.1 M in deuterated solvent (as indicated), irradiated at 350 nm for 60 min. [b]The yields were obtained by ^{1}H NMR spectroscopy using ethyl trifluoracetate as an internal standard. [c]The conversions were obtained by ^{1}H NMR spectroscopy using ethyl trifluoracetate as an internal standard. [d]Chemical shifts in acetone and acetonitrile were obtained from PDC-F of **2.26** with NFSI and thermal decomposition of **2.25** in the presence of NFSI.

Having determined that dichloromethane was also a suitable solvent for hypervalent iodine mediated fluorodecarboxylation; optimisation of PDC-F was investigated in the chlorinated solvent. The parameters screened included the amount, and type, of iodine reagent needed in dichloromethane with aryloxyacetic acid substrate **3.42** (Table 3.3). Unfortunately, fluoroether **3.43** yields in dichloromethane (entries 4 to 6, 10 to 12) were lower than fluoroether **3.43** yields benzene (entries 1 to 3, 7 to 9). The yields of fluoroether product **3.43** decreased as more hypervalent iodine reagent was added further supporting the hypothesis that excess iodine (III) would oxidize the intermediary radical

and reduce the yields of fluorination product. As a final observation, DIB (entries 7 to 12) provided superior yields to PIFA (entries 1 to 6) for this photochemical transformation.

Table 3.3.PDC-F with DIB and PIFA: Equivalents of I (III) in C_6D_6 and CD_2Cl_2

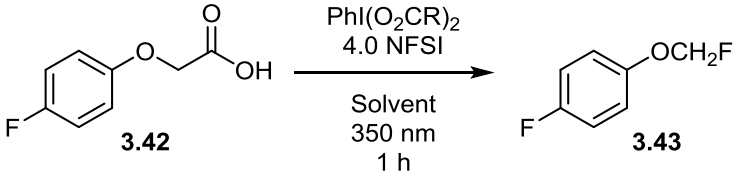

3.42 **3.43**

entry[a]	R	equivalents of I (III)	solvent	yield[b]
1	CF_3	0.5	C_6D_6	49[c]
2	CF_3	0.75	C_6D_6	38
3	CF_3	1.0	C_6D_6	60
4	CF_3	0.5	CD_2Cl_2	37
5	CF_3	0.75	CD_2Cl_2	27
6	CF_3	1.0	CD_2Cl_2	14
7	CH_3	0.5	C_6D_6	69
8	CH_3	0.75	C_6D_6	63
9	CH_3	1.0	C_6D_6	56
10	CH_3	0.5	CD_2Cl_2	51
11	CH_3	0.75	CD_2Cl_2	45
12	CH_3	1.0	CD_2Cl_2	39

[a]Reaction conditions: DIB or PIFA (as indicated), NFSI (4.0 equiv), **3.42** (1.0 equiv, 0.1 mmol) at 0.1 M in deuterated solvent (as indicated), irradiated at 350 nm for 1 h. [b]The yields were obtained by ^{1}H NMR spectroscopy using ethyl trifluoracetate as an internal standard. [c]Average yield of 2 trials.

In the exploratory reactions detailed in Table 3.1, both sunlamp light and 350 nm lamp light were tested for fluorodecarboxylation. Further investigation revealed that UV light emitted from a sunlamp, 300 nm lamps or 350 nm lamps inside a photoreactor were all equally suitable for DIB-mediated fluorodecarboxylation. The only stipulation was that reactions carried out with a sunlamp required the reaction vessel to be an NMR tube. At this point, the working conditions for the iodine

(III)-mediated fluorodecarboxylation reaction was aryloxyacetic acid (1.0 equiv.), DIB (0.5 equiv.) in benzene irradiated for 1 h under 300 nm, 350 nm, or sunlamp light.

Investigations into the DIB-mediated fluorodecarboxylation reaction for the synthesis of mono-fluoromethoxy arenes are summarized in Scheme 3.11. As work was still mostly exploratory, I was primarily interested in ^{1}H and ^{19}F NMR spectroscopic detection of the fluoromethoxy moiety and yields were not obtained. Once the characteristic doublet was obtained after Fourier-transform of the free induction decay obtained by a normal ^{1}H pulse sequence, the ^{1}H $\{^{19}F\}$ pulse sequence was executed to test if the doublet coalesced. *para*-Substituted phenoxyacetic acids (**2.26**, **3.43**, **3.45**, **3.46**) showed clean conversion to the corresponding fluoromethyl ether. Aryloxy acid substrates **3.48**, and **3.49** indicated the presence of a fluorodecarboxylation product, but also the presence of other unidentifiable fluorinated products. 2-Naphthyloxyacetic acid (**3.47**) displayed poor solubility in benzene; nevertheless, fluorodecarboxylation product 2-fluoromethoxynaphthalene was detected and no signals corresponding to ring-fluorinated products were observed.

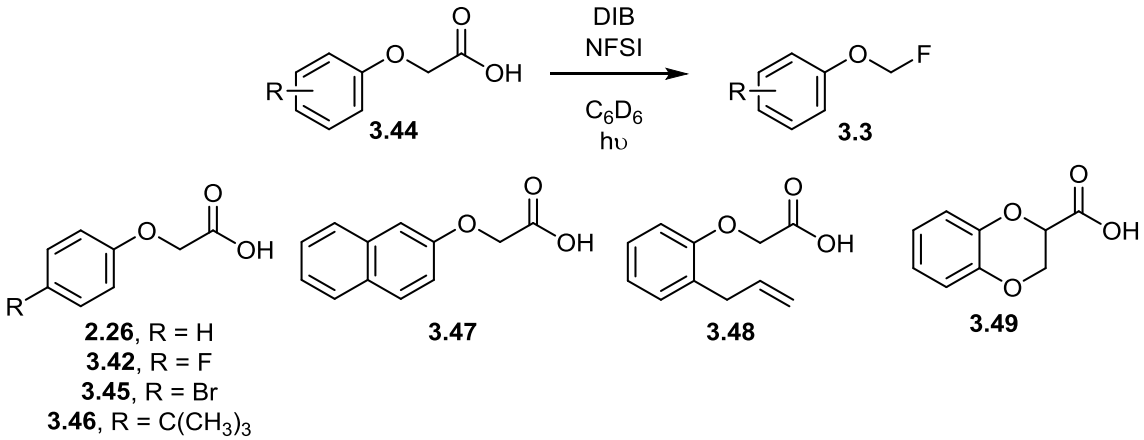

Scheme 3.11. Successful substrates for DIB-mediated fluorodecarboxylation

Having investigated the use of iodine (III) for the synthesis of a variety of aryl monofluoromethyl ethers (**3.3**), attention was given to aryl difluoromethyl ethers (**3.4**) synthesis. My investigations began with the synthesis of the α-fluoro phenoxyacetic acids (**3.51**, Scheme 3.12). S_N2 displacement of bromide from ethyl fluorobromoacetate by the potassium aryloxide salt of **3.1**, followed by saponification of α-fluoro ester **3.50**, delivered the required α-fluoro acids (**3.52-3.55**) in a facile two-step procedure.

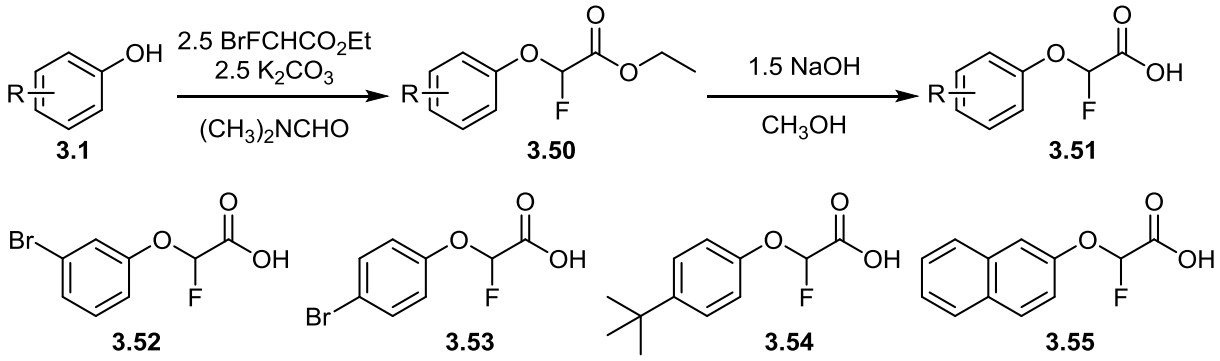

Scheme 3.12. Synthesis of alpha-fluoro phenoxyacetic acids

4-Bromophenoxy acid **3.53** was chosen as the optimisation substrate for difluoromethoxyarene synthesis with PIFA as the iodine (III) source (Table 3.4). PIFA was employed in place of DIB because **3.53** was anticipated to be a better I (III) ligand than trifluoromethylacetate whereas a reverse argument may be true with acetate. Conditions similar to those for monofluoromethyl ether synthesis (entry 1) provided small amounts of fluorination product **2.40** as determined by ^1H and $^1H\{^{19}F\}$ NMR analysis. Increasing the stoichiometry of PIFA (entries 2 to 6) lead to increases in the yield of difluoromethoxy ether **2.40** with a highest observed yield of 48% with 2.0 equivalents (entry 4). With 3 equivalents of PIFA, all of the starting material is consumed but the yield of fluorination product does not increase (entry 6).

Interesting observations were found when the equivilants of NFSI were changed (entries 7 to 10). The ratio of starting material **3.53** to fluorination product **2.40** was monitored because the 'control' experiment with no NFSI added (entry 10) was anticipated to also function as a t=0 entry. Having more NFSI did not significantly change the **3.53**: **2.40** ratio (entries 7, 8); however, NFSI was unnecessary for decarboxylative fluorination (entry 10)! Difluoro ether **2.40** could be isolated as a mixture with iodobenzene (^{1}H and ^{1}H{^{19}F} NMR, $M^{\bullet+}$ with characteristic bromine isotope ratio observed). When the reaction was run with 3 equivalents of PIFA in the absence of NFSI, aryl difluoromethyl ether **2.40** was observed in 15% NMR yield (entry 11).

Table 3.4. PIFA-mediated difluoromethyl ether synthesis

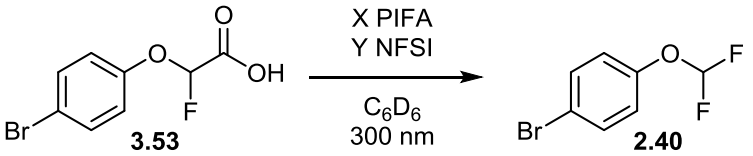

3.53 **2.40**

entry[a]	PIFA (X equiv.)	NFSI (Y equiv.)	Ratio **3.53**: **2.40**	Yield of **2.40** (%)	Conv. of **3.53** (%)
1	0.5	3.0	1 : 0.2	no data	no data
2	1.0	3.0	1 : 0.7	29	60
3	1.5	3.0	1 : 2.0	43	88
4	2.0	3.0	1 : 4.7	48	90
5	2.5	3.0	1 : 9.6	47	95
6	3.0	3.0	only **2.40**	46	100
7	2.0	5.0	1 : 4.5	no data	no data
8	2.0	3.0	1 : 4.2	no data	no data
9	2.0	1.0	1 : 2.7	no data	no data
10	2.0	0.0	1 : 1.6	no data	no data
11	3.0	0.0	only **2.40**	15	100

[a]Reaction conditions: Reaction conditions: PIFA (as specified), NFSI (as specified), **3.53** (1.0 equiv, 0.05 mmol) in benzene (0.1 M), irradiated for 1 h at 300 nm in an NMR tube. [b] NMR yields and conversions were obtained using ethyl trifluoroacetate as an internal standard.

To explain the observed phenomena of decarboxylative fluorination in the absence of a radical fluorinating agent, the mechanism depicted in Scheme 3.13 is proposed. Intermediate **3.57**, obtained by

radical decarboxylation, can be further oxidized by PIFA to oxonium **3.58** which is trapped by trifluoromethylacetate generating dioxyfluoromethane **3.59**. However, the presence of oxonium **3.58** may induce **3.59** to act as a source of fluoride, thus generating difluoromethoxyarene **3.4**. The resulting oxonium **3.60** can ultimately decompose to phenol by attack with another oxygen-centered nucleophile. There are 3 pieces of evidence in support of this mechanism: (1) bromophenol is detected by TLC, (2) higher amounts of PIFA are needed for complete conversion of **3.53**, (3) SET oxidation of radicals is a well-established pathway for hypervalent iodine.[178]

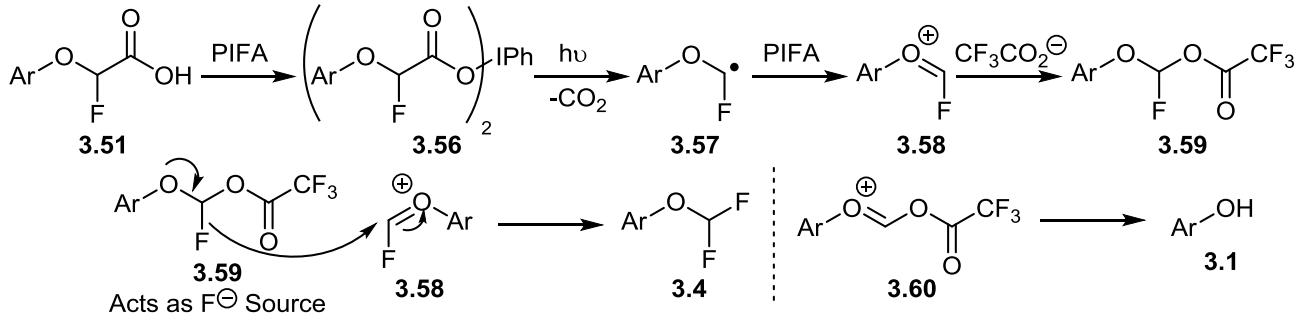

Scheme 3.13. Mechanism for difluoromethyl ether formation in the absence of NFSI

Without an addition source of fluoride, the starting carboxylic acid acts as both substrate and fluoride source resulting in a theoretical yield of 50%. A selection of inorganic fluorides were screened as alternative sources of fluoride (Scheme 3.14) including tetrabutylammonium triphenylsilyl-difluoride and tetrabutylammonium triphenylstannyldifluoride. Unfortunately, no increases in yield were observed relative to the background reaction without additive. Given that yields of **2.40** as high as 48% were observed in the presence of NFSI (Table 3.4, entry 4), a radical fluorination reaction was likely also active. Therefore, experiments towards better understanding the role of I (III) were resumed.

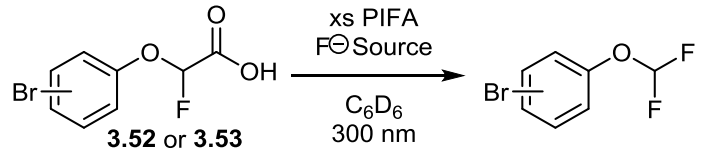

Scheme 3.14. Alternative fluoride sources screened for difluoromethyl ether synthesis

After completing the investigations into PDC-F with Sel-F and sensitized PDC-F with NFSI, I briefly resumed work on DIB-mediated PDC-F with NFSI (Scheme 3.15). Unlike the solvent-screen experiments reported in Table 3.2 (where acetonitrile was not suitable for DIB-mediated fluorodecarboxylation) the addition of 2, 6 di-*tert*-butyl pyridine (DtBuPy) aids in the formation and preservation of the fluorination products. Furthermore, it was found that some NFSI-mediated PDC-F reactions could be catalyzed by the presence of a photosensitizer such as acetone or benzophenone (see subsection 3.4.3). The successful PDC-F of **3.55** (left portion) and **3.62** (right portion) in acetonitrile with UV-light from a tropical terrarium lamp suggests that DIB may also be acting as a photosensitizer similar to acetone or benzophenone. Exclusive to DIB, fluoromethoxy ether **3.63** can be obtained, whereas such a transformation cannot be performed with Sel-F or NFSI in acetone. Ideas for further work on hypervalent iodine-mediated monofluoromethoxyarene and difluoromethoxyarene synthesis will be elaborated upon in Chapter 5.

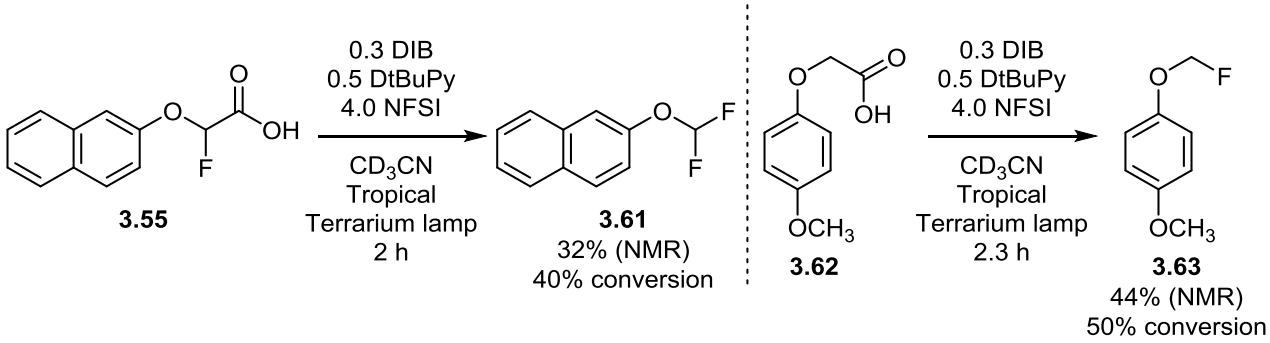

Scheme 3.15. Resumed work on DIB-mediated PDC-F with NFSI

3.2.3 DIB-mediated fluorodecarboxylation of non-aryloxyacetic acid substrates

Unfortunately, the carboxylic acid substrates depicted in Figure 3.3 failed to produce appreciable amounts of fluorodecarboxylation product. As the reaction is mediated by radicals, the failure of 4-nitrophenoxyacetic acid (**3.80**) is not surprising as nitrobenzene is a known radical scavenger. The fluorodecarboxylation product of diphenoxyacetic acid **3.81** was not observed, and may have been unstable under the reaction conditions (fluoride elimination to the doubly-stabilized oxonium). Photochemical treatment of styrene **3.78** lead to a complex mixture of unidentifable compounds. The failure of thiophenoxyacetic acid (**3.71**) and 4-iodophenoxyacetic acid (**3.79**) can be explained by a competitive oxidation reaction of the sulphur or iodine by DIB or NFSI. As DIB is primarily an oxidant, a literature search revealed that benzylic oxidation and lactone formation can be accomplished by the action of DIB on substrate **3.67**.[182]

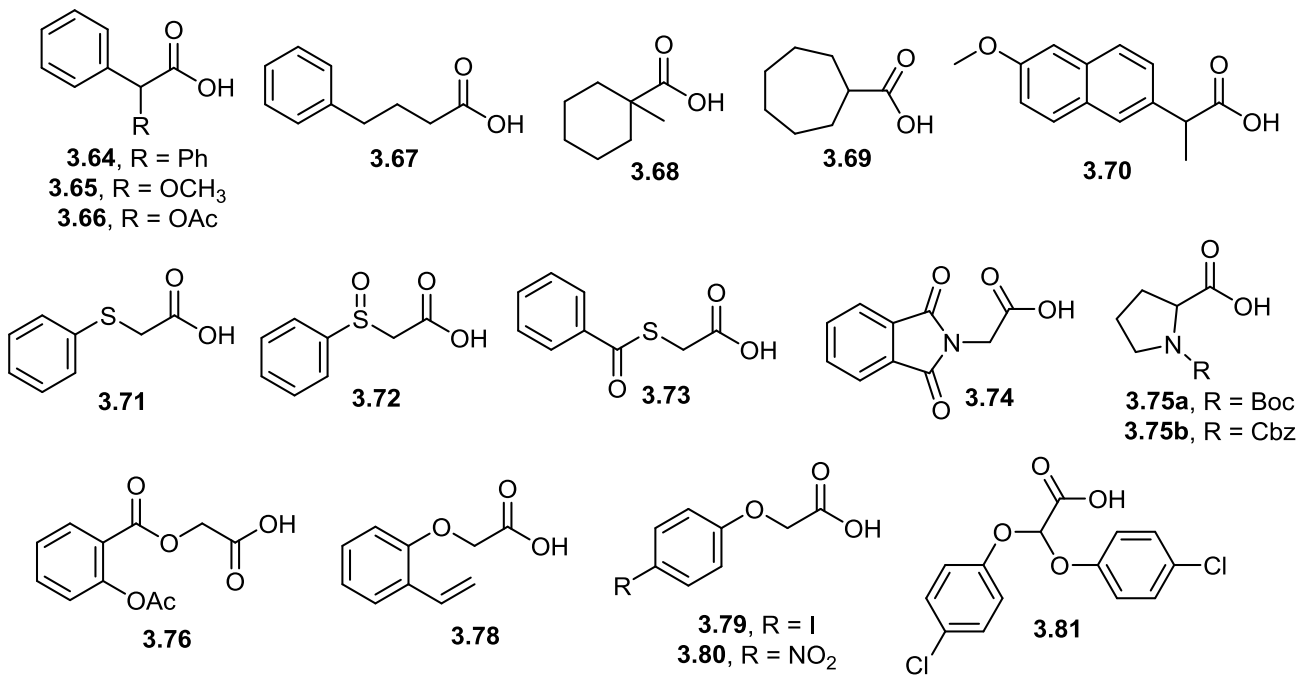

Figure 3.3. Carboxylic acids which did no undergo DIB-mediated fluorodecarboxylation

However, if the reaction mechanism depicted in Scheme 3.10 is correct, the failure of the remaining carboxylic acid substrates is difficult to explain. It may be that higher energy wavelengths of light are required to decompose the ligand-exchanged intermediates, or that the ligand-exchanged intermediates were not formed at all with DIB, and required PIFA.

In all of the stoichiometry reaction screens, it was assumed that the minimum requirement for DIB (or PIFA) was 0.5 equivalents. When DIB-mediated PDC-F with NFSI was investigated using fewer than 0.5 equivalents of DIB (Table 3.5), the assumption was found to be incorrect. According to scheme 3.2.4, with only 0.1 equivalents of DIB, the theoretical yield is 20%; yet, experimentally, 24% yield of **3.43** is observed (entry 1). Similarly, the yields of **3.43** obtained with 0.15 to 0.25 equivalents of DIB (entries 2 to 4) all violate the maximum theoretical yield predicted by Scheme 3.2.4. Furthermore, the optimal amount of DIB for PDC-F appears to be 0.3 equivalents (entry 5).

Table 3.5.Photodecarboxylative fluorination with less than 0.5 equivalents of DIB

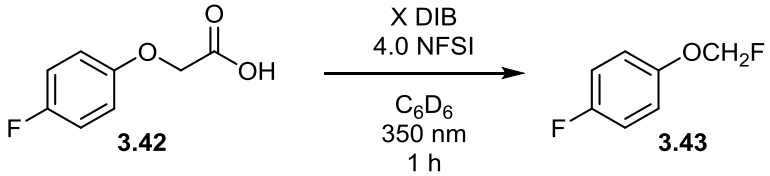

entry[a]	DIB (X equiv.)	theoretical yield (%)[b]	yield (%)[c]	conversion (%)[c]
1	0.10	20	24	35
2	0.15	30	44[d]	63[d]
3	0.20	40	51	73
4	0.25	50	56[d]	87[d]
5	0.3	60	57[d]	95[d]
6	0.35	70	53[d]	>95[d]
7	0.4	80	47	>95

[a]Reaction conditions: PIFA (as indicated), NFSI (as indicated), **3.42** (1.0 equiv, 0.05 mmol) at 0.1 M in deuterobenzene, irradiated for 1 h with light source as indicated. [b]Maximum theoretical yield of **3.43** as predicted by the mechanism in Scheme 3.10 [c]The yields and conversions were obtained by ^{1}H NMR spectroscopy using ethyl trifluoracetate as an internal standard. [d] Average of 2 trials.

It is clear that the mechanism proposed in Scheme 3.10 is not entirely correct. I had overlooked that formation of ligand exchanged intermediate **3.39** is accompanied by formation of acetate, which is a weak base. However, acetate is a sufficently strong base to deprotonate a small amount of phenoxyacetic acid (**2.26**); thus, the addition of DIB is effectively the addition of small amounts of acetate base. When stronger amine bases were investigated in place of DIB at 350 nm, no PDC-F was observed. The breakthrough occurred when the light source was switched to 300 nm (Scheme 3.16). A benzene solution containing only carboxylic acid **3.42**, radical fluorination agent NFSI, and triethylamine base irradiated at 300 nm overnight in a photoreactor provided 44% yield of the PDC-F product **3.43**.

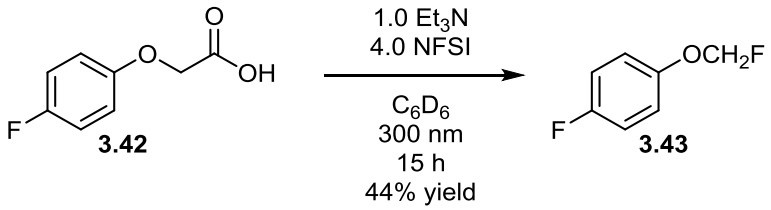

Scheme 3.16. Photofluorodecarboxylation in the absence of DIB or PIFA

Surprisingly, DIB or PIFA was not necessary for photodecarboxylative fluorination! The desired transformation can be accomplished through the mechanism depicted in Scheme 3.17. Direct excitation of the deprotonated aryloxyacetate (**3.82** is demonstrated for simplicity) to **3.83** allows for a single electron transfer oxidation event. Rapid decarboxylation of **3.84** produces phenoxymethyl radical (**2.33**) which intercept the radical fluorination pathway discussed in Chapter 2. A detailed discussion of the PDC-F mechanism can be found in subsections 3.3.6 and 3.4.3.

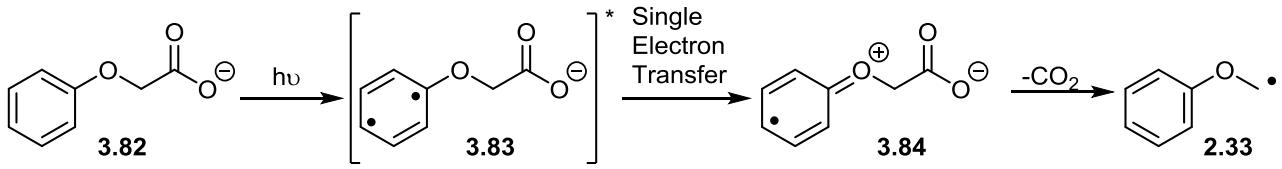

Scheme 3.17. Direct photodecarboxylation of phenoxyacetate

Soon after obtaining the result in Scheme 3.16, I was joined by Julian West, an undergraduate summer research student placed under my supervision. While explaining the discovery that DIB was not necessary for PDC-F,[f] I immediately realised that the generic nature of the mechanism in Scheme 3.17 could tolerate *small* changes to the reaction conditions. By changing the solvent from benzene to aqueous sodium hydroxide solution, and using Sel-F, it was possible to obtain fluoroether **3.43** in superior yields (Scheme 3.18).

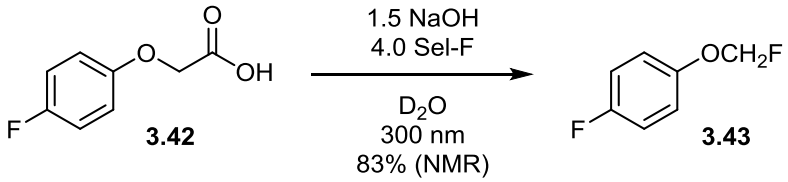

Scheme 3.18. PDC-F of 4-fluorophenoxyacetic acid with Sel-F

[f] J. West asked why I did not use sodium hydroxide as the base. The simple answer was that sodium hydroxide would not dissolve in benzene; however, switching the solvent to water would enable the use of sodium hydroxide.

3.3 Photodecarboxylative fluorination utilising Sel-F

3.3.1 Literature precedence for photodecarboxylation

Photodecarboxylation (PDC) of aryl acetic acids has been studied extensively in the early 1970's and continues to generate interest to this day.[183] The driving force behind modern studies has been the decomposition of bioactive small molecules in the environment. As textbooks exist on photoinduced electron transfer (PET),[184,185] only the photodecarboxylation of phenoxyacetic and (**2.26**) phenylacetic acid (**3.40a**) and the role of ionization potentials in electron transfer reactions will be discussed. The mechanisms of **2.26** and **3.40a** photodecarboxylation are most related to my investigations on the PDC-F of 2-aryl (**3.40**) and 2-aryloxyacetic acids (**3.44**) by Sel-F.

Photoionization of aromatic compounds in aqueous solution by ultraviolet light leads to a solvated electron and radical products. Joschek and Grossweiner have surveyed a variety of solvated aromatic compounds in water by flash photolysis and found that phenoxyacetate (**3.82**) and phenylacetate (**3.85a**) undergo decarboxylation reactions to produce the corresponding phenoxymethyl (**2.33**) and benzyl (**3.86a**) radicals (Scheme 3.19).[186] Filter experiments showed that photoionization is induced by irradiation in the longest wavelength aromatic band and that the electron is not released directly from the carboxylate.[186]

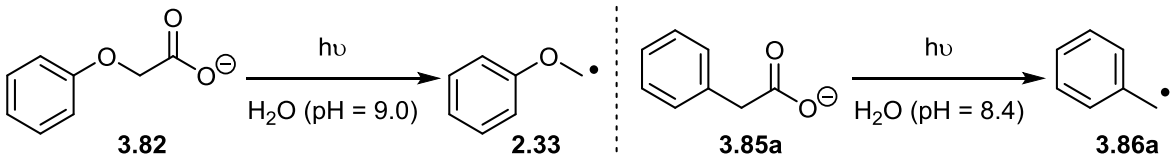

Scheme 3.19. Photodecarboxylation of phenoxyacetate and phenylacetate

Related to this work, Epling and Lopes studied the photodecarboxylation of sodium phenylacetate (**3.87**) and found that the solvated electron rapidly recombines with benzyl (**3.86a**) leading to benzyl anion **3.88** and ultimately to toluene (**1.68**).[187] The observation of toluene was previously thought to be evidence of an ionic hydrodecarboxylation reaction. It is more accurate to view the decarboxylation as a radical process with rapid recombination of the alkyl radicals generated with the solvated electron (Scheme 3.20).

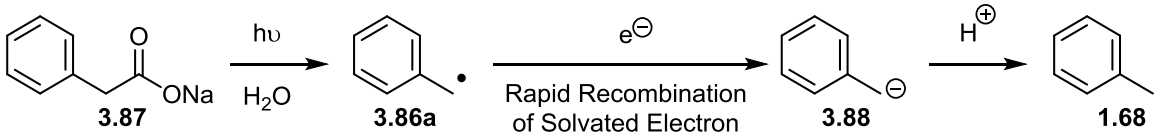

Scheme 3.20. Photodecarboxylation and rapid recombination with the solvated electron

Gilbert and coworkers studied the aqueous photodecarboxylation of phenyl ethanoic, propanoic, and butanoic acids and found that the same radical intermediates could be generated by oxidation of the aromatic ring with a strong single electron transfer oxidant such as the sulphate radical anion.[188] They explained the formation of alkyl radical **3.86** from decarboxylation of **3.89** after an internal electron transfer from the carboxylate anion to the oxidized benzene ring (**3.90**, Scheme 3.21). More recently, Bietti and Capone have postulated that the aryl oxidation and internal electron transfer steps might be coupled when formation of the aryl cation is relatively costly.[189]

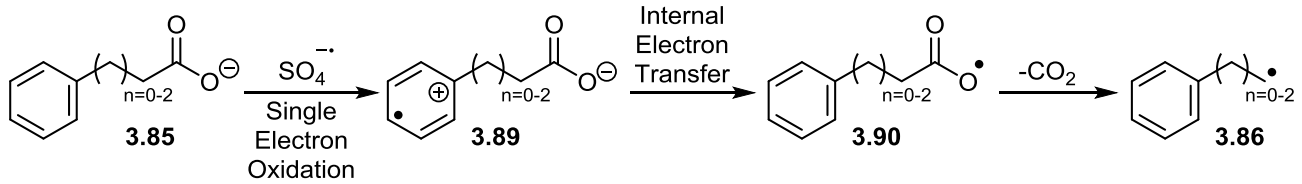

Scheme 3.21.Radical intermediates of photodecarboxylation generated by single electron oxidation

Davidson discovered that aromatic ketones[190] (such as benzophenone) and quinones[191] sensitize the photodecarboxylation of certain carboxylic acids with ionisation potentials below 9 eV.[191b] Photodecarboxylation of phenoxyacetic acid (**2.26**) in benzene can be sensitized by benzophenone (**3.91**) and radical decarboxylation products **3.92** and **3.93** were obtained along with reduced benzophenone dimer **3.94** (Scheme 3.22). The mechanism proposed by Davidson[191] (further supported by McLauchlan and coworkers[192]) involves excitation of benzophenone to di-radical **3.95** followed by reversible electron transfer oxidation of oxygen on **2.26** to **3.98**. The resulting radical anion **3.96** then abstracts a proton from **3.98** triggering a decarboxylation event to phenoxymethyl (**2.33**). Radical abstraction of hydrogen produces anisole (**3.92**), dimerisation of **2.33** leads to 1, 2-diphenoxyethane (**3.93**), and dimerization of reduced benzophenone **3.97** produces glycol **3.94**. An important observation, reported by Davidson and coworkers, was that the addition of thiophenol dramatically increases the yield of anisole (Scheme 3.23).[191a] Thiophenol is an excellent radical hydrogen donor and can quench phenoxymethyl (**2.33**) to anisole (**3.92**).

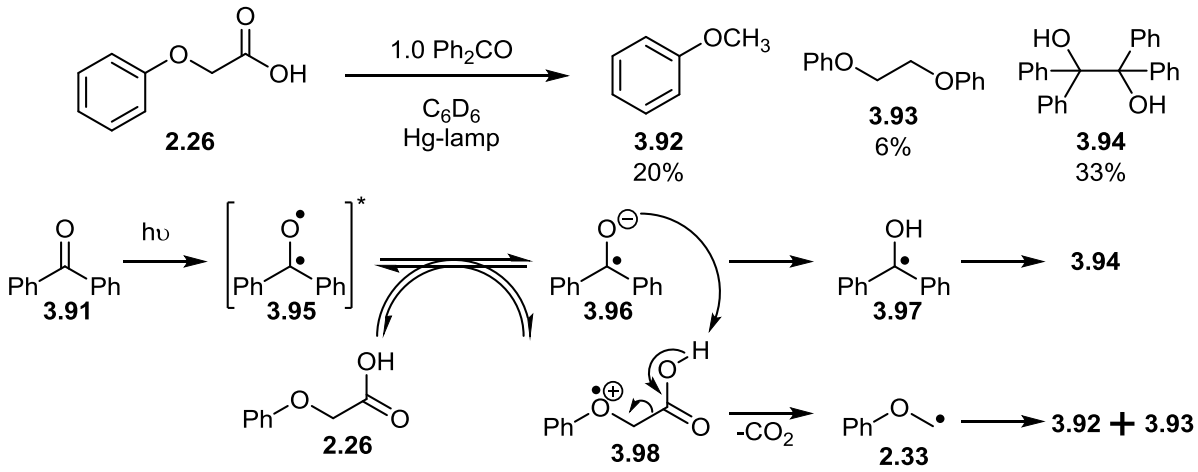

Scheme 3.22. Benzophenone-sensitized PDC of phenoxyacetic acid

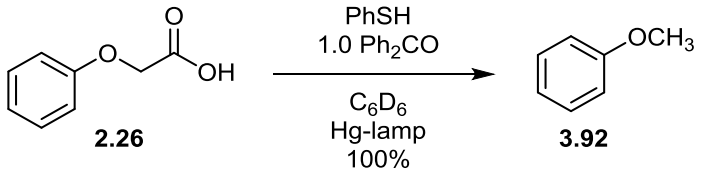

Scheme 3.23. Sensitized PDC of phenoxyacetic acid in the presence of thiophenol

All of the decarboxylation reactions described involve electron transfer processes. In the case of aqueous photoionization of phenylacetic acid (**3.40a**) and phenoxyoxyacetic acid (**2.26**), the aromatic ring acts as the donor and the electron is ionised with no acceptor.[186-189] In the studies by Gilbert with the sulphate anion, photoexcitation was not necessary to induce electron transfer from the donor arylacetic acid to the sulphate anion acceptor.[188] The electron transfer system of sensitized PDC by Davidson places benzophenone (**3.91**) as the photoexcited acceptor and the phenoxyacetic acid (**2.26**) as the ground-state donor.[190,191]

The feasibility of electron transfer between an excited state molecule and a quencher is determined by the overall change in free energy(ΔG) of the reaction according to eqn. 3.5, where IP_{D^*} is the ionisation potential of the excited-state donor (eqn. 3.6), $E_{D^*}$is the energy absorbed by the donor, and $EA_A$is the electron affinity of the acceptor.[184,193] This scenario is applicable to the photodecarboxylative fluorination reactions with Sel-F and NFSI where the donor acids (**3.44**) are excited. The reverse equation is true if the electron transfer is triggered by excitation of the acceptor (as in the case of sensitized PDC with benzophenone or acetone). In the gas phase, IP_D and EA_A are typically estimated from the energies of the highest occupied and lowest unoccupied molecular orbitals respectively.

$$\Delta G = IP_{D^*} - EA_A \quad (3.5)$$

$$IP_{D^*} = IP_D - E_{D^*} \quad (3.6)$$

In the solution phase, IP_D and EA_A can be related to the redox potentials of the donor and acceptor according to eqn. 3.7 and 3.8 where $E(D\cdot^+/D)$ is the reduction potential of the donor, $E(A/A\cdot^-)$ is the reduction potential of the acceptor, $\Delta G(D\cdot^+)$ and $\Delta G(A\cdot^-)$ are the individual solvation energies. If the solvent has a large dielectric constant, some Coulombic energy terms can be neglected and a simplified equation for the free energy of electron transfer in solution can be given by eqn. 3.9. Electron transfer is allowed if $\Delta G < 0$.

$$IP_D = E(D\cdot^+/D) - \Delta G(D\cdot^+) + \text{constant} \quad (3.7)$$

$$EA_A = E(A/A\cdot^-) - \Delta G(A\cdot^-) + \text{constant} \quad (3.8)$$

$$\Delta G(kcal/mol) = 23.06[E(D\cdot^+/D) - E(A/A\cdot^-)] - E_{D^*} \quad (3.9)$$

3.3.2 Optimisation of photodecarboxylative fluorination with Sel-F

Although Sel-F was reported in Chapter 2 to be a viable source of atomic fluorine, it only gave satisfactory yields as a fluorine transfer agent with the *tert*-butyl perester **2.25**. As a reagent for PDC-F of aryloxyacetic acids, Sel-F performs admirably (Scheme 3.18). Photochemical irradiation at 300 nm of 4-fluorophenoxyacetic acid (**3.42**) and Sel-F in an alkaline aqueous solution for 2 hours yielded the desired PDC-F product 1-fluoro-4-(fluoromethoxy)benzene (**3.43**) in 83% NMR yield (Scheme 3.18). The control reaction in a foil-covered NMR tube showed no decarboxylation occurs in the absence of light (Scheme 3.24).

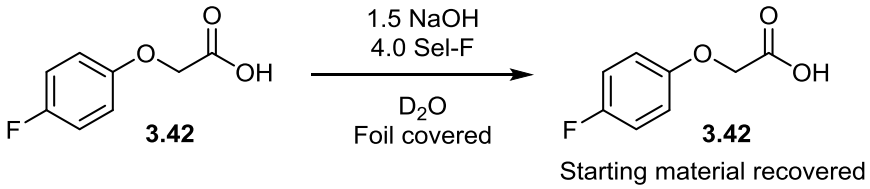

Scheme 3.24. Necessity of light for decarboxylative fluorination

Having established the necessity of light, I investigated the wavelength required for this transformation (Table 3.6). 300 nm lamps provided the best yields for PDC-F (entry 3) and the reaction run at 254 nm (entry 1) or 350 nm (entry 3) showed lower efficiency at PDC-F with Sel-F. Ultraviolet light was necessary for PDC-F as experiments employing an incandescent tungsten lamp or a compact fluorescent lamp failed to deliver appreciable amounts of **3.43** (entries 4, 5). As the absorption maxima for the sodium salt of **3.42** in water are near 278 nm and 284 nm, the emission profile of the 300 nm lamps provide the optimal fit for PDC-F with Sel-F. Given the requirement of light near 300 nm, alternative light sources such as direct sunlight (entry 5) and terrarium lamps (entry 6, 7), were investigated; however, the yields obtained were less satisfactory.

Table 3.6. Photodecarboxylative fluorination with Sel-F: Wavelength studies

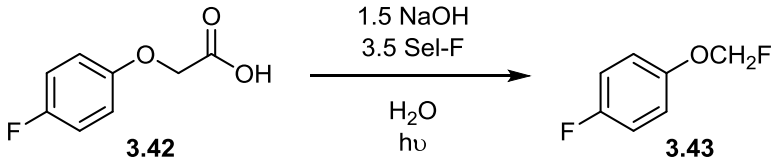

3.42 **3.43**

entry[a]	wavelength[b]	NMR yield[c]
1	254 nm	25%
2	300 nm	94%[d]
3	350 nm	47%
4	sunlamp	4%
5	compact fluorescent lamp	0%
6	sunlight	42%
7	desert terrarium lamp[e]	0%
8	tropical terrarium lamp[f]	0%

[a]Reaction conditions: NaOH (1.5 equiv.), Sel-F (3.5 equiv), **3.42** (1.0 equiv, 0.1 mmol) in water (0.1 M), irradiated for 1 h at the indicated wavelength in a 15ml polypropylene centrifuge tube . [b]Light sources utilized for these experiments are not strictly monochromatic. The indicated wavelength refers to the maximum light intensity emitted. [c]The NMR yields were obtained using trimethoxybenzene as an internal standard. [d]The reported yield is an average of 3 runs. [e]The desert terrarium lamp emitts broad spectrum UV light with a higher precentage in the UVA region. [f]The tropical terrarium lamp emitts broad spectrum UV light with a higher precentage in the UVB region.

The next parameter investigated was the equivalents of Sel-F required (Table 3.7). Yields for **3.43** are comparable with 2.0, 2.5 or 3.0 equivalents of Sel-F (entries 1-3) with the highest yield obtained employing 3.5 equivalents of Sel-F (entry 4). Further increases in Sel-F (entry 5) do not show improvement in yield. 3.5 Equivalents of Sel-F was found to be optimal, and the amounts of Sel-F could be reduced to 3.0 equivalents upon reaction scale-up.

Table 3.7. Photodecarboxylative fluorination with Sel-F: Optimisation of Sel-F equivalents

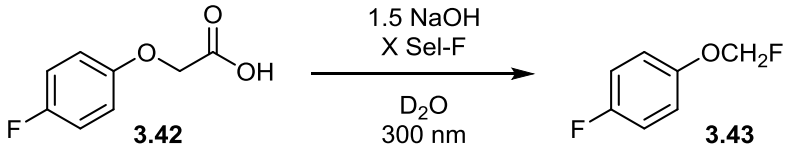

3.42 **3.43**

entry[a]	amount of Sel-F	NMR yield[b]
1	2.0 equiv.	86%
2	2.5 equiv.	87%
3	3.0 equiv.	87%
4	3.5 equiv.	90%
5	4.0 equiv.	88%

[a]Reaction conditions: NaOH (1.5 equiv.), Sel-F (as specified in table), **3.42** (1.0 equiv, 0.05 mmol) in deuterium oxide (0.1 M), irradiated at 300 nm for 1 h. [b]The NMR yields were obtained using trimethoxybenzene as an internal standard.

The effect of base on PDC-F with Sel-F was examined next. The addition of a base was necessary to facilitate solution of aryloxy acetic acids into water. Substituting sodium hydroxide for lithium hydroxide, potassium hydroxide or potassium carbonate did not have any appreciable effect on the NMR yield of **3.43**. However, the use of potassium bases decreased the solubility of **3.42** after the addition of Sel-F and the precipitation of aryloxyacetate salts was observed. As sodium hydroxide was the most cost-efficient base, it was selected for further optimisation studies (Table 3.8). An excess of sodium hydroxide increased the rate of solubility of aryloxacetic acids but was detrimental to the yield of PDC-F (entry 1). Stoichiometric use of base (entry 3) provided nearly quantitative yields of the fluorinated product **3.43** but it took a long time to dissolve the starting acid.

Increasing the amount of base to 1.5 equivalents accelerated the solubility process. The PDC-F of **3.42** is effective with sub-stoichiometric amounts of base (entry 4) or even in the absence of sodium hydroxide (entry 5) when acetonitrile is employed as the solvent. However, solutions containing Sel-F are slightly alkaline because trace amounts of trialkylamine base **1.199** are typically found in reagent bottles of Sel-F. Furthermore, decomposition of Sel-F is observed under the photochemical conditions

and generates additional trialkylamine base **1.199**. For practical reasons, 1.5 equivalents of sodium hydroxide was chosen as the optimal conditions because solubilisation of **3.42** was relatively quick and mixed solvent systems were not necessary.

Table 3.8. Photodecarboxylative fluorination with Sel-F: Optimisation of NaOH equivalents

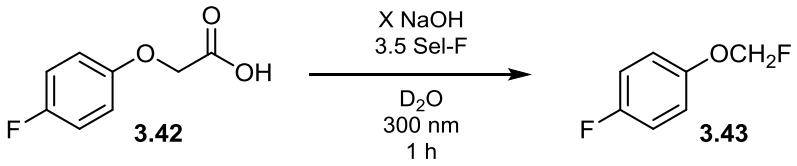

3.42 **3.43**

entry[a]	equivalents $NaOH_{(aq)}$	NMR yield[b]
1	5.0 equiv.	74%
2	1.5 equiv.	92%
3	1.0 equiv.	>95%
4 [c]	0.5 equiv.	90%
5 [c]	0.0 equiv.	90%

[a]Reaction conditions: NaOH (as specified in table), Sel-F (3.5 equiv), **3.42** (1.0 equiv, 0.05 mmol) in deuterium oxide (0.1 M), irradiated at 300 nm for 1 h. [b]The NMR yields were obtained using trimethoxybenzene as an internal standard [c]Reaction was run in a mixture of water and acetonitrile-*d3*.

Sel-F is a doubly charged cationic salt and the deprotonated carboxylic acid is a singly charged anionic compound. Both of these two compounds are critical components to PDC-F and water is a logical choice for solvating charged species. Two other solvents were investigated: acetone and acetonitrile. With pure acetone, Sel-F was moderately soluble but difficulties were encountered solvating the carboxylate salts. With pure acetonitrile, Sel-F had a poor solubility profile but the related compound F-TEDA-PF_6 was a suitable substitute; however, the yields of PDC-F were moderate (~45%). Water appears to be a desirable solvent for this reaction.

The order of reagent addition was found to be important in facilitating complete solution of reactants. The most efficient procedure calls for completely dissolving the carboxylic acid in aqueous

basic solution first. Finely powered Sel-F is added in one portion with vigorous stirring. In this manner, a homogeneous solution may be formed for many aryloxyacetic acids.

While I was optimising the conditions for PDC-F of **3.42**, J. West investigated the problem of solubility with substrate **3.46** that contained larger hydrophobic substituent. When **3.46** was exposed to aqueous sodium hydroxide, a viscous gel was formed. Employing lithium hydroxide or potassium carbonate as the aqueous base allowed for smooth formation of an aqueous solution of 3**.46** as the carboxylate salt; however, precipitation of aryloxyacetate occurred immediately upon addition of Sel-F. The problem was addressed by employing acetonitrile as a co-solvent. J. West found that PDC-F yields decreased slightly as the amounts of acetonitrile increased. We decided that 3:1 ratio of water: acetonitrile was the best general conditions for PDC-F with Sel-F.

The last parameter investigated was reaction time (Table 3.9). Within 30 minutes, the reaction progresses to 79% NMR yield with 90% conversion (entry 1), and after 45 minutes, the reaction is complete on the 0.1 mmol scale (entry 2). Prolonged exposure to 300 nm light lead to a slight decrease in yields (entries 4, 5). It was decided that 1 hour of irradiation was sufficient to ensure complete conversion of starting material. For PDC-F on larger scales, longer exposure times would be required.

Table 3.9. Photodecarboxylative fluorination studies: reaction time.

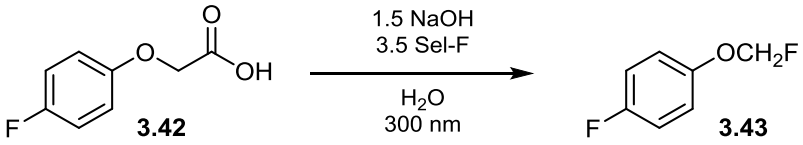

3.42 **3.43**

entry[a]	irradiation time	NMR yield[b]	Conversion[b]
1	30 min	79%	90%
2	45 min	86%	100%
3	60 min	86%	100%
4	75 min	84%	100%
5	90 min	83%	100%

[a]Reaction conditions: NaOH (1.5 equiv.), Sel-F (3.5 equiv), **3.42** (1.0 equiv, 0.1 mmol) in water (0.1 M), irradiated for 1 h at 300nm in a 15ml polypropylene centrifuge tube . [b] The NMR yields and conversions were obtained using trimethoxybenzene as an internal standard.

In summary, the general optimized condition for PDC-F with Sel-F was established to be: 1.0 equivalents of aryloxyacetic acid (**3.44**), 3.5 equivalents of Sel-F, 1.5 equivalents of sodium hydroxide, and water as the solvent. If solubility becomes an issue, a 3:1 mixture of water: acetonitrile may be employed as the reaction medium. A discussion of the reaction mechanism can be found in subsection 3.3.6.

3.3.3 Synthesis of aryl monofluoromethyl ethers

Photodecarboxylative fluorination of aryloxyacetic acids (**3.44**) is an excellent reaction for the synthesis of aryl monofluoromethoxy arenes (Scheme 3.25). Monofluoromethoxy arenes containing bromine or fluorine on the aryl moiety can be obtained in 57 – 60% yields (**3.43** isolated by me, **3.101** isolated by C. Chatalova-Sazepin, **3.102** isolated by C. Chatalova-Sazepin). An oxygen heteratom attatched to the benzene ring can be tolerated if electron density is removed by conversion of the phenol to a mesylate (**3.100**). PDC-F can be performed effectively at the 2.0 mmol scale with **1.113**

synthesized in 86% isolated yield. With a mixture of electron donating and electron withdrawing substituents on the benzene ring, poor yields of **3.105** were obtained using PDC-F with Sel-F.

In the presence of benzylic protons, PDC-F with Sel-F is less effective as optimized conditions found by J. West provided NMR evidence for **3.104** at 34 % yield. However, the related *tert*-butyl analogue **3.103** (isolated by J. West) is an excellent substrate for PDC-F with Sel-F. Fluoromethyl ether **3.99** was detected by NMR in 38% yield; however, isolation of the fluoroether was not possible as only the enol ether product of fluorine elimination could be obtained.

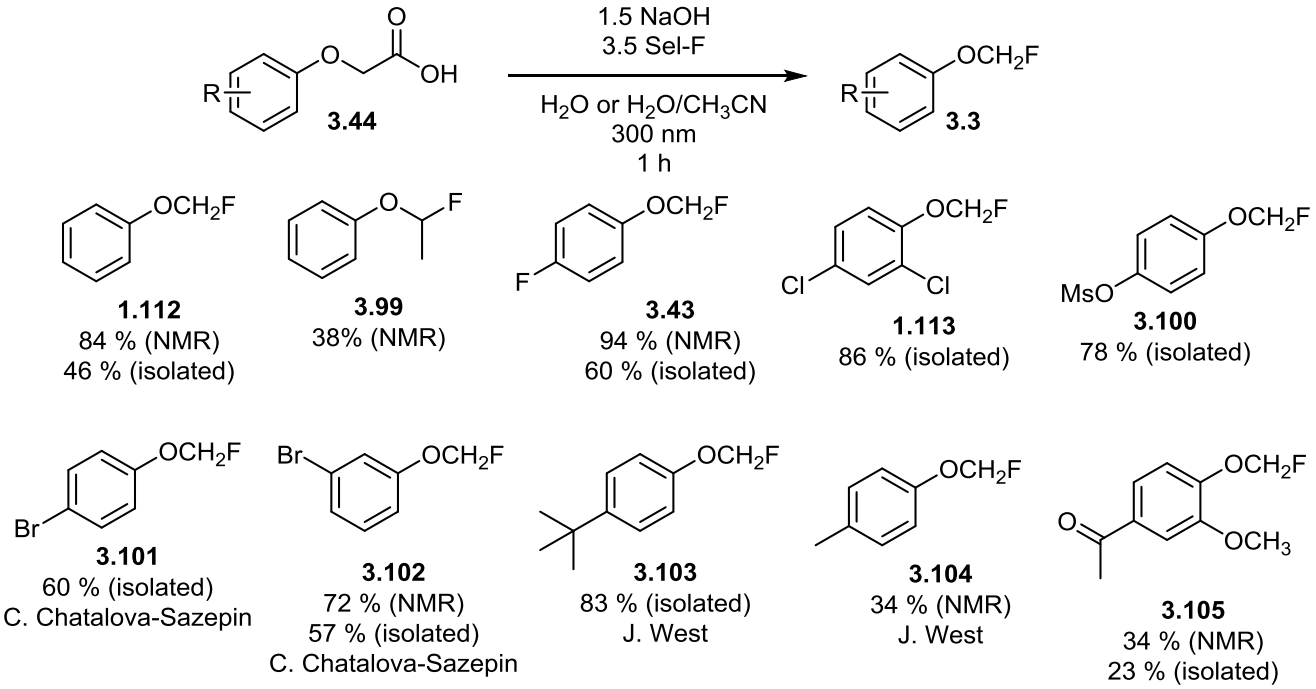

Scheme 3.25 Monofluoromethyl aryl ethers successfully synthesized by PDC-F with Sel-F

Unfortunately, the aryloxyacetic acid substrates depicted in Scheme. 3.26 failed to produce appreciable amounts of fluorodecarboxylation product under the standard PDC-F with Sel-F conditions. As the reaction is mediated by radicals, the failure of 4-nitrophenoxyacetic acid (**3.80**) is,

again, not surprising as nitrobenzene is a known radical scavenger. Biphenyloxyacetic acid (**3.106**) provided low yields of fluorodecarboxylation product as solubility of the acid was problematic. The failure of the remaining aryloxyacetic acids can be related to the ionic fluorination strength or oxidation power of Sel-F. 4-Methoxy acid **3.62**, and the napthoxy acids **3.47**, **3.107**, and **3.109** are fluorinated by Sel-F through electrophilic aromatic substitution in competition with fluorodecarboxylation. Mesityl acid **3.108** and allyl acid **3.48** showed signs of benzylic oxidation whereas styrene acid **3.78** and estrone acid **3.110** lead to complex product mixtures likely caused by non-specific fluorination.

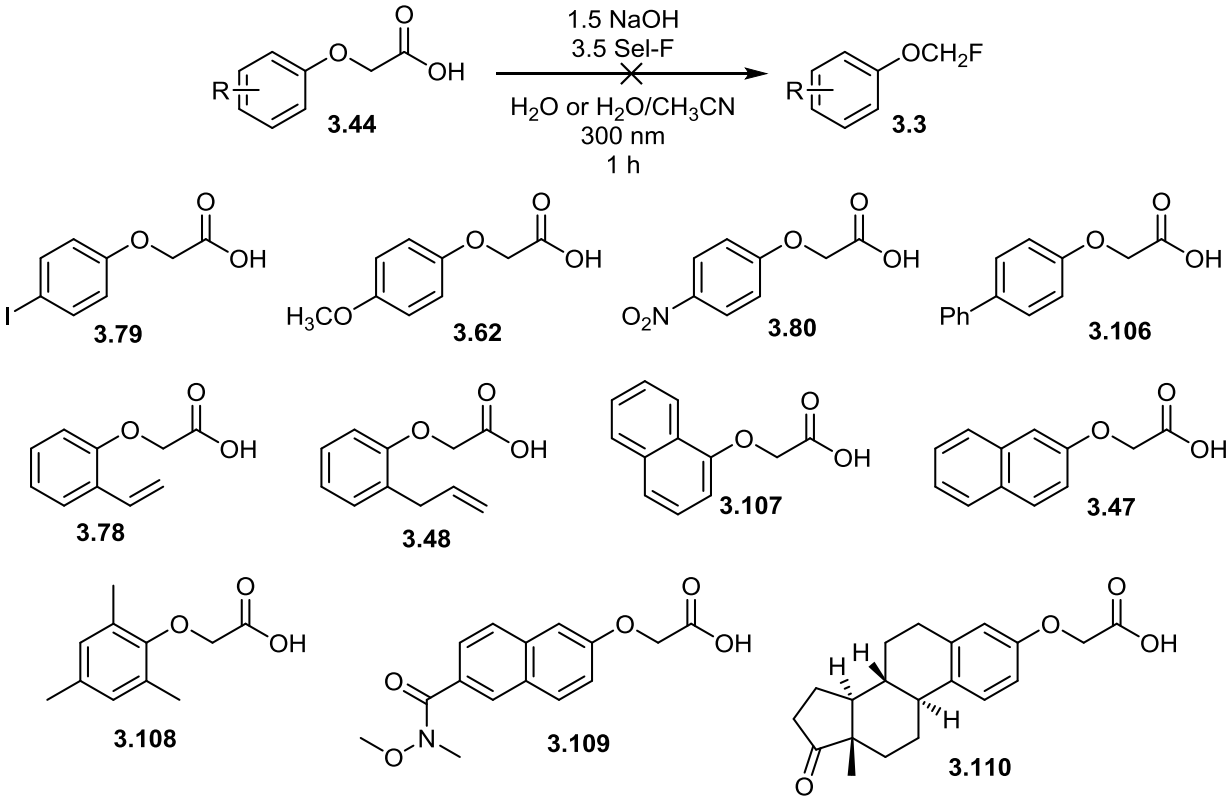

Scheme 3.26. Aryloxyacetic acids which failed to undergo PDC-F with Sel-F

Substrates outside the scope of aryloxyacetic acids were also examined (Scheme 3.27 and 3.28). In the absence of a photoactive aryl moiety, alkyl acid salt **3.111** failed to undergo PDC-F. Radical fluorobenzene synthesis failed as benzoic acid (**2.54**) was not a viable substrate for PDC-F (Scheme 3.27, middle). The observation that PDC-F of phenylthioacetic acid (**3.71**) lead to only trace amounts of fluoroproduct **3.112** is possibly explained by Sel-F mediated sulphur oxidation.[119] With *N*-phthaloyl glycine (**3.74**), a 25% yield of PDC-F product **1.119** was observed (Scheme 3.28). The implications of this experiment will be discussed in subsection 3.3.6. Gratifyingly, PDC-F with phenylacetic acid (**3.40a**) produced benzyl fluoride (**1.70**) in nearly quantitative yields allowing for an expansion of the PDC-F methodology (Table 3.10, entry 1).

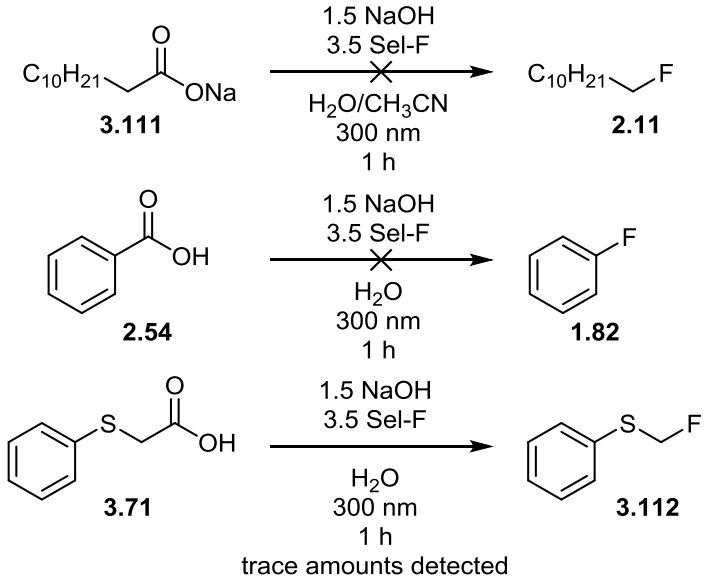

Scheme 3.27. Expansion of PDC-F with Sel-F to alternate classes of carboxylic acids

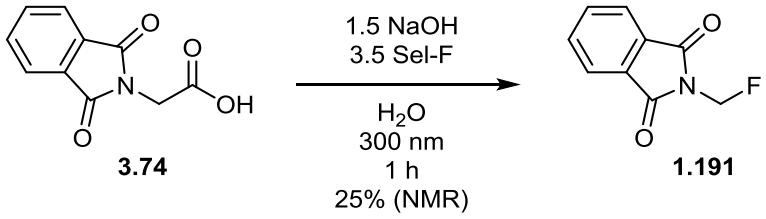

Scheme 3.28. PDC-F of *N*-phthaloylglycine

3.3.4 Synthesis of benzyl fluorides

The scope of PDC-F with Sel-F is not limited to aryloxyacetic acids (**3.44**). Phenylalkyl fluorides (**3.114**) can be synthesized effectively by PDC-F from the corresponding arylalkyl acid (**3.113**) under the same aqueous alkaline conditions (Table 3.10). Oxygenation on the aromatic ring is tolerated by either an electron-donating methoxy substituent (entry 2) or an electron-withdrawing mesyloxy substituent (entry 3) although the reaction is not complete within 1 hour. A free hydroxyl substituent on the phenyl (entry 4) ring does not facilitate PDC-F as the main reaction product with Sel-F is predominately ionic ring fluorination. Interestingly, photodecarboxylative fluorination can be employed to generate the homobenzyl fluoride **1.115b** (entry 5); however, PDC-F of further chain-elongated acetic acids fail to produce the fluorinated product (entry 6). The implications entry 5 will be discussed in subsection 3.3.6.

Table 3.10. Photofluorodecarboxylation studies of aryl acetic acids

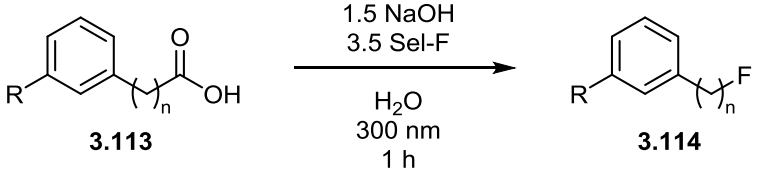

3.113 **3.114**

entry[a]	R	n	comment[b]
1 (**3.40a**)	H	1	(**1.70**) >95% NMR yield, 72% isolated yield
2 (**3.113a**)	OCH_3	1	(**3.114a**) 84% NMR yield
3 (**3.113b**)	OMs	1	(**3.114b**) 20% NMR yield
4 (**3.113c**)	OH	1	(**3.114c**) Not observed.
5 (**3.40b**)	H	2	(**1.115b**) 70% NMR yield, 53% isolated yield
6 (**3.40c**)	H	3	(**1.115c**) Not observed.

[a]Reaction conditions: NaOH (1.5 equiv.), Sel-F (3.5 equiv), **3.40** or **3.113** (1.0 equiv, 0.1 mmol) in water (0.1 M), irradiated for 1 h at 300 nm in a 15ml polypropylene centrifuge tube. [b]The NMR yields and conversions were obtained using trimethoxybenzene as an internal standard.

The implications of oxygen substitution adjacent to the carboxylic acid were then examined (Scheme 3.29). Preliminary ^{1}H NMR studies showed that oxygenation with an acetoxy substituent in the alpha position is tolerated although yields were low. Further studies of this reaction were conducted by C. Chatalova-Sazepin and her optimised conditions employed a milder base (sodium carbonate) obtaining the desired PDC-F product **3.115** in 68% isolated yield.

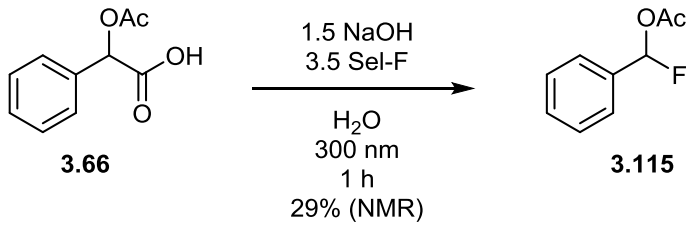

3.66 **3.115**

Scheme 3.29. Photodecarboxylative fluorination of 3.66 with Sel-F

Similar to the studies on PDC-F with Sel-F of naphthyloxyacetic acids (**3.47**, **3.107**), subjecting naproxen (**3.70**) to PDC-F with Sel-F conditions did not yield any naphthyl fluoride by ^{1}H NMR analysis (Scheme 3.30). The methoxynaphthyl ring proves too electron rich and a mixture of products resulting from non-specific electrophilic aromatic substitution were observed.

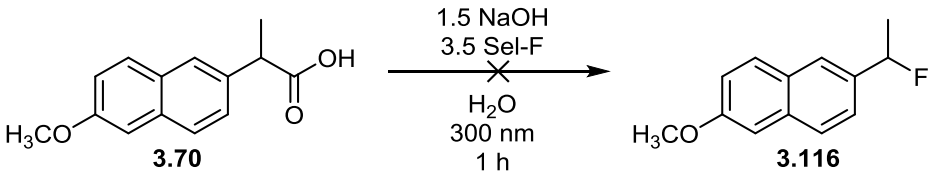

3.70 **3.116**

Mixture of products resulting from ring fluorination observed

Scheme 3.30. Failed attempt at PDC-F of naproxen

As a logical extension of this methodology, I explored the synthesis of benzyl difluoride **3.118** through a double decarboxylation strategy. Subjecting an alkaline solution of phenyl malonic acid

(**3.117**) saturated with Sel-F for 2 hours at 300 nm provided trace amounts of difluoromethyl-benzene (**3.118**) by NMR analysis. (Scheme 3.31) No α-fluoro phenylacetic acid was observed, which would be the presumed intermediate to the formation of difluoromethyl benzene. The vast majority of phenyl malonic acid remained unreacted. This method of difluoromethyl benzene synthesis shows promise and optimization of the reaction conditions will likely require 254 nm light.

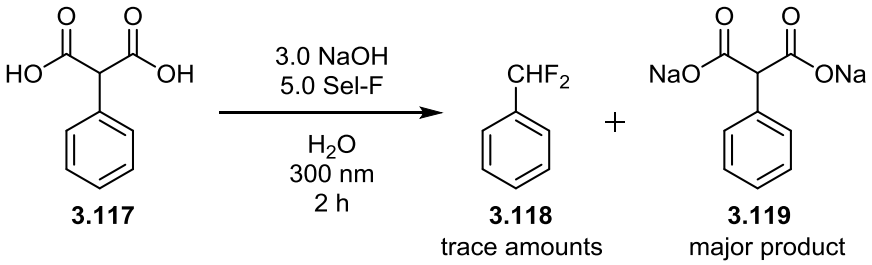

Scheme 3.31. Double PDC-F of phenylmalonic acid

3.3.5 Synthesis of aryl difluoromethyl and aryl trifluoromethyl ethers

Shortly after the PDC-F with Sel-F control experiment in a foil covered reaction vessel to verify the necessity of light (Scheme 3.24), I briefly turned my attention to the synthesis of aryl difluoro-methyl ethers (**3.4**). Fluoroacid **3.54** was subjected to irradiation in an alkaline aqueous suspension with Sel-F and gratifyingly, difluoroether **3.120** was observed 38% NMR yield (Scheme 3.32).

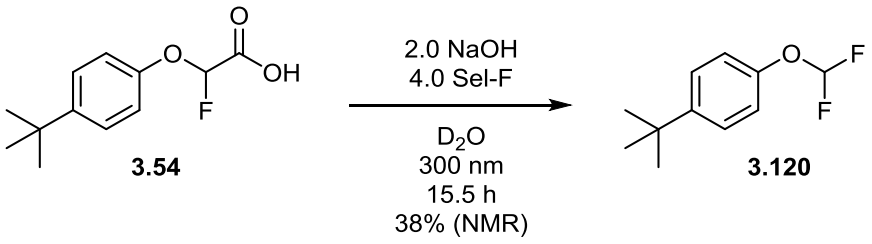

Scheme 3.32. Exploratory aryl difluoromethyl ether synthesis

After the general procedure for PDC-F with Sel-F was obtained, I briefly resumed synthetic studies on difluoromethyl ether with **3.52** and noticed that the reaction did not go to completion after 1 hour (Table 3.11, entry 1). A time-screen experiment showed that the reaction required 3 hours for completion with a best yield of 50% (entry 4). My studies on the PDC-F reaction were then diverted towards the synthesis of aryl trifluoromethyl ethers (**3.13**) and the synthesis of aryl difluoromethyl ethers was delegated to, C. Chatalova-Sazepin. Her optimized conditions were used to synthesize 3-bromo-1-difluoromethoxy benzene (**3.121**) in 40% isolated yield. PDC-F with Sel-F is an excellent method for the synthesis of difluoromethoxy arenes and a variety of aryl difluoromethyl ethers can be synthesized in good yields (Scheme 3.33). I isolated compound **3.121**, compounds **3.122**, **3.123**, **2.40** were isolated by C. Chatalova Sazepin, and **3.120** was isolated by J. West.

Table 3.11. Photodecarboxylative fluorination synthesis of 3.121: reaction time screen

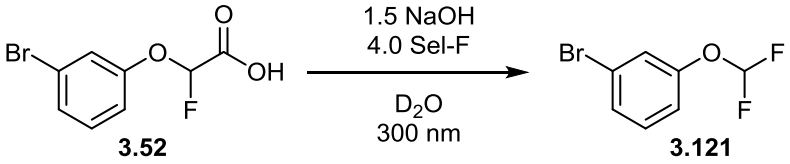

3.52 **3.121**

entry[a]	time (h)	yield (%)[b]
1	1	26[c]
2	1.5	44[c]
3	2	46[c]
4	3	50[c]
5	15	38

[a]Reaction conditions: NaOH (1.5 equiv.), Sel-F (4.0 equiv), **3.52** (1.0 equiv, 0.05 mmol or 0.1 mmol) in deuterium oxide (0.1 M), irradiated at 300 nm for the specified time. [b]The NMR yields were obtained using trimethoxybenzene as an internal standard. [c]Average yield over 2 trials.

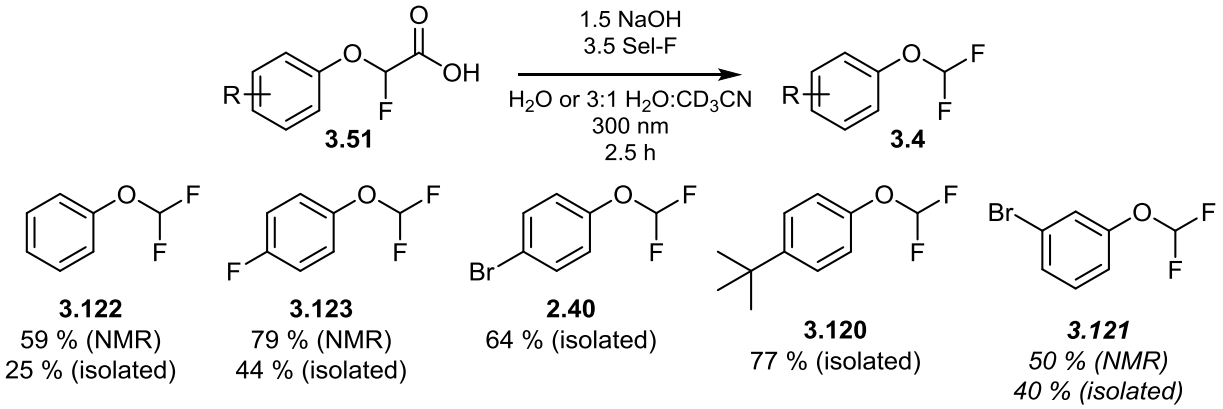

Scheme 3.33. Synthesis of aryl difluoromethyl ethers by PDC-F with Sel-F[a]

[a]My contribution is in *italics*. The remaining compounds were isolated by C. Chatalova-Sazepin or J. West.

Similar to the attempted PDC-F of **3.47**, exposure of **3.55** in a mixture of water: acetonitrile to the PDC-F with Sel-F conditions failed to produce **3.61** (Scheme 3.34). ^{1}H and ^{19}F analysis of the crude reaction mixture reveals fluorination at multiple positions on the naphthylene ring as the dominant reaction pathway.

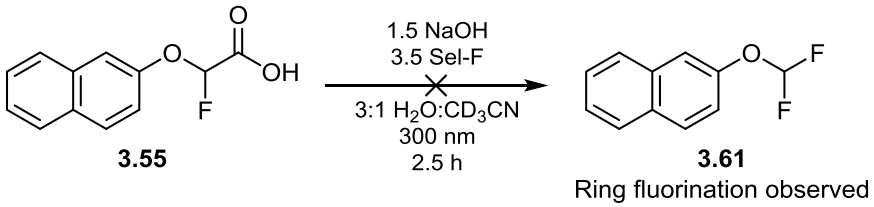

Scheme 3.34. Failed synthesis of 2-difluoromethoxynaphthalene by PDC-F with Sel-F

I next focused my efforts towards the synthesis of aryl trifluoromethyl ethers (**3.13**). Investigations began with the synthesis of the α-difluoro phenoxyacetic acids (**3.125**). Attempted synthesis of 4-bromophenoxy **3.125f** by adapting literature protocols for other related difluorophenoxy acids failed to produce the desired difluoroacid. However, small amounts of **3.125a** could be isolated

when 4-fluorophenol was used as the starting phenol. I was then able to develop a generalized procedure for the synthesis of a variety of difluorophenoxy acetic acids (**3.125a-e**, Scheme 3.35).[g]

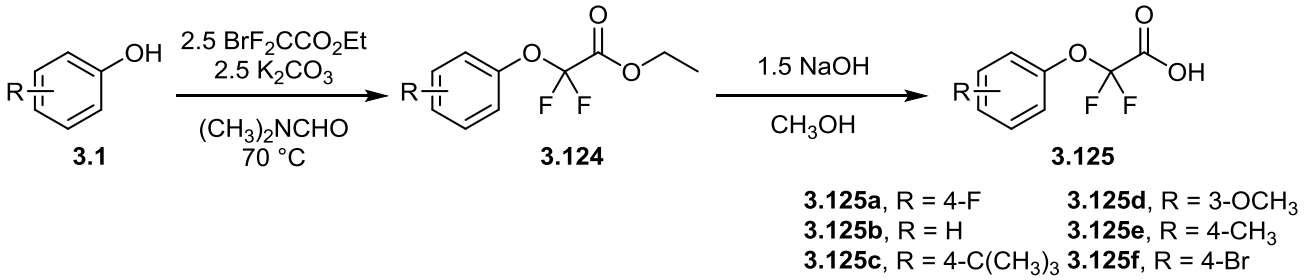

Scheme 3.35. Synthesis of aryloxy difluoroacetic acids

To test the applicability of PDC-F with Sel-F for the synthesis of trifluoromethoxy arenes, studies employed **3.125a** and ^{19}F NMR analysis was carried out on deuterochloroform extracts of the crude reaction mixture (Table 3.12). Trace amounts of **3.126** were observed after irradiation of solution containing **3.125a** and Sel-F under the standard PDC-F conditions, albeit the vast majority of starting difluoroacid **3.125a** was recovered unreacted (entry 1). Prolonged irradiation lead to complete consumption of the starting diacid with an increase in integration at -58.6 ppm corresponding to **3.126** (entry 2); however, an assortment of other significant peaks appeared in the ^{19}F spectrum indicating the formation of multiple undesired byproducts. When the reaction was run in acetone or acetonitrile (entries 3, 4), no **3.126** was detected by ^{19}F NMR.

[g] Analytically pure material for complete characterization of **3.125** was never obtained. The suspected decomposition pathway leads to carbon dioxide, phenol and difluoromethyl carbene (**3.5**).

Table 3.12. Studies on PDC-F: 4-fluoro trifluoromethoxybenzene formation

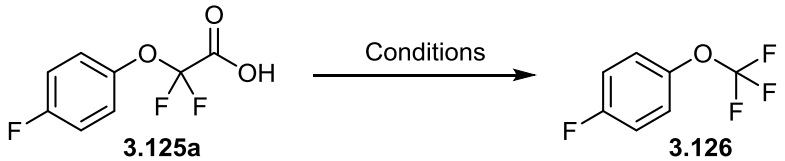

3.125a **3.126**

entry	conditions	comments[a]
1	1.5 NaOH, 3.5 Sel-F, in D_2O, 1 h @ 300 nm in a Falcon tube.	Trace amounts of **3.126** at -58.6 ppm. Ratio of **3.125a**: **3.126** is 16:1
2	1.5 NaOH, 3.5 Sel-F, in D_2O, 21 h @ 300 nm in a Falcon tube.	More **3.126** observed at -58.6 ppm. Significant peaks at -65.8 ppm (d), -76.5ppm, -77.8 ppm, -81.0 ppm, -81.3 ppm.
3	1.5 NaOH, 3.5 Sel-F, in $(CD_3)_2CO$, 21 h @ 300 nm in a microwave vial.	No **3.126** detected. New peak at -61.9 ppm.
4	1.5 NaOH, 3.5 Sel-F, in CD_3CN, 21 h@ 300 nm in a microwave vial.	No **3.126** detected. New peak at -61.9 ppm.
5	1.0 DtBuPy, 3.5 F-TEDA-PF_6, in CD_3CN, 3h @ 250 nm + 300 nm lamps in a cuvette.	Small amounts of **3.126**. Ratio of **3.125a**: **3.126** = 6: 1
6	1.5 NaOH, 3.5 Sel-F, in D_2O, 2.5 h @ 250 nm + 300 nm lamps in a cuvette.	10% NMR yield based on PhF trace amounts of **3.125a** detected
7	1.5 NaOH, 5.0 Sel-F, in D_2O, 2.5 h @ 250 nm + 300 nm lamps in a cuvette.	10% NMR yield based on $PhOCF_3$ trace amounts of **3.125a** detected

[a] ^{19}F NMR spectra referenced to BF_4 at -150.4 ppm

Before proceeding further, a definitive study was carried out with phenoxydifluoroacetic acid (**3.125b**) employing an authentic sample of trifluoromethoxybenzene (**1.83**) in an NMR spike experiment. Experiments in Table 3.12 relied on the reasonable assumption that the monitored ^{19}F NMR peak was the trifluoromethoxy signal of **3.126**. However, as only trace amounts of **3.126** had been observed, rigorous proof of the existence of **3.126** by isolation was not possible.

An aqueous solution containing **3.125b**, sodium hydroxide, and saturated with Sel-F was irradiated at 300 nm for 19 hours and the deuterochloroform extract was immediately subject to ^{19}F NMR analysis. As seen in Figure 3.4, the top ^{19}F NMR spectrum is the crude reaction mixture and shows signals for both unreacted starting material at -77.3 ppm and the **1.83** trifluoromethoxy signal at

-58.1 ppm. Immediately below is the ^{19}F NMR spectrum of an authentic sample of trifluoromethoxy benzene (**1.83**) with a signal for the trifluoromethoxy moiety at -58.1 ppm. The bottom ^{19}F NMR spectrum shows the effect of adding a small amount of the authentic **1.83** sample to the crude reaction mixture. The peak at -58.1 ppm greatly increases in magnitude, strongly supporting the hypothesis that the candidate peak in the crude reaction mixture was indeed trifluoromethoxy benzene. Furthermore, the successful fluorodecarboxylation of **3.125b** supports the assertion that the peak at -58.6 ppm is the fluorodecarboxylation product of **3.126**.

Examination of the UV-VIS absorption spectra for fluoroacid salt **3.129** shows that the addition of fluorine causes a hypsochromic shift in respect to the des-fluoro acid salt **3.127** (Figure 3.5). Therefore, 254 nm lamps were placed into the photoreactor and the reaction vessel was changed to a quartz cuvette thereby allowing the reaction mixture to be exposed to lower wavelength light. Within 3 hours, fluoroacid **3.125a** was entirely consumed (Table 3.12, entries 6, 7). With the addition of known quantities of fluorobenzene or trifluoromethoxybenzene into the deuterochloroform extracts, an NMR yield of 10% was obtained for **3.126**. When the reaction was carried out in acetonitrile, lower yields and conversions were observed (entry 4).

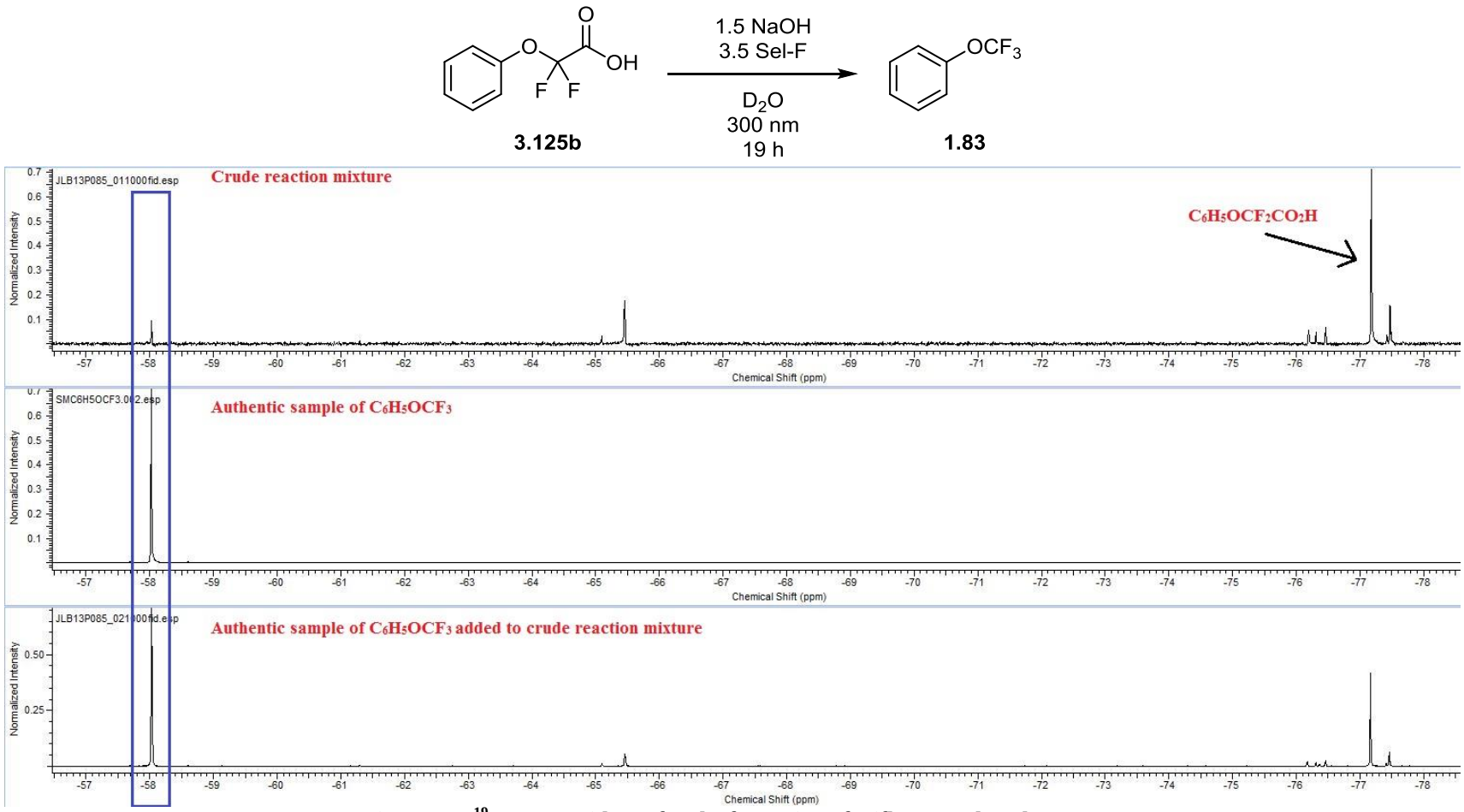

Figure 3.4. ^{19}F NMR evidence for the formation of trifluoromethoxybenzene

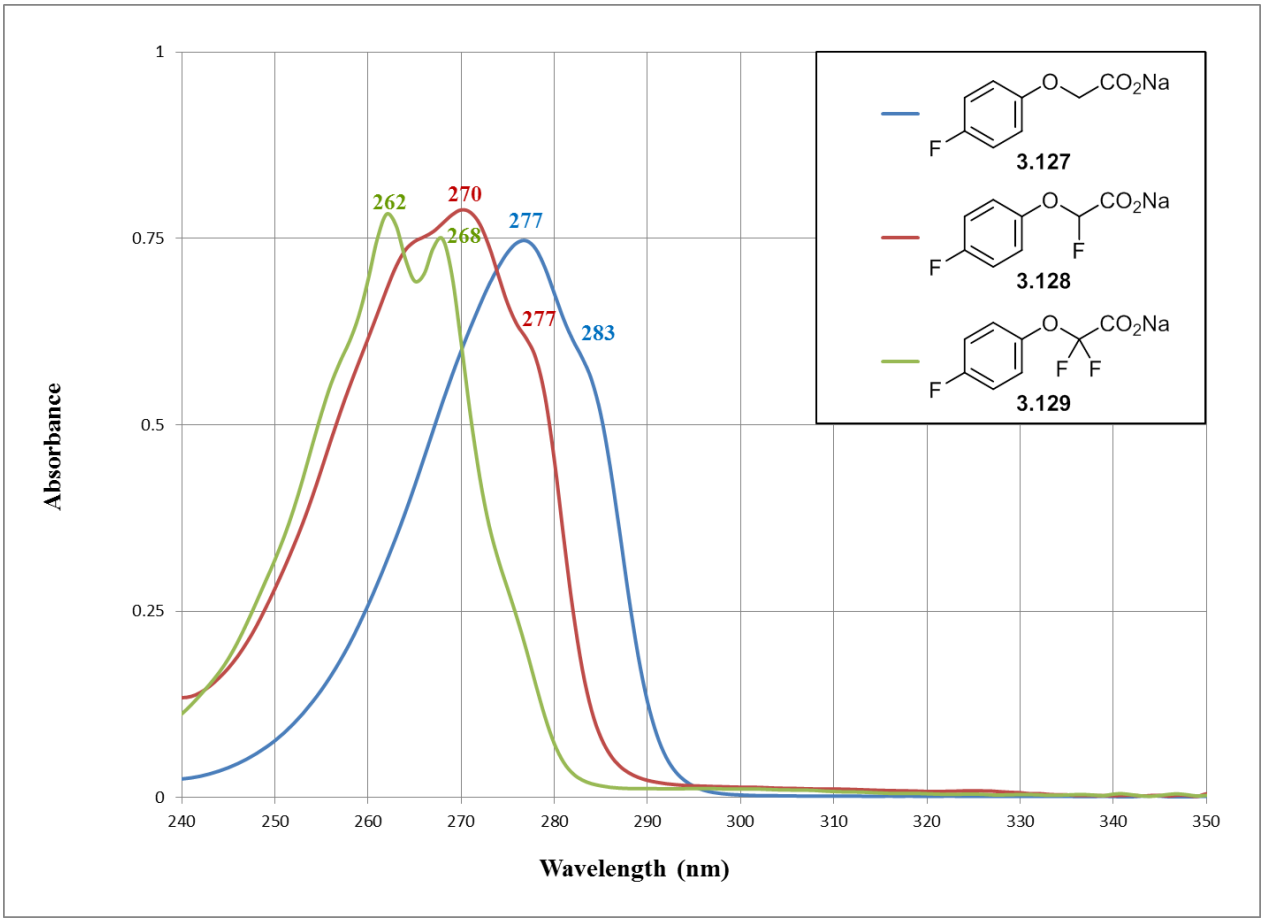

Figure 3.5. UV-VIS spectra for 4-fluorophenoxyacetic acids (0.001M in H_2O)

Having established that PDC-F with Sel-F of phenoxy difluoroacetic acids could yield the trifluoromethoxy arenes, semi-purified samples of **3.125c-e** were subjected to the best PDC-F reaction conditions obtained from studies on **3.125a** in Table 3.12 (Scheme 3.36). Only **3.125c** produced ^{19}F signals which could correspond to the PDC-F product. The low yields of trifluoromethoxybenzene products thus far might be explained by the addition of two fluorine atoms to the acid, making oxidation of the aromatic core more difficult. In subsection 3.3.3, PDC-F of methoxy acid **3.62** and napthyloxy acid **3.47** containing acids failed to undero PDC-F because the aryl ring was too electron rich (Scheme 3.26). Since the installation of two inductively withdrawing fluorine atoms on the acids caused a hypsochromic shift in the UV-absorption spectrum, the counterbalance of electron densities in

the benzenoid core could aid in the formation of fluorodecarboxylation product. Unfortunately, PDC-F of **3.125d** and **3.125e** did not yield detectable amounts of aryl trifluoromethyl ether (Scheme 3.36, lower section).

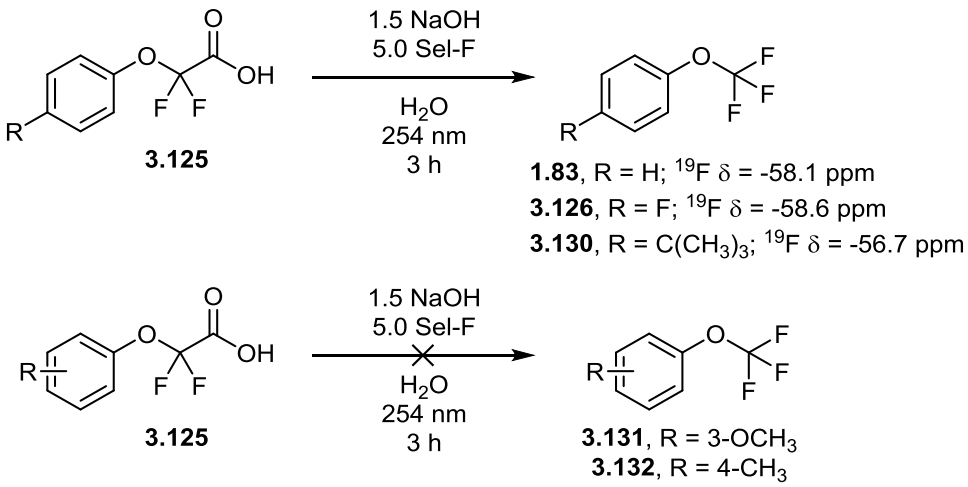

Scheme 3.36. PDC-F for aryl trifluoromethyl ether synthesis

Having obtained proof-of-concept for PDC-F with Sel-F as a candidate reaction for the synthesis of trifluoromethoxy arenes, my studies on aryl trifluoromethyl ethers ended. I will elaborate on ideas regarding the future direction of trifluoromethoxybenzene synthesis in Chapter 5.

3.3.6 Mechanism of photodecarboxylative fluorination with Sel-F

In Chapter 1, acyl hypofluorites (**1.55**) were discussed as intermediates for radical decarboxylative fluorination with fluorine gas (Scheme 1.10).[36,39] It is reasonable to suggest that radical decarboxylative fluorination is mediated by photochemical decomposition of acyl hypofluorites (**1.55**) similar to the Hunsdieker reaction (Scheme 3.37). In support of this hypothesis is the observation that aqueous sodium carboxylates are suitable nucleophiles for the formation of acyl hypofluorites when a stream of fluorine gas is bubbled through the solution.[37] PDC-F with Sel-F is also an aqueous reaction

employing sodium carboxylates and Sel-F has also been demonstrated to transfer fluorine to heteroatomic nucleophiles such as nitrogen.[194]

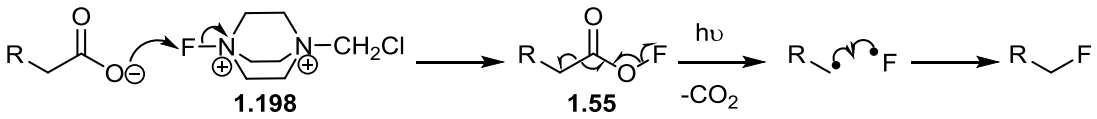

Scheme 3.37. Hypofluorite-mediated mechanism for PDC-F with Sel-F

However, it is unlikely that acyl hypofluorites are responsible for PDC-F with Sel-F because there is overwhelming evidence to discount hypofluorite decomposition as the main reaction pathway. Although the argument may be made that hypofluorites are too unstable to observe at 25 °C, acyl hypofluorite signals have never been observed in my ^{19}F NMR studies. In Scheme 3.27, sodium dodecanoate (**3.111**) was unsuitable for PDC-F. If acyl hypofluorites could be formed from arylacetic acids and aryloxyacetic acids, there is no reasonable explanation for why **3.111** could not also form the hypofluorite. Lastly, if acyl hypofluorites were involved, thermolysis of the acyl hypofluorite would also generate the requisite benzyl or phenoxymethyl radical for fluorination. As demonstrated in Scheme 3.24, photochemical stimulation is required for fluorodecarboxylation. Based on these observations, the involvement of acyl hypofluorites in PDC-F is improbable.

The following mechanism is proposed for the non-sensistized photodecarboxylative fluorination of aryloxyacetic acids with Sel-F (Scheme 3.38). Excitation of the B band transition of the aryloxy nucleus of **3.82** (for simplicity, phenoxyacetic acid is depicted) generates an excited state **3.83** which is shown as a triplet diradical since intersystem crossing of anisole derivatives is rapid.[195] This activated intermediate may be reversibly oxidized by Sel-F to a zwitterionic species **3.84** that will decarboxylate irreversibly to the phenoxymethyl radical (**2.33**) which is then fluorinated by Sel-F or **3.135**.

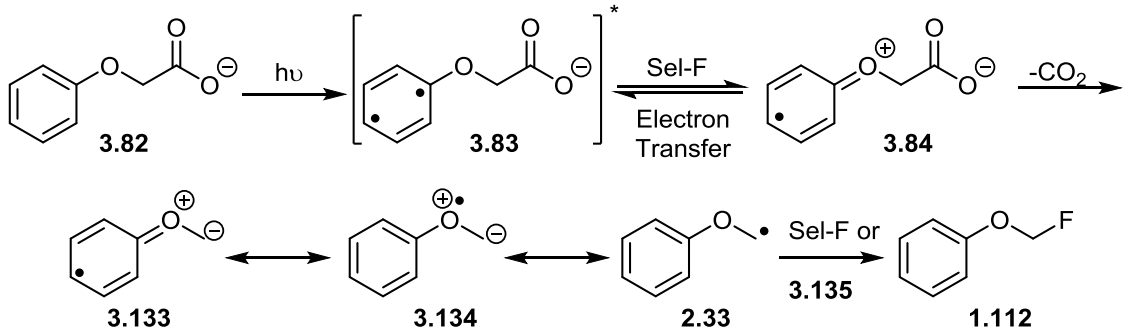

Scheme 3.38. Proposed mechanism for PDC-F with Sel-F

From computational studies on the radical intermediate represented by resonance structures **3.133**, **3.134**, **2.33** (see section 3.5), **2.33** is the most accurate representation of the intermediate and the fluorination step is likely radical in nature. However, it is unclear wither the final fluorination step resembles an S_H2 reaction with Sel-F (Scheme 3.39 A), an S_H2 reaction with **3.135** (Scheme 3.39 B), or if other reactions involving further SET processes are involved (Scheme 3.39 C, D).

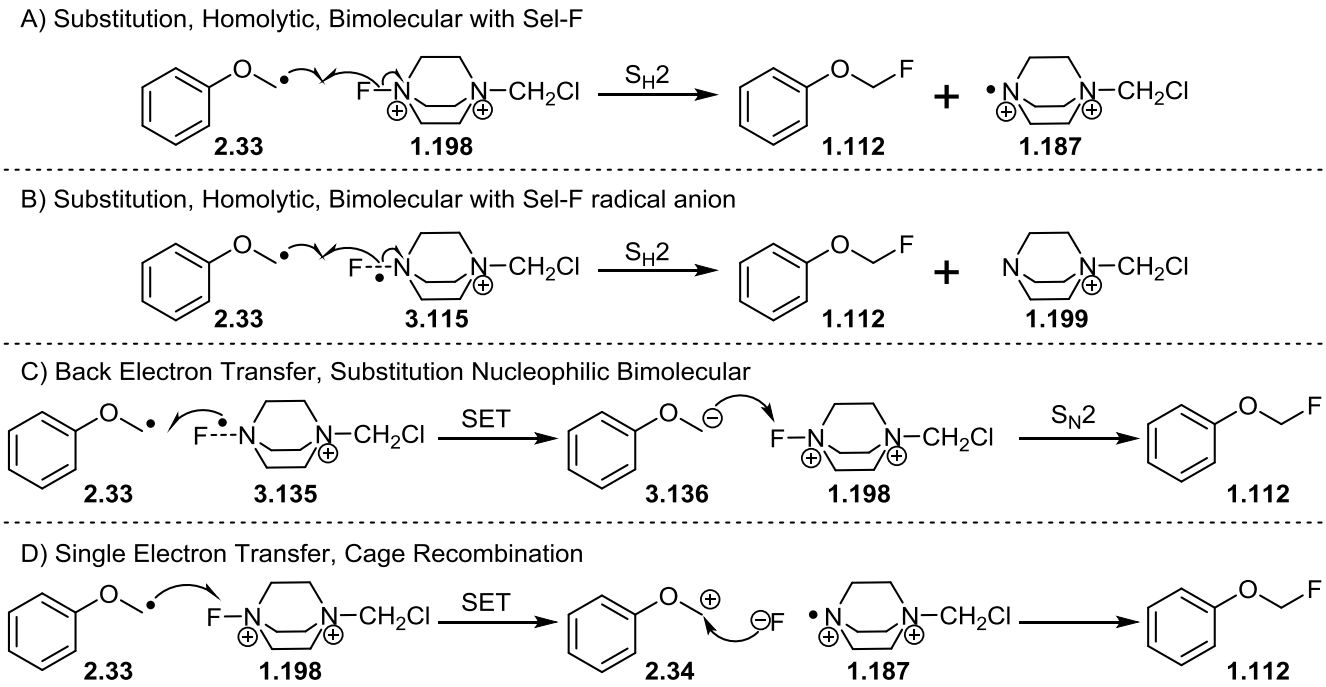

Scheme 3.39. Possible fluorination pathways for phenoxymethyl with Sel-F

The proposed photoelectron transfer mechanism is supported by wavelength studies in Table 3.6 and the 350 nm experiment in Scheme 3.40. At 300 nm, both **3.42** and **3.40a** are effectively photodecarboxylated in >95% yields after one hour of irradiation. After one hour of irradiation at 350 nm, **3.43** is observed in 38% yield and 19% yield of **1.70** is obtained. A comparison of the UV-VIS absorption spectra of **3.87** and **3.127** (Figure 3.6) with the emission profile spectra for Rayonet 350 nm (RPR-3500) photoreactor lamps (Figure 3.7, obtained from the Rayonet website)[196] shows that only a small proportion of light can be absorbed by **3.127** and even less may be absorbed by **3.87**. The low yields of **3.43** (and even lower yields of **1.70**) can be explained if the mechanism of PDC-F requires photoexcitation of the aromatic ring. Given the poor overlap between acid absorption spectra and lamp emission spectra, few photons of light are available to initiate PDC-F. In contrast, the emission profile of the Rayonet 300 nm (RPR-3000) lamps almost completely covers the absorption spectrum of both acids with yields of PDC-F product in near quantitative yields for both **3.43** and **1.70**.

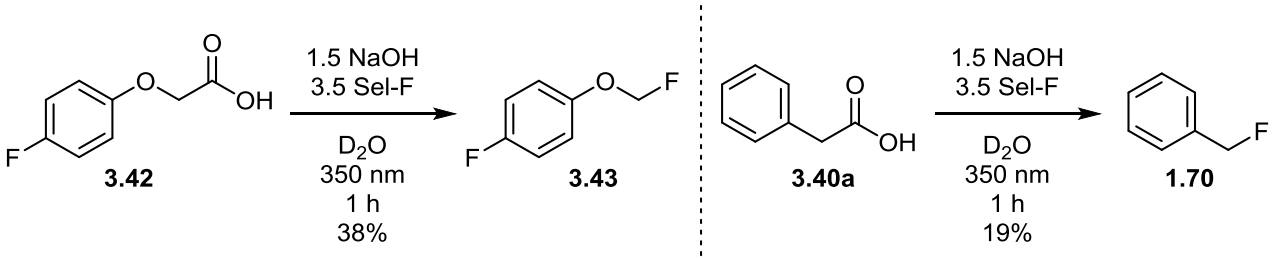

3.42 **3.43** **3.40a** **1.70**

Scheme 3.40. PDC-F with Sel-F at 350nm

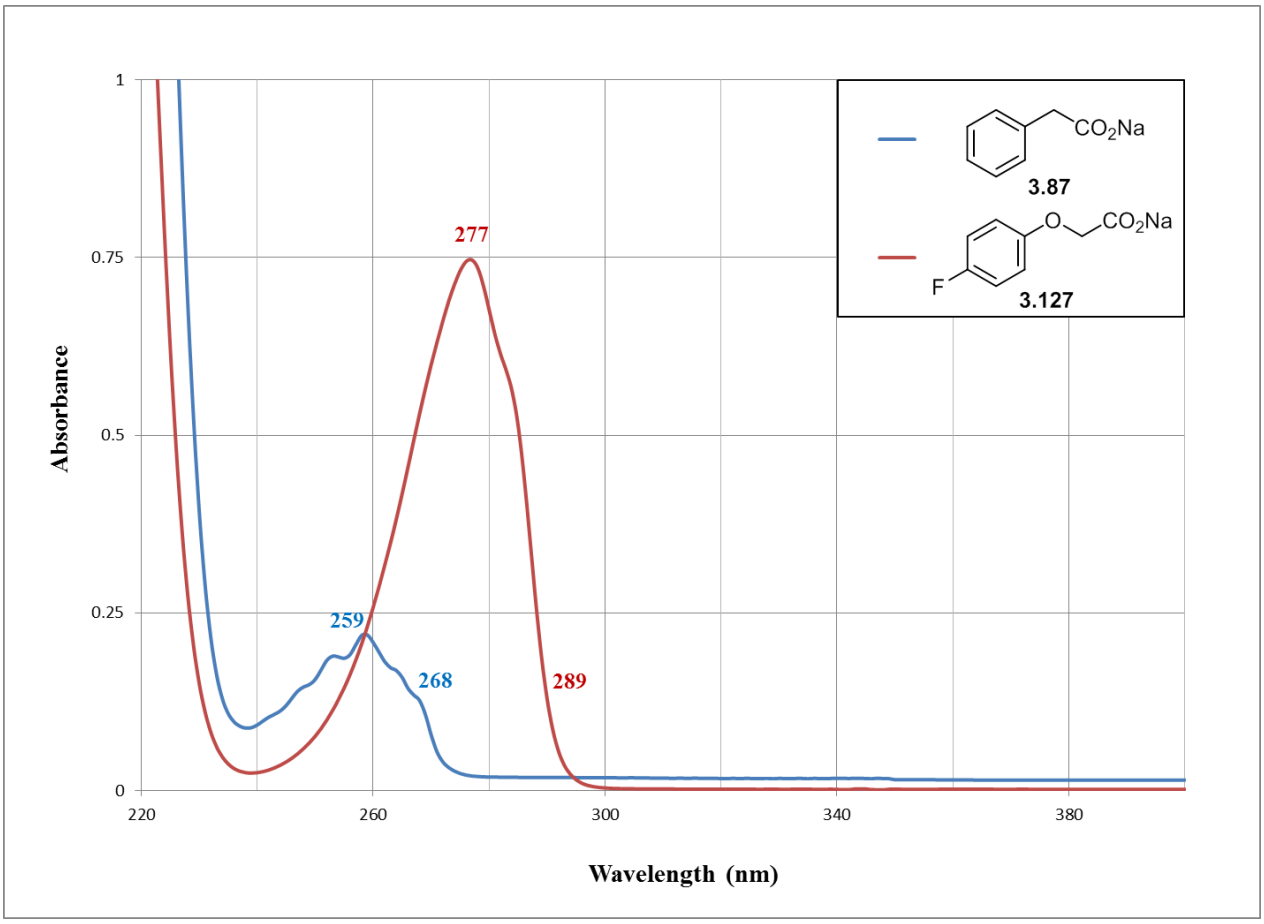

Figure 3.6.UV-VIS spectral comparison of 3.87 and 3.127 (0.001M in H_2O)

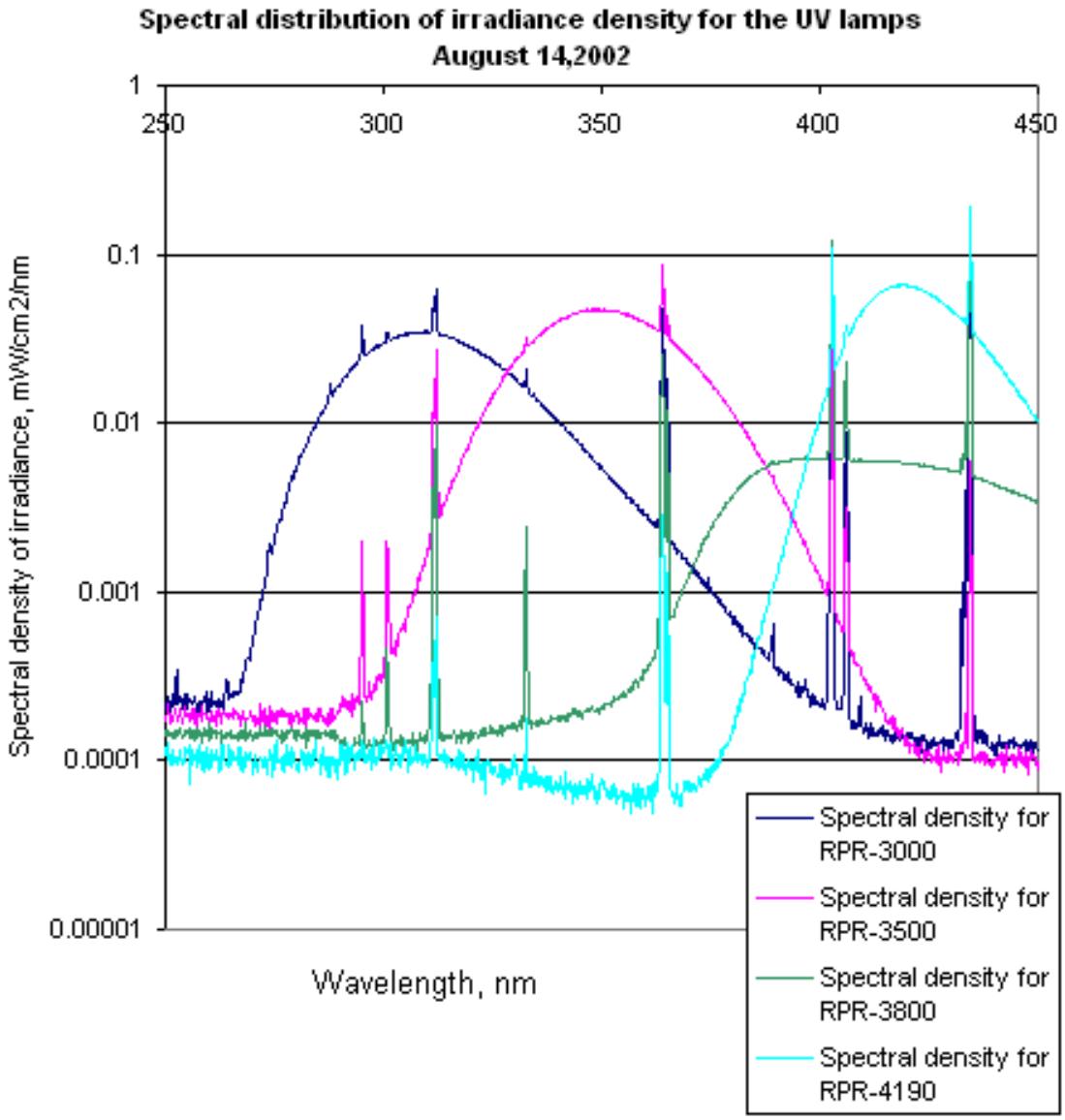

Figure 3.7 Spectral distribution of irradiance density for Rayonet UV lamps[196]

Examination of the overlaps between emission spectra for the photoreactor lamps (Figure 3.7) and UV-VIS absorption spectra of 4-fluorophenoxy acetic acids **3.127**-**3.129** (Figure 3.5) provide further supporting evidence for the PET-mechanism. A similar irradiation time to wavelength correlation can be drawn for **3.128** as was drawn from **3.127** with 300 nm and 350 nm light. The absorption range for the α-fluoro acid **3.128** experiences a hypsochromic shift of 7 nm and longer

reaction times are required for optimal fluorodecarboxylation. Reflecting this trend, α-difluoro acid **3.129** experiences a further hypsochromic shift of 8 nm resulting in the need for 254 nm lamps for effective PDC-F.

The PET mechanism adequately explains why some of the substrates in Scheme 3.27, failed to photodecarboxylate. Alkyl acid **3.111** does not contain a photoactive aryl-moiety; and therefore, cannot participate in PDC-F. Single electron oxidation of benzoic acid (**2.54**) is considerably more difficult than oxidation of aryoxy acetic acids and aryl acetic acids.[197] Strong evidence to support the mechanism in Scheme 3.3.20 can be obtained from the experiments with *N*-phthaloylglycine (**3.74**) (Scheme 3.28). Unlike the phenoxy moiety, it is well established that the phthaloyl moiety acts as an oxidant when photoexcited.[183b,198] Thus, the excitation of **3.137** with 300 nm light leads to an internal electron transfer event from the tethered carboxylate to the phthaloyl diradical **3.138** (Scheme 3.41). The resulting decarboxylation intermediate **3.140** can be better expressed as anionic resonance structure **3.142** which can be quenched by a proton source resulting predominately in *N*-methyl phthalimide (**3.143**). PDC-F product **1.191** can be obtained from quenching **3.142** by Sel-F and is the minor reaction pathway for PDC of **3.74**.

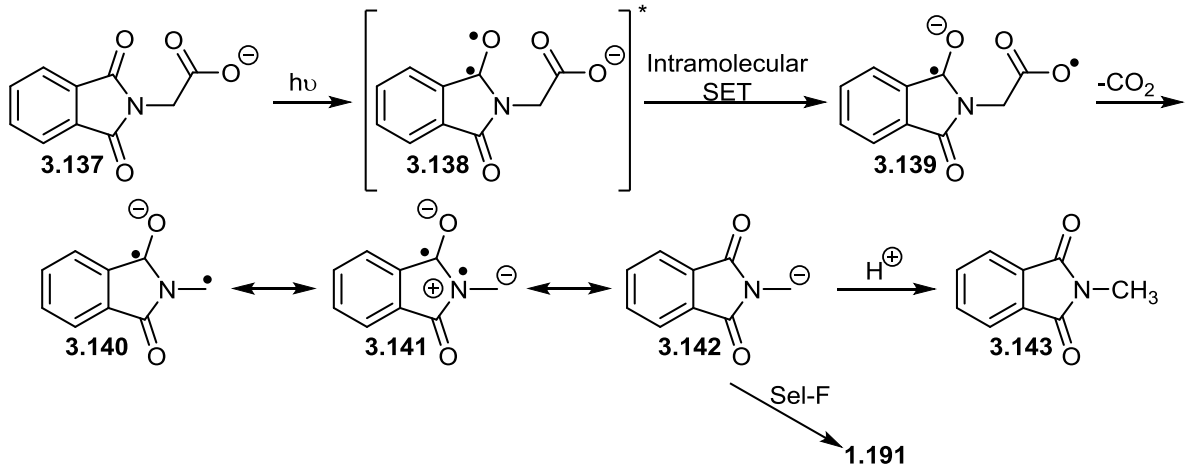

Scheme 3.41. Alternative mechanism for PDC-F of *N*-phthaloylglycine

Taking into consideration the literature precedent for photodecarboxylation of sodium phenylacetate (**3.87**), PDC-F with Sel-F of arylacetic acids is postulated to occur through a slightly different mechanism than PDC-F of aryloxyacetic acids (Scheme 3.42). Excitation of the benzenoid nucleus to the singlet state is followed by oxidation by Sel-F to generate intermediate **3.89a**. An internal electron transfer event occurs from the carboxylate to the phenylium[188] generating carboxy radical **3.90a** which rapidly decarboxylates to phenylmethyl (**3.86a**). Fluorine transfer to the phenylmethyl radical would resemble any of the S_H2 or SET pathways presented in Scheme 3.3.21. Evidence presented in support of a photoelectron transfer mechanism for **3.82** is also applicable to the PDC-F of arylacetic acids with Sel-F. The observed PDC-F of **3.40b** supports the mechanism of internal electron transfer as this is the simplest explanation for radical generation at the homobenzylic position (Table 3.10, entry 5).

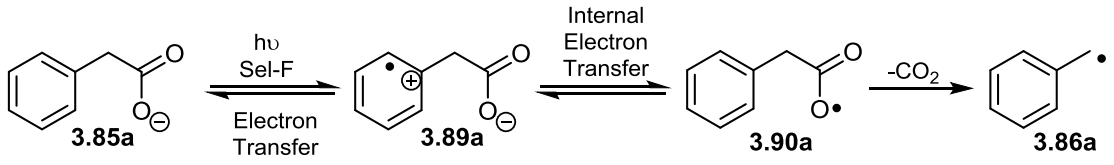

Scheme 3.42. Proposed mechanism for PDC-F of phenylacetic acid with Sel-F

3.4 Photodecarboxylative fluorination utilising NFSI

Studies on PDC-F with Sel-F substrate scope in the previous section highlight a deficiency of the PDC-F reaction: the inability to fluorodecarboxylate electron-rich aromatics such as napthoxyacetic acid **3.47** and **3.107**, and substrates that contain benzylic protons such as **3.108** and **3.110**. ^{1}H and ^{19}F NMR experiments detected ionic ring fluorination of electron-rich aromatics and non-selective fluorination of weak C-H bonds. Both of these reactions are characteristic of the desired ionic fluorinating ability of Sel-F and are responsible for the popularity of Sel-F as an electrophilic fluorination agent.[6,10,108]

It has been postulated that the electrophilic reactivity of the fluorinating agents correlates with higher reduction potentials.[10c,f] The challenge is that most of the known sources of atomic fluorine, such as elemental fluorine and xenon difluoride, have significantly higher reduction potentials (E°= 2.87 V and 2.64V respectively)[199] than Selectfluor™ (E° = 0.33V (SCE))[110] (Figure 3.8), and thus will likely have more significant substrate limitations. Substitution of NFSI for Sel-F is a potential solution as NFSI is a weaker oxidant with a lower measured reduction potential of E° =-1.24V (SCE).[110] There are multiple conflicting reports for the reduction potential of both Sel-F and NFSI and the most recently reported values are presented.[110a]

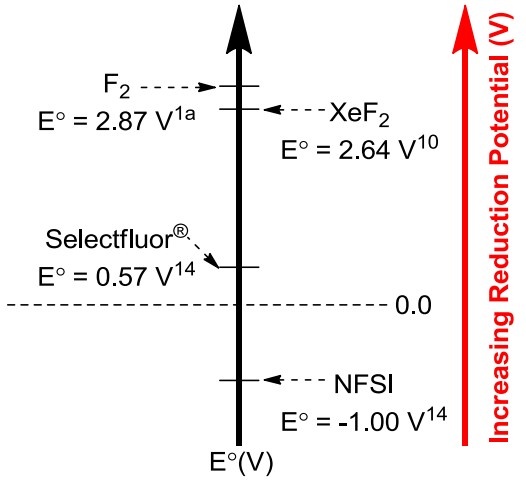

Figure 3.8. Comparison of radical fluorinating agents by increasing reduction potential (referenced to the standard hydrogen electrode)

In Scheme 3.18, a combination of NFSI and triethylamine was shown to affect PDC-F of phenoxyacetic acid (**2.26**) in benzene irradiated by 300 nm light. Studies resumed on this system with the hypothesis that NFSI could serve as both the PET oxidant and radical fluorine transfer agent in place of Sel-F through an identical reaction mechanism. During the course of optimization studies, it became clear that employing acetone as a solvent enabled an alternate reaction pathway that did not involve direct excitation of the carboxylic acid substrates. This section aims to simultaneously describe two reaction systems: a non-sensitized PDC-F with NFSI in acetonitrile, and a sensitized PDC-F with NFSI in acetone.

3.4.1 Optimisation of photodecarboxylative fluorination with NFSI

Studies on the PDC-F with NFSI resumed with the screening of a variety of organic amine bases for PDC-F with NFSI (Table 3.13). As expected, the control experiment (in the absence of base) of PDC-F with NFSI gave low yields as observed by ^{1}H NMR spectroscopy (entry 1). The addition of triethylamine (**3.146**) improved the yield to 46% (entry 2). A distinct colour change was observed in

the reaction mixture immediately upon the addition of base. Furthermore, this coloured intermediate was no longer present after photochemical stimulation of the reaction mixture. ^{19}F NMR spectroscopic analysis at t=0 for triethylamine (entry 2) showed the formation of fluorotrialkylammonium species **3.144** (~63 ppm), which suggests a fluorine transfer between amines is occurring (Scheme 3.43). *N*-Fluorine transfer reactions are known for Sel-F,[194] and under these reaction conditions, is occurring reversibly with NFSI. Sel-F is a trifluoroalkylammonium species that is also an atomic fluorine transfer agent for PDC-F. Therefore, the new fluorotriethylammonium (**3.144**), formed *in-situ* by the reaction of triethylamine (**3.146**) with NFSI, was examined for atomic fluorine transfer abilities.

A PDC-F reaction with sufficient triethylamine base to consume all of the NFSI and deprotonate all of the carboxylic acid was executed (entry 3). ^{19}F NMR spectroscopic analysis at t=0 showed complete conversion of NFSI to fluorotriethylammonium (**3.144**); however, no PDC-F product was observed after 2 hours of irradiation at 300 nm, which confirms that **3.144** is not a novel source of atomic fluorine. NFSI is the active reagent for PDC-F and the optimization target was to find a base that would selectively deprotonate the carboxylic acid substrate **3.44** but not react with NFSI.

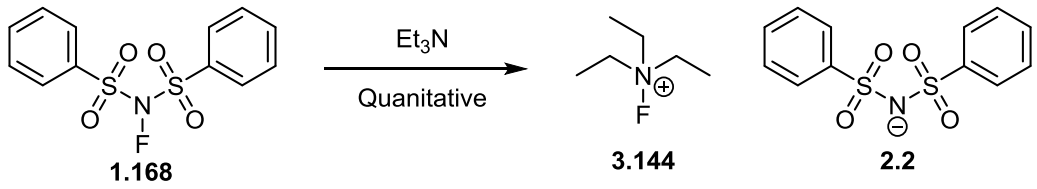

Scheme 3.43. Formation of a fluorotriethylammonium species at ~63 ppm (^{19}F NMR)

Next, the more hindered amine base diisopropylethylamine (**3.147**) was tested for PDC-F with NFSI (entry 4). The characteristic brown-red colour was also observed upon addition of base, indicating that NFSI and base had reacted. The yield of PDC-F product was moderate after 2 hours of irradiation at 300 nm. While proton-sponge **3.148** is known to be selective at abstracting acidic protons,

the molecule itself is rather electron-rich and was observed to react with NFSI (entry 6). The amidate base DBU (**3.145**) also produced the characteristic brown-red colour upon addition to the NFSI solution. Prolonged stirring of the solution (~10 min) restored the solution to a light yellow colour and suggests the N-F transfer reaction from NFSI to DBU is not thermodynamically favourable. Correspondingly, the yield of PDC-F product after 2 hours of irradiation at 300 nm was higher than observed with **3.146** or **3.147** as a base (61%, entry 5).

Table 3.13 PDC-F with NFSI: base screen

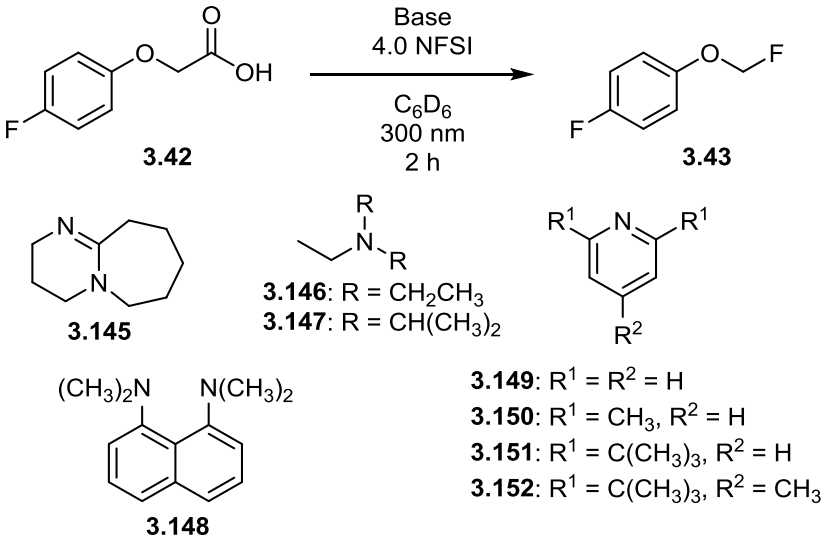

entry[a]	base	equivalents	yield[b]	entry[a]	base	equivalents	yield[b]
1	no base	0	7	7	**3.149**	1.0	55
2	**3.146**	1.0	46[c]	8	**3.150**	1.0	80
3	**3.146**	5.0	0	9	**3.151**	1.0	75[e]
4	**3.147**	1.0	43[c]	10	**3.152**	1.0	81[e]
5	**3.145**	1.0	61[c]	11	**3.152**	0.5	81[e]
6	**3.148**	1.0	0[d]	12	**3.152**	0.25	65[f]

[a]Reaction conditions: Base (as indicated), NFSI (4.0 equiv.), **3.42** (1.0 equiv, 0.05 mmol) at 0.1 M in deuterobenzene, irradiated at 300 nm for 2 h. [b]The yields were obtained by ^{1}H NMR spectroscopy using ethyl trifluoracetate as an internal standard. [c]NFSI reacts with base forming an ammonium fluoride. [d]Electrophilic aromatic fluorination of base observed. [e]Average value of 3 trials. [f]Average value of 2 trials.

Investigations into nitrogen bases continued with pyridine and pyridine derivatives (entries 7-12). Hindered pyridine bases, with substituents at the 2 and 6 positions, provided superior yields of the

PDC-F products than the parent compound pyridine (**3.149**, entry 7). PDC-F with lutidine (**3.150**) provided high yields of **3.43** in benzene (entry 8); however, it was found to precipitate with the carboxylate salt of **3.42** in solvents such as acetone. More sterically hindered di-*tert*-butyl pyridine bases **3.151** (DtBuPy) and **3.152** (DtBuMPy) were considered best for PDC-F with NFSI (entries 9, 10) and high yields could be maintained with even sub-stoichiometric amounts of **3.152** (entry 11).

PDC-F with NFSI was investigated over a broad range of solvents (Table 3.14). High yields of fluorination products could be achieved in non-polar solvents (entries 1-4); however, with polar solvents, solubility problems were encountered. Mixed-solvent systems, such as aqueous acetone (entry 5), aqueous acetonitrile (entry 6), and neat methanol (entry 7), failed to solubilize NFSI and failed to deliver PDC-F product. As expected, PDC-F did not occur in neat DMSO as the solvent begins to absorb UV light at 330 nm (entry 8); however, trace amounts of DMSO could be added into acetone or acetonitrile to improve substrate solubility when necessary. A suitable balance of effective PDC-F and reagent solubility was found for neat acetone and neat acetonitrile (entries 9, 10) providing fluoroether **3.43** in high yields for both solvents.

Unlike acetonitrile, acetone is a known triplet sensitizer[184,185] and has been shown to catalyze the photodecarboxylation of alkyl carboxylates in the presence of SET acceptors, such as phthalimide.[183b] At this point, I realized that the PDC-F in acetone (entry 9) may be operating under a different mechanism than the PDC-F reaction in acetonitrile (entry 10). Both PDC-F with NFSI in acetone and PDC-F with NFSI in acetonitrile were examined in all subsequent reaction optimization investigations as different reactions operating under different reaction mechanisms.

Table 3.14. PDC-F with NFSI: solvent screen

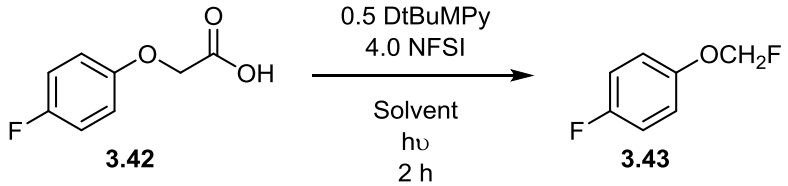

entry[a]	solvent	yield[b]	entry	solvent	yield[b]
1	C_6D_6	81	6	CD_3CN: D_2O 1:1	0[c]
2	$C_6D_5CD_3$	69	7	CD_3OD	0[c]
3	CD_2Cl_2	85	8	$(CD_3)_2SO$	0
4	$CDCl_3$	81	9	CD_3CN	80[d]
5	$(CD_3)_2CO$: D_2O 1:1	0[c]	10	$(CD_3)_2CO$	82[d]

[a]Reaction conditions: DtBuMPy (0.5 equiv), NFSI (4.0 equiv), **3.42** (1.0 equiv, 0.05 mmol) at 0.1 M in deuterated solvent, irradiated at 300 nm for 2 h. [b]The yields were obtained by ^{1}H NMR spectroscopy using ethyl trifluoracetate as an internal standard. [c]NFSI not sufficiently soluable. [d]Average value of 4 trials.

Continuing the optimisation studies in acetonitrile, possible light sources for PDC-F with NFSI were examined. As shown in Table 3.15, a variety of light sources ranging from ultraviolet (entries 1, 2, 6, 7) to visible (entries 3-5) were tested. Only entry 1, PDC-F under high intensity 300 nm light from the photoreactor, provided fluoromethyl ether **3.43**. Many sources of visible light also emit trace amounts of UV light, but they failed to promote PDC-F with NFSI. Photochemical stimulation of aryloxyacetic acids by 350 nm UV light could still initiate the PDC-F with Sel-F as the stronger oxidant ability of Sel-F may facilitate the PET event. Being a weaker oxidant, NFSI is less able to facilitate the PET event and this may explain by irradiation with 350 nm light is insufficient to initiate PDC-F with NFSI (entry 2). This observation supports the original hypothesis that PDC-F with NFSI could allow access to aryl fluoromethyl ethers containing oxidation-sensitive aromatic ring.

Table 3.15 PDC-F with NFSI in acetonitrile: wavelength screen

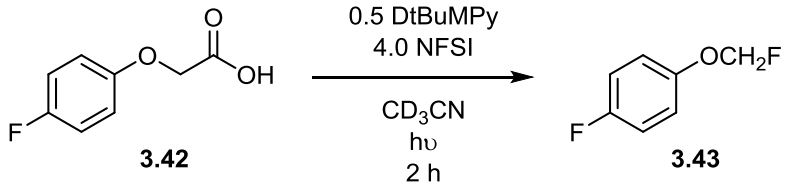

3.42 **3.43**

entry[a]	light source[b]	yield[c]
1	300 nm	82[d]
2	350 nm	0
3	compact fluorescent	0
4	halogen	0
5	incandescent tungsten lamp	0
6	Desert lamp	0
7	Tropical lamp	0

[a]Reaction conditions: DtBuMPy (0.5 equiv), NFSI (4.0 equiv), **3.42** (1.0 equiv, 0.05 mmol) at 0.1 M in deuterated acetonitrile, irradiated by light source (as indicated) for 2 h. [b]The light sources utilized for these experiments were not strictly monochromatic. The indicated wavelength refers to the maximum light intensity emitted. [c]The yields were obtained by ^{1}H NMR spectroscopy using ethyl trifluoracetate as an internal standard. [d]Average value of 4 trials.

Light source optimisation studies of PDC-F with NFSI in acetone show this reaction to be very different than the reaction in acetonitrile (Table 3.16). While the trace amounts of UV light emitted from visible light sources (entries 3-5) did not initiate photodecarboxylation, all other UV light sources promoted the photodecarboxylative fluorination reaction (entries 1,2, 6-8). The difference in viable light sources between acetone and acetonitrile can be explained by treating acetone as the primary photoactive compound. Acetone has an absorption maximum at 270 nm and tails to 330 nm making it photoactive within both the 300 nm and 350 nm lamps emission profiles (entries 1, 2). Employing a photoactive solvent maximizes the absorption of UV light and enables commercially available terrarium lamps to be a viable light source for the photosensitized PDC-F with NFSI (entries 6-8). Prolonged irradiation of **3.42** with a tropical terrarium lamp allows for the synthesis of **3.43** in 71% NMR yield suggesting that photosensitized PDC-F with NFSI could be accessible without specialized photochemical apparatus.

Table 3.16. PDC-F with NFSI in acetone: wavelength screen

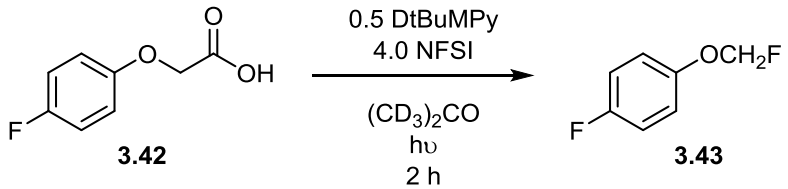

3.42 **3.43**

entry[a]	light source[b]	yield[c]
1	300 nm	80[d]
2	350 nm	85
3	compact fluorescent	0
4	halogen	0
5	incandescent tungsten	0
6	desert terrarium[e]	trace
7	tropical terrarium[f]	15
8	tropical terrarium[f] 16hr	71

[a]Reaction conditions: DtBuMPy (0.5 equiv), NFSI (4.0 equiv), **3.42** (1.0 equiv, 0.05 mmol) at 0.1 M in deuterated acetonitrile, irradiated by light source (as indicated) for 2 h. [b]The light sources utilized for these experiments were not strictly monochromatic. The indicated wavelength refers to the maximum light intensity emitted. [c]The yields were obtained by ^{1}H NMR spectroscopy using ethyl trifluoracetate as an internal standard.[d]Average value of 4 trials. [e]The desert terrarium lamp emitts broad spectrum UV light with a higher precentage in the UVA region. [f]The tropical terrarium lamp emitts broad spectrum UV light with a higher precentage in the UVB region.

I next investigated the stoichiometry of NFSI required for this transformation (Table 3.17). PDC-F with NFSI in acetonitrile does not proceed to completion when less than 2 equivalents of NFSI are employed (entries 1, 2). Interestingly, when 4 or more equivalents of NFSI are added to the reaction mixture, only one equivalent (approximately) of NFSI is consumed and PDC-F of **3.42** goes to completion. Acceptable yields are obtained employing as little as 3 equivalents of NFSI (entry 3) and yields are marginally better with 5 equivalents of NFSI. 4 equivalents of NFSI was the optimal amount for PDC-F with NFSI in acetonitrile and that the lower limit for successful PDC-F with NFSI was 3 equivalents. As shown in Table 3.18, PDC-F with NFSI in acetone appears to be more efficient. The reaction goes to completion with as little as 2 equivalents of NFSI (entry 2) and the best yields of PDC-F product occur with 3 equivalents of NFSI (entry 3). Monitoring the amount of NFSI consumed was not productive as prolonged irradiation of the acetone solution at 300 nm lead to degradation of NFSI.

Table 3.17. PDC-F with NFSI in acetonitrile: NFSI equivalents screen

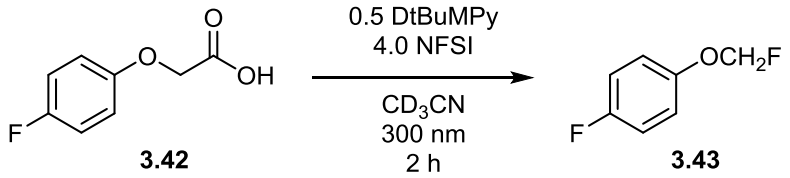

3.42 **3.43**

entry[a]	NFSI (equiv.)	NFSI consumed (equiv.)	conversion of **3.42** (%)[b]	yield (%)[c]
1	1	1	70	45
2	2	2	93	70
3	3	not determined	98	80
4	4	1.1	100	82[d]
5	5	1.1	100	86

[a]Reaction conditions: DtBuMPy (0.5 equiv), NFSI (as indicated), **3.42** (1.0 equiv, 0.05 mmol) at 0.1 M in deuterated acetonitrile, irradiated at 300 nm for 2 h. [b]The conversions were obtained by ^{1}H NMR spectroscopy using ethyl trifluoracetate as an internal standard. [c]The yields were obtained by ^{1}H NMR spectroscopy using ethyl trifluoracetate as an internal standard. [d]Average value of 4 trials.

Table 3.18. PDC-F with NFSI in acetone: NFSI equivalents screen

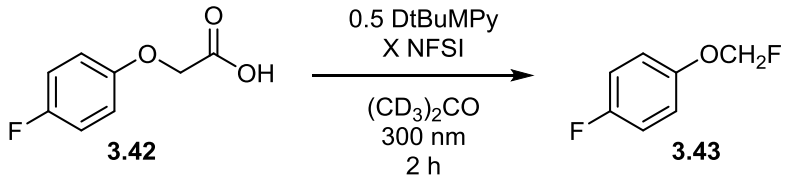

3.42 **3.43**

entry[a]	NFSI (equiv)	conversion[b]	yield[c]
1	1	81	41
2	2	100	72
3	3	100	82
4	4	100	80[d]

[a]Reaction conditions: DtBuMPy (0.5 equiv), NFSI (as indicated), **3.42** (1.0 equiv, 0.05 mmol) at 0.1 M in deuterated acetone, irradiated at 300 nm for 2 h. [b]The conversions were obtained by ^{1}H NMR spectroscopy using ethyl trifluoracetate as an internal standard. [c]The yields were obtained by ^{1}H NMR spectroscopy using ethyl trifluoracetate as an internal standard. [d]Average value of 4 trials.

The last parameter to be investigated was reaction time (Table 3.19). PDC-F with NFSI in acetonitrile is a slower reaction than PDC-F with Sel-F in water. Whereas the reaction with Sel-F is complete in 45 minutes, PDC-F with NFSI in acetonitrile requires approximately 2 hours for completion (entry 4). The reaction is >90% complete within 1 hour or irradiation (entry 3) and continuous irradiation for 3 hours is required for complete consumption of **3.43** (entry 5).

Table 3.19. PDC-F with NFSI: time screen.

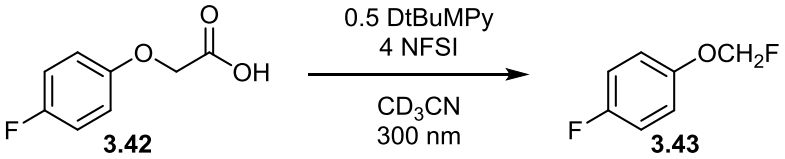

entry[a]	irradiation time	NMR yield[b]	Conversion[b]
1	10 min	26	30
2	30 min	65	77
3	60 min	78	92
4	120 min	80	95
5	3 h	80	100

[a]Reaction conditions: DtBuMPy (0.5 equiv), NFSI (4.0 equiv.), **3.42** (1.0 equiv, 0.05 mmol) at 0.1 M in deuterated acetonitrile, irradiated at 300 nm for the time specified. [b]The yields and conversions were obtained by ^{1}H NMR spectroscopy using ethyl trifluoracetate as an internal standard.

In stark contrast to the previous two PDC-F reactions, the PDC-F of **3.42** with NFSI in acetone is very fast (Table 3.20). Within 5 minutes, more than half of the starting carboxylic acid substrate is consumed (entry 2) and the reaction is nearly complete in 10 minutes (entry 4). This rate increase further supports the assertion that acetone is participating in the mechanism of photodecarboxylative fluorination. As the solvent, acetone is present in vast excess of the carboxylic acid substrate. While the coefficient of absorption for acetone is low, the amount of acetone present produces an effective increase in photon absorption from the photoreactor, leading to an increase in rate of PDC-F.

Table 3.20. Sensitized PDC-F with NFSI: time screen

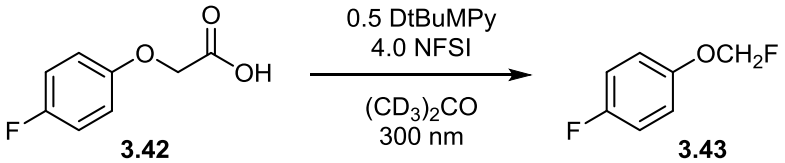

entry[a]	irradiation time	NMR yield[b]	Conversion[b]
1	2.5 min	14	15
2	5 min	46	57
3	7.5 min	57	69
4	10 min	80	97
5	30 min	81	100

[a]Reaction conditions: DtBuMPy (0.5 equiv.), NFSI (4.0 equiv.), **3.42** (1.0 equiv., 0.05 mmol) at 0.1 M in deuterated acetone, irradiated at 300 nm for the time specified. [b]The yields and conversions were obtained by ^{1}H NMR spectroscopy using ethyl trifluoracetate as an internal standard.

In summary, the general optimized conditions for PDC-F with NFSI was established to be 1.0 equivalents of substrate, 4.0 equivalents of NFSI, 0.5 equivalents of DtBuMPy in a 0.15 M solution in acetonitrile or acetone. In acetonitrile, a minimum of 1 hour irradiation with 300 nm light in a photoreactor is required for a successful PDC-F reaction and this reaction is similar to PDC-F with Sel-F. In acetone, a mere 15 minutes of irradiation with 300 nm light in a photoreactor is necessary for sensitized PDC-F. A tropical terrarium lamp may be used in place of a photoreactor for the PDC-F with NFSI in acetone, although the reaction requires much longer reaction times. A detailed discussion of the reaction mechanism in both acetone and acetonitrile can be found in subsection 3.4.3.

3.4.2 Synthesis of fluoromethoxyarenes by PDC-F with NFSI

Having established that PDC-F with NFSI is possible, I applied the sensitized PDC-F reaction to substrates which could be effectively fluorodecarboxylated in the presence of Sel-F as a benchmark for comparison (Scheme 3.44). PDC-F synthesis of **1.112** with NFSI (82% NMR yield) is comparible with results obtained by Sel-F (84% NMR yield). NFSI mediated synthesis of *meta*-butyl **3.153** in 84% isolated yield is almost identical to *para*-butyl **3.103** obtained in 83% yield with Sel-F. Brominated fluoromethyl ethers (**3.101**, **3.102**) were also obtained with NFSI in comparible yields to PDC-F with Sel-F. From all of the optimisation studies, yields of **3.42** obtained with NFSI were lower than yields obtained with Sel-F. Further electronic deactivation of the aryloxy ring with two chlorine substituents reduces the effectiveness of PDC-F with NFSI and **1.113** was obtained in 70% NMR yield using NFSI while the Sel-F system could deliver **1.113** in 86% isolated yield. Overall, the reactivity of the two methods is comparable.

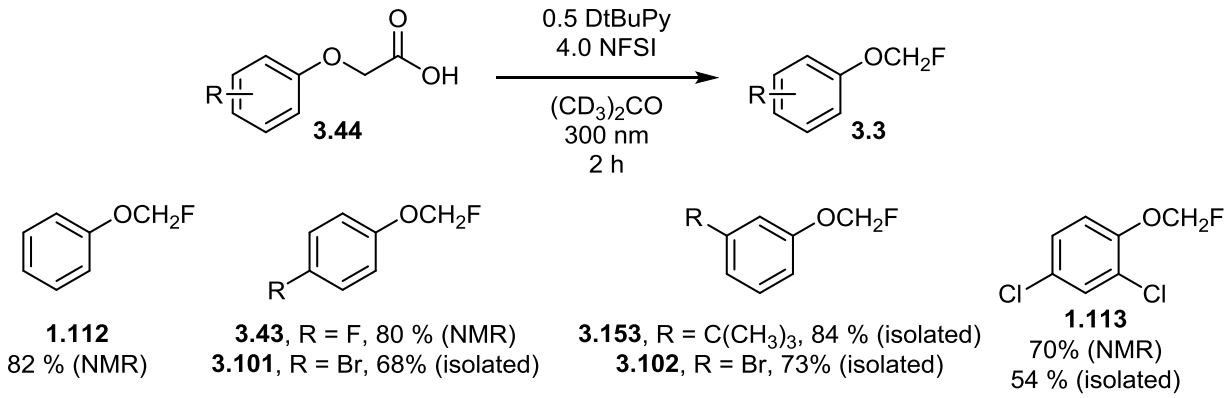

Scheme 3.44. Sensitized PDC-F with NFSI of substrates accessible by PDC-F with Sel-F

The hypothesis regarding NFSI's lower reduction potential enabling PDC-F of more electron-rich aryloxy acetic acids was tested next. All of the substrates shown in Scheme 3.45 provided either low yields or failed completely under PDC-F conditions with Sel-F (Schemes 3.25 and 3.26). Synthesis of fluoromethyl **3.104** was problematic under Sel-F conditions with ring fluorination as the predominant side product. Under the new sensitized PDC-F conditions with NFSI, **3.104** could be obtained in 75% NMR yield (54% isolated yield) and competitive ring fluorination was not observed. Similarly, PDC-F of **3.108** with Sel-F produced three different major fluorine-containing products whereas sensitized PDC-F with NFSI delivered **3.154** in 64% isolated yield.

Sensitized photofluorodecarboxylation of naphthyloxyacetic acids (**3.47**, **3.107**), an incompatible PDC-F substrate class with Sel-F, proceeded excellently with NFSI. This validates the hypothesis that a weaker oxidant such as NFSI would enable access to more electron-rich aryl fluoromethyl ethers. Fluoromethoxy napthalene **3.157** was isolated in near quantitative yields, **3.156** and **3.159** were isolated in 60 and 68% yield respectively, and the difluoromethyl ether **3.61** could be accessed in 40% NMR yield.

Apocynin derivative **3.105** was a more complex target as the counterbalance of the electron-donating (2-methoxy) and electron-withdrawing (4-methylketo) substituents on the aryl ring provided

an intriguing test for photodecarboxylative fluorination. PDC-F under aqueous Sel-F conditions only provided **3.105** in 23% isolated yield (34% by NMR analysis, Scheme 3.25). However, sensitized PDC-F with NFSI in acetone was very successful, providing **3.105** in 73% isolated yield.

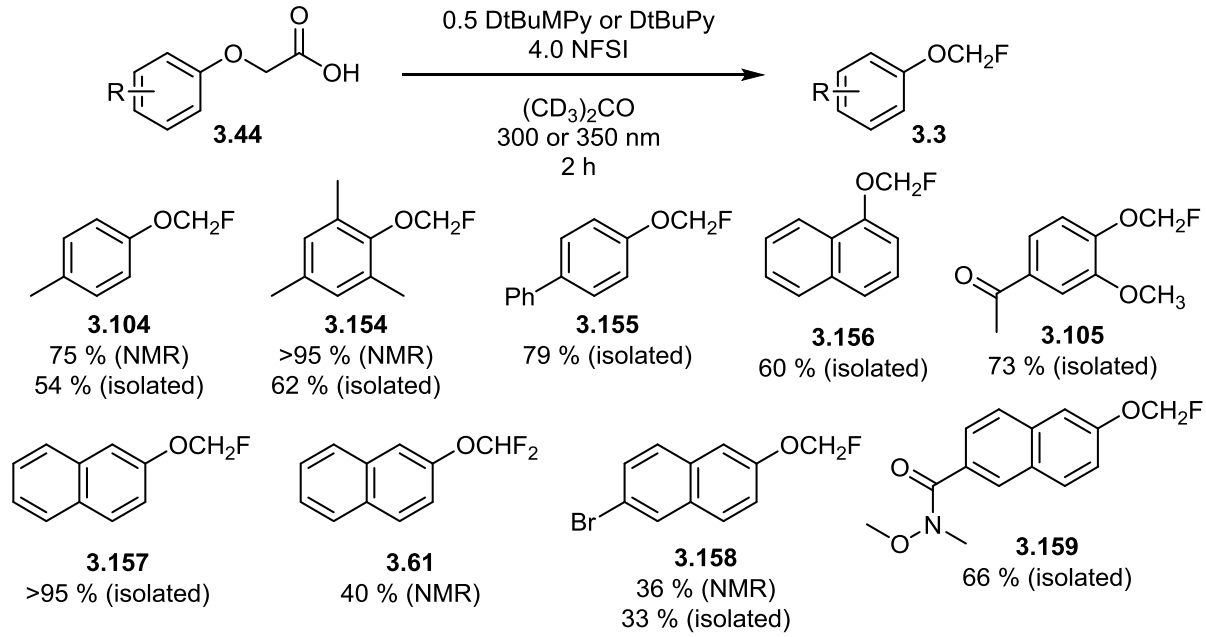

Scheme 3.45. Sensitized PDC-F with NFSI of substrates previously inaccessible by PDC-F with Sel-F

Exploring the limitations of sensitized PDC-F with NFSI, the fluorodecarboxylation of naproxen (**3.70**) and *sec*-butyl acid **3.160** were attempted (Scheme 3.46). PDC-F of **3.70** delivered a complex mixture of fluorinated compounds, but peaks corresponding to naphthyl fluoride **3.116** could be detected in 35% by ^{1}H NMR spectroscopy (top reaction). While the conditions with NFSI are milder, benzylic fluorination was still observed to some extent with PDC-F of **3.160**. The overall yield of sensitized PDC-F with NFSI was 88% and a 2:1 mixture of **3.161**: **3.162** was detected by ^{1}H and ^{19}F NMR spectroscopy (bottom reaction).

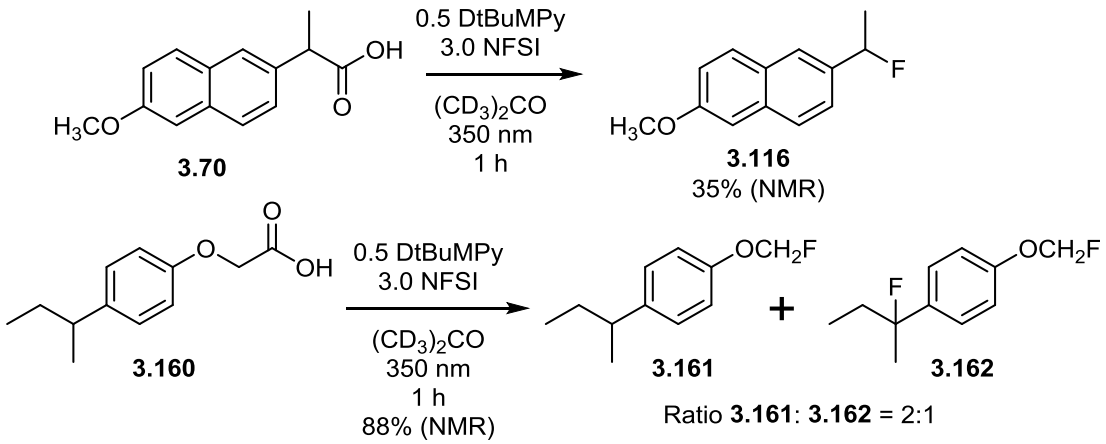

Scheme 3.46. Limits of sensitized PDC-F with NFSI

Emplying the milder reagent, NFSI, allowed for the construction of natural product analogs such as estrone fluoromethyl ether **3.163** (Scheme 3.47). Estrone acid **3.110** was easily prepared in two steps from estrone by S_N2 displacement of ethyl bromoacetate followed by saponification. PDC-F of this steroid derivative presented a formidable challenge to the Sel-F-mediated system as the tertiary benzylic position can be readily oxidized, the enolizable α-keto position is succeptable to electrophilic fluorination, and the aromatic ring is activated for electrophilic aromatic substituion. Gratifyingly, sensitized PDC-F employing NFSI successfully provided **3.163** in 49% isolated yield whereas PDC-F with Sel-F could not produce **3.163** selectively.

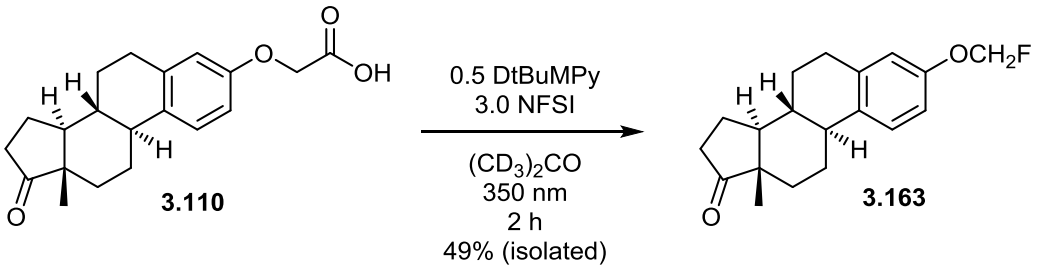

Scheme 3.47. Photosensitized decarboxylative fluorination of estrone acid 3.110

While sensitized PDC-F with NFSI yielded many fluoromethyl ethers which were inaccessable by PDC-F with Sel-F, some aryloxyacetic acids still remained a challenge (Scheme 3.48). 4-Iodophenoxyacetic acid (**3.79**) did not fluorodecarboxylate with NFSI in either acetone or acetonitrile, nor did dichloronaphthyloxy acid **3.164**. Sensitized PDC-F of 2-vinyl and 2-allyl acids **3.78** and **3.48** with NFSI delivered complex reaction mixtures similiar to PDC-F with Sel-F. Increasing the electron density of the aryloxy moiety further with a 4-methoxy substituent (**3.62**) was still a limitation, and as similarly observed with Sel-F, non-specific aryl fluorination competed with the desired PDC-F. It is interesting to note that **3.78** and **3.62** could be photofluorodecarboxylated using DIB in section 3.2 (Scheme 3.11, Scheme 3.15).

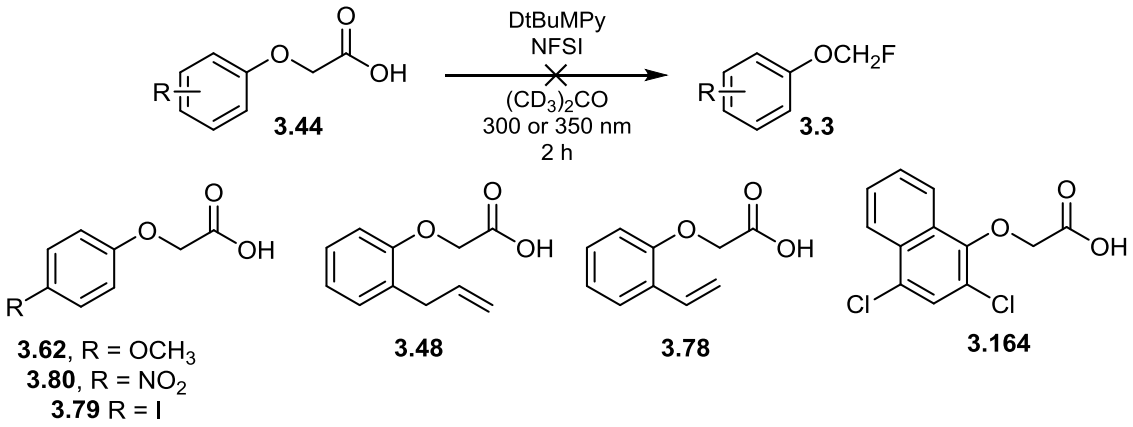

Scheme 3.48. Failed substrates for sensitized PDC-F with NFSI

In summary, employing the milder oxidant NFSI in sensitized PDC-F greatly broadens the substrate scope. Electron-rich aryloxyacid acids can be successfully fluorodecarboxylated and even complex natural product-like fluoromethyl ethers (**3.105**, and **3.163**) can be obtained.

3.4.3 Mechanism of photodecarboxylative fluorination with NFSI

The study of PDC-F with NFSI consists of two different reaction mechanisms which converge to the same aryoxymethyl radical which is fluorinated by NFSI. Non-sensitised photodecarboxylative fluorination of aryloxyacetic acids with NFSI and is proposed to be analogous to the mechanism of PDC-F with Sel-F (Scheme 3.49). Excitation of the B band transition of the aryloxy nucleus of **3.82** (for simplicity, phenoxyacetic acid is depicted) generates an excited di-radical state **3.83**. This activated intermediate may be reversibly oxidized by NFSI to a zwitterionic species **3.84** that will decarboxylate irreversibly to the phenoxymethyl radical (**2.33**). Fluorination by the NFSI radical anion, directly through an S_H2-like mechanism (Scheme 3.50 A), or through back electron transfer followed by an S_N2-like reaction (Scheme 3.50 B) delivers the fluoromethyl ether product **1.112**. Evidence in support of the NFSI radical anion being the active source of fluorine is found in Table 3.4-5.

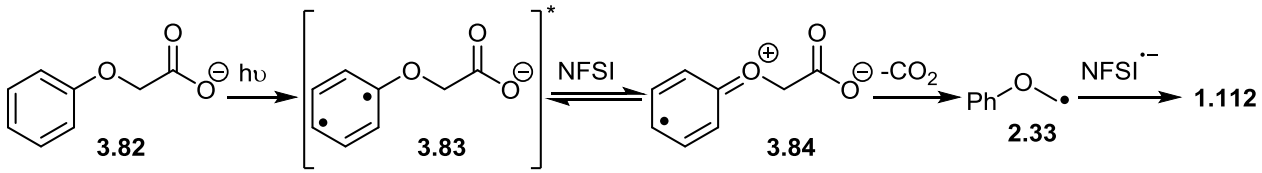

Scheme 3.49. Proposed mechanism for non-sensitized PDC-F with NFSI

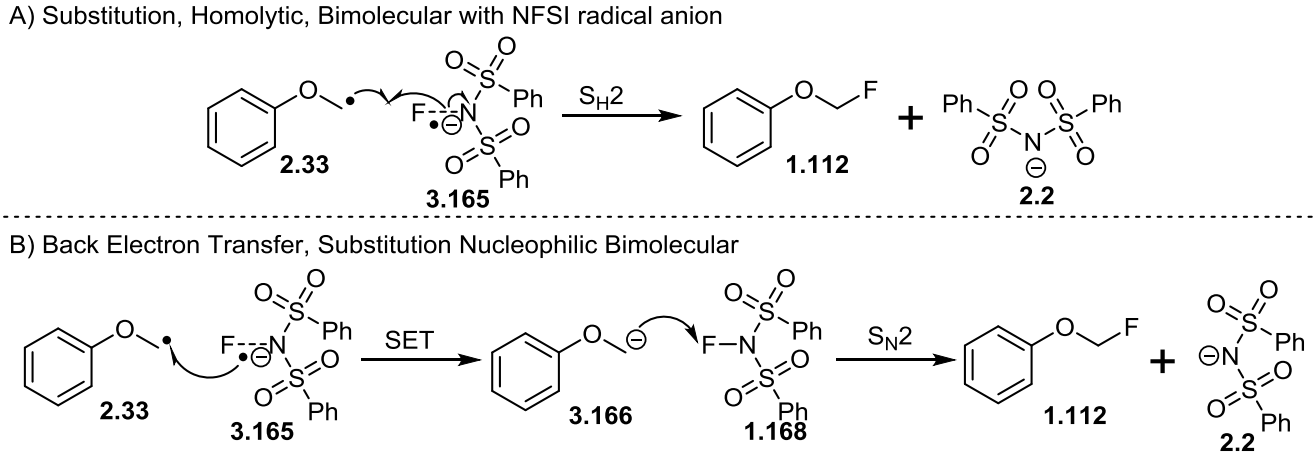

Scheme 3.50. Possible fluorination pathways for phenoxymethyl with NFSI

As established by the experiments in Table 3.4-1 and Scheme 3.51 (top reaction), efficient non-sensitized PDC-F with NFSI requires the addition of base. Deprotonation of the carboxylic acid facilitates an irreversible decarboxylation of **3.84**, which supports the necessity of a carboxylate for either a Strecker-type decarboxylation[200] mechanism or an internal electron transfer and radical decarboxylation mechanism analogous to PDC-F with Sel-F (Scheme 3.38). Furthermore, no reaction is observed under thermal conditions, which implies that the reaction does not go through a Hunsdieker-type reaction[38] with acyl hypofluorite intermediates.

Under the standard PDC-F with NFSI in acetonitrile conditions, no reactivity was observed with phenylacetic acid (**3.40a**) nor 1-adamantyloxyacetic acid (**3.167**) (Scheme 3.51). In both experiments, the starting acids were completely recovered. These experiments reveal the following information: (1) they further support the assertion that hypofluorites are not involved in the reaction mechanism, (2) they suggest that direct oxidation of the carboxylate by NFSI does not occur, (3) if photoexcitation of NFSI occurs (NFSI absorbs at 270 nm with a shoulder at 277 nm, Figure 3.9), it is not sufficient to initiate decarboxylation of the acids, and (4) they support the necessity of an aryloxy moiety. Having an aryl chromophore or having an oxidizable oxygen alone are not sufficient to initiate PDC with NFSI. The observation that **3.40a** is a viable substrate for PDC-F with Sel-F further highlights the oxidant power differences between NFSI and Sel-F.

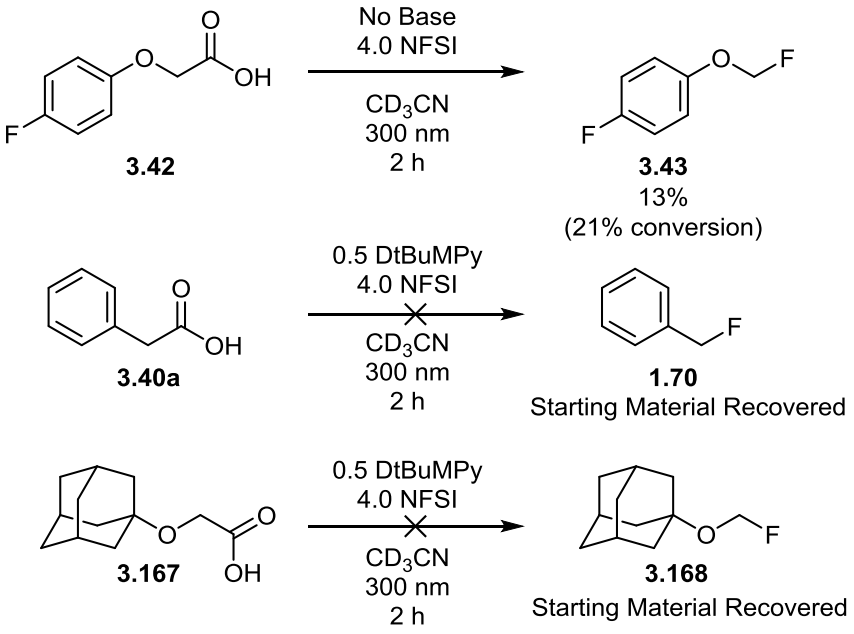

Scheme 3.51. Mechanistic investigations into PDC-F with NFSI in acetonitrile

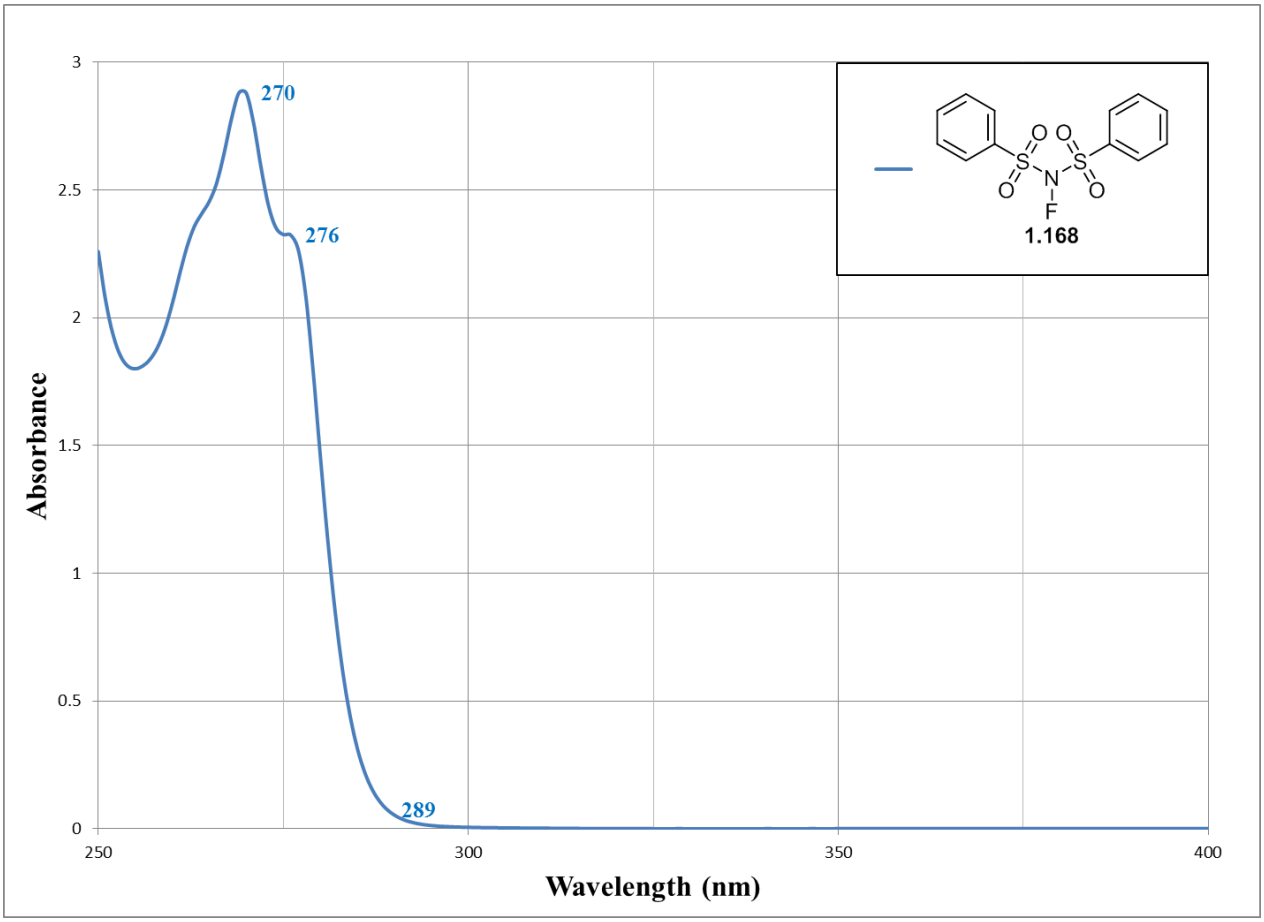

Figure 3.9 UV-Vis absorption spectrum of NFSI (0.001 M in CH_3CN)

Throughout this section, acetone has been treated as a photosensitizer; although it is a very poor photosensitizer as the molar absorptivity coefficient for acetone (ε = 12.4 l mol^{-1} cm^{-1} @ 280 nm)[197] is relatively low when compared to commonly employed photosensitizers such as rose bengal (ε = 90,400 l mol^{-1} cm^{-1} @ 559 nm).[184] To negate the hypothesis that observed rate increases in acetone are the result of an extreme solvent or polarity effect, an experiment was conducted test the role a photosensitizer might have in PDC-F with NFSI.

An increase in rate would strongly suggest that the photosensitizer is a key component of the reaction mechanism. The test experiment was carried out in acetonitrile with catalytic amounts of a benzophenone (Scheme 3.52). Benzophenone (**3.91**) was chosen as the triplet sensitization for PDC with phenoxyacetic acid (**2.26**) has already been established.[191] After only 10 minutes, the benzophenone-sensitized reaction in acetonitrile resembled the PDC-F reaction in acetone, both in conversion and yield, refuting the solvent effect/polarity hypothesis.

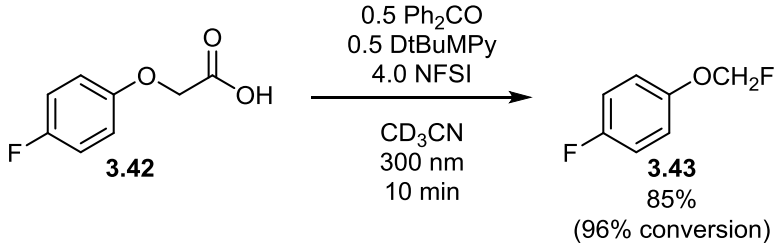

Scheme 3.52. Sensitized PDC-F with benzophenone in acetonitrile

As a photosensitizer, acetone can alter the reaction mechanism in three possible ways: facilitate intersystem crossing, mediate energy transfer, or serve as a single electron oxidant. It is unlikely that the photosensitizer is facilitating intersystem crossing as the quantum yield for anisole intersystem crossing is high.[195] Both the observation that the viable wavelengths for PDC-F have broadened (due to the broader absorbance range of acetone) and the increase in rate at 300 nm (due to the effective

increase in quantum yield because both substrate and acetone can absorb light in this range) are consistent with both energy transfer and reversible single electron oxidation.

If acetone is mediating energy transfer, then the overall reaction mechanism will be similar to the non-sensitized mechanism presented in Scheme 3.49, with the exception that acetone could facilitate the excitation of acid **3.82** to **3.83**. If acetone is acting as an intermediary oxidant between acid **2.26** and NFSI, then the overall reaction mechanism would resemble the depiction in Scheme 3.53. Triplet acetone (**3.170a**, R= CH_3) or benzophenone (**3.170b**, R = Ph) participates in reversible single electron transfer with aryloxyacetic acid **3.44** effectively oxidizing the oxygen. Upon deprotonation by base, intermediate **3.173** rapidly decarboxylates to aryloxymethyl radical **3.175** and is fluorinated by NFSI or the NFSI radical anion (**3.165**). The photosensitizer can be regenerated by reducing NFSI to the NFSI radical anion (**3.165**).

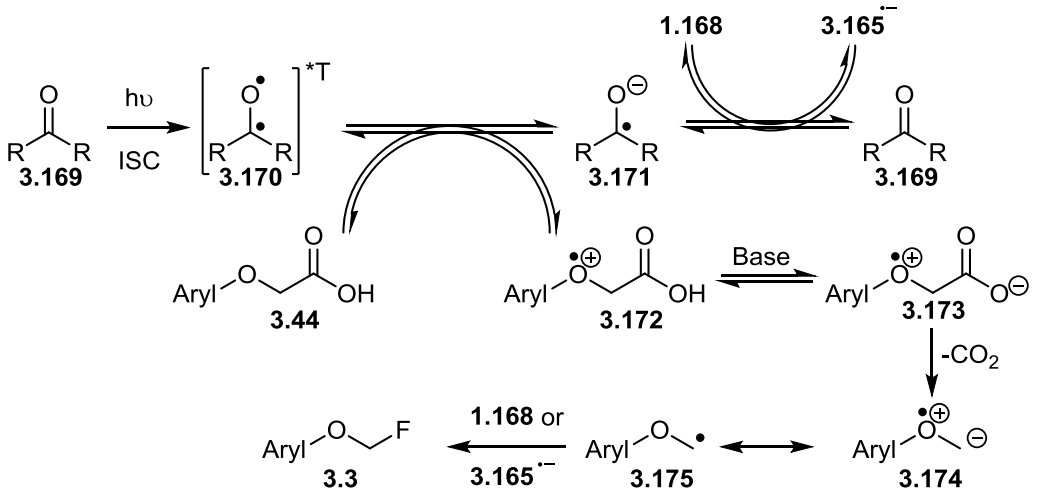

Scheme 3.53. Proposed mechanism for sensitized PDC-F with NFSI

To differentiate between these two mechanistic possibilities, PDC-F of α-alkoxy acid derivative **3.167** was examined (Scheme 3.54). If acetone acts as a mediator for energy transfer, this substrate should not undergo decarboxylation as there is no aryloxy moiety to activate. However, if acetone acts

as an oxidant, this substrate should undergo decarboxylation although fluorination might not be observed due to the instability of alkyl fluoromethyl ethers. Subjecting **3.167** to PDC-F with NFSI in acetone yielded several products resulting from decarboxylation of **3.167**. This strongly suggests that a chromophore on the substrate is not necessary for the reaction and photoexcited acetone **3.170** has replaced NFSI as the initial SET oxidant.

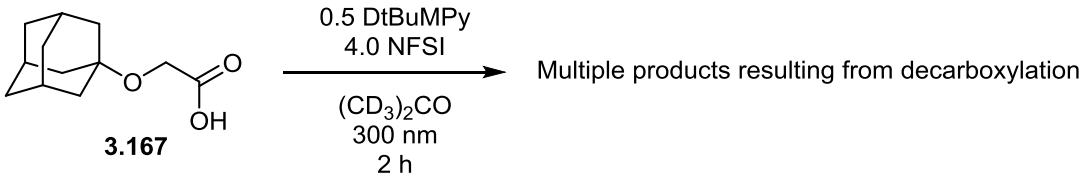

Scheme 3.54. Sensitized photodecarboxylation of 1-adamantyloxyacetic acid

There are two possible sites that can be oxidized in **3.44**: the ether oxygen or the carboxylate. To test which is being oxidized, PDC-F of **3.76** and phenylacetic acid (**3.40a**) were investigated (Scheme 3.55). Aspirin derivative **3.76** possesses a carboxylic acid with similar electronic properties to **3.44**, but the oxygens are more difficult to oxidize. Phenylacetic acid has the carboxylic acid, but is lacking the ether oxygen. Both of these substrates were not viable in the PDC-F in acetone, which suggests the ether oxygen is crucial for reactivity.

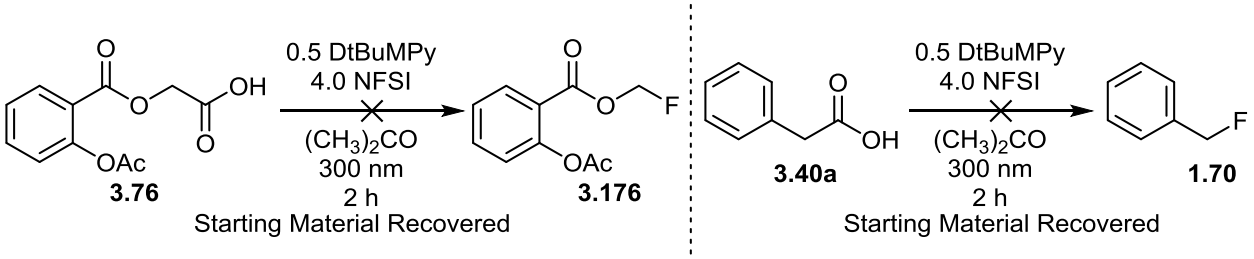

Scheme 3.55. Attempted sensitized PDC-F of oxidation resistant acids

Based on the mechanism depicted in Scheme 3.53, radical anion **3.171** could act as the base and facilitate decarboxylation. Sensitized PDC-F, both in acetone and in acetonitrile (with catalytic amounts of benzophenone), proceeded smoothly to give high conversions of **3.42** after only 10 minutes (Scheme 3.56), thus supporting the mechanism in which the photosensitizer promotes the photodecarboxylation as both an oxidant and a base.

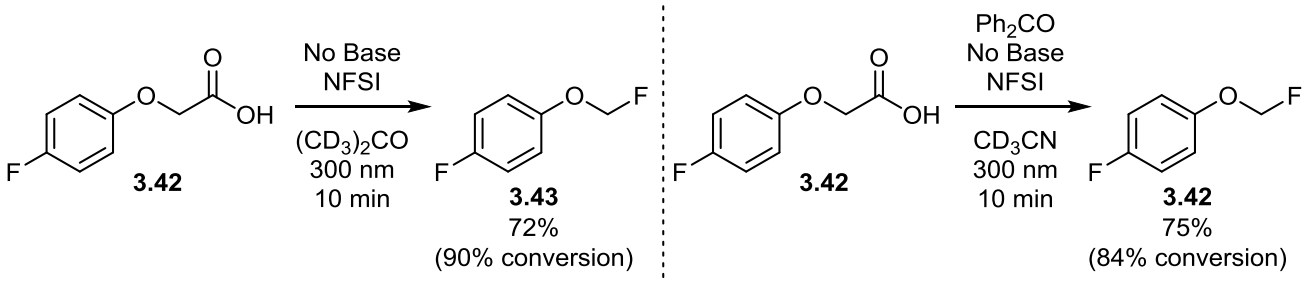

Scheme 3.56. Sensitized PDC-F in the absence of hindered pyridine bases

While sensitized PDC-F is successful without the addition of a pyridine base, the addition DtBuMPy (**3.152**)**,** reduces the number of products related to non-specific fluorination and acts as a stabilizer for fluoromethyl ether product **3.3** (Figure 3.10). Photosensitized PDC-F without **3.152,** under prolonged periods of irradiation with 300 nm light, leads to the complete loss of fluoroether products (Figure 3.10, top 2 spectra). Furthermore, sensitized PDC-F with **3.152** leads to the following changes as observed by NMR spectroscopy: ^{1}H NMR shows that the aryl C-H protons are absent, the 4-methyl singlet broadens, and the *tert*-butyl singlet shifts downfield by 0.1 ppm (Figure 3.10, lower 2 spectra). Analysis of the ^{19}F NMR spectrum reveals a new signal in the region of a cyclohexyl C-F bond. The identity of this compound is uncertain as isolation of this compound failed (**3.152** is recovered by flash column chromatography). The exact role of pyridine base in this reaction is uncertain, but it is clear that the addition of base is beneficial to photosensitized PDC-F and required for non-sensitized PDC-F.

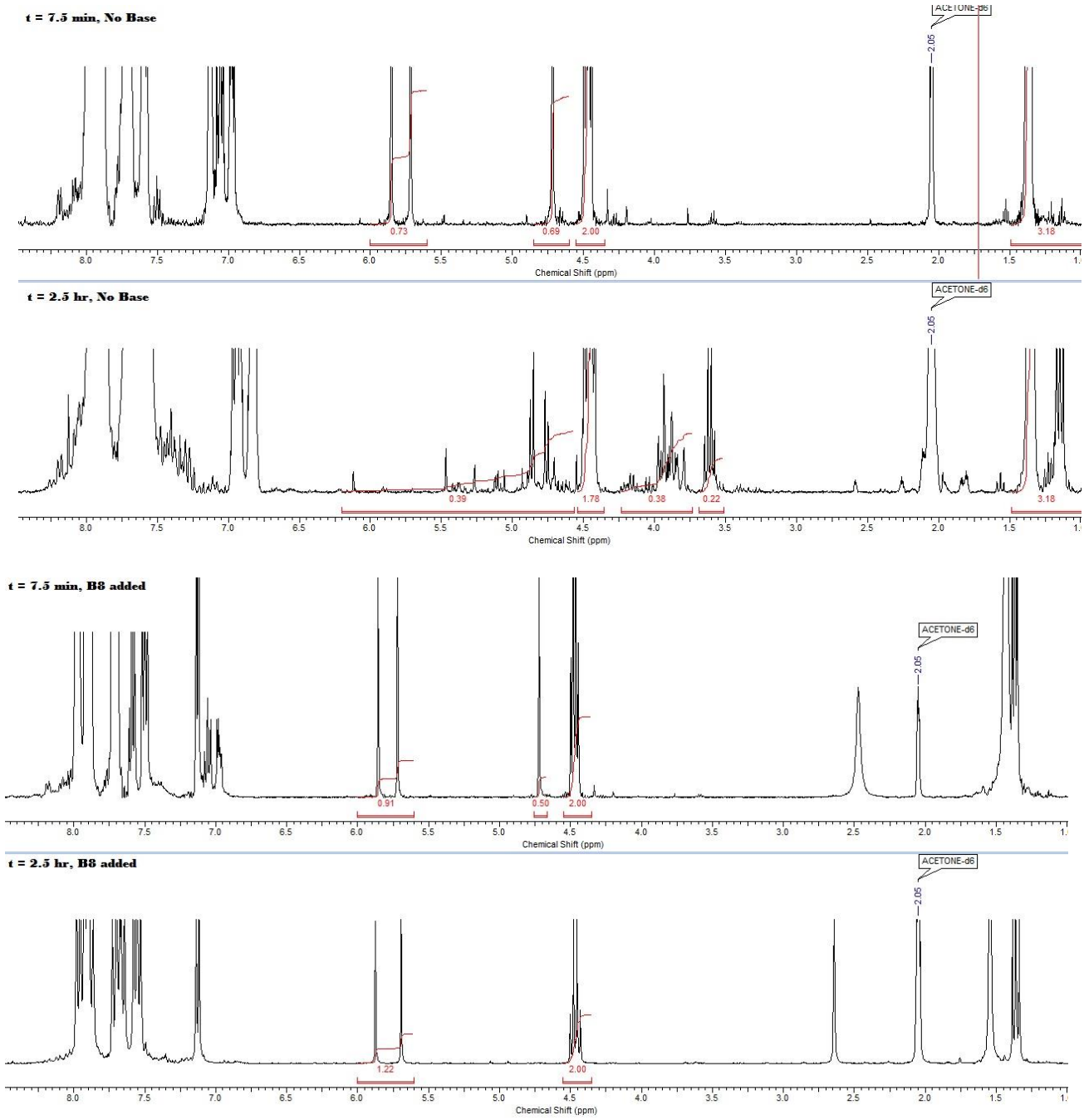

Figure 3.10 PDC-F in acetone with, and without, DtBuMPy[a]

[a]From top to bottom: ^{1}H NMR spectrum (400 MHz, $(CH_3)_2CO$) for PDC-F of **3.42** in acetone with no base additive (after 7.5 minutes of 300 nm irradiation), ^{1}H NMR spectrum (300 MHz, $(CH_3)_2CO$) for PDC-F of **3.42** in acetone with no base additive (after 2.5 hours of 300 nm irradiation), ^{1}H NMR spectrum (400 MHz, $(CH_3)_2CO$) for PDC-F of **3.42** in acetone with 0.5 equivalents of DtBuMPy (after 7.5 minutes of 300 nm irradiation), ^{1}H NMR spectrum (300 MHz, $(CH_3)_2CO$) for PDC-F of **3.43** in acetone with 0.5 equivalents of DtBuMPy (after 2.5 hours of 300 nm irradiation).

3.5 Density Functional Theory calculations

DFT calculations through the ORCA computational package were executed to investigate the ionised carboxylic acid intermediate and to study the decarboxylated phenoxymethyl intermediate common to all PDC-F reactions. DFT geometry optimisation calculations were performed at the B3LYP/TZVP level[201,125] in the gas phase from 3D structures obtained using the Cambridge Chembio3D ultra 13.0 program. The Becke 3 parameter hybrid DFT functional was selected for its demonstrated efficient and accurate calculation of ground state geometries for small organic molecules.[201] Ahlrichs's basis set with a single polarization function was selected to allow the calculation to localize the spin density on a single atom or share the spin density over multiple atoms if desirable. The RI approximation (RIJCOSX)[165] was employed to accelerate calculations on ORCA and the COSMO solvation model was employed for studies on the decarboxylated radical intermediate.[126]

Calculations were performed to understand where ionization occurs on the carboxylic acid substrates. The global spin density maps for phenylacetic acid radical cation (**3.177**) and phenoxyacetic acid radical cation (**3.98**) are presented in Figure 3.11. The orbital in blue depicts the resulting SOMO after ionization and indicates where the ionized partner originated. Calculations show that the remaining electron in **3.177** resides mostly on the phenyl ring, but also partially on the carbonyl oxygen (Figure 3.11 left portion).

The remaining electron in **3.98** resides predominately on the oxygen and carbons in the phenyl ring corresponding to positions that would be predicted by resonance delocalization (Figure 3.11, right portion). Studies on sensitized PDC-F of aryl- or alkyl-oxyacetic acids demonstrated that oxygen ionization was required to induce a subsequent decarboxylation event. The calculated SOMO picture of **3.98** also supports oxygen ionization with the resulting radical greatly stabilized by the phenyl ring.

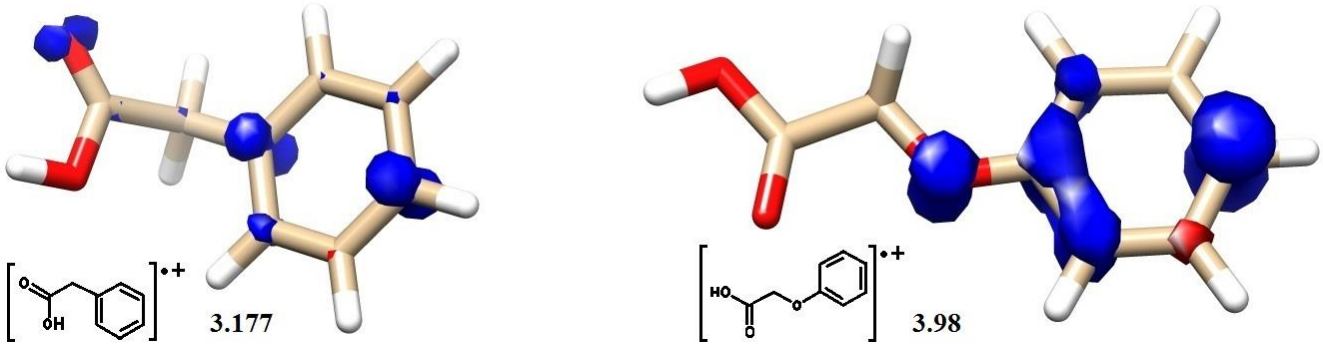

Figure 3.11. Spin density maps for single electron oxidized phenylacetic acid (left) and phenoxyacetic acid (right)

Calculations related to the fate of the oxidized electron were successful for reduced Sel-F (**3.135**) but not for the reduced NFSI radical anion (**3.165**).[h] An examination of the spin density on **3.135** shows the extra electron is equally shared between N and F, supporting the existence of **3.135** despite an elongated N-F distance (Figure 3.12). If dissociation of **3.135** occurs rapidly, then the mechanism of the final fluorination step should involve oxidation of phenoxymethyl (**2.33**) by **1.187** followed by trapping of the oxonium with fluoride. As the reaction with Sel-F is aqueous, trapping of the oxymethyl cation by the solvent could be expected to some extent, but this has yet to be observed. Thus, the calculations do not support mechanism D in Scheme 3.39.

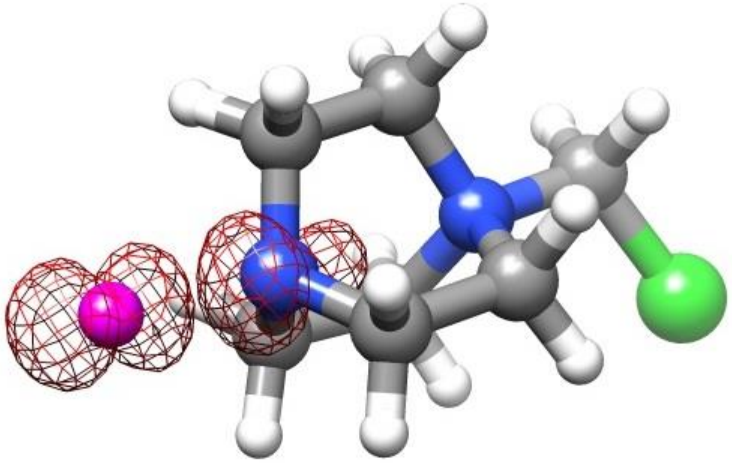

Figure 3.12. Spin density map for single electron reduced Sel-F

[h] Calculations on **3.165** failed as N-S bond cleavage was found whereas N-F bond cleavage is the experimental result.[110]

All of the mechanistic investigations on PDC-F, wither sensitized or non-sensitized, and with Sel-F or NFSI, converge on a common decarboxylated intermediate. The identity of the major resonance contributor may provide insight on the final steps of the reaction mechanism. If the predominant resonance form resembles zwitterionic intermediate **3.134**, it is likely that the fluorination step resembles ionic electrophilic fluorination through an S_N2-like pathway. If the predominant resonance form resembles intermediate **2.33**, the fluorination step would be highly radical in nature either through an S_H2-like pathway or SET mediated pathway.

DFT calculations were performed at the B3LYP/TZVP level[201,125] employing the COSMO solvation model for acetone.[126] Solvation with a continuum model for acetone was selected as these computational studies were performed alongside investigations into the sensitized PDC-F with NFSI reaction. The calculations show phenoxymethyl intermediate **2.33** as the predominant resonance structure. The greatest spin density is found on the oxymethyl group and a significant amount of spin sharing is found on the oxygen (Figure 3.13). A relaxed scan of the dihedral angle (formed by the methoxy carbon, oxygen, carbon 1 and carbon 2 of the benzene ring) by 30 degrees in either direction finds less than 1 kcal/mol change in the overall energy of the molecule suggesting that the phenyl ring does not participate significantly in stabilizing the radical. The overall electron density map further supports structure **2.33** as it does not show a build-up of charge density anywhere on the molecule (Figure 3.14).

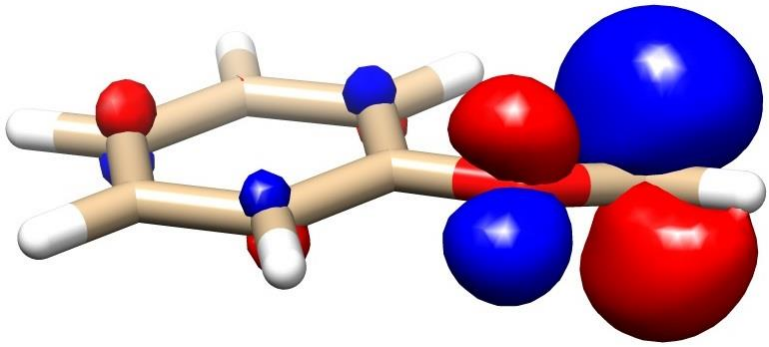

Figure 3.13. Calculated global spin density of decarboxylated intermediate resembling 2.33 (contour value = 0.05)

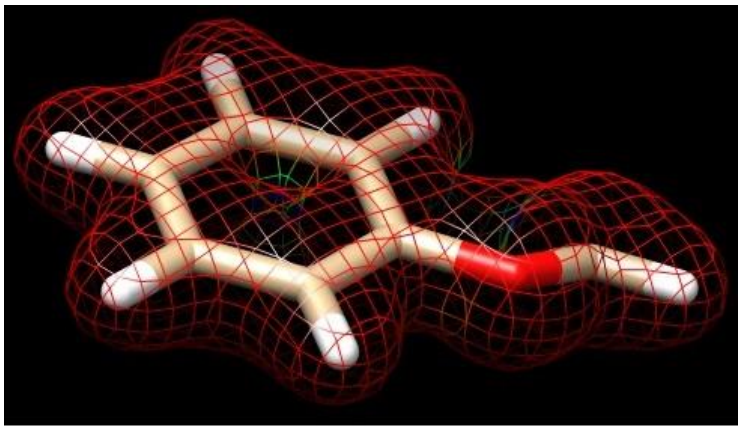

Figure 3.14. Calculated electron density of decarboxylated intermediate resembling 2.33 (contour value = 0.05)

These calculations show strong evidence for radical behaviour of the decarboxylated aryloxymethyl intermediate and discredit the S_N2-like ionic fluorination pathway. However, they do not rule out the possibility of further single electron transfer events between **2.33** and the fluorinating agent prior to fluorine transfer. Further computational studies on the PDC-F mechanism would aim to elucidate the transition state for fluorine transfer and I will elaborate in Chapter 5.

3.6 Experimental

3.6.1 General experimental

All chemicals were purchased from commercial sources and used as received. Aryloxyacetic acid synthesis reactions were performed in regular air atmosphere at ambient conditions with air-dried glassware. All photochemical reactions were performed under argon atmosphere in argon-sparged solvents in a Rayonet RPR-100 immersion photoreactor with 15 lamps (RPR-2500Å for 254 nm, RPR-3000Å for 300nm, RPR-3500Å for 350nm). Photochemical reactions on the 0.05 mmol scale were performed in Norell alumino-borosilicate glass NMR tubes (standard series, length = 7 inch; OD = 4.97 ± 0.025 mm; ID = 4.20 ± 0.025 mm). Photochemical reactions on 0.4 mmol scale were performed in Wilmad borosilicate glass NMR/EPR tubes (thin-walled, length = 8 inch; OD = 9.9935 ± 0.0065 mm; ID = 9.070 ± 0.013 mm; wall thickness = 0.46 mm) or Falcon 15 ml polypropylene centrifuge tubes.

Melting points were performed using a Mel-Temp II apparatus (Lab devices USA) and are uncorrected. Infrared (IR) spectra were obtained using a Thermo Nicolet 4700 FT-IR spectrometer or a Perkin Elmer Frontier FT-IR. Ultraviolet-Visable (UV/VIS) spectra were obtained using a Varian Cary 5000 spectrophotometer. Proton and carbon nuclear magnetic resonance (^{1}H and ^{13}C NMR) spectra were recorded in deuterated solvents using a Bruker AV-400 or AV-300 spectrometer. Fluorine nuclear magnetic resonance (^{19}F NMR) spectra were recorded in deuterated solvents using a Bruker AV-300 spectrometer. Chemical shifts are reported in parts per million (ppm) and are referenced to the centerline of deuterochloroform (7.27 ppm ^{1}H NMR; 77.0 ppm ^{13}C NMR), deuterobenzene (7.16 ppm ^{1}H NMR; 128.4 ppm ^{13}C NMR), acetone-d_6 (2.05 ppm ^{1}H NMR; 29.9 ppm ^{13}C NMR), acetonitrile-d_3 (1.94 ppm ^{1}H NMR; 118.7 ppm ^{13}C NMR). High resolution mass spectra (HRMS) were recorded on either a Waters or Micromass LCT spectrometer.

3.6.2 Experimental procedures related to DFT calculations

Initial structures were obtained from the CambridgeSoft Chem 3D Office program. Geometry optimization was performed using density functional theory (DFT) with the ORCA computational package[127] using the B3LYP functional,[201] TZV/P basis set for all the atoms,[125] the RIJCOSX approximation,[165] and COSMO dielectric continuum model for solvent effects.[126] Increased integration grids (Grid4) and tight SCF convergence criteria (TightSCF) were also used. Numerical frequency calculations at the same level of theory indicated that the fully optimized geometry was obtained. All figures and diagrams were produced with the Chimera or Mol-Den programs.

3.6.3 Synthesis of carboxylic acid test substrates

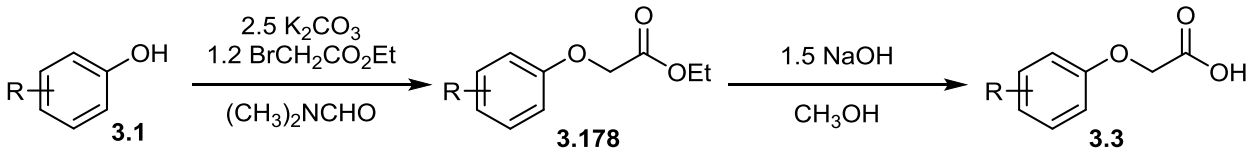

General procedure for the synthesis of aryloxyacetic acids: To a suspension of potassium carbonate (2.5 equiv.) in a solution of phenol (1.0 equiv.) in dimethyl formamide (0.5M with respect to phenol) was added ethyl bromoacetate (1.2 equiv.) in100 µl portions every 10 min at ambient temperature. After addition was completed, the reaction was allowed to stir an additional 2 hours. The reaction mixture was poured into water and extracted with 3 x Et_2O. The organic layers were combined and washed with 2 x $NaOH_{(aq)}$ (3.0M) and brine. The organic extract was dried over Na_2SO_4, filtered and concentrated by rotary evaporation to afford the crude ethyl ester which was used immediately.
To a solution of the crude ester in methanol (0.2 M with respect to phenol) was added $NaOH_{(aq)}$ (1.5 equiv., 3.0M) at ambient temperature. The reaction was monitored by TLC for completion then poured into Et_2O and extracted with water and 2 x $NaOH_{(aq)}$ (1.0 M). The aqueous layers were combined and

acidified with $HCl_{(aq)}$ (10 wt%) and extracted with 3 x Et_2O or EtOAc. The organic layers were combined, washed with brine, dried over Na_2SO_4, filtered and concentrated by rotary evaporation to afford a solid which was recrystallized in hexanes/EtOAc.

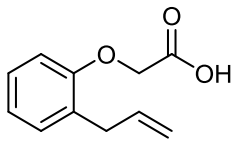

3.48

2-(2-allylphenoxy)acetic acid (**3.48**): 2-allylphenol (537 mg, 4.0 mmol) was subjected to the general aryloxyacetic acids synthesis procedure. Recrystallization from hexanes-Et_2O (3:1) yielded 2-(2-allylphenoxy)acetic acid (**3.48**) as white crystals (590 mg, 77%).

^{1}H NMR (400MHz; C_6D_6): δ = 7.05 (dd, *J* = 1.7, 7.5 Hz, 1 H), 6.94 (dt, *J* = 1.7, 7.9 Hz, 1 H), 6.82 (dt, *J* = 1.0, 7.3 Hz, 1 H), 6.30 (dd, *J* = 0.7, 8.2 Hz, 1 H), 5.06 (qd, *J* = 1.7, 17.1 Hz, 1 H), 5.01 (qd, *J* = 1.7, 10.1 Hz, 1 H), 4.01 (s, 2 H), 3.45 (d, *J* = 6.5 Hz, 2 H) ppm.

^{13}C NMR (101MHz; C_6D_6): δ = 156.0, 137.6, 131.0, 129.7, 127.9, 122.4, 116.0, 111.9, 65.0, 35.2 ppm.

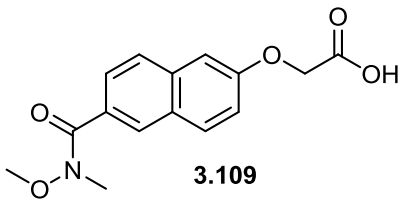

3.109

2-((6-(methoxy(methyl)carbamoyl)naphthalen-2-yl)oxy)acetic acid (**3.109**): To a solution of N,O-dimethylhydroxylamine hydrochloride (536 mg, 5.5 mmol, 1.1 equiv.) in CH_2Cl_2 (20 ml), cooled to 0 °C in ice/water bath, was added 1,8-diazabicycloundec-7-ene (900 µl, 6.0 mmol, 1.2 equiv.) over 10 sec. To this colourless solution was added 6-hydroxy-2-naphthoic acid (941 mg, 5.0 mmol, 1.0 equiv.) in one portion followed by DCC (1.1 g, 5.5 mmol, 1.1 equiv.). The cold bath was removed and the suspension was stirred for 3 days. The reaction mixture was filtered through a plug of celite, washed

with EtOAc (3 x 20 ml) then concentrated by rotary evaporation. The solids obtained were re-suspended in EtOAc, filtered through a plug of celite, and concentrated by rotary evaporation to obtain crude a naphthol which was used without further purification. The crude naphthol was subjected to the general aryloxyacetic acids synthesis procedure. Recrystallization from hexanes-EtOAc yielded 2-((6-(methoxy(methyl)carbamoyl)naphthalen-2-yl)oxy)acetic acid (**3.109**) as grey solid (420 mg with trace amounts of EtOAc, 29% yield over 3 steps).

m.p.: 125.0 - 127.0 ºC

IR (neat): 2967, 2934, 2591, 1726, 1640, 1626, 1480, 1464, 1425, 1396, 1365, 1257, 1232, 1190, 1079, 1001, 930, 896, 884, 870, 815, 801, 764, 739, 673 cm^{-1}.

^{1}H NMR (400MHz; $(CD_3)_2CO$): δ = 8.19 (s, 1 H), 7.95 (d, *J* = 9.0 Hz, 1 H), 7.84 (d, *J* = 8.5 Hz, 1 H), 7.72 (dd, *J* = 1.7, 8.5 Hz, 1 H), 7.36 (d, *J* = 2.6 Hz, 1 H), 7.29 (dd, *J* = 2.6, 9.0 Hz, 1 H), 4.89 (s, 2 H), 3.60 (s, 3 H), 3.34 (s, 3 H) ppm.

^{13}C NMR (101MHz; $(CD_3)_2CO$): δ = 170.4, 170.0, 158.3, 136.5, 131.4, 131.1, 129.2, 127.3, 126.8, 120.2, 107.9, 65.5, 61.3, 33.9 ppm.

HRMS-ESI (m/z): $[M+H]^+$ calcd for $C_{15}H_{16}NO_5$: 290.1028. Found: 290.1024.

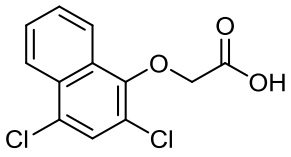

3.164

2-((2,4-dichloronaphthalen-1-yl)oxy)acetic acid (**3.164**): 2,4-dichloronaphthalen-1-ol (532 mg, 2.5 mmol) was subjected to the general aryloxyacetic acids synthesis procedure. Recrystallization from hexanes-EtOAc yielded 2-((2,4-dichloronaphthalen-1-yl)oxy)acetic acid (**3.164**) as light wispy solids (157 mg, 23%).

^{1}H NMR (400MHz; $(CD_3)_2CO$): δ = 8.59 - 8.45 (m, 1 H), 8.28 - 8.16 (m, 1 H), 7.79 - 7.72 (m, 2 H), 7.71 (s, 1 H), 4.87 (s, 2 H), 2.81 (br. s., 1 H) ppm.

^{13}C NMR (101MHz; $(CD_3)_2CO$): δ = 169.8, 157.9, 131.3, 130.7, 129.2, 129.0, 128.5, 128.0, 125.2, 124.1, 122.8, 70.8 ppm.

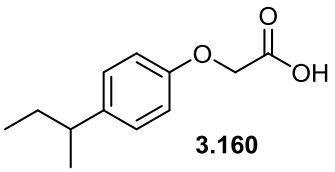

3.160

2-(4-*sec*-butylphenoxy)acetic acid (**3.160**): 4-*sec*-butylphenol (376 mg, 2.5 mmol) was subjected to the general aryloxyacetic acids synthesis procedure. Recrystallization from hexanes yielded 2-(4-*sec*-butylphenoxy)acetic acid (**3.160**) as white crystals (270 mg, 52%).

^{1}H NMR (400MHz; $CDCl_3$): δ = 7.13 (d, *J* = 8.7 Hz, 2 H), 6.87 (d, *J* = 8.7 Hz, 2 H), 4.67 (s, 2 H), 2.57 (sxt, *J* = 7.0 Hz, 1 H), 1.57 (quin, *J* = 7.3 Hz, 2 H), 1.22 (d, *J* = 7.0 Hz, 3 H), 0.82 (t, *J* = 7.4 Hz, 3 H) ppm.

^{13}C NMR (101MHz; $CDCl_3$): δ = 173.5, 155.4, 141.5, 128.1, 114.5, 65.0, 40.8, 31.2, 21.9, 12.2 ppm.

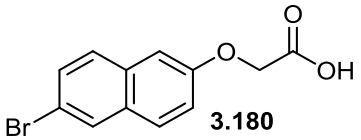

3.180

2-((6-bromonaphthalen-2-yl)oxy)acetic acid (**3.180**): To a suspension of potassium carbonate (1.8 g, 18.5 mmol, 2.5 equiv.) in a solution of 6-bromonaphthalen-2-ol (1.12 g, 5.0 mmol, 1.0 equiv.) in dimethyl formamide (10 ml) was added ethyl bromoacetate (660 µl, 6.0 mmol, 1.2 equiv.) in100 µl portions every 10 min at ambient temperature. After addition was completed, the reaction was allowed to stir an additional 2 hours. The reaction mixture was poured into water and extracted with 3 x EtOAc. The organic layers were combined and washed with 2 x $NaOH_{(aq)}$ (3.0M) and brine. The organic extract was dried over Na_2SO_4, filtered and concentrated by rotary evaporation. Recrystallization from hexanes-Et_2O provided the ethyl ester intermediate as white crystals (1.3 g, 83%).

^{1}H NMR (400MHz; $CDCl_3$): δ = 7.94 (d, *J* = 0.9 Hz, 1 H), 7.69 (d, *J* = 9.0 Hz, 1 H), 7.63 - 7.55 (m, 1 H), 7.52 (dd, *J* = 1.7, 8.8 Hz, 1 H), 7.30 - 7.20 (m, 1 H), 7.05 (d, *J* = 2.3 Hz, 1 H), 4.74 (s, 2 H), 4.31 (q, *J* = 7.2 Hz, 2 H), 1.32 (t, *J* = 7.2 Hz, 3 H) ppm.

^{13}C NMR (101MHz; $CDCl_3$): δ = 168.6, 156.0, 132.7, 130.4, 129.8, 129.7, 128.8, 128.5, 119.6, 117.6, 107.1, 65.4, 61.5, 14.2 ppm.

To a solution of the ethyl ester (309 mg, 1.0 mmol, 1.0 equiv.) in THF (5 ml) was added lithium hydroxide (1.2 ml, 1.0 M solution in H_2O, 1.2 mmol, 1.2 equiv.) in one portion. After 24 h, the reaction was poured into 1.0 M $HCl_{(aq)}$ (50 ml) and extracted with CH_2Cl_2 (3 x 20 ml). The organic extracts were washed with brine (20 ml), dried over Na_2SO_4, filtered, concentrated by rotary evaporation and recrystallized from EtOAc to yield 2-((6-bromonaphthalen-2-yl)oxy)acetic acid (**3.180**) as a white solid (196 mg 70%).

^{1}H NMR (400MHz; $(CD_3)_2CO$: $CDCl_3$ mix): δ = 7.99 (d, *J* = 1.7 Hz, 1 H), 7.78 (d, *J* = 8.7 Hz, 1 H), 7.71 (d, *J* = 8.8 Hz, 1 H), 7.50 (dd, *J* = 2.0, 8.7 Hz, 1 H), 7.30 - 7.20 (m, 2 H), 4.81 (s, 2 H) ppm.

^{13}C NMR (101MHz; $(CD_3)_2CO$: $CDCl_3$ mix): δ = 169.8, 157.2, 133.8, 131.1, 130.2, 130.2, 129.5, 129.4, 120.5, 117.7, 107.9, 65.3 ppm.

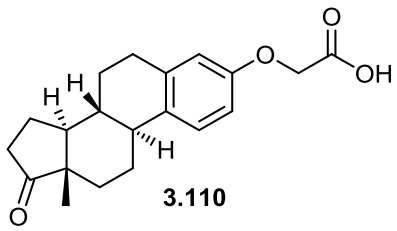

3.110

3-*O*-Carboxymethylestrone (**3.110**): Estrone (810 mg, 3.0 mmol) was subjected to the general aryloxyacetic acids synthesis procedure. Recrystallization from hexanes-EtOAc yielded 3-*O*-carboxymethylestrone (**3.110**) as white crystals (695 mg, 71% yield over 2 steps). The compound obtained matched literature characterization data.[267]

^{1}H NMR (400MHz; $CDCl_3$): δ = 7.23 (d, *J* = 8.9 Hz, 1 H), 6.74 (dd, *J* = 2.7, 8.5 Hz, 1 H), 6.68 (d, *J* = 2.7 Hz, 1 H), 4.66 (s, 2 H), 2.95 - 2.85 (m, 2 H), 2.52 (dd, *J* = 8.5, 18.8 Hz, 1 H), 2.45 - 2.36 (m, 1 H), 2.31 - 2.22 (m, 1 H), 2.22 - 1.90 (m, 4 H), 1.73 - 1.37 (m, 6 H), 0.92 (s, 3 H) ppm.

^{13}C NMR (101MHz; $CDCl_3$): δ = 221.4, 173.7, 155.4, 138.1, 133.5, 126.6, 114.8, 112.0, 64.8, 50.4, 48.0, 43.9, 38.2, 35.9, 31.5, 29.6, 26.4, 25.8, 21.6, 13.8 ppm.

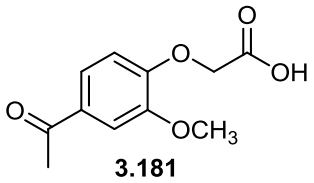

3.181

2-(4-Acetyl-2-methoxyphenoxy)acetic acid (**3.181**): Apocynin (832 mg, 5.0 mmol) was subjected to the general aryloxyacetic acids synthesis procedure. Recrystallization from EtOAc yielded 2-(4-acetyl-2-methoxyphenoxy)acetic acid (**3.181**) as white crystals (682 mg, 61% yield over 2 steps). This compound is commercially available; however, no characterization data could be located.

m.p.: 165.0 - 167.0 ºC

IR (neat): 2965, 2911, 2755, 2620, 2548, 1772, 1737, 1645, 1585, 1514, 1413, 1281, 1268, 1206, 1177, 1145, 1084, 1066, 1027, 876, 812, 798, 659, 641cm^{-1}.

^{1}H NMR (400MHz; $(CD_3)_2CO$): δ = 7.60 (dd, *J* = 2.0, 8.5 Hz, 1 H), 7.55 (d, *J* = 1.8 Hz, 1 H), 7.00 (d, *J* = 8.5 Hz, 1 H), 4.84 (s, 2 H), 3.90 (s, 3 H), 2.52 (s, 3 H) ppm.

^{13}C NMR (101MHz; $(CD_3)_2CO$): δ = 196.5, 169.9, 152.8, 150.4, 132.3, 123.5, 113.4, 112.1, 66.0, 56.3, 26.4 ppm.

HRMS-ESI (m/z): $[M+Na]^+$ calcd for $C_{11}H_{12}NaO_5$: 247.0582 Found: 247.0582.

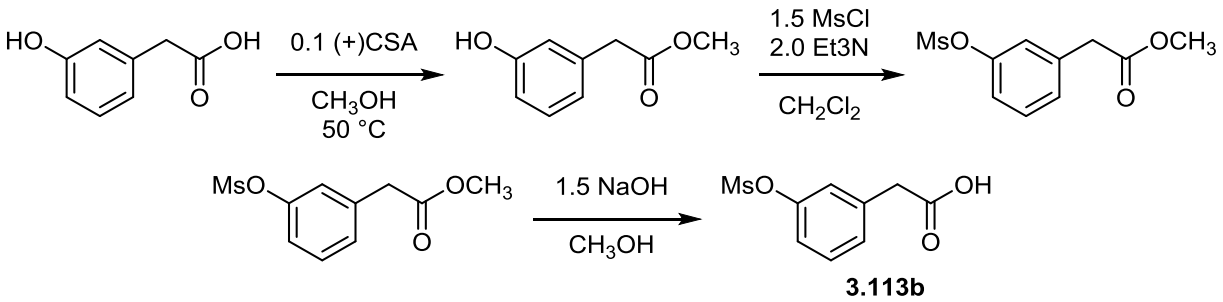

3.113b

2-(3-((methylsulfonyl)oxy)phenyl)acetic acid (**3.113b**): To a solution of 2-(3-hydroxyphenyl)acetic acid (455 mg, 3.0 mmol, 1.0 equiv.) in methanol (15 ml) was added (+) camphorsulfonic acid (70 mg, 0.3 mmol, 0.1 equiv.) in one portion and the reaction was placed in an 50 °C oil bath. After 19 h, the reaction was poured into EtOAc (80 ml), washed with water (3 x 25 ml), brine (20 ml), dried over Na_2SO_4, filtered, and concentrated by rotary evaporation to the crude methyl ester. This oil was dissolved in CH_2Cl_2 (12 ml) and cooled to 0 °C in an ice/water bath and mesyl chloride (350 µl, 4.5 mmol, 1.5 equiv.) was added over 30 s. Triethylamine (840 µl, 6.0 mmol, 2.0 equiv.) was added slowly over 3 min resulting in a cloudy yellow-white suspension. After 1.5 h, the orange reaction was quenched with water (1 ml), poured into EtOAc (80 ml), washed with water (25 ml), 1.0 M $HCl_{(aq)}$ (2 x 20 ml), brine (20 ml), dried over Na_2SO_4, filtered, and concentrated by rotary evaporation to the crude mesylated methyl ester.

To a solution of the crude ester in methanol (15 ml) was added $NaOH_{(aq)}$ (1.5 ml, 3.0 M in H_2O, 4.5 mmol, 1.5 equiv.) at ambient temperature. The reaction was monitored by TLC for completion then poured into Et_2O (60 ml) and extracted with water (20 ml) and 1.0 M $NaOH_{(aq)}$ (2 x 20 ml). The aqueous layers were combined and acidified with $HCl_{(aq)}$ (10 wt%) and extracted with EtOAc (3 x 20 ml). The organic layers were combined, washed with brine, dried over Na_2SO_4, filtered and concentrated by rotary evaporation to afford 2-(3-((methylsulfonyl)oxy)phenyl)acetic acid (**3.113b**) as a white solid (314 mg, 46% yield over 3 steps).

^{1}H NMR (400MHz; CD_3OD): δ = 7.47 - 7.39 (m, 1 H), 7.36 - 7.30 (m, 2 H), 7.25 (dd, *J* = 1.2, 8.1 Hz, 1 H), 3.71 (s, 2 H), 3.27 (s, 3 H) ppm.

^{13}C NMR (101MHz; CD_3OD): δ = 172.3, 150.7, 138.4, 130.7, 129.4, 124.2, 121.5, 40.7, 37.7 ppm.

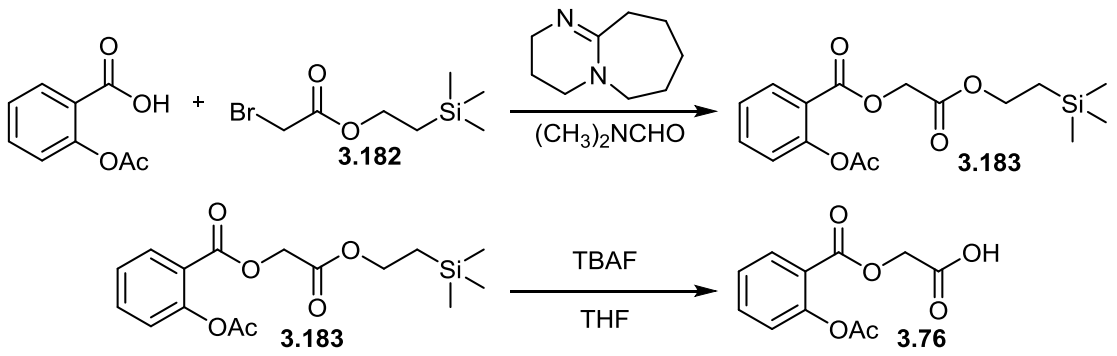

2-((2-acetoxybenzoyl)oxy)acetic acid (**3.76**): To a solution of 2-(trimethylsilyl)ethanol (280 µl, 2.0 mmol, 1.0 equiv.) in CH_2Cl_2 (8 ml, 0.25 M), cooled to 0 °C in ice/water bath, was added 2-bromoacetyl chloride (220 µl, 2.6 mmol, 1.3 equiv.) in one portion, then triethylamine (370 µl, 2.6 mmol, 1.3 equiv.) was added over 1 min. The reaction mixture turns from a clear colourless solution to off-white solids suspended in a yellow liquid. After 3 h, the reaction was quenched with water (500 µl) then poured into hexanes (60 ml). The organic layer was washed sequentially with water (20 ml), 1.0 M $HCl_{(aq.)}$ (2 x 15 ml), brine (15 ml), then dried over Na_2SO_4. The organic layer was filtered and concentrated by rotary evaporation to afford bromide (**3.182**) which was used without further purification.

To a solution bromide (**3.182**) in DMF (5 ml) was added 2-acetoxybenzoic acid (540 mg, 3.0 mmol, 1.5 equiv.) in one portion, then 1,8-diazabicycloundec-7-ene (450 µl, 3.0 mmol, 1.5 equiv.) was added dropwise over 10 s. The reaction mixture turns from yellow solution to orange-brown solution. After 3 days, the reaction mixture was poured into water (100 ml) and extracted with Et_2O (3 x 20 ml). The combined yellow-brown organic extract was washed sequentially with 10% w/w $HCl_{(aq.)}$ (20 ml), 3.0M $NaOH_{(aq.)}$ (20 ml), brine (20 ml), then dried over Na_2SO_4. The organic layer was filtered, concentrated

by rotary evaporation and semi-purified by flash chromatography (6:1 hexanes: EtOAc, Rf = 0.26, visualization = $KMnO_4$, UV) to afford silane (**3.183**) as a pale yellow-brown oil.

To a solution silane (**3.183**) in THF (14 ml) was added tetrabutylammonium fluoride (2.1 ml, 2.1 mmol, 1.0 M in THF) in one portion. The reaction mixture turns from yellow-brown solution to clear colourless solution. After 3 h, the reaction mixture was quenched with water (15 ml) then poured into1.0M $HCl_{(aq.)}$ (75 ml) and extracted with Et_2O (3 x 20 ml). The combined organic extract was washed with brine (20 ml), dried over Na_2SO_4, filtered, and concentrated by rotary evaporation. Recrystallization from hexanes- Et_2O yielded 2-((2-acetoxybenzoyl)oxy)acetic acid (**3.76**) as white needles (173 mg, 36% yield over 3 steps).

m.p.: 124.0 - 125.0 ºC

IR (neat): 3204, 3005, 2951, 1749, 1722, 1606, 1488, 1426, 1411, 1374, 1276, 1262, 1239, 1190, 1169, 1136, 1094, 1044, 1030, 1008, 957, 929, 882, 838, 779, 758, 702, 686, 657 cm^{-1}.

^{1}H NMR (400MHz; CD_3OD): δ = 8.08 (dd, *J* = 1.7, 7.9 Hz, 1 H), 7.65 (dt, *J* = 1.7, 7.9 Hz, 1 H), 7.39 (dt, *J* = 1.2, 7.6 Hz, 1 H), 7.18 (dd, *J* = 1.2, 8.0 Hz, 1 H), 4.81 (s, 2 H), 2.30 (s, 3 H) ppm.

^{13}C NMR (101MHz; CD_3OD): δ = 171.5, 171.0, 165.5, 152.4, 135.6, 132.9, 127.3, 125.2, 124.2, 62.2, 21.1 ppm.

HRMS-ESI (m/z): $[M+Na]^+$ calcd for $C_{11}H_{10}O_6Na$: 261.0375. Found: 261.0377.

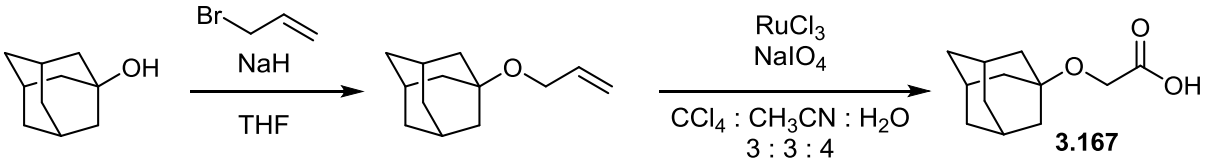

3.167

2-(adamantan-1-yloxy)acetic acid (**3.167**): To a solution of 1-adamantanol (761 mg, 5.0 mmol, 1.0 equiv.) in THF (20 ml, 0.25 M), was added allylbromide (2.2 ml, 25.0 mmol, 5 equiv.) in one portion,

then sodium hydride (400 mg, 10.0 mmol, 2.0 equiv, 60 wt% in mineral oil) was added in two equal portions with a 90 minute interval. The reaction mixture turns from a clear colourless solution to white solids suspended in a yellow liquid. The reaction mixture was refluxed for 20 hours then cooled to ambient temperature, poured into water (80 ml) and extracted with Et_2O (2 x 20 ml) then EtOAc (2 x 20 ml). The combined organic extract was washed with brine (20 ml), dried over Na_2SO_4, filtered, concentrated by rotary evaporation and purified by flash column chromatography (15:1 hexanes : EtOAc, Rf = 0.42, visualization = $KMnO_4$) to afford 1-(allyloxy)adamantane as a clear colourless oil (420 mg, 44%). The compound obtained matched literature characterization data.[268]

To a biphasic mixture of 1-(allyloxy)adamantane (370 mg, 1.9 mmol, 1.0 equiv.) and ruthenium (III) chloride hydrate (10 mg, ~0. 05 mmol, ~0.025 equiv.) in CCl_4 : CH_3CN : water (6 ml : 6 ml: 8 ml, total volume = 20 ml), was added sodium periodate (3.4 g, 15.3 mmol, 8 equiv.) in two equal portions with a 60 min interval. The reaction mixture turns from a brown-yellow mixture with suspended white solids to a cloudy white-brown emulsion. The reaction mixture was stirred for 2 hours then poured into CH_2Cl_2 (50 ml) and washed with 1.0 M $HCl_{(aq.)}$ (40 ml), brine (20 ml), then dried over Na_2SO_4 and decolourizing carbon. Recrystallization from hexanes yielded 2-(adamantan-1-yloxy)acetic acid (**3.167**) as a grey solid (156 mg, 39%).

m.p.: 128.5 - 130.5 ºC

IR (neat): 2907, 2853, 1738, 1432, 1358, 1215, 1185, 1108, 1088, 1062, 973, 916, 900, 677cm^{-1}.

^{1}H NMR (400MHz; $CDCl_3$): δ = 4.08 (s, 2 H), 2.20 (br. s., 3 H), 1.78 (s, 3 H), 1.78 (s, 3 H), 1.72 - 1.55 (m, 6 H) ppm.

^{13}C NMR (101MHz; $CDCl_3$): δ = 172.4, 75.0, 58.4, 41.2, 36.0, 30.4 ppm.

HRMS-EI (m/z): $[M]^+$• calcd for $C_{12}H_{18}O_3$: 210.12559. Found: 210.12538.

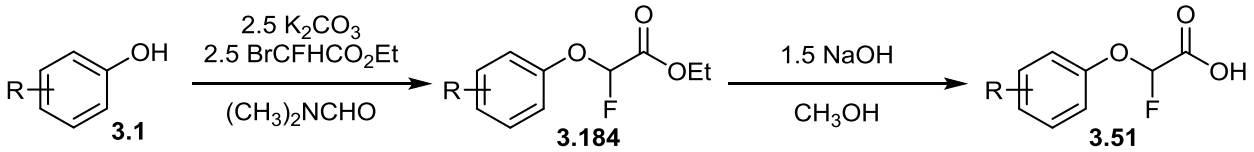

3.1 3.184 3.51

General procedure for the synthesis of aryloxy fluoroacetic acids: To a suspension of potassium carbonate (2.5 equiv.) in a solution of phenol (1.0 equiv.) in dimethyl formamide (0.5M with respect to phenol) was added ethyl bromofluoroacetate (2.5 equiv.) in100 μl portions every 10 min at ambient temperature. After addition was completed, the reaction was allowed to stir an additional 2 hours. The reaction mixture was poured into water and extracted with 3 x Et_2O. The organic layers were combined and washed with 2 x $NaOH_{(aq)}$ (3.0M) and brine. The organic extract was dried over Na_2SO_4, filtered and concentrated by rotary evaporation to afford the crude ethyl ester which was used immediately. To a solution of the crude ester in methanol (0.2 M with respect to phenol) was added $NaOH_{(aq)}$ (1.5 equiv., 3.0M) at ambient temperature. The reaction was monitored by TLC for completion then poured into Et_2O and extracted with water and 2 x $NaOH_{(aq)}$ (1.0M). The aqueous layers were combined and acidified with $HCl_{(aq)}$ (10 wt%) and extracted with 3 x Et_2O or EtOAc. The organic layers were combined, washed with brine, dried over Na_2SO_4, filtered and concentrated by rotary evaporation to afford a solid which was recrystallized in hexanes/EtOAc.

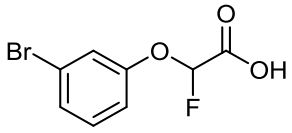

3.52

2-(3-bromophenoxy)-2-fluoroacetic acid (**3.52**): 3-bromophenol (523 mg, 3.0 mmol) was subjected to the general aryloxy fluoroacetic acids synthesis procedure. 2-(3-bromophenoxy)-2-fluoroacetic acid (**3.52**) was obtained as white crystals (520 mg, 70% yield).

^{1}H NMR (400MHz; C_6D_6): δ = 7.14 (s, 1 H), 6.93 (d, *J* = 7.6 Hz, 1 H), 6.65 (dd, *J* = 1.8, 8.2 Hz, 1 H), 6.53 (t, *J* = 7.9 Hz, 1 H), 5.46 - 5.14 (m, 2 H) ppm.

^{13}C NMR (101MHz; C_6D_6): δ = 166.6 (d, *J* = 31.0 Hz), 156.8, 131.4, 128.1, 123.5, 121.4, 116.6, 102.4 (d, *J* = 232.5 Hz) ppm.

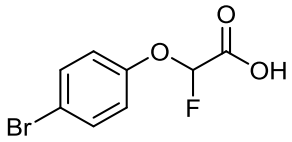

3.53

2-(4-bromophenoxy)-2-fluoroacetic acid (**3.53**): 4-bromophenol (350 mg, 2.0 mmol) was subjected to the general aryloxy fluoroacetic acids synthesis procedure. 2-(4-bromophenoxy)-2-fluoroacetic acid (**3.53**) was obtained as off white crystals (305 mg, 61% yield).

^{1}H NMR (300MHz; $CDCl_3$): δ = 7.56 - 7.36 (m, 2 H), 7.04 (d, *J* = 8.8 Hz, 9 H), 5.97 (d, *J* = 58.1 Hz, 2 H), 4.84 (br. s., 1 H) ppm.

^{13}C NMR (101MHz; $CDCl_3$): δ = 166.6 (d, *J* = 31.5 Hz), 154.6, 132.9, 119.3, 117.5, 102.1 (d, *J* = 232.8 Hz) ppm.

^{19}F (282 MHz; $CDCl_3$): δ = -130.5 (d, *J* = 58.7 Hz).

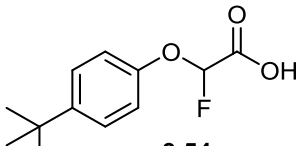

3.54

2-(4-(*tert*-butylphenoxy)-2-fluoroacetic acid (**3.54**): 4-*tert*-Butylphenol (350 mg, 3.0 mmol) was subjected to the general aryloxy fluoroacetic acids synthesis procedure. 2-(4-(*tert*-butylphenoxy)-2-fluoroacetic acid (**3.54**) was obtained as off white crystals (305 mg, 61% yield).

^{1}H NMR (400MHz; $CDCl_3$): δ = 9.57 (br. s., 1 H), 7.07 (d, *J* = 8.9 Hz, 2 H), 6.93 (d, *J* = 8.9 Hz, 2 H), 5.60 (d, *J* = 59.4 Hz, 1 H), 1.14 (s, 9 H) ppm.

^{13}C NMR (101MHz; $CDCl_3$): δ = 168.5 (d, *J* = 30.7 Hz), 154.4, 147.7, 127.3, 117.7, 103.1 (d, *J* = 231.6 Hz), 34.6, 31.7 ppm.

^{19}F (282 MHz; $CDCl_3$): δ = -129.6 (d, *J* = 59.7 Hz).

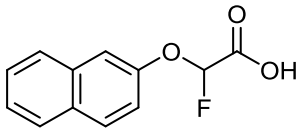

3.55

2-fluoro-2-(naphthalen-2-yloxy)acetic acid (**3.55**): 2-Naphthol (360 mg, 3.0 mmol) was subjected to the general aryloxy fluoroacetic acids synthesis procedure. 2-fluoro-2-(naphthalen-2-yloxy)acetic acid (**3.55**) was obtained as off white crystals (325 mg, 59% yield).

^{1}H NMR (400MHz; $CDCl_3$): δ = 7.92 (br. s., 1 H), 7.88 - 7.79 (m, 3 H), 7.57 - 7.43 (m, 3 H), 7.33 (dd, *J* = 2.4, 8.8 Hz, 1 H), 6.31 - 6.07 (m, *J* = 59.1 Hz, 1 H) ppm.

^{13}C NMR (101MHz; $CDCl_3$): δ = 168.1 (d, *J* = 32.1 Hz), 153.4, 133.9, 130.7, 130.2, 127.7, 127.4, 126.9, 125.4, 118.5, 112.6, 102.2 (d, *J* = 232.5 Hz) ppm.

^{19}F (282 MHz; $CDCl_3$): δ = -129.4 (d, *J* = 57.4 Hz).

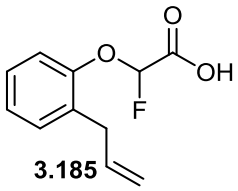

3.185

2-(2-allylphenoxy)-2-fluoroacetic acid (**1.185**): 2-Allylphenol (537 mg, 4.0 mmol) was subjected to the general aryloxy fluoroacetic acids synthesis procedure. 2-(2-allylphenoxy)-2-fluoroacetic acid (**3.185**) was obtained as off white crystals (400 mg, 48% yield).

^{1}H NMR (400MHz; $CDCl_3$): δ = 9.72 (br. s, 1H), 7.31 - 7.22 (m, 2 H), 7.21 - 7.10 (m, 2 H), 6.15 - 5.82 (m, 2 H), 5.17 - 5.00 (m, 2 H), 3.69 - 3.28 (m, 2 H) ppm.

^{13}C NMR (101MHz; $CDCl_3$): δ = 168.7 (d, *J* = 32.2 Hz), 153.8 (d, *J* = 3.1 Hz), 136.3, 130.7, 127.8, 125.0, 116.5, 116.1, 102.6 (d, *J* = 232.3 Hz), 34.1 ppm.

^{19}F (282 MHz; $CDCl_3$): δ = -128.2 (d, *J* = 57.4 Hz).

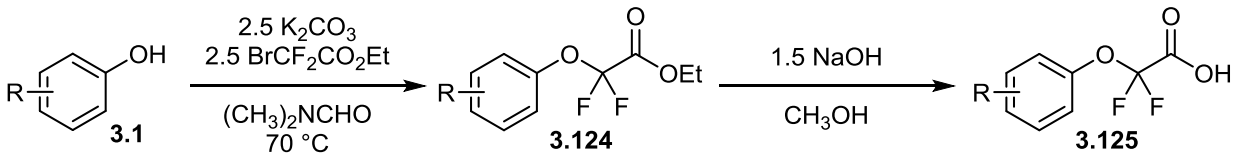

General procedure for the synthesis of aryloxy difluoroacetic acids: To a suspension of potassium carbonate (2.5 equiv.) in a solution of phenol (1.0 equiv.) in dimethyl formamide (0.5M with respect to phenol) heated to 70 °C was added ethyl bromodifluoroacetate (2.5 equiv.) in100 µl portions every 10 min. After addition was completed, the reaction was allowed to stir an additional 12 hours. The reaction mixture was poured into water and extracted with 3 x Et_2O. The organic layers were combined and washed with 2 x $NaOH_{(aq)}$ (3.0M) and brine. The organic extract was dried over Na_2SO_4, filtered and concentrated by rotary evaporation to afford the crude ethyl ester which was used immediately. To a solution of the crude ester in methanol (0.2 M with respect to phenol) was added $NaOH_{(aq)}$ (1.5 equiv., 3.0M) at ambient temperature. The reaction was monitored by TLC for completion then poured into Et_2O and extracted with water and 2 x $NaOH_{(aq)}$ (1.0M). The aqueous layers were combined and neutralized with $HCl_{(aq)}$ (10 wt%,) and washed with 3 x DCM. The pH was then adjusted to 6 and washed with 4 x DCM. The aqueous layer was then acidified (pH < 2) and extracted with 3 x DCM. The final organic extracts were combined, washed with brine, dried over Na_2SO_4, filtered and concentrated by rotary evaporation in a cold water bath (15 °C) to afford an oil which should be stored in the freezer.

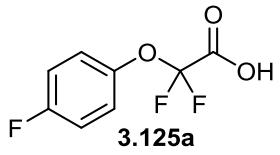

2,2-difluoro-2-(4-fluorophenoxy)acetic acid (**3.125a**): 4-Fluorophenol (336 mg, 3.0 mmol) was subjected to the general aryloxy difluoroacetic acids synthesis procedure. 2,2-difluoro-2-(4-

fluorophenoxy)acetic acid (**3.125a**) was obtained as a colourless oil which froze upon standing in the freezer (173 mg, 28% yield).

^{1}H NMR (300MHz; $CDCl_3$): δ = 7.25 - 7.17 (m, 2H), 7.12 - 6.95 (m, 4H) ppm.

^{19}F (282 MHz; $CDCl_3$): δ = -77.5 (s), -115.8 - -115.9 (m) ppm.

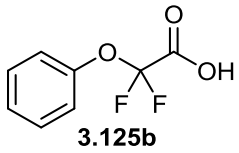

3.125b

2,2-difluoro-2-phenoxyacetic acid (**3.125b**): Phenol (282 mg, 3.0 mmol) was subjected to the general aryloxy difluoroacetic acids synthesis procedure. 2,2-difluoro-2-phenoxyacetic acid (**3.125b**) was obtained as a colourless oil containing multiple unknown impurities (371 mg, 66% yield).

^{1}H NMR (300MHz; $CDCl_3$): δ = 7.47 - 7.33 (m, 2 H), 7.32 - 7.18 (m, 3 H) ppm.

^{19}F (282 MHz; $CDCl_3$): δ = -77.0 (s) ppm.

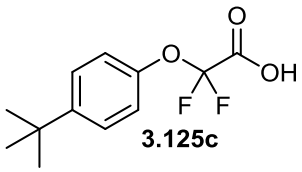

3.125c

2,2-difluoro-2-(4-*tert*-butylphenoxy)acetic acid (**3.125c**): 4-*tert*-butylphenol (451 mg, 3.0 mmol) was subjected to the general aryloxy difluoroacetic acids synthesis procedure. 2,2-difluoro-2-(4-*tert*-butylphenoxy)acetic acid (**3.125c**) was obtained as a colourless oil which froze in the freezer (~300 mg, 40% yield).

^{1}H NMR (300MHz; $CDCl_3$): δ = 7.44 - 7.32 (m, 2 H), 7.15 (dd, *J* = 3.3, 8.8 Hz, 2 H), 1.32 (s, 9 H) ppm.

^{19}F (282 MHz; $CDCl_3$): δ = -76.6 (s) ppm.

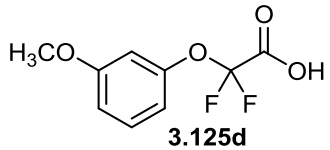

3.125d

2,2-difluoro-2-(3-methoxyphenoxy)acetic acid (**3.125d**): 3-Methoxyphenol (372 mg, 3.0 mmol) was subjected to the general aryloxy difluoroacetic acids synthesis procedure. 2,2-difluoro-2-(3-methoxyphenoxy)acetic acid (**3.125d**) was obtained as a light brown oil contain Et_2O (128 mg, 20% yield).

^{1}H NMR (300MHz; $CDCl_3$): δ = 7.40 - 7.10 (m, 1 H), 6.93 - 6.67 (m, 3 H), 6.26 (br. s., 1 H), 3.82 (s, 3 H) ppm.

^{19}F (282 MHz; $CDCl_3$): δ = -77.0 (s) ppm.

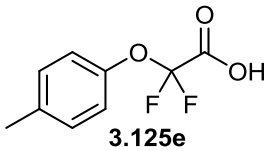

3.125e

2,2-difluoro-2-(4-methylphenoxy)acetic acid (**3.125e**): 4-methylphenol (541 mg, 3.0 mmol) was subjected to the general aryloxy difluoroacetic acids synthesis procedure. 2,2-difluoro-2-(4-methylphenoxy)acetic acid (**3.125e**) was obtained as a light yellow oil containing Et_2O (285 mg, 28% yield).

^{1}H NMR (300MHz; $CDCl_3$): δ = 7.23 - 6.97 (m, 5 H), 2.36 (s, 3 H) ppm.

^{19}F (282 MHz; $CDCl_3$): δ = -77.0 (s) ppm.

3.6.4 Experimental procedures related to fluorodecarboxylation mediated by iodine(III)

Experimental procedure for reactions reported in Tables 3.1, 3.2, 3.3, 3.5, Scheme 3.11, Figure 3.3: To a 0.5-2.5 ml microwave vial filled with argon was added carboxylic acid substrate (1.0 equiv, 0.1 mmol), PIFA or DIB (as indicated), NFSI (as indicated), and deuterated solvent (as indicated) to a concentration of 0.1 M of acid in solvent and ethyl trifluoroacetate or nitromethane (as an internal standard). An aliquot was kept for the t=0 timepoint for ^{1}H NMR analysis. The reaction mixture was partitioned into an NMR tube and irradiated for 1 h with a light source as indicated, and the crude reaction mixtures were subject to NMR analysis. Isolation of fluorinated compounds was never attempted for hypervalent iodine mediated aryl monofluoromethyl ether syntheses.

Experimental procedure for reactions reported in Tables 3.4 and Scheme 3.14: To a 0.5-2.5 ml microwave vial filled with argon was added phenoxyfluoroacetic acid (1.0 equiv, 0.1 mmol), PIFA or DIB (as indicated), NFSI or fluoride source (as indicated), deuterobenzene (0.1 M in acid) and ethyl trifluoroacetate (as an internal standard). An aliquot of the acid solution was kept for the t=0 timepoint for ^{1}H NMR analysis. The reaction mixture was partitioned into an NMR tube and irradiated at 300 nm for 1 h, and the crude reaction mixtures were subject to NMR analysis.

The reaction in Table 3.4, entry 6, was concentrated by rotary evaporation and filtered through a plug of silica (100% hexanes, visualization by UV) to afford a 1: 8 mixture of 4-bromodifluoromethyl benzene (**2.40**) and iodobenzene.

3.6.5 Experimental procedures related to PDC-F with NFSI or Sel-F

PDC-F Method A (NFSI): To an argon filled Wilmad tube (10 mm diameter EPR tube) equipped with stirbar was added aryloxyacetic acid (**3.44**) (0.4 mmol, 1.0 equiv.), DtBuPy (41 mg, 0.2 mmol, 0.5 equiv.), NFSI (500 mg, 1.6 mmol, 4.0 equiv.), and acetone (argon sparged, 2.7 ml, 0.15 M in **3.44**). The tube was capped and the reaction mixture was stirred until all solids were dissolved (~3 min). The reaction vessel was placed in the photoreactor and exposed to 300 nm light for 3 hours, producing a yellow-orange solution. The reaction mixture was concentrated by rotary evaporation in an ambient temperature (25 ºC) water bath under reduced pressure to roughly 1 mL, then subject to flash column chromatography (Et_2O/pet. ether). The appropriate fractions were collected and concentrated by rotary evaporation in an ambient temperature water bath under reduced pressure to afford the fluorinated products.

PDC-F Method B (NFSI): To an argon filled Wilmad tube (10 mm diameter EPR tube) equipped with stirbar was added aryloxyacetic acid (**3.44**) (0.4 mmol, 1.0 equiv.), DtBuMPy (41 mg, 0.2 mmol, 0.5 equiv.), NFSI (378 mg, 1.2 mmol, 3.0 equiv.), and acetone (argon sparged, 2.7 ml, 0.15 M in **3.44**). The tube was capped and the reaction mixture was stirred until all solids were dissolved (~3 min). The reaction vessel was placed in the photoreactor and exposed to 350 nm light for one hour, producing a light yellow solution. The reaction mixture was concentrated by rotary evaporation in an ambient temperature (25 ºC) water bath under reduced pressure to roughly 1 mL, then subject to flash column chromatography (Et_2O/pet. ether). The appropriate fractions were collected and concentrated by rotary evaporation in an ambient temperature water bath under reduced pressure to afford the fluorinated products.

PDC-F Method C (Sel-F): To an argon filled 15mL Falcon tube (15 mL polypropylene centrifuge tube) equipped with stirbar was added aryloxyacetic acid (**3.44**) (0.5 mmol, 1.0 equiv.) water (argon sparged, 5 ml), and 5.0 M $NaOH_{(aq)}$ (150 µl, 0.75 mmol, 1.5 equiv.). The tube was capped and the reaction mixture was stirred until all of the acid was dissolved (~5 min). Freshly powdered Sel-F (620 mg, 1.75 mmol, 3.5 equiv.) was added and the reaction mixture was stirred until all solids were dissolved (~5 min). The reaction vessel was placed in the photoreactor and exposed to 300 nm light for one hour, producing a cloudy yellow-orange or white emulsion. The reaction mixture was poured into water (20 ml) and extracted with Et_2O (3 x 10 ml). The organic layers were combined and washed with 3.0 M $NaOH_{(aq)}$ (2 x 10 mL) and brine (15 ml). The organic extracts were dried over Na_2SO_4, filtered and concentrated by rotary evaporation in a cold (10 ºC) water bath to roughly 1 ml. The solution was washed through a short plug of silica with chloroform and the solvent was removed by rotary evaporation in a cold (10 ºC) water bath to afford the fluorinated product.

PDC-F Method D (Sel-F): To an argon filled 15mL Falcon tube (15 mL polypropylene centrifuge tube) equipped with stirbar was added aryloxyacetic acid (**1**, **3** or **5**) (0.1 mmol, 1.0 equiv.) and deuterium oxide (argon sparged, 1 ml) [or deuterium oxide:deuteroacetonitrile 2:1 (argon-sparged, 1 ml)] then 5.0M $NaOH_{(aq)}$ (30 µl, 0.15 mmol, 1.5 equiv.) The tube was capped and the reaction mixture was stirred until all of the acid was dissolved (~5 min). Freshly powdered Selectfluor® (124 mg, 0.35 mmol, 3.5 equiv.) was added and the reaction mixture was stirred until all solids were dissolved (~5 min). The reaction vessel was placed in the photoreactor and exposed to 300 nm light for one hour, producing a cloudy yellow-orange or white emulsion. The reaction mixture was extracted with a deuterochloroform solution (700 µl) containing a known amount of 1,3,5-trimethoxybenzene and immediately analyzed by NMR spectroscopy.

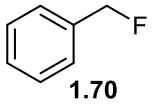

1.70

Benzyl fluoride (**1.70**): Phenylacetic acid (**3.40a**) (70 mg, 0.5 mmol) was subjected to general PDC-F method C. Benzyl fluoride was obtained as a slightly yellow oil with trace amounts of ether (40 mg, 72% yield). The compound obtained matched literature characterization data.[269]

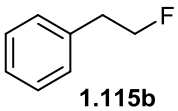

1.115b

Homobenzyl fluoride (**1.115b**): Hydrocinnamic acid (**3.40b**) (75 mg, 0.5 mmol) was subjected to general PDC-F method C. Homobenzyl fluoride was obtained as a yellow oil (33 mg, 53% yield). The compound obtained matched literature characterization data.[83b]

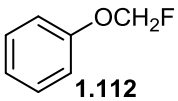

1.112

(Fluoromethoxy)benzene (**1.112**): 2-Phenoxyacetic acid (**2.26**) (76 mg,) was subjected to general PDC-F method C. (Fluoromethoxy)benzene (**1.112**) was obtained as a yellow oil (29 mg, 46% yield). The compound obtained matched literature characterization data.[83b]

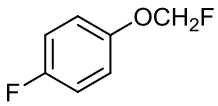

3.43

1-Fluoro-4-(fluoromethoxy)benzene (**3.43**): 2-(4-fluorophenoxy)acetic acid (**3.42**) (85 mg,) was subjected to general PDC-F method C. 1-fluoro-4-(fluoromethoxy)benzene (**3.42**) was obtained as a yellow oil with trace amounts of ether (44 mg, 60% yield). The compound obtained matched literature characterization data.[264]

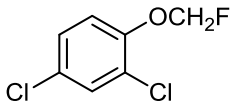

1.113

2, 4-dichloro-1-(fluoromethoxy)benzene (**1.113**): 2-(2,4-Dichlorophenoxy)acetic acid (88 mg,) was subjected to general PDC-F Method A. 2,4-Dichloro-1-(fluoromethoxy)benzene (**1.113**) was obtained as a white solid (45 mg, 54% yield).

2, 4-dichloro-1-(fluoromethoxy)benzene (**1.113**): To an argon filled 15mL Falcon tube equipped with stirbar was added 2-(2,4-dichlorophenoxy)acetic acid (443mg, 2.0 mmol, 1.0 equiv.) and a 2:1 water : acetonitrile mixture (argon-sparged, 10 ml) then 5.0M $NaOH_{(aq)}$ (600 µl, 3.0 mmol, 1.5 equiv.) The tube was capped and the reaction mixture was stirred until all of the acid was dissolved (~25 min). Freshly powdered Sel-F (2.1 g, 6.0 mmol, 3.0 equiv.) was added and the reaction mixture was stirred until all solids were dissolved (~5 min). The screw-top cap was replaced with a rubber septum pieced with a venting needle and then the reaction vessel was placed in the photoreactor and exposed to 300 nm light for 1.5 h producing a cloudy white reaction mixture with an orange phase on the bottom. The reaction mixture was poured into water (75 ml) and extracted with Et_2O (3 x 20 ml). The organic layers were combined and washed with 3.0M $NaOH_{(aq)}$ (2 x 20 ml) and brine (25 ml). The organic extracts were dried over Na_2SO_4, filtered and concentrated by rotary evaporation in a cold (10 ºC) water bath under reduced pressure to roughly 3 ml. The reduced organic phase was washed through a short plug of silica with chloroform and concentrated by rotary evaporation in a cold (10 ºC) water bath under reduced pressure to afford **1.113** as an orange solid (337mg, 86% yield).

m.p.: 46.5 - 47.5 ºC

IR (neat): 3105, 3084, 3017, 2952, 1476, 1390, 1296, 1234, 1108 cm^{-1}.

^{1}H NMR (300MHz; $CDCl_3$): δ = 7.43 (d, *J* = 2.4 Hz, 1H), 7.24 (dd, *J* = 8.8, 2.4 Hz, 1H), 7.15 (dd, *J* = 8.8, 0.7 Hz, 1H), 5.72 (d, *J* = 53.9, 2H) ppm.

^{13}C NMR (75MHz; $CDCl_3$): δ = 151.2 (d, *J* = 3.0 Hz), 130.3, 129.2, 128.0, 125.1 (d, *J* = 2.2 Hz), 118.4 (d, *J* = 1.7 Hz), 101.1 (d, *J* = 222.0 Hz) ppm.

^{19}F (282 MHz; $CDCl_3$): δ = -149.9 (t, *J* = 54.2 Hz) ppm.

HRMS-EI (m/z): $[M]^{+\bullet}$ calcd for $C_7H_5O_1Cl_2F_1$: 193.97015. Found: 193.97045.

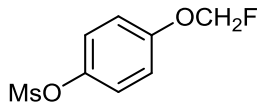

3.100

4-(Fluoromethoxy)phenyl methanesulfonate (**3.100**): 2-(4-((methylsulfonyl)oxy)phenoxy)acetic acid (123 mg,) was subjected to general PDC method C. 4-(fluoromethoxy)phenyl methanesulfonate (**3.100**) was obtained as a white-yellow solid (86 mg, 78% yield).

m.p.: 36-38 ºC

IR (neat): 3028, 2945, 1500, 1417, 1369, 1335, 1306, 1238 cm^{-1}.

^{1}H NMR (300MHz; $CDCl_3$): δ = 7.23 - 7.30 (m, 2H), 7.09 - 7.17 (m, 2H), 5.71 (d, *J* = 54.2 Hz, 2H), 3.14 (s, 2H) ppm.

^{13}C NMR (101MHz; $CDCl_3$): δ = 155.6 (d, *J* = 3.1 Hz), 144.7, 123.35, 118.0 (d, *J* = 1.5 Hz), 100.7 (d, *J* = 217.8 Hz), 37.2 ppm.

^{19}F (282 MHz; $CDCl_3$): δ = -149.9 (t, *J* = 52.4 Hz) ppm.

HRMS-ESI (m/z): $[M+H]^{+}$ calcd for $C_8H_9FNaO_4S$: 243.0103. Found: 243.0108.

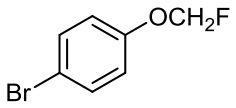

3.101

1-bromo-4-(fluoromethoxy)benzene (**3.101**): 2-(4-Bromophenoxy)acetic acid (92 mg,) was subjected to general PDC-F method A. 1-Bromo-4-(fluoromethoxy)benzene (**3.101**) was obtained as a colourless oil (56 mg, 68% yield). The compound obtained matched literature characterization data.[264]

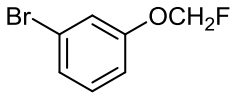

3.102

1-bromo-3-(fluoromethoxy)benzene (**3.102**): 2-(3-Bromophenoxy)acetic acid (92 mg,) was subjected to general PDC-F method A. 1-Bromo-3-(fluoromethoxy)benzene (**3.102**) was obtained as a colourless oil (60 mg, 73% yield). The compound obtained matched literature characterization data.[265]

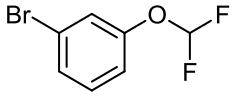

3.121

1-Bromo-3-(difluoromethoxy)benzene (**3.121**): 2-(3-bromophenoxy)-2-fluoroacetic acid (**3.52**) (125 mg) was subjected to general PDC-F method C with 2.5 hours irradiation. 1-bromo-3-(difluoromethoxy)benzene (**3.121**) was obtained as a slightly yellow oil (44 mg, 40% yield).

^{1}H NMR (300MHz; $CDCl_3$): δ = 7.43 - 7.17 (m, 3 H), 7.07 (d, *J* = 8.2 Hz, 1 H), 6.50 (t, *J* = 73.4 Hz, 1 H) ppm.

^{19}F (282 MHz; $CDCl_3$): δ = -81.56 (t, *J*=73.4) ppm.

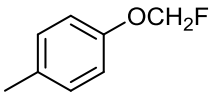

3.104

1-(Fluoromethoxy)-4-methylbenzene (**3.104**): 2-(4-Methylphenoxy)acetic acid (67 mg,) was subjected to general PDC-F method A. 1-(Fluoromethoxy)-4-methylbenzene (**3.104**) was obtained as a colourless oil (29 mg, 52% yield). The compound obtained matched literature characterization data.[264]

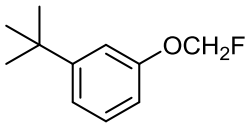

3.153

1-(*tert*-Butyl)-3-(fluoromethoxy)benzene (**3.153**): 2-(3-(*tert*-Butyl)phenoxy)acetic acid (84 mg,) was subjected to PDC-F method A. 1-(*tert*-Butyl)-3-(fluoromethoxy)benzene (**3.153**) was obtained as a colourless oil (61 mg with trace amounts of EtOAc, 84% yield).

IR (neat): 2964, 2870, 1610, 1584, 1488, 1439, 1411, 1395, 1365, 1295, 1274, 1216, 1203, 1117, 1099, 967, 893, 876, 782, 700 cm^{-1}.

^{1}H NMR (400MHz; $CDCl_3$): δ = 77.33 - 7.21 (m, 1 H), 7.15 (d, *J* = 7.9 Hz, 1 H), 7.11 (d, *J* = 1.5 Hz, 1 H), 6.93 (d, *J* = 8.1 Hz, 1 H), 5.73 (d, *J* = 55.0 Hz, 2 H), 1.33 (s, 9 H) ppm.

^{13}C NMR (101MHz; $CDCl_3$): δ = 156.7 (d, *J*=3.1 Hz), 153.4, 129.2, 120.6, 114.3 (d, *J*=1.5 Hz), 113.2, 100.9 (d, *J*=217.8 Hz), 34.8, 31.2 ppm.

^{19}F (282 MHz; $CDCl_3$): δ = -148.2 (t, *J*=54.8 Hz) ppm.

HRMS-EI (m/z): $[M]^{+\bullet}$ calcd for $C_{11}H_{15}OF$: 182.11069. Found: 182.11051.

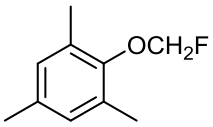

3.154

2-(Fluoromethoxy)-1, 3, 5-trimethylbenzene (**3.154**): 2-(Mesityloxy)acetic acid 20 mg,) was subjected to PDC-F method D in water/acetonitrile. ^{1}H NMR analysis shows conversion to a mixture of up to 4 distinct fluorinated compounds.

2-(Mesityloxy)acetic acid (78 mg,) was subjected to PDC-F method B. 2-(fluoromethoxy)-1,3,5-trimethylbenzene (**3.154**) was obtained as a colourless oil (42 mg, 62% yield).

IR (neat): 2971, 2922, 2862, 1491, 1474, 1411, 1378, 1311, 1207, 1165, 1140, 1081, 1036, 966, 853, 755, 724 cm^{-1}.

^{1}H NMR (400MHz; $CDCl_3$): δ = 6.86 (d, *J* = 0.7 Hz, 2 H), 5.54 (d, *J* = 55.0 Hz, 2 H), 2.27 (s, 3 H), 2.25 (s, 6 H) ppm.

^{13}C NMR (101MHz; $CDCl_3$): δ = 151.9 (d, *J*=1.5 Hz), 134.5, 130.4, 129.5, 104.4 (d, *J*=219.3 Hz), 20.6, 16.6, 16.6 ppm.

^{19}F (282 MHz; $CDCl_3$): δ = -146.8 (t, *J*=55.1) ppm.

HRMS-EI (m/z): $[M]^{+}$• calcd for $C_{10}H_{13}FO$: 168.09504 Found: 168.09519.

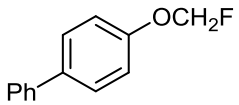

3.155

4-(Fluoromethoxy)-1,1'-biphenyl (**3.155**): 2-([1,1'-Biphenyl]-4-yloxy)acetic acid (23 mg,) was subjected to PDC-F method D in water/acetonitrile. Significant solubility problems were encountered; nevertheless, the suspension was subject irradiation. ^{1}H NMR analysis shows low conversion to **3.155**.

2-([1,1'-Biphenyl]-4-yloxy)acetic acid (92 mg, suspended in 200µl DMSO) was subjected to general PDC-F method B. 4-(Fluoromethoxy)-1,1'-biphenyl (**3.155**) was obtained as a white solid (64 mg, 79% yield). The compound obtained matched literature characterization data.[266]

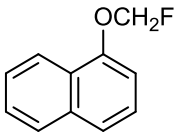

3.156

1-(Fluoromethoxy)naphthalene (**3.156**): 1-Naphthyloxyacetic acid (21 mg,) was subjected to PDC-F method D in water/acetonitrile. Undesired reactions were observed to occur even before irradiation. ^{1}H NMR analysis shows no conversion to the desired fluoroether **3.156**.

1-Naphthyloxyacetic acid (81 mg,) was subjected to general PDC-F method A. **3.156** was obtained as a colourless oil (42 mg, 60% yield). The compound obtained matched literature characterization data.[266]

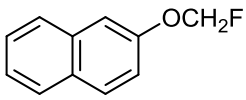

3.157

2-(Fluoromethoxy)naphthalene (**3.157**): 2-Naphthyloxyacetic acid (21 mg,) was subjected to PDC-F method D in water/acetonitrile. Undesired reactions were observed to occur even before irradiation. ^{1}H NMR analysis shows no conversion to **3.157**.

2-Naphthyloxyacetic acid (82 mg,) was subjected to general PDC-F method A. 2-(Fluoromethoxy)naphthalene (**3.157**) was obtained as a white solid (69 mg, >95% yield). The compound obtained matched literature characterization data.[266]

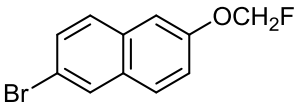

3.158

2-Bromo-6-(fluoromethoxy)naphthalene (**3.158**): 2-((6-bromonaphthalen-2-yl)oxy)acetic acid (**3.180**) 112 mg) was subjected to general PDC-F method B. 2-Bromo-6-(fluoromethoxy)naphthalene (**3.158**) was obtained as a white solid (34 mg, 33% yield).

^{1}H NMR (400MHz; $CDCl_3$): δ = 77.98 (d, *J* = 1.8 Hz, 1 H), 7.73 (d, *J* = 8.8 Hz, 1 H), 7.66 (d, *J* = 8.8 Hz, 1 H), 7.55 (dd, *J* = 2.0, 8.7 Hz, 1 H), 7.43 (d, *J* = 2.4 Hz, 1 H), 7.28 (dd, *J* = 2.4, 9.1 Hz, 1 H), 5.84 (d, *J* = 54.5 Hz, 2 H) ppm.

^{13}C NMR (101MHz; $CDCl_3$): δ = 154.8 (d, *J* = 3.1 Hz), 132.6, 131.2, 130.0, 129.7, 128.9, 119.6 (d, *J* = 1.5 Hz), 118.5, 111.0 (d, *J* = 1.5 Hz), 100.7 (d, *J* = 220.0 Hz) ppm.

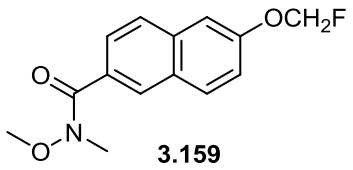

3.159

6-(Fluoromethoxy)-N-methoxy-N-methyl-2-naphthamide (**3.159**): **3.109** (29 mg,) was subjected to PDC-F method D in water. ^{1}H NMR analysis shows conversion to a mixture of up to 3 distinct fluorinated compounds.

3.109 (116 mg,) was subjected to PDC-F method B. 6-(Fluoromethoxy)-N-methoxy-N-methyl-2-naphthamide (**3.109**) was obtained as a thick colourless oil (69 mg, 66% yield).

IR (neat): 2934, 1630, 1605, 1479, 1420, 1385, 1362, 1281, 1257, 1221, 1182, 1145, 1124, 1079, 971, 959, 930, 903, 867, 811, 763, 736 cm^{-1}.

^{1}H NMR (400MHz; $CDCl_3$): δ = 8.21 (s, 1 H), 7.87 (d, *J* = 9.3 Hz, 1 H), 7.82 - 7.75 (m, 2 H), 7.47 (d, *J* = 2.3 Hz, 1 H), 7.29 (dd, *J* = 2.5, 8.9 Hz, 1 H), 5.85 (d, *J* = 54.4 Hz, 2 H), 3.57 (s, 3 H), 3.42 (s, 3 H) ppm.

^{13}C NMR (101MHz; $CDCl_3$): δ = 169.7, 155.7, 135.2, 130.8, 130.2, 129.1, 128.6, 126.9, 126.0, 119.1, 110.6, 100.5 (d, *J* = 217.8 Hz), 61.1, 33.8 ppm.

^{19}F (282 MHz; $CDCl_3$): δ = -149.88 (t, *J* = 55.1) ppm.

HRMS-EI (m/z): $[M]^{+\bullet}$ calcd for $C_{14}H_{14}NO_3F$: 263.09577. Found: 263.09570.

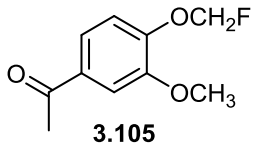

3.105

1-(4-(Fluoromethoxy)-3-methoxyphenyl)ethanone (**3.105**): 2-(4-Acetyl-2-methoxyphenoxy)acetic acid (**3.181**) (112 mg,) was subjected to PDC-F method C. **3.105** was obtained as an off-white solid (23 mg, 23% yield).

3.181 (91 mg,) was subjected to PDC-F method B. 1-(4-(Fluoromethoxy)-3-methoxyphenyl)ethanone (**3.105**) was obtained as an off-white solid (58 mg, 73% yield).

m.p.: 99 - 100.5 ºC.

IR (neat): 2947, 1670, 1593, 1511, 1492, 1462, 1415, 1282, 1265, 1242, 1216, 1179, 1152, 1088, 1028, 979, 950, 901, 878, 815, 763, 674, 644 cm^{-1}.

^{1}H NMR (400MHz; $CDCl_3$): δ = 7.52 - 7.60 (m, 2 H), 7.17 (dd, *J*=8.2, 1.0 Hz, 1 H), 5.79 (d, *J*=53.6 Hz, 2 H), 3.94 (s, 3 H), 2.59 (s, 3 H) ppm.

^{13}C NMR (101MHz; $CDCl_3$): δ = 196.75, 149.67 (d, *J*=2.2 Hz), 133.31, 122.65, 115.65, 111.11, 100.55 (d, *J*=220.8 Hz), 56.06, 26.34 ppm.

^{19}F (282 MHz; $CDCl_3$): δ = -150.23 (t, *J*=54.2) ppm.

HRMS-ESI (m/z): $[M+H]^+$ calcd for $C_{10}H_{12}O_3F$: 199.0770. Found: 199.0776.

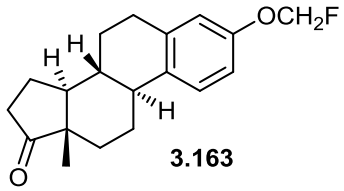

3.163

3-O-Fluoromethylestrone (**3.163**): 3-*O*-Carboxymethylestrone (**3.110**) (33 mg,) was subjected to PDC-F method D in water/acetonitrile mixture. ^{1}H NMR analysis shows a complex mixture of fluorinated compounds deriving from **3.110**. Although likely present in the mixture, **3.163** could not be unambiguously identified.

3-*O*-Carboxymethylestrone (**3.110**) (131 mg,) was subjected to PDC-F method B. 3-*O*-

Fluoromethylestrone (**3.163**) was obtained as a white solid (59 mg, 49% yield).

m.p.: 85 - 88 ºC.

$[\alpha]_D^{20\,°C}$: + 141° (acetonitrile, c = 23.8 mg/ml).

IR (neat): 2962, 2938, 2868, 1736, 1611, 1580, 1493, 1451, 1285, 1238, 1213, 1165, 1147, 1118, 1078, 1002, 972, 889, 868, 815, 778 cm^{-1}.

^1H NMR (400MHz; $CDCl_3$): δ = 7.25 (d, J = 8.5 Hz, 1 H), 6.89 (dd, J = 2.4, 8.5 Hz, 1 H), 6.84 (d, J = 2.4 Hz, 1 H), 5.69 (d, J = 55.0 Hz, 2 H), 2.92 (dd, J = 3.9, 8.7 Hz, 2 H), 2.52 (dd, J = 8.9, 19.1 Hz, 1 H), 2.46 - 2.37 (m, 1 H), 2.33 - 2.23 (m, 1 H), 2.21 - 1.92 (m, 4 H), 1.71 - 1.37 (m, 7 H), 0.92 (s, 3 H) ppm.

^{13}C NMR (101MHz; $CDCl_3$): δ = 220.8, 154.8, 138.2, 135.0, 126.6, 116.8, 114.2, 100.9(d, *J* = 217.8 Hz), 50.4, 48.0, 44.0, 38.2, 35.8, 31.5, 29.6, 26.4, 25.9, 21.6, 13.8 ppm.

^{19}F (282 MHz; $CDCl_3$): δ = -148.22 (t, *J*=55.1) ppm.

HRMS-EI (m/z): $[M]^+\bullet$ calcd for $C_{19}H_{23}O_2F$: 302.16821. Found: 302.16830.

Chapter 4: Alkoxy radical mediated processes

Prior to my work on radical fluorination, I studied the synthetic utility of alkoxyl radicals. In this chapter, selected works from studies on competition kinetic and alkoxyl radical mediated relay cyclizations will be discussed.

4.1 Introduction

4.1.1 Generation of alkoxyl radicals

Alkoxyl radicals are a sub-class of oxygen centered radicals whereby the oxygen atom possessing an unpaired electron is bound to an alkyl carbon.[202] Based on the degree of substitution of the linking carbon atom, alkoxyl radicals are classified as primary, secondary or tertiary.[202c] Regardless of the degree distinction, all alkoxyl radicals that cannot be stabilized by resonance delocalization are highly reactive electrophilic species[203] and rapidly undergo addition, homolytic substitution/cleavage or electron transfer reactions.

The three most commonly encountered alkoxyl radical mediated reactions are depicted in Scheme 4.1. If a radical stabilizing group (such as a phenyl ring or a heteroatom) is present beta to an alkoxyl radical, or a significant amount of ring strain can be released, fragmentation to a carbonyl and an alkyl radical will be favourable (homolytic cleavage).[204] If an alkene is present in the molecule, cyclization to form a 3, 4, or 5 membered ring is favourable (addition).[202c,e] While oxirane formation is rapid and reversible,[205] tetrahydrofuran formation is rapid and irreversible.[202e] If an accessible hydrogen is present in the delta position, an internal 1, 5-hydrogen atom transfer (1, 5-HAT) is kinetically favourable (homolytic substitution).[206] 1, 6-HAT is favourable only if the C-H bond is activated by the presence of a heteroatom such as oxygen.[206e]

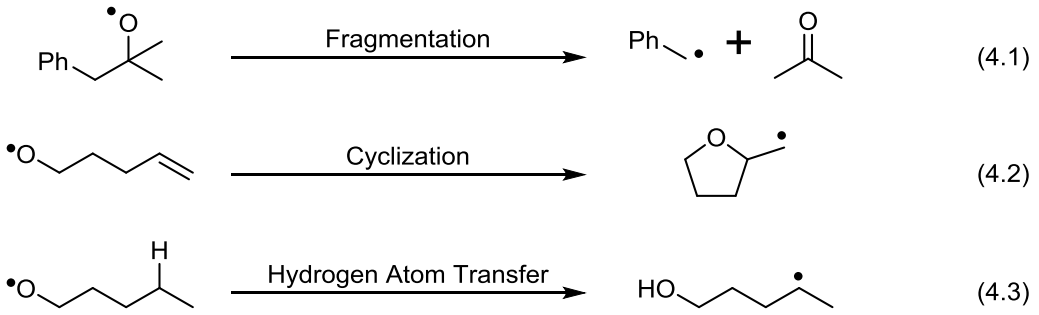

Scheme 4.1. Commonly encountered alkoxyl radical reactions

Practical, controlled generation of alkoxyl radicals typically relies on the corresponding alkyl alcohol **4.1** (by oxidation or functional group conversion to a homolytically cleavable oxygen-heteroatom bond) or rearrangement of an alkyl radical (by addition to a carbonyl or the fragmentation of a strained oxacycle). Oxidation of an alcohol to the alkoxyl radical can be carried out directly with $Pb(OAc)_4$,[207] $Ag_2S_2O_8$,[208] $(NH_4)_2[Ce(NO_3)_6]$[209] or through homolysis of a hypohalite intermediate.[210-213]

Activated intermediates, formed through a formal oxidation of the corresponding alkyl alcohol, can be homolyzed to an alkoxyl radical by photochemical or thermal stimulation (Scheme 4.2). Conversion to a hypoiodite (**4.2a**, X = I)[210] intermediate can be performed under relatively mild conditions with reagent combinations such as I_2/ hypervalent iodine (Suarez reaction)[179] or I_2/HgO.[211] A hypobromite (**4.2b**, X = Br)[212] intermediate can be formed by the action of a metal alkoxide salt on Br_2. Oxidation to an isolatable hypochlorite (**4.2c**, X = Cl)[213] is also possible and hypofluorite formation is only practical for perfluoroalcohols as covered in Chapter 1.

Peroxide (**4.2d**, X = OR')[133] formation is also a formal oxidation of the corresponding alkyl alcohol, although it is typically generated by displacement of an alcohol derivative with a hydroperoxide or the trapping of an alkyl radical with O_2. Formation of a nitrite ester (**4.2e**, X = NO)[214] or nitro ester (**4.2f**, X = NO_2)[215] is accomplished through a similar displacment reaction.

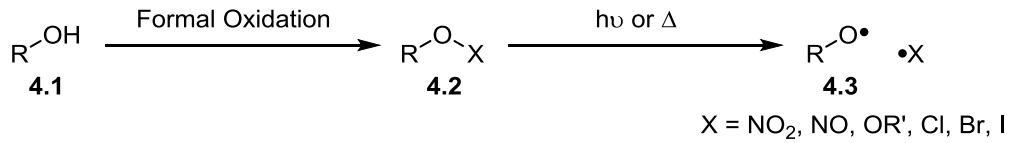

Scheme 4.2. Alkoxyl radical generation by homolysis of weak O-X bonds

Weak O-N and O-S bonds in alkoxyl radical precursors **4.2** (Scheme 4.3) can be cleaved under mild conditions for the generation of alkoxyl radicals. *N*-Alkoxyphthalimides (**4.2g**) are readily obtained by a Mitsunobu reaction from the corresponding alkyl alcohol with *N*-hydroxypthalimide or an S_N2 displacement employing the phthalimide *N*-oxide salt and suitable electrophile.[216] Cleavage of the O-N bond can be accomplished under radical conditions with trialkylstannyl radicals or tristrimethylsilylsilyl radicals.[216b]

N-Alkoxypyridinethiones (**4.2h**) can be obtained from S_N2 displacement of an alkyl tosylate with a 2-thioxopyridine *N*-oxide salt[217] although S-alkylation is a significant competing reaction which results in low yields of the thiohydroxamic acid esters (**4.2h**). In addressing this problem, Hartung has developed N-alkoxythiazolethiones (**4.2i**) as an alternative to **4.2h** where S-alkylation does not readily compete with the desired O-alkylation.[218] Both **4.2h** and **4.2i** can be homolyzed to alkoxyl radicals with visible light. Sulfenic acid *O*-esters (**4.2j**, **4.2k**, **4.2l**) can be obtained by subjecting an appropriate sulfenyl chloride with the desired alkyl alcohol in the presence of a weak base.[219,220] Cleavage of the O-S bond can be accomplished under radical conditions employing a trialkylstannyl radical or UV light.

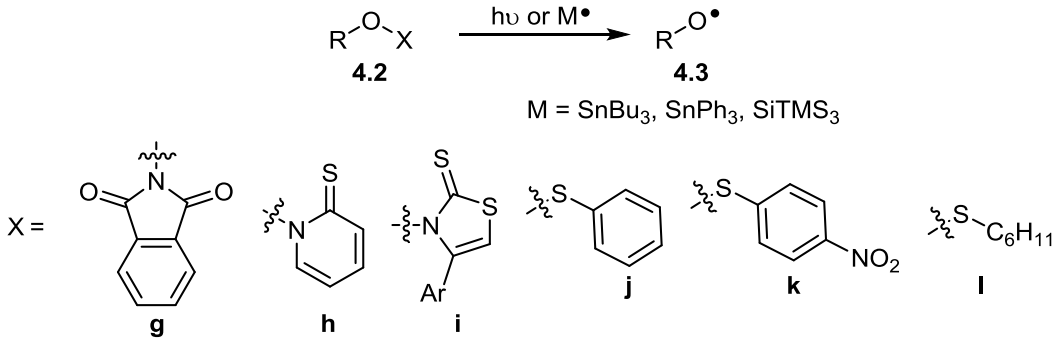

Scheme 4.3. Selection of alkoxyl radical precursors

The most commonly employed method of alkoxyl radical generation for synthetic transformations is the rearrangement of an alkyl radical (Scheme 4.4).[202,204,205] An alkyl radical adjacent to an oxirane can fragment to an alkoxyl radical and an alkene (eqn. 4.4), which is the reverse of 3-exo alkoxyl radical cyclization.[205] Both reactions occur rapidly and are reversible; however, oxirane fragmentation can be biased by a secondary irreversible reaction involving the alkoxyl radical. Alkoxyl radical formation can also be accomplished by the intramolecular addition of an alkyl radical into a carbonyl functionality (eqn. 4.5), which is the reverse of alkoxyl radical fragmentation (eqn. 4.1). This method of alkoxyl radical generation is particularly useful for ring expansion (Dowd-Beckwith reaction).[204]

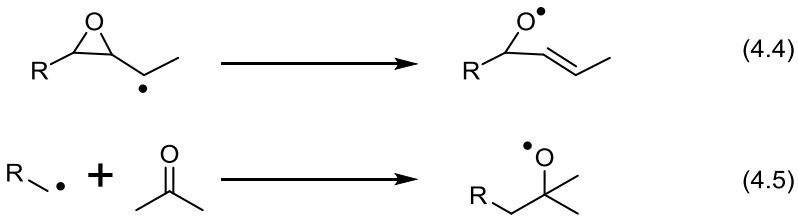

Scheme 4.4. Alkoxyl radical formation by alkyl radical rearrangement

4.1.2 Synthetic utility of alkoxyl radicals

Useful synthetic applications of alkoxyl radicals abound in the literature and a selection of methodologies and synthetic applications, which demonstrates the breadth of alkoxyl radical chemistry, will be presented in the order of cyclization,[202c,e] fragmentation,[204] and hydrogen atom transfer.[206]

Cyclization of the simplest suitable alkoxyl radical substrate, the 4-pentenyloxyl radical (**4.4**), has been studied extensively (Table 4.1).[217,219,221-223] Alkoxyl radical generation from 4-pentenol under oxidative conditions provided the lepidine alkylated tetrahydrofuran in high yields (entry 1).[208]

Photolytic cyclization of the 4-pentenol nitrite ester has been studied by Surzur and coworkers, leading to tetrahydrofuranyl oxime in 50% yield (entry 2).[221]

Rieke and Moore obtained the tetrahydrofuranyl oxime in 68% yield (entry 3).[222a] By varying the radical trapping agent, methyl halogenated tetrahydrofurans could be obtained in reasonable yields (entries 4, 5).[222b] Cyclization of *N*-pent-4-en-oxypyridinethione under photochemical conditions provides the S-alkylated tetrahydrofuran in 63% yield (entry 6)[223] while under reductive conditions, 2-methyltetrahydrofuran is obtained in 80% yield (entry 7).[217] Cyclization of arylsulfenic acid O-esters by thermal reductive conditions or photochemical conditions leads to tetrahydrofuran products in good yield (entries 8, 9).[219]

Table 4.1. Cyclization of the 4-pentenyloxyl radical

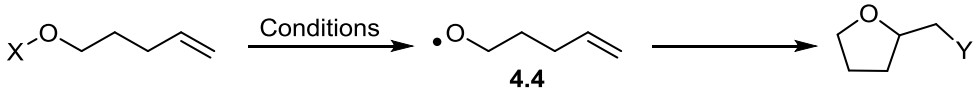

4.4

entry	X	conditions	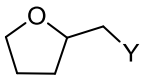	yield (%)
1	H	Δ, $Ag_2S_2O_8$, CH_3CN/H_2O	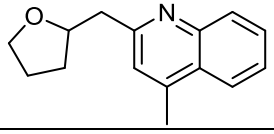	90%[208]
2	NO	hυ, C_6H_6	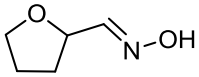	50%[221]
3	NO	hυ, C_6H_6	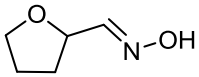	68%[222a]
4	NO	hυ, $BrCCl_3$, C_6H_6	Y = Br	51%[222b]
5	NO	hυ, I_2, C_6H_6	Y = I	61%[222b]
6	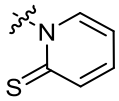	hυ, C_6H_6	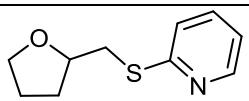	64%[223]
7	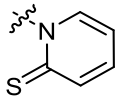	Δ, AIBN, Bu_3SnH, C_6H_6	Y = H	80%[217]
8	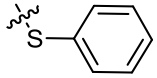	Δ, AIBN, Bu_3SnH, C_6H_6	Y = H	73%[219a]
9	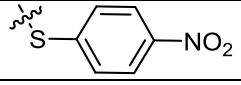	hυ, C_6D_6	Y = X	75%[219b]

Cyclization of alkoxyl radicals generated by oxirane fragmentation has been studied by the groups of Murphy and Walton independently (Scheme 4.5).[224] Radicals generated alpha to an oxirane (**4.5**) (by radical abstraction of bromide or through a Barton-McCombie deoxygenation)[225] rearrange to produce an alkoxyl radical (**4.8**), which can participate in an irreversible 5-*exo* cyclization to yield tetrahydrofuran **4.6**.[224] Alkoxyl radicals generated in this manner, by necessity, produce a second radical acceptor which can also participate in a second 5-*exo* alkyl radical cyclization (**4.10**) to yield bicycle **4.7**.[224]

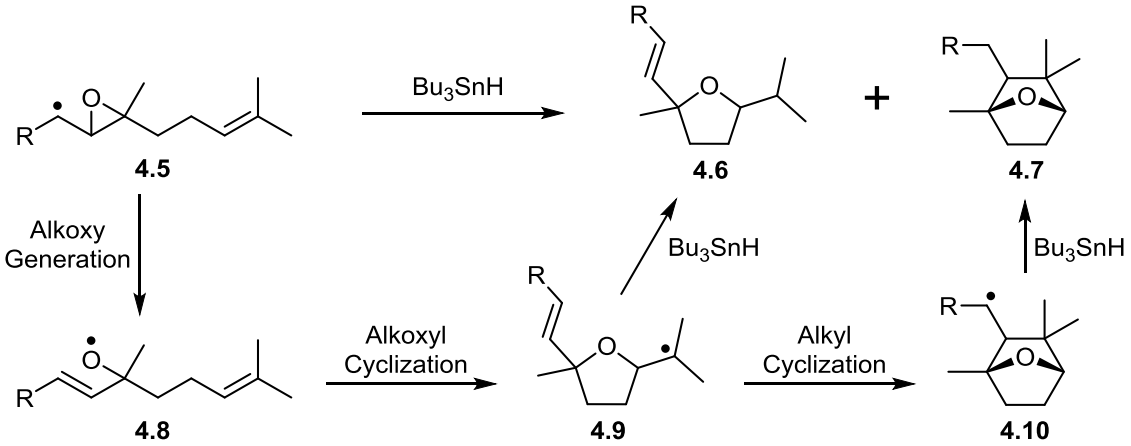

Scheme 4.5. 5-*exo* Cyclization of alkoxyl radicals generated by oxirane opening

More recently, the groups of Hartung and Sammis have both studied the 5-*exo* cyclization of alkoxyl radicals generated directly from the homolysis of N-O bonds (Scheme 4.6). Under photochemical conditions, *N*-alkoxythiazolethione **4.11** smoothly cyclizes to tetrahydrofuran **4.12**[202f] while *N*-alkoxyphthalimide **4.13** was cyclized to tetrahydrofuran **4.14** in the presence of tributylstannyl radical.[226] Only the *trans*-cyclization product was observed when a large alkyl substituent is present in the gamma position. Moderate to poor cyclization diastereoselectivity is observed with substitution at the alpha or beta positions of the alkoxyl chain. In the vast majority of cases, cyclization diastereoselectivity can be predicted by the model derrived from studies performed independently by

Beckwith and Houk.[227] Exceptions in diastereoselectivity can be predicted by the model proposed by Hartung.[228]

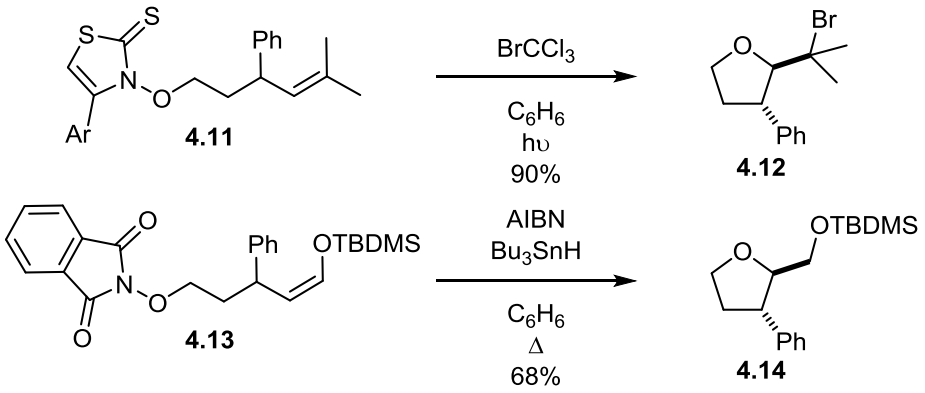

Scheme 4.6. 5-*exo* cyclization of alkoxyl radical precursors 4.11 and 4.13

Alkoxyl radical 6-*exo* cyclization is a more-difficult transformation (Scheme 4.7). In every 6-*exo* alkoxyl cyclization where the delta position possesses a hydrogen atom, 1, 5-HAT is a competing elementary alkoxyl reaction (eqn. 4.3). Indeed, the 5-hexenoxyl radical participates exclusively in 1, 5-HAT.[221,226] Hartung and Gottwald found that increasing the electron density of the radical acceptor with additional alkyl substituents (**4.15**) lead to moderate yields of tetrahydropyran product **4.16** (Scheme 4.7, top reaction).[229]

By changing the radical acceptor to an alkyne (**4.17**) in combination with Thorpe-Ingold effects,[230] Johns and Murphy were able to affect 6-*exo* cyclization (Scheme 4.7, middle reaction).[224a] Tetrahydropyran product **4.18** was subjected to further heating and the Claisen-rearrangement product **4.19** was obtained in 70% yield over 2 steps.

Sammis and coworkers were able to solve the chemoselectivity issue by employing a silyl enol ether as the radical acceptor (Scheme 4.7, bottom reaction, **4.20** to **4.21**).[226] The addition of a heteroatom in the radical acceptor further increases the electron density and accelerates the relative rate for cyclization over 1, 5-HAT.

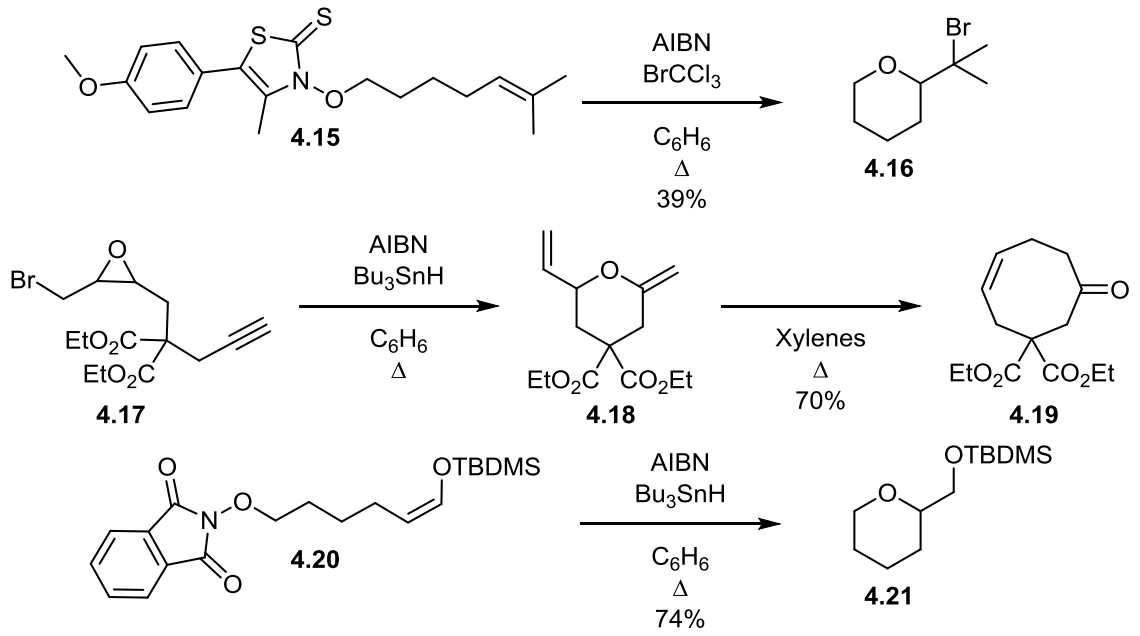

Scheme 4.7. Selected 6-*exo* alkoxyl radical cyclization strategies

The fragmentation of alkoxyl radicals is a powerful synthetic tool, though it may first appear to be counterintuitive. Selectively breaking a carbon-carbon bond is harder to do than breaking a carbon-heteratom bond or forming a carbon-carbon bond. Suarez has developed many useful transformations involving the fragmentation of carbohydrate-derived alkoxyl radicals.[231] A representative example is depicted in Scheme 4.8. When **4.22** is subject to Suarez's photochemical hypervalent iodine/I_2 system,[179] the intermediate hypoiodite **2.24** formed by oxidation of the anomeric hydroxyl, fragments to form alkoxyl radical **4.25**.[231] Selective fragmentation of the carbon-carbon bond and radical trapping with iodine provides high yields of dihaloalkane **4.23**. In one synthetic transformation, a stereocenter-rich cyclic system is transformed into a linear polyfunctional di-haloalkane with no epimerisation at the alcoholic stereocenters.

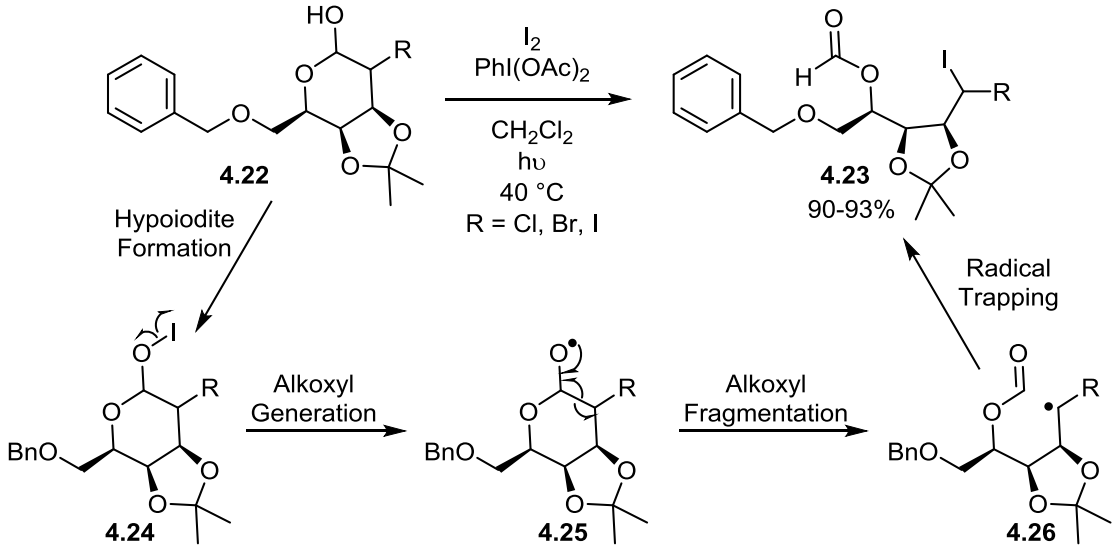

Scheme 4.8. Fragmentation of anomeric alkoxyl radicals

Where alkoxyl radical fragmentation may lead to multiple products, a common assumption is fragmentation to the most stabilized radical is favoured. However, Beckwith and coworkers have shown that temperature can greatly affect fragmentation selectivity (Scheme 4.9).[232] At lower temperatures, fragmentation of **4.27** to the more stable secondary alkyl radical is indeed favoured, leading exclusively to bromoketone **4.28**. At higher temperatures, fragmentation to the higher-energy primary alkyl radical is possible and this higher-energy intermediate is rapidly quenched by halogen transfer (**4.29**).[233] Barton and coworkers were able to observe the same fragmentation selectivity with cholesterol derivative **4.30** (Scheme 4.10).[234] Fragmentation of tertiary alkoxyl **4.33** generated by oxirane opening, delivered the primary alkyl radical **4.34** which re-cyclized to provide ketone **4.31**.

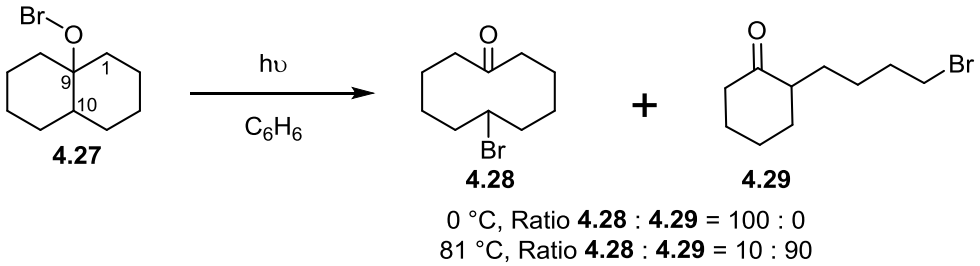

Scheme 4.9. Fragmentation of hypobromite 4.27

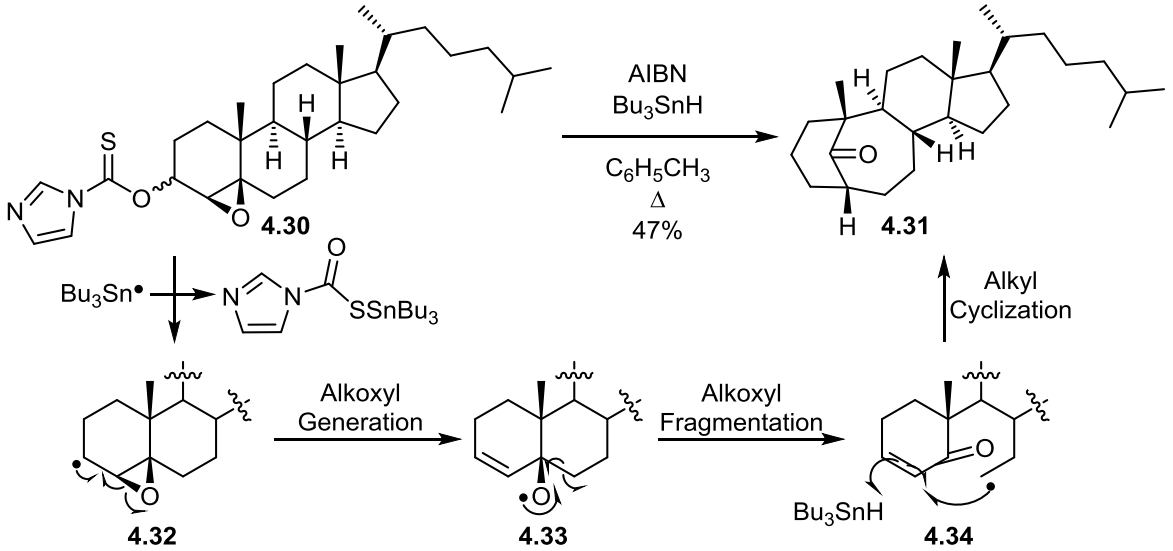

Scheme 4.10. Skeletal rearrangement of cholesterol derivative 4.30

Kim and Lee have developed a ring expansion methodology based on this reaction for the synthesis of cyclopentanones and cyclohexanones (Scheme 4.11).[235] Addition of a stannyl radical into a vinyl epoxide induces fragmentation of the spirocyclic oxirane **4.37**. Release of ring-strain facilitates alkoxyl fragmentation of the cyclobutanoxyl or cyclopentanoxyl to vinyl ketone **4.40**. Cyclization of alkyl radical **4.40** onto the allylic stannane, followed by elimination of stannyl radical, produces a carbonyl-insertion product **4.38**. This methodology is unsuitable for the synthesis of cycloheptanones.

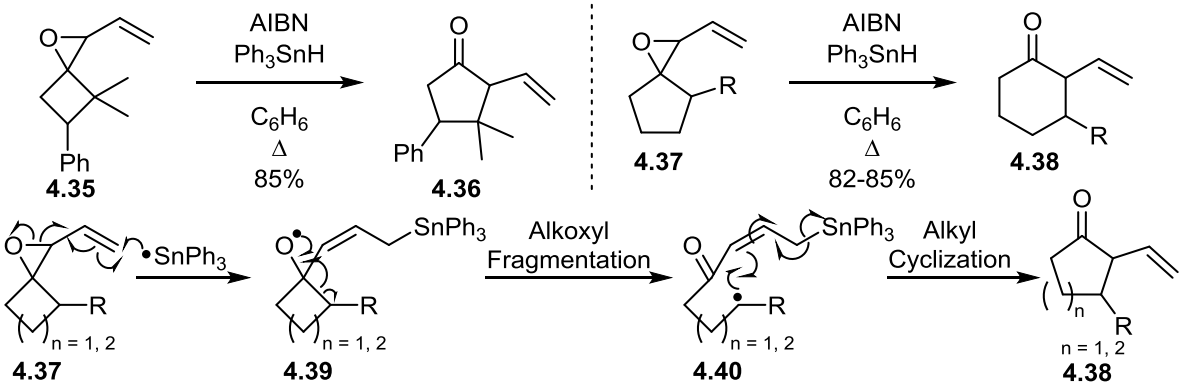

Scheme 4.11. Ring expansion synthesis of cyclopentanones and cyclohexanones

A general procedure for one carbon ring expansion of cyclic ketoesters **4.41** was developed simultaneously, and independently, by Dowd and Beckwith (Scheme 4.12).[236,237] Alkylation with a methyl radical precursor in the 2 position of a 1, 3 dicarbonyl is a relatively straight-forward transformation to obtain the rearrangement precursor **4.41**. Bromine,[236] iodine or phenyl selenide[237] is readily abstracted by stannyl radical and the resulting methyl radical **4.43** cyclizes onto the adjacent ketone. Alkoxyl radical fragmentation to release cyclopropyl ring strain provides a stabilized α-carbonyl radical **4.45** and quenching with a hydride source delivers the one carbon ring expansion product **4.42**. This methodology may be successfully extended to ring expansion of three or four carbons (two carbon extensions fail)[236b] and to the expansion of heterocycles.[238]

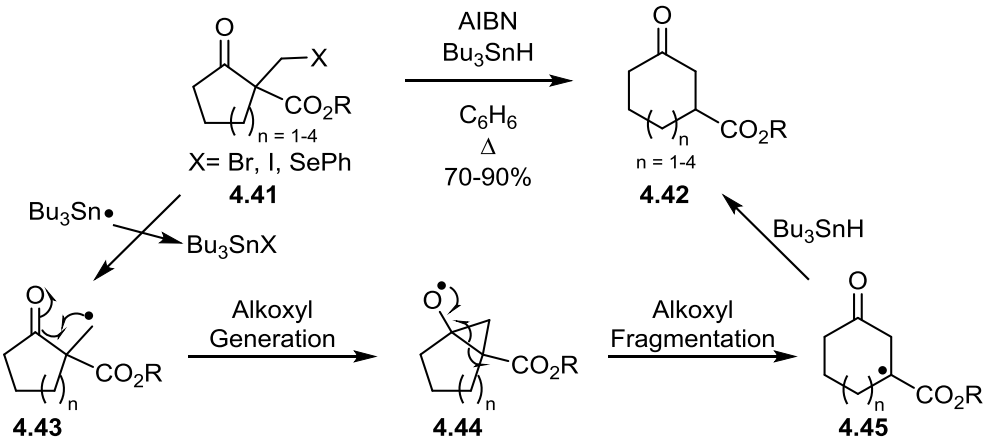

Scheme 4.12. Dowd-Beckwith ring expansion

An elegant application of alkoxyl fragmentation is Nishida's synthesis of 8, 5-bicyclic **4.47** (Scheme 4.13).[239] Treatment of alkynyl cyclohexanone **4.46** with stannyl radical provides vinyl radical **4.48**, which cyclizes onto the ketone to generate alkoxyl radical **4.49**. Fragmentation to the datively stabilized radical **4.50**, followed by 5-exo-trig cyclization, provides methyl radical **4.51**, which undergoes a second ring expansion sequence to provide **4.53**. The chain is finally terminated by elimination of stannyl radical to provide **4.47** in 51% after 7 bond-making or bond-breaking events.

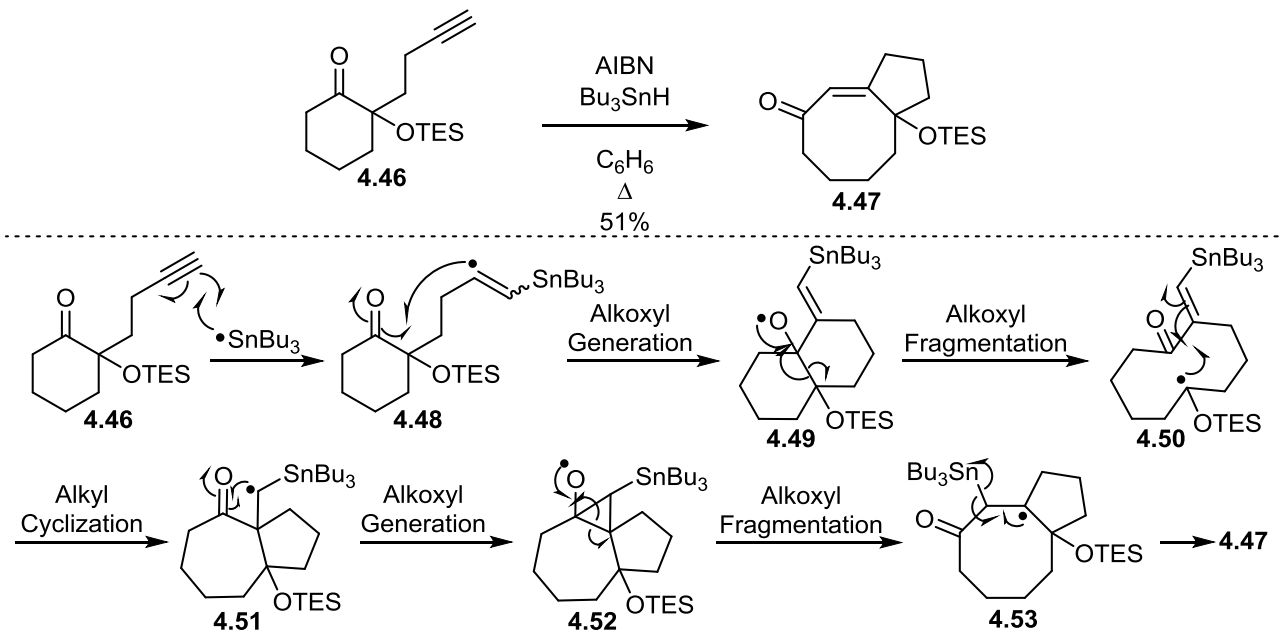

Scheme 4.13. Double alkoxyl fragmentation - ring expansion sequence

Transposition of an alkoxyl radical to the remote non-activated δ-carbon or the remote activated ε-carbon is the most utilized synthetic alkoxyl radical mediated reaction. Hydrogen atom transfer is enthalpicly favourable because the bond dissociation energy of an alkoxyl O-H bond is considerably higher than those of most alkyl C-H bonds. According to theoretical calculations, 1, 5-HAT is favoured entropicly[240] as an envelope like transition state can be reached with a migratory C-H-O bond angle of 153° (Figure 4.1, left). 1, 6-HAT occurs through a chair-like arrangement of the carbon backbone with a migratory C-H-O bond angle of 165°, which is closer to the ideal of linearity (Figure 4.1, right). Manipulation of conformational effects, available kinetic energy and reaction enthalpy can change the entropic 1, 5 bias.

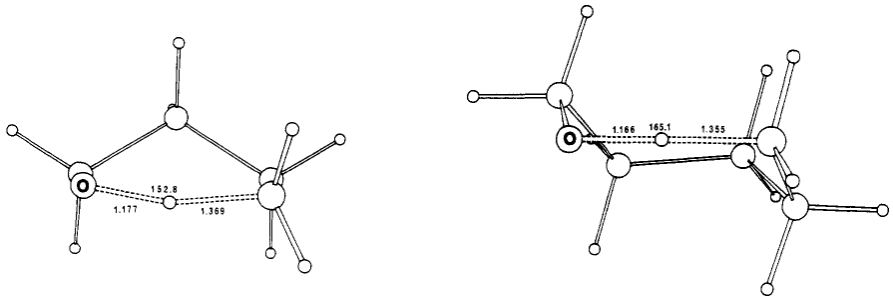

Figure 4.1. Calculated transition states for 1, 5-HAT and 1, 6-HAT by Houk[240b]

Barton was the first to demonstrate the synthetic utility of 1, 5-HAT when he disclosed a method for the remote oxidation of axial steroidal methyl groups[241] followed by the elegant 3 step semi-synthesis of aldosterone acetate (**4.59**) from readily available corticosterone acetate (**4.54**).[242] Photolysis of nitrite ester **4.55** generates alkoxyl radical **4.56** which participates in 1, 5-HAT to produce alkyl radical **4.57** that is subsequently trapped by nitosyl (Scheme 4.14). Impressively, oxime **4.58** is isolated in 21% yield because: (a) corticosterone acetate contains a vinyl ketone which is a good radical acceptor, (b) alkoxyl radical **4.56** can undergo fragmentation in competition with 1, 5-HAT, and (c) there is a second, activated, axial methyl that is equidistant to the desired axial methyl for aldersterone.

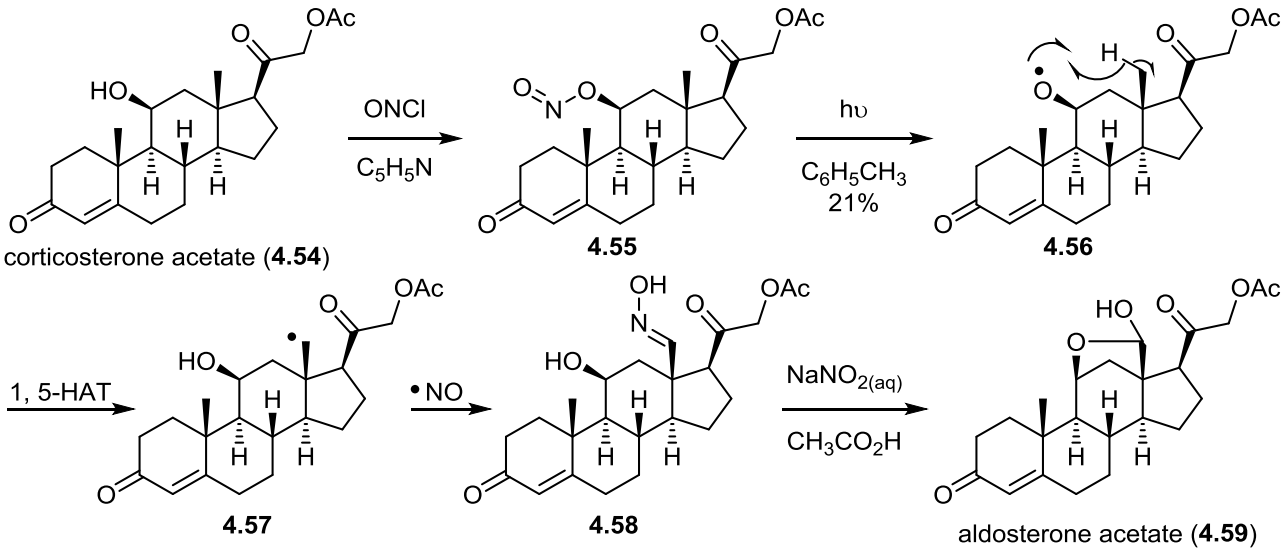

Scheme 4.14. Barton's synthesis of aldosterone acetate

The synthesis of tetrahydrofurans and tetrahydropyrans by alkoxyl radicals may be accomplished by 1, 5-HAT (or 1, 6-HAT) followed by oxidative trapping of the resulting relayed radical **4.63** (Scheme 4.15).[206d] This transformation was studied extensively[243] as the oxygen analogue to the Hofmann-Loffler-Freytag reaction.[244] The alkoxyl radical **4.62** (typically generated by *in-situ* oxidation of the corresponding alcohol) affects 1, 5-HAT and the resulting alkyl radical **4.63** may be trapped by a halogen (**4.65**, typical with Cl and Br) and internally displaced,[212b,213a,b,d] or further oxidized to the carbocation **4.64** and trapped by the alcohol (SET oxidation pathway).[245]

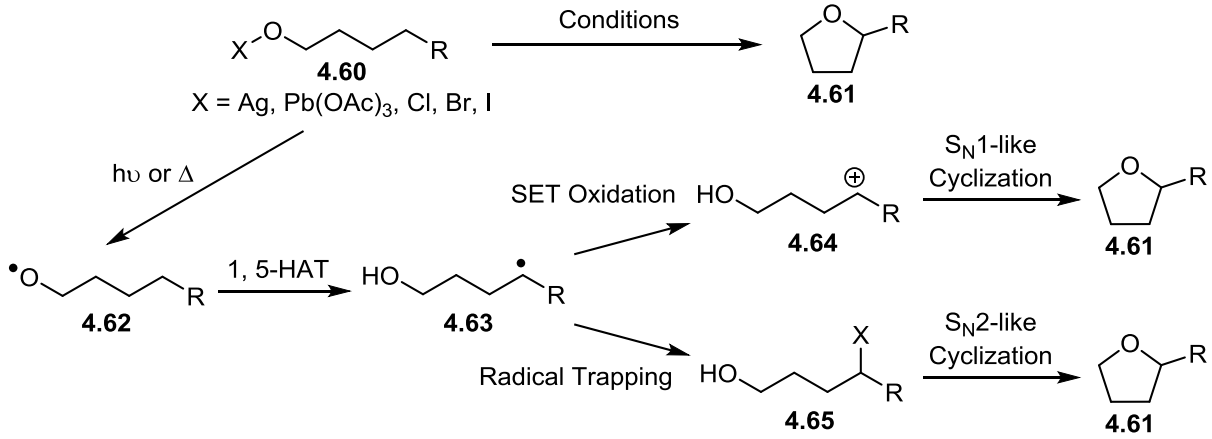

Scheme 4.15. Tetrahydrofuran synthesis mediated by 1, 5-HAT

One particularly useful application of 1, 5-HAT mediated oxidative cyclisation is the synthesis of spirocyclic oxacycles (Scheme 4.16). Using the methodology developed by Suarez,[245b-e] Brimble was able to affect the double oxidative cyclization of **4.66** to **4.69** in high overall yields.[246] The cyclization diastereoselectivity was poor; however, many natural products containing this type of motif adopt the most thermodynamically stable confirmation in the native state. Thus, after the alkene was epoxidized to resemble the native state, a spontaneous rearrangement corrected the 1: 1: 1: 1 mixture to the desired spirocyclic configuration in an isolated yield of 62%.[246]

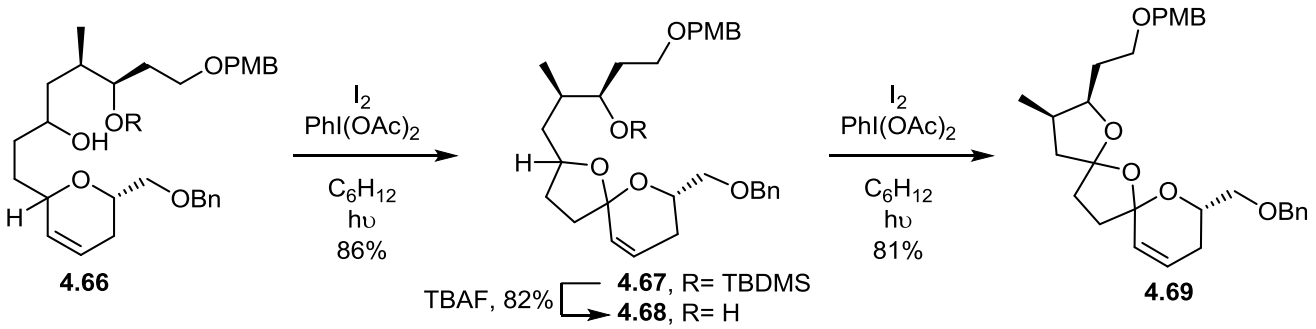

Scheme 4.16. Double 1, 5-HAT oxidative cyclization of 4.66

As shown by the selected examples in Scheme 4.17, the transposed alkyl radical may undergo carbon-carbon bond formation. Cekovic was able to obtain the addition product of acrylonitrile (**4.71)** to the 1, 5-HAT intermediate from nitrite **4.70** (Scheme 4.17, top reaction).[220] Ryu was able to trap a molecule of carbon monoxide followed by oxidative lactonization to obtain **4.73** (Scheme 4.17, middle reaction).[247] Suarez was able to utilize dative stabilization to effect both 1, 5-HAT and 1, 6-HAT for the allylation of methylated carbohydrate **4.74** (Scheme 4.17, bottom reaction).[248] The success of intermolecular addition is the employment of vast excesses of radical trapping agent. Cekovic employed 60 equivalents of acrylonitrile, Ryu employed a pressurized carbon monoxide bomb, and Suarez employed 10 equivalents of tributylallylstanne.

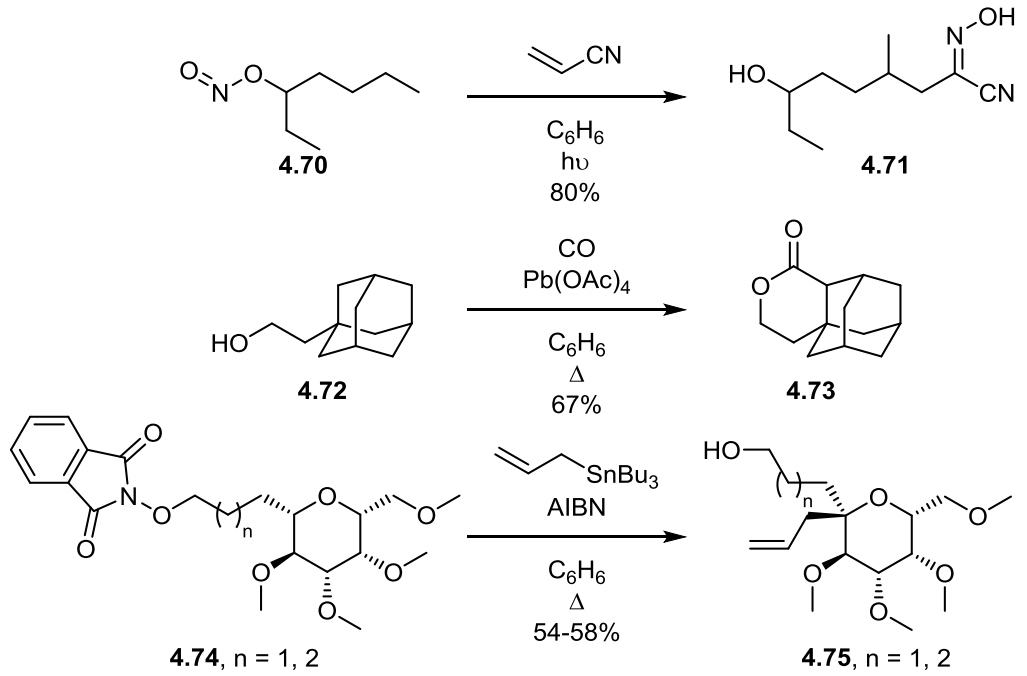

Scheme 4.17. Selected examples of intermolecular trapping of the 1, 5-HAT relayed radical

Before we entered the field, only two examples of alkoxyl mediated radical relay cyclization with linear substrates were known. Early work by Cekovic showed that simple nitrite esters and hypochlorites (**4.76**) could be cyclized in low to moderate yields.[249] Homolysis of the O-X bond followed by 1, 5-HAT provides intermediate radical **4.79** which cyclizes to **4.77** in 5-*exo* or 6-*exo* fashion (Scheme 4.18).[249] This is excellent proof of concept for relay cyclization and we thought that a slower, more controlled, generation of alkoxyl radicals would improve the cyclization selectivity. The other system of alkoxyl radical mediated relay cyclization was disclosed by Rawal (Scheme 4.19).[250] Generation of alkoxyl radical **4.83** by oxirane fragmentation creates the radical acceptor for the ultimate 5-*exo* cyclization (**4.85**). The elegance of simultaneous radical acceptor and alkoxyl formation is also the drawback of this system, as the radical acceptor scope is limited. Furthermore, only one linear example (**4.81** to **4.82**) was provided by Rawal and it is the lowest yielding relay cyclization of his disclosure.[250]

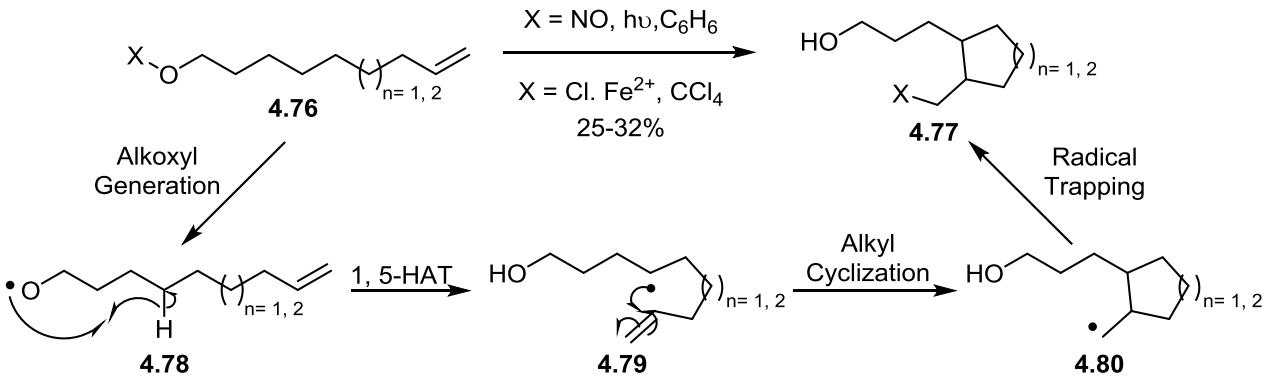

Scheme 4.18. Cekovic's alkoxyl radical relay cyclization methodology

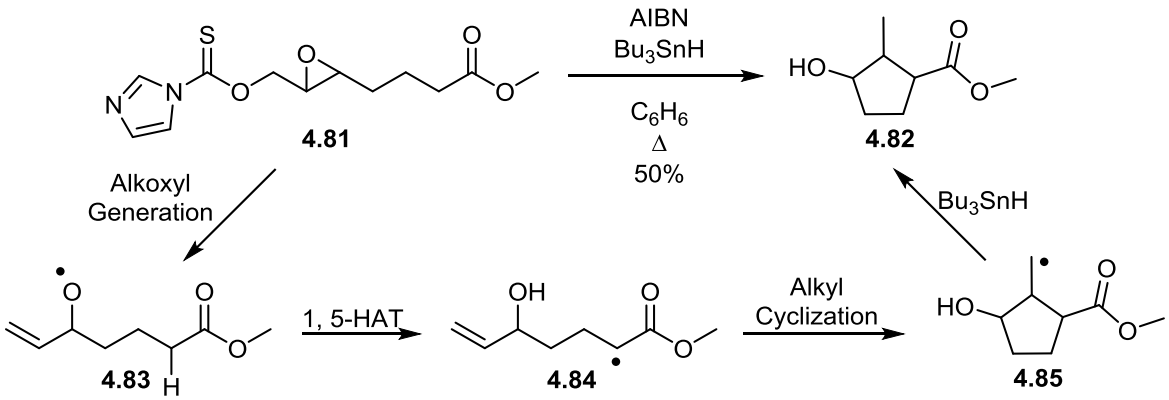

Scheme 4.19. Rawal's alkoxyl radical relay cyclization methodology

Nevertheless, alkoxyl mediated relay cyclization is an excellent methodology for the synthesis of carbobicyclic systems[251] as demonstrated by a succession of publications from Rawal and Kim in the early 1990s (Scheme 4.20).[252-255] Addition of phenylsulfenyl to enol ether **4.86** induces oxirane fragmentation to alkoxyl radical and alkene radical acceptor **4.91**. 1, 5-HAT followed by 5-exo cyclization provides good yields of 5, 5 carbobicycles (**4.87a**, n = 1) and even better yields of 6, 5 carbobicycles (**4.87b**, n = 2).[252.253] Shortly thereafter, both Rawal and Kim disclosed that transformation of the ketone to an enol ether was unnecessary with the use of stannyl radical. However, only 6, 5 carbobicycles (**4.89b**, n = 2) can be generated in this fashion.[254,255] Rawal showed that the

analogous 5, 5 carbobicycles (**4.89a**, n = 1) could only be generated in low yields.[255] This is likely the result of a competing alkoxyl fragmentation of the intermediate cyclopentenyloxyl radical.

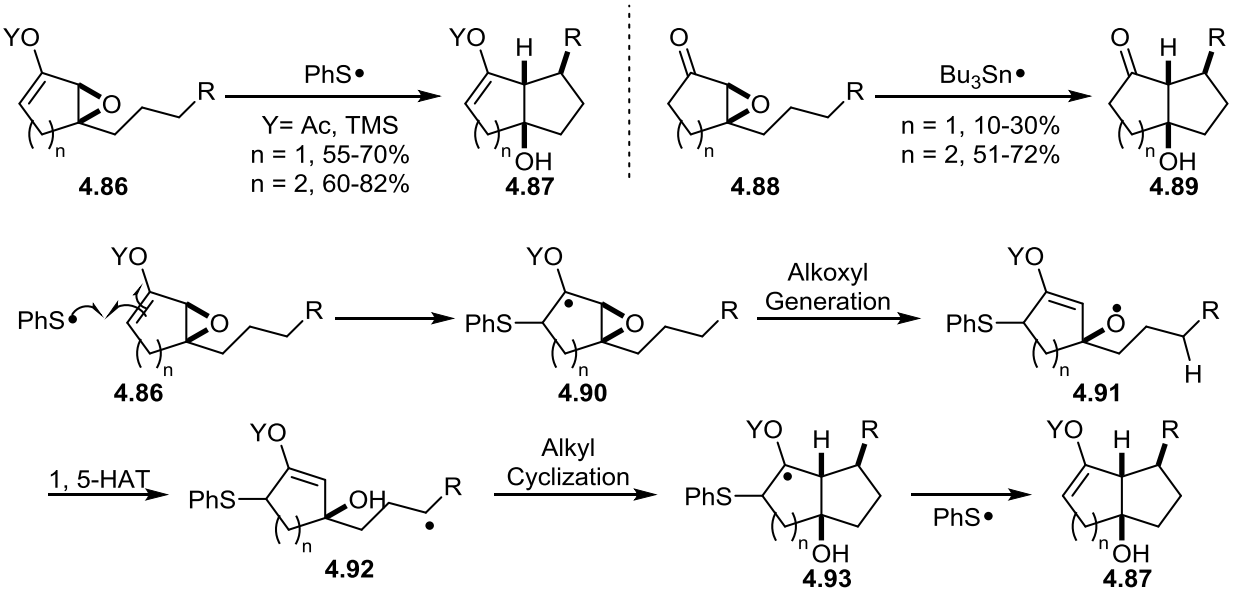

Scheme 4.20. Alkoxyl radical relay cyclization for the synthesis of carbobicyclic compounds

4.2 Competition kinetics of alkoxy radicals

Alkoxy radical mediated tetrahydropyran synthesis (**4.21**) presents a difficult question of chemoselectivity as 1, 5-HAT, leading to **4.94**, is usually a faster process (Scheme 4.2.1). [221] Flash photolysis studies by Newcomb and coworkers on alkoxy radical 1, 5-HAT of unactivated C-H bonds, extrapolated to 80 °C, estimates a rate of 8.6 x 10^7 s^{-1},[256] which provides a minimum-rate estimate of the 1, 5-HAT as the hydrogen in the 6-*exo* cyclization case is an activated allylic hydrogen. Thus, the successful 6-*exo* cyclization must be occurring at approximately 9 x 10^8 s^{-1}, an order of magnitude faster than1, 5-HAT.

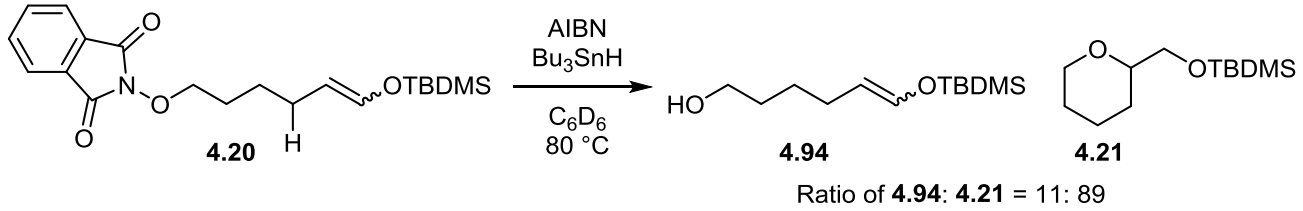

Scheme 4.21. 6-*exo* Alkoxy radical cyclization onto a silyl enol ether acceptor

The inherent question of chemoselectivity in 6-*exo* cyclization onto silyl enol ethers highlighted the problem of relative rates in competing alkoxy radical processes. If alkoxy radical 6-*exo* cyclization onto a silyl enol ether is faster than 1, 5-HAT, then what could compete with the cyclization? The principle of least motion gives the answer of 5-*exo* cyclization onto a silyl enol ether. Without changing the other variable (the radical acceptor), less molecular reorganisation (lower entropic barrier) is required in 5 member ring formation. To elucidate the relative rate of 6-exo cyclization onto a silyl enol ether, the relative rate of 5-exo cyclization can be used as a radical clock. Thus, the most important question to ask is: "how fast is an alkoxy radical 5-*exo* cyclization onto a silyl enol ether"?

4.2.1 Competition between direct cyclization and fragmentation

One method which may be employed to estimate the rate of a reaction is to design a competition experiment between the reaction in question and a second reaction with well-established rates within two orders of magnitude. The first attempt at elucidating the relative rate of 5-*exo* alkoxy radical cyclization was a competition experiment between two radical acceptors: a silyl enol ether, and a simple terminal alkene. From the initial publication by our group on alkoxy radical cyclizations, it was concluded that cyclization onto a silyl enol either (in the presence of a simple terminal alkene) was exclusive,[226] suggesting a rate two orders of magnitude faster than the pentenyloxyl clock of 5.2×10^8 s^{-1} at 80 °C (eqn. 4.2).[219a]

Fragmentation of alkoxy radical **4.95** to formaldehyde and a stabilized benzyl radical **4.96** (Scheme 4.22) could compete with cyclization to **4.97**, providing a ratio for fragmentation to cyclization of 1: 5.3 for **4.98a** (Table 4.2, entry 1).[226] While the rate of alkoxy radical fragmentation was unknown, the rate could be estimated through a competition experiment involving fragmentation and cyclization onto a terminal alkene. Both the alkoxy radical fragmentation and the alkoxy radical cyclization are irreversible processes; therefore, measuring the product ratio of alkene formation to tetrahydrofuran formation results in an accurate measurement of the relative rates of these two processes.

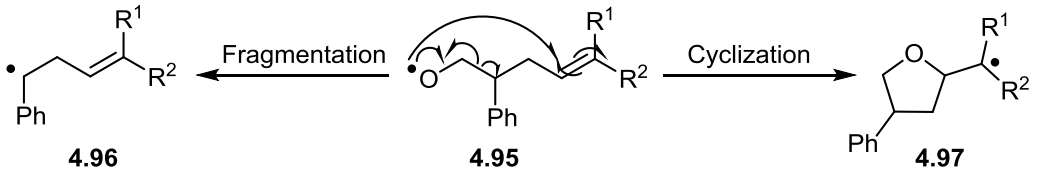

4.96 **4.95** **4.97**

Scheme 4.22. Design of fragmentation vs cyclization substrates 4.98

The synthesis of competition substrate **4.98b** followed the general synthetic procedure for substrate **4.98a** utilized by M. Zlotorszynka (Scheme 4.23).[226] Methyl phenylacetate (**4.101**) was prenylated under basic conditions followed by lithium aluminum hydride reduction to alcohol **4.103**. A Mitsunobu reaction was employed to install the phthalimide moiety to yield competition substrate **4.98b** in 27%. Competition substrate **4.98c** was an intermediate employed by M. Zlotorszynska for the synthesis of competition substrate **4.98a** and sufficient amounts were available from the communal laboratory library.

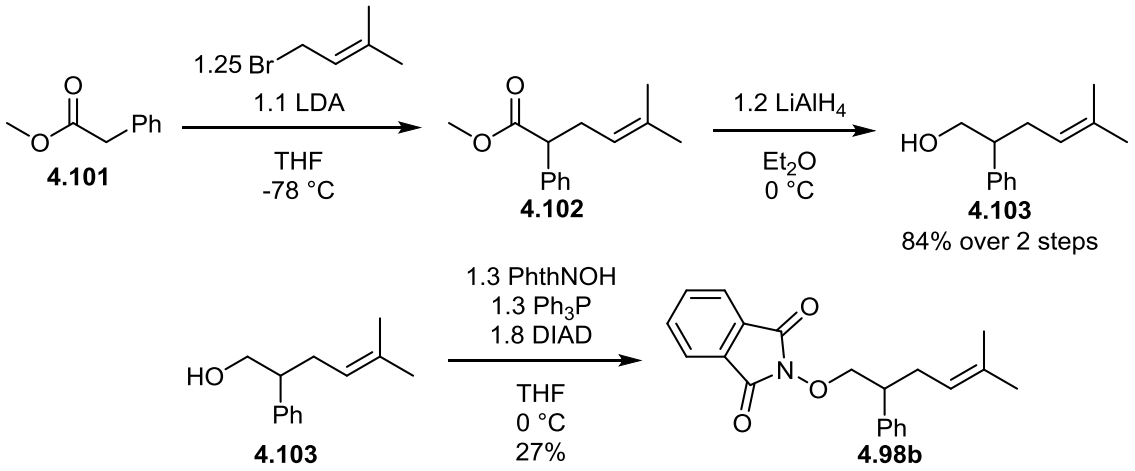

Scheme 4.23. Synthesis of competition substrate 4.98b

The results of fragmentation experiments are summarized in Table 4.2. The ratio of fragmentation to cyclization for a silyl enol ether is (**4.99a**: **4.100a**) 1: 5.3 (entry 1). For a trisubstituted alkene, the ratio of fragmentation to cyclization (**4.99b**: **4.100b**) is 1: 5.1 (entry 2) which indicates that the 5-*exo* cyclization of a primary alkoxy radical onto a silyl enol either is only slightly faster than 5-*exo* cyclization onto a trisubstituted alkene. The ratio of fragmentation to cyclization obtained with a simple terminal alkene (**4.99c**: **4.100c**) is 1: 2.4 (entry 3) and indicates that 5-*exo* cyclization of a primary alkoxy radical onto a silyl enol either is about twice as fast as cyclization onto a terminal alkene.

Given the rate of alkoxy radical cyclization onto a terminal alkene at reflux in benzene has been measured to be 5.2 x 10^8 s^{-1} at 80 °C,[219a] the rate of alkoxy radical fragmentation to formaldehyde and a benzylic radical is calculated to be 2 x 10^8 s^{-1} at 80 °C. Furthermore, the rate of primary alkoxy radical cyclization onto a silyl enol ether is 1 x 10^9 s^{-1} at 80 °C and the rate of primary alkoxy radical cyclization onto a trisubstituted alkene is also 1 x 10^9 s^{-1} at 80 °C. A loose comparison to the literature value of alkoxy radical cyclization on a trisubstituted alkene by Hartung and Gallou (between 2 to 5 x 10^9 s^{-1}) shows the estimated value falls within an order of magnitude.[223]

Table 4.2. Primaryl alkoxyl competition: cyclization vs fragmentation

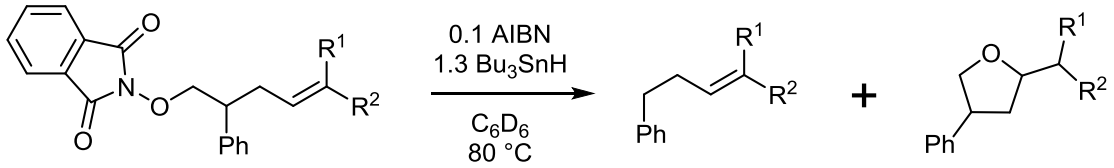

4.98 **4.99** **4.10**

entry[a]	substrate	R^1	R^2	ratio[b] **4.99** : **4.10**
1[226]	**4.98a**	OTBDMS	H	1 : 5.3
2	**4.98b**	CH_3	CH_3	1 : 5.1
3	**4.98c**	H	H	1 : 2.4

[a]Reaction conditions: AIBN (0.1 equiv), Bu_3SnH (1.3 equiv), **4.98** (1.0 equiv, 0.25 mmol) at 0.02 M in N_2-sparged deuterobenzene, refluxed for 18 h. [b]The ratio was obtained by ^1H NMR spectroscopy using the phthalimide-tin adduct as an internal standard.

However, these fragmentation studies contradict the conclusions that initiated this competition study.[266] According to Table 4.2, cyclization onto the terminal alkene should have been easily observable as the predicted competition outcome of simple terminal alkene against silyl enol ether is 1: 2.2. If the rate of 5-*exo* alkoxy radical cyclization onto a silyl enol ether is only slightly faster than the cyclization onto a trisubstituted alkene, the predicted competition outcome of simple terminal alkene against silyl enol ether is 1: 9 based on the cyclization rates reported by Hartung and Gallou.[223]

A critical examination of the fragmentation substrate reveals that the reactive intermediate was a primary alkoxy radical whereas both Sammis[226] and Hartung[223] employed secondary alkoxy radicals. Conventional wisdom assumed that the high reactivity of alkoxy radicals would override other effects. The practise of approximating the rate of hydrogen atom transfer from tributyltin hydride to any alkoxy radical with the rate of hydrogen abstraction by *tert*-butyloxyl (a tertiary alkoxy radical) from tributyltin hydride is quite common.[202f] While undesirable, this approximation must be made as hydrogen transfer from tributyltin hydride to *tert*-butyloxyl is the only known alkoxy radical stannyl hydride transfer studied to date.[257]

Perhaps the rate difference between the fragmentation studies and the work of Hartung and Gallou[223] could be explained as the difference between a primary and secondary alkoxy radical. A 1, 5-HAT rate study by Newcomb and coworkers showed that the rate of 1, 5-HAT by a primary alkoxy radical was approximately twice as fast as 1,5-HAT by a tertiary alkoxy radical.[256] Before returning to the rate question of 5-*exo* alkoxy radical cyclization, the hypothesis that primary and secondary alkoxy radicals have distinctly different cyclization reactivity was tested.

As will demonstrated in the following sections, there is a noticeable difference in reactivity between primary and secondary alkoxy radicals in cyclization and 1, 5-HAT. However, the direct competition study of primary alkoxy radical cyclization onto a simple terminal alkene vs a silyl enol ether is 1: 4.8 (Scheme 4.29), and not 1: 2.2 as predicted by the fragmentation studies (Table 4.2). There is still a discrepancy between the two competition experiments that cannot be easily explained. The transition state for cyclization may be related to one of the many possible transition states for fragmentation, thereby skewing the results in favour of fragmentation. Perhaps the choice of this particular set of reactions as the basis for competition was flawed. Nevertheless, the competition studies involving cyclization and fragmentation provide useful information for synthetic planning. It is clear from these studies that homobenzylic alkoxy radicals are prone to fragmentation and should be avoided in radical cyclization onto simple terminal alkenes.

4.2.2 Differences in reactivity between primary and secondary alkoxy radicals

The hypothesis that primary alkoxyl radicals react differently than secondary alkoxyl radicals is based on the fact that alkoxyl radicals are electrophilic.[203] An additional alkyl substituent might stabilize the electrophilic alkoxy radical through induction or hyper-conjugative effects. Thus, the

primary alkoxy radical would be more reactive than a secondary alkoxy radical with the consequence that cyclization of a primary alkoxyl radical may be faster than cyclization of a secondary alkoxyl radical. For example, in a cyclization competition experiment between the simple terminal alkene and a silyl enol ether, we would expect the primary alkoxyl cyclization reaction would be less selective overall; that is, the secondary alkoxyl radical to have a greater ratio of cyclization onto the silyl enol ether vs terminal alkene than the ratio obtained by a primary alkoxyl radical.

In the previous subsection, I concluded that fragmentation and cyclization were an unsuitable pair of experiments for competition studies. Before embarking on studies to investigate the differences between primary and secondary alkoxy radicals, it was necessary to validate the competition experiments. As both the rate of secondary alkoxy radical cyclization onto a simple terminal alkene and secondary alkoxy radical cyclization onto a disubstituted alkene were reported by Hartung and Gallou,[223] it is possible to predict a competition ratio for the cyclization of secondary alkoxy radical **4.104** favouring the disubstituted alkene of 1 : 5.1 (Figure 4.2). Thus, competition substrate **4.107** became the first synthetic target.

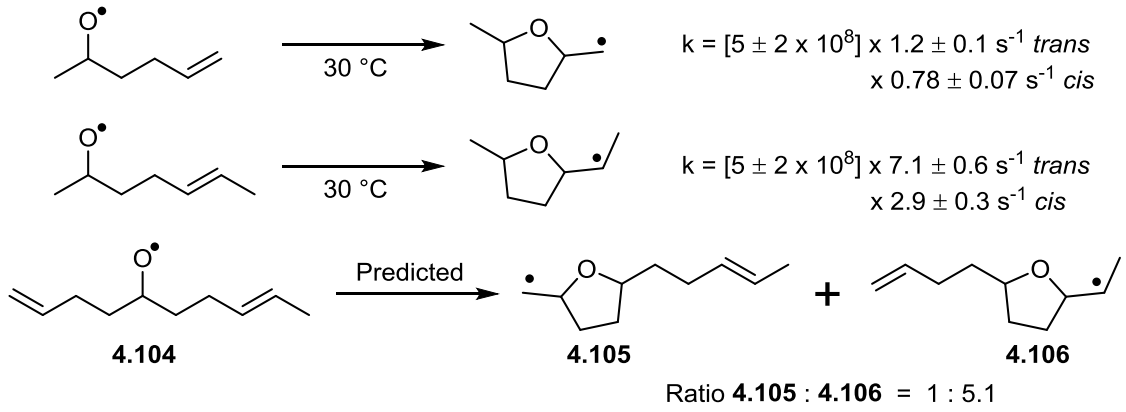

Figure 4.2 Predicted behaviour of secondary alkoxy radical 4.104.[223]

Three generations of synthesis for validation substrate **4.107** were explored (Scheme 4.24). The first generation synthesis (Scheme 4.24 A) was designed to be divergent, allowing access to both **4.107** and competition substrate **4.112**. Copper catalyzed opening of triethylsilyl protected alcoholic oxirane **4.108** followed by Mitsunobu installation of the phthalimide moiety and deprotection, provided **4.111** as the point of divergence. However, conversion of **4.112** to **4.107** proved unmanageable as after the Appel-type transformation of the alcohol **4.111** to iodide **4.112**, I was unable to selectively eliminate the halide for substrate **4.107** (the phthalimide moiety could not be maintained).

The second generation synthesis (Scheme 4.24 B) was designed as a reliable method to obtain **4.107**. Malonate alkylation with **4.113** followed by Krapcho decarboxylation provided ester **4.115** which was reduced to aldehyde **4.116** and quickly transformed to alcohol **4.117** through a copper-mediated Grignard addition. A Mitsunobu reaction was used to install the phthalimide moiety providing access to the validation substrate **4.107** in 7% overall yield in 5 steps. Having obtained the validation substrate in this manner, a third generation synthesis was devised (Scheme 4.24 C) as a more efficient route for scale-up production of **4.107**.

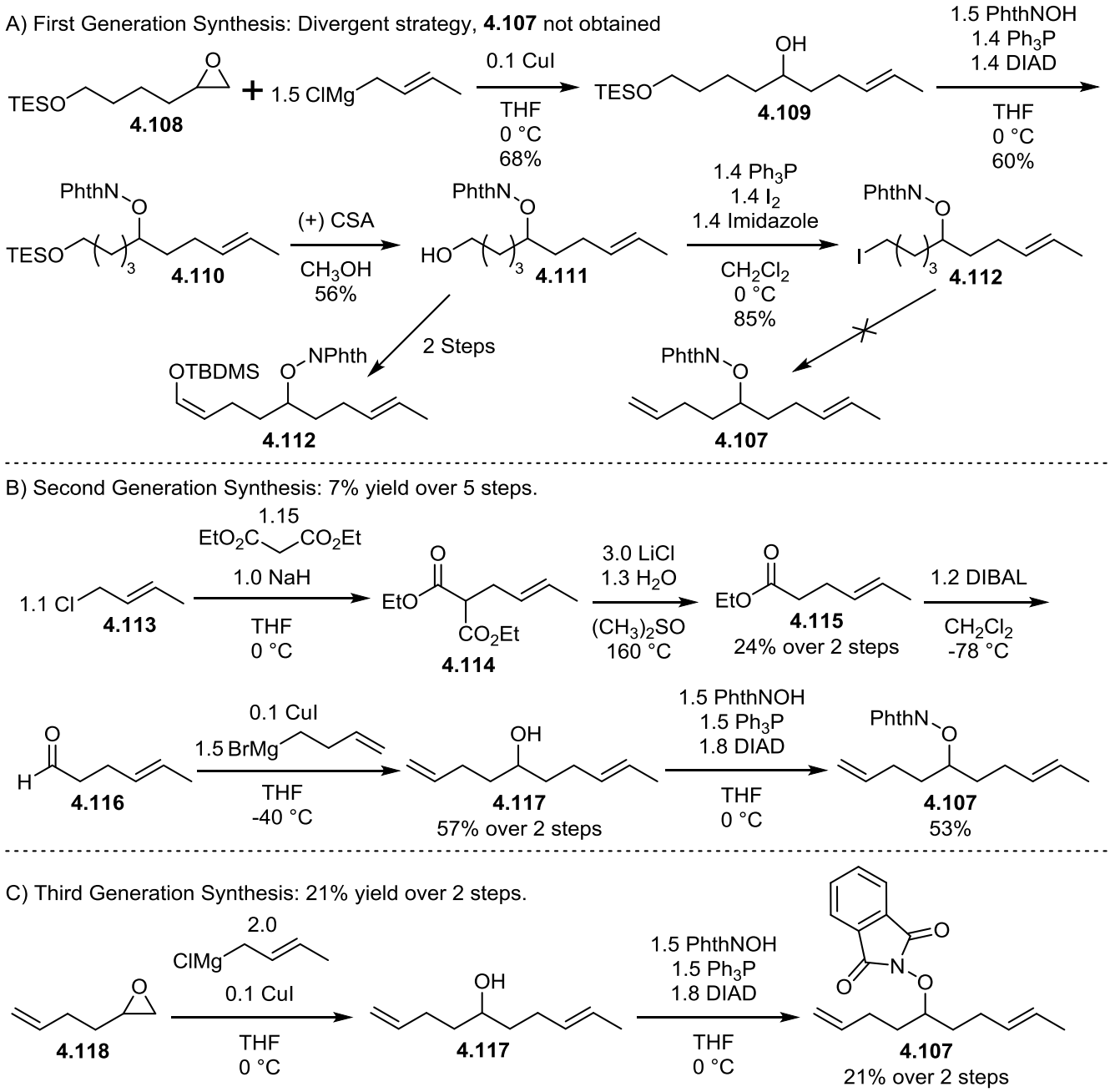

Scheme 4.24. Three generations of synthesis for validation substrate 4.107.

Validation substrate **4.107** was subject to reflux in benzene with slow addition of excess tributyltin hydride and catalytic amounts of AIBN (Scheme 4.25). Slow addition of tributyltin hydride was necessary to ensure the concentration of stannyl hydride was low and prevent premature quenching

of the alkoxy radical prior to cyclization. The ratio of secondary alkoxy radical cyclization onto a simple terminal alkene vs a disubstituted alkene (**4.119**: **4.120**) was 1: 4.8 (average of 3 trials) which is very close to the predicted value of 1: 5.1 (Figure 4.2).

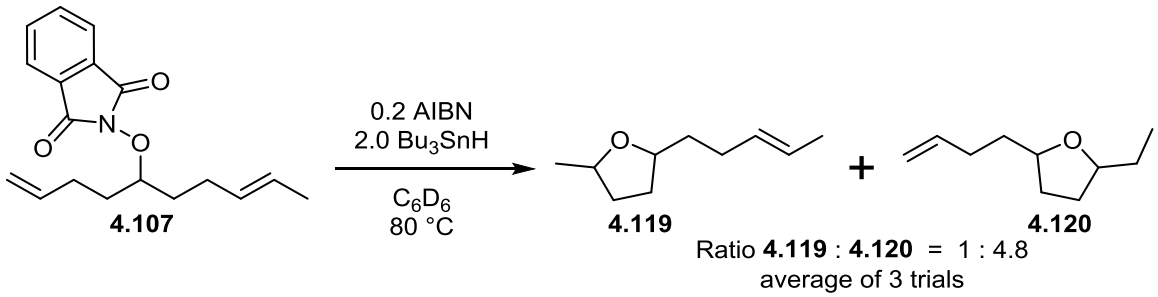

Scheme 4.25. Secondary alkoxy radical competition: simple terminal alkene vs disubstituted alkene.

Having validated this method of competition, M. Rueda-Becerril reinvestigated secondary alkoxy radical competition cyclization between a simple terminal alkene and a silyl enol ether (competition substrate **4.121**) while I investigated primary alkoxy radical competition cyclization between a simple terminal alkene and a silyl enol ether (competition substrate **4.122**).

Primary alkoxy competition substrate **4.122** was synthesized in a six step procedure starting from protected acrolein equivalent **4.123** (Scheme 4.26). Alkylation of diethylmalonate **4.124** at elevated temperatures resulted in a mixture of ester **4.126** and malonate **4.125** which was subjected to Krapcho decarboxylation conditions to obtain ester **4.126** in a combined 64% yield over 3 steps. Ester **4.126** was reduced to alcohol **4.127** by lithium aluminum hydride and transformed to alkoxyphthalimide **4.128** through a Mitsunobu reaction in 53% yield over 2 steps. Acid mediated hydrolysis of the acetal followed by treatment with TBDMS triflate provided competition substrate **4.122** (1: 7 *E*: *Z*) in 39% yield over 2 steps.

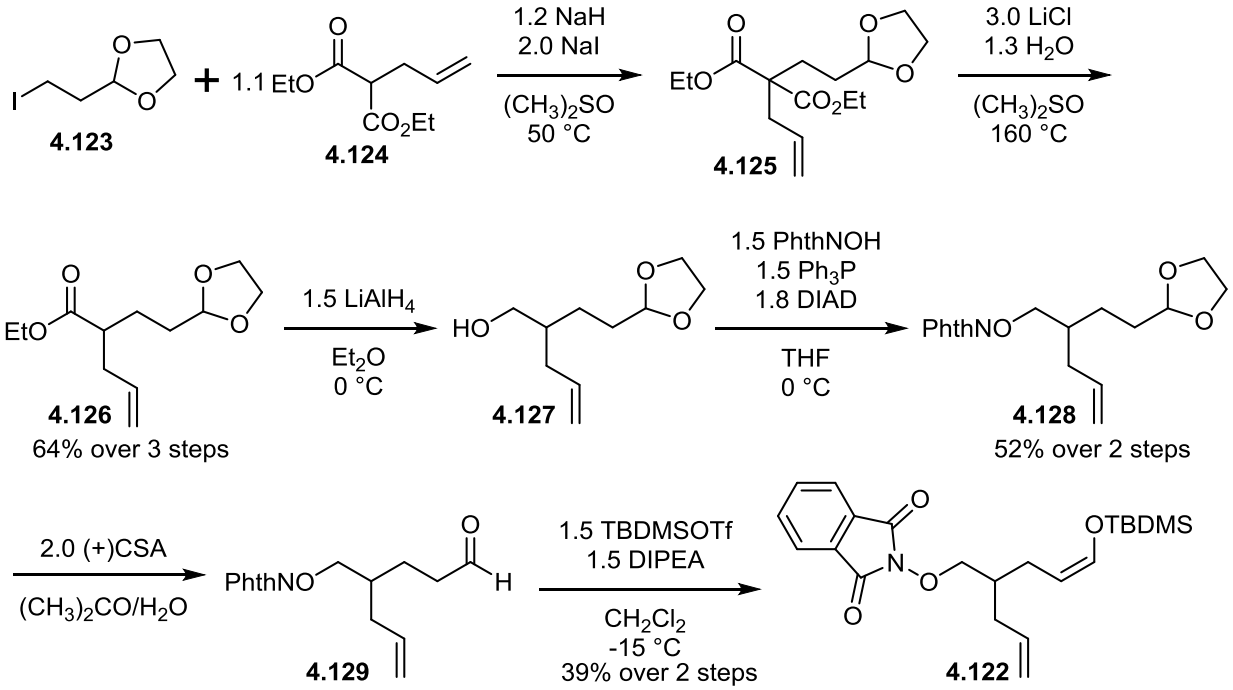

Scheme 4.26. Synthesis of competition substrate 4.122

Secondary alkoxy radical competition substrate **4.121** was investigated by M. Rueda-Becerril. After an average of 2 trials, she found that the ratio of cycliation between simple terminal alkene and silyl enol ether (**4.130**: **4.131**) was 1: 8.1 and that there was no difference between *E* silyl enol ether and *Z* silyl enol ether (Scheme 4.27). Furthermore, re-examination of previously published data revealed that certain ^{1}H NMR signals were incorrectly assigned. Product peaks corresponding to cyclization onto the terminal alkene were misinterpreted as unreacted starting material from an incomplete cyclization experiment and corrected ratio is 1: 11.

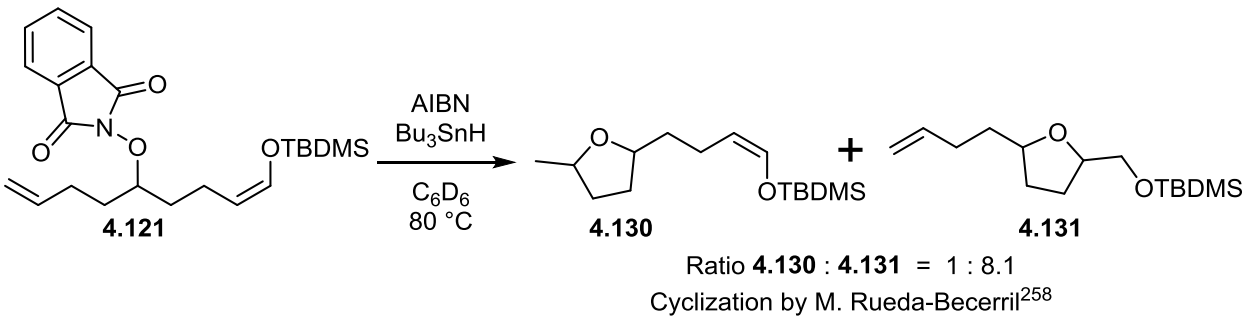

Scheme 4.27. Secondary alkoxy radical competition: simple terminal alkene vs silyl enol ether

When primary alkoxy radical competition substrate **4.122** was subject to competition cyclization conditions, a complex mixture of cyclization products was obtained (Scheme 4.28). Treatment of competition substrate **4.122** produces primary alkoxyl radical **4.132** that participates in the irreversible cyclization reaction of interest (Scheme 4.28 A). The subsequent radicals **4.133**, **4.134** can be quenched by tributyltin hydride to yield products **4.135**, **4.136**. However, radicals **4.133a** and **4.134a** can participate in a second cyclization event as shown in Scheme 4.28 B and C respectively. A secondary cyclization event by **4.134a**, after quenching by tributyltin hydride, leads to double cyclization products **4.140**. A secondary cyclization even by **4.133a** leads to double cyclization product **4.138** after quenching with tributyltin hydride. Flash chromatography provided fractions which were enriched with double cyclization products **4.140**. NMR spectrometry (COSY + HSQC) lead to the identification of protons H' and H" in all 4 of the double cyclization products resulting from initial cyclization onto the silyl enol ether (Scheme 4.28 C). Thus each of the 6 possible products resulting from cyclization onto the silyl enol ether (**4.136a,b**; **4.140a-d**) were identified.

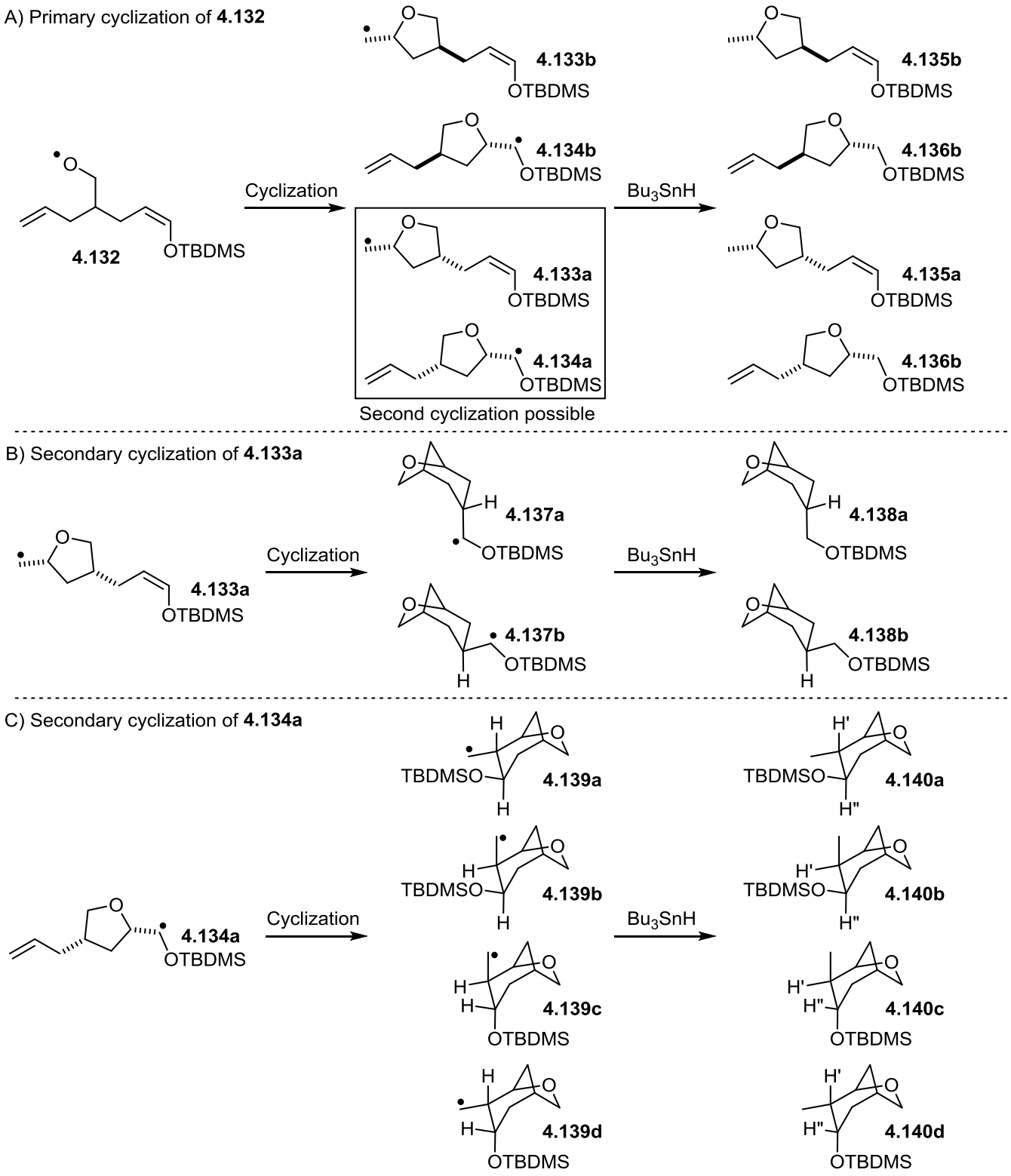

Scheme 4.28. Multiple cyclization pathways for 4.132

The ^{1}H NMR spectra of crude reaction mixtures from two separate trials (cyclization of substrate **4.122**) are shown in Figure 4.3. The multiplets at 7.55 ppm and 6.92 ppm correspond to protons from the tributyltin-phthalimide adduct which can be utilized as an internal standard. Signals at 5.6 ppm correspond to vinyl protons found only on **4.136**; signals at 5.25ppm, 3.80 ppm and 2.95 ppm correspond to protons found on double cyclization products **4.140**. One proton from each of the two major diastereomers, resulting from initial cyclization on the silyl enol ether acceptor, overlap at 5.25 ppm while the two minor diastereomers each have one proton that resonates at 3.80 ppm and 2.95 ppm respectively. Summation of the proton signals at 5.6 ppm, 5.25 ppm, 3.80 ppm, and 2.95 ppm accurately accounts for the products resulting from initial alkoxy radical cyclization onto the silyl enol ether acceptor (**4.134**). The remaining proton balance accounts for the products resulting from initial alkoxy radical cyclization on the terminal alkene acceptor (**4.133**). Thus, primary alkoxy radical competition substrate **4.122** revealed a ratio of cyclization products resulting from initial cyclization onto the simple terminal alkene and cyclization products resulting from initial cyclization onto the silyl enol ether as 1 : 4.8 (average of 4 trials, 2 of which were performed by M. Rueda-Becerril) (Scheme 4.29).

From the two cyclization competition studies by primary alkoxyl substrate **4.122** and secondary alkoxyl substrate **4.121,** there is clear evidence for alkoxyl-substitution related selectivity differences. Secondary substrate **4.121** is approximately twice as selective for cyclization onto a silyl enol ether as the primary alkoxyl radical counterpart (**4.122**). Relating this to rate arguments, the rate of primary alkoxyl radical cyclization onto a silyl enol ether is approximately five times faster than primary alkoxyl radical cyclization onto a terminal alkene and the rate of secondary alkoxyl radical cyclization onto a silyl enol ether is approximately eight times faster than secondary alkoxyl radical cyclization onto a terminal alkene.

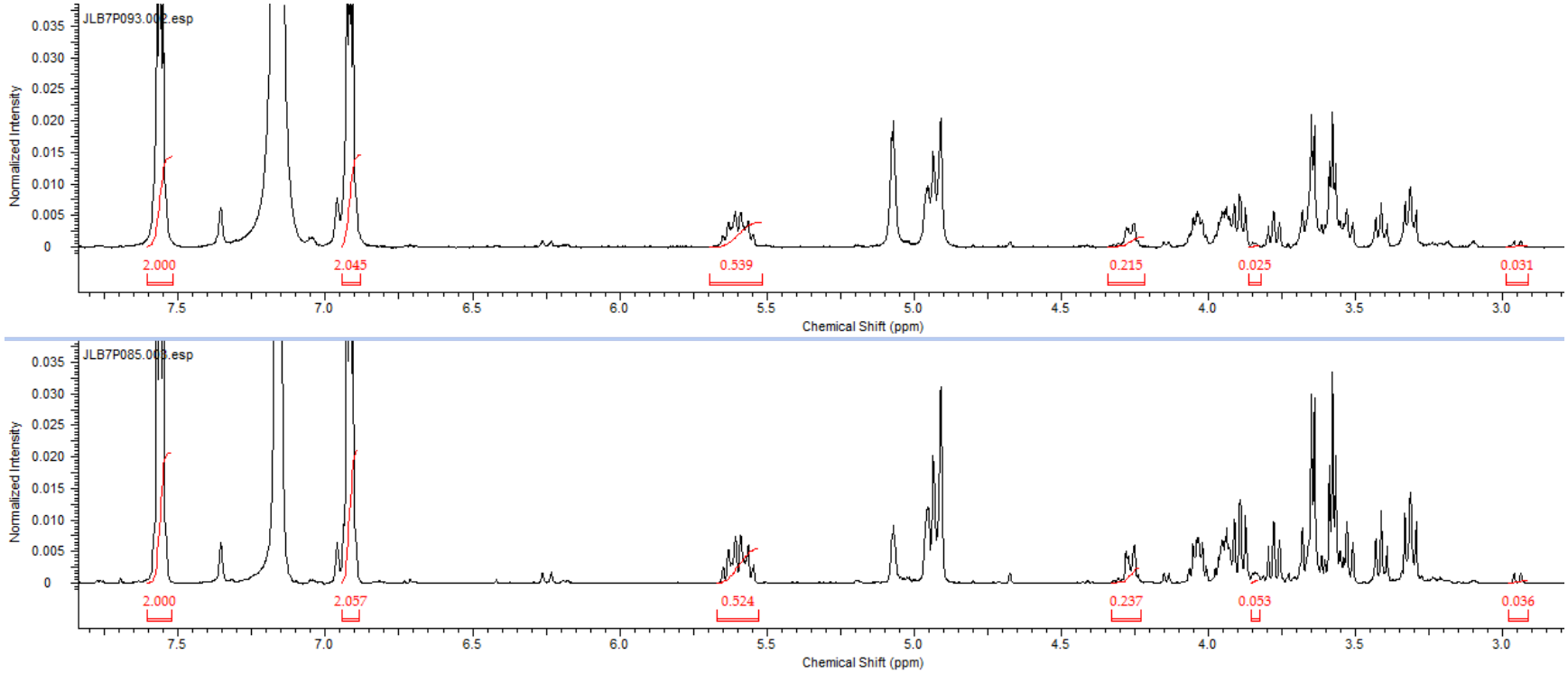

Figure 4.3. Primary alkoxyl radical competition: terminal alkene vs silyl enol ether

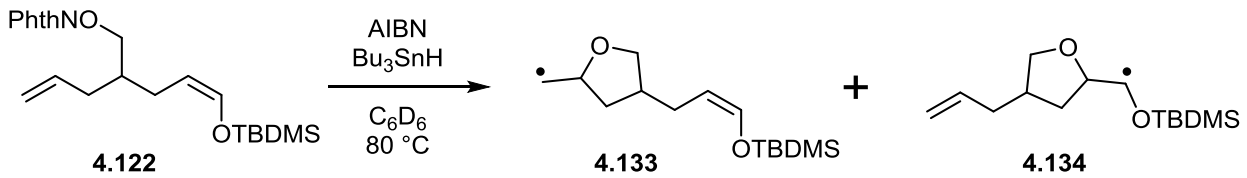

Ratio of products from **4.133** : **4.134** = 1: 4.8

Scheme 4.29. Primary alkoxy radical competition: simple terminal alkene vs silyl enol ether

Two explanations can be proposed that match with all of selectivity observations from cyclization of **4.121** and **4.122**: (A) the relative rate of secondary alkoxyl radical cyclization onto a silyl enol ether is significantly faster than the relative rate of primary alkoxyl radical cyclization onto a silyl enol ether, or (B) the relative rate of primary alkoxy radical cyclization onto a terminal alkene is significantly faster than the relative rate of secondary alkoxyl radical cyclization onto a terminal alkene. Since explanation A relies on a very fast reaction (primary alkoxyl cyclization onto silyl enol ether) being even faster, it less likely to be correct than explanation B. Explanation B can be manifest in two equally reasonable ways: (B1) that the 'slowest' reaction (primary alkoxyl cyclization onto a terminal alkene, eqn. 4.2) is faster than previously thought, or (B2) that the equally fast secondary alkoxyl cyclization onto a terminal alkene is slower than previously measured. Investigations into the competition between alkoxyl radical cyclization onto a terminal alkene and 1, 5-HAT were carried out to acquire more data.

Primary alkoxy competition substrate **4.144** was rapidly synthesized in 37% overall yield in 3 steps. Ester **4.142** was obtained through a Johnson-Claisen rearrangement of hexenyl alcohol **4.141** and reduced to alcohol **4.143** by action of lithium aluminum hydride. A Mitsunobu reaction was employed to install the phthalimide moiety producing primary alkoxy radical competition substrate **4.144** for 1,5-HAT vs cyclization (Scheme 4.30). Secondary alkoxy competition substrate **4.147** was synthesized in 59% overall yield in 2 steps. Oxirane **4.145** was opened by a copper-catalyzed addition of allyl magnesium bromide followed by a Mitsunobu reaction to install the phthalimide moiety (Scheme 4.31).

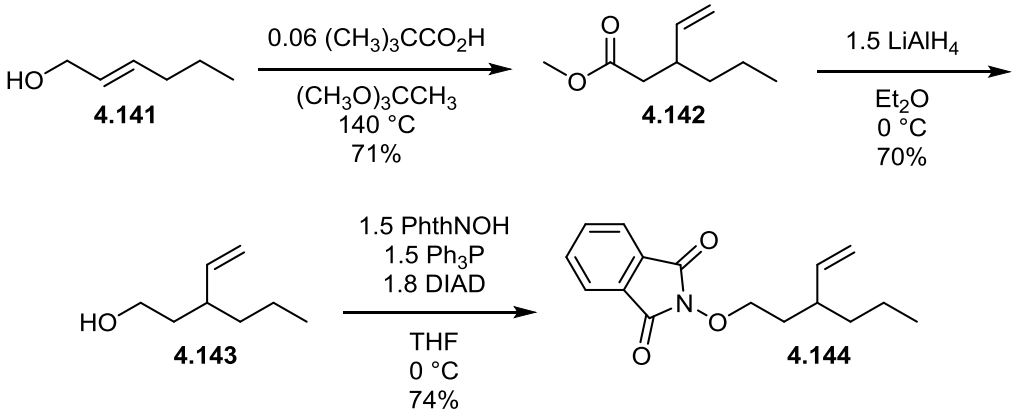

Scheme 4.30. Synthesis of competition substrate 4.144

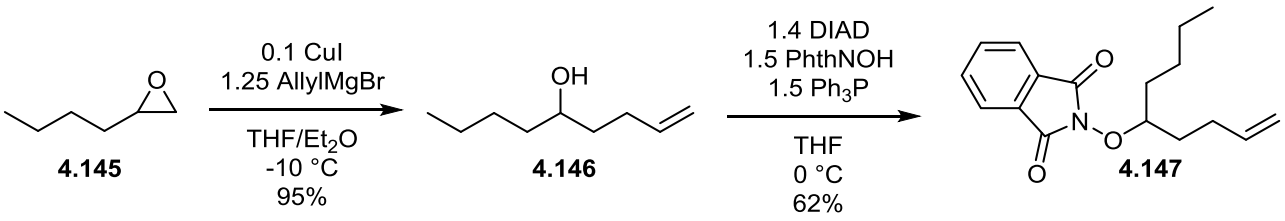

Scheme 4.31. Synthesis of competition substrate 4.147

Treatment of secondary alkoxy competition substrate **4.147** with tributyltin hydride and AIBN in refluxing benzene lead to a ratio of cyclization product **4.148** to 1, 5-HAT product **4.146** of 8.1: 1 (Scheme 4.32). Newcomb and coworkers did not publish the rate of secondary alkoxyl radical 1,5-HAT; however, it can be reasonably assumed that the rate of secondary alkoxyl radical 1, 5-HAT is located between the rate of primary (8.6×10^7 s^{-1}) and tertiary (3.7×10^7 s^{-1}) alkoxyl radical 1, 5-HAT.[256] Based on this assumption, the rate of secondary alkoxyl radical cyclization onto a simple terminal alkene is $5 \pm 2 \times 10^8$ s^{-1}, which matches to the rates obtained by Hartung and Gallou.[223]

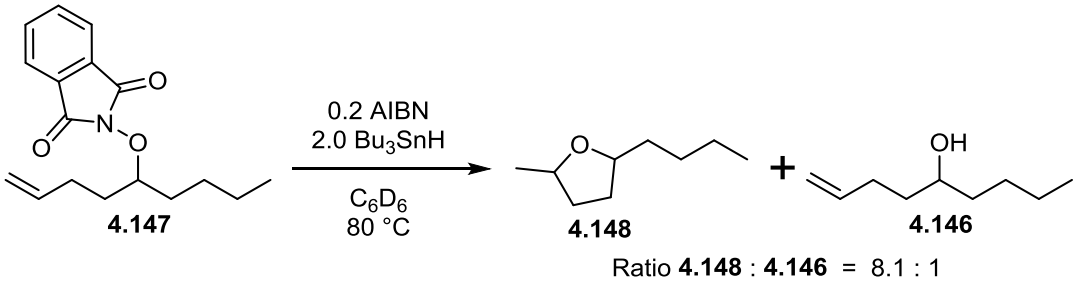

Scheme 4.32. Secondary alkoxy radical competition: 1, 5-HAT vs cyclization

Treatment of primary alkoxy competition substrate **4.144** with tributyltin hydride and AIBN in refluxing benzene lead to a ratio of cyclization product **4.147** to 1, 5-HAT products **4.143** and **4.151** of 15 ± 1: 1 (average of 3 trials) (Scheme 4.33). The crude reaction mixture of 3 separate trials of substrate **4.144** cyclization is shown in Figure 4.4. The two terminal vinyl protons (5.01 - 4.89 ppm) were integrated against protons corresponding from tin-bound phthalimide (doublets at 7.55 ppm and 6.92 ppm) and the integral value divided by 2 (each alcohol has 2 protons in that region). The remaining mass balance was attributed to cyclization onto the terminal alkene.

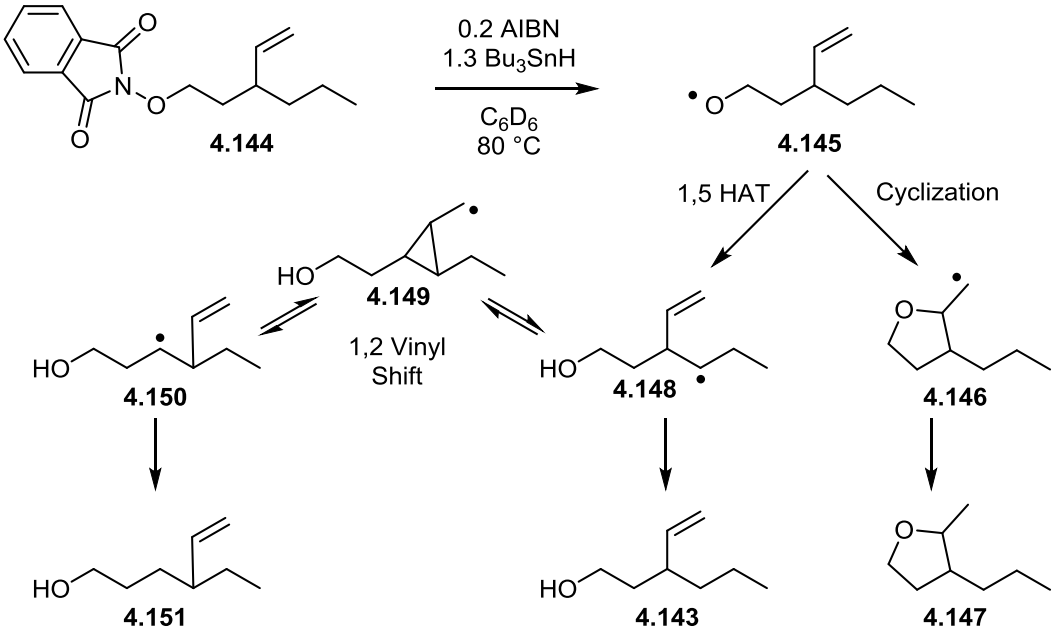

Scheme 4.33. Primary alkoxy radical competition: 1, 5-HAT vs cyclization

With primary alkoxy competition substrate **4.144**, there is clear evidence that the 1, 5-HAT intermediate **4.148** is generated as a 1, 2- vinyl shift[259] can be observed (leading to a mixture of alcohols **4.143** and **4.151**). Maintaining a low concentration of tributyltin hydride throughout the competition experiment was designed to prevent premature quenching of the alkoxy radical. Thus, all of the alcohol generated are products of 1, 5-HAT.

As these experiments were conducted on NMR scales, it was impractical to confirm the presence of **4.151** by isolation. Only small amounts of alcohol are generated in each reaction and it is unlikely that the isomeric mixture of alcohols could be separated. To prove the existence of **4.151**, it was synthesized according to Scheme 4.34. Dimethyl ethyl malonate (**4.152**) was alkylated with 3-bromopropanol (**4.153**) and subject to acid mediated decarboxylation to lactone **4.155**. Reduction to lactol **4.156** followed by a Wittig reaction provided an authentic sample of alcohol **4.151**. Evidence for the presence of alcohols **4.143** and **4.151** is presented in Figure 4.5. The top two ^{1}H NMR spectra contain pure samples of **4.151** and **4.143** respectively. Next, the alkene region from one of the crude reaction mixtures is presented followed by a 1:1 mixture of alcohols **4.143** and **4.151** below. The pattern of signals from the two bottom spectra are nearly identical except for the small signal at 5.025 ppm (caused by leaching from a plastic syringe during the slow addition tributyltin hydride/AIBN).

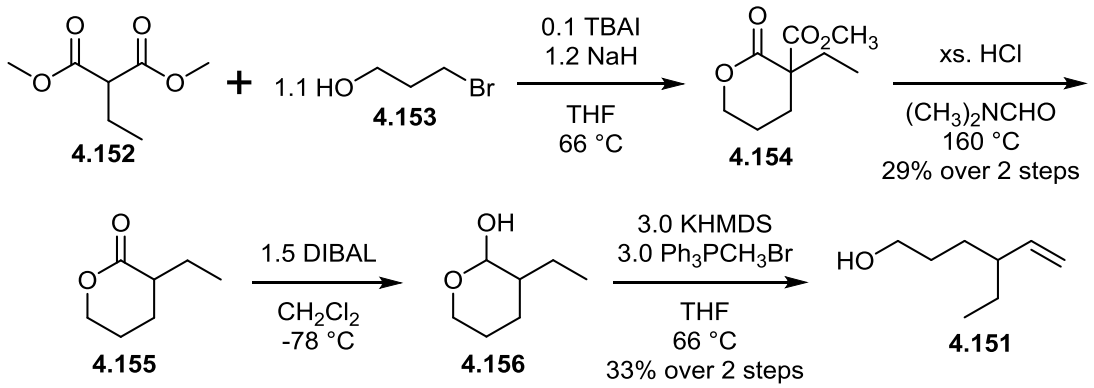

Scheme 4.34. Synthesis of 1, 2-vinyl shift product 4.151.

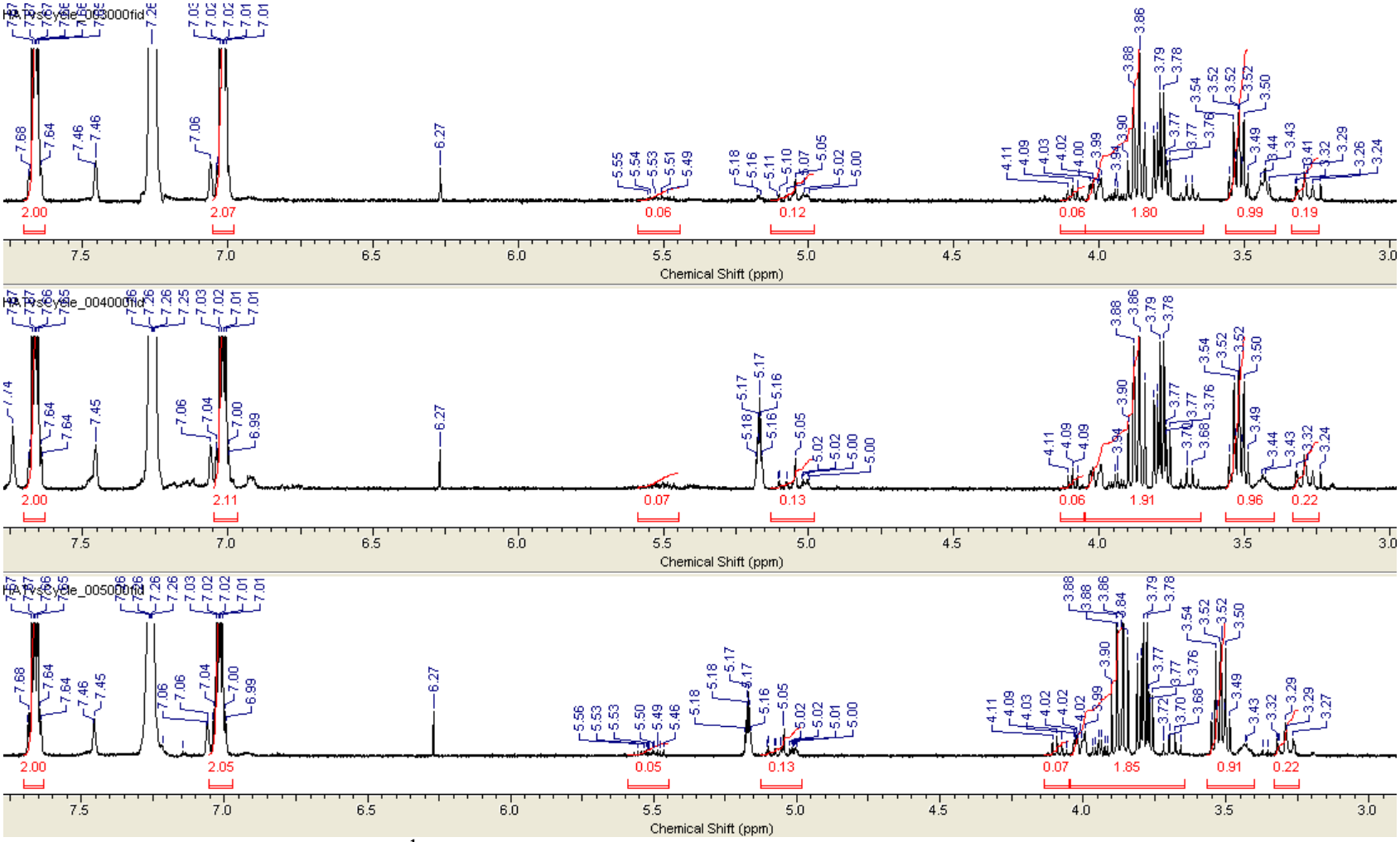

Figure 4.4. ^{1}H NMR (400MHz, C_6D_6) spectra of the crude reaction of substrate 4.144

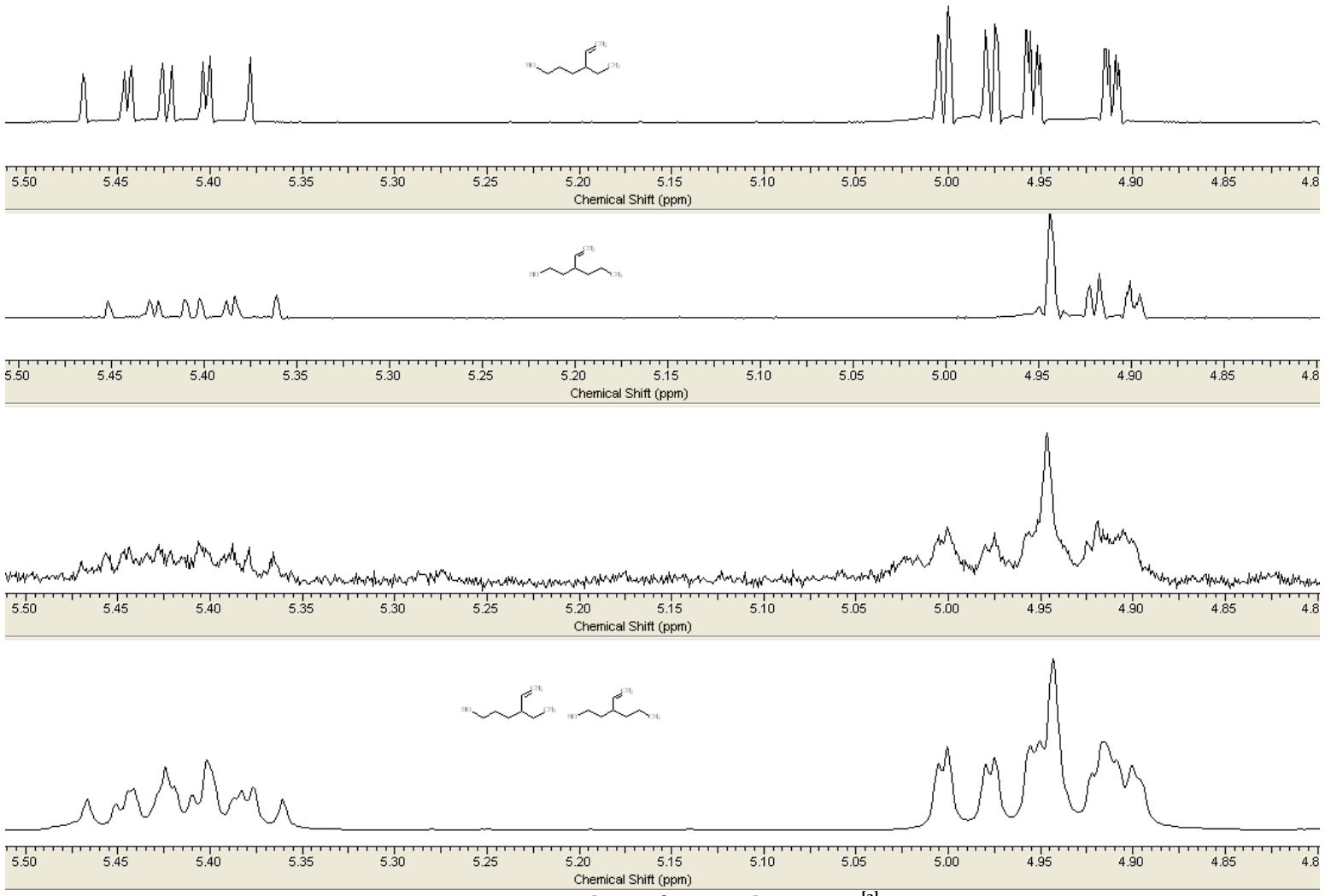

Figure 4.5 Evidence of 1, 2 vinyl migration[a]

[a]From top to bottom: ^{1}HNMR(400MHz, C_6D_6) spectrum of alkene region for 4-vinyl hexanol (**4.151**), ^{1}HNMR(400MHz, C_6D_6) spectrum of alkene region for 3-vinyl hexanol (**4.143**), ^{1}HNMR (400MHz, C_6D_6) spectrum of alkene region after cyclization study (peak at 5.025 ppm is leaching from the plastic syringe used for slow addition of Bu_3SnH/AIBN solution), ^{1}HNMR(400MHz, C_6D_6) spectrum of alkene region for 1:1 mixture of the two alcohols.

Employing a similar rate approximation analysis to the primary alkoxyl radical cyclization vs 1, 5-HAT competition experiment, the rate of cyclization is 15 times faster than hydrogen abstraction. Based on the extrapolated rate for a primary alkoxy radical 1, 5-HAT of 8.6×10^7 s^{-1} at 80 °C, the rate of primary alkoxyl cyclization onto a simple terminal alkene is 1×10^9 s^{-1} at 80 °C. This rate is faster than the previously measured rate of 5.2×10^8 s^{-1} at 80 °C by Beckwith and coworkers.[219a] The fast rate for primary alkoxyl radical 5-*exo* cyclization onto a simple terminal alkene is further evidence to support explanation B2 from the cyclization acceptor competition experiments: the 'slowest' reaction (primary alkoxyl cyclization onto a terminal alkene) is faster than previously thought.

4.3 Use of 1, 5-hydrogen atom transfer for relay cyclizations

4.3.1 Tin-mediated cleavage of *N*-alkoxyphthalimides for alkoxy radical relay cyclizations

Seminal studies on the radical cyclization of transposed alkoxyl radicals by Cekovic and Ilijev (Scheme 4.18) highlight the problem of chemoselectivity inherent to all radical processes.[249] Low yields of the relay cyclization product can be mostly explained by the lack of control in the radical chain propagation process. Studies on relay cyclization by Rawal and Kim (Scheme 4.20)[251-255] were highly successful for bridged bicyclic systems but suffered from lack of generality in that molecular complexity could not be built from a linear substrate and the cyclization acceptor was limited to the alkene formed from oxirane opening.[250] Our studies on alkoxyl 1, 5-HAT radical relay cyclization aimed to address all of these shortcomings to produce a general and effective relay cyclization methodology.

The problem of controlling alkoxyl radical formation was solved by employing *N*-alkoxyphthalimides as radical precursors (Scheme 4.35). Controlled generation of tributylstannyl (**4.159**) through slow addition of tributyltin hydride in solution with AIBN as a radical initiator to a dilute solution containing **4.157** at reflux would provide a steady source of alkoxyl **4.78**. The by-product from alkoxyl generation is tin-phthalimide adduct **4.160**, which is inert under the reaction conditions. Alteration of the radical cyclization acceptor is possible because our methodology cleanly provides alkoxyl radicals without the concomitant creation of a radical acceptor. By maintaining low concentrations of tributyltin hydride in solution, alkoxyl radical **4.78** undergoes 1, 5-HAT without alkoxyl radical quenching (to **4.160**) and 5-*exo* cyclization of transposed radical **4.79** is maximized. Thus, we have a general and flexible system for alkoxyl 1, 5-HAT radical relay cyclization.

By the time I joined the radical relay project, optimisation studies on this system by H. Zhu were complete for **4.158a** synthesis (n= 1, 5-*exo* cyclization) and the one carbon extended analogue **4.158b** (n= 2, 6-*exo* cyclization) was in progress. Studies in the Sammis group culminated in a multi-author publication and the results are summarized in Scheme 4.36.[260] The following section will be limited to my contributions to the paper (depicted in italics) and unpublished results relating the construction of cyclohexanes and nitrogen-containing heterocycles.

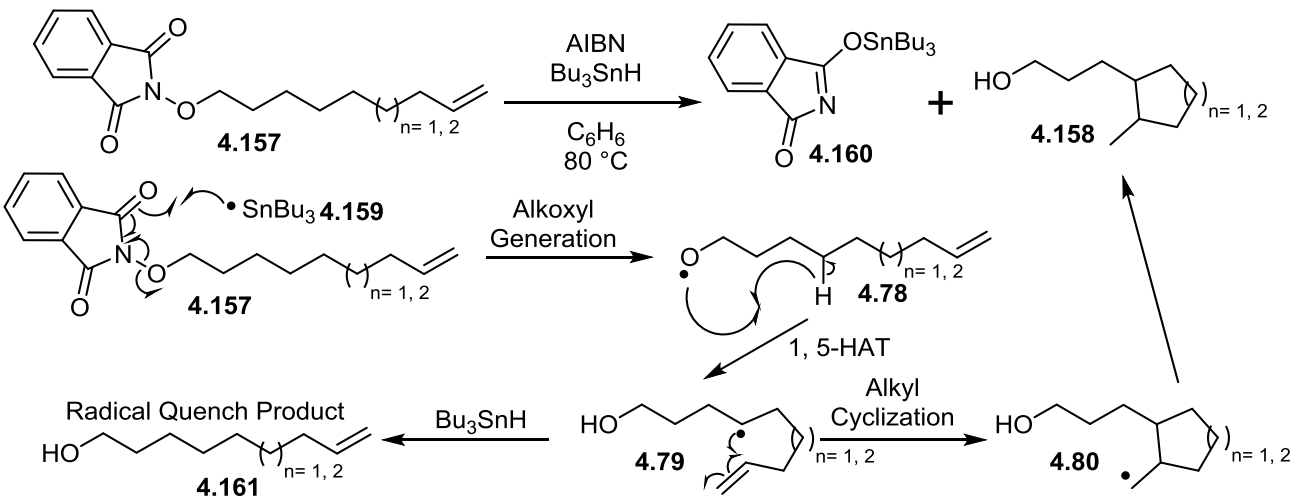

Scheme 4.35. Mechanism of the Alkoxy 1, 5-HAT Radical Relay Cyclization

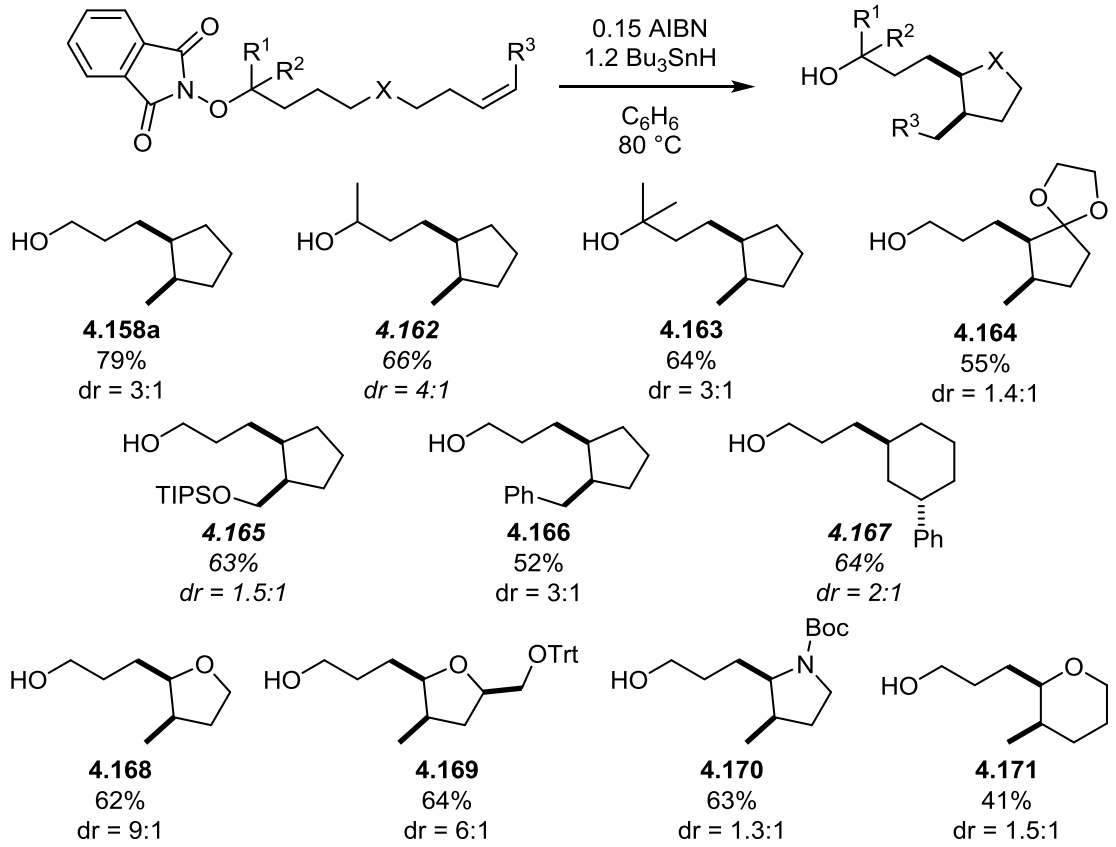

Scheme 4.36. Summary of alkoxyl 1, 5-HAT radical relay cyclization[a]

[a]My contributions are in *italics*.

4.3.2 Synthesis of 5-membered rings

Having obtained the optimized conditions for alkoxyl 1, 5-HAT radical relay cyclization from H. Zhu, I was tasked with exploring the viability of secondary and tertiary alkoxyl radicals as mediators of 1, 5-HAT for relay cyclization. Cyclization test substrate **4.174** was designed to evaluate the effectiveness of secondary alkoxyl radicals in relay cyclization (Scheme 4.37). Synthesis of **4.174** commenced with the Swern oxidation of 8-noneneol (**4.161a**) to the corresponding aldehyde (**4.172**) followed by nucleophilic attack by a Gilman reagent to deliver **4.173**. A cuprate nucleophile was chosen for the addition to reduce the possibility of a competing aldol reaction (methyllithium being a strong base). The alkoxyphthalimide moiety was installed by a Mitsunobu reaction in 80% yield.

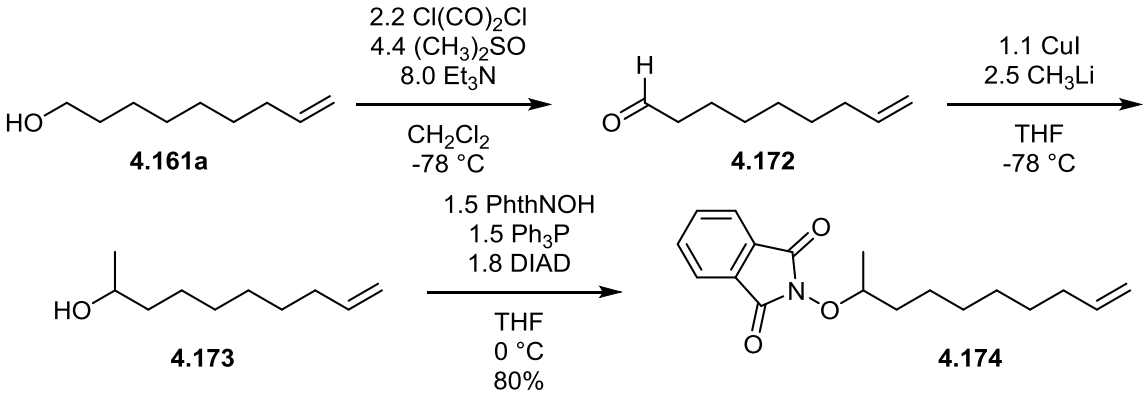

Scheme 4.37. Synthesis of relay cyclization substrate 4.174

All cyclization precursors were subject to the two step general cyclization procedure developed by H. Zhu for 5-*exo* cyclization (see experimental section). Secondary alkoxyl relay substrate **4.174** was cyclized according to the general procedure and inspection of the crude reaction mixture by ^{1}H NMR spectroscopy revealed a cyclization to linear quench ratio of 5.7: 1. Cyclization product **4.162** was isolated in 66% yield as a complex mixture of diastereomers (Scheme 4.38). The relative

configuration of the secondary alcohol could not be determined and the diastereomeric ratio (dr) for cyclization was 4: 1 *cis*: *trans*. The diastereomeric ratio was determined by ^{1}H NMR analysis of the methyl doublets in analogy to cyclopentane **4.158a**.

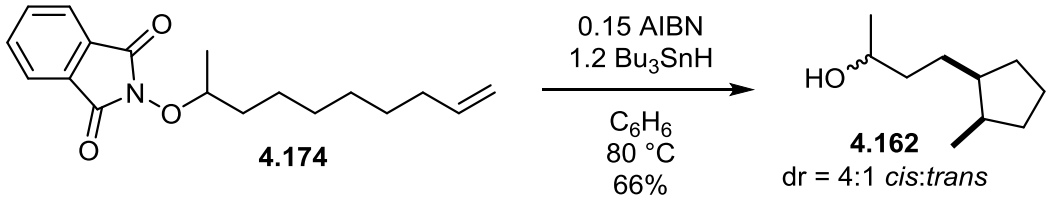

Scheme 4.38. Successful relay cyclization of 4.174

During studies on the 1, 5-HAT radical relay cyclization reaction, I was joined by an undergraduate student named Kayli Johnson. Under my supervision, K. Johnson synthesized tertiary alkoxyl substrate **4.176a** (for 5-*exo* relay cyclization) according to the procedure I had developed for tertiary alkoxyl substrate **4.176b** (for 6-*exo* relay cyclization) (Scheme 4.39); and substrate **4.178** (for 6-*endo* relay cyclization) according to the procedure I had developed for substrate **4.179** (for 7-*endo* relay cyclization) (Scheme 4.49).

Cyclization test substrate **4.176a** was designed to evaluate the effectiveness of tertiary alkoxy radicals in relay cyclizations. I did not participate in the execution of the synthetic steps to obtain **4.176a**, nevertheless, I contributed to most of the synthetic planning and reaction design. Installation of the *N*-alkoxyphthalimide moiety (**4.175** to **4.176**) was a particularly challenging transformation and deserves commentary. We had found literature precedence for an S_N1 reaction to install the alkoxyphthalimide; however, replication of the procedure for alcohol **4.175** produced very low yield of **4.176**. When I executed the S_N1 reaction, 6-*exo* substrate **4.178b** was obtain in only 20% yield.

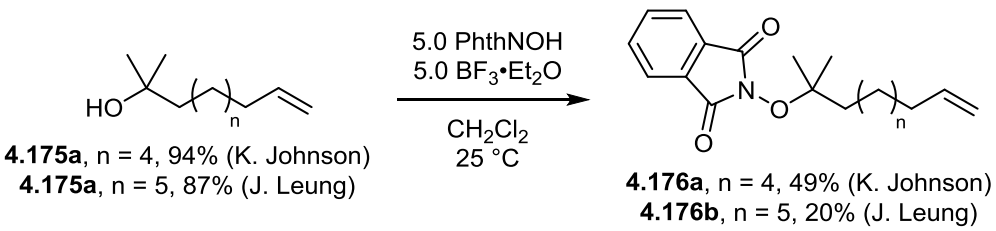

Scheme 4.39. Synthesis of relay cyclization substrate 4.176

In both reactions (Scheme 4.39), *N*-hydroxyphthalimide was not dissolving effectively in dichloromethane. Other solvents were examined for the transformation, but many of the available solvents contained Lewis basic heteroatoms which could interfere with boron trifluoride coordinating to the tertiary alcohol. I suggested the procedural modification of allowing the suspension of *N*-hydroxyphthalimide in dichloromethane to stir overnight in an attempt to maximize the amount of dissolved nucleophile prior to addition of the alcohol and boron trifluoride. Gratifyingly, this procedure allowed K. Johnson to obtain **4.176a** in a more reasonable yield.[260] Application of this modified procedure to substrate **4.176b** was unnecessary as 6-*exo* relay cyclizations were not attempted.

Cyclization of **4.176a** under the general relay conditions lead to an excellent ratio of cyclization to linear quench of 10: 1 (Scheme 4.40). Cyclopentane **4.163** was isolated in 64% yield as a 3: 1 *cis*: *trans* ratio of diastereomers by K. Johnson.[260] The successful synthesis of cyclopentanes **4.158a**, **4.162** and **4.163** indicate that alkoxyl radicals of any degree can be employed for relay cyclization. Reflecting on the studies detailed in subsection 4.2.1, only alkoxyl radicals not prone to fragmentation should be employed, although further work by H. Zhu has shown that fragmentation can be mitigated by lowering the reaction temperature for cyclization.[261]

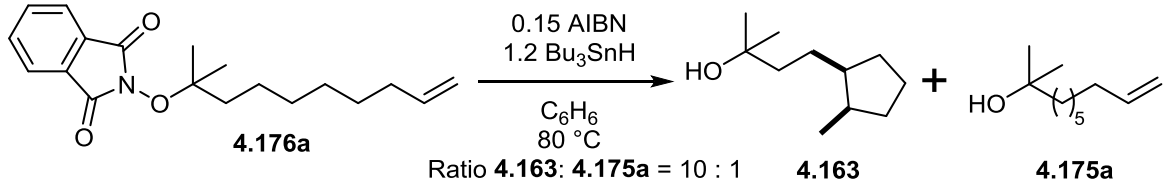

Scheme 4.40. Successful relay cyclization of 4.176a.

Incorporation of a heteroatom into the cyclization precursor alkyl chain for the synthesis of heterocycles was next explored. Cyclization precursor **4.184** was synthesized in 26% overall yield in 4 steps from valerolactone (Scheme 4.41). Nucleophillic acyl substitution of lactone **4.180** with allylamine followed by lithium aluminum hydride reduction and protection of secondary amine **4.182** provided alcohol **4.183**. A Mitsunobu reaction was employed to produce *N*-alkoxyphthalimide **4.184** in 83% yield.

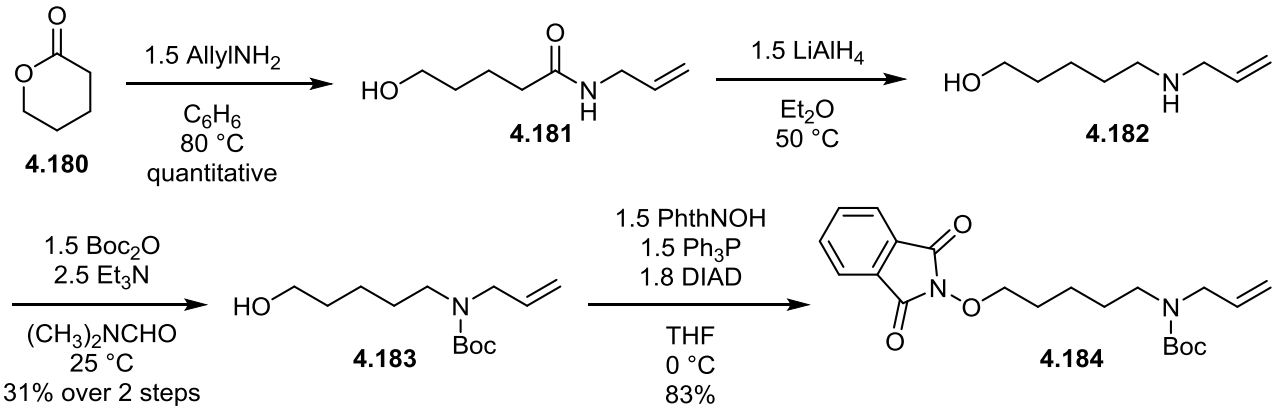

Scheme 4.41. Synthesis of relay cyclization substrate 4.184

Cyclization of **4.184** under the general radical relay conditions lead to the isolation of trace amounts of pyrrolidine **4.185**. However, ^{1}H NMR analysis of the crude reaction mixture suggests a 53% conversion to **4.185** with relatively poor diastereoselectivity (Scheme 4.42). At the time, this

reaction was not further pursued as the oxacycle analogue had failed to produce any cyclization products. 1, 6-HAT was likely occurring and the resulting 4-*exo* cyclization is unfavourable.[261]

The 1, 6-HAT relay is well established for activated ether C-H bonds.[206e] However, substrate **4.184** is different in that the 1, 6-HAT relay is less likely to occur. Unlike the ether C-H bond, the carbamate C-H bond is not activated for abstraction since there is less dative stabilization of the resulting radical. Furthmore, trace amounts of cyclization product **4.185** could be isolated and further investigation of this reaction is merited.

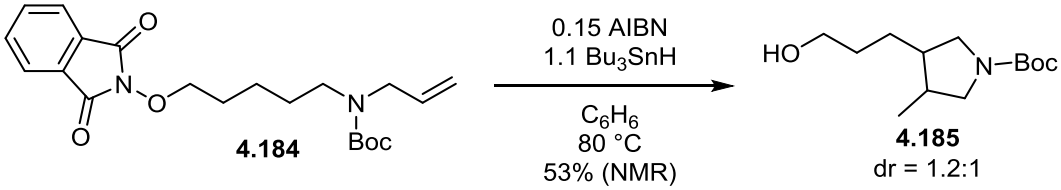

Scheme 4.42 Relay cyclization of 4.184 as evidenced by ^{1}H NMR spectroscopy

One of the many advantages of our relay cyclization methodology over the Rawal-Kim system[252-255] is the ability to alter the radical acceptor. Relay cyclization onto a silyl enol ether was examined as the resulting carbocycle would contain a silyl protected alcohol (a useful functional group handle). Cyclization precursor **4.189** synthesized in 61% overall yield in 3 steps from tosylated nonanediol **4.186** (Scheme 4.43). Swern oxidation of the primary alcohol followed by soft enolization provided intermediate silyl enol ether **4.188**. Nucleophilic displacement of tosylate with the DBU salt of alkoxyphthalimide delivered *N*-alkoxyphthalimide **4.189**.

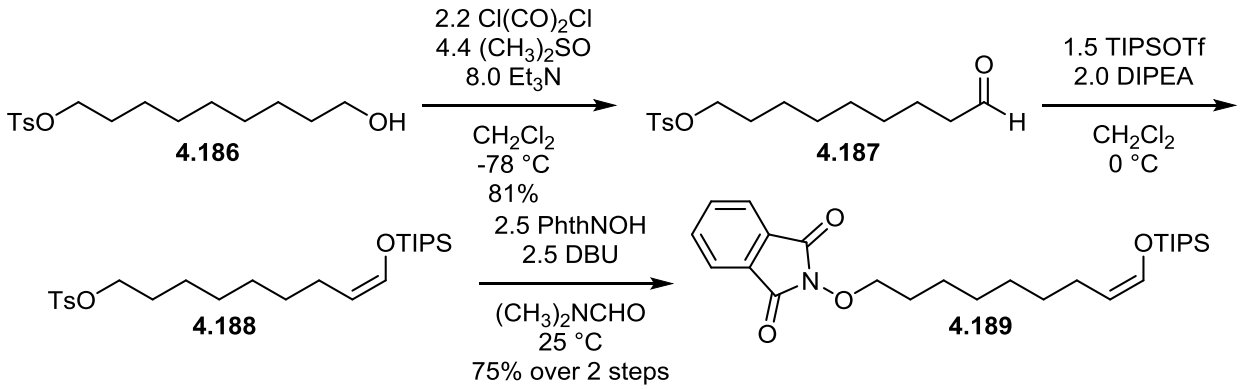

Scheme 4.43. Synthesis of relay cyclization substrate 4.189

Cyclization of **4.189** under radical relay conditions lead to a linear quench to cyclization ratio of 4.3 : 1 with a 63% isolated yield of cyclopentane **4.165** (Scheme 4.44). As the ^{1}H NMR signals of the protons adjacent to the free alcohol and the silyl ether overlapped, further transformation was necessary to elucidate the diastereomeric ratio. Purified **4.165** was benzoylated and desilylated to cyclopentane **4.191** in 69% yield over 2 steps. The diastereomeric ratio of **4.191** was 1.5: 1 *cis*: *trans*, which is assumed to be the dr of cyclopentane **4.165** obtained from relay cyclization.

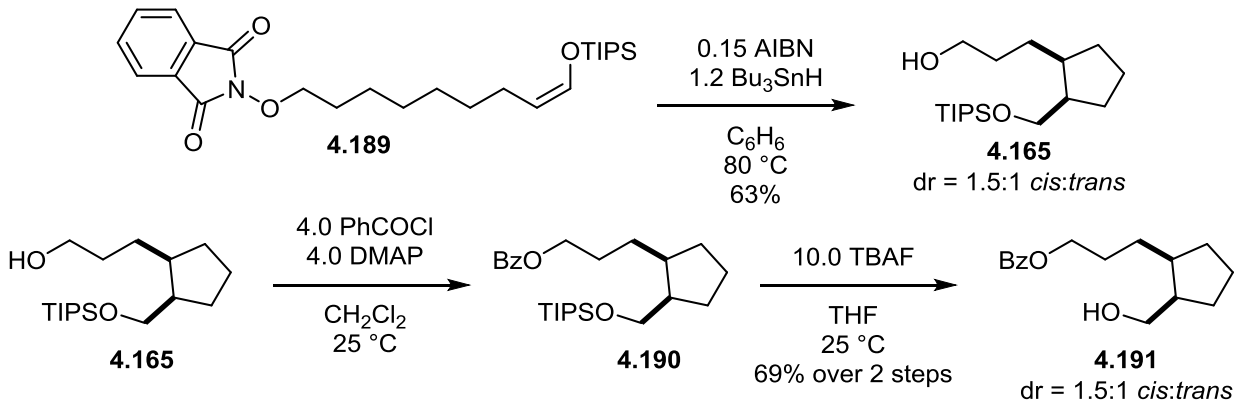

Scheme 4.44. Relay cyclization of 4.189 and transformation to 4.191 for dr elucidation

The low diastereoselectivity of this cyclization is disappointing; however, conversion of the silyl ether functionality to a carbonyl would render a cyclopentyl proton acidic and prone to

epimerization. In this manner, it may be possible to alter the inherent *cis*-selectivity of relay cyclization to the thermodynamically favourable *trans*-diastereomer (Scheme 4.45). Such a transformation may not be the most efficient way of accessing a 1, 2-*trans* cyclopentane; nevertheless, this strategy partially addresses the critiques that relay cyclization can only access *cis*-cyclopentanes.

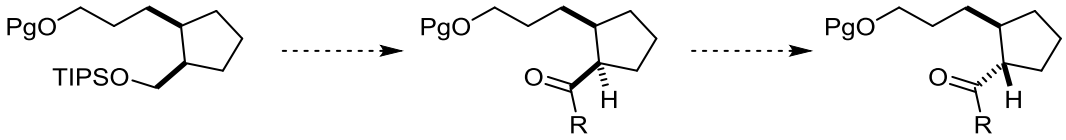

Scheme 4.45. Strategy to obtain the *trans* radical relay product

4.3.3 Synthesis of 6-membered rings

When studies began on 1, 5-HAT radical relay cyclization, it was anticipated that the methodology could be applied to cyclohexane construction. Unfortunately, after extensive optimization studies by H. Zhu, an acceptable procedure for cyclohexane synthesis could not be obtained. The best result for 6-*exo* cyclization was obtained by J. Wickenden for oxacycle **4.171**.[260] The moderate level of success achieved with oxacycle **4.171** can be rationalized by the shortened distance between the radical intermediate and the alkene acceptor (C-O bonds are shorter than C-C bonds). Thus, the 3 substrates I had synthesized for testing 6-*exo* (**4.177**, **4.176b**) and 7-*endo* (**4.179**) 1, 5-HAT radical relay cyclization were not utilized (Figure 4.6).

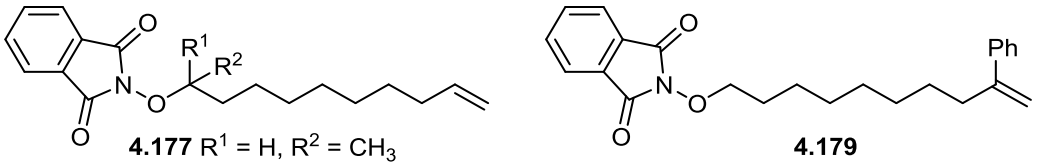

4.177 R^1 = H, R^2 = CH_3
4.176b R^1 = R^2 = CH_3
4.179

Figure 4.6 Substrates prepared for 6-*exo* and 7-*endo* cyclizations

Given the relative success in relay cyclization synthesis of tetrahydropyran **4.171**, the nitrogen analogue was explored as C-N bonds are also shorter than C-C bonds.[7] Protected 4-aminobutanol **4.192** was *N*-alkylated to **4.193** followed by acid catalyzed removal of the silyl ether to alcohol **4.194**. A Mitsunobu reaction provided *N*-alkoxyphthalimide **4.195** in 82% yield (Scheme 4.46).

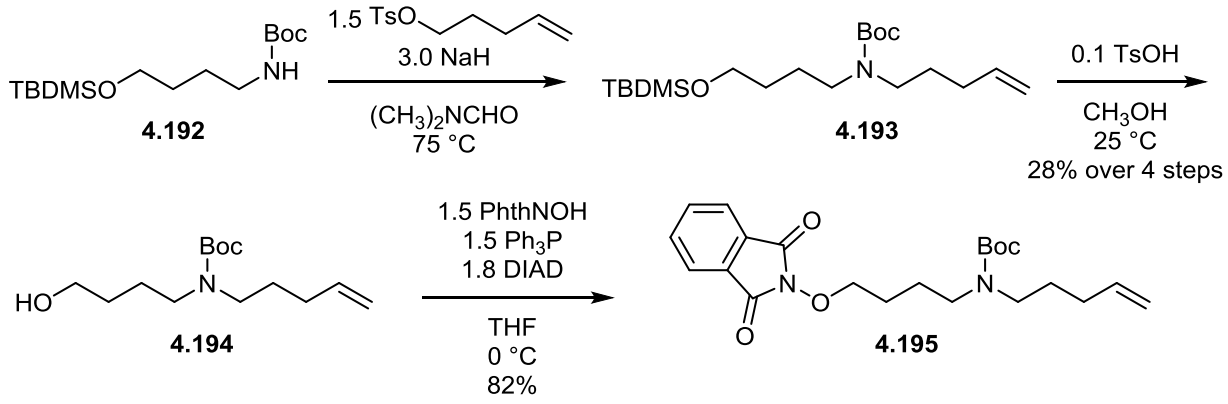

Scheme 4.46. Synthesis of relay cyclization substrate 4.195

Cyclization of 6-*exo* substrate **4.195** (under the optimised conditions for 5-*exo* radical relay cyclization) resulted in a linear quench to cyclization ratio of 1: 10, and a 70% isolated yield of cyclization products (Scheme 4.47). After oxidative treatment and purification, a third compound was present in addition to the two diastereomers resulting from 6-*exo* cyclization (**4.196**). Using the ^{1}H NMR signals for protons adjacent to a heteroatom as an integration reference of 5 protons, the two doublets corresponding to 6-*exo* cyclization products accounted for only half of the mass balance. ^{13}C NMR analysis of the purified material revealed signals in excess of the expected 24 singlets accounting for the two piperidine diastereomers of **4.196**.

Esterification of the alcohol with benzoyl chloride followed by a second purification by flash chromatography did not alter the integration ratio between protons adjacent to a heteroatom and the

methyl protons (Scheme 4.48). Furthermore, the ^{13}C NMR spectra distinctly showed 3 sets of carbon signals for the carbons label 1, 4, 5 which can be correlated to protons in the heteroatom region by HSQC. By these observations, cyclization of 6-*exo* substrate **4.195** yielded a mixture of 6-*exo* (**4.196**) and 7-*endo* (**4.197**) products in a 1: 1 ratio with an overall yield of 70%. Integration of the methyl doublets shows a diastereomeric ratio of 4:1; however, the relative configuration of the major or minor piperidine diastereomers of **4.196** or **4.198** could not be determined.

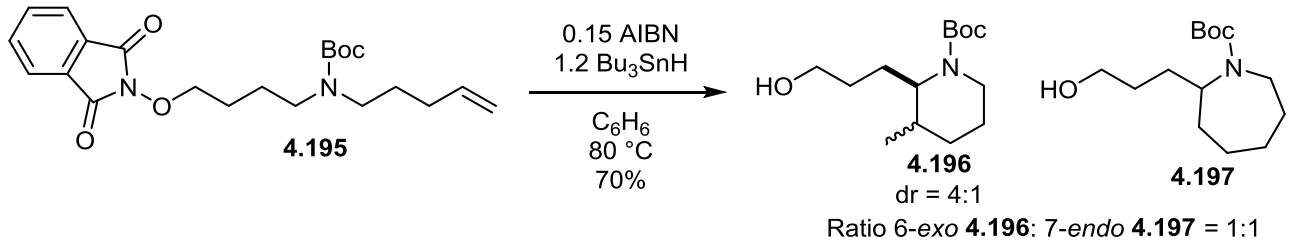

Scheme 4.47 Successful relay cyclization of 4.195

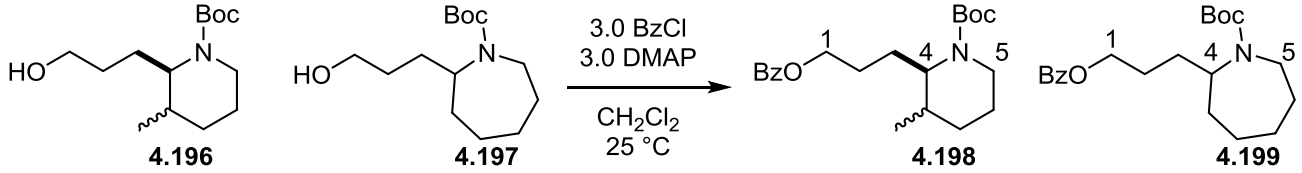

Scheme 4.48 Derivatization of 4.195 cyclization products for detailed NMR analysis

Another strategy for the synthesis of cyclohexanes is to employ a 6-*endo* mode of radical cyclization. Installation of a radical stabilizing substituent (such as a phenyl group or carbonyl group) on the internal position of the alkene acceptor reverses the kinetic bias for 5-*exo* cyclization. K. Johnson's synthesis of 6-*endo* cyclization substrate **4.178** did not yield adequate amounts of compound for the final cyclization to be performed on scale; however, she was able fully characterize all of the

intermediates. I resynthesized substrate **4.178** by telescoping from intermediate **4.201** to **4.206** in 51% yield, followed by a Mitsunobu reaction to furnish *N*-alkoxyphthalimide **4.178** (Scheme 4.49).

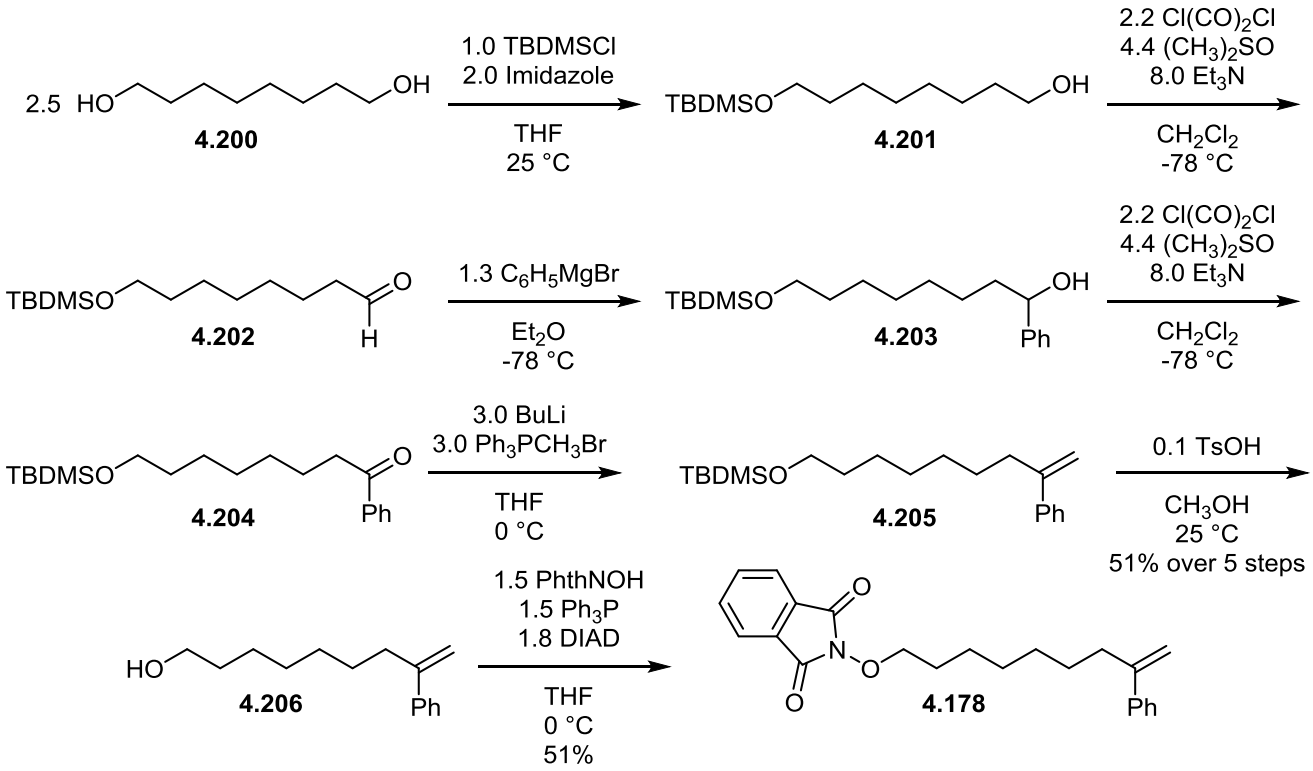

Scheme 4.49. Synthesis of relay cyclization substrate 4.178

Cyclization of 6-*endo* substrate **4.178** under the optimised conditions for 5-*exo* radical relay cyclization resulted in a linear quench to 6-*endo* cyclization ratio of 1: 4.8. No 5-*exo* cyclization product was observed and cyclohexane **4.167** was isolated in 71% yield as a 1: 2 *cis*: *trans* mixture of diastereomers (Scheme 4.50). The relative stereochemistry was determined by observing an nOe correlation between the benzylic proton and the alkyl branching tertiary cyclohexyl proton, indicating a *cis*-configuration for the minor diastereomer.

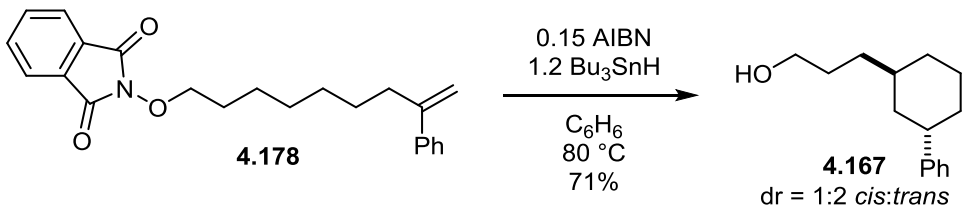

Scheme 4.50. Successful relay cyclization of 4.178

4.4 Future work and conclusions

The two major alkoxyl reaction pathways which I studied (5-*exo* cyclization and 1, 5-HAT) are powerful tools for building molecular complexity from simple linear chains. Numerous potential applications towards the synthesis of polyketide natural products exist as the predominate diastereoselectivity of alkoxyl 5-exo cyclization and alkoxyl 1, 5-HAT relay cyclization are orthogonal, allowing access to virtually all tetrahydrofuran substitution patterns (Figure 4.7).

Figure 4.7. Diastereoselectivity comparison between alkoxyl 5-exo cyclization and 1, 5-HAT relay cyclization

One advantage of 1, 5-HAT relay cyclization over 5-*exo* alkoxyl cyclization to be further explored is the applicability to alkaloid synthesis. Radical relay 6-*exo* cyclization and 7-*endo* cyclization is possible with carbamate protected nitrogen in the ring (Scheme 4.47), and suggests that minor changes to the radical cyclization acceptor could bias the cyclization towards either the piperdine **4.208** or azepane **4.209** product (Scheme 4.51). The placement of a radical stabilizing group on the external alkene position (**4.207a**, R^1 = H, R^2 = Ph) should favour 6-*exo* cyclization to piperidine **4.208**

with good diastereoselectivity. Conversely, the placement of a radical stabilizing group on the internal position (**4.207b**, R^1 = Ph, R^2 = H) should favour 7-*endo* cyclization to access azepane **4.209**.

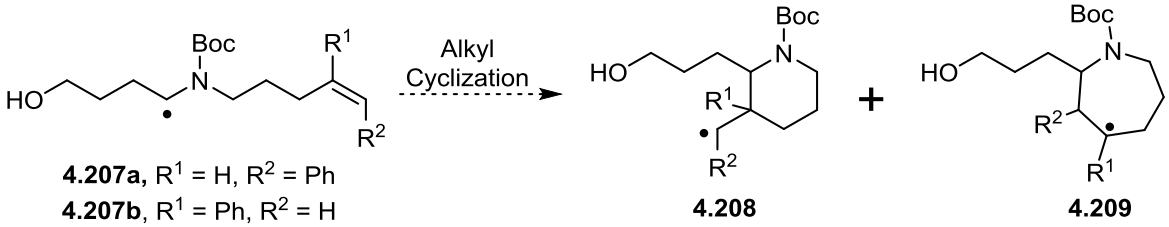

4.207a, R^1 = H, R^2 = Ph
4.207b, R^1 = Ph, R^2 = H

4.208 **4.209**

Scheme 4.51. Predicted 6-exo or 7-endo cyclization bias

Efforts towards the synthesis of pyrrolidine **4.185** were prematurely halted, partially because only trace amounts could be isolated (Scheme 4.42). However, further investigation into relay cyclization substrate **4.184** should be performed because the crude NMR shows promise and **4.185** could be obtained. If **4.185** can be isolated above 51% yield (the NMR yield was 53%), a powerful application of this methodology is the synthesis of azabicycles (Scheme 4.52). Cyclization of **4.210** onto an allyl ether radical acceptor would provide a synthetic handle for further manipulation. Functional group transformation of the ether or alcohol to a suitable nucleophile followed by internal displacement by the liberated amine could rapidly furnish azabicyclo[3.2.1]octane **4.213** or azabicyclo[2.2.1]heptane **4.214** in as few as 3 steps from a linear relay cyclization precursor.

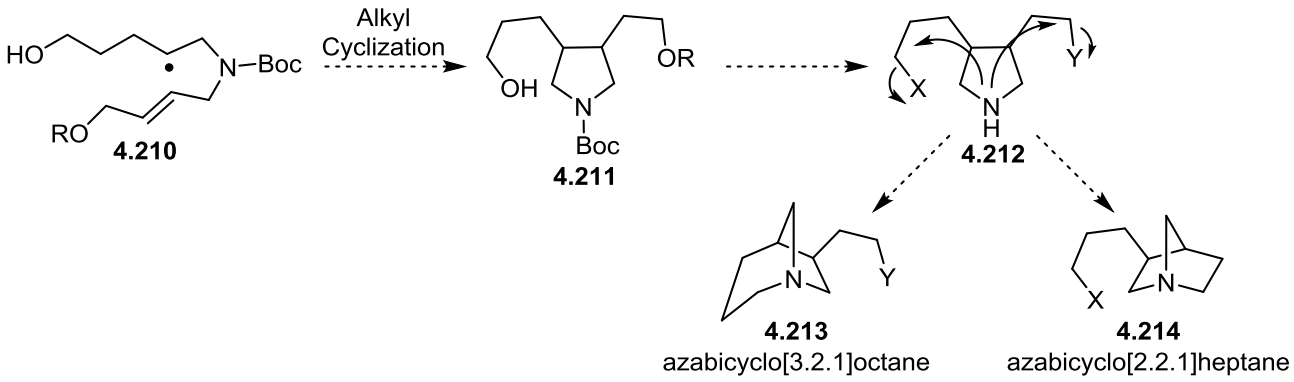

4.210 **4.211** **4.212**

4.213 azabicyclo[3.2.1]octane

4.214 azabicyclo[2.2.1]heptane

Scheme 4.52. Application of pyrrolidine synthesis to azabicycles

In summary, I have utilized three types of alkoxyl radical competition experiments to investigate the rates of alkoxyl radical cyclization onto a silyl enol ether acceptor and investigated alkoxyl radical 1, 5-HAT relay cyclizations. Alkoxyl radical 5-*exo* cyclization onto a silyl enol ether (both primary and secondary alkoxyl) is marginally faster than alkoxyl radical 5-*exo* cyclization onto a trisubstituted alkene. Primary alkoxyl radical 5-*exo* cyclization onto a terminal alkene is likely faster than previously estimated (at reflux in benzene) and results in poorer cyclization chemoselectivity than a secondary or tertiary alkoxyl radical. Primary, secondary, and tertiary alkoxyl radicals are suitable for participation in relay cyclization and this methodology can accommodate the synthesis of 5 and 6 membered carbocycles (5-*exo* and 6-*endo* modes of cyclisation) and selected nitrogen containing 5-7 membered heterocycles.

4.5 Experimental

4.5.1 General experimental

All chemicals were purchased from commercial sources and used as received. Proton and carbon nuclear magnetic resonance (^{1}H and ^{13}C NMR) spectra were recorded in deuterated solvents using a Bruker AV-400 or AV-300 spectrometer. Chemical shifts are reported in parts per million (ppm) and are referenced to the centerline of deuterochloroform (7.27 ppm ^{1}H NMR; 77.0 ppm ^{13}C NMR) or deuterobenzene (7.16 ppm ^{1}H NMR; 128.4 ppm ^{13}C NMR). Melting points were performed using a Mel-Temp II apparatus (Lab devices USA) and are uncorrected. Infrared (IR) spectra were obtained using a Thermo Nicolet 4700 FT-IR spectrometer or a Perkin Elmer Frontier FT-IR. High resolution mass spectra (HRMS) were recorded on either a Waters or Micromass LCT spectrometer.

4.5.2 Experimentals pertaining to competition kinetic studies

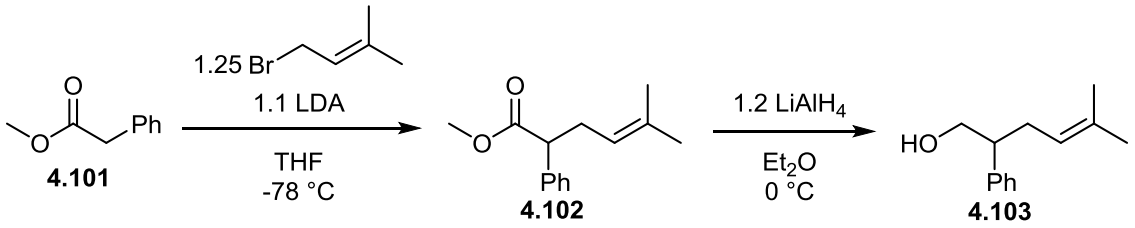

5-Methyl-2-phenylhex-4-en-1-ol (**4.103**): To a solution of diisopropylamide (1.7 ml, 12.0 mmol, 1.2 equiv.) in THF (22 ml) cooled to -78 °C in an acetone/dry ice bath was added *n*-butyllithium (6.9 ml, 1.6 M in hexane, 11.0 mmol, 1.1 equiv.) over 1 min. The resulting solution of LDA was removed from the cold bath and allowed to warm to ambient temperature over 30 min. The solution was returned to the acetone/dry ice bath and methyl phenylacetate (1.4 ml, 10.0 mmol, 1.0 equiv.) was added over 4 min resulting in a yellow solution. After 10 min, the reaction mixture (a suspension with white solids) was removed from the cold bath and allowed to warm to ambient temperature over 20 min resulting in a bright yellow solution. This solution was cooled to 0 °C in an ice/water bath and 1-bromo-3-methylbut-2-ene (1.45 ml, 12.5 mmol, 1.25 equiv.) was added in one portion resulting in a colourless solution. The cold bath was removed and the reaction mixture was allowed to warm to ambient temperature. After 40 min, the reaction was quenched with saturated $NH_4Cl_{(aq)}$ (5 ml), poured into Et_2O (150 ml). The organic layer was washed with 0.5M $HCl_{(aq)}$ (3 x 40 ml), brine (30 ml), dried over Na_2SO_4, filtered, and concentrated by rotory evaporation to provide crude **4.102** as a yellow-orange oil. To a solution of crude **4.102** in Et_2O (20 ml) cooled to 0 °C in an ice/water bath was added lithium aluminum hydride (0.46 g, 12.0 mmol, 1.2 equiv.) slowly over 5 min. Vigorous gas release was observed. The grey suspension was removed from the bath and allowed to warm to ambient temperature. After 40 min, the reaction mixture was returned to the cold bath and quenched with sodium sulphate decahydrate (5 g) slowly over 10 min. Vigorous gas release was observed. The

resulting suspension was filtered through a plug of silica and the solids washed with Et_2O (200 ml). The combined organic layer was concentrated by rotary evaporation and purified by flash chromatography (2:1 hexane: Et_2O, Rf = 0.27, visualization by $KMnO_4$ stain) to provide **4.103** as a clear colourless oil (1.6 g, 84% yield over 2 steps).

^{1}H NMR (400MHz; $CDCl_3$): δ = 7.40 - 7.32 (m, 2 H), 7.31 - 7.21 (m, 3 H), 5.16 - 5.07 (m, 1 H), 3.91 - 3.70 (m, 2 H), 2.85 (quin, *J* = 6.8 Hz, 1 H), 2.52 - 2.41 (m, 1 H), 2.36 - 2.24 (m, 1 H), 1.69 (s, 3 H), 1.61 (s, 3 H), 1.43 - 1.36 (m, 1 H) ppm.

^{13}C NMR (101MHz; $CDCl_3$): δ = 142.4, 133.1, 128.5, 128.0, 126.6, 121.9, 67.0, 48.8, 30.9, 25.7, 17.8 ppm.

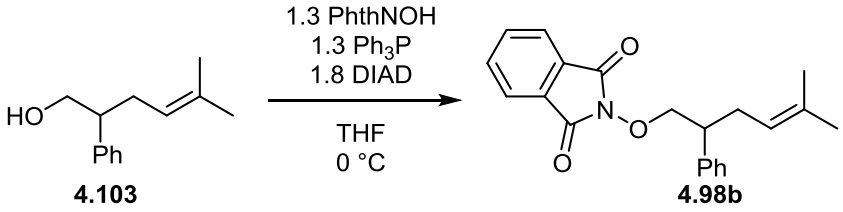

4.103 **4.98b**

2-((5-Methyl-2-phenylhex-4-en-1-yl)oxy)isoindoline-1,3-dione (**4.98b**): To a solution of alcohol **4.103** (1.6 g, 8.3 mmol, 1.0 equiv.), *N*-hydroxypthalimide (1.8 g, 10.8 mmol, 1.3 equiv.), and triphenyl-phosphine (2.8 g, 10.8 mmol, 1.3 equiv.), in THF (33 ml) cooled to 0 °C in an ice/water bath was added diisopropyl azodicarboxylate (2.5 ml, 12.5 mmol, 1.8 equiv.) over 55 min turning the solution to an orange-red colour. After 18 h, the light-yellow solution was poured into Et_2O (150 ml), washed with 50% saturated $NaHCO_{3(aq)}$ (3 x 50 ml, orange coloured aqueous layer), brine (40 ml), dried over Na_2SO_4, filtrated and concentrated by rotary evaporation. Triphenylphosphineoxide was precipitated with a 1:1 mixture of hexane : Et_2O (100 ml), triterated with hexanes until no colour remained, and the collected organics were concentrated by rotary evaporation. Purification by flash chromatography (5:2 hexanes: Et_2O, Rf = 0.31, visualization by UV or $KMnO_4$ stain) yielded *N*-alkoxypthalimide **4.98b** as a colourless oil that solidifies upon standing (761 mg, 27%).

^{1}H NMR (400MHz; $CDCl_3$): δ = 7.88 - 7.71 (m, 4 H), 7.41 - 7.18 (m, 5 H), 5.19 - 5.07 (m, 1 H), 4.51 (dd, *J* = 7.2, 8.9 Hz, 1 H), 4.38 (dd, *J* = 7.2, 8.9 Hz, 1 H), 3.22 (quin, *J* = 7.2 Hz, 1 H), 2.75 - 2.63 (m, 1 H), 2.48 - 2.36 (m, 1 H), 1.68 (s, 3 H), 1.59 (s, 3 H) ppm.

^{13}C NMR (101MHz; $CDCl_3$): δ = 163.4, 141.2, 134.3, 133.6, 128.8, 128.3, 127.8, 126.6, 123.3, 121.0, 81.1, 45.0, 31.7, 25.7, 17.8 ppm.

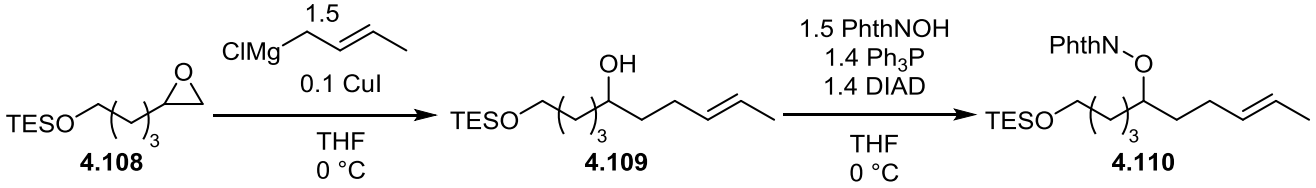

(*E*)-2-((1-((Triethylsilyl)oxy)dec-8-en-5-yl)oxy)isoindoline-1,3-dione (**4.110**): To a two-neck flask equipped with reflux condenser containing magnesium churnings (0.74 g, 28.8 mmol, 2.5 equiv.) and a small crystal of iodine was added crotyl chloride (1.7 ml, 17.3 mmol, 1.5 equiv.) in THF (20 ml + 15 ml rinse) at such a rate to maintain a gentle reflux. The resulting cloudy grey suspension was refluxed for 1 h to provide the Grignard solution. To a separate flask containing copper (I) iodide (243 mg, 1.12 mmol, 0.1 equiv.) and **4.108** (2.69 g, 11.5 mmol, 1.0 equiv.) was added THF (11.5 ml) and cooled to 0°C in an ice/water bath. To the cloudy grey suspension was added the Grignard solution over 15 min. Colour in the reaction mixture changed from cloudy grey to bright yellow to orange-red to red-black. After 18 h, the blue-black solution was quenched with 50% saturated $NH_4Cl_{(aq)}$ (100 ml) and extracted with Et_2O (3 x 50 mL). Colourless organics were washed with brine (25 ml), dried over Na_2SO_4, filtrated and concentrated by rotary evaporation. Purification by flash chromatography (3:1 Hexanes: Et_2O, Rf = 0.26, visualization by $KMnO_4$ stain) provided 2.25 g of a colourless oil consistent with alcohol **4.109** by LCMS-ESI analysis.

To alcohol **4.109** (2.25 g, 7.8 mmol, 1.0 equiv.) was added *N*-hydroxypthalimide (1.91 g, 11.7 mmol, 1.5 equiv.), triphenylphosphine (2.83 g, 10.9 mmol, 1.4 equiv.), and THF (80 ml). The solution was

cooled to 0 °C in an ice/water bath and diisopropyl azodicarboxylate (2.2 ml, 10.9 mmol, 1.4 equiv.) was added in two portions over 20 min turning the solution to an orange-red colour. After 18 h, the light-yellow solution was poured into EtOAc (250 ml), washed with 50% saturated $NaHCO_{3(aq)}$ (3 x 70 ml, orange coloured aqueous layer), brine (50 ml), dried over Na_2SO_4, filtrated and concentrated by rotary evaporation. Triphenylphosphineoxide was triterated with hexanes until no colour remained and the collected organics were concentrated by rotary evaporation. Purification by flash chromatography (4:1 Hexanes: Et_2O, Rf = 0.28, visualization by UV or $KMnO_4$ stain) yielded *N*-alkoxypthalimide **4.110** as a colourless oil (2.0 g, 40% over 2 steps).

IR ($CDCl_3$): 2952, 2875, 1791, 1737, 1731, 1467, 1371, 976, 701 cm^{-1}.

^{1}H NMR (400MHz; $CDCl_3$): δ = 7.91 - 7.66 (m, 4 H), 5.56 - 5.29 (m, 2 H), 4.24 (quin, J = 6.1 Hz, 1 H), 3.62 (t, J = 5.5 Hz, 2 H), 2.38 - 2.06 (m, 2 H), 1.84 - 1.66 (m, 4 H), 1.63 (d, J = 5.8 Hz, 3 H), 1.60 - 1.45 (m, 4 H), 0.95 (t, J = 8.0 Hz, 9 H), 0.59 (q, J = 8.0 Hz, 6 H) ppm.

^{13}C NMR (101MHz; C_6D_6): δ = 164.3, 134.3, 130.4, 129.6, 129.1, 125.5, 124.5, 123.4, 87.7, 62.6, 32.9, 32.3, 32.2, 28.0, 21.2, 17.9, 6.8, 4.4 ppm.

HRMS-ESI (m/z): $[M+Na]^+$ calcd for $C_{24}H_{37}NO_4NaSi$: 454.2390. Found 454.2397.

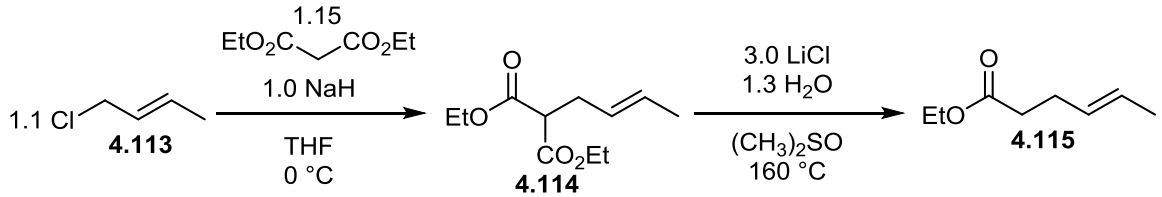

(*E*)-ethyl hex-4-enoate (**4.115**): To a suspension of sodium hydride (0.81 g, 60 wt% in mineral oil, 20 mmol, 1.0 equiv.) in THF (40 ml) cooled to 0 °C in an ice/water bath was added diethyl malonate (3.5 ml , 23.0 mmol, 1.15 equiv.) over 5 min. Gas evolution was observed as the suspension turns to a colourless solution. After 5 min, crotyl chloride (5.1 ml, 22.0 mmol, 1.1 equiv.) was added in one

portion and the bath was removed. After 18 h, the colourless suspension with white precipitate was quenched with 50% $NH_4Cl_{(aq)}$ (2 ml) then poured into water (80 ml). The aqueous mixture was extracted with Et_2O (3 x 30 ml) and the combined organic extracts washed with brine (30 ml), dried over Na_2SO_4, filtrated and concentrated by rotary evaporation to provide crude malonate **4.114** as a colourless oil. To flask containing crude malonate **4.114** was added DMSO (40 ml), lithium chloride (2.6 g, 60 mmol, 3.0 equiv.) and water (470 µl, 26 mmol, 1.3 equiv.), then heated to reflux. The reaction was stirred at reflux for 5 h then allowed to cool to ambient temperature. The yellow-brown solution was poured into 0.5M $HCl_{(aq)}$ (150 ml) and extracted with pet. ether (3 x 50 ml). The yellow organic extracts were washed with 1.0M $HCl_{(aq)}$ (30 ml), brine (30 ml), dried over Na_2SO_4, filtrated and concentrated by rotary evaporation (45°C @ 300 Torr) to provide a yellow oil. Purification by flash chromatography (10:1 pet. ether: Et_2O, Rf = 0.42, visualization by $KMnO_4$ stain) provided ~400 mg (24% over 2 steps) of ester **4.115** as a colourless oil (containing ~ 20% Et_2O).

^{1}H NMR (400MHz; $CDCl_3$): δ = 5.60 - 5.29 (m, 2 H), 4.14 (q, *J* = 7.1 Hz, 2 H), 2.44 - 2.24 (m, 4 H), 1.71 - 1.60 (m, 3 H), 1.26 (t, *J* = 7.1 Hz, 3 H) ppm.

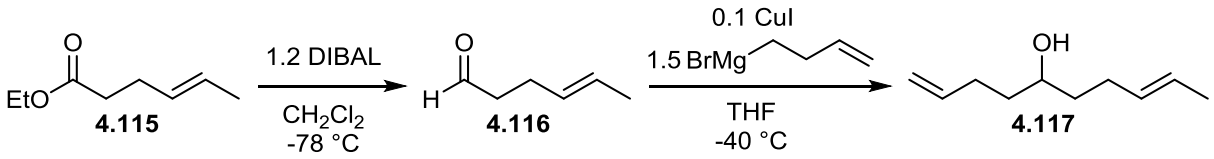

(*E*)-deca-1,8-dien-5-ol (**4.117**): To a solution of **4.115** (426 mg, 3.0 mmol, 1 equiv.) in CH_2Cl_2 (12 ml) cooled to –78 °C in a dry ice/acetone bath was added diisobutylaluminum hydride (3.6 ml, 1.0 M in hexanes, 3.6 mmol, 1.2 equiv.) over 2 minutes. After stirring for 30 minutes the reaction mixture was quenched with aqueous methanol (50% v/v methanol in water, 3 ml). The cooling bath was removed and the mixture was stirred for an additional 30 minutes, dried over Na_2SO_4, and filtrated. The solids

washed with Et_2O (5 x 5 ml) and the combined colourless organic extracts were distilled off through a 15 cm vigeraux column (60 °C). To the crude aldehyde **4.116**, cooled to –40 °C in a dry ice/acetonitrile bath, was added copper (I) iodide (63 mg, 0.3 mmol, 0.1 equiv.) in one portion and homoallylmagnesium bromide solution (9 ml, 0.5 M in THF, 4.5 mmol, 1.5 equiv.) over 5 min. Cooling bath was removed and the blue-grey reaction mixture was stirred for 18 h. The blue-black suspension was quenched with saturated $NH_4Cl_{(aq)}$ (1 ml), poured into EtOAc (100 ml), washed with 50% saturated $NH_4Cl_{(aq)}$ (3 x 20 ml), brine (20 ml), dried over Na_2SO_4, filtered and concentrated by rotary evaporation. Purification by flash chromatography (3:1 hexanes: Et_2O, Rf = 0.29, visualization by $KMnO_4$ stain) yielded 264 mg of alcohol **4.117** as a colourless oil (57% over 2 steps).

IR ($CDCl_3$): 3374, 2927, 2855, 2067, 2996, 966, 920, 772 cm^{-1}.

^1H NMR (400 MHz; $CDCl_3$): δ = 5.91 - 5.79 (m, 1 H), 5.58 - 5.37 (m, 2 H), 5.10 - 5.02 (m, 1 H), 5.02 - 4.96 (m, 1 H), 3.70 - 3.61 (m, 1 H), 2.33 - 2.02 (m, 4 H), 1.75 - 1.45 (m, 9 H) ppm.

^{13}C NMR (101MHz; C_6D_6): δ = 138.6, 130.9, 125.4, 114.7, 71.1, 37.1, 36.5, 30.0, 28.9, 17.9 ppm.

Mass peak was unobtainable by either EI or ESI. Only fragmentation was observed.

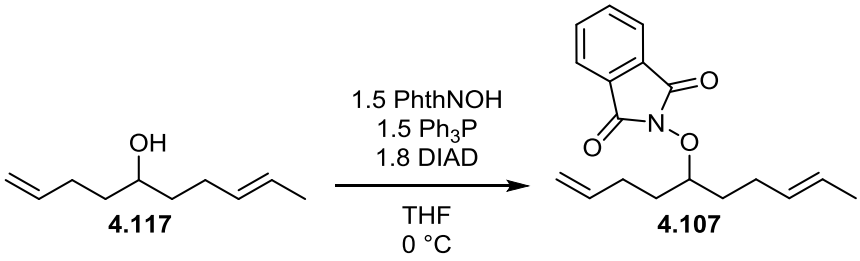

(*E*)-2-(deca-1,8-dien-5-yloxy)isoindoline-1,3-dione (**4.107**) [Route B]: To alcohol **4.117** (260 mg, 1.7 mmol, 1.0 equiv.) was added *N*-hydroxypthalimide (417 mg, 2.5 mmol, 1.5 equiv.), triphenylphosphine (666 mg, 2.5 mmol, 1.5 equiv.), and THF (17 ml). The solution was cooled to 0 °C in an ice/water bath

and diisopropyl azodicarboxylate (0.6 ml, 3.0 mmol, 1.8 equiv.) was added over 20 min producing an orange-red solution during addition. After 18 h of stirring, the light-yellow solution was poured into 50% saturated $NaHCO_{3(aq)}$ (100 ml, orange coloured aqueous layer) and extracted with Et_2O (3 x 30 ml). The yellow organic extracts were washed with 50% saturated $NaHCO_{3(aq)}$ (40 ml), brine (30 ml), dried over Na_2SO_4, filtrated and concentrated by rotary evaporation. Triphenylphosphineoxide was triterated with hexanes until no colour remained and the collected organics were concentrated by rotary evaporation. Purification by flash chromatography (3:1 hexanes: Et_2O, Rf = 0.37, visualization by UV or $KMnO_4$ stain) yielded 265 mg *N*-alkoxypthalimide **4.107** as a colourless oil (53%).

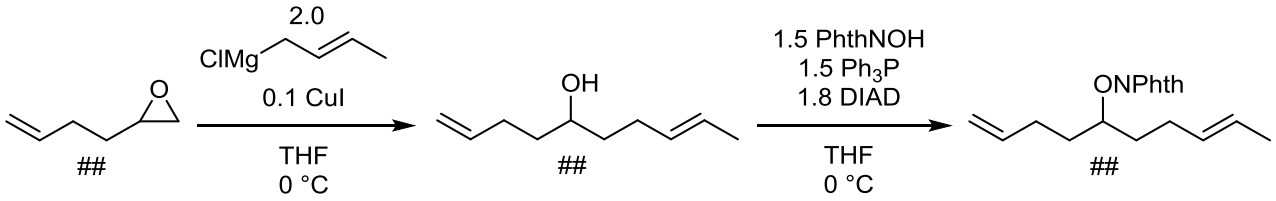

(*E*)-2-(deca-1,8-dien-5-yloxy)isoindoline-1,3-dione (**4.107**) [Route C]: To a two-neck flask equipped with reflux condenser containing magnesium churnings (480 mg, 20 mmol, 4.0 equiv.) and a small crystal of iodine was added crotyl chloride (975 µl, 10.0 mmol, 2.0 equiv.) in THF (10 ml + 1 ml rinse) at such a rate to maintain a gentle reflux. The resulting cloudy grey suspension was refluxed for 1 h to provide the Grignard solution. To a separate flask containing copper (I) iodide (137 mg, 0.5 mmol, 0.1 equiv.) and **4.118** (560 µl, 5.0 mmol, 1.0 equiv.) was added THF (5.0 ml) and cooled to 0°C in an ice/water bath. To the cloudy grey suspension was added the Grignard solution over 10 min (4 ml THF rinse). Colour in the reaction mixture changed from cloudy grey to bright yellow to blue-black and the cold bath was removed after 30 min. After 22 h, the blue-black solution was quenched with saturated $NH_4Cl_{(aq)}$ (10 ml), poured into Et_2O (100 ml) washed with water (25 ml), 1.0 M $HCl_{(aq)}$(2 x 25 ml),

brine (25 ml), dried over Na_2SO_4, filtrated and concentrated by rotary evaporation. Alcohol **4.117** was obtained as a colourless oil and used without further purification.

To crude alcohol **4.117** in THF (50 ml) was added *N*-hydroxypthalimide (1.22 g, 7.5 mmol, 1.5 equiv.) and triphenylphosphine (1.93 g, 7.5 mmol, 1.5 equiv.). The solution was cooled to 0 °C in an ice/water bath and diisopropyl azodicarboxylate (1.8 ml, 9.0 mmol, 1.8 equiv.) was added over 50 min producing an orange-red solution during addition. After 20 h of stirring, the light-yellow solution was quenched with 50% saturated $NaHCO_{3(aq)}$ (50 ml, orange coloured aqueous layer), poured into Et_2O (100 ml), washed with 50% saturated $NaHCO_{3(aq)}$ (2 x 50 ml), brine (50 ml), dried over Na_2SO_4, filtrated and concentrated by rotary evaporation. Triphenylphosphineoxide was triterated with hexanes until no colour remained and the collected organics were concentrated by rotary evaporation. Purification by flash chromatography (3:1 hexanes: Et_2O, Rf = 0.37, visualization by UV or $KMnO_4$ stain) yielded *N*-alkoxypthalimide **4.107** as a colourless oil (315 mg, 21% over 2 steps).

IR (neat): 2923, 2854, 1772, 1730, 1700, 1639, 1653, 1188, 976, 701 cm^{-1}.

^1H NMR (400MHz; $CDCl_3$): δ = 7.91 - 7.69 (m, 4 H), 5.92 - 5.78 (m, 1 H), 5.56 - 5.34 (m, 2 H), 5.08 (qd, *J* = 1.7, 17.2 Hz, 1 H), 4.98 (dd, *J* = 1.7, 10.3 Hz, 1 H), 4.26 (quin, *J* = 6.1 Hz, 1 H), 2.43 - 2.09 (m, 4 H), 1.89 - 1.66 (m, 4 H), 1.64 (d, *J* = 5.7 Hz, 3 H) ppm.
^{13}C NMR (101MHz; $CDCl_3$): δ = 164.3, 138.0, 134.4, 130.3, 129.5, 129.0, 125.6, 124.6, 123.4, 115.0, 87.2, 32.4, 31.7, 29.1, 28.0, 17.9 ppm.

HRMS-ESI (*m/z*): $[M+Na]^+$ calcd for $C_{18}H_{21}NO_3Na$: 322.1419. Found: 322.1409.

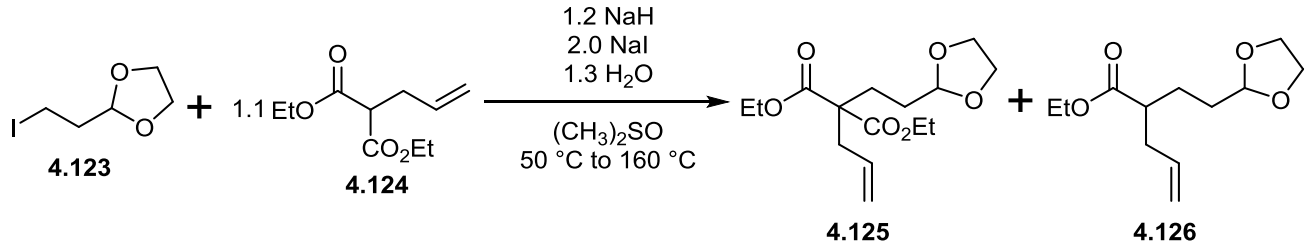

Diethyl 2-(2-(1,3-dioxolan-2-yl)ethyl)-2-allylmalonate (**4.125**): To a solution of crude **4.123**[i] (1.74g, 10 mmol, 1.0 equiv) in dimethylsulfoxide (20 ml) was added diethyl allylmalonate (2.2 ml, 11 mmol, 1.1 equiv), sodium iodide (3 g, 20 mmol, 2.0 equiv) then sodium hydride (480 mg, 12 mmol, 1.2 equiv) over 5 minutes. Vigorous gas release was observed. The suspension was heated to 50 °C for 5 h, then water (235 μl, 13 mmol, 1.3 equiv) was added and the reaction mixture was brought to reflux in a 160 °C oil bath for one day, then poured into $HCl_{(aq)}$ (150 ml) and extracted with Et2O (3 x 50 ml). The combined organic layers were washed with $HCl_{(aq)}$ (50 ml), brine (50 ml), dried over Na_2SO_4, and concentred by rotary evaporation. Purification by flash chromatography (2:1 hexane: Et_2O, visualization by KMnO4 stain) yielded ethyl ester **4.126** (223 mg, Rf = 0.31, 10% over 4 steps) and diethyl malonate **4.125** (1.5 g, Rf = 0.24, 57% over 3 steps).

^{1}H NMR (300 MHz, $CDCl_3$): δ = 5.78 - 5.52 (m, 1 H), 5.21 - 5.00 (m, 2 H), 4.86 (t, *J* = 4.6 Hz, 1 H), 4.18 (q, *J* = 7.1 Hz, 4 H), 4.07 - 3.68 (m, 4 H), 2.64 (d, *J* = 7.3 Hz, 2 H), 2.08 - 1.91 (m, 2 H), 1.68 - 1.51 (m, 2 H), 1.24 (t, *J* = 7.1 Hz, 6 H) ppm.

^{13}C NMR (75 MHz, $CDCl_3$): δ = 171.0, 132.3, 119.0, 104.0, 64.9, 61.2, 56.9, 37.0, 28.5, 26.4, 14.1 ppm.

[i] Prepared according to: Larson, G. L.; Klesse, R. *J. Org. Chem.* **1985**, *50*, 3627.

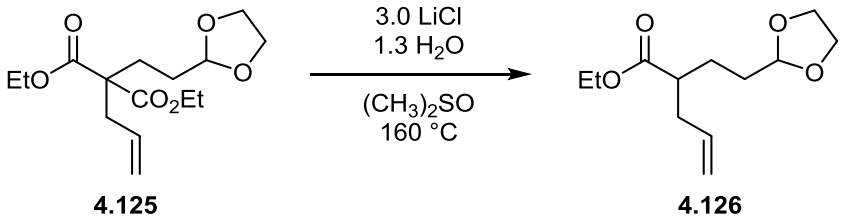

4.125 **4.126**

Ethyl 2-(2-(1,3-dioxolan-2-yl)ethyl)pent-4-enoate (**4.126**): To a solution of diethyl malonate **4.125** (1.5 g, 5 mmol, 1.0 equiv) in dimethylsulfoxide (10 ml) was added lithium chloride (636 mg, 15 mmol, 3.0 equiv) and water (120 µl, 6.5 mmol, 1.3 equiv). The resulting solution was heated to reflux in a 160 °C oil bath for 2 days, then poured into $HCl_{(aq)}$ (125 ml) and extracted with Et_2O (3 x 40 ml). The combined organic layers were washed with brine (40 ml), dried over Na_2SO_4, and concentred by rotary evaporation. Purification by flash chromatography (2:1 hexane: Et_2O, Rf = 0.31, visualization by KMnO4 stain) yielded ethyl ester **4.126** (1.2 g, >95%) as a slightly yellow oil.

^{1}H NMR (300 MHz, $CDCl_3$): δ = 5.82 - 5.64 (m, 1 H), 5.13 - 4.95 (m, 2 H), 4.85 (t, *J* = 4.6 Hz, 1 H), 4.14 (q, *J* = 7.1 Hz, 2 H), 4.01 - 3.77 (m, 4 H), 2.53 - 2.30 (m, 2 H), 2.30 - 2.17 (m, 1 H), 1.79 - 1.57 (m, 4 H), 1.25 (t, *J* = 7.1 Hz, 3 H) ppm.

^{13}C NMR (75 MHz, $CDCl_3$): δ = 175.2, 135.3, 116.8, 104.1, 64.9, 64.8, 60.2, 45.0, 36.5, 31.5, 25.9, 14.3 ppm.

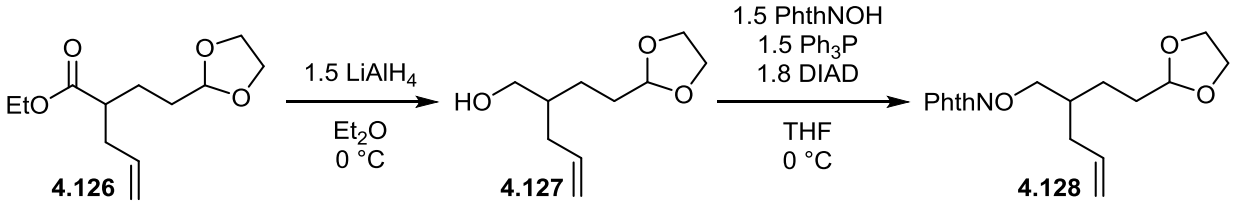

4.126 **4.127** **4.128**

2-((2-(2-(1,3-Dioxolan-2-yl)ethyl)pent-4-en-1-yl)oxy)isoindoline-1,3-dione (**4.128**): To a solution of **4.126** (453 mg, 2.0 mmol, 1.0 equiv) in Et_2O (10 ml) cooled to 0 °C in an ice/water bath was added lithium aluminum hydride (124 mg, 3.0 mmol, 1.5 equiv) over 1 min. Vigorous gas release was observed. After 5 min, the grey suspension was removed from the bath and allowed to warm to ambient

temperature. After 1 h, the mixture was slowly quenched with saturated $NH_4Cl_{(aq)}$ (5 ml), poured into 1.0 M $HCl_{(aq)}$ (75 ml) and extracted with Et_2O (3 x 20 ml). The combined organic extracts were washed with brine (25 ml), dried over Na_2SO_4, filtered, concentrated by rotary evaporation to provide **4.127** as a colourless oil which was carried forward immediately.

To a solution of alcohol **4.127** in THF (20 ml) was added *N*-hydroxypthalimide (498 mg, 3.0 mmol, 1.5 equiv.) and triphenylphosphine (787 mg, 3.0 mmol, 1.5 equiv.). The solution was cooled to 0 °C in an ice/water bath and diisopropyl azodicarboxylate (710 μL, 3.6 mmol, 1.8 equiv) was added dropwise over 30 min. The colourless solution turned to an orange-red solution during addition. After 16 h, the ambient temperature light-yellow solution was poured into 50% saturated $NaHCO_3$ (80 ml) and extracted with Et_2O (3 x 30 ml). The combined aqueous extracts were washed with brine (25 ml), dried over Na_2SO_4, filtrated, concentrated by rotary evaporation. Purification by flash chromatography (1:1 hexanes: Et_2O, Rf = 0.22, visualization by UV or $KMnO_4$ stain) yield *N*-alkoxypthalimide **4.128** (351 mg, 53% over 2 steps) as a colourless oil.

^{1}H NMR (400 MHz, $CDCl_3$): δ = 7.87 - 7.80 (m, 2 H), 7.78 - 7.71 (m, 2 H), 5.85 (tdd, *J* = 7.3, 10.1, 17.1 Hz, 1 H), 5.14 (qd, *J* = 1.6, 17.1 Hz, 1 H), 5.08 (tdd, *J* = 0.9, 2.1, 10.1 Hz, 1 H), 4.90 (t, *J* = 4.7 Hz, 1 H), 4.16 - 4.08 (m, 2 H), 4.01 - 3.94 (m, 2 H), 3.88 - 3.82 (m, 2 H), 2.40 - 2.21 (m, 2 H), 1.98 (td, *J* = 6.3, 12.7 Hz, 1 H), 1.87 - 1.72 (m, 2 H), 1.71 - 1.50 (m, 2 H) ppm.

^{13}C NMR (101MHz, $CDCl_3$): δ = 174.0, 163.5, 142.7, 135.6, 134.4, 129.0, 123.4, 117.2, 104.6, 80.4, 64.8, 37.0, 35.1, 31.0, 24.8 ppm.

HRMS-ESI (*m/z*): $[M+Na]^+$ calcd for $C_{18}H_{21}NO_5Na$: 354.1317 Found: 354.1309.

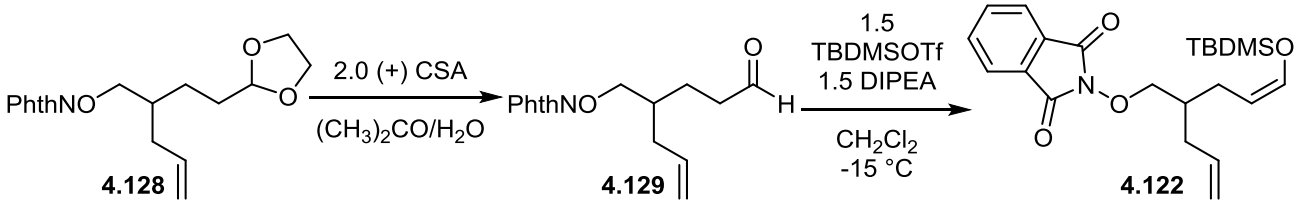

(*Z*)-2-((2-Allyl-5-((*tert*-butyldimethylsilyl)oxy)pent-4-en-1-yl)oxy)isoindoline-1,3-dione (**4.122**): To a solution of **4.128** (339 mg, 1.0 mmol, 1.0 equiv) in aqueous acetone (10 ml, 4:1 acetone: water) was added (+) camphorsulfonic acid (460 mg, 2.0 mmol, 2.0 equiv). The resulting solution was stirred at ambient temperature for 16 h, then quenched with 50% saturated $NaHCO_{3(aq)}$ (100 ml), and extracted with Et_2O (3 x 25 ml). The combined organics were washed with brine (25 ml), dried over Na_2SO_4, filtered, and concentrated by rotary evaporation to provide **4.129** as a colourless oil. To a solution of **4.129** and diisopropylethylamine (260 µl, 1.5 mmol, 1.5 equiv) in dichloromethane (10 ml) cooled to -15 °C in an ethylene glycol/ dry ice bath was added *tert*-butyldimethylsilyl triflate (340 µl, 1.5 mmol, 1.5 equiv) over 10 minutes. After 2 h, the cold bath was removed and the reaction was stirred a further 2 h at ambient temperature. The reaction was quenched with saturated $NaHCO_{3(aq)}$ (1 ml), poured into Et2O (100 ml), washed with 50% saturated $NaHCO_{3(aq)}$ (25 ml), 1.0 M $HCl_{(aq)}$ (2 x 25 ml), brine (25 ml), dried over Na2SO4, filtered, and concentrated by rotary evaporation. Purification by flash chromatography (3:1 hexanes: Et_2O, Rf = 0.36, visualization by UV or $KMnO_4$ stain) yielded **4.122** as a colourless oil (339 mg, E: Z = 1: 7, 39% over 2 steps).

IR (neat): 3080, 2932, 2859, 1736, 1554, 1473, 1444, 1256, 1163, 1006, 839, 783 cm^{-1}

^1H NMR (400 MHz, C_6D_6): δ = 7.31 - 7.25 (m, 2 H), 6.82 - 6.74 (m, 2 H), 6.52 (d, *J* = 11.9 Hz, 0.11 H), 6.22 (d, *J* = 6.1 Hz, 0.86 H), 6.01 - 5.87 (m, 0.82 H), 5.84 - 5.71 (m, 0.12 H), 5.32 - 5.00 (m, 2.28 H), 4.63 (dt, *J* = 5.8, 7.5 Hz, 0.88 H), 4.24 - 4.10 (m, 1.81 H), 4.10 - 3.99 (m, 0.37 H), 2.56 - 2.01 (m, 5.2 H), 1.87 - 1.75 (m, 0.12 H), 0.98 (s, 1.24 H), 0.92 (s, 7.9 H), 0.03 (s, 0.73 H), 0.02 (s, 5.2 H) ppm.

^{13}C NMR (101MHz, C_6D_6): (Z isomer only) δ = 163.6, 140.6, 137.0, 134.0, 129.9, 123.3, 117.4, 108.0, 81.2, 38.7, 35.9, 26.1, 25.4, 18.7, -5.0 ppm.

HRMS-ESI (*m/z*): $[M+Na]^+$ calcd for $C_{22}H_{31}NO_4SiNa$: 424.1920 Found: 424.1925.

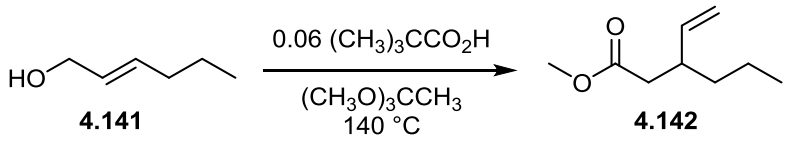

4.141 **4.142**

Methyl 3-vinylhexanoate (**4.142**): To a 2-5 ml microwave vial equipped with stir bar was added a solution of *trans*-hex-2-enol (300 mg, 3.0 mmol, 1 equiv.) and pivalic acid (20 mg, 0.2 mmol, 0.06 equiv.) in trimethoxyorthoacetate (3.8 mL, 20 mmol, 10 equiv.). The vial was capped and heated to 140 °C for 14 h in a microwave reactor. The resulting colourless solution was transferred to a 25 ml round bottom flask and quenched with 1.0 M $HCl_{(aq)}$ (4 ml) while immersed in an ambient temperature water bath to maintain 20 °C. After 1 h, the resulting emulsion was poured into 1.0 M $HCl_{(aq)}$ (80 ml) and extracted with Et_2O (3 x 25 ml). The combined colourless organic extracts were washed with saturated $NaHCO_{3(aq)}$ (25 ml), brine (25 ml), dried over Na_2SO_4, filtrated and concentrated by rotary evaporation to provide a yellow oil. Purification by flash chromatography (10:1 hexanes: Et_2O, Rf = 0.42, visualization by $KMnO_4$ stain) yielded ester **4.142** as a colourless oil (333 mg, 71%). The compound obtained matched literature characterization data.[270]

^{1}H NMR (400 MHz, $CDCl_3$): δ = 5.74-5.53 (m, 1H), 5.12-4.88 (m, 2H), 3.66 (s, 3H), 2.62-2.22 (m, 2H), 1.42-1.20 (m, 4H), 0.94-0.84 (m, 3H).

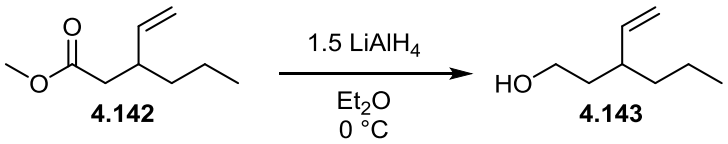

3-Vinyl hexanol (**4.143**): To a solution of ester **4.142** (174 mg, 1.1 mmol, 1 equiv.) in Et_2O (11 ml, 0.1 M) cooled to 0 °C in ice/water bath was added lithium aluminum hydride (64 mg, 1.7 mmol, 1.5 equiv.) in small portions over 30 seconds. The grey suspension was stirred for 30 minutes, then quenched with the slow addition of Na_2SO_4 decahydrate (1g) over 3 minutes (violent bubbling observed during quenching). The suspension was filtered through a plug of $MgSO_4$ and the solids were washed with Et_2O (5 x 40 ml). The combined organic extracts were concentrated by rotary evaporation to yield alcohol **4.143** as a colourless oil (100 mg, 70%).

IR (neat): 3331, 3076, 2958, 2930, 1640, 1466, 1458, 1419, 1379, 1046, 995, 912 cm^{-1}

^1H NMR (400 MHz, C_6D_6): δ = 5.49-5.32 (m, 1H), 4.94 (s, 1H), 4.93 - 4.88 (m, 1H), 3.47-3.33 (m, 2H), 2.12-1.96 (m, 1H), 1.51-1.40 (m, 1H), 1.36-1.07 (m, 5H), 0.86 (t, *J* = 7.0 Hz, 3H), 0.64 (bs, 1H) ppm.

^{13}C NMR (101 MHz, C_6D_6): δ = 143.6, 115.0, 61.2, 41.3, 38.6, 38.0, 20.9, 14.6 ppm.

HRMS-ESI (*m/z*) $[M+H]^+$ calcd for $C_8H_{17}O$: 129.1279. Found: 129.1277.

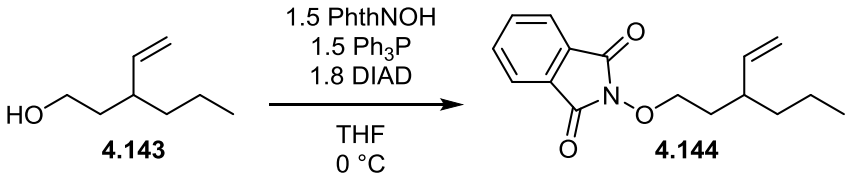

2-(3-Vinylhexyloxy)isoindoline-1,3-dione (**4.144**): To a solution of alcohol **4.143** (98mg, 0.77 mmol, 1.0 equiv.) in THF (7.7 ml, 0.1 M) was added *N*-hydroxypthalimide (189 mg, 1.16 mmol, 1.5 equiv.) and triphenylphosphine (301 mg, 1.16 mmol, 1.5 equiv.). The solution was cooled to 0 °C in an ice/water bath and diisopropyl azodicarboxylate (280 µl, 1.4 mmol, 1.8 equiv.) was added dropwise

over 10 min. The colourless solution turned to an orange-red solution during addition. The reaction was stirred for 18 h and allowed to warm to ambient temperature. The light-yellow solution was poured into Et_2O (75 ml), washed with 50% saturated $NaHCO_3$ (2 x 25 ml, orange coloured aqueous layer), and brine (25 ml). The yellow organic extract was dried over Na_2SO_4, filtrated, concentrated by rotary evaporation, purified by flash chromatography (7:2 hexanes: Et_2O, Rf = 0.30, visualization by UV or $KMnO_4$ stain) followed by recrystallization from cold pentanes (–10 °C) to yield two crops of *N*-alkoxypthalimide **4.144** as fluffy white needles (156 mg combined, 74%).

mp: 44-45.5 °C

IR ($CHCl_3$): 3683, 3621, 1790, 1732, 1468, 1188, 878, 703 cm^{-1}

^1H NMR (400 MHz, C_6D_6): δ = 7.30 (dd, *J* = 5.4, 3.0 Hz, 2H), 6.80 (dd, *J* = 5.4, 3.0 Hz, 2H), 5.41-5.26 (m, 1H), 5.10 (dd, *J* = 17.1, 1.8 Hz, 1H), 4.99 (dd, *J* = 10.3, 1.8 Hz, 1H), 4.29-3.90 (m, 2H), 2.41-2.13 (m, 1 H), 1.88-1.74 (m, 1H), 1.55-1.40 (m, 1H), 1.38-1.06 (m, 4H), 0.85 (t, *J* = 7.0 Hz, 1H) ppm.

^{13}C NMR (100 MHz, C_6D_6): δ = 163.7, 142.5, 134.1, 129.8, 123.4, 116.0, 77.1, 40.9, 37.8, 33.9, 20.9, 14.6 ppm

HRMS-ESI (*m/z*) $[M+Na]^+$ calcd for $C_{16}H_{19}NO_3Na$: 296.1263. Found: 296.1265.

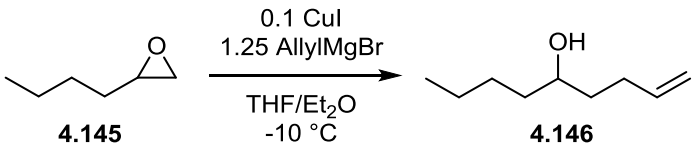

4.145 **4.146**

Non-1-en-5-ol (**4.146**): To a suspension of copper (I) iodide (150 mg, 0.8 mmol, 0.1 equiv.) in THF (10 ml), cooled to –10 °C in an ice/brine bath, was added allylmagnesium bromide (10 ml, 1.0 M in Et_2O, 10.0 mmol, 1.25 equiv.) over 5 min resulting in a blue-black solution. 1-Hexene oxide (965 µl, 8.0 mmol, 1.0 equiv.) was added over 4 minutes and the cooling bath was removed. After 2 h, the blue-black suspension was quenched with saturated $NH_4Cl_{(aq)}$ (5 ml), poured into Et_2O (150 ml), washed

with 50% saturated $NH_4Cl_{(aq)}$ (3 x 40 ml), brine (30 ml), dried over Na_2SO_4, filtered and concentrated by rotary evaporation. Purification by filtration through a plug of silica (wash with 3 x 50 ml, 2:1 hexanes: Et_2O) yielded alcohol **4.146** (1.3 g, 95%) as a colourless oil contaminated with ~10% oxirane starting material.

IR (neat): 3356, 2957, 2930, 2860, 1641, 1455, 1417, 1379, 1125, 1038, 995, 910 cm^{-1}.

^{1}H NMR (400MHz; $CDCl_3$): δ = 5.85 (tdd, *J* = 6.7, 10.3, 17.0 Hz, 1 H), 5.06 (qd, *J* = 1.7, 17.1 Hz, 1 H), 4.98 (qd, *J* = 1.7, 10.2 Hz, 1 H), 3.62 (br. s., 1 H), 2.30 - 2.07 (m, 2 H), 1.66 - 1.26 (m, 8 H), 0.99 - 0.85 (m, 3 H) ppm.

^{13}C NMR (101MHz; C_6D_6): δ = 138.7, 114.7, 71.5, 37.2, 36.5, 30.1, 27.8, 22.7, 14.0 ppm.

Mass peak was unobtainable by either EI or ESI. Only fragmentation was observed.

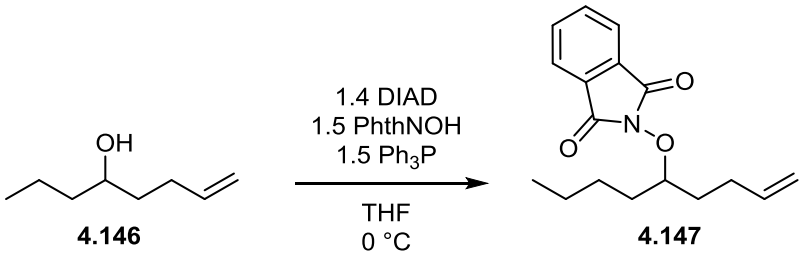

4.146 **4.147**

2-(non-1-en-5-yloxy)isoindoline-1,3-dione (**4.147**): To a solution of alcohol **4.146** (711 mg, 5.0 mmol, 1.0 equiv.) in THF (33 ml, 0.15 M) was added *N*-hydroxypthalimide (1.26 g, 7.5 mmol, 1.5 equiv.) and triphenylphosphine (1.99 g, 7.5 mmol, 1.5 equiv.). The solution was cooled to 0 °C in an ice/water bath and diisopropyl azodicarboxylate (1.4 ml, 7.0 mmol, 1.4 equiv.) was added over 10 min. The colourless solution turned to an orange-red solution during addition. After 5.5 h, the light-yellow solution was poured into 50% saturated $NaHCO_3$ (100 ml, orange coloured aqueous layer) and extracted with Et_2O (3 x 50 ml). The combined organic extracts were washed with 50% saturated $NaHCO_3$ (2 x 40 ml),

brine (30 ml), dried over Na_2SO_4, filtrated, and concentrated by rotary evaporation. Purification by flash chromatography (2:1 hexanes: Et_2O, Rf = 0.43, visualization by UV or $KMnO_4$ stain) yielded *N*-alkoxypthalimide **4.147** as a colourless oil (894 mg, 62%).

IR (neat): 3077, 2955, 2871, 1789, 1738, 1727, 1684, 1653, 1641, 1467, 1457, 1448, 1437, 1418, 1372, 1188, 1121, 1082, 1015, 977, 912, 878, 785, 702 cm^{-1}.

^1H NMR (400MHz; $CDCl_3$): δ = 7.88 - 7.70 (m, 4 H), 5.92 - 5.78 (m, 1 H), 5.07 (d, *J* = 17.4 Hz, 1 H), 4.97 (d, *J* = 10.2 Hz, 1 H), 4.25 (quin, *J* = 5.8 Hz, 1 H), 2.42 - 2.18 (m, 2 H), 1.88 - 1.60 (m, 4 H), 1.58 - 1.27 (m, 4 H), 0.91 (t, *J* = 7.2 Hz, 3 H) ppm.

^{13}C NMR (101MHz; $CDCl_3$): δ = 164.3, 138.0, 134.3, 129.0, 123.4, 114.9, 87.6, 32.1, 31.6, 29.1, 27.0, 22.7, 14.0 ppm.

HRMS-ESI (m/z): [M+Na]+ calcd for $C_{17}H_{21}NO_3Na$: 310.1419. Found: 310.1415.

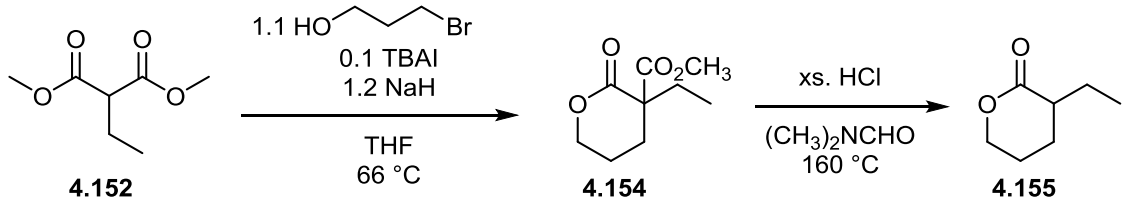

4.152 **4.154** **4.155**

3-Ethyltetrahydro-2H-pyran-2-one (**4.155**): To a suspension of sodium hydride (243 mg, 60 wt% in mineral oil, 6.0 mmol, 1.2 equiv.) in THF (10 ml) cooled to 0 °C in an ice/water bath was added dimethyl ethylmalonate (750 µl , 5.0 mmol, 1.0 equiv.) over 1 minute (gas evolution was observed). After 5 min, 3-bromopropanol (500 µl, 5.5 mmol, 1.1 equiv.) was added in one portion followed by tetrabutylammonium iodide (180 mg, 0.5 mmol, 0.1 equiv.) in one portion and the reaction was brought to reflux. After 19 h, the yellow suspension with white precipitate was cooled to ambient temperature, quenched with 50% $NH_4Cl_{(aq)}$ (2 ml), poured into water (80 ml) and extracted with Et_2O (3 x 30 ml). The combined yellow organic extracts were washed with brine (30 ml), concentrated by rotary evaporation and taken up in DMF (9 ml). To the solution of crude **4.154** in DMF was added

concentrated $HCl_{(aq)}$ (1 ml) and the reaction mixture was refluxed for 2 days. The light-yellow solution was poured into water (150 ml) and extracted with Et_2O (3 x 30 ml). The combined organic extracts were washed with 1.0M $HCl_{(aq)}$ (30 ml), brine (30 ml), dried over Na_2SO_4, filtrated and concentrated by rotary evaporation. Purification by flash chromatography (1:2 hexanes: Et_2O, Rf = 0.37, visualization by $KMnO_4$ stain) provided lactone **4.155** as a colourless oil (184 mg, 29% over 2 steps). The compound obtained matched literature characterization data.[271]

^{1}H NMR (400 MHz, $CDCl_3$): δ = 4.37-4.24 (m, 2 H), 2.47-2.33 (m, 1 H), 2.10 (dq, *J* = 6.7, 13.4 Hz, 1 H), 1.99-1.80 (m, 3 H), 1.62-1.49 (m, 2 H), 0.99 (t, *J* = 7.4 Hz, 3 H) ppm.

^{13}C NMR (100 MHz, $CDCl_3$) δ =174.5, 68.3, 41.0, 24.2, 24.1, 22.0, 11.3 ppm.

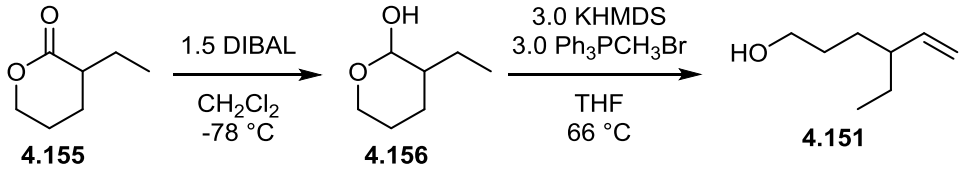

4.155 **4.156** **4.151**

4-Vinyl hexanol (**4.151**): To a solution of **4.155** (169 g, 1.3 mmol, 1 equiv.) in CH_2Cl_2 (6.5 ml) cooled to -78 °C using a dry ice/acetone bath was added diisobutylaluminum hydride (1.0 M in hexanes, 2 ml, 2.0 mmol, 1.5 equiv.) over 2 minutes. After 30 min, the reaction mixture was quenched with aqueous methanol (50% v/v methanol in water, 2 ml). After an additional 30 minutes, the mixture was poured into 1.0M $HCl_{(aq)}$ (80 ml) and extracted with Et_2O (3 x 25 ml). The combined colourless organic extracts were washed with brine (20 ml), dried over Na_2SO_4, filtrated and concentrated by rotary evaporation to provide crude lactol **4.156** as a colourless oil. To a flask containing potassium hexamethyldisilazide (789 mg, 3.9 mmol, 3.0 equiv.) and methyltriphenylphosphonium bromide (1.4 g, 3.9 mmol, 3.0 equiv.) kept at ambient temperature with an oil bath was added THF (10 ml) over 30 seconds. To the bright yellow suspension was added crude lactol **4.156** (solution in 2 ml THF, 1 ml

rinse) over 3 minutes. The suspension was refluxed for 20 h and became an orange suspension with light-brown solids. The reaction mixture was poured into 0.5M $HCl_{(aq)}$ (100 ml) and extracted with Et_2O (3 x 30 ml). The combined colourless organic extracts were washed with brine (30 ml), dried over Na_2SO_4, filtrated and concentrated by rotary evaporation. Purification by flash chromatography (1:1 hexanes: Et_2O, Rf = 0.32, visualization by $KMnO_4$ stain) yielded alcohol **4.151** as a colourless oil (55 mg, 33% over 2 steps). The compound obtained matched literature characterization data.[272]

^{1}H NMR (400 MHz, C_6D_6): δ = 5.42 (ddd, *J* = 8.8, 10.4, 17.1 Hz, 1 H), 4.99 (dd, *J* = 2.1, 10.4 Hz, 1 H), 4.93 (ddd, *J* = 0.6, 2.1, 17.1 Hz, 1 H), 3.33 (t, *J* = 6.4 Hz, 2H), 1.81-1.66 (m, 1 H), 1.52-1.25 (m, 4 H), 0.85 (t, *J* = 7.4 Hz, 3 H), 0.68 (bs, 1 H) ppm.

^{13}C NMR (100 MHz, C_6D_6) δ = 143.5, 115.0, 63.2, 46.4, 31.4, 31.2, 28.4, 12.2 ppm.

General procedure for reaction of competition kinetic experiments: A solution of tributyltin hydride (35 ml, 1.3 mmol, 1.3 equiv.) and AIBN (1.6 mg, 0.01 mmol, 0.1 equiv.) in deuterobenzene (2 ml) was added at a rate of 1.00 ml/h to a refluxing solution of *N*-alkoxypthalimide (1.0 mmol, 1.0 equiv.) in deuterobenzene (5ml, 0.05 M). The reaction was performed under ambient pressure with reaction temperature monitored to be 78 ± 1 °C using an internal probe. Reaction mixture was refluxed a minimum of 4 h before cooling to ambient temperature. An aliquot was taken directly from the reaction vessel for NMR analysis with a Bruker AV400 inverse spectrometer (20 scans, 4 sec pulse sequence).

4.5.3 Experimentals pertaining to alkoxyl 1 5-HAT radical relay cyclization

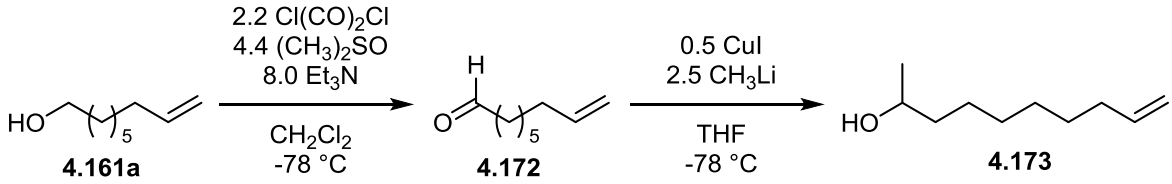

Dec-9-ene-2-ol (**4.173**): To a solution of oxalyl chloride (960 µl, 11 mmol, 2.2 equiv.) in dry CH_2Cl_2 (50 mL) cooled to -78 °C in an acetone/dry ice bath was added dimethylsulfoxide (1.6 ml, 22 mmol, 4.4 equiv.) over 1 min. After 30 min, 8-nonene-1-ol (840 µl, 5.0 mmol, 1.0 equiv.) was added over 30 seconds. After 90 min, triethylamine (5.6 mL, 40 mmol, 8.8 equiv.) was added over 1 min. After 16 h, the ambient temperature yellow slurry was poured into water (100 ml) and extracted with CH_2Cl_2 (3 x 40 ml). The combined organic extracts were washed with brine (30 ml), dried over Na_2SO_4 and concentrated by rotary evaporation to yield aldehyde **4.172** as a yellow oil which was used without further purification. To a suspension of crude **4.172** and copper (I) iodide (475 mg, 2.5 mmol, 0.5 equiv.) in THF (10 mL) cooled to -78 °C in an acetone/dry ice bath was added methyllithium (7.6 ml, 1.6 M in hexane, 12.5 mmol, 2.5 equiv.) over 5 min. After 16 h, the green reaction mixture was quenched with 2% $HCl_{(aq)}$ (5 ml) and poured into Et_2O (100 ml). The organic layer was washed with 2% aqueous $HCl_{(aq)}$ (3 x 40 mL), brine (30 mL), dried over Na_2SO_4, and concentrated by rotary evaporation. Purification by flash chromatography (1:1 pet. ether: Et_2O, Rf = 0.48, visualization by $KMnO_4$ stain) provided alcohol **4.173** as a colorless oil (540 mg, 69% over 2 steps). The compound obtained matched literature characterization data.[273]

^{1}H NMR (400MHz; $CDCl_3$): δ = 5.75-5.88 (m, 1 H), 5.00 (dd, *J* = 17.0, 1.4 Hz, 1 H), 4.93 (d, *J* = 10.2 Hz, 1 H), 3.74-3.84 (m, 1 H), 1.97-2.11 (q, *J* = 7.2 Hz, 2 H), 1.27-1.52 (m, 11 H), 1.19 (d, *J* = 6.3 Hz, 3 H) ppm.

^{13}C NMR (101MHz; $CDCl_3$): δ = 140.1, 115.2, 69.2, 40.4, 34.8, 30.5, 30.1, 29.9, 26.7, 24.5 ppm.

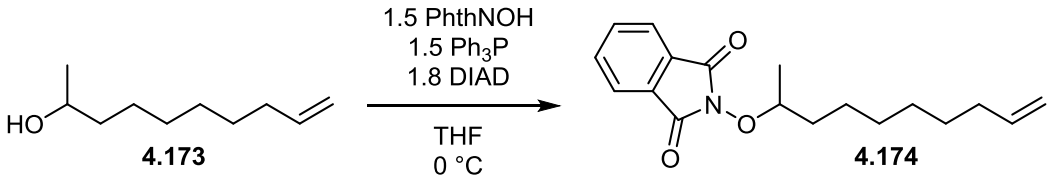

2-(Dec-9-en-2-yloxy)isoindoline-1,3-dione (**4.174**): To a solution of alcohol **4.173** (211 mg, 1.35 mmol, 1.0 equiv.) in THF cooled to 0 °C in an ice/water bath was added triphenylphosphine (534 mg, 2.0 mmol, 1.5 equiv.) and *N*-hydroxypthalimide (332 mg, 2.0 mmol, 1.5 equiv.). Diisopropyl azodicarboxylate (480 µl, 2.4 mmol, 1.8 equiv.) was added by syringe to maintain a pale yellow to colorless solution for the first 300 µl and the remaining 180 µl was added in one portion. The reaction was then stirred for an additional 2 h, whereupon the reaction became a suspension of white precipitate in a yellow solution. After 16h, the reaction was poured into Et_2O (100 ml), washed with saturated $NaHCO_{3(aq)}$ (3 x 40 mL), brine (30 mL), dried over Na_2SO_4 and concentrated by rotary evaporation. Purification by flash chromatography (3:1 pet. ether: Et_2O, Rf = 0.50, visualization by UV or $KMnO_4$ stain) yielded phthalimide **4.174** as a yellow oil that partially solidified upon standing (371 mg, 80%).

IR (neat): 2976, 2928, 2855, 1790, 1734, 1467, 1375, 1188, 1122, 1082 cm^{-1}.

^1H NMR (400MHz; $CDCl_3$): δ = 7.70-7.88 (m, 4 H), 5.70-5.92 (m, 1 H), 4.99 (dd, *J* = 17.2, 2.0 Hz, 1 H), 4.93 (d, *J* = 10.2 Hz, 1 H), 4.38 (sextet, *J* = 6.3 Hz, 1 H), 2.00-2.10 (m, 2 H), 1.74-1.88 (m, 1 H), 1.55-1.67 (m, 1 H), 1.29-1.54 ppm (m, 11 H) ppm.

^{13}C NMR (101MHz; $CDCl_3$): δ = 139.1, 134.4, 129.0, 123.4, 114.2, 100.0, 84.5, 34.9, 33.8, 29.4, 29.0, 28.8, 25.2, 18.8 ppm.

HRMS-ESI (m/z): [M+Na]+ calcd for $C_{18}H_{23}NO_3Na$: 324.1576. Found: 324.1572.

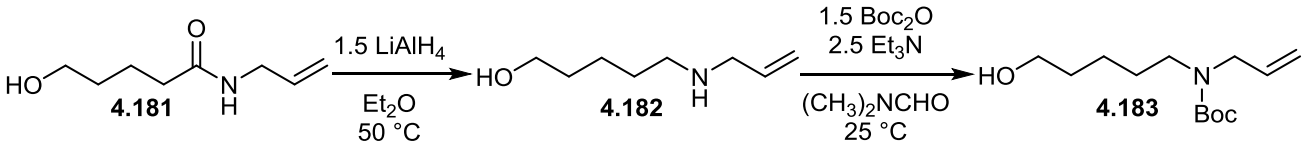

tert-Butyl allyl(5-hydroxypentyl)carbamate (**4.183**): To an emulsion of **4.181** (5.5 g, 35 mmol, 1.0 equiv.) in Et_2O (90 ml) cooled to 0 °C in an ice/water bath, was added lithium aluminum hydride (53 ml, 1.0 M in Et_2O, 53 mmol, 1.5 equiv.) over 30 min. Violent gas release was observed. The cold bath was removed and the reaction mixture was brought to reflux. After 24 h, the reaction was cooled to ambient temperature and quenched with 1.0 M $NaOH_{(aq)}$ (5 ml) slowly with violent gas release observed. The reaction mixture was brought to reflux and after 1 h, Na_2SO_4 (20 g) was added. After 10 min at reflux, the reaction was cooled to ambient temperature, filtered, and concentrated to provide crude amino alcohol **4.182** (4.5 g) as a thick oil which was carried forward immediately.

To a solution of **4.182** in DMF (20 ml) cooled to 0 °C in an ice/water bath, was added *tert*butylcarbonic anhydride (3.34 g, 15.3 mmol, 1.5 equiv.) in one portion and triethylamine (3.6 ml, 25.5 mmol, 2.5 equiv.) over 30 sec. The resulting solution was stirred at ambient temperature for 20 h. The solution was poured into Et_2O (80 ml), washed with 2% $HCl_{(aq)}$ (3 x 30 ml), brine (30 ml), dried over Na_2SO_4, filtered and concentrated by rotary evaporation. Purification by flash chromatography (1:4 pet. ether: Et_2O, Rf = 0.42, visualization by ninhydrin or $KMnO_4$ stain) yielded **4.183** as a colorless oil (764 mg, 31% over 2 steps).

^{1}H NMR (300MHz; $CDCl_3$): δ = 5.96 - 5.62 (m, 1 H), 5.09 (d, *J* = 11.6 Hz, 1 H), 3.78 (br. s., 2 H), 3.62 (t, *J* = 6.5 Hz, 2 H), 3.16 (br. s., 2 H), 1.90 (br. s., 1 H), 1.67 - 1.26 (m, 15 H) ppm.

^{13}C NMR (75MHz; $CDCl_3$): δ = 155.6, 134.3, 79.4, 79.0, 62.6, 46.4, 32.3, 28.4, 28.4, 11.2 ppm.

HRMS-ESI (m/z): [M+Na]+ calcd for $C_{13}H_{25}NO_3Na$: 266.1732. Found: 266.1725.

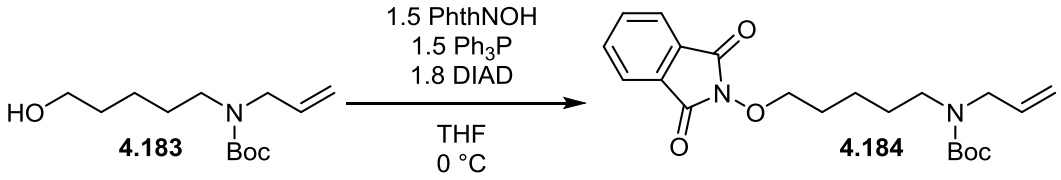

tert-Butyl allyl(5-((1,3-dioxoisoindolin-2-yl)oxy)pentyl)carbamate (**4.184**): To a solution of alcohol **4.183** (730 mg, 3.0 mmol, 1.0 equiv.) in THF (30 ml) cooled to 0 °C in an ice/water bath was added triphenylphosphine (1.18 g, 4.5 mmol, 1.5 equiv.) and *N*-hydroxypthalimide (734 mg, 4.5 mmol, 1.5 equiv). Diisopropyl azodicarboxylate (1 ml, 5.4 mmol, 1.8 equiv) was added *via* syringe pump at a rate of 0.2 ml/h. After 20 h, the reaction was poured into Et_2O (80 ml), washed with saturated $NaHCO_{3(aq)}$ (3 x 40 ml), brine (30 ml), dried over Na_2SO_4 and concentrated by rotary evaporation. Purification by gradient flash chromatography (4:1 to 3: 2 pet. ether: Et_2O, Rf = 0.50 at 3:2 pet. ether: Et_2O, visualization by UV or $KMnO_4$ stain) yielded **4.184** as a colourless oil (956 mg, 83%).

^{1}H NMR (400MHz; $CDCl_3$): δ = 7.89 - 7.67 (m, 4 H), 5.77 (dddd, *J* = 16.7, 10.8, 5.9, 5.5 Hz, 1 H), 5.18 - 5.01 (m, 2 H), 4.19 (t, *J* = 6.8 Hz, 2 H), 3.82 (br. s., 2 H), 3.18 (br. s., 2 H), 1.88 – 1.74 (m, 2 H), 1.67-1.36 (m, 13 H) ppm.

^{13}C NMR (101MHz; $CDCl_3$): δ = 163.6, 155.5, 134.4, 128.9, 123.4, 79.3, 78.3, 77.2, 46.3, 28.4, 27.8, 22.9 ppm.

HRMS-ESI (m/z): [M+Na]+ calcd for $C_{21}H_{28}N2O_5Na$: 411.1896. Found: 411.1890.

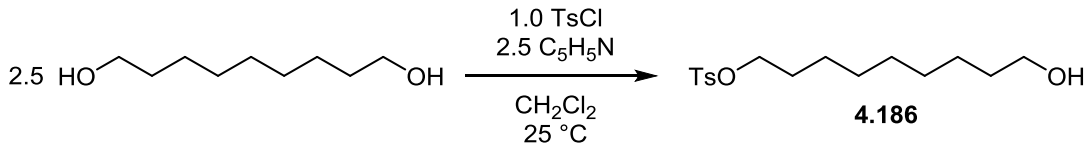

9-Hydroxynonyl 4-methylbenzenesulfonate (**4.186**): To a solution of 1,9-nonanediol (1.60 g, 10.0 mmol, 2.5 equiv) and *para*-toluenesulfonyl chloride (766 mg, 4 mmol, 1.0 equiv.) in CH_2Cl_2 (20 ml) was added pyridine (810 µl, 10 mmol, 2.5 equiv.) in one portion. After 16h, the reaction mixture

was concentrated by rotary evaporation and the crude oil was dissolved in Et_2O (100 mL), washed with 2% $HCl_{(aq)}$ (3 x 40 ml), brine (30 ml), dried over Na_2SO_4, and concentrated by rotary evaporation. Purification by flash chromatography (1:3 pet. ether: Et_2O, Rf = 0.38, visualization by UV or $KMnO_4$ stain) yielded tosyl alcohol **4.186** as a colorless oil (898 mg, 71%).

IR (neat): 3385, 2929, 2856, 1598, 1465, 1358, 1189, 1176, 1122, 1097, 1035, 1010 cm^{-1}.

^1H NMR (400MHz; $CDCl_3$): δ = 7.72-7.85 (m, 2 H), 7.36 (d, *J* = 8.2 Hz, 2 H), 4.02 (t, *J* = 6.5 Hz, 2 H), 3.63 (t, *J* = 6.7 Hz, 2 H), 2.45 (s, 3 H), 1.59-1.68 (m, 2 H), 1.51-1.59 (m, 2 H), 1.42 (br. s., 1 H), 1.20-1.38 (m, 10 H) ppm.

^{13}C NMR (101MHz; $CDCl_3$): δ = 144.6, 133.2, 129.8, 127.8, 70.6, 63.0, 32.7, 29.3, 29.2, 28.8, 25.6, 25.3, 21.6 ppm.

HRMS-ESI (m/z): [M+Na]+ calcd for $C_{16}H_{26}O_4NaS$: 337.1450. Found: 337.1450.

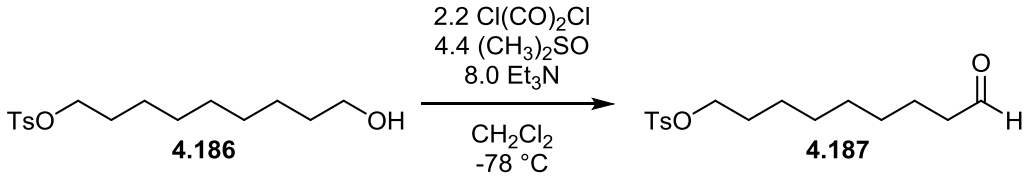

9-Oxononyl 4-methylbenzenesulfonate (**4.187**): To a solution of oxalyl chloride (540 µl, 6.2 mmol, 2.2 equiv.) in dry CH_2Cl_2 (25 mL) cooled to -78 °C in an acetone/dry ice bath was added DMSO (880 µl, 12.4 mmol, 4.4 equiv.) dropwise over 1 min. After 30 min, a solution of monotosylate **4.186** (880 mg, 2.8 mmol, 1.0 equiv.) in CH_2Cl_2 (3 ml) was added over 5 min. After 90 min, triethylamine (3.15 ml, 22.4 mmol, 8.0 equiv.) was then added and the solution was allowed to warm to ambient temperature. After 12 h, the reaction was poured into H_2O (100 ml) and extracted with CH_2Cl_2 (3 x 40 ml). The combined organic extracts were washed with brine (30ml), dried over Na_2SO_4 and concentrated by rotary evaporation. Purification by flash chromatography (3:2 pet. ether : Et_2O, Rf = 0.44, visualization by UV or $KMnO_4$ stain) yielded aldehyde **4.187** as a colorless oil (898 mg, 71%).

IR (neat): 2977, 2856, 1706, 1426, 1412, 1358, 1300, 1188, 1173, 1096 cm^{-1}.

^{1}H NMR (400MHz; $CDCl_3$): δ = 9.76 (s, 1 H), 7.79 (d, *J* = 8.0 Hz, 2 H), 7.36 (d, *J* = 8.0 Hz, 2 H), 4.01 (t, *J* = 6.6 Hz, 2 H), 2.45 (s, 3 H), 2.41 (td, *J* = 7.3, 1.5 Hz, 2 H), 1.52-1.71 (m, 4 H), 1.16-1.39 (m, 8 H) ppm.

^{13}C NMR (101MHz; $CDCl_3$): δ = 202.7, 144.6, 133.2, 129.8, 127.8, 70.6, 43.8, 29.1, 28.9, 28.7, 28.7, 25.2, 21.9, 21.6 ppm.

HRMS-ESI (m/z): [M+Na]+ calcd for $C_{16}H_{24}O_4NaS$: 335.1293. Found: 335.1284.

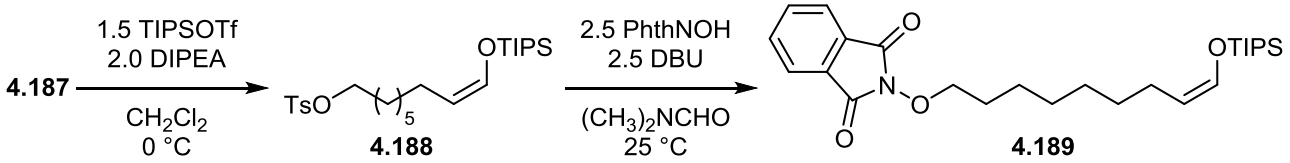

(Z)-2-(9-(Triisopropylsilyloxy)non-8-enyloxy)isoindoline-1,3-dione (**4.189**): To a solution of aldehyde **4.187** (874 mg, 2.8 mmol, 1.0 equiv.) and *N*,*N*-diisopropylethylamine (980 µl, 5.6 mmol, 2.0 equiv.) in CH_2Cl_2 (14 ml) cooled to 0 °C in an ice/water bath was added triisopropylsilyl trifluoro-methanesulfonate (1.15 ml, 4.2 mmol, 1.5 equiv.) over 5 min. After 45 min, the reaction mixture was concentrated by rotary evaporation and used without further purification. To a solution of *N*-hydroxypthalimide (1.15 g, 7.0 mmol, 2.5 equiv.) in DMF (7 ml) was added 1, 8-diazabicyclo[5.4.0] undec-7-ene (1.05 ml, 7.0 mmol, 2.5 equiv.) in one portion resulting in a dark purple solution. After 30 min, a solution of crude silyl enol ether **4.188** in DMF (7 ml) was added in one portion. After 21 h, the reaction mixture was poured into a mixture of 1:8 pet. ether: Et_2O (90 ml), washed with saturated $NaHCO_{3(aq)}$ (3 x 40 ml), brine (30 ml), dried over Na_2SO_4 and concentrated by rotary evaporation. Purification by flash chromatography (5:1 pet. ether: Et_2O, Rf = 0.31, visualization by UV or $KMnO_4$ stain) yielded *N*-alkoxyphthalimide **4.189** as a colorless oil (374 mg, 75% over 2 steps).

IR (neat): 2942, 2866, 1791, 1736, 1654, 1466, 1398, 1369, 1258, 1187, 1127, 1092 cm^{-1}.

^{1}H NMR (400MHz; $CDCl_3$): δ = 7.72-7.87 (m, 4 H), 6.26 (d, *J* = 5.9 Hz, 1 H), 4.38 (q, *J* = 5.9 Hz, 1 H), 4.20 (t, *J* = 6.8 Hz, 2 H), 2.06-2.14 (m, 2 H), 1.79 (qd, *J* = 7.3, 7.0 Hz, 2 H), 1.42-1.53 (m, 2 H), 1.31-1.39 (m, 6 H), 1.10-1.20 (m, 3H), 1.05-1.10 (m, 18 H) ppm.

^{13}C NMR (101MHz; $CDCl_3$): δ = 163.6, 138.9, 134.4, 129.0, 123.4, 109.9, 78.6, 29.5, 29.2, 28.1, 25.5, 23.5, 17.7, 12.0 ppm.

HRMS-ESI (m/z): [M+H]+ calcd for $C_{26}H_{42}NO_4Si$: 460.2883. Found: 460.2888.

Characterization data for 6-*exo* and 7-*endo* substrates synthesized but not cyclized

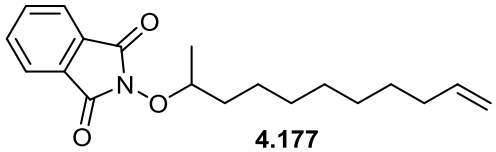

4.177

2-(Undec-10-en-2-yloxy)isoindoline-1,3-dione (**4.177**):

IR (neat): 3077, 2975, 2928, 2855, 1791, 1734, 1639, 1467, 1376, 1188, 1123, 1083, 1016, 977, 911, 879, 786, 703 cm^{-1}.

^{1}H NMR (400MHz; $CDCl_3$): δ = 7.88 - 7.78 (m, 2 H), 7.78 - 7.70 (m, 2 H), 5.80 (tdd, *J* = 6.7, 10.2, 17.0 Hz, 1 H), 4.98 (qd, *J* = 1.7, 17.2 Hz, 1 H), 4.92 (qd, *J* = 1.1, 10.2 Hz, 1 H), 4.37 (sxt, *J* = 6.2 Hz, 1 H), 2.03 (q, *J* = 6.8 Hz, 2 H), 1.86 - 1.74 (m, 1 H), 1.65 - 1.53 (m, 1 H), 1.52 - 1.43 (m, 2 H), 1.41 - 1.26 (m, 11 H) ppm.

^{13}C NMR (101MHz; $CDCl_3$): δ = 164.4, 136.4, 134.4, 129.0, 123.4, 114.1, 84.5, 34.9, 33.8, 29.5, 29.3, 29.0, 28.9, 25.3, 18.8 ppm.

HRMS-ESI (m/z): [M+Na]+ calcd for $C_{19}H_{25}NO_3Na$: 338.1732. Found: 338.1740.

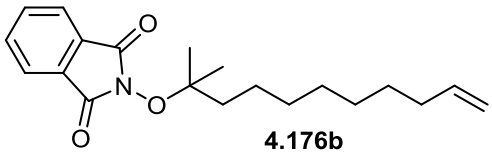

4.176b

2-((2-Methylundec-10-en-2-yl)oxy)isoindoline-1,3-dione (**4.176b**):

^{1}H NMR (400MHz; $CDCl_3$): δ = 7.88 - 7.71 (m, 4 H), 5.83 (tdd, *J* = 6.7, 10.3, 17.1 Hz, 1 H), 5.00 (qd, *J* = 1.7, 17.1 Hz, 1 H), 4.94 (td, *J* = 1.0, 10.2 Hz, 1 H), 2.05 (q, *J* = 6.9 Hz, 2 H), 1.77 - 1.67 (m, 2 H), 1.53 - 1.18 (m, 16 H) ppm.

^{13}C NMR (101MHz; $CDCl_3$): δ = 165.8, 139.2, 134.3, 129.4, 123.4, 114.1, 89.0, 40.5, 33.8, 30.1, 29.7, 29.4, 29.1, 28.9, 25.1, 24.5 ppm.

HRMS-ESI (m/z): [M+Na]+ calcd for $C_{20}H_{27}NO_3Na$:352.1889. Found: 352.1900.

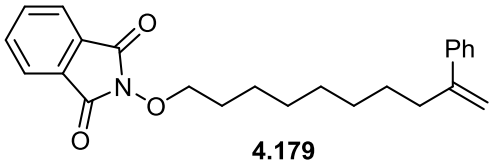

4.179

2-((9-Phenyldec-9-en-1-yl)oxy)isoindoline-1,3-dione (**4.179**):

^{1}H NMR (300MHz; $CDCl_3$): δ = 7.87 - 7.61 (m, 4 H), 7.41 - 7.16 (m, 5 H), 5.21 (s, 1 H), 5.01 (d, *J* = 0.9 Hz, 1 H), 4.15 (t, *J* = 6.9 Hz, 2 H), 2.46 (t, *J* = 7.3 Hz, 2 H), 1.83 - 1.65 (m, 2 H), 1.50 - 1.18 (m, 10 H) ppm.

^{13}C NMR (75MHz; $CDCl_3$): δ = 163.7, 148.7, 141.4, 134.4, 129.0, 128.2, 127.2, 126.1, 123.5, 112.0, 78.6, 35.3, 29.2, 29.2, 28.2, 28.1, 25.5 ppm.

HRMS-ESI (m/z): [M+H]+ calcd for $C_{24}H_{28}NO_3$: 378.2069. Found: 378.2072.

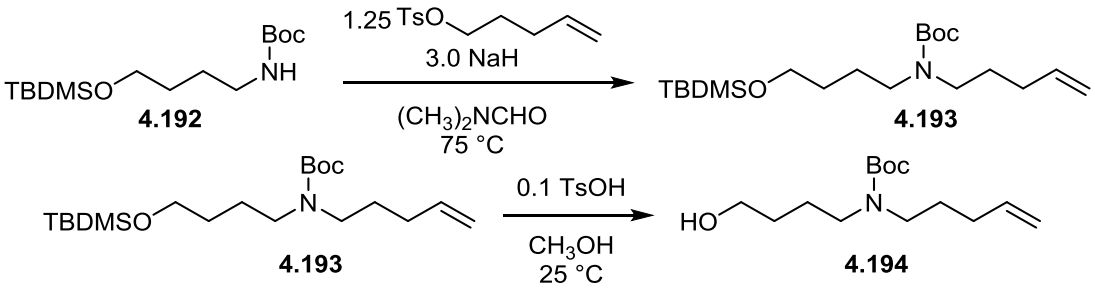

tert-Butyl (4-hydroxybutyl)(pent-4-en-1-yl)carbamate (**4.194**): To a suspension of sodium hydride (0.6 g, 60 wt% in mineral oil, 15 mmol, 3.0 equiv., washed with 3 x 10 ml pet. ether) in DMF (10 ml) cooled to 0 °C in an ice/water bath was added a solution of crude **4.192** (1.5 g, 5.0 mmol, 1.0 equiv., obtained in 2 steps from 4-aminobutanol) in DMF (5 ml + 5 ml wash) over 10 min. To the creamy brown slurry was added pent-4-enyl tosylate (1.5 g, 6.3 mmol, 1.25 equiv.) over 30 seconds. The cold bath was removed and the solution heated to 75 °C in an oil bath for 12 h. The reaction was quenched with saturated $NH_4Cl_{(aq)}$ (5ml), poured into Et_2O (200 ml), washed with 50% saturated $NH_4Cl_{(aq)}$ (100 ml), saturated $NaHCO_{3(aq)}$ (2 x 50 ml), brine (50 ml), dried over Na_2SO_4, filtered, and concentrated by rotary evaporation to a crude oil which was used without further purification.

To the crude oil containing **4.193** was added methanol (10 ml) and tosic acid monohydrate (95 mg, 0.5 mmol, 0.1 equiv.). After 2 h of stirring at ambient temperature, the yellow-brown solution was concentrated by rotary evaporation. Purification by flash chromatography (1:4 pet ether: Et_2O, Rf = 0.32, visualization by $KMnO_4$ stain) yielded alcohol **4.194** as a yellow oil (366 mg, 28% over 4 steps).

IR (neat): 3431, 2975, 2932, 2867, 1693, 1673, 1479, 1455, 1420, 1366, 1254, 1167, 1069, 911 cm^{-1}.

^1H NMR (400MHz; $CDCl_3$): δ = 5.89 - 5.74 (m, 1 H), 5.03 (d, *J* = 17.4 Hz, 1 H), 4.98 (d, *J* = 9.9 Hz, 1 H), 3.68 (br. s., 2 H), 3.29 - 3.11 (m, 4 H), 2.05 (q, *J* = 7.3 Hz, 2 H), 1.69 - 1.50 (m, 7 H), 1.46 (s, 9 H) ppm.

^{13}C NMR (101MHz; $CDCl_3$): δ = 183.1, 138.0, 114.9, 79.2, 77.2, 62.6, 46.7, 31.0, 28.5, 24.9 ppm.

HRMS-ESI (*m/z*): $[M+Na]^+$ calcd for $C_{14}H_{27}NO_3Na$: 280.1889. Found: 280.1887.

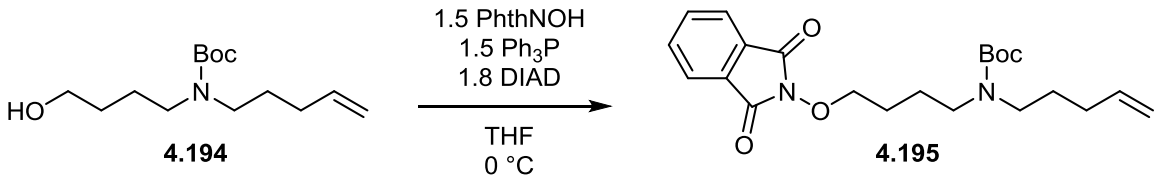

tert-Butyl (4-((1,3-dioxoisoindolin-2-yl)oxy)butyl)(pent-4-en-1-yl)carbamate (**4.195**): To a solution of alcohol **4.194** (360 mg, 1.4 mmol, 1.0 equiv.) in THF (14 ml) was added *N*-hydroxypthalimide (360 mg, 2.1 mmol, 1.5 equiv.) and triphenylphosphine (552 g, 2.1 mmol, 1.5 equiv.). The solution was cooled to 0 °C in an ice/water bath and diisopropyl azodicarboxylate (0.5 ml, 2.5 mmol, 1.8 equiv.) was added by syringe pump at a rate of 0.5 ml/h. The colourless solution turned to an orange-red solution during addition. After 12 h, the ambient temperature light-yellow solution was concentrated by rotary evaporation. Triphenylphosphineoxide was precipitated with a 1:1 mixture of hexane: Et_2O (100 ml), triturated with hexanes until no colour remained, and the collected organics were concentrated by rotary evaporation. Purification by gradient flash chromatography (3:1 to 1:1 pet. ether: Et_2O, Rf = 0.45 @ 1: 1 pet. ether: Et_2O, visualization by UV or $KMnO_4$ stain) yield *N*-alkoxypthalimide **4.195** as a thick colourless oil (460 mg, 82%).

IR (neat): 2974, 2932, 1790, 1735, 1689, 1468, 1417, 1366, 1255, 1186, 1172, 1082, 1017, 983, 878, 702 cm^{-1}.

^1H NMR (400MHz; $CDCl_3$): δ = 7.87 - 7.79 (m, 2 H), 7.78 - 7.69 (m, 2 H), 5.82 (tdd, *J* = 6.8, 10.2, 16.9 Hz, 1 H), 5.03 (dd, *J* = 1.2, 17.2 Hz, 1 H), 4.96 (d, *J* = 10.6 Hz, 1 H), 4.22 (br. s., 2 H), 3.33 - 3.11 (m, 4 H), 2.05 (q, *J* = 7.4 Hz, 2 H), 1.76 (br. s., 4 H), 1.63 (quin, *J* = 7.4 Hz, 2 H), 1.45 (s, 9 H) ppm.

^{13}C NMR (101MHz; $CDCl_3$): δ = 163.6, 155.6, 138.1, 134.4, 128.9, 123.5, 114.8, 79.2, 78.1, 77.2, 46.5, 31.0, 28.4, 25.5 ppm.

HRMS-ESI (*m/z*): $[M+K]^+$ calcd for $C_{22}H_{30}N_2O_5K$: 441.1792. Found: 441.1805.

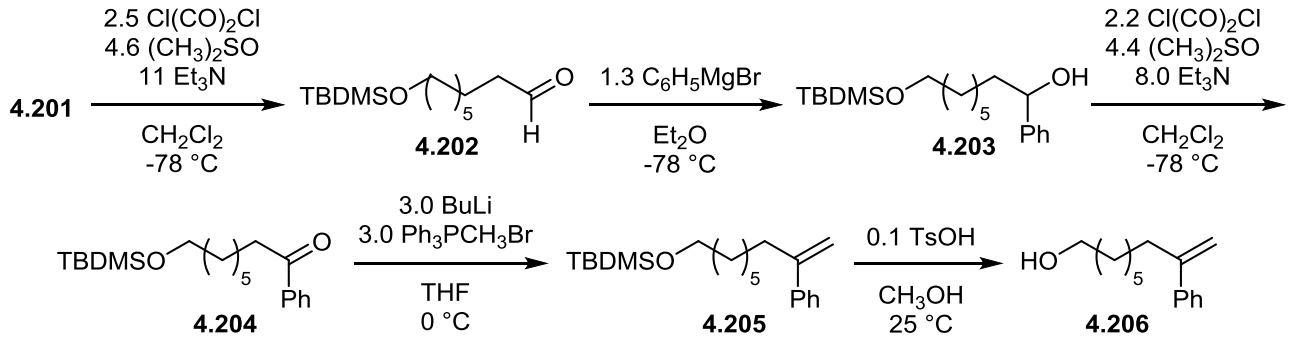

8-phenylnon-8-en-1-ol (**4.206**): To a solution of oxalyl chloride (3.4 ml, 32 mmol, 2.5 equiv.) in dry CH_2Cl_2 (130 ml) cooled to -78 °C in an acetone/dry ice bath was added DMSO (1.6 ml, 60 mmol, 4.6 equiv) over 5 min. After 30 min, alcohol **4.201** (3.36 g, 12.9 mmol, 1.0 equiv.) was added over 1 min. After 90 min, triethylamine (20 ml, 143 mmol, 11 equiv.) was added over 5 min. After 16 h, the ambient temperature yellow slurry was poured into water (200 ml) and extracted with CH_2Cl_2 (3 x 75 ml). The combined organic extracts were washed with brine (50 ml), dried over Na_2SO_4 and concentrated by rotary evaporation to yield aldehyde **4.202** which was carried forward immediately. To a solution of **4.202** in Et_2O (130 ml) cooled to -78 °C in an acetone/dry ice bath was added phenyl-magnesium bromide (5.6 ml, 3.0 M in Et_2O, 16.8 mmol, 1.3 equiv.) over 3 min. After 17 h, the solution was quenched with saturated $NH_4Cl_{(aq)}$ (10 ml) and poured into Et_2O (50 ml). The organic layer was washed with 50% saturated $NH_4Cl_{(aq)}$ (100 ml), 2% $HCl_{(aq)}$ (2 x 50 ml), brine (50 ml), dried over Na_2SO_4 and concentrated by rotary evaporation to yield alcohol **4.203** which was carried forward immediately. Alcohol **4.203** was subjected to a standard Swern oxidation protocol (similar to the first step in this sequence) with oxalyl chloride (2.5 ml, 28 mmol, 2.2 equiv.), DMSO (4.0 ml, 57 mmol, 4.4 equiv.) in CH_2Cl_2 (110 ml) followed by addition of **4.203** as a solution in CH_2Cl_2 (20 ml) and triethylamine (14.5 ml, 103 mmol, 8 equiv.). Concentration by rotary evaporation yielded ketone **4.204** as reddish brown oil which was carried forward immediately. To a suspension of methyltriphenyl-

phosphonium bromide (13.9 g, 38.7 mmol, 3.0 equiv.) in THF (100 ml) cooled to -78 °C in an acetone/dry ice bath was added butyllithium (25 ml, 1.6 M in hexane, 38.7 mmol, 3.0 equiv.) over 7 min resulting in a bright yellow slurry. The cold bath was removed and the reaction mixture was allowed to warm to ambient temperature. After 90 min, the reaction was again cooled to -78 °C in an acetone/dry ice bath and a solution of ketone **4.204** in THF (20 ml) was added over 5 min. After 10 h, the reaction mixture was quenched with 2% $HCl_{(aq)}$ (10 ml) and poured into a 4:1 mixture of pet. ether and Et_2O (250 ml). The organic layer was washed with 2% $HCl_{(aq)}$ (3 x 100 ml), water (100 ml), brine (75 ml), dried over Na_2SO_4 and concentrated by rotary evaporation. The crude oil was filtered through a plug of silica (elution with 39:1 pet. ether: Et_2O) and concentrated by rotary evaporation to provide 2.9 g of crude alkene **4.205** as a yellow oil. Alkene **4.205** was taken up in a solution of tosic acid monohydrate (179 mg, 0.86 mmol, 0.1 equiv.) in methanol (17 ml) and stirred at ambient temperature for 1 h. Methanol was removed by rotary evaporation and purification by automated flash chromatography (SNAP 100g cartridge, elution gradient of 5% to 40% EtOAc in hexanes over 10 column volumes, Rf = 0.19 in 5:1 hexane: EtOAc, visualization with UV or $KMnO_4$ stain) yielded alcohol **4.206** as a slightly yellow oil (1.44 g, 51% over 5 steps). The compound obtained matched characterization data obtained by K. Johnson.[260]

^{1}H NMR (300MHz; $CDCl_3$): δ = 77.52 - 7.20 (m, 5 H), 5.31 (s, 1 H), 5.10 (s, 1 H), 3.67 (t, *J* = 6.4 Hz, 2 H), 2.55 (t, *J* = 7.1 Hz, 2 H), 1.70 - 1.32 (m, 11 H) ppm.

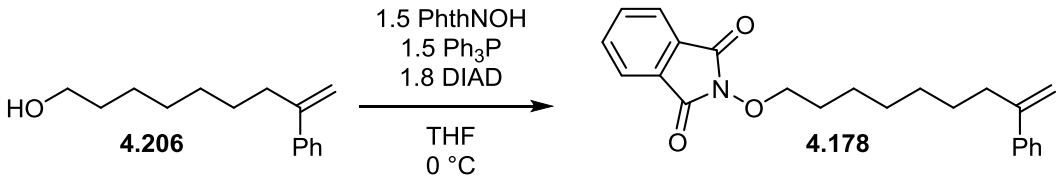

2-((8-Phenylnon-8-en-1-yl)oxy)isoindoline-1,3-dione (**4.178**): To a solution of alcohol **4.206** (873 mg, 4.0 mmol, 1.0 equiv) in THF (20 ml) was added *N*-hydroxypthalimide (994 mg, 6.0 mmol, 1.5 equiv.) and triphenylphosphine (1.57 g, 6.0 mmol, 1.5 equiv.). The solution was cooled to 0 °C in an ice/water bath and diisopropyl azodicarboxylate (1.5 ml, 7.2 mmol, 1.8 equiv.) was added by syringe pump at a rate of 1.5 ml/h. The colourless solution turned to an orange-red solution during addition. After 16 h, the ambient temperature light-yellow solution was poured into Et_2O (150 ml), washed with 50% saturated $NaHCO_3$ (3 x 50 ml), brine (25 ml), dried over Na_2SO_4, filtrated, concentrated by rotary evaporation. Purification by flash chromatography (2:1 pet. ether: Et_2O, Rf = 0.50, visualization by UV or $KMnO_4$ stain) yield *N*-alkoxypthalimide **4.178** as a colourless oil (744 mg, 51%). The compound obtained matched characterization data obtained by K. Johnson.[260]

^{1}H NMR (300MHz; $CDCl_3$): δ = 7.90 - 7.61 (m, 4 H), 7.42 - 7.11 (m, 5 H), 5.21 (s, 1 H), 5.00 (s, 1 H), 4.13 (t, *J* = 6.9 Hz, 2 H), 2.45 (t, *J* = 7.3 Hz, 2 H), 1.73 (quin, *J* = 7.0 Hz, 2 H), 1.49 - 1.21 (m, 8 H) ppm.

General alkoxyl 1, 5-HAT radical relay cyclization procedure (1, 5-HAT relay procedure): To a solution of *N*-alkoxyphthalimide (1 equiv.) in benzene (0.02 M, nitrogen-sparged) at reflux was added a solution of AIBN (0.15 equiv.) and tributyltin hydride (1.2 equiv.) in benzene (0.2 M in tributyltin hydride, nitrogen-sparged) by syringe pump (0.5 ml/h). After the addition was complete, the reaction was refluxed for an additional hour. The resulting solution was allowed to cool to ambient temperature, concentrated using rotary evaporation, and purified by flash chromatography to afford a mixture of cyclized and linear alcohol products. The product mixture was taken up in CH_2Cl_2 (0.3 M), cooled to 0

°C in an ice/water bath, and *meta*-chloroperbenzoic acid (3.0 equiv.) was added in one portion. After 16 h, the reaction was quenched with 2.0 M $Na_2S_2O_3$ (10 ml), washed with saturated aqueous Na_2CO_3 (3 x 5 ml), H_2O (5 mL), dried over Na_2SO_4, concentrated by rotary evaporation, and purified again by flash chromatography.

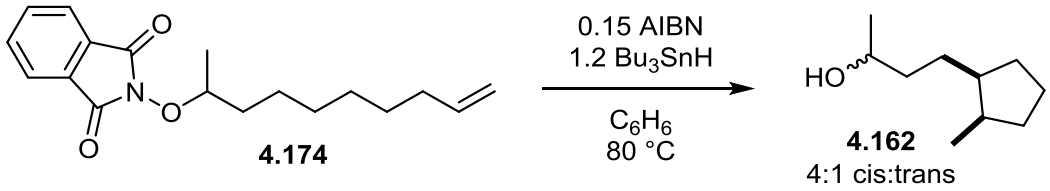

4-(2-Methylcyclopentyl)butan-2-ol (**4.162**): *N*-Alkoxyphthalimide **4.174** (108 mg, 0.34 mmol) was subjected to the general 1, 5-HAT relay procedure. Purification by flash chromatography (4:1 pet. ether/ Et_2O, Rf = 0.20, visualization by $KMnO_4$ stain) afforded cyclopentane **4.162** as a colorless oil (35 mg, 66%, *cis:trans* = 4:1) with ~20% diethyl ether.

IR (neat): 3345, 2929, 2863, 1460, 1375, 1067 cm^{-1}.

^1H NMR (400MHz; $CDCl_3$): δ = 3.80 (s, 1 H), 2.09 - 1.94 (m, 0.88 H), 1.88 - 1.09 (m, 18.4 H), 0.97 (d, *J* = 6.3 Hz, 0.56 H), 0.80 (d, *J* = 7.0 Hz, 2.44 H) ppm.

^{13}C NMR (101MHz; $CDCl_3$): δ = 68.6, 68.5, 43.4, 43.3, 38.6, 35.9, 35.9, 33.5, 29.8, 29.7, 26.6, 23.5, 23.5, 23.4, 22.5, 14.8, 14.7 ppm.

HRMS-ESI (*m/z*): $[M+Na]^+$ calcd for $C_{10}H_{20}ONa$: 179.1412. Found: 179.1416.

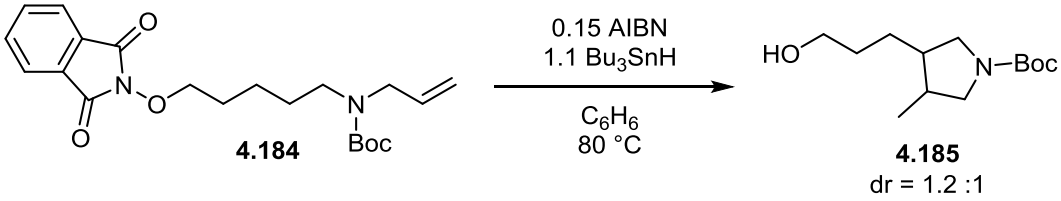

tert-Butyl 3-(3-hydroxypropyl)-4-methylpyrrolidine-1-carboxylate (**4.185**): *N*-Alkoxyphthalimide **4.184** (438 mg, 1.13 mmol) was subjected to the general 1, 5-HAT relay procedure. Purification by flash column chromatography (1:4 pet. ether/ Et_2O, Rf = 0.23, visualization by $KMnO_4$ stain.) afforded trace amounts of pyrrolidine **4.185** as a colorless oil (53% by NMR analysis of crude reaction mixture).

^{1}H NMR (400MHz; $CDCl_3$): δ = 3.71 - 3.33 (m, 3.6 H), 3.18 - 3.11 (m, 0.25 H), 3.09 - 2.79 (m, 1.6 H), 2.28 - 2.17 (m, 0.49 H), 2.16 - 2.02 (m, 0.46 H), 1.84 - 1.50 (m, 4.7 H), 1.47 - 1.14 (m, 11.3 H), 1.02 (dd, *J* = 2.2, 6.6 Hz, 1.3 H), 0.91 (dd, *J* = 2.2, 7.0 Hz, 1.9 H) ppm.

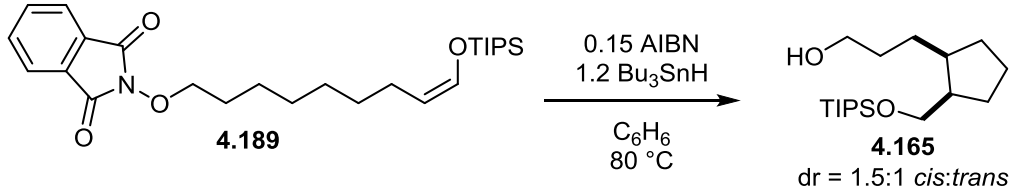

3-(2-((Triisopropylsilyloxy)methyl)cyclopentyl)propan-1-ol (**4.165**): *N*-Alkoxyphthalimide **4.189** (356.8 mg, 0.78 mmol) was subjected to the general 1, 5-HAT relay procedure. Purification by flash column chromatography (3:1 pet. ether/ Et_2O, Rf = 0.26, visualization by $KMnO_4$ stain) afford silyl ether **4.165** as a colorless oil (155 mg, 63%, *cis*:*trans* = 1.5:1).

IR (neat): 3328, 2942, 2865, 1463, 1386, 1099, 1065, 1013 cm^{-1}.

^{1}H NMR (400MHz; $CDCl_3$): δ = 3.51-3.73 (m, 4 H), 2.04-2.15 (m, 0.6 H), 1.16-1.96 (m, 13.8 H), 0.98-1.14 ppm (m, 22.0 H) ppm.

^{13}C NMR (101MHz; $CDCl_3$): δ = 66.8, 63.7, 63.4, 63.3, 48.2, 44.7, 41.8, 41.6, 32.9, 32.2, 31.8, 31.0, 29.3, 28.0, 25.8, 24.4, 22.9, 18.1, 17.7, 12.0 ppm.

HRMS-ESI (*m/z*): $[M+Na]^+$ calcd for $C_{18}H_{38}O_2SiNa$: 337.2539. Found: 337.2528.

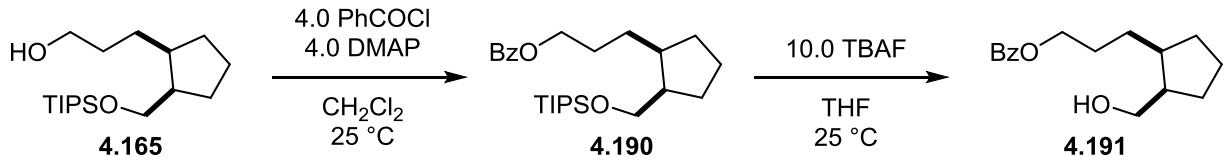

3-(2-(hydroxymethyl)cyclopentyl)propyl benzoate (**4.191**): To a solution of silyl ether **4.165** (106 mg, 0.35 mmol, 1.0 equiv.) in CH_2Cl_2 (3.5 ml) was added DMAP (171 mg, 1.4 mmol, 4.0 equiv.) and benzoyl chloride (170 µl, 1.4 mmol, 4.0 equiv.). After 9 h, the reaction was quenched with saturated $NaHCO_{3(aq)}$ (1 ml). The crude mixture was extracted with Et_2O (60 ml), and the combined organic extracts were washed with saturated $NaHCO_{3(aq)}$ (3 x 30 ml), brine (30 ml), dried over Na_2SO_4, filtered and concentrated by rotary evaporation. To ester **4.190** was added a solution of TBAF (3.5 ml, 1.0 M in THF, 3.5 mmol, 10 equiv.). The reaction was warmed to 50 °C and stirred for 12 h. The reaction was poured into Et_2O (60 ml), washed with saturated $NaHCO_{3(aq)}$ (3 x 30 ml), brine (30 ml), dried over Na_2SO_4, filtered and concentrated by rotary evaporation. Purification by automated flash chromatography (gradient 5% - 40% EtOAc in hexanes, Rf = 0.18 in 4:1 hexanes/EtOAc, visualization by UV and $KMnO_4$ stain) yielded **4.191** as a colorless oil (63 mg, 69% over 2 steps).

IR (neat): 3399, 2947, 2868, 1451, 1315, 1114, 1070, 1026 cm^{-1}.

^1H NMR (400MHz; $CDCl_3$): δ = 8.05 (d, *J* = 7.3 Hz, 2 H), 7.60-7.54 (m, 1 H), 7.45 (t, *J* = 7.6, 2 H), 4.41 - 4.25 (m, 2 H), 3.71 (dd, *J* = 6.4, 10.4 Hz, 0.60 H), 3.64 (dd, *J* = 5.5, 10.7 Hz, 0.40 H), 3.54 - 3.43 (m, 1 H), 2.20 - 2.09 (m, 0.59 H), 2.07 - 1.93 (m, 0.64 H), 1.93 - 1.18 (m, 10.4 H), 0.99 (t, *J* = 7.3, 0.40 H) ppm.

^{13}C NMR (101MHz; $CDCl_3$): δ = 166.7, 132.8, 130.4, 129.5, 128.3, 66.5, 65.2, 65.1, 63.3, 48.1, 44.5, 41.7, 41.3, 32.6, 31.9, 30.8, 29.3, 28.0, 27.9, 27.7, 26.1, 24.3, 22.8 ppm.

HRMS-ESI (*m/z*): $[M+Na]^+$ calcd for $C_{16}H_{22}O_3Na$: 285.1467. Found: 285.1462.

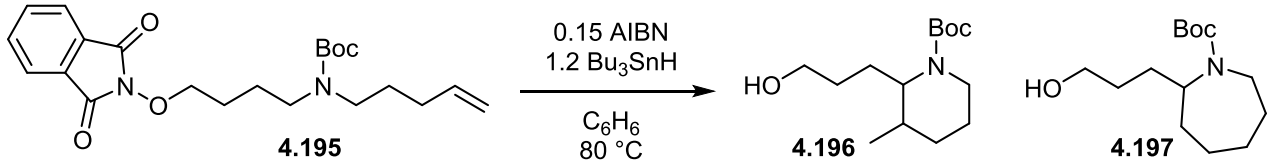

4.195 4.196 4.197

<u>*tert*-Butyl 2-(3-hydroxypropyl)-3-methylpiperidine-1-carboxylate (**4.196**) and *tert*-Butyl 2-(3-hydroxypropyl)azepane-1-carboxylate (**4.197**):</u> *N*-Alkoxyphthalimide 4.195 (233 mg, 0.58 mmol) was subjected to the general 1, 5-HAT relay procedure. Purification by flash chromatography (1:7 pet. ether/Et_2O, Rf = 0.44, visualization by $KMnO_4$ stain) afforded nitrogen heterocycles **4.196** and **4.197** as a colorless oil (100 mg, 70%, *cis*:*trans* = 4:1, exo:endo = 1:1).

^{1}H NMR (400MHz; $CDCl_3$): δ = 4.33 - 3.81 (m, 1.7 H), 3.76 - 3.53 (m, 3.2 H), 3.29 - 3.10 (m, 0.1 H), 2.81 - 2.54 (m, 1.2 H), 2.41 (br. s., 0.4 H), 2.14 - 1.94 (m, 1.0 H), 1.90 - 1.09 (m, 25 H), 1.03 (d, *J* = 7.0 Hz, 0.5 H), 0.88 (d, *J* = 7.0 Hz, 1.1 H) ppm.

^{13}C NMR (101MHz; $CDCl_3$): δ = 79.2, 79.1, 79.1, 62.9, 62.8, 62.7, 55.0, 54.1, 41.6, 41.3, 34.9, 34.6, 31.7, 31.3, 29.9, 29.8, 29.5, 29.0, 28.8, 28.5, 28.5, 28.4, 28.3, 27.3, 27.1, 25.1, 25.0, 24.9, 18.1 ppm.

HRMS-ESI (*m/z*): $[M+Na]^+$ calcd for $C_{14}H_{27}NO_3Na$: 280.1889. Found: 280.1893.

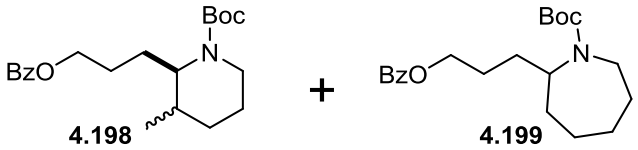

4.198 + 4.199

<u>*tert*-Butyl -2-(3-(benzoyloxy)propyl)-3-methylpiperidine-1-carboxylate (**4.198**) and *tert*-Butyl 2-(3-(benzoyloxy)propyl)azepane-1-carboxylate (**4.199**):</u>

^{1}H NMR (400MHz; $CDCl_3$) δ = 8.10 - 7.97 (m, 2 H), 7.61 - 7.51 (m, 1 H), 7.48 - 7.38 (m, 2 H), 4.41 - 4.25 (m, 2.2 H), 4.21 - 3.84 (m, 1.3 H), 3.80 - 3.72 (m, 0.3 H), 3.66 - 3.56 (m, 0.3 H), 2.82 - 2.55 (m, 1 H), 2.14 - 1.10 (m, 21.5 H), 1.04 (d, *J* = 7.2 Hz, 0.4 H), 0.88 (d, *J* = 6.8 Hz, 1.1 H) ppm.

^{13}C NMR (101MHz; $CDCl_3$) δ = 166.5, 156.1, 155.7, 155.1, 132.8, 132.8, 132.8, 132.7, 130.5, 130.3, 129.6, 129.5, 129.5, 129.5, 128.3, 128.2, 79.2, 79.1, 78.8, 65.0, 64.8, 64.7, 54.8, 53.9, 41.6, 41.3, 34.8,

34.5, 31.5, 31.4, 29.8, 28.9, 28.5, 28.5, 28.5, 28.5, 28.4, 28.4, 27.4, 25.7, 25.6, 25.1, 25.0, 24.8, 20.0, 18.9, 18.1 ppm.

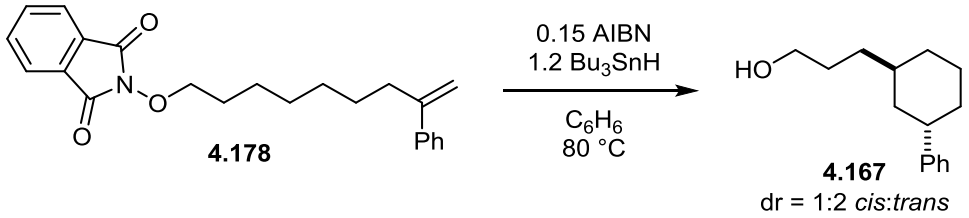

3-(3-Phenylcyclohexyl)propan-1-ol (**4.167**)**:** *N*-Alkoxyphthalimide **4.178** (218 mg, 0.6 mmol) was subjected to the general 1, 5-HAT relay procedure. Purification by flash chromatography (3:1 pet. ether/Et_2O, Rf = 0.3, visualization by $KMnO_4$ stain) afforded cyclohexane **4.167** as a colorless oil (78 mg, 71%, *cis*:*trans* = 1:2).

IR (neat): 3330, 2923, 2851, 1493, 1449, 1057 cm^{-1}.

^1H NMR (400MHz; $CDCl_3$): δ = 7.15-7.34 (m,5.10 H), 3.60-3.77 (m, 2 H), 2.72-2.84 (m, 0.36 H), 2.46-2.60 (m, 0.56 H), 1.78-1.99 (m, 3.09 H), 1.72-1.78 (m, 0.75 H), 1.19-1.67 (m, 9.55 H), 1.11 (q, *J*=12.2 Hz, 0.60 H), 0.89-1.02 (m,0.58 H) ppm.

^{13}C NMR (101MHz; $CDCl_3$): δ = 147.8, 147.4, 128.3, 126.9, 126.8, 125.8, 125.7, 63.3,44.4, 41.2, 38.0, 37.9, 34.2, 33.8, 33.4, 33.2, 32.8, 31.1, 30.1, 30.0, 28.3, 26.6, 21.3 ppm.

HRMS-EI (*m/z*): $[M\bullet]^+$ calcd for $C_{15}H_{22}O$: 218.16707. Found: 218.16725.

Chapter 5: Future work and conclusions

5.1 Radical fluorination to synthesize aryl fluorides

In the follow-up study on the fluorodesilylation of trimethylsilylarenes, Ramsden and co-workers performed some experiments employing arylboronates (Scheme 5.1)[92] hoping to demonstrate SET activity with XeF_2 and fluorination intercepting the originally proposed mechanism involving an arylxenon intermediate as proposed in their original report employing trimethylsilylarenes.[89] Trace amounts of 4-fluorotoluene (*p*-**1.69**) were detected with tolylbornic acid (**5.1**) and the reaction with aryl boronate **5.2** delivered significant amounts of 4-chlorotoluene (**5.6**) suggesting the formation of aryl radicals. Unfortunately, it does not appear that aryl radicals are fluorinated under conditions employing XeF_2 as the fluorine source; however, Sel-F or NFSI might. One avenue to explore is a mixed reaction system employing XeF_2 to effect the same oxidation transformation to generate aryl radicals.

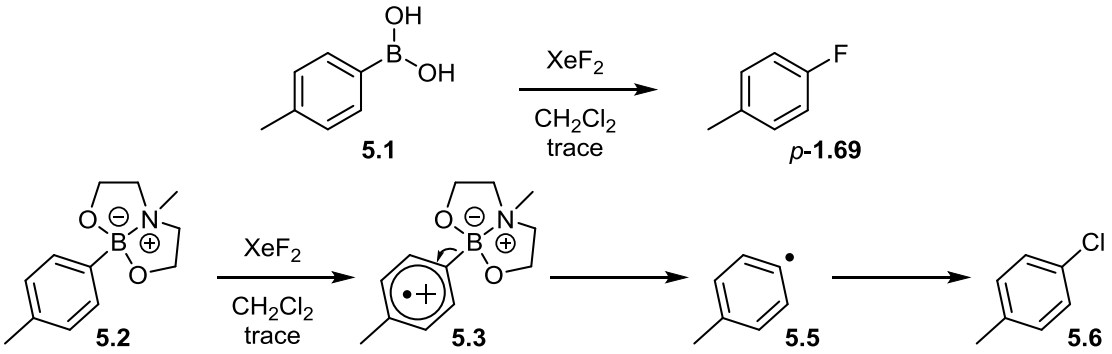

Scheme 5.1. Reaction of XeF_2 with arylboron compounds

At the close of section 2.3.3, I stated that there are similarities between the reaction of arylboronic acids with Sel-F and phenoxyacetic acids with PIFA and NFSI. In the I (III) systems, optimisation under thermal conditions did not lead to any appreciable increases in yield from the first observed thermal reactions (Scheme 3.9). However, switching to a photochemical system greatly

improved the yields, and finally, when I (III) was removed, the PDC-F reaction was uncovered. Analogously, the thermal reaction of arylbornic acids with Mn(III) and Sel-F did not lead to any appreciable increases in yield until Mn(III) was removed leaving only Sel-F. After extensive screening of additives under thermal conditions, the yields still remained low.

If fluorodeborylation requires SET oxidation, Sel-F may be a suitable oxidant and perhaps a photochemical system analogous to PDC-F with **3.44** is possible. Comparing the steps of PDC-F to arylboronic acids in Scheme 5.2, a parrallel to decarboxylation can be envisioned for each step of deborylation. Therefore, if aryl radicals can truly be fluorinated by Sel-F, photochemical stimulation of arylboronic acids is a potential alternative to thermochemical stimulation.

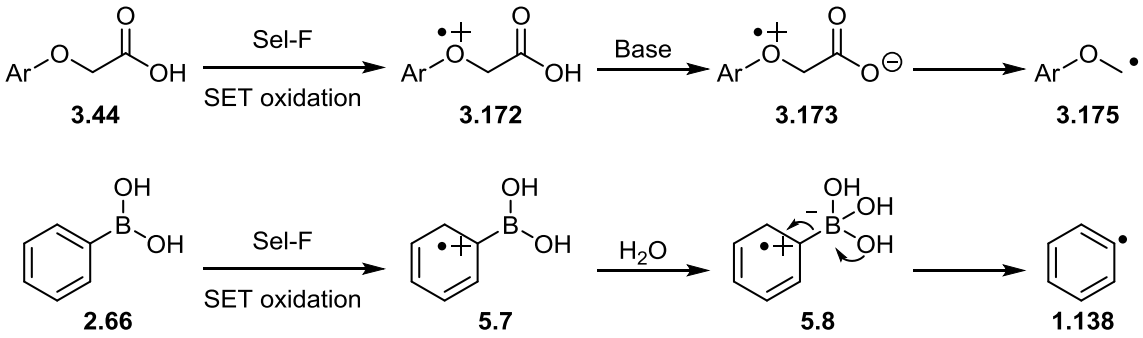

Scheme 5.2. Comparison of photodecarboxylation to aryldeborylation

5.2 Fluorination employing hypervalent iodine

In section 3.2, I stated that the mechanism for hypervalent iodine-mediated PDC-F was still unclear. Based on the reactions in Scheme 3.15, there is evidence to support that I (III) is acting as a photosensitizer. UV-VIS spectroscopy of DIB and mixtures containing DIB and carboxylic acid substrate in acetonitrile show no detectable shifts in absorbance. At higher concentrations of DIB, absorption of light is detected beginning at 320 nm. PDC-F of phenoxyacetic acids was observed with

irradiation from a terrarium lamp, similar to sensitized reactions carried out in acetone. Therefore, it is very likely that DIB is the principal chromophore in this reaction.

Fluorodecarboxylation of 4-methoxyphenyoxyacetic acid (**3.62**) to aryl fluoromethyl ether **3.63** has only been observed with DIB, suggesting that this system may further expand the substrate scope for fluorodecarboxylation (Scheme 5.3). Given that oxidation of 4-methoxylated anisole derivatives may lead to quinone formation,[105] DIB may be activating **3.62** for PDC-F by an alternate pathway. More work is needed on this system to understand the role of I (III).

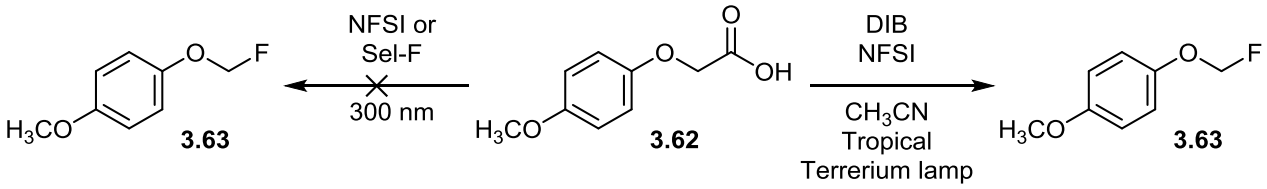

Scheme 5.3. PDC-F of 4-methoxyphenoxyacetic acid

The addition of excess PIFA to the PDC-F of phenoxyfluoroacetic acids demonstrated that aryl difluoromethyl ethers could be obtained even in the absence of a radical fluorinating agent. While higher yields could be obtained in the presence of NFSI (Table 3.4), the proposed alternate mechanism invoking oxidation of the phenoxymethyl radical to the cation and trapping with a source of fluoride is more appealing (Scheme 3.13). An ionic mechanism of fluorination is amenable to radiotracer synthesis as it is much easier to generate radioactive [^{18}F]-fluoride than [^{18}F]-NFSI or [^{18}F]-Sel-F. Initial experiments were carried out in benzene (Scheme 3.14), which is hardly a good solvent for anionic fluoride. If carbocationic intermediates are generated, the use of nucleophilic polar solvents such as alcohols or acetonitrile may be problematic; however, non-nucleophilic polar solvents such as perfluoroethanol or tetrahydrofuran in combination with a phase transfer agent may increase the

amount of solvated fluoride nucleophile. Furthermore, the list of nucleophilic fluoride sources was not screened exhaustively. A more thorough investigation of this reaction manifold is worthy of consideration.

5.3 Photodecarboxylative halogenation

All of the mechanistic understanding gained from studies performed on photodecarboxylative fluorination leads me to believe that a generalized halogenation reaction is possible. In place of Sel-F or NFSI, one could substitute an equivalent source of radical chlorine, bromine or iodine. Preliminary attempts to expand the reaction scope from a photodecarboxylative fluorination into a generalized photodecarboxylative halogenation reaction for the synthesis benzyl halides showed promise for bromination (Scheme 5.4). Irradiation of an acetone solution containing **3.40a**, *N*-bromosuccinimide and DtBuPy for one hour at 300 nm yielded 33% (by ^{1}H NMR analysis) of benzyl bromide (**5.10**) and 69% conversion of phenylacetic acid (by ^{1}H NMR analysis). When phenylacetic acid was irradiated at 300 nm in solution with *N*-chlorosuccinimide or *N*-iodosuccinimide, no benzyl chloride (**5.9**) nor benzyl iodide (**5.11**) was observed.

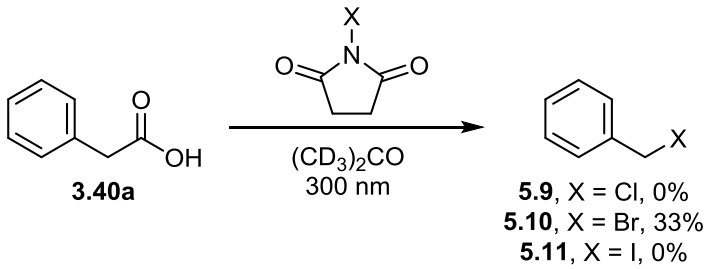

Scheme 5.4. Photodecarboxylative halogenation of phenylacetic acid

Preliminary attempts to expand the reaction scope from a photodecarboxylative fluorination into a generalized photodecarboxylative halogenation reaction for the synthesis aryl halomethyl ethers

showed promise for iodination (Scheme 5.5). When phenoxyacetic acid was irradiated at 300 nm in solution with N-chlorosuccinmide or N-bromosuccinimide, selective electrophilic aromatic substitution was observed in the 4-position of the phenoxy ring leading to good yields of 4-chlorophenoxyacetic acid (**5.15**) and 4-bromophenyoxyacetic acid (**3.45**). Under conditions of photolysis, it is possible that chlorine and bromine were generated, leading to the aromatic halogenation reactions. A control reaction employing phenoxyacetic acid with bromine in place of *N*-bromosuccinimide lead to the same reaction behaviour as the phenoxyacetic acid irradiated in the presence of *N*-bromosuccinimide, providing an explanation for the lack of photodecarboxylation.

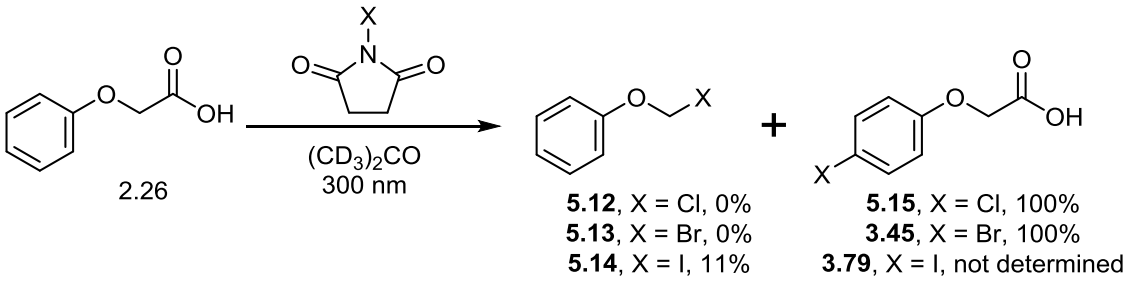

Scheme 5.5. Photodecarboxylative halogenation of phenoxyacetic acid

While there are many methods to synthesize benzyl halides and aryl halomethyl ethers, photodecarboxylation appears to be a new avenue for exploration especially given the wealth of knowledge on photodecarboxylation. The Hunsdieker reaction accomplishes a similar transformation through homolysis (thermal or photochemical) of an intermediate carboxylic hypohalite intermediate. Schemes 5.4 and 5.5 suggest that a PET-mediated decarboxylative halogenation reaction may exist. Thus far, research has focused on the photodecarboxylative pathways for aryloxyacetic acids and arylacetic acids, but employing the resulting radical (or ionic) decarboxylated species in a meaningful synthetic transformation may warrant attention. Davidson has demonstrated the addition of thiophenol

efficiently leads to photodecarboxylative hydrogenation.[191a] I have demonstrated the addition of NFSI and Sel-F efficiently leads to photodecarboxylative fluorination. There is room for someone to demonstrate that efficient photodecarboxylative chlorination, bromination, or iodination can be accomplished without formation of a hypohalite intermediate.

5.4 Computational studies

The ultimate question to be answered in future computational studies is the mechanism of fluorination. My studies indicate that the phenoxymethyl radical is formed and that the radical character is significantly localized on the oxymethyl oxygen and carbon. This intermediate is present in both the photosensitized and non-sensitized variant with both Sel-F and NFSI. It has been repeatedly asserted that NFSI and Sel-F are radical fluorinating agents as they will ultimately deliver a fluorine atom to an alkyl radical; however, the radical intermediate may be susceptible to further redox activity prior to fluorination.

If Sel-F and NFSI deliver fluorine by an S_H2 mechanism (Scheme 5.6), the required calculations would be straight-forward. A relaxed scan can be performed where the distance between radical **2.33** and fluorinating agent are reduced until a global energy minimum is found. Once located, a transition state search may be performed at higher levels of theory to find the transition state whereby one vibration will form a C-F bond while simultaneously breaking the N-F bond. This strategy can be utilized to ascertain the mechanism of perester mediated fluorodecarboxylation in addition to the mechanism of photofluorodecarboxylation. However, if this calculation method is unable to locate a transition state, then single electron transfer processes prior to fluorine transfer are likely active and collaboration with an expert at computational chemistry will be required.

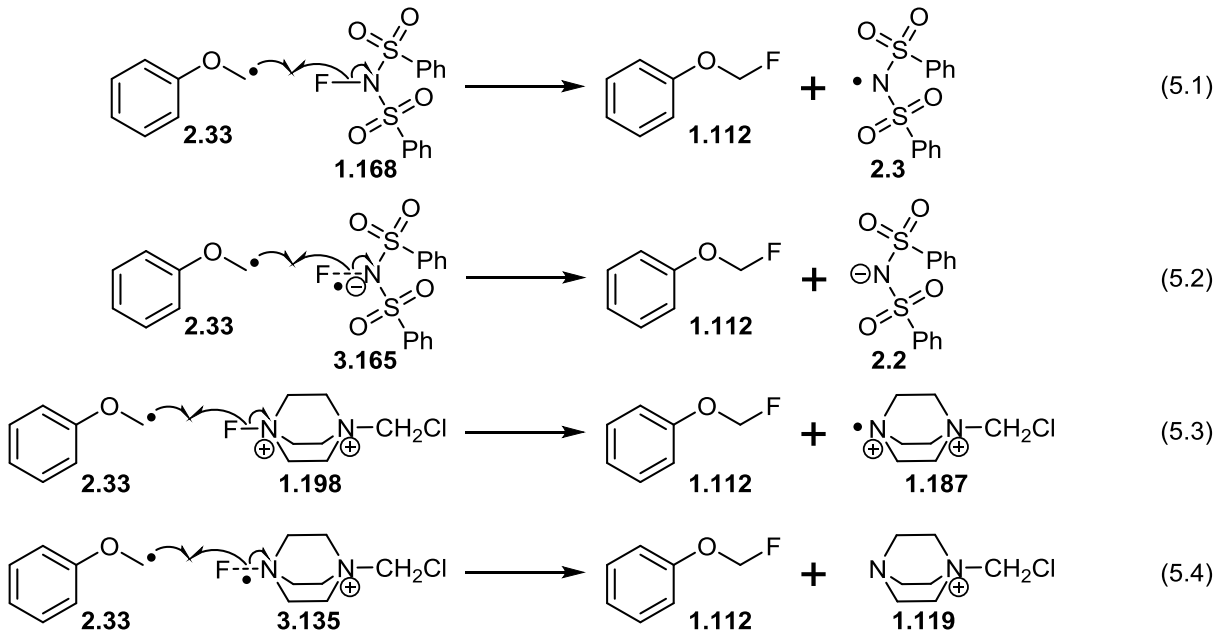

Scheme 5.6. S_H2 Mechanisms for radical fluorination

There is a very high probability that eqn. 5.2 and 5.4 are active because SET mechanisms for the fluorination of anionic substrates by NFSI and Sel-F have been reported.[108a,262] If anionic substrates are fluorinated through a SET mechanism, the intermediate radical coupling step exactly resembles the step in eqn. 5.2 and 5.4 (Scheme 5.7). There is already strong evidence to support SET-mediated mechanisms for Sel-F,[108a,117] and circumstantial evidence for NFSI.[263]

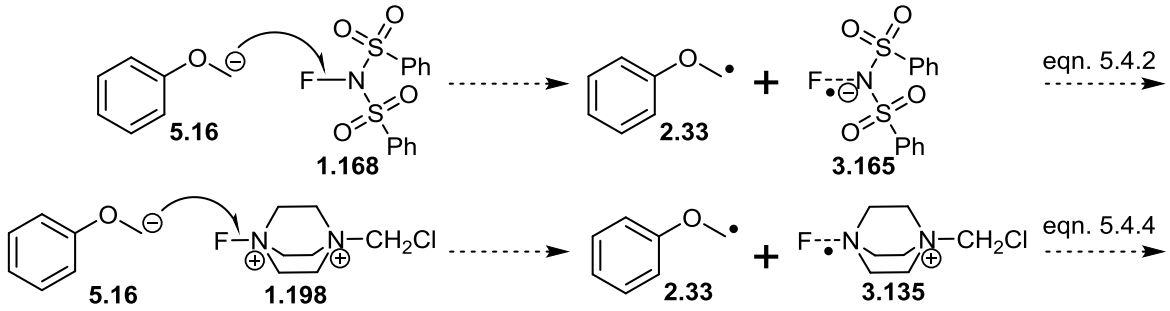

Scheme 5.7. Hypothetical SET mediated fluorination of the phenoxymethyl anion

5.5 Photodecarboxylative fluorination employing Sel-F or NFSI

PDC-F for the synthesis of benzyl fluorides was established (Table 3.10), but by no means, explored. Furthermore, it appears that hydrocinnamic acids are also capable of PDC-F and this work has yet to be published. Silver-mediated decarboxylative fluorination of phenylacetic acid (and fluorinated derivatives)[103-104] has already been established, suggesting that a photochemically promoted strategy is possible (Scheme 5.8). A PDC-F variant would be superior in that elevated temperatures or catalysts are unnecessary.

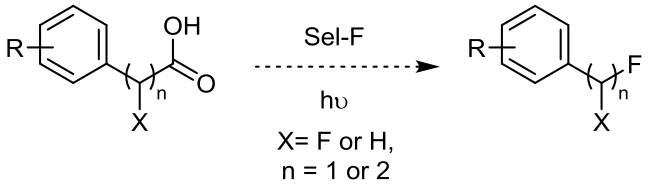

Scheme 5.8. Detailed investigations into PDC-F or phenylacetic acids and hydrocinnamic acids

While I was able to demonstrate that small amounts of aryl trifluoromethyl ether can be synthesized by photodecarboxylative fluorination, the problem is by no means solved (Figure 3.4). The problem of trying to optimise a reaction using a volatile reaction product can be easily solved by testing compounds which would produce higher molecular weight trifluoromethyl ethers. However, both the O-alkylation/saponification synthesis of difluorophenoxyacetic acids was low yielding, as was the fluorodecarboxylation step. Additionally, the acids synthesized were never pure because either the decomposition of the difluoro acids occur during purification, or residual solvent from purification was present in all of the test samples. It is possible that this contamination had detrimental effects on the PDC-F reaction. During the work on sensitized PDC-F, methyl phenoxyacetate did not undergo PDC-F and, without a carboxylate (or carboxylic acid), decarboxylation in general does not occur. Thus, one

improvement would be to develop a PDC-F procedure which relies on in-situ saponification of **3.124** in the photoreactor allowing for immediate PDC-F of the **3.125** (Scheme 5.9).[j]

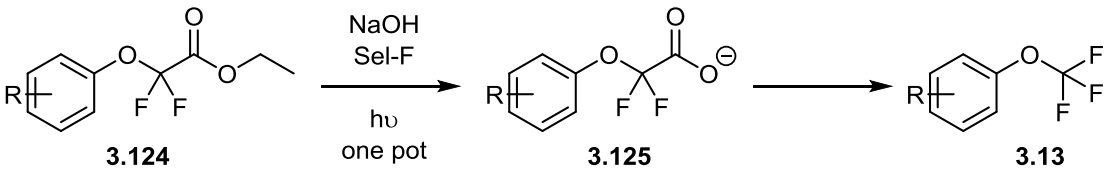

Scheme 5.9. One-pot procedure for saponification and PDC-F

Under the best conditions obtained, PDC-F required photochemical stimulation by a relatively broad spectrum 254 nm light source. With the assumption that not all wavelengths of light will trigger photoionization, it is reasonable to assume that other wavelengths of light might promote side reactions. Ultraviolet light is very energetic, and it is possible that this broad spectrum irradiation is delivering enough energy (especially if two photons are absorbed) to promote substrate degradation. Another strategy to increase the yields of aryl trifluoromethyl ether lies in designing a system whereby monochromatic light is used. A corrleation study between monochromatic irradiation and yield might reveal that only a narrow range of wavelengths promote photooxidation and decarboxylation. Tuning the irradiation wavelength might decrease undesired reactions from excitation of the wrong transition.

From the studies on photosensitized PDC-F, I have demonstrated that direct excitation of the substrate is not necessary to promote a decarboxylation. Benzophenone and acetone have allowed reactions which would otherwise require 300nm light to be performed with 350nm light. A natural

[j] Ongoing work in the Sammis research group by C. Chatalova-Sazepin have already produced such a procedure.

progression would be to identify a sensitizer which would be suitably activated by visible light.[k] A photosensitization strategy might also be suitable for aryl trifluoromethyl ether synthesis (Scheme 5.10). As it is still unclear what the role of hypervalent iodine is to fluorodecarboxylation, perhaps the addition of PIFA might improve aryl trifluoromethyl ether synthesis.

Having established that an aryl substituent is unnecessary for photodecarboxylation in acetone (or in the presence of a benzophenone), it may be possible to expand the scope of PDC-F to alkyl difluoromethyl and trifluoromethyl ethers (Scheme 5.11). The mechanistic investigations with adamantyloxyacetic acid **3.167** would have produced alkyl monofluoro ethers that are unstable towards isolation (Scheme 3.54), but dilfuoromethyl and trifluoromethyl ethers are more robust. With the correct choice of photosensitizer, it may even be possible to promote such a reaction with visible light.

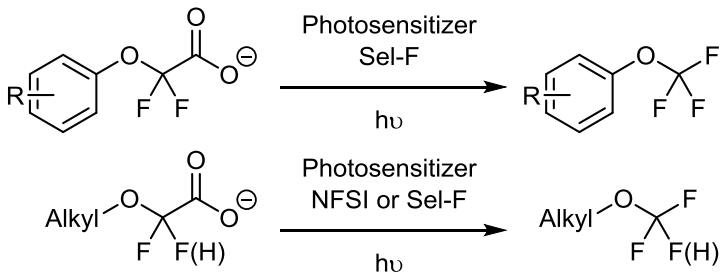

Scheme 5.10. Photosensitized PDC-F with Sel-F

Finally (although the possibilities are practically limitless), while radicals have been implicated in fluorination, the rich chemistry of alkyl radicals has not touched. Prior to fluorination, alkyl radicals can be utilized for addition reactions, fragmentation reactions, rearrangements, cyclizations, and relay cyclizations to name but a few examples. Verily, there is much to look forward to!

---

[k] Ongoing work in the Sammis research group by M. Rueda-Becerril has already identified a suitable ruthenium-based photosensitizer.

5.6 Conclusions

In times past, radical fluorination was avoided as the reagents capable of transferring fluorine to an alkyl radical were also capable of discrete fluorine radical generation. Generation of fluorine radicals could lead to uncontrollable combustion-like reactions and many have sought non-radical routes to fluorine incorporation. I have discovered that Sel-F is capable of delivering fluorine to alkyl radicals. The Sammis group has demonstrated that *N*-fluorobenzensulfonimide is also capable of such a transformation. It is very likely that other "electrophilic" fluorinating agents might also function as "radical" fluorinating agents.

In my synthetic studies on aryl fluoromethyl ether synthesis, I have discovered two new reactions. Photochemical (UV-light including sunlight, the most abundant and renewable energy source known to earth) stimulation of aqueous (water, the most abundant solvent on earth) alkaline solutions containing 2-aryloxyacetic acids and in the presence of Sel-F will promote a decarboxylative fluorinating reaction which yields aryl fluoromethyl ethers, aryl difluoromethyl ethers, and great potential for aryl trifluoromethyl ethers. In the second discovery, photochemical stimulation of acetone solutions containing 2-aryloxyacetic acids in the presence of NFSI will promote a different, milder, photosensitized decarboxylative fluorination reaction capable of delivering more electron rich aryl fluoromethyl ethers, aryl difluoromethyl ethers, and potential for alkyl fluoromethyl ethers. DFT calculations support the assertion that a radical intermediate is fluorinated.

This work contributes significantly to the growing field of fluorine chemistry and allows for many avenues of exploration into the fluorination of alkyl radicals and the synthesis of aryl fluoromethyl ethers.

Bibliography

1. (a) Tressaud, A. *Angew. Chem. Int. Ed.* **2006**, *45*, 6792.; (b) Moissan, H. *C. R. Hebd Seances Acad. Sci.* **1886**, *102*, 1543.; (c) Moissan, H. *C. R. Hebd. Seances Acad. Sci*. **1886**, *103*. 202.; (d) Moissan, H. *C. R. Hebd Seances Acad. Sci.* **1886**, *103*, 256.
2. Kirk, K. L. *Org. Process Res. Dev.* **2008**, *12*, 305.
3. Deng, H.; O'Hagan, D.; Schaffrath, C. *Nat. Prod. Rep.* **2004**, 773.
4. (a) Jeschke, P.; Baston, E.; Leroux, F. R. *Mini-Rev. Med. Chem.* **2007**, *7*, 1027. (b) Hagmann,W. K. *J. Med. Chem.* **2008**, *51*, 4359.
5. (a) Purser, S.; Moore, P. R.; Swallow, S.; Gouverneur, V. *Chem. Soc. Rev.* **2008**, *37*, 320. (b) Gladysz, J. A.; Jurisch M. *Top. Curr. Chem.* **2012**, *308*, 1.
6. (a) R. D. Chambers, *Fluorine in Organic Chemistry*, Blackwell Publishing: Oxford, 2000.; (b) Hiyama, T. *Organofluorine compounds: chemistry and applications;* Springer-Verlag: New York, 2000.
7. Smith, M. B.; March, J. *March's advanced organic chemistry: reactions, mechanisms, and structure;* 6th ed. John Wiley & Sons: Hoboken, 2007.
8. Sharts, C. M. *J. Chem. Educ.* **1968**, *45*, 185.
9. For a review on Cytochrome P450 monooxygenases see: Coon, M. J. *Annu. Rev. Pharmacol. Toxicol.* **2005**, *45*, 1.
10. For reviews on fluorination methods see: (a) Resnati, G. *Tetrahedron* **1993**, *49*, 9385. (b) Rozen, S. *Chem. Rev.* **1996**, *96*, 1717. (c) Lal, G. S.; Pez, G. P.; Syvret, R. G. *Chem. Rev.* **1996**, *96*, 1737. (d) Hutchinson, J.; Sandford, G. *Top. Curr. Chem.* **1997**, *193*, 1. (e) Ma, J.-A.; Cahard, D. *Chem. Rev.* **2004,** *104*, 6119.; Ma, J.-A.; Cahard, D. *Chem. Rev.* **2008,** *108*, PR1. (f) Furuya, T.; Kuttruff C. A.; Ritter, T. *Curr. Opin. Drug Discovery Dev.* **2008**, *11*, 803. (g) Manteau, B.; Pazenok, S.; Vors, J.; Leroux, F. R. *J. Fluorine Chem.* **2010**, *131*, 140. (h) Gakh, A. A. *Top. Heterocycl. Chem.* **2012**, *27*, 33.
11. Bucher, G.; Scaiano, J. C. *J.* Am. Chem. *Soc.* **1994**,*116*, 10076.
12. Lagow, R. T.; Margrave, J. L. *Prog. Inorg. Chem.* **1979**, *26*, 161.
13. (a) Rozen, S. *Acc. Chem. Res.* **2005,** *38*, 803.; (b) Rozen, S. *Acc. Chem. Res.* **1988**, *21***,** 307.
14. Rueda-Becerril, M.; Chatalova-Sazepin, C.; Leung, J. C. T.; Okbinoglu, T.; Kennepohl, P.; Paquin, J.-F.; Sammis, G. M. *J. Am. Chem. Soc.* **2012**, *134*, 4026.
15. (a) Burdon, J.; Parsons, I. W.; Tatlow, J. C. *Tetrahedron* **1972**, *28*, 43. (b) Chambers, R. D.; Clark, D.T.; Holmes, T.F.; Musgrave, W.K.R.; Ritchie, I. *J. Chem. Soc., Perkin Trans. 1* **1974**, 114.
16. Nagase, S. *Fluorine Chem. Rev.* **1967**, *1*, 77.
17. Bigelow, L. A. *Chem. Rev.* **1947**, *40*, 51.

18. Moissan, H.; Chavanne G. *C. R. Hebd. Seances Acad. Sci.***1905**, *140*, 407.
19. (a) Calfee, J. D.; Bigelow, L. A. *J. Am. Chem. Soc.* **1937**, *59*, 2072.; (b) Calfee, J. D.; Fukuhara, N.; Bigelow, L. A. *J. Am. Chem. Soc.* **1939**, *61*, 3552.; (c) Young, DeW. S.; Fukuhara, N.; Bigelow, L. A. *J. Am. Chem. Soc.* **1940**, *62*, 1171.
20. Hadley, E. H.; Bigelow, L. A. *J. Am. Chem. Soc.* **1940**, *62*, 3302.
21. Henne, A. L. *J. Am. Chem. Soc.* **1937**, *59*, 1200.
22. Miller, W. T. Jr.; Calfee, J. D.; Bigelow, L. A. *J. Am. Chem. Soc.* **1937**, *59*, 198.
23. (a) Bockemuller, W. *Justus Liebigs Ann. Chem.* **1933**, *506*, 20.; (b) Miller, W. T. Jr. *J. Am. Chem. Soc.* **1940**, *62*, 341.
24. Miller, W. T. Jr.; Koch, S. D. Jr. *J. Am. Chem. Soc.* **1957**, *79*, 3084.
25. (a) Bigelow, L. A.; Pearson, J. H.; Cook, L. B.; Miller, W. T. Jr. *J. Am. Chem. Soc.* **1933**, *55*, 4614.; (b) Tompson, R. Y.; Tarrant, P.; Bigelow, L. A. *J. Am. Chem. Soc.* **1946**, *68*, 2187. (c) Grakauskas, V. *J. Org. Chem.* **1969**, *34*, 2835.
26. Fukuhara, N.; Bigelow, L. A. *J. Am. Chem. Soc.* **1941**, *63*, 2792.
27. (a) Bigelow, L. A.; Pearson, J. H. *J. Am. Chem. Soc.* **1934**, *56*, 2773.; (b) Fukuhara, N.; Bigelow, L. A. *J. Am. Chem. Soc.* **1938**, *60*, 427.
28. (a) Lagow, R. J.; Margrave, J. L. *Proc. Natl. Acad. Sci.* **1970**, *67*, 4. (b) Lagow, R. J.; Margrave, J. L. *Chem. Eng. News* **1970**, 40.
29. For a review on fluorination using microreactors, see: Lob, P.; Lowe, H.; Hessel, V. *J. Fluorine Chem.* **2004**, *125*, 1677.
30. For selected examples see: (a) Moldavskii, D. D.; Bispen, T. A.; Kaurova, G. I.; Furin, G. G. *J. Fluorine Chem.* **1999**, *94*, 157.; (b) Chambers, R. D.; Joel, A. K.; Rees, A. J. *J. Fluorine Chem.* **2000**, *101*, 97.
31. For a review on the topic of perfluorination see: Kharitonov, A. P; Taege, R.; Ferrier, G.; Teplyakov, V. V.; Syrtsova, D. A.; Koops, G.-H. *J. Fluorine Chem.* **2005**, *126*, 251.
32. McEwan, W. E.; Guzikowski, A. P.; Wolf, A. P. *J. Fluorine Chem.* **1984**, *25*, 169.
33. Kharasch, M. S.; Brown, H. C. *J. Am. Chem. Soc.* **1940**, *62*, 925.
34. Barton, D. H. R.; Hesse, R. H.; Markwell, R. E.; Pechet, M. M.; Rozen S *J. Am. Chem. Soc.* **1976**, *98*, 3036.
35. (a) Purrington, S. T.; Kagen B. S.; Patrick, T. B. *Chem. Rev.* **1989**, *86*, 997. (b) Olah, G. A.; Chambers, R. D.; Prakash, G. K S. (eds) *Synthetic Fluorine Chemistry;* John Wiley & Sons: New York, 1992.
36. Grakauskas, V. *J. Org. Chem.* **1969**, *34*, 2443.
37. Rozen, S.; Hebel, D. *J. Org. Chem.* **1990**, *55*, 2621.
38. For a review on the Hunsdieker reaction, see: Johnson, R. G.; Ingham, R. K. *Chem. Rev.* **1956**, *56*, 219.
39. Marchionni, G.; Staccione, A.; Gregorio, G. *J. Fluorine Chem.* **1990**, *47*, 515.
40. Fukuhara, N.; Bigelow, L. A. *J. Am. Chem. Soc.* **1941**, *63*, 788.

41. (a) Chambers, R. D.; Spink, R. C. H. *Chem. Commun.* **1999**, *10*, 883.; (b) Chambers, R. D.; Holling, D.; Spink, R. C. H.; Sandford, G. *Lab Chip* **2001**, *1*, 132.
42. Chambers, R. D.; Fox, M. A.; Holling, D.; Nakano, T.; Okazoe, T.; Sandford, G. *Chem. Eng. Technol.* **2005**, *28*, 344.
43. Gal, C.; Rozen, S. *Tetrahedron Lett.* **1984**, *25*, 449.
44. Jahnisch, K.; Baerns, M.; Hessel, V.; Ehrfeld, W.; Haverkamp, V.; Lowe, H.; Wille, Ch.; Guber, A. *J. Fluorine Chem.* **2000**, *105*, 117.
45. de Mas, N.; Gunther, A.; Schmidt M. A.; Jensen, K. F. *Ind. Eng. Chem. Res.* **2003**, *42*, 698.
46. (a) Grakauskas, V. *J. Org. Chem.* **1970**, *35*, 723.; (b) Cacace, F.; Wolf, A. P. *J. Am. Chem. Soc.* **1978**, *100*, 3639.
47. Kellogg, K. B.; Cady, G. H. *J. Am. Chem. Soc.* **1948**, *70*, 3986.
48. (a) Barton, D. H. R.; Godinho, L. S.; Hesse, R. H.; Pechet, M. M. *Chem. Commun.* **1968**, 804. (b) Barton, D. H. R.; Ganguly, A.K.; Hesse, R. H.; Loo, S. N.; Pechet, M. M. *Chem. Commun.* **1968**, 806.
49. For reviews on CF_3OF, see: (a) Mukhametshin, F. M. *Russ. Chem. Rev.* **1980**, *49*, 668.; (b) Navarrini, W.; Tortelli, V.; Russo, A.; Corti. S. *J. Fluorine Chem.* **1999**, *95*, 27.; Francesco V.; Sansotera, M.; Navarrini W. *J. Fluorine Chem.* **2013**, *155*, 2.; and reference 10b.
50. Aymonino, P. J. *Photochem. Photobiol.* **1968**, *7*, 761.
51. Shoiket, A. A.; Teitelboim, M. A,; Vedneev, V. I. *Kinet. Katal.* **1983**, *24*, 225.
52. Wang, N.-Y.; Rowland, F. S. *J. Phys. Chem.* **1985**, *89*, 5154.
53. (a) dos Santos Afonso, M.; Schumacher, H. J. *Z. Phys. Chem.* **1988**,*158* ,15.; (b) dos Santos Afonso, M.; Czarnowski, J. *Z. Phys. Chem.* **1988**,*158* ,25.; (c) Czarnowski, Z.; Czarnowski, J. *J. Chem. Soc., Faraday Trans.* **1993**, *89*, 451. (d) Navarinni, W.; Russo, A.; Tortelli, V. *J. Org. Chem.* **1995**, 60, 6441.; (e) Conti, F.; Corvaja, C.; Cremonese, F. *J. Chem. Soc., Faraday Trans.* **1995** ,*91*, 3813.
54. Johri, K. K.; DesMarteau, D. D. *J. Org. Chem.* **1983**, 48, 242.
55. Porter, R. S.; Cady, G. H. *J. Am. Chem. Soc.* **1957**, *79*, 5625.
56. Allison, J. A. C.; Cady G. H. *J. Am. Chem. Soc.* **1959**, *81*, 1089.
57. dos Santos Afonso, M.; Schumacher, H. J. *Int. J. Chem. Kinet.* **1984**, *16* ,103
58. Sekiya A.; Ueda, K. *Chem. Lett.* **1990**, 609.
59. Di Loreto, H.; Czarnowski, J. *J. Fluorine Chem.* **1994**, *66*, 1.
60. Corvaja, C.; Cremonese, F.; Navarrini, W.; Tonelli, C.; Tortelli, V. *Tetrahedron Lett.* **1995**, *36*, 3543.
61. Levy, J. B.; Sterling, D. M. *J. Org. Chem.* **1985**, *50*, 5615.
62. Kollonitsch, J.; Barash, L; Doldouras, G. A. *J. Am. Chem. Soc.* **1970**, *92*, 7494.
63. For an account by Kollonitsch, see: Kollonitsch, J. *Isr. J. Chem.* **1978**, *17*, 53.
64. (a) Kollonitsch, J.; Barash, L; Kahan, F. M.; Kropp, H. *Nature* **1973**, *243*, 346.; (b) Kollonitsch, J.; Barash, L *J. Am. Chem. Soc.* **1976**, *98*, 5591.

65. Pragar, J. H.; Thompson, P G. *J. Am. Chem. Soc.* **1965**, *87*, 230.
66. (a) Hohorst, F. A.; Shreeve, J. M. *J. Am. Chem. Soc.* **1967**, *89*, 1809.; (b) Cauble, R. L.; Cady, G. H. *J. Am. Chem. Soc.* **1967**, *89*, 1962.
67. (a) Menefee, A.; Cady, G. H. *J. Am. Chem. Soc.* **1954**, *76*, 2020. (b) Steward, R. D.; Cady, G. H. *J. Am. Chem. Soc.* **1955**, *77*, 6110.
68. Barnette, W. E.; Wheland, R. C.; Middleton, W. J.; Rozen, S. *J. Org. Chem.* **1985**, *50*, 5698.
69. Visser, G. W. M.; Bakker, C. N. M.; Halteren, B. W.; Herscheid, J. D. M.; Brinkman, G. A.; Hoekstra, A. *Recl. Trav. Chim. Pays-Bas* **1986**, *105*, 214.
70. Rozen, S.; Lerman, O.; Kol, M. *J. Chem. Soc., Chem. Commun.* **1981**, 443.
71. Appelman, E. H.; Mendelsohn, M. H.; Kim, H. *J. Am. Chem. Soc.* **1985**, *107*, 6515.
72. Hebel, D.; Lerman, O.; Rozen, S. *J. Fluorine Chem.* **1985**, *30*, 141.
73. For reviews, see: Hesse. R. H. *Isr. J. Chem.* **1978**, *17*, 60.; reference 13 and reference 35a
74. (a) Visser, G. W. M.; von Halteren, B. W.; Herscheid, J. M. D.; Brinkman, G. A.; Hoekstra, A. *J. Chem. Soc., Chem. Commun.* **1984**, 655.; (b) Visser, G. W. M.; Boele, S.; von Halteren, B. W.; Knops, G. H. J. N.; Herscheid, J. M. D.; Brinkman, G. A.; Hoekstra, A. *J. Org. Chem.* **1986**, *51*, 1466.; (c) Visser, G. W. M.; Bakker, C. N. M.; von Halteren, B. W.; Herscheid, J. M. D.; Brinkman, G. A.; Hoekstra, A. *J. Org. Chem.* **1986**, *51*, 1886.; (d) Visser, G. W. M.; Herder, R. E.; de Kanter, F. J. J.; Herscheid, J. M. D. *J. Chem. Soc., Perkin Trans. 1* **1988**, 1203.
75. Williamson, S. M.; Cady, G. H. *Inorg. Chem.* **1962**, *1*, 673.
76. Williamson, S. M. *Inorg. Chem.* **1963**, *2*, 421.
77. Place, R. D.; Williamson, S. M. *J. Am. Chem. Soc.* **1968**, *90*, 2550.
78. (a) Weeks, J. L.; Chernick, C. L.; Matheson, M. S. *J. Am. Chem. Soc.* **1962**, *84*, 4612.; (b) Williamson, S. M.; Sladky, F. O.; Bartlett, N. *Inorg. Synth.* **1968**, *11*, 147.
79. For reviews on XeF_2, see: (a) Tius, M. A. *Tetrahedron* **1995**, *51*, 6605.; (b) Brel, V. K.; Pirkuliev, N. Sh.; Zefirov, N. S. *Russ. Chem. Rev.* **2001**, *70*, 231.
80. (a) Ramsden, C. A.; Smith, R. G. *J. Am. Chem. Soc.* **1998**, *120*, 6842.; (b) Ramsden, C. A.; Shaw, M. M. *Tetrahedron Lett.* **2009**, *50*, 3321.
81. Tamura, M.; Quan, H.-d.; Sekiya, A. *Eur. J. Org. Chem.* **1999**, 3151 and references therein.
82. Dukat, W. W.; Holloway, J. H.; Hope, E. G.; Townson, P. J.; Powell, R. L. *J. Fluorine Chem.* **1993**, *62*, 293.
83. (a) Patrick, T. B.; Johri, K. K.; White, D. H. *J. Org. Chem.* **1983**, *48*, 4158. (b) Patrick, T. B.; Johri, K. K.; White, D. H.; Bertrand, W. S.; Mokhtar, R.; Kilbourn, M. R.; Welch, M. J. *Can. J. Chem.* **1986**, *64*, 138.
84. Patrick, T. B.; Khazaeli, S.; Nadji, S.; Hering-Smith, K.; Reif, D. *J. Org. Chem.* **1993**, *58*¸705.
85. Vasdev, N.; Pointer, B. E.; Chirakal, R.; Schrobilgen, G. J. *J. Am. Chem. Soc.* **2002**, *124*, 12863.

86. For reviews on radical clocks, see: (a) Griller, D.; Ingold, K. U. *Acc. Chem. Res.* **1980**, *13*, 317.; (b) Newcomb, M. *Tetrahedron* **1993**, *49*¸1151.
87. Tanabe, Y.; Matsuo, N.; Ohno, N. *J. Org. Chem.* **1988**, *53*, 4582.; (b) Brel, V. K.; Uvarov, V. I.; Zefirov, N. S.; Stang, P. J.; Caple, R. *J. Org. Chem.* **1993**, *58*, 6922.; (c) Brel, V. K.; Koz'min, A. S.; Martynov, I. V.; Uvarov, V. I.; Zefirov, N. S.; Zhdankin, V. V.; Stang, P. J. *Tetrahedron Lett.* **1990**, *31*, 4799.
88. Gregorcic, A.; Zupan, M. *J. Org. Chem.* **1979**, *44*, 4120.
89. Lothlian, A. P.; Ramsden, C. A. *Synlett* **1993**, 753.
90. Bardin, V. V.; Frohn, H. J. *J. Fluorine Chem.* **1998**, *90*, 93.
91. Nongkunsarn, P.; Ramsden, C. A. *J. Chem. Soc., Perkin Trans. 1* **1996**, 121.
92. Lothlian, A. P.; Ramsden, C. A.; Shaw, M. M.; Smith, R. G. *Tetrahedron* **2011**, *67*¸ 2788.
93. Tsushima, T.; Kawada, K.; Tsuji, T. *Tetrahedron Lett.* **1982**, *23*, 1165.
94. Zajc, B.; Zupan, M. *J. Org. Chem.* **1982**, *47*, 573.
95. Differding, E.; Ruegg, G. M. *Tetrahedron Lett.* **1991**, *32*, 3815.
96. Zajc, B.; Zupan, M. *J. Chem. Soc., Chem Commun.* **1980**, 759.
97. Ramsden, C. A.; Smith, R. G. *Org. Lett.* **1999**, *1*, 1591.
98. (a) Cantrell, G. L.; Filler, R. *J. Fluorine Chem.***1985**, *27*, 35.; (b) Patrick, T. B.; Mortezania, R. *J. Org. Chem.* **1988**, *53*, 5153.; (c) Garrett, G. S.; Emge, T. J.; Lee, S. C.; Fischer, E. M.; Dyehouse K.; McIver, J. M. *J. Org. Chem.* **1991**, *56*, 4823.; and reference 93.
99. (a) Tselinskii, I. V.; Mel'nikov, A. A.; Varyagina, L G.; Trubitsin, A. E. *Zh. Org. Khim.* **1985**, *21*, 2490. (b) Tselinskii, I. V.; Mel'nikov, A. A.; Trubitsin, A. E. *Zh. Org. Khim.* **1987**, *23*, 1657. (c) Tselinskii, I. V.; Mel'nikov, A. A.; Trubitsin, A. E. *Zh. Org. Khim.* **1988**, *24*, 688.
100. Barker, T. J.; Boger, D. L. *J. Am. Chem. Soc.* **2012,** *134*, 13588.
101. (a) Bloom, S.; Pitts, C. R.; Miller, D. C.; Haselton, N.; Holl, M. G.; Urheim, E.; Lectka, T. *Angew. Chem., Int. Ed.* **2012,** *51*, 10580.; (b) Bloom, S.; Pitts, C. R.; Woltornist, R.; Griswold, A.; Holl, M. G.; Lectka, T. *Org. Lett.* **2013,** *15*, 1722.
102. Amaoka, Y.; Nagatomo, M.; Inoue, M. *Org. Lett.* **2013,** *15*, 2160.
103. Yin, F.; Wang, Z.; Li, Z.; Li, C. *J. Am. Chem. Soc.* **2012**, *134*, 10401.
104. Mizuta, S.; Stenhagen, I. S. R.; O'Duill, M.; Wolstenhulme, J.; Kirjavainen, A. K.; Forsback, S. J.; Tredwell, M.; Sandford, G.; Moore, P. R.; Huiban, M.; Luthra, S. K.; Passchier, J.; Solin, O.; Gouverneur, V. *Org. Lett.* **2013**, *15*, 2648.
105. Li, Z.; Song, L.; Li, C. J. Am. Chem. Soc. 2013, 135, 4640.
106. (a) Liu, W.; Huang, X.; Cheng, M.; Nielsen, R. J.; Goddard, W. A., III; Groves, J. T. *Science* **2012,** *337*, 1322.; (b) Liu, W.; Groves, J. T. *Angew. Chem., Int. Ed.* **2013**, *52*, 6024.
107. Liu, W.; Groves, J. T. *J. Am. Chem. Soc.* **2010**, 132, 12847.
108. (a) Nyffeler, P. T.; Duron, S. G.; Burkart, M. D.; Vincent, S. P.; Wong, C.-H. *Angew. Chem. Int. Ed.* **2004**, *43*, 192.; (b) Singh, R. P.; Shreeve, J. M. *Acc. Chem. Res.* **2004**, *37*, 31.
109. Differding, E.; Ofner, H. *Synlett* **1991**, 187.

110. (a) Girina, G. P.; Fainzil'berg, A. A.; Feoktistov, L. G. *Russ. J. Electrochem.* **2000**, *36*, 162.; (b) Gilicinski, A. G.; Pez, G. P.; Syvret, R. G.; Lal, G. S. *J. Fluorine Chem.* **1992**, *59*, 157.; (c) Differding, E.; Bersier, P., M. *Tetrahedron* **1992**, *48*, 1595.
111. Vincent, S. P.; Burkart, M. D.; Tsai, C.-Y.; Zhang, Z.; Wong, C.-H. *J. Org. Chem.* **1999**, *64*, 5264.
112. (a) R. E. Banks, S. N. Mohialdin-Khaffa, G. S. Lal, I. Sharif, R. G. Syvret, *J. Chem. Soc., Chem. Commun.* **1992**, *8*, 595.; (b) Hart. J. J.; Syvret, R. G. *J. Fluorine Chem.* **1999**, *100*, 157.
113. Banks, R. E.; Sharif, I.; Pritchard, R. G. *Acta Cryst.***1993**, *C49*¸ 492.
114. McKinney, T. M.; Geske, D. H. *J. Am. Chem. Soc.* **1965**, *87*, 3013.
115. Hoffmann, R.; Imamura, A.; Hehre, W. J. *J. Am. Chem. Soc.* **1968**, *90*, 1499.
116. Wolfe, S.; Shi, Z.; Brion, C. E.; Rolke, J.; Zheng, Y.; Cooper, G.; Chong, D. P.; Hu, C. Y. *Can. J. Chem.* **2002**, *80*, 222.
117. (a) Piana, S.; Devillers, I.; Togni, A.; Rothlisberger, U. *Angew. Chem. Int. Ed.* **2002**, *41*, 979.; (b) Zhang, X.; Wang, H.; Gou, Y. *Rapid Commun. Mass Spectrom.* **2006**, *20*, 1877.
118. Syvret, R. G.; Butt, K. M.; Nguyen, R. P.; Bulleck, V. L; Rieth, R. D. *J. Org. Chem.* 2002, 67, 4487.
119. Liu, J.; Wong, C.-H. *Tetrahedron Lett.* 2002, *43*, 4037.
120. Banks, R. E.; Lawrence, N. J.; Popplewell, A. L. *Synlett* **1994**, 831.
121. Darwent, B. deB. *Bond dissociation energies in simple molecules;* National Bureau of Standards: Washington D. C, 1970. (NSRDS-NBS 31)
122. (a) Czarnowski, J.; Schumacher, H. J. *Z. Phys. Chem.* **1970**,73, 68.; (b) Kennedy, R. C.; Levy, J. B. *J. Phys. Chem.* **1972**, *76*, 3480.
123. Neese, F. *ORCA-An Ab Initio, Density Functional and Semiempirical Program Package* (v. 2.80); Universitat Bonn: Bonn, Germany, 2011.
124. (a) Perdew, J. P. *Phys. Rev. B.* **1986**, *33*, 8822.; (b) Perdew, J. P. *Phys. Rev. B* **1986**, *34*, 7406.; (c) Becke, A. D. *Phys. Rev. A.* **1988**, *38*, 3098.
125. Schafer, A.; Huber, C.; Ahlrichs, R. *J. Chem. Phys.* **1994**, *100*, 5829.
126. Klamt, A., Schurmann, G. *J. Chem. Soc., Perkin Trans.* **1993**, *2*, 799.
127. Neese, F. *ORCA-An Ab Initio, Density Functional and Semiempirical Program Package* (v. 2.90); Universitat Bonn: Bonn, Germany, 2012.
128. Olsen, J. F. *J. Fluorine Chem.* **1977**, *9*, 471.
129. Diodati, F. P.; Bartell, L. S. *J. Molec. Struct.* **1971**, *8*, 395.
130. Czarnowski, J.; Castellano, E.; Schumacher, H. J. *Chem Commun.* **1968**, 1255.
131. Banks, R. E.; Besheesh, M. K.; Pritchard, R. G. *Acta Cryst.***2003**, *C59*¸ m141.
132. Fraenk, W.; Klapotke, T. M.; Banks, R. E.; Besheesh, M. K. *J. Fluorine Chem.* **2001**, *108*, 87.
133. (a) Walling, C.; Waits, H. P.; Milovanovic, J.; Pappiaonno, C. G. *J. Am. Chem. Soc.* **1970**, *92*, 4927.; (b) Sanchez, J.; Myers, T. N. *Peroxides and Peroxide Compounds, Organic Peroxides*.

In Kirk-Othmer Encyclopedia of Chemical Technology, vol. 18. John Wiley & Sons: New York, 2000.
134. For reviews on radical atom transfer, see: (a) Curran, D. P. *Synthesis* **1988**, *7*, 489.; (b) Clark, A. J. *Chem. Soc. Rev.* **2002**, *31*, 1.; (c) Pintauer, T.; Matyjaszewski, K. *Chem. Soc. Rev.* **2008**, *37*, 1087.
135. (a) Walling, C.; Wagner, P. J. *J. Am. Chem. Soc.* **1964**, *86*, 3368.; (b) Bacha, J. D.; Kochi, J. K. *J. Org. Chem.* **1965**, *30*, 3272.
136. Borodkin, G. I.; Shubin, U. G. *Russ. Chem. Rev.* **2010**, *79*, 259.
137. Cramer, J. A.; Rowland, F. S. *J. Am. Chem. Soc.* **1974**, *96*, 6579.
138. Pratsch, G.; Heinrich, M. R. *Top. Curr. Chem.* **2012**, *320*, 33 and references therein.
139. Serguchev, Yu. A.; Beletskaya, I. P. *Russ. Chem. Rev.* **1980**, *49*, 1119.
140. Anslyn, E. V.; Dougherty, D. A. *Modern Physical Organic Chemistry*; University Science Books: Sausalito, CA, 2000.
141. Chateauneuf, J.; Lusztyk, J.; Ingold, K. U. *J. Am. Chem. Soc.* **1988**, *110*, 2886.
142. Hilborn, J. W.; Pincock, J. A. *J. Am. Chem. Soc.* **1991**, *113*, 2683.
143. RajanBabu, T. V.; Gagosz, F. *Dibenzoyl peroxide* In Encyclopedia of reagents for organic synthesis, John Wiley & Sons: New York, 2005. DOI: 10.1002/047084289X.rd022.pub2
144. Hammond, G. S. *J. Am. Chem. Soc.* **1950**, *72*, 3737.; (b) Hammond, G. S.; Soffer, L. M. *J. Am. Chem. Soc.* **1950**, *72*, 4711.
145. Dou, H. J. M.; Lynch, B. M. *Tetrahedron Lett.* **1965**, *14*, 897.
146. Allen, K. J.; Bolton, R.; Williams, G. H. *J. Chem. Soc., Perkin Trans. 2* **1983**, 691.
147. Walling, C. *Tetrahedron* **1985**, *41*, 3887.
148. For reviews on dediazoniation of aryldiazoniums, see: (a) Galli, C. *Chem. Rev.* **1988**, *88*, 765-792.; (b) Heinrich, M. R. *Chem. Eur. J.* **2009**, *15*, 820.
149. Sandmeyer, T. *Ber. Dtsch. Chem. Ges.* **1884**, *17*, 1633.
150. For a review on the Sandmeyer reaction, see: Hodgson, H. H. *Chem. Rev.* **1947**, *40*, 251.
151. Balz, G.; Schiemann, G. *Ber.* **1927**, *60*, 1186.
152. Flood, D. T. *Org. Syn. Coll.* **1943**, *2*, 295.
153. Griess. J. P. *Ann. Chem.* **1866**, *137*, 67.
154. Gulliver, D. J.; Levason, W.; Webster. W. *Inorg. Chim. Acta* **1981**, *52*, 153.
155. Zlotorzynska, M.; Sammis, G. M. *Org. Lett.* **2011**, *13*, 6264.
156. Abramovitch, R. A.; Robson, A. *J. Chem. Soc. C* **1967**, 1101.
157. Filimonov, V. D.; Trusova, M.; Postnikov, P.; Krasnokutskaya, E. A.; Lee, Y. M.; Hwang, H. Y.; Kim, H.; Chi, K.-W. *Org. Lett.* **2008**, *10*, 3961.
158. (a) Demir, A. S.; Reis, O.; Emrullahoglu, M. *J. Org. Chem.* **2003**, *68*, 578.; (b) Demir, A. S.; Findik, H.; Saygili, N.; Subasi, N. T. *Tetrahedron* **2010**, *66*, 1308.
159. Guchhait, S. K.; Kashyap, M.; Saraf, S. *Synthesis* **2010**, *7*, 1166.

160. (a) Lockner, J. W.; Dixen, D. D.; Risgaard, R.; Baran, P. S. *Org. Lett.* **2011**, *13*, 5628.; (b) Wang, J.; Wang, S.; Wang, G.; Zhang, J.; Yu, X.-Q. *Chem. Commun.* **2012**, *48*, 11769.
161. Dickschat, A.; Studer, A. *Org. Lett.* **2010**, *12*, 3972.
162. Petasis, N. A.; Yudin, A. K.; Zavialov, I. A.; Prakash, G. K. S.; Olah, G. A. *Synlett* **1997**, 606.
163. Cazorla, C.; Metay, E.; Andrioletti, B.; Lemaire, M. *Tetrahedron Lett.* **2009**, *50*, 3936.
164. Sun, A. D. *Doctoral dissertation*, University of British Columbia: 2013.
165. Neese, F.; Wennmohs, F.; Hansen, A.; Becker, U. *Chem. Phys.* **2009**, *356*, 98.
166. (a) Leroux, F. R.; Jeschke, P.; Schlosser, M. *Chem. Rev.* **2005**, *105*, 827.; (b) Leroux, F. R.; Manteau, B.; Vors, J.; Pazenok, S. *Beilstein J. Org. Chem.* **2008**, *4*. doi:10.3762/bjoc.4.13.; (c) Hu, J.; Huang, W.; Wang, F. *Chem. Commun.* **2009**, 7465.
167. Prakash, G. K. S.; Ledneczki, I.; Chacko, S.; Olah, G. A. *Org. Lett.* **2008**, *10*, 557.
168. Zhang, M.-R.; Ogawa, M.; Furutsuka, K.; Yoshida, Y.; Suzuki, K. *J. Fluorine Chem.* **2004**, *125*, 1879.
169. (a) Zhang, M.-R.; Haradahira, T.; Maeda, J.; Okauchi, T.; Kida, T.; Obayashi, S.; Suzuki, K.; Suhara, T. *J. Labelled Compd. Radiopharm.* **2002**, *45*, 857.; (b) Zhang, M.-R.; Maeda, J.; Furutsuka, K.; Yoshida, Y.; Ogawa, M.; Suhara, T.; Suzuki, K. *Bioorg. Med. Chem. Lett.* **2003**, *13*, 201.; (c) Zhang, M.-R.; Maeda, J.; Ito, T.; Okauchi, T.; Ogawa, M.; Noguchi, J.; Suhara, T.; Halldin, C.; Suzuki, K. *Bioorg. Med. Chem.* **2005**, *13*, 1811.; (d) Hamill, T. G.; Burns, H. D. *J. Labelled Compd. Radiopharm.* **2004**, *47*, 99.; (e) Hamill, T. G.; McCauley, J. A.; Burns, H. D. *J. Labelled Compd. Radiopharm.* **2005**, *48*, 1.; (f) Donohue, S. R.; Halldin, C.; Pike, V. W. *Bioorg. Med. Chem.* **2006**, *14*, 3712.; (g) Chin, F. T.; Morse, C. L.; Shetty, H. U.; Pike, V. W. *J. Labelled Compd. Radiopharm.* **2006**, *49*, 17.
170. For seminal work on difluoromethyl carbene insertion into phenols, see: Miller, T. G.; J. W. Thanassi, J. W. *J. Org. Chem.* **1960**, *25*, 2009.
171. For selected examples, see: (a) Fuchibe, K.; Koseki, Y.; Aono, T.; Sasagawa, H.; Ichikawa, J. *J. Fluorine Chem.* **2012**, *133*, 52 (and references therein).; (b) Sperry, J. B.; Sutherland, K. *Org. Process Res. Dev.* **2011**, *15*, 721.; (c) Zafrani, Y.; Sod-Moriah, G.; Segall, Y. *Tetrahedron* **2009**, *65*, 5278.; (d) Wang, F.; Huang, W.; Hu, J. *Chin. J. Chem.* **2011**, *29*, 2717 (and references therein).
172. For selected examples see: (a) Guay, D.; Hamel, P.; Blouin, M.; Brideau, C.; Chan, C. C.; Chauret, N.; Ducharme, Y.; Huang, Z.; Girard, M.; Jones, T. R.; Laliberte, F.; Masson, P.; McAuliffe, M.; Piechuta, H.; Silva, J.; Young, R. N.; Girard, Y. *Bioorg. Med. Chem. Lett.* **2002**, *12*, 1457.; (b) Zheng, S.; Kaur, G.; Wang, H.; Li, M.; Macnaughtan, M.; Yang, X.; Reid, S.; Prestegard, J.; Wang, B.; Ke, H. *J. Med. Chem.* **2008**, *51*, 7673.; (c) Hartz, R. A.; Ahuja, V. T.; Rafalski, M.; Schmitz, W. D.; Brenner, A. B.; Denhart, D. J.; Ditta, J. L.; Deskus, J. A.; Yue, E. W.; Arvanitis, A. G.; Lelas, S.; Li, Y-W.; Molski, T. F.; Wong, H.; Grace, J. E.; Lentz, K. A.; Li, J.; Lodge, N. J.; Zaczek, R.; Combs, A. P.; Olson, R. E.; Mattson, R. J.; Bronson, J. J.; Macor, J. E. *J. Med. Chem.* **2009**, *52*, 4161.

173. (a) Stavber, S.; Koren, Z.; Zupan, M. *Synlett* **1994**, 265.; (b) Tamura, M.; Takagi, T.; Quan, H-D.; Sekiya, A. *J. Fluorine Chem.* **1999**, *98*, 163.
174. Ochiai, M.; Yoshimura, A.; Hoque, Md. M.; Okubo, T.; Saito, M.; Miyamoto, K. *Org. Lett.* **2011**, *13*, 5568.
175. (a) Kuroboshi, M.; Suzuki, K.; Hiyama, T. *Tetrahedron Lett.* **1992**, *33*, 4173.; (b) Kanie, K.; Tanaka, Y.; Suzuki, K.; Kuroboshi, M.; Hiyama, T. *Bull. Chem. Soc. Jpn.* **2000**, *73*, 471.
176. Huang, C.; Liang, T.; Harada, S.; Lee, E.; Ritter, T. *J. Am. Chem. Soc.* **2011**, *133*, 13308.
177. Navarrini, W.; Tortelli, V.; Zedda, A. *J. Fluorine Chem.* **1992**, *58*, 143.
178. For reviews on hypervalent iodine reagents, see: (a) Varvoglis, A. *Chem. Soc. Rev.* **1981**, 377.; (b) Wirth, T., Ed. *Hypervalent iodine compounds*; Topics in Current Chemistry 224; Springer-Verlag: New York, 2003.; (c) Zhdankin, V. V.; Stang, P. J. *Chem. Rev.* **2008**, *108*, 5299.
179. Concepcion, J. I.; Francisco, C. G.; Freire, R.; Hernandez, R.; Salazar, J. A.; Suarez, E. *J. Org. Chem.* **1986**, *51*, 403.
180. (a) Togo, H.; Aoki, M.; Yokoyama, M. *Chem. Lett.* **1992**, 2169.; (b) Togo, H.; Aoki, M.; Yokoyama, M. *Tetrahedron.* **1993**, *49*, 8241.
181. Sutherland, A.; Vederas, J. C. *Chem. Commun.* **2002**, 224.
182. Dohi, T.; Takenaga, N.; Goto, A.; Maruyama, A.; Kita, Y. *Org. Lett.* **2007**, *9*, 3129.
183. For reviews on photodecarboxylation, see: (a) Budac, D.; Wan, P. *J. Photochem. Photobiol. A: Chem.* **1992**, *67*, 135.; (b) Griesbeck, A. G. *Chimia* **1998**, *52*, 272-283.
184. Turro, N. J. *Modern Molecular Photochemistry;* University Science Books: 1991.
185. For reviews on photoinduced electron transfer, see: (a) Mattay, J.; Eaton, D. F., Eds. *Photoinduced Electron Transfer Volume 1*; Topics in Current Chemistry 156; Springer-Verlag: New York, 1990. (b) Mattay, J., Ed. *Photoinduced Electron Transfer Volume 5*; Topics in Current Chemistry 168; Springer-Verlag: New York, 1993.; (c) Prier, C. K.; Rankic, D. A.; MacMillan, D. W. C. *Chem. Rev.* **2013**, *113*, 5322.
186. Joschek, H.-I.; Grossweiner, L. I. *J. Am. Chem. Soc.* **1966**, *88*, 3261.
187. Epling, G. A.; Lopes, A. *J. Am. Chem. Soc.* **1977**, *99*, 2700.
188. Gilbert, B. C.; Scarratt, C. J.; Thomas, B.; Young, J *J. Chem. Soc., Perkin Trans. 2* **1987**, 371.
189. Bietti, M.; Capone, A. *J. Org. Chem.* **2004**, *69*, 482.
190. (a) Davidson, R. S.; Steiner, P. R. *Chem Commun.* **1971**, 1115.; (b) Davidson, R. S.; Harrison, K.; Steiner, P. R. *J. Chem. Soc. C* **1971**, 3480.
191. (a) Davidson, R. S.; Steiner, P. R. *J. Chem. Soc. C* **1971**, 1682.; (b) Davidson, R. S.; Steiner, P. R. *J. Chem. Soc., Perkin Trans. 2* **1972**, 1357.
192. Bowers, P. R.; McLauchlan, K. A.; Sealy, R. C. *J. Chem. Soc., Perkin Trans. 2* **1976**, 915.
193. Kavarnos, G. J.; Turro, N. J. *Chem. Rev.* **1986**, *86*, 401.
194. Singh, R. P.; Shreeve, J. M. *Chem. Commun.* **2001**, 1196.
195. Carroll, F. A.; Quina, F. H. *J. Am. Chem. Soc.* **1972**, *94*, 6246.
196. http://www.rayonet.org/graphscharts.htm (retrieved on September 5, 2013).

197. Linstrom, P. J.; Mallard, W. G. Eds., *NIST Chemistry WebBook, NIST Standard Reference Database Number 69*, National Institute of Standards and Technology, http://webbook.nist.gov, (retrieved September 30, 2013).
198. Yoon, U. C.; Mariano, P. S. *Acc. Chem. Res.* **200l**, *34*, 523.
199. Bard, A. J.; Parsons, R.; Jordan, J. *Standard potentials in aqueous solution;* CRC press: 1985; Vol. 6.; and reference 6a.
200. For a review on the Strecker degradation, see: Schonberg, A.; Moubasher, R. *Chem. Rev.* **1952**, *50*, 261.
201. (a) Becke, A. D. *J. Chem. Phys.* **1993**, *98*, 5648. (b) Lee, C.; Yang, W.; Parr, R. G. *Phys. Rev. B: Condens. Matter* **1988**, *37*, 785.
202. For reviews on alkoxyl radicals see: (a) Walling, C. *Pure Appl. Chem.* **1967**, *15*, 69-80.; (b) Brun, P.; Waegell, B. In *Reactive Intermediates*, Vol 3; Abramovitch, R. A. Ed.; Plenum Press: New York, 1983, 367.; (c) Hartung, J. In *Radicals in Organic Synthesis*, Vol. 2; Renaud, P.; Sibi, M. P., Eds.; Wiley-VCH: New York, 2001, 425.; (d) Suarez, E.; Rodriguez, M. S. *ibid*, 440.; (e) Hartung, J. *Eur. J. Org. Chem.* **2001**, 619.; (f) Hartung, J.; Gottwald, T.; Špehar, K. *Synthesis*. **2002**, 1469.; (g) Cekovic, Z. *J. Serb. Chem. Soc.* **2005**, *70*, 287-318.
203. De Vleeschouwer, F.; Van Speybroeck, V.; Waroquier, M.; Geerlings, P.; De Proft, F. *Org. Lett.* **2007**, *9*, 2721.
204. For reviews on alkoxyl fragmentation, see: Dowd, P.; Zhang, W. *Chem. Rev.* **1993**, *93*, 2091.; and reference 202d
205. Ziegler, F. E.; Petersen, A. K. *J. Org. Chem.* **1995**, *60*, 2666.
206. For reviews on internal hydrogen atom transfer, see: (a) Majetich, G.; Wheless, K. *Tetrahedron* **1995**, *51*, 7095.; (b) Robertson, J.; Pillai, J.; Lush, R. K. *Chem. Soc. Rev.* **2001**, *30*, 94.; (c) Cekovic, Z. *Tetrahedron* **2003**, *59*, 8073.; (d) Sperry, J.; Liu, Y.-C. (W.); Brimble, M. A. *Org. Biomol. Chem.* **2010**, *8*, 29.; (e) Tsunoi, S.; Ryu, I.; Okuda, T.; Tanaka, M.; Komatsu, M.; Sonoda. N. *J. Am. Chem. Soc.* **1998**, *120*, 8692 and reference therein; and reference 202g.
207. For selected examples, see: (a) Micovic, V. M.; Mamuzic, R. I.; Jeremic, D.; Mihailovic, M. Lj. *Tetrahedron* **1964**, *20*, 2279 and references therein.; (b) Mihailovic, M. Lj.; Jakoljevic, M.; Cekovic, Z. *Tetrahedron* **1969**, *25*, 2269.; (c) Bertrand, M. P.; Surzur, J. M.; Boyer, M.; Mihailovic, M. Lj. *Tetrahedron* **1979**, *35*, 1365.; and reference 206e.
208. Clerici, A.; Minisci, F.; Ogawa, K.; Surzur, J. M. *Tetrahedron Lett.* **1978**, 1149.
209. For a review, see: Ho, T. L. In *Organic Synthesis by Oxidation with Metal Compounds*; Mijs, W. J.; De Jong, C. R. H. I., Eds.; Plenum Press: New York, **1986**, 569.
210. Courtneidge, J. L.; Lusztyk, J.; Page, D. *Tetrahedron Lett.* **1994**, *35*, 1003.
211. For a review, see: Kalvoda, J.; Heusler, K. *Synthesis* **1971**, 501.
212. For selected examples, see: (a) Akhtar, M.; Barton, D. H. R. *J. Am. Chem. Soc.* **1964**, *86*, 1528. (O-I, but also OBr).; (b) Mihailovic, M. Lj.; Cekovic, Z.; Stankovic, J. *J. Chem. Soc.*,

Chem. Commun. **1969**, 981.; (c) Sneen, R. A.; Matheny, N. P. *J. Am. Chem. Soc.* **1969**, *86*, 3905.; (d) Sneen, R. A.; Matheny, N. P. *J. Am. Chem. Soc.* **1969**, *86*, 5503.; (e) Walling, C.; Padwa, A. *J. Org. Chem.* **1962**, *27*, 2976.

213. For selected examples, see: (a) Walling, C; Padwa, A. *J. Am. Chem. Soc.* **1961**, *83*, 2207.; (b) Walling, C; Padwa, A. *J. Am. Chem. Soc.* **1963**, *85*, 1593.; (c) Walling, C; Padwa, A. *J. Am. Chem. Soc.* **1963**, *85*, 1597.; (d) Walling, C.; Bristol, D. *J. Org. Chem.* **1972**, *37*, 3514. (e) Cekovic, Z.; Djokic, G. *Tetrahedron* **1981**, *37*, 4263.
214. For an account of his discovery, see: Barton, D. H. R. *Pure Appl. Chem.* **1968**, *16*, 1.
215. Francisco, C. G.; Leon, E. I.; Moreno, P.; Suarez, E. *Tetrahedron: Asymmetry* **1998**, *9*, 2975 and references therein.
216. (a) Barton, D. H. R.; Blundell, P.; Jaszberenyi, J. C. *Tetrahedron Lett.* **1989**, *30*, 2341.; (b) Kim, S.; Lee, T. A.; Song, Y. *Synlett* **1998**, 471-472.
217. Beckwith, A. L. J.; Hay, B. P. *J. Am. Chem. Soc.* **1988**, *110*, 4415.
218. (a) Hartung, J.; Schwarz, M. *Synlett* **1997**, 848.; (b) Hartung, J.; Kneuer, R.; Schwarz, M; Svoboda, I.; Feuss, H. *Eur. J. Org. Chem.***1999**, 97.; (c) Hartung, J.; Schwarz, M; Svoboda, I.; Feuss, H.; Duarte M.-T. *Eur. J. Org. Chem.***1999**, 1275.
219. (a) Beckwith A. L. J.; Hay, B. P; Williams, G. M. *Chem. Commun.* **1989**, 1202.; (b) Pasto, D. J.; Cottard, F *Tetrahedron Lett.* **1994**, *35*, 4303.
220. (a) Petrovic, G.; Cekovic, Z. *Tetrahedron Lett.* **1997**, *38*, 627. (b) Petrovic, G.; Cekovic, Z. *Tetrahedron* **1999**, *55*, 1377.
221. Surzur, J.-M.; Bertrand, M.-P.; Nouguier, R. *Tetrahedron Lett.* **1969**, *48*, 4197.
222. (a) Rieke, R. D.; Moore, N. D. *Tetrahedron Lett.* **1969**, *25*, 2035.; (b) Rieke, R. D.; Moore, N. D. *J. Org. Chem.* **1972**, *37*, 314.
223. Hartung, J.; Gallou, F. *J. Org. Chem.* **1995**, *60*, 6706.
224. (a) Johns, A.; Murphy, J. A. *Tetrahedron Lett.* **1988**, *29*, 837. (b) Gash, R. C.; MacCorquodale, F.; Walton, J. C. *Tetrahedron* **1989**, *45*, 5531.
225. Barton, D. H. R.; McCombie, S. W. *J. Chem. Soc., Perkin Trans. 1* **1975**, *16*, 1574.
226. Zlotorzynska, M.; Zhai, H.; Sammis, G. M. *Org. Lett.* **2008**, *10*, 5083.
227. (a) Beckwith, A. L. J.; Schiesser, C. H. *Tetrahedron Lett.* **1985**, *26*, 373.; (b) Beckwith, A. L. J.; Schiesser, C. H. *Tetrahedron* **1985**, *41*, 3925.; (c) Spellmeyer, D. C.; Houk, K. N. *J. Org. Chem.* **1987**, *52*, 959.
228. Hartung, J.; Daniel, K.; Rummey, C.; Bringmann, G. *Org. Biomol. Chem.* **2006**, *4*, 4089.
229. Hartung, J.; Gottwald, T. *Tetrahedron Lett.* **2004**, *45*, 5619.
230. Beesley, R. M.; Ingold, C. K.; Thorpe, J. F. *J. Chem. Soc., Trans.* **1915**, *107*, 1080.
231. Gonzalez, C. C.; Kennedy, A. R.; Leon, E. I.; Riesco-Fagundo, C.; Suarez, E. *Angew. Chem. Int. Ed.* **2001**, *40*, 2326.
232. Beckwith, A. L. J.; Kazlauskas, R.; Syner-Lyons, M. R. *J. Org. Chem.* **1983**, *48*, 4718.

233. Beckwith was not the first to make this observation, see also: (a) Holmquist, H. E.; Rothrock, H. S.; Theobald, C. W.; Englund, B. E. *J. Am. Chem. Soc.* **1956**, *78*, 5339. (b) Macdonald, T. L.; O'Dell, D. E. *J. Org. Chem.* **1981**, *46*, 1501.
234. Barton, D. H. R.; Hay Motherwell, R. S.; Motherwell, W. B. *J. Chem. Soc., Perkin Trans. 1* **1981**, 2363.
235. Kim, S.; Lee, S. *Tetrahedron Lett.* **1991**, *32*, 6575.
236. (a) Dowd, P.; Choi, S.-C. *J. Am. Chem. Soc.* **1987**, *109*, 3493.; (b) Dowd, P.; Choi, S.-C. *J. Am. Chem. Soc.* **1987**, *109*, 6548.
237. (a) Beckwith, A. L. J.; O'Shea, D. M.; Gerba, S.; Westwood, S. W. *J. Chem. Soc., Chem. Commun.* **1987**, 666.; (b) Beckwith, A. L. J.; O'Shea, D. M.; Westwood, S. W. *J. Am. Chem. Soc.* **1988**, *110*, 2565
238. (a) Dowd, P.; Choi, S.-C. *Tetrahedron Lett.* **1989**, *30*, 6129.; (b) Dowd, P.; Choi, S.-C. *Tetrahedron* **1991**, *27*, 4847.
239. Nishida, A.; Takahashi, H.; Takeda, H.; Takada, N.; Yonemitsu, O. *J. Am. Chem. Soc.* **1990**, *112*, 902.
240. (a) Dorigo, A. E.; Houk, K. N. *J. Am. Chem. Soc.* **1987**, *109*, 2195.; (b) Dorigo, A. E.; Houk, K. N. *J. Org. Chem.* **1988**, *53*, 1650.
241. Barton, D. H. R.; Beaton, J. M.; Geller, L. E.; Pechet, M. M. *J. Am. Chem. Soc.* **1960**, *82*, 2640.
242. (a) Barton, D. H. R.; Beaton, J. M. *J. Am. Chem. Soc.* **1960**, *82*, 2641.; (b) Barton, D. H. R.; Beaton, J. M.; Geller, L. E.; Pechet, M. M. *J. Am. Chem. Soc.* **1961**, *83*, 4076.
243. For a comprehensive list, see: Table 2 in reference 206c.
244. For a review, see: Wolff, M. E. *Chem. Rev.* **1963**, *63*, 55.
245. (a) Mihailovic, M. Lj.; Cekovic, Z.; Maksimovic, Z.; Jeremic, D.; Lorenc, Lj.; Mamuzic, R. I. *Tetrahedron* **1965**, *21*, 2799.; (b) Concepcion, J. I.; Francisco, C. G.; Hernandez, R.; Salazar, J. A.; Suarez, E. *Tetrahedron Lett.* **1984**, *25*, 1953.; (c) de Armas, P.; Concepcion, J. I.; Francisco, C. G.; Hernandez, R.; Salazar, J. A.; Suarez, E. *J. Chem. Soc., Perkin Trans. 1* **1989**, 405.; (d) Dorta, R. L.; Martin, A.; Salazar, J. A.; Suarez, E. *Tetrahedron Lett.* **1996**, *37*, 6021.; (e) Francisco, C. G.; Freire, R.; Herrera, A. J.; Perez-Martin, I.; Suarez, E. *Org. Lett.* **2002**, *4*, 1959.
246. (a) Meilert, K.; Brimble, M. A. *Org. Lett.* **2005**, *7*, 3497.; (*b*) Meilert, K.; Brimble, M. A. *Org. Biomol. Chem.*, 2006, **4**, 2184‑2192.
247. Tsunoi, S.; Ryu, I.; Sonoda, N. *J. Am. Chem. Soc.* **1994**, *116*, 5473.; and reference 206e.
248. Martin, A.; Perez-Martin, I.; Quintanal, L. M.; Suarez, E. *Tetrahedron Lett.* **2008**, *49*, 5179.
249. Cekovic, Z.; Ilijev, D. *Tetrahedron Lett.* **1988**, *29*, 1441.
250. Rawal, V. H.; Newton, R. C.; Krishnamurthy, V. *J. Org. Chem.* **1990**, *55*, 5181.
251. Rawal, V. H.; Iwasa, S. *Tetrahedron Lett.* **1992**, *33*, 4687.

252. Rawal, V. H.; Krishnamurthy, V. *Tetrahedron Lett.* **1992**, *33*, 3439.
253. Kim, S.; Koh, J. S.. *Tetrahedron Lett.* **1992**, *33*, 7391.
254. Kim, S.; Koh, J. S.. *J. Chem. Soc., Chem Commun.* **1992**, 1377.
255. Rawal, V. H.; Krishnamurthy, V.; Fabre, A. *Tetrahedron Lett.* **1993**, *34*, 2899.
256. Horner, J. H.; Choi, S.-Y.; Newcomb, M. *Org. Lett.* **2000**, *2*, *3369*.
257. Scaiano, J. C. *J. Am. Chem. Soc.* **1980**, *102*, 5400.
258. Rueda-Becerril, M.; Leung, J. C. T.; Dunbar, C. R.; Sammis, G. M. *J. Org. Chem.* **2011**, *76*, 7720.
259. For kinetic studies on 1, 2 migration, see: (a) Newcomb, M.; Glenn, A. G.; Williams, W. G. *J. Org. Chem.***1989**, *54*, 2675.; (b) Beckwith, A. L. J.; Bowry, V. W. *J. Org. Chem.***1989**, *54*, 2681.
260. Zhu, H.; Wickenden, J. G.; Campbell, N. E.; Leung, J. C. T.; Johnson, K. M.; Sammis, G. M. *Org. Lett.* **2009**, *11*, 2019.
261. Zhu, H. *Doctoral dissertation*, University of British Columbia: 2013.
262. Differding, E.; Wehrli, M. *Tetrahedron Lett.* **1991**, *32*, 3819.
263. Yamada, S.; Gavryushin, A.; Knochel, P. *Angew. Chem. Int. Ed.* **2010**, *49*, 2215.
264. Ochiai, M.; Yoshimura, A.; Miyamoto, K. *Tetrahedron Lett.* **2009**, *50*, 4792.
265. Leung, J. C. T.; Chatalova-Sazepin, C.; West, J. G.; Rueda-Becerril, M; Paquin, J.-F.; Sammis, G. M. *Angew. Chem. Int. Ed.* **2012**, *51*, 10804.
266. Zhang, W.; Zhu, L.; Hu, J. *Tetrahedron* **2007**, *63*, 10569.
267. Katzenellenbogen, J. A.; Myers, H. N.; Johnson, H. J. Jr. *J. Org. Chem.* **1973**, *38*, 3525.
268. Kropp, P. J.; Fryxell, G. E.; Tubergen, M. W.; Hager, M. W.; Harris, G. D. Jr.; McDermott, T. P. Jr.; Tornero-Velez, R. *J. Am. Chem. Soc.* **1991**, *113*, 7300.
269. M. Mąkosza, R. Bujok, *J. Fluorine Chem.* **2005**, *126*, 209.
270. Franck, G.; Brodner, K.; Helmchen, G. *Org. Lett.* **2010**, *12*, 3886.
271. Molander, G. A.; Harris, C. R. *J. Org. Chem.***1997**, *62*, 7418.
272. Liang, B.; Negishi, E. *Org. Lett.***2008**, *10*, 193.
273. Trollsas, M.; Orrenius, C.; Sahlen, F.; Gedde, U. W. ; Norin, T.; Hult, A.; Hermann, D.; Rudquist, P.; Komitov, L.: Lagerwall, S. T.; Lindstrom, J. *J. Am. Chem. Soc.* **1996**, *118*, 8542.

Appendices

Appendix A Selected NMR spectra for Chapter 2 and 3

2.21

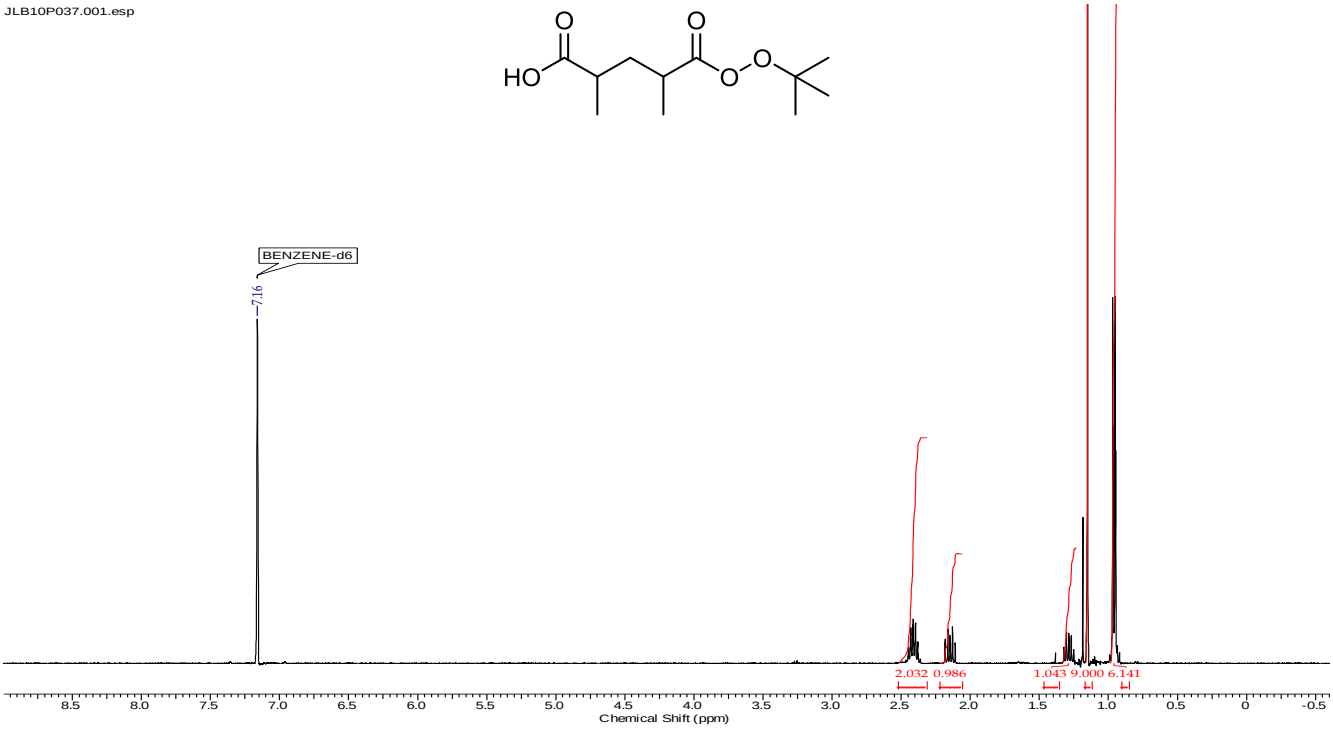
JLB10P037.001.esp
HO
O
O
O
O
BENZENE-d6
7.16
2.032
0.986
1.043
9.000
6.141
Chemical Shift (ppm)

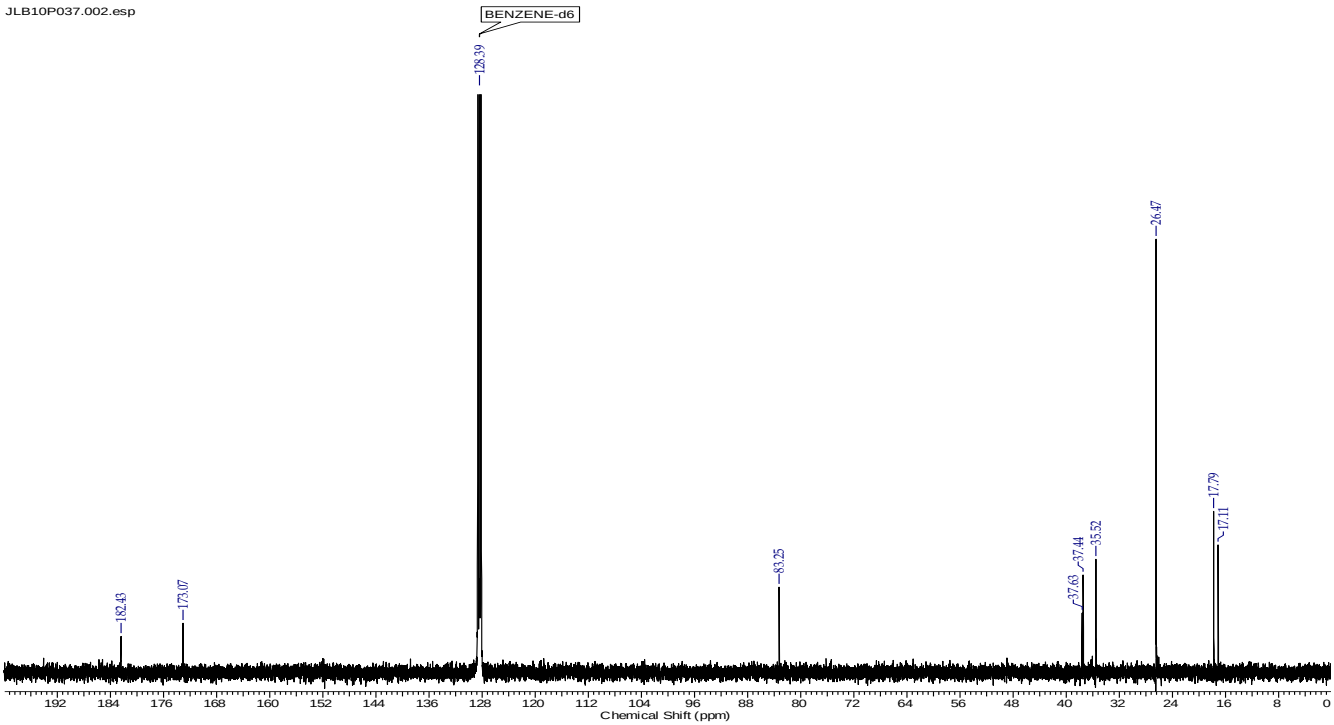
JLB10P037.002.esp
BENZENE-d6
128.39
182.43
173.07
83.25
37.63
37.44
35.52
26.47
17.79
17.11
Chemical Shift (ppm)

2.25

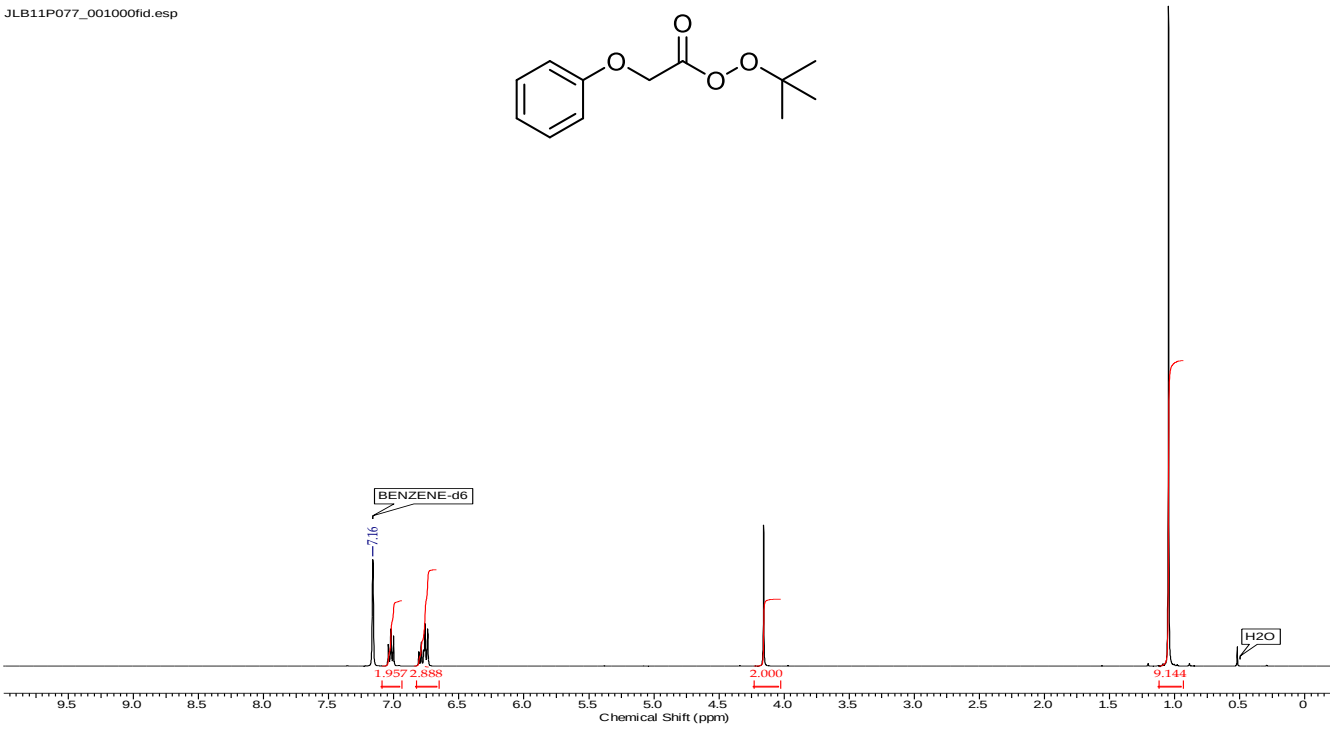
JLB11P077_001000fid.esp
BENZENE-d6
7.16
1.957
2.888
2.000
9.144
H2O
Chemical Shift (ppm)

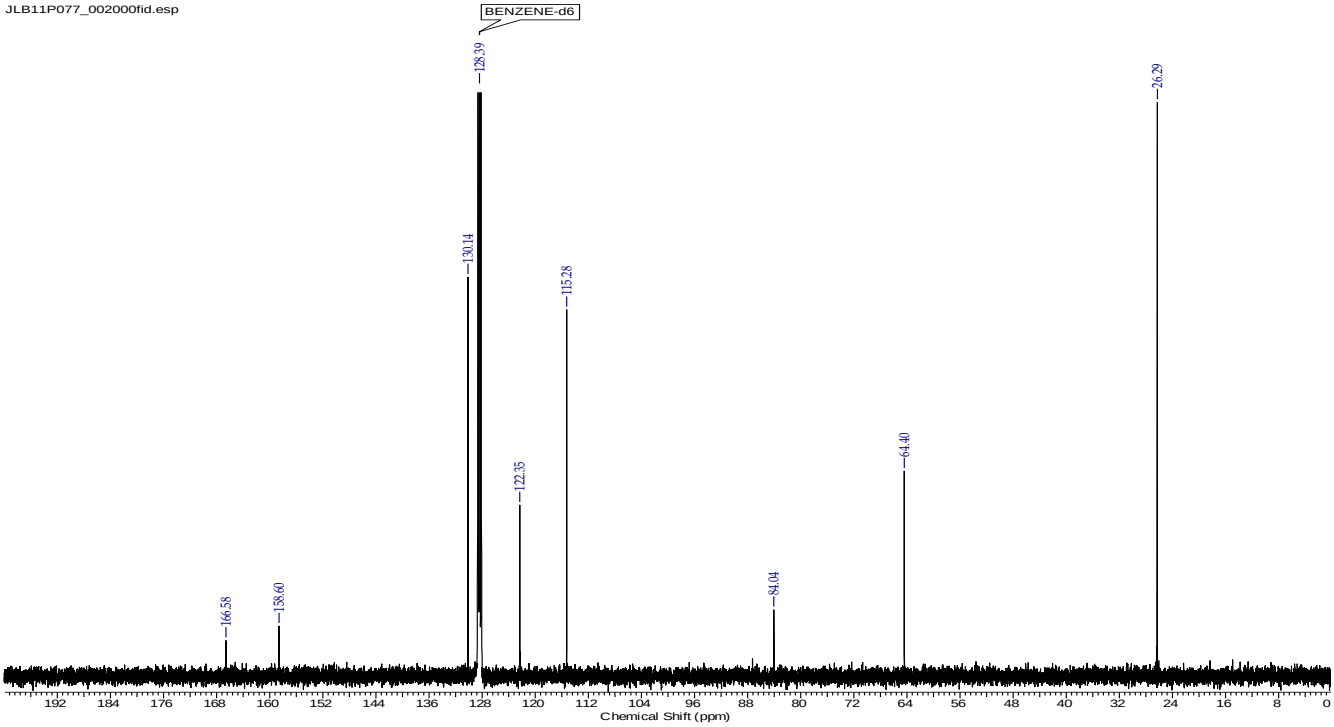
JLB11P077_002000fid.esp
BENZENE-d6
128.39
130.14
115.28
122.35
64.40
26.29
166.58
138.60
84.04
Chemical Shift (ppm)

2.28

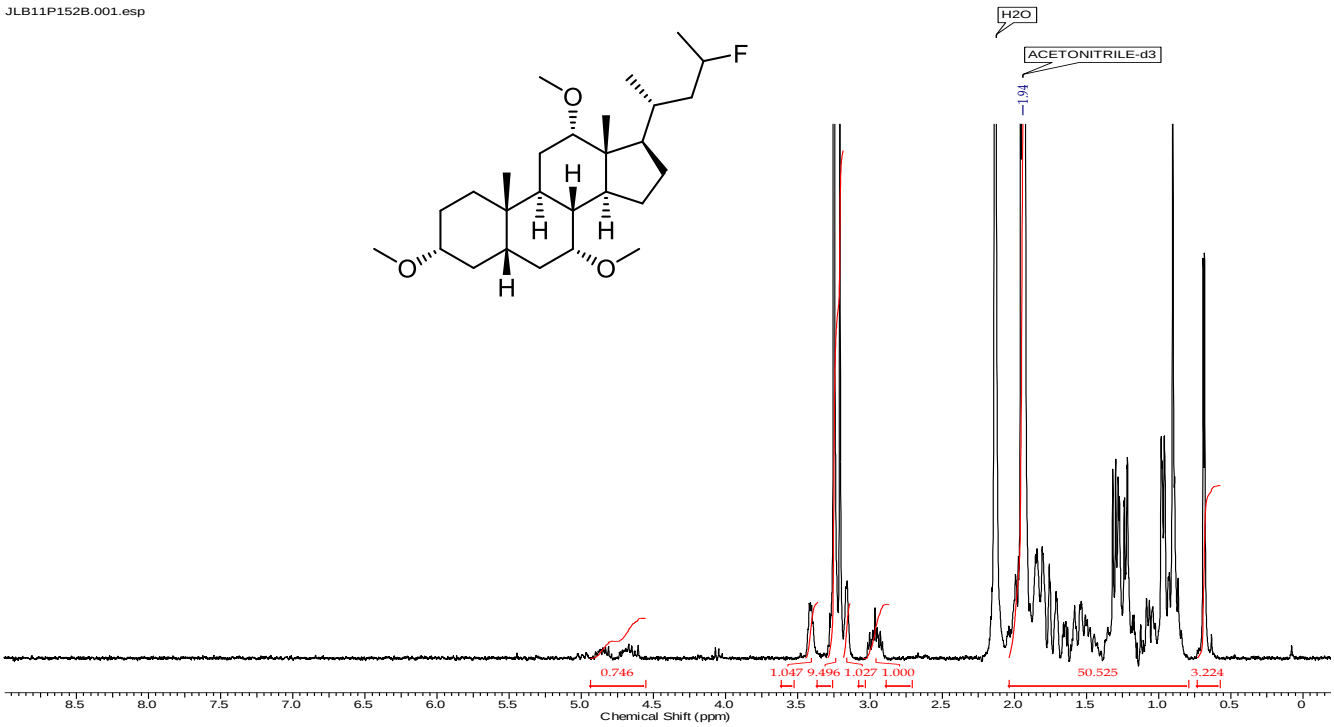
JLB11P152B.001.esp
H2O
ACETONITRILE-d3
1.94
F
O
H
H
H
O
O
H
0.746
1.047
9.496
1.027
1.000
50.525
3.224
Chemical Shift (ppm)

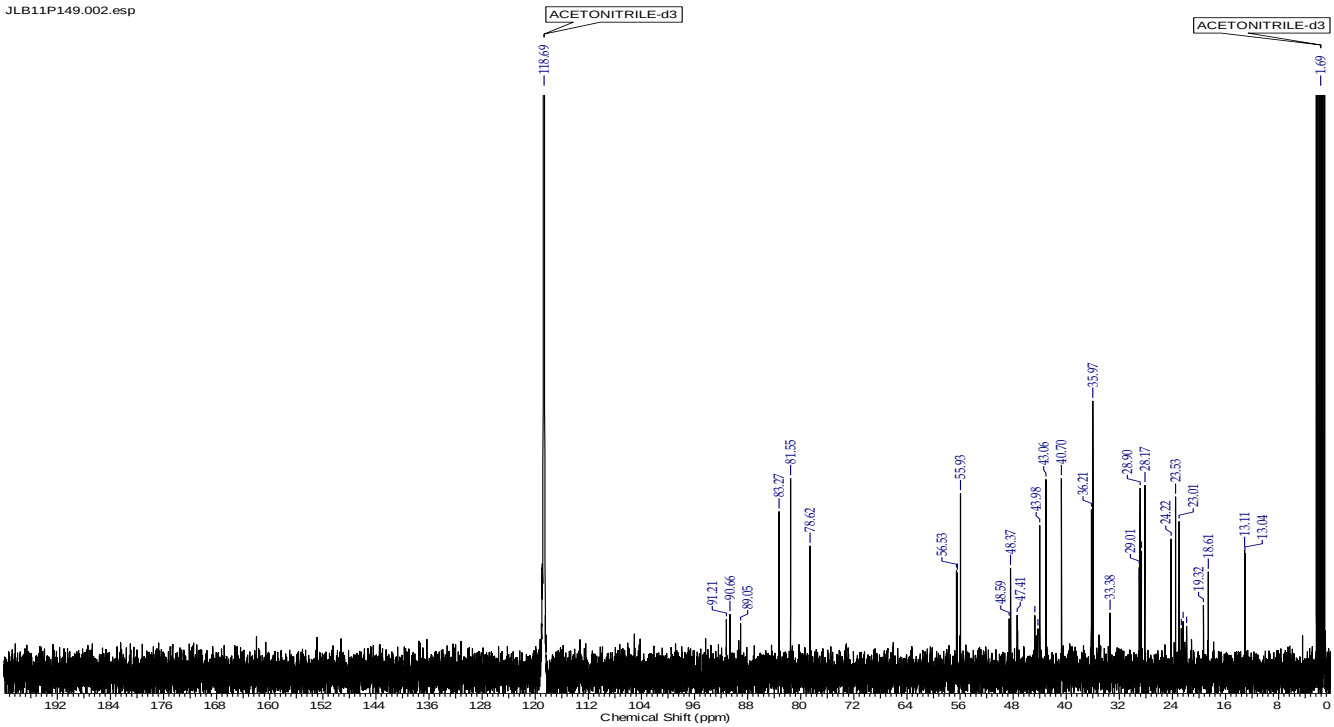
JLB11P149.002.esp
ACETONITRILE-d3
ACETONITRILE-d3
118.69
1.69
91.21
90.66
89.05
83.27
81.55
78.62
56.53
55.93
48.59
48.37
47.41
43.98
43.06
40.70
36.21
35.97
33.38
29.01
28.90
28.17
24.22
23.53
23.01
19.32
18.61
13.11
13.04
Chemical Shift (ppm)

3.48

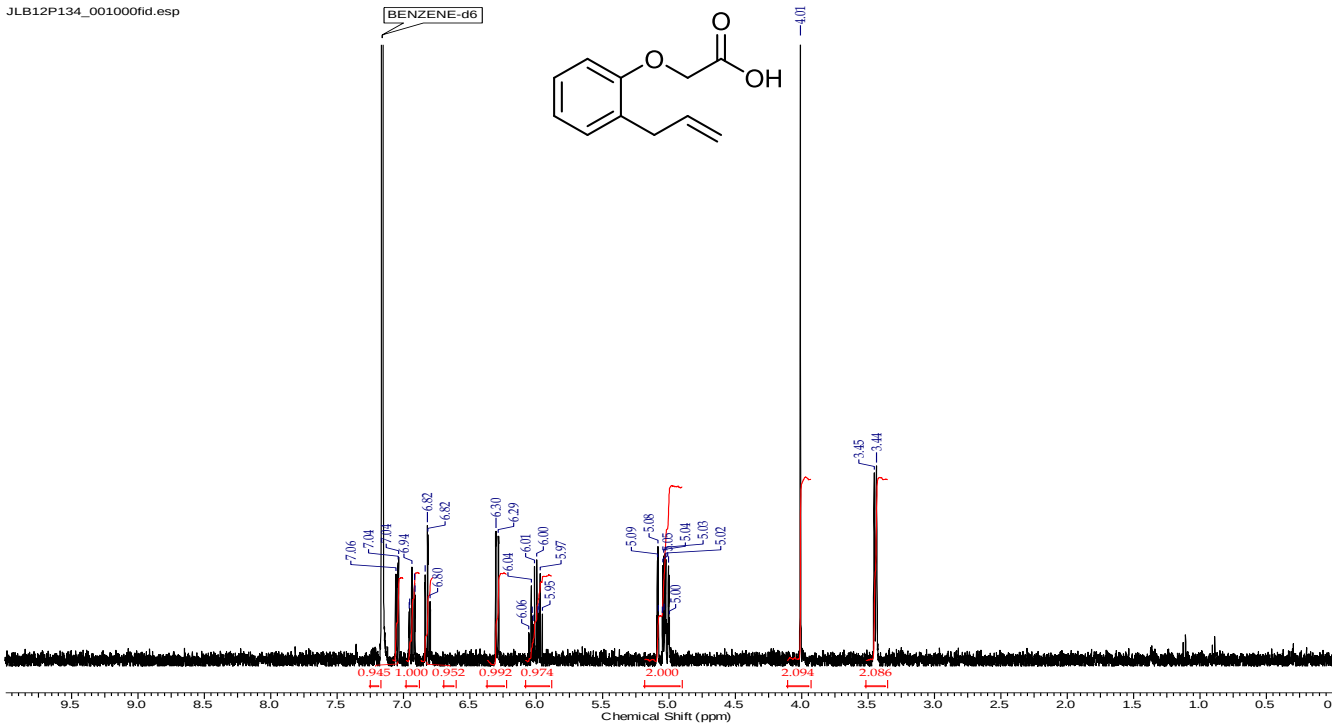
JLB12P134_001000fid.esp
BENZENE-d6
O
O
OH
4.01
3.45
3.44
7.06
7.04
7.04
6.94
6.82
6.82
6.80
6.30
6.29
6.04
6.01
6.00
6.06
5.97
5.95
5.09
5.08
5.05
5.04
5.03
5.02
5.00
0.945
1.000
0.952
0.992
0.974
2.000
2.094
2.086
Chemical Shift (ppm)

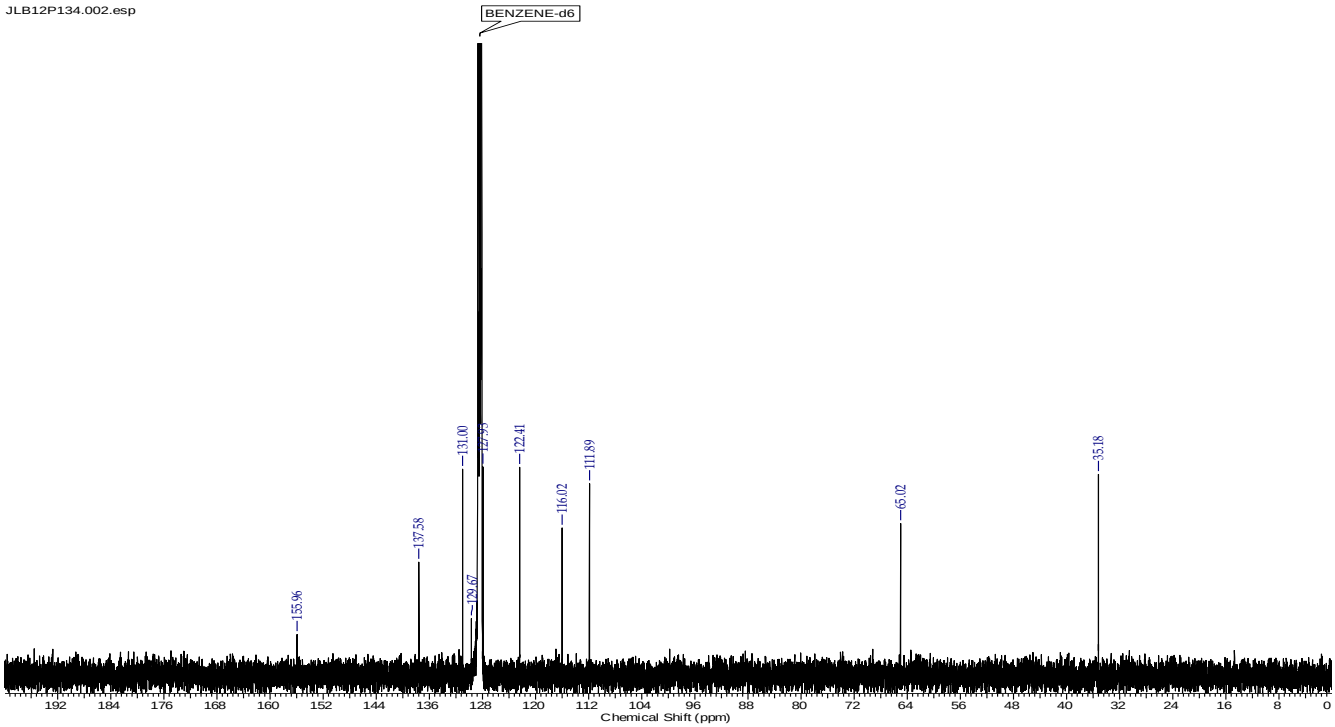
JLB12P134.002.esp
BENZENE-d6
155.96
137.58
131.00
129.67
122.41
116.02
111.89
65.02
35.18
Chemical Shift (ppm)

3.109

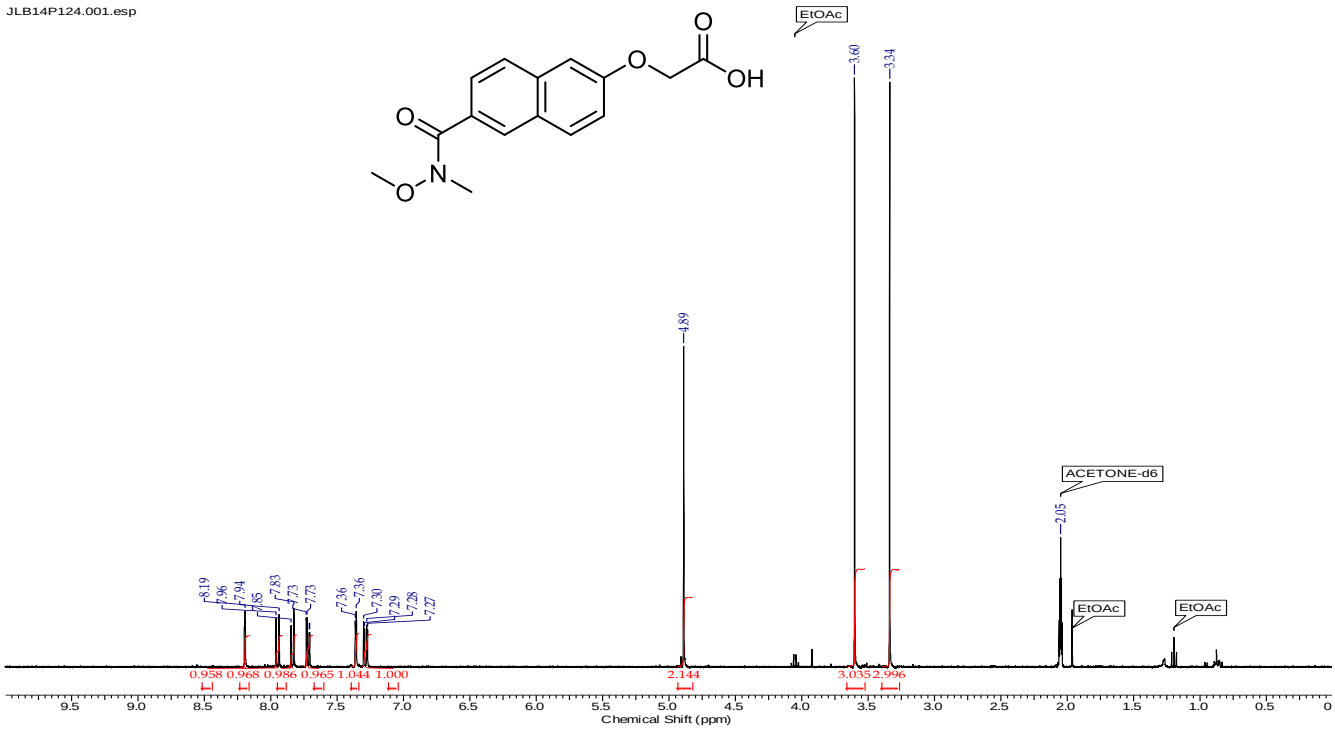
JLB14P124.001.esp
EtOAc
3.60
3.34
4.89
ACETONE-d6
2.05
EtOAc
EtOAc
8.19
7.96
7.94
7.85
7.83
7.73
7.73
7.36
7.36
7.30
7.29
7.28
7.27
0.958 0.968 0.986 0.965 1.044 1.000
2.144
3.035 2.996
Chemical Shift (ppm)

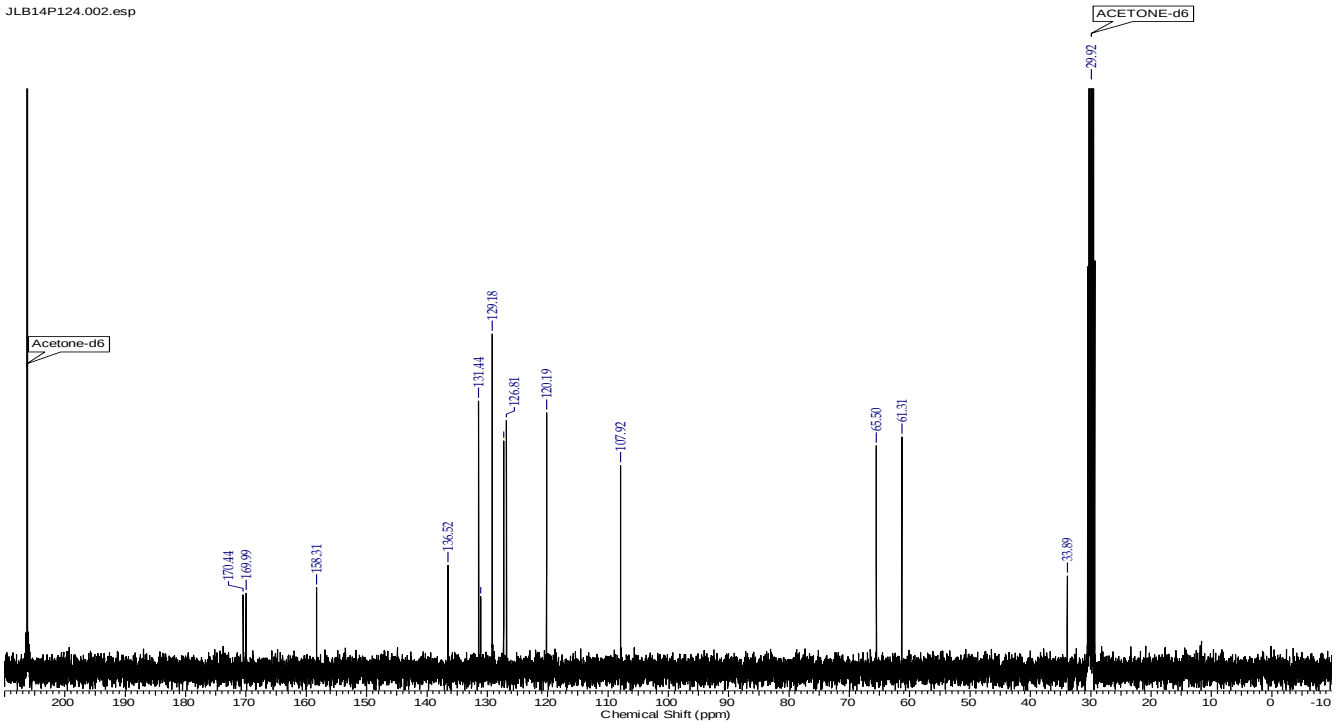
JLB14P124.002.esp
ACETONE-d6
29.92
Acetone-d6
170.44
169.99
158.31
136.52
131.44
129.18
126.81
120.19
107.92
65.50
61.31
33.89
Chemical Shift (ppm)

3.160

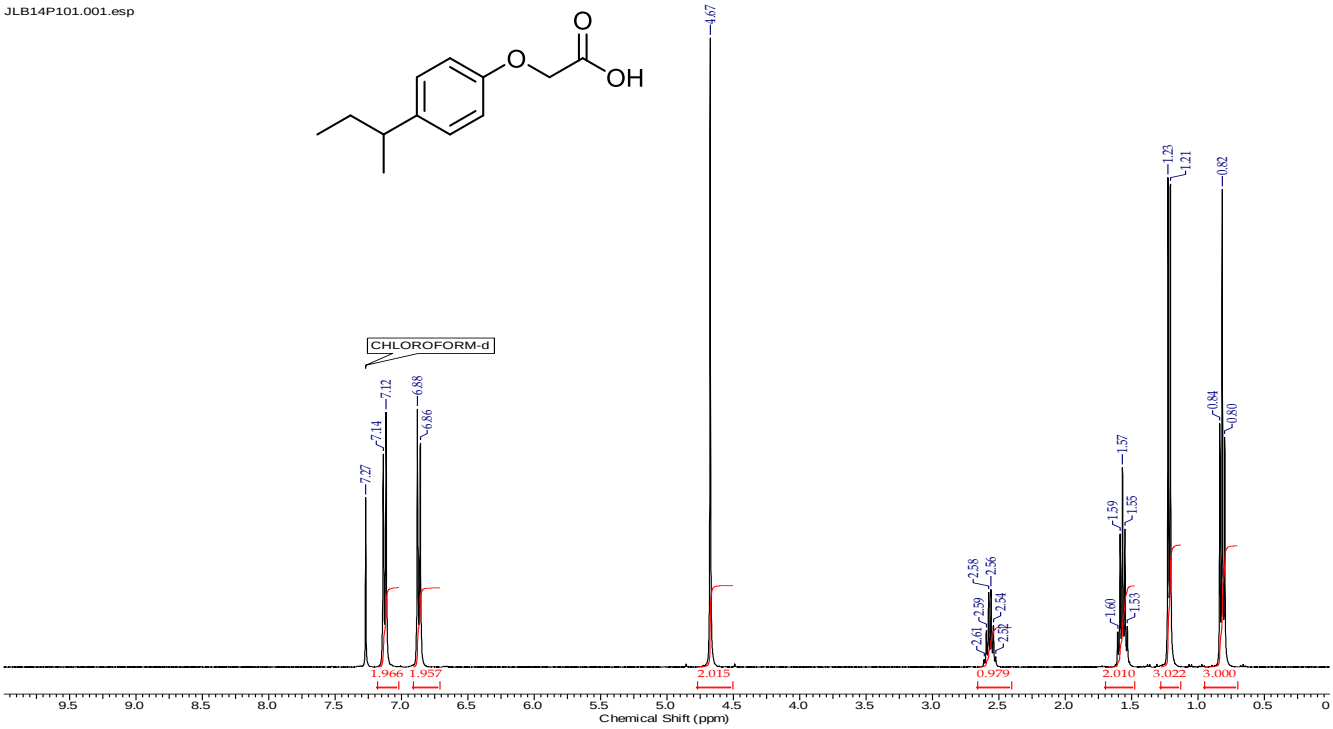
JLB14P101.001.esp
O
O
OH
CHLOROFORM-d
7.27
7.14
7.12
6.88
6.86
4.67
2.61
2.59
2.58
2.56
2.54
2.52
1.60
1.59
1.57
1.55
1.53
1.23
1.21
0.84
0.82
0.80
1.966
1.957
2.015
0.979
2.010
3.022
3.000
Chemical Shift (ppm)

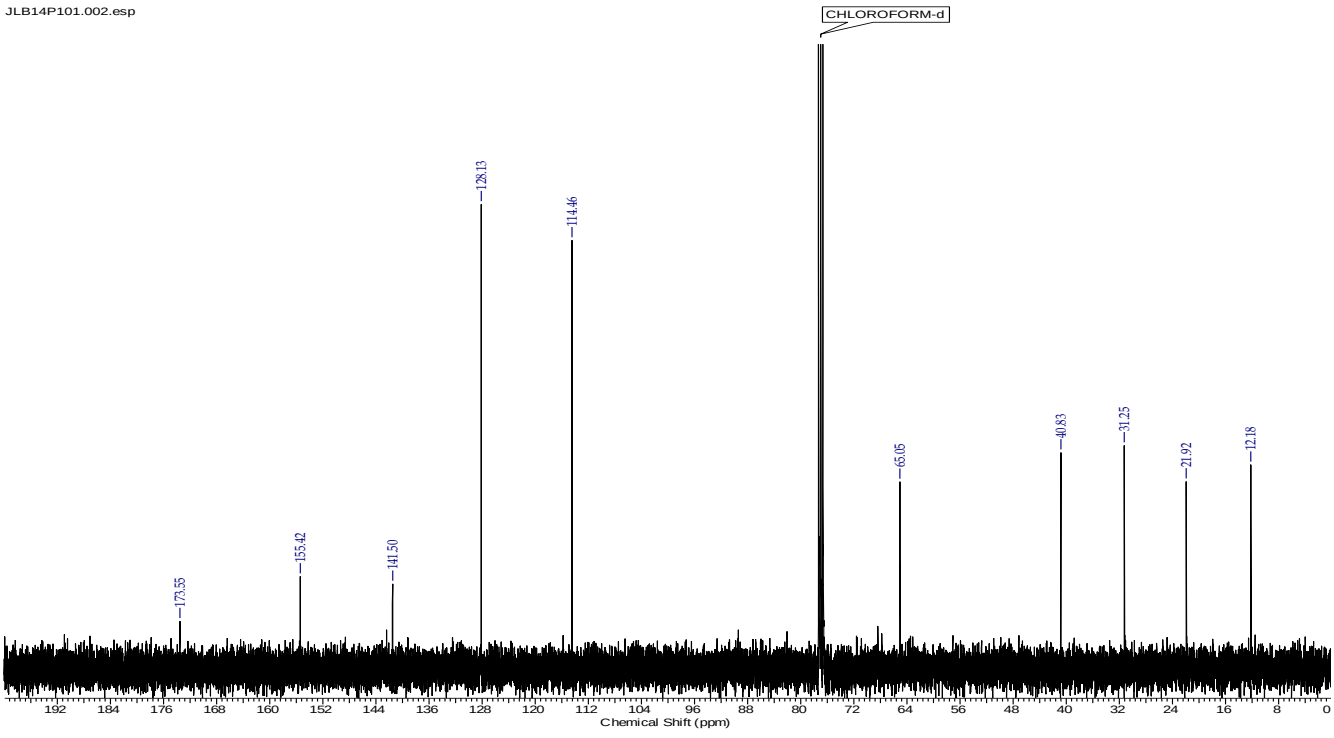
JLB14P101.002.esp
CHLOROFORM-d
173.55
155.42
141.50
128.13
114.46
65.05
40.83
31.25
21.92
12.18
Chemical Shift (ppm)

3.164

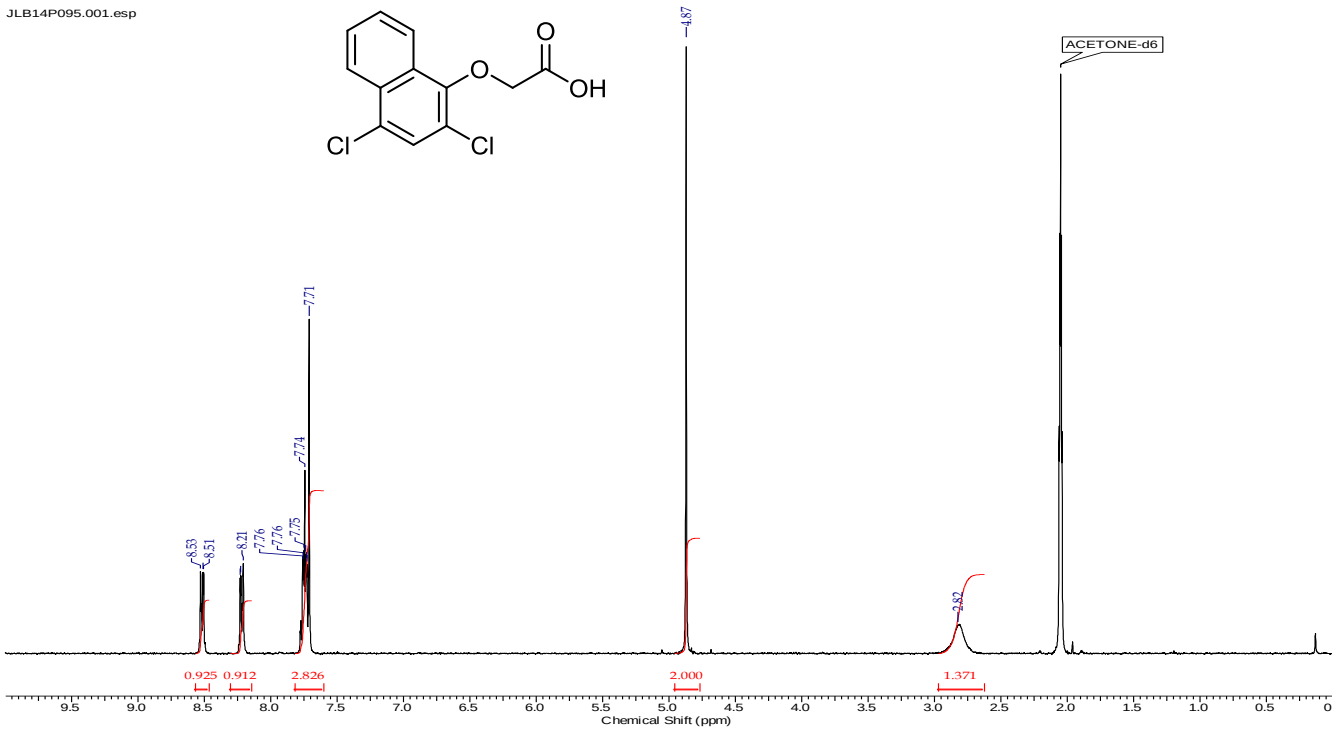
JLB14P095.001.esp
O
O
OH
Cl
Cl
4.87
ACETONE-d6
7.71
7.74
8.53
8.51
8.21
7.76
7.76
7.75
2.82
0.925
0.912
2.826
2.000
1.371
Chemical Shift (ppm)

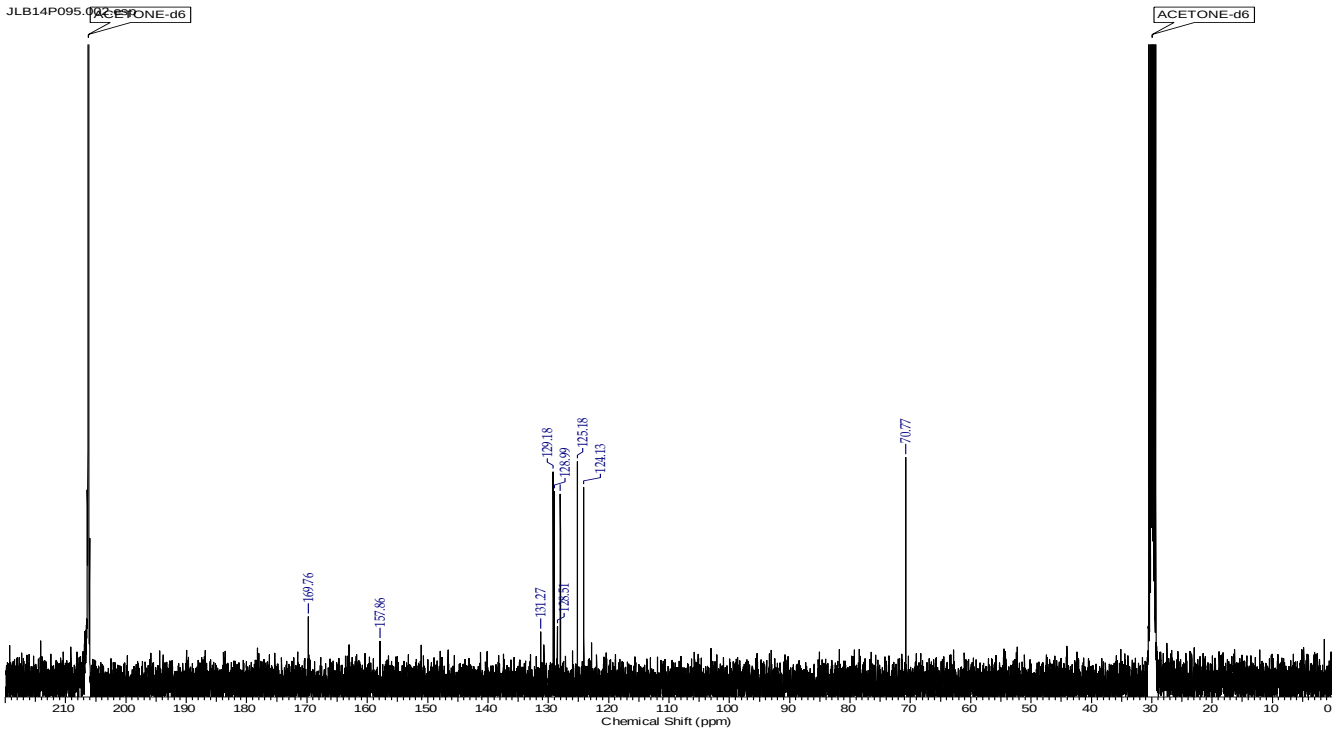
JLB14P095.002.esp
ACETONE-d6
ACETONE-d6
129.18
128.99
125.18
124.13
70.77
169.76
157.86
131.27
128.51
Chemical Shift (ppm)

3.180

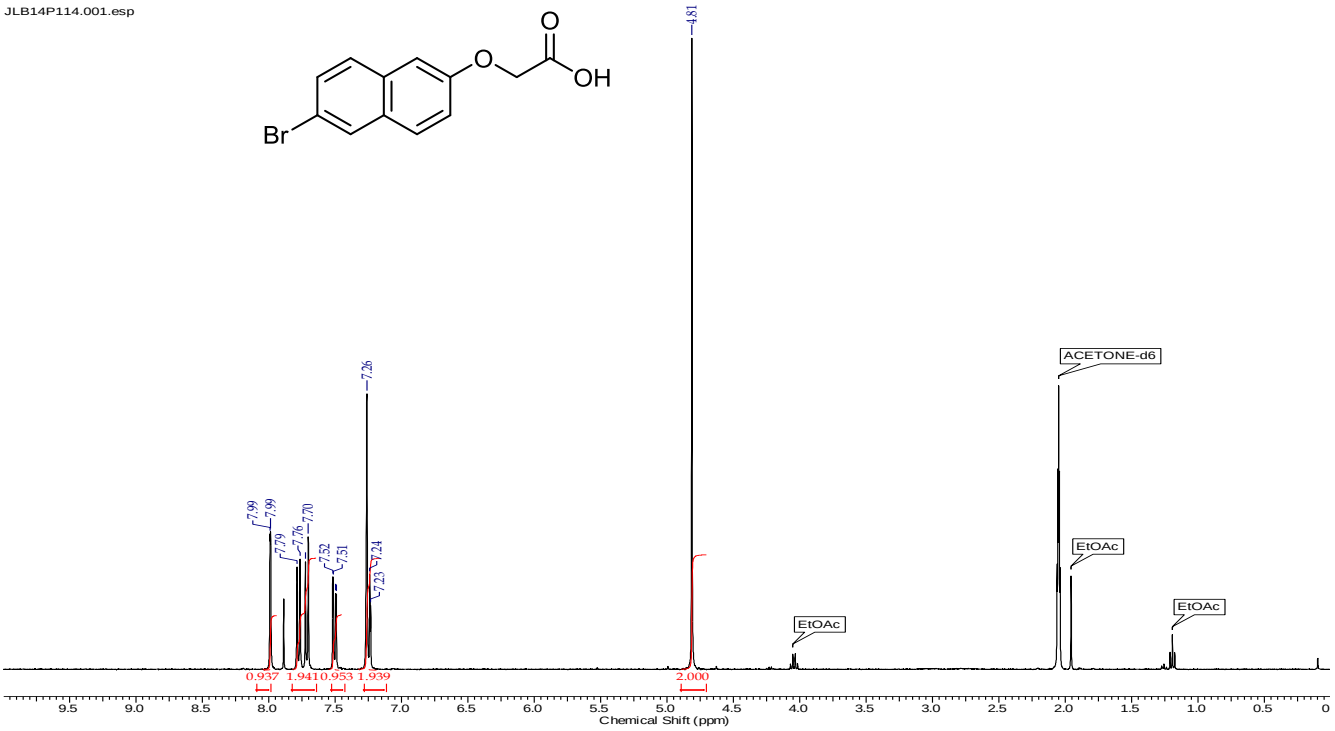
JLB14P114.001.esp
O
O
OH
Br
4.81
7.26
7.99
7.99
7.79
7.76
7.70
7.52
7.51
7.24
7.23
ACETONE-d6
EtOAc
EtOAc
EtOAc
0.937
1.941
0.953
1.939
2.000
Chemical Shift (ppm)

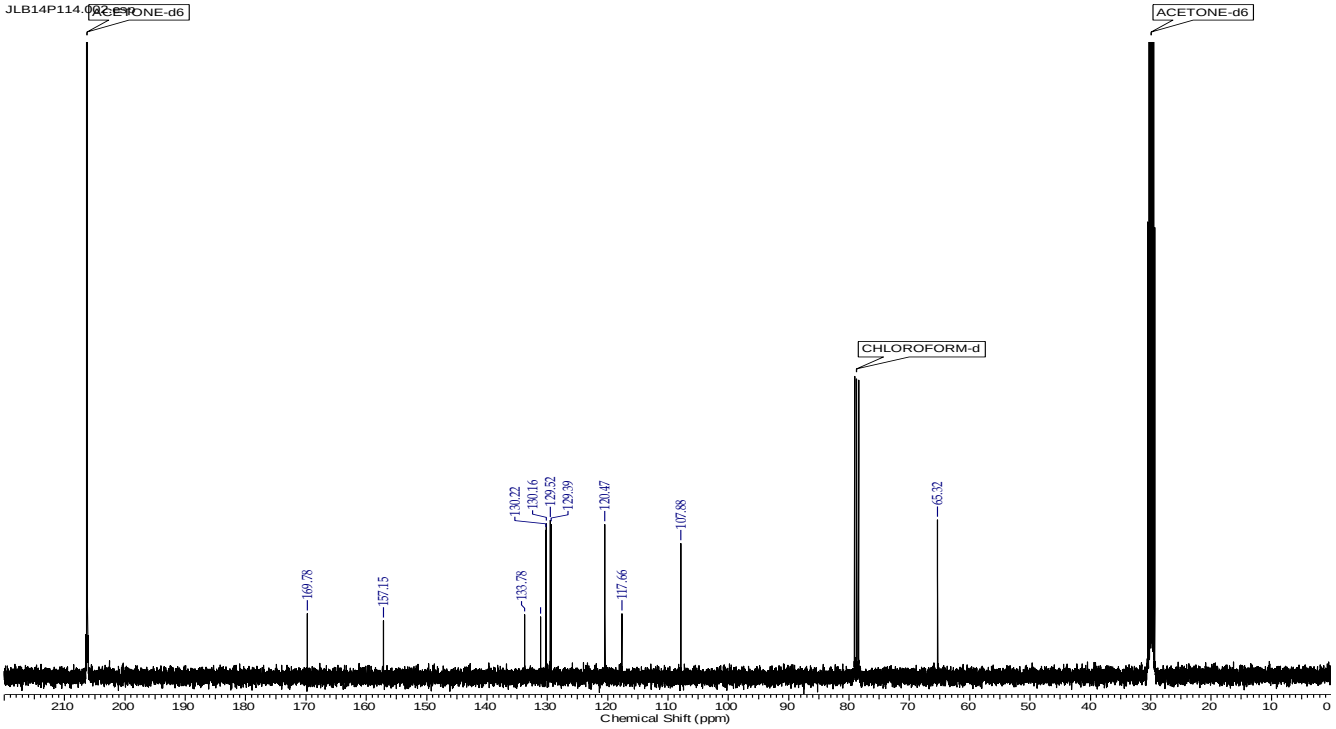
JLB14P114.002.esp
ACETONE-d6
ACETONE-d6
CHLOROFORM-d
169.78
157.15
133.78
130.22
130.16
129.52
129.39
120.47
117.66
107.88
65.32
Chemical Shift (ppm)

3.110

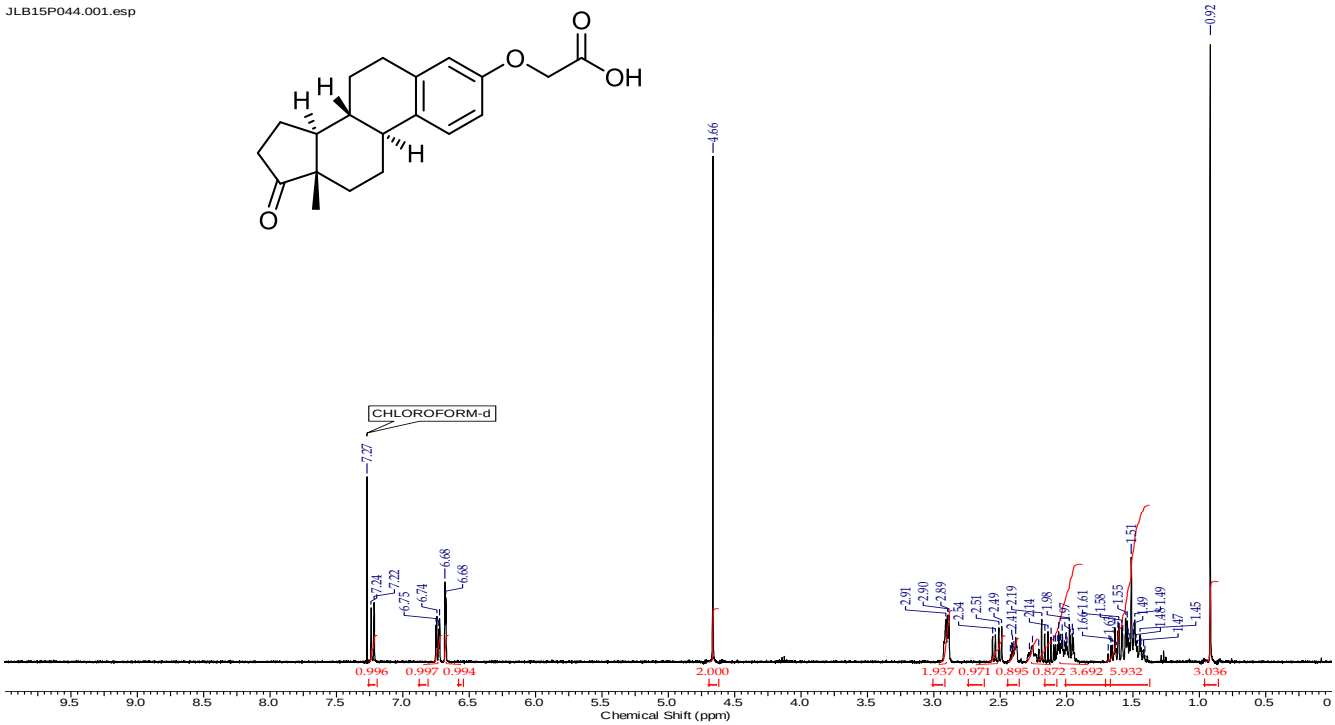
JLB15P044.001.esp
CHLOROFORM-d
Chemical Shift (ppm)

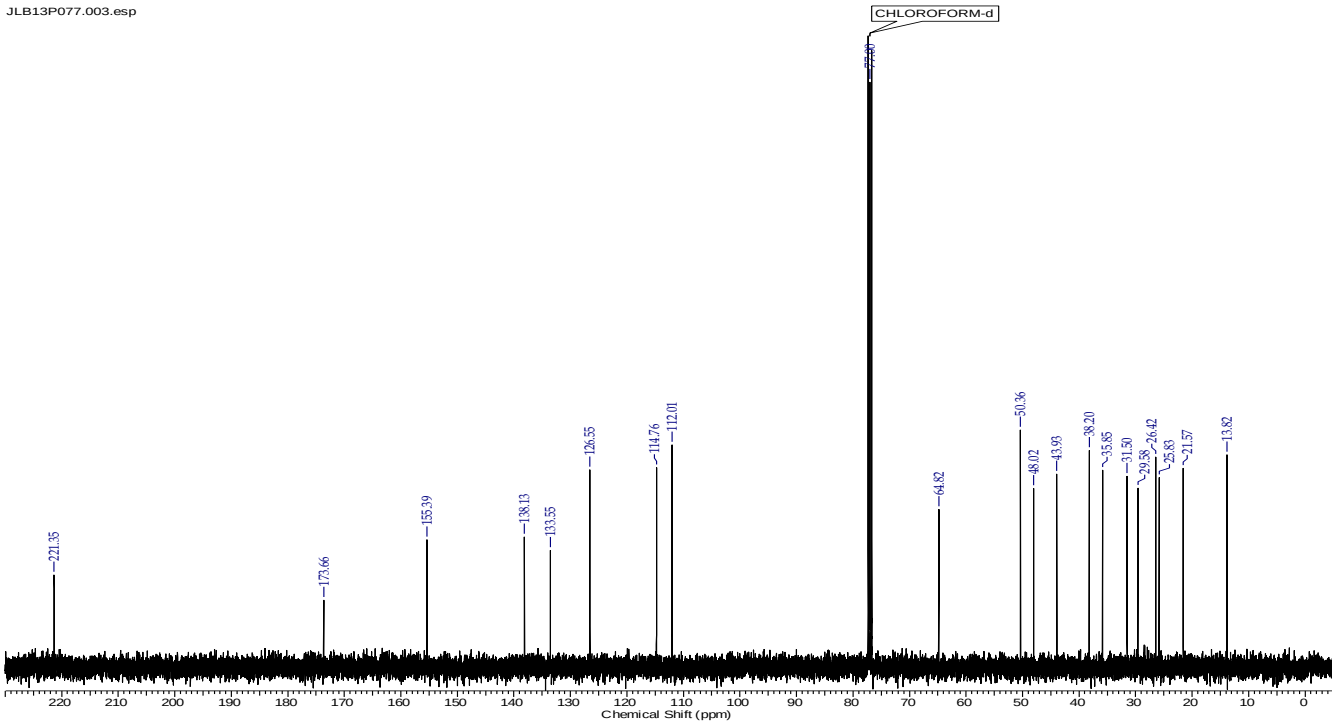
JLB13P077.003.esp
CHLOROFORM-d
Chemical Shift (ppm)

3.181

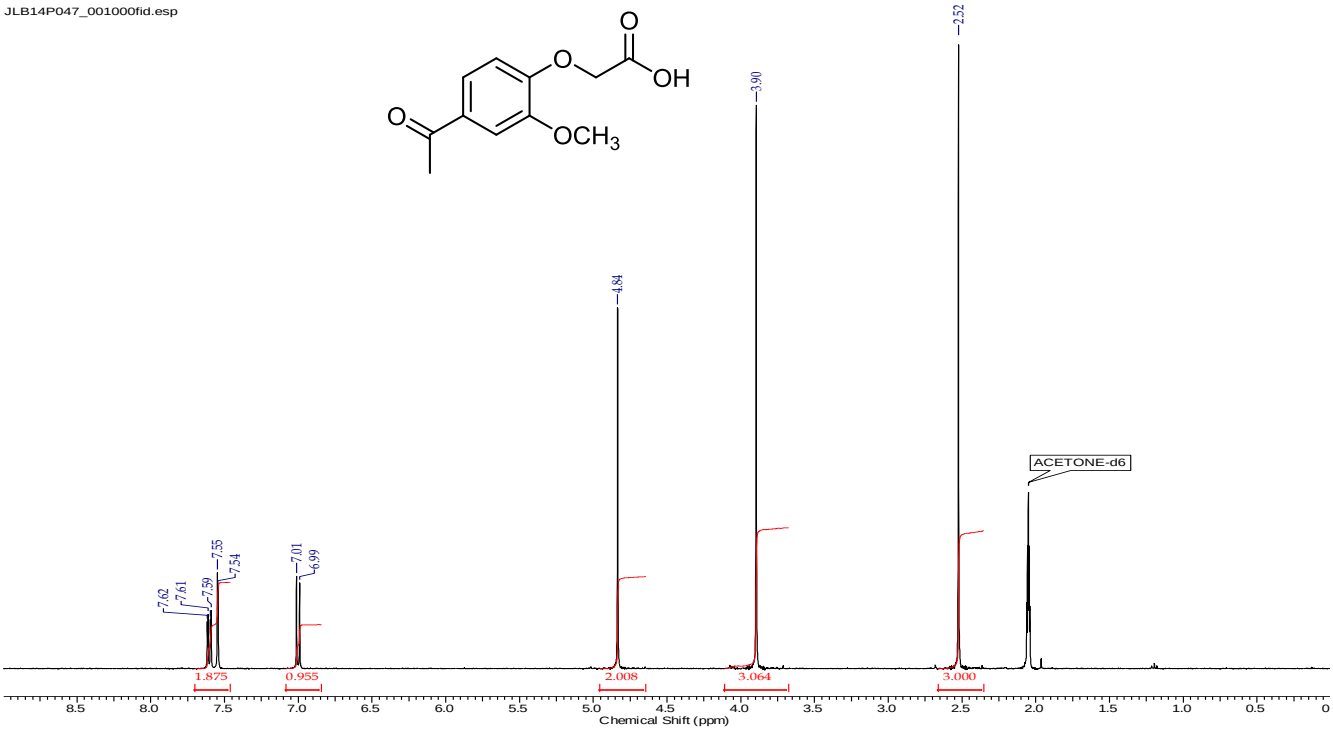
JLB14P047_001000fid.esp
O
O
OH
O
OCH3
2.52
3.90
4.84
ACETONE-d6
7.62
7.61
7.59
7.55
7.54
7.01
6.99
1.875
0.955
2.008
3.064
3.000
Chemical Shift (ppm)

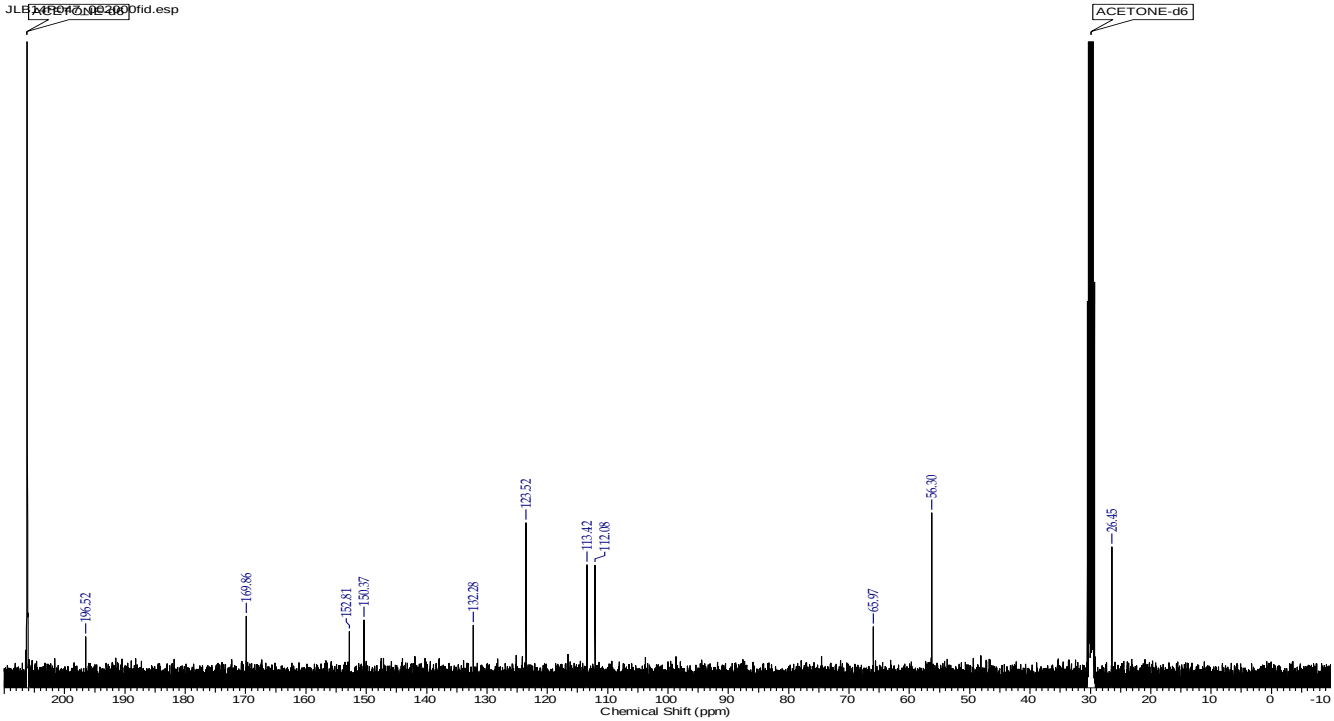
ACETONE-d6
196.52
169.86
152.81
150.37
132.28
123.52
113.42
112.08
65.97
56.30
26.45
Chemical Shift (ppm)

3.113b

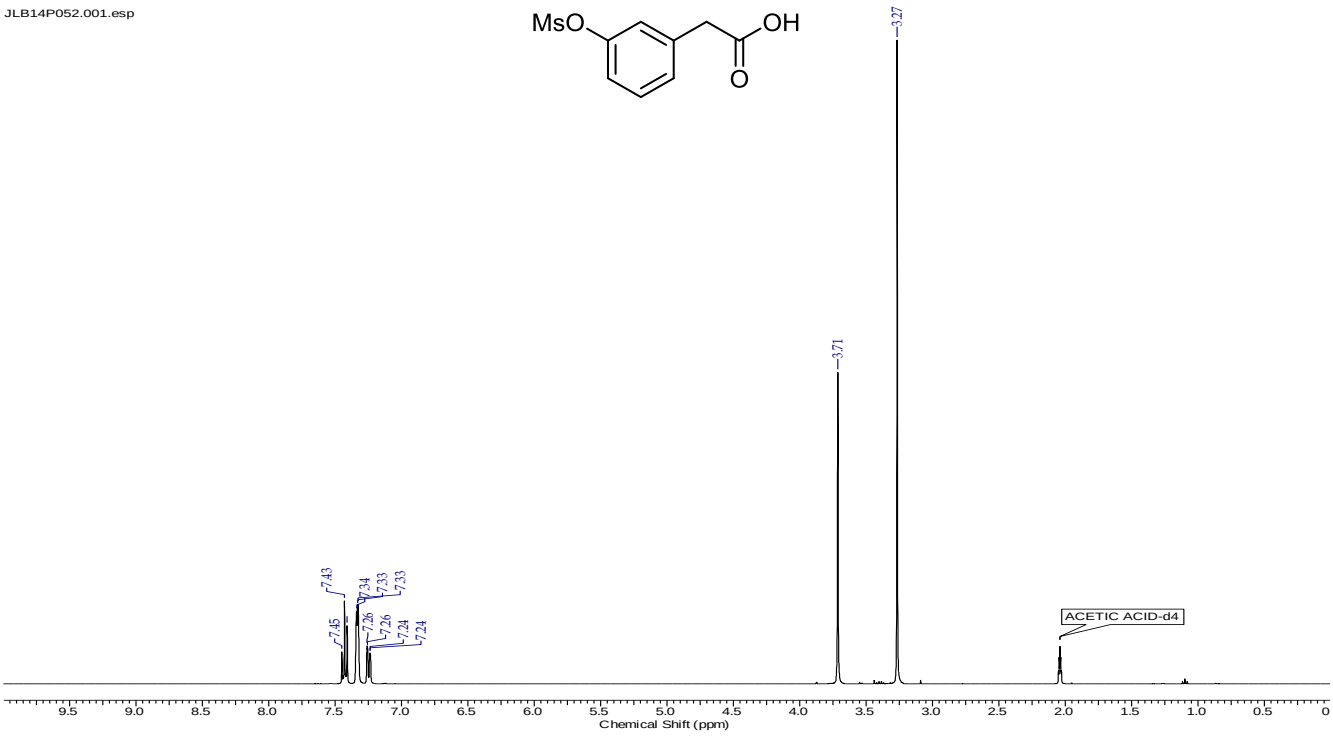
JLB14P052.001.esp
MsO
OH
O
3.27
3.71
7.43
7.45
7.34
7.33
7.33
7.26
7.26
7.24
7.24
ACETIC ACID-d4
Chemical Shift (ppm)

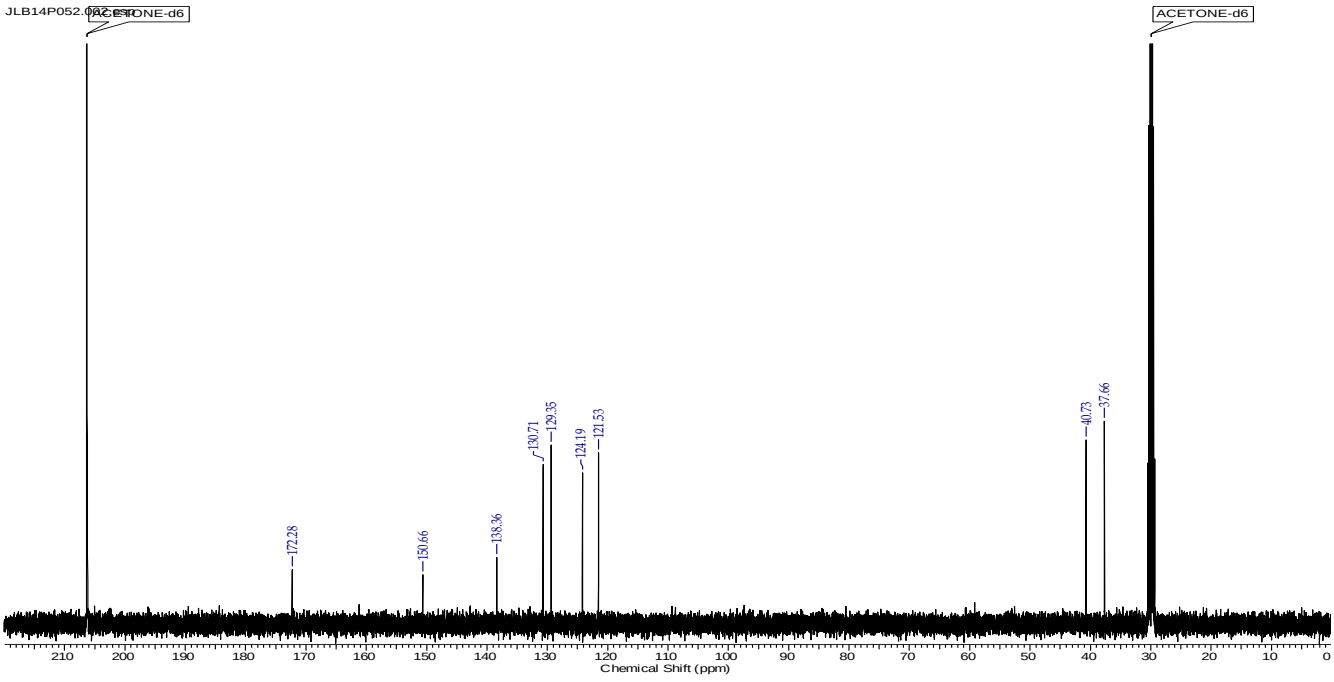
ACETONE-d6
ACETONE-d6
172.28
150.66
138.36
130.71
129.35
124.19
121.53
40.73
37.66
Chemical Shift (ppm)

3.76

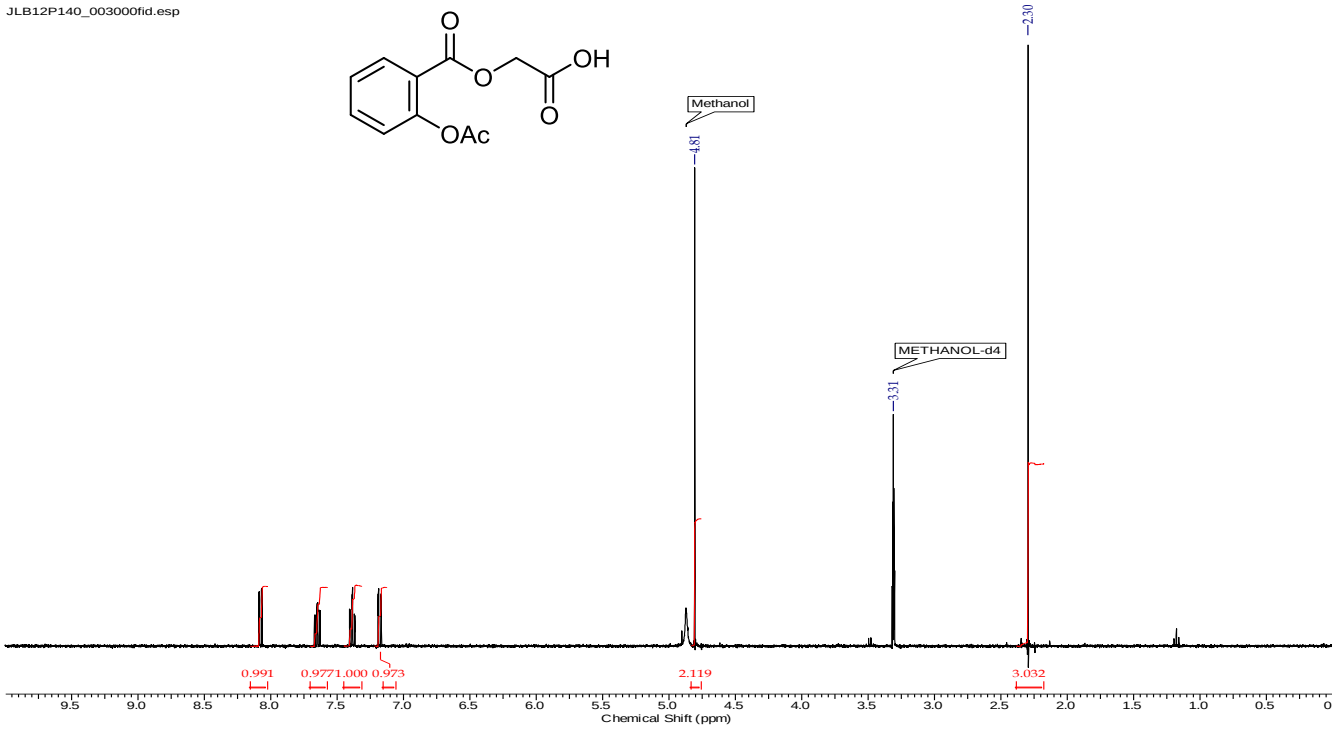
JLB12P140_003000fid.esp
O
O
OH
O
OAc
Methanol
4.81
2.30
METHANOL-d4
3.31
0.991
0.977
1.000
0.973
2.119
3.032
Chemical Shift (ppm)

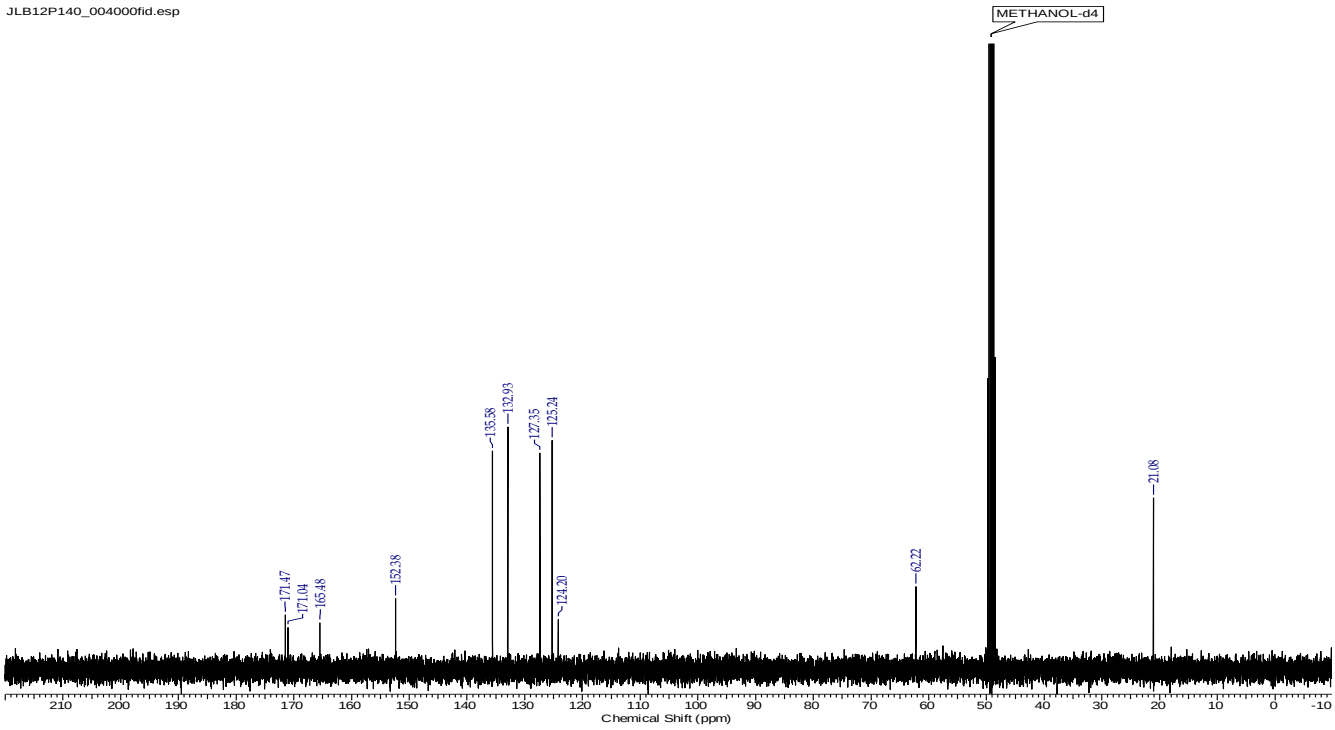
JLB12P140_004000fid.esp
METHANOL-d4
171.47
171.04
165.48
152.38
135.58
132.93
127.35
125.24
124.20
62.22
21.08
Chemical Shift (ppm)

3.167

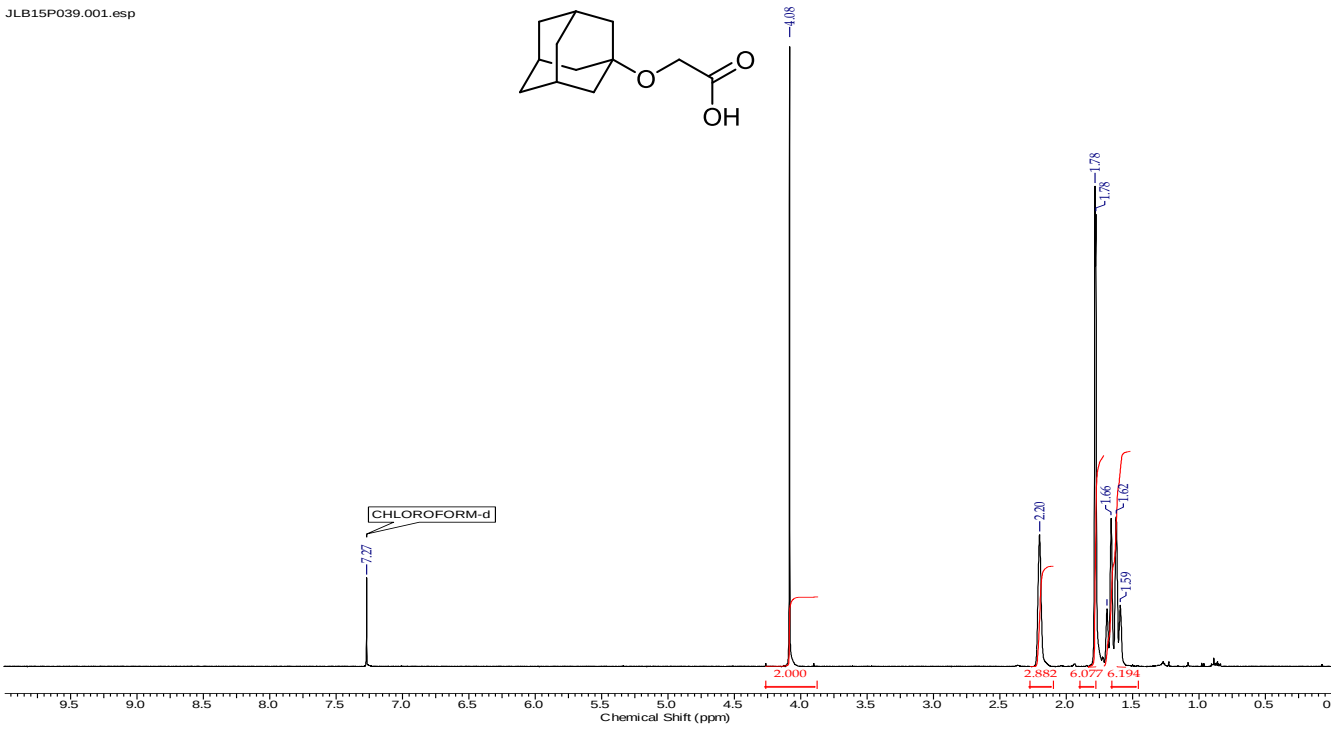
JLB15P039.001.esp
O
OH
4.08
1.78
1.78
CHLOROFORM-d
7.27
2.20
1.66
1.62
1.59
2.000
2.882
6.077
6.194
Chemical Shift (ppm)

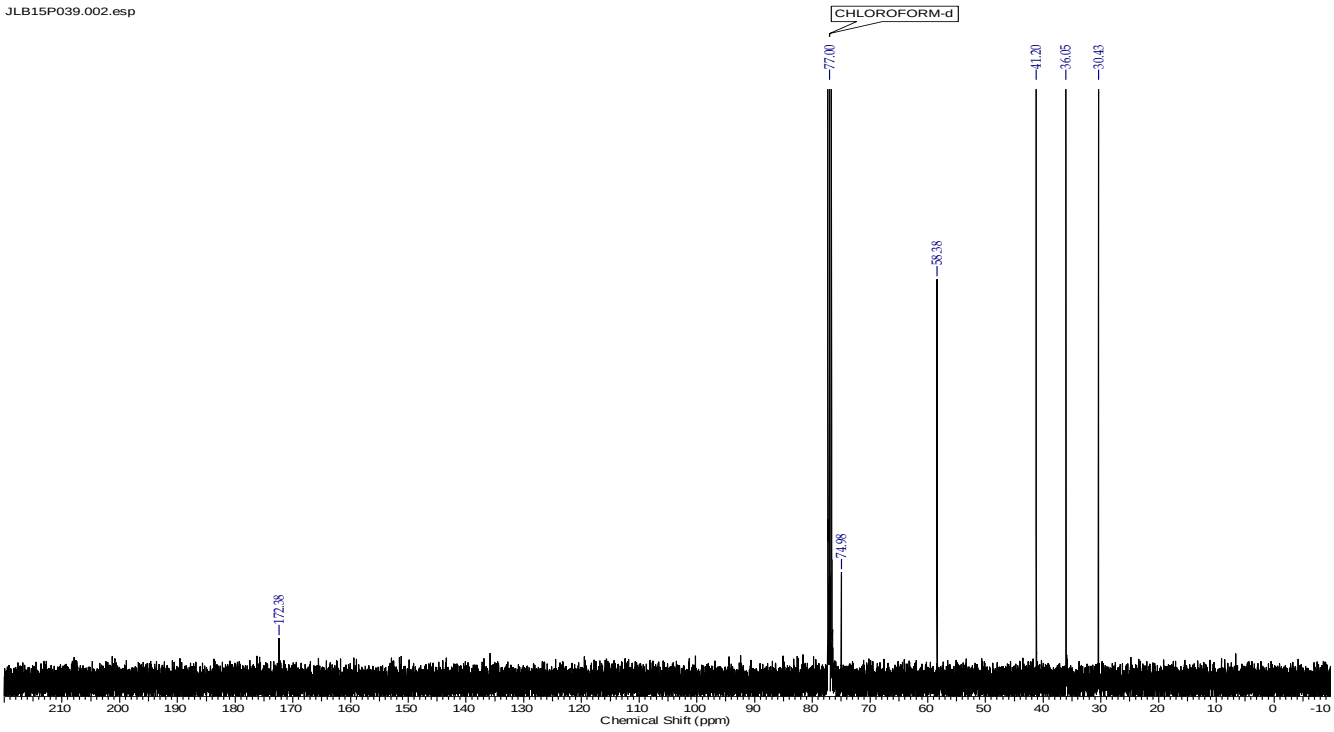
JLB15P039.002.esp
CHLOROFORM-d
77.00
41.20
36.05
30.43
58.38
74.98
172.38
Chemical Shift (ppm)

3.52

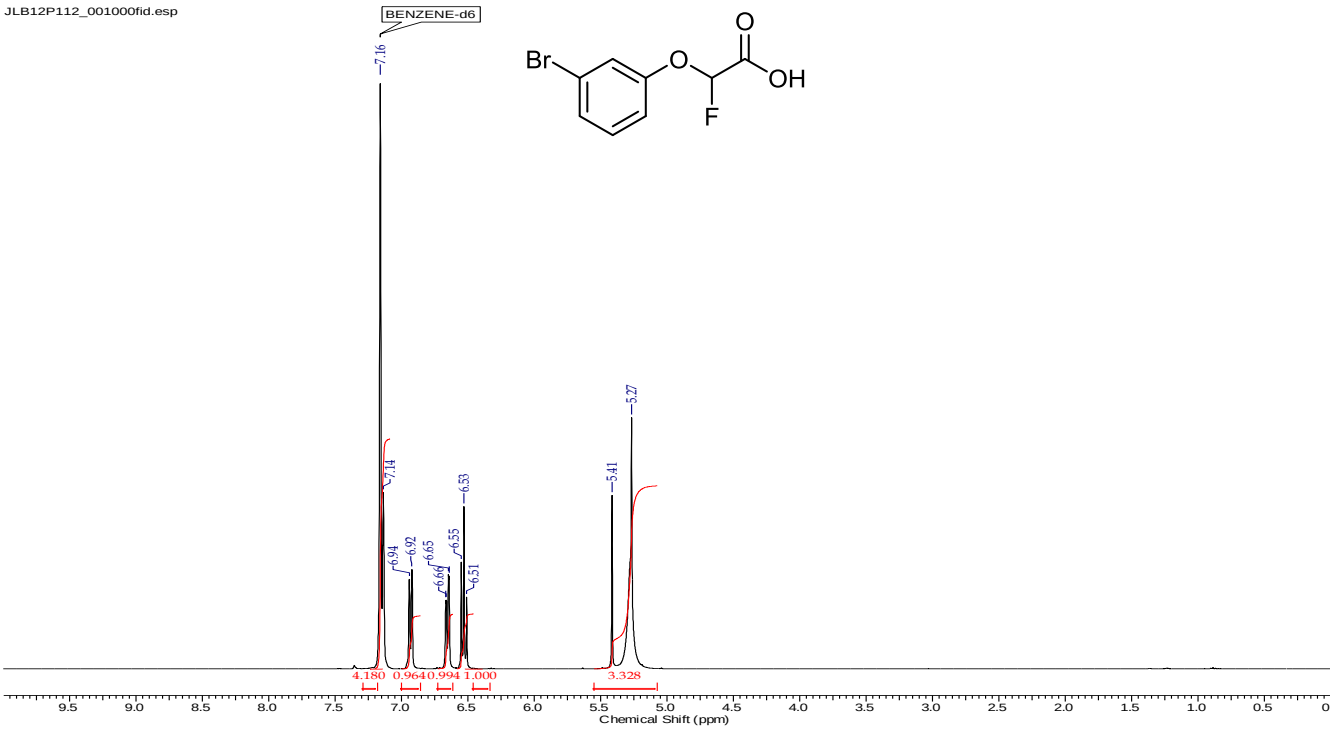
JLB12P112_001000fid.esp
BENZENE-d6
Br
O
OH
F
7.16
7.14
6.94
6.92
6.85
6.69
6.55
6.53
6.51
5.41
5.27
4.180
0.964
0.994
1.000
3.328
Chemical Shift (ppm)

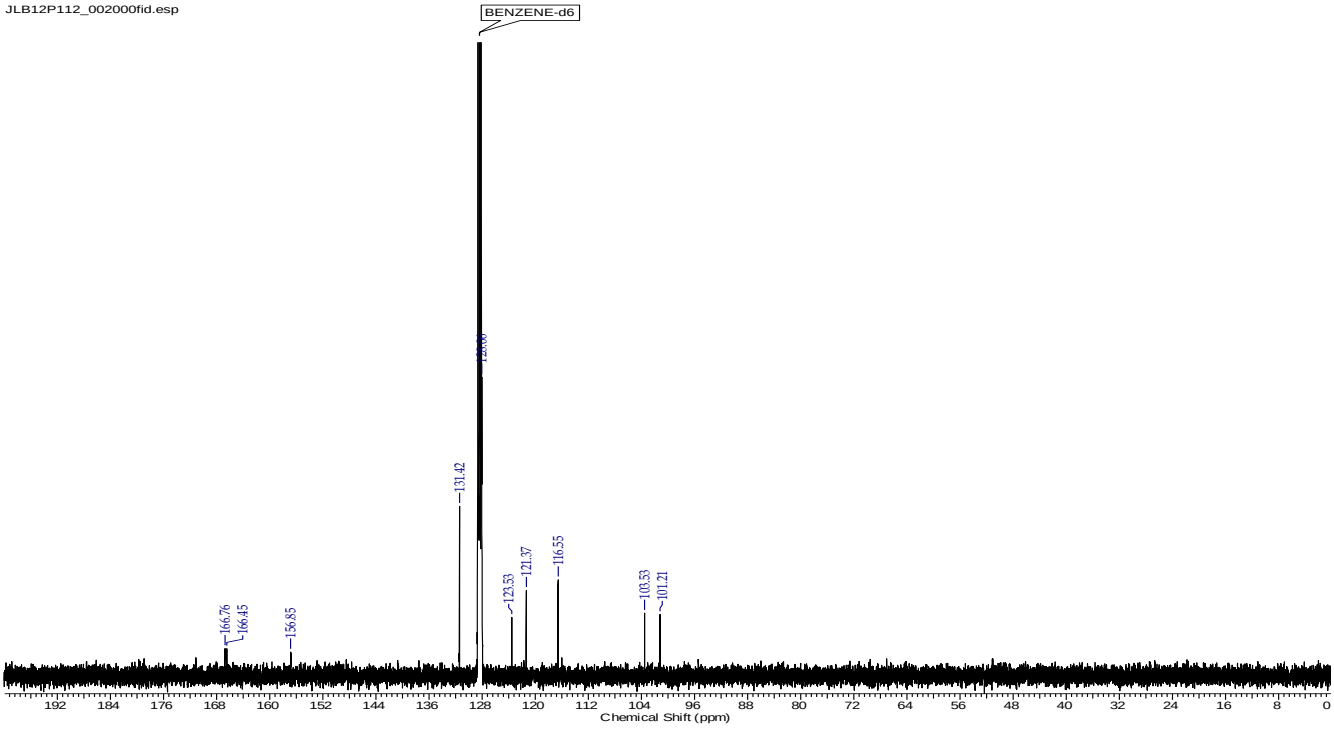
JLB12P112_002000fid.esp
BENZENE-d6
131.42
123.53
121.37
116.55
103.53
101.21
166.76
166.45
136.85
Chemical Shift (ppm)

3.53

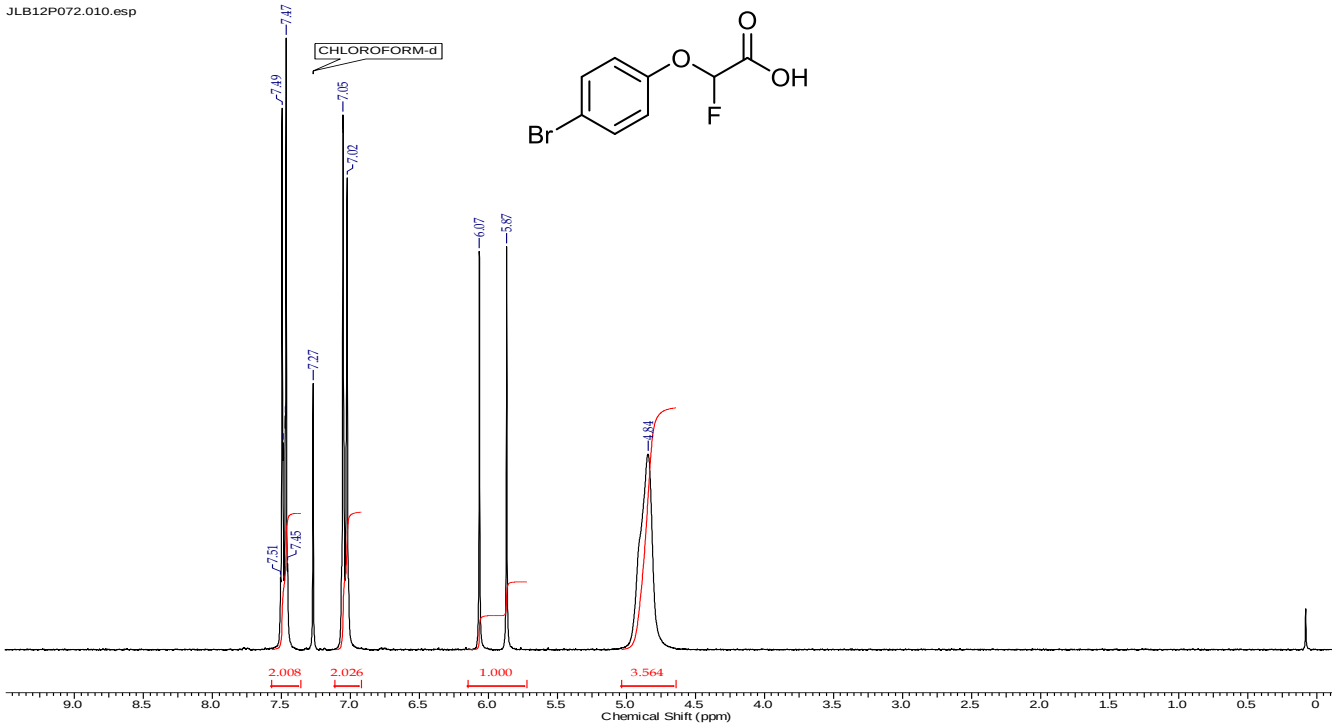
JLB12P072.010.esp
CHLOROFORM-d
7.47
7.49
7.05
7.02
6.07
5.87
7.27
4.84
7.51
7.45
2.008
2.026
1.000
3.564
Chemical Shift (ppm)

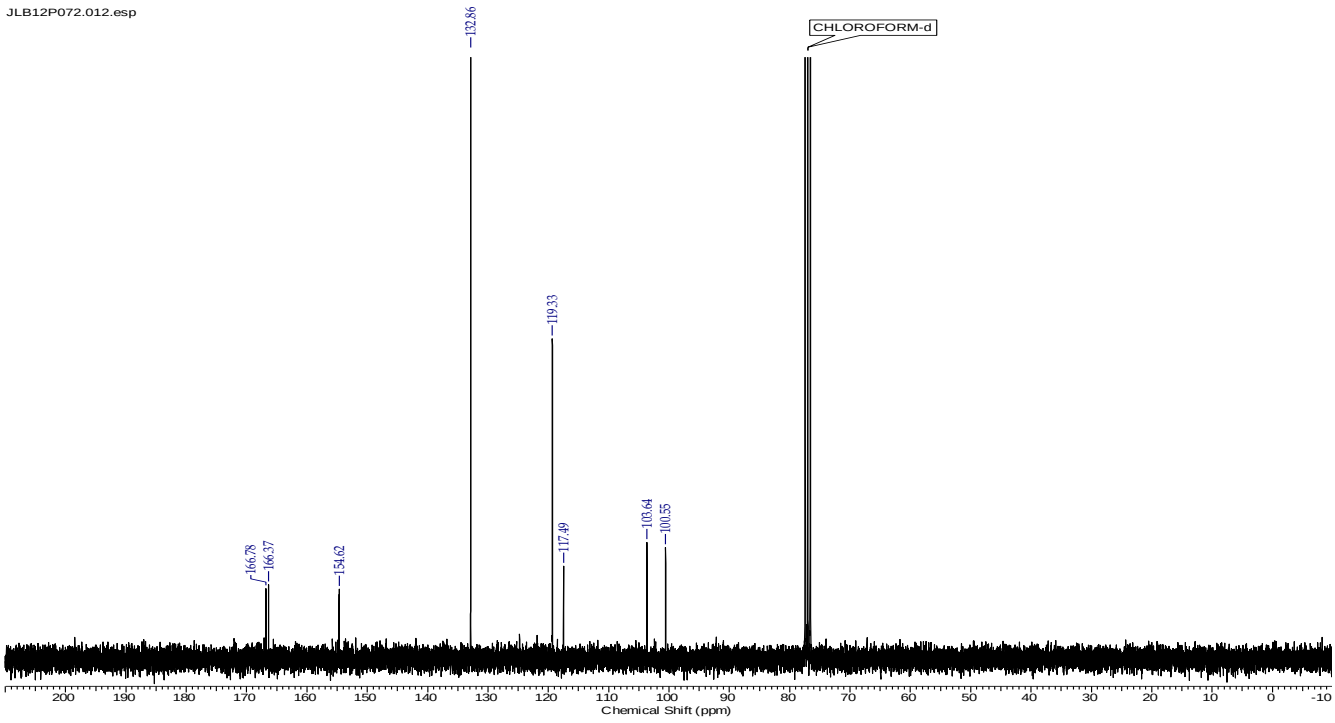
JLB12P072.012.esp
132.86
CHLOROFORM-d
119.33
103.64
100.55
117.49
166.78
166.37
154.62
Chemical Shift (ppm)

3.55

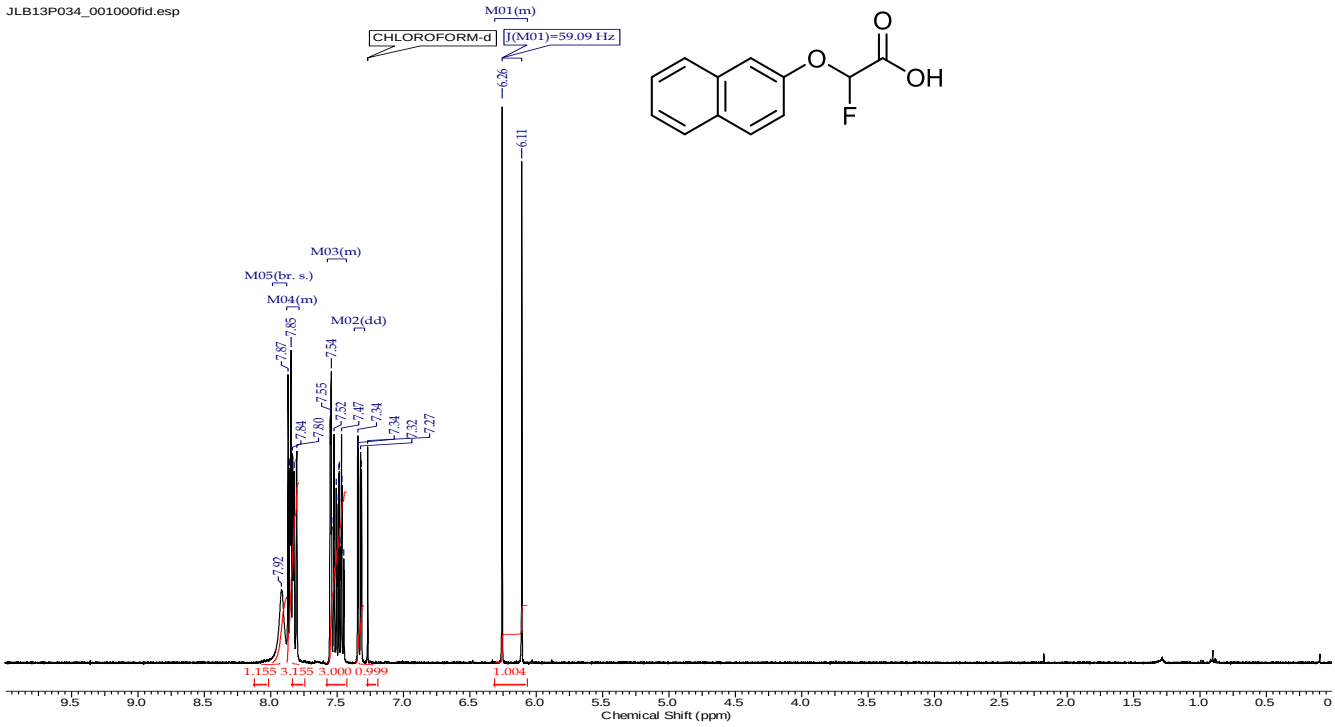
JLB13P034_001000fid.esp
M01(m)
CHLOROFORM-d
J(M01)=59.09 Hz
6.26
6.11
M03(m)
M05(br. s.)
M04(m)
M02(dd)
7.87
7.85
7.84
7.80
7.54
7.55
7.52
7.47
7.34
7.34
7.32
7.27
7.92
1.155 3.155 3.000 0.999
1.004
Chemical Shift (ppm)

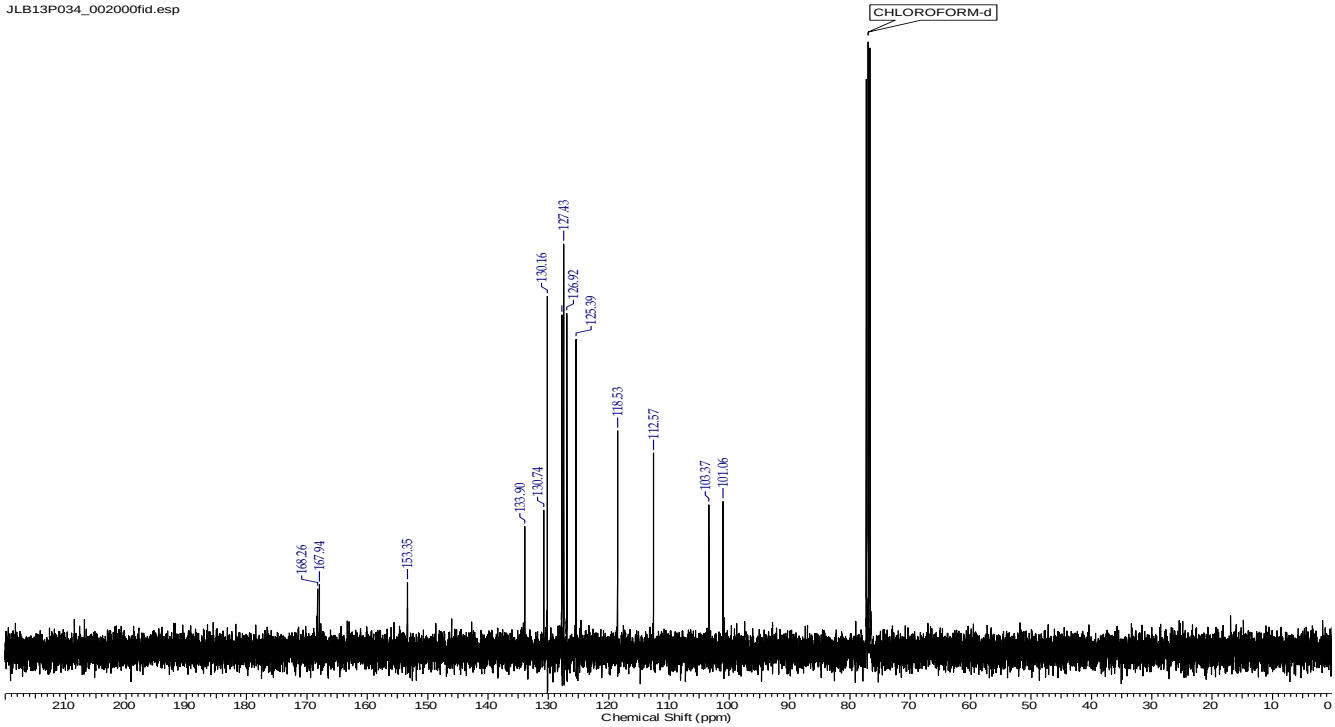
JLB13P034_002000fid.esp
CHLOROFORM-d
168.26
167.94
153.35
133.90
130.74
130.16
127.43
126.92
125.39
118.53
112.57
103.37
101.06
Chemical Shift (ppm)

3.185

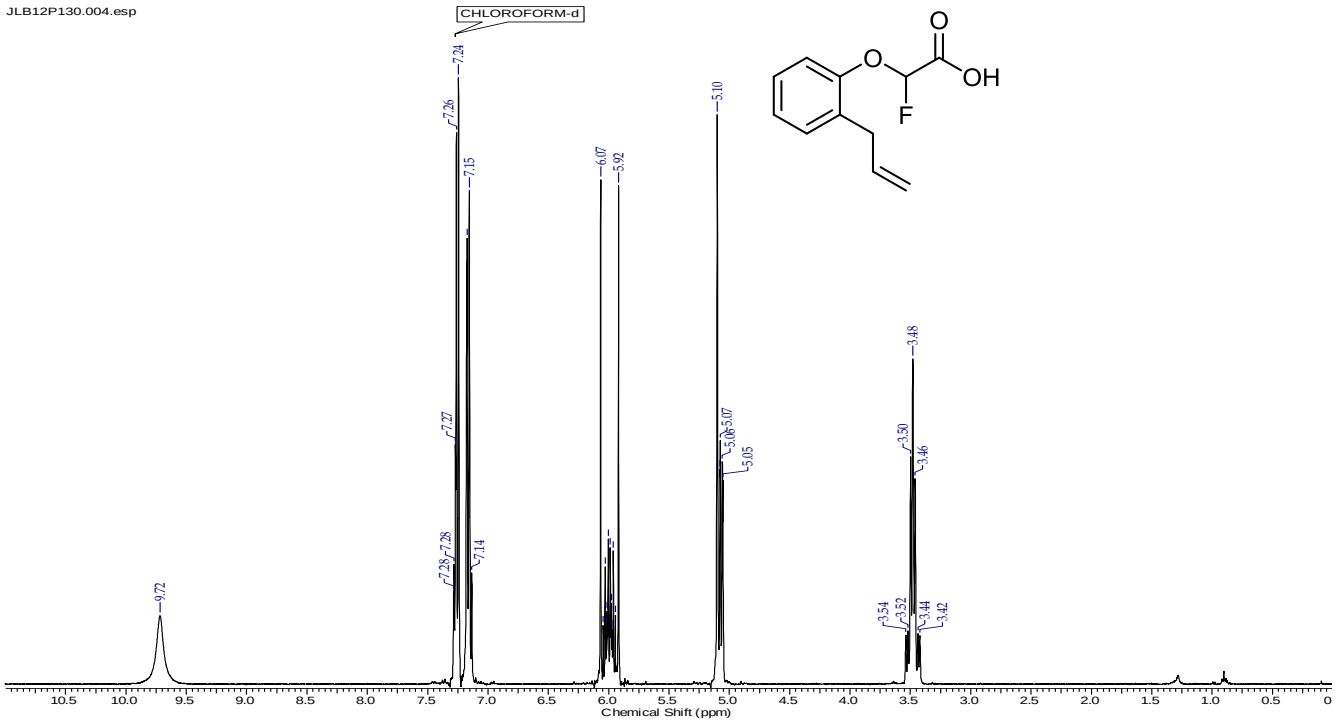
JLB12P130.004.esp
CHLOROFORM-d
O
O
OH
F
7.24
7.26
7.15
6.07
5.92
5.10
7.27
7.28
7.28
7.14
5.08
5.07
5.05
3.48
3.50
3.46
9.72
3.54
3.52
3.44
3.42
Chemical Shift (ppm)

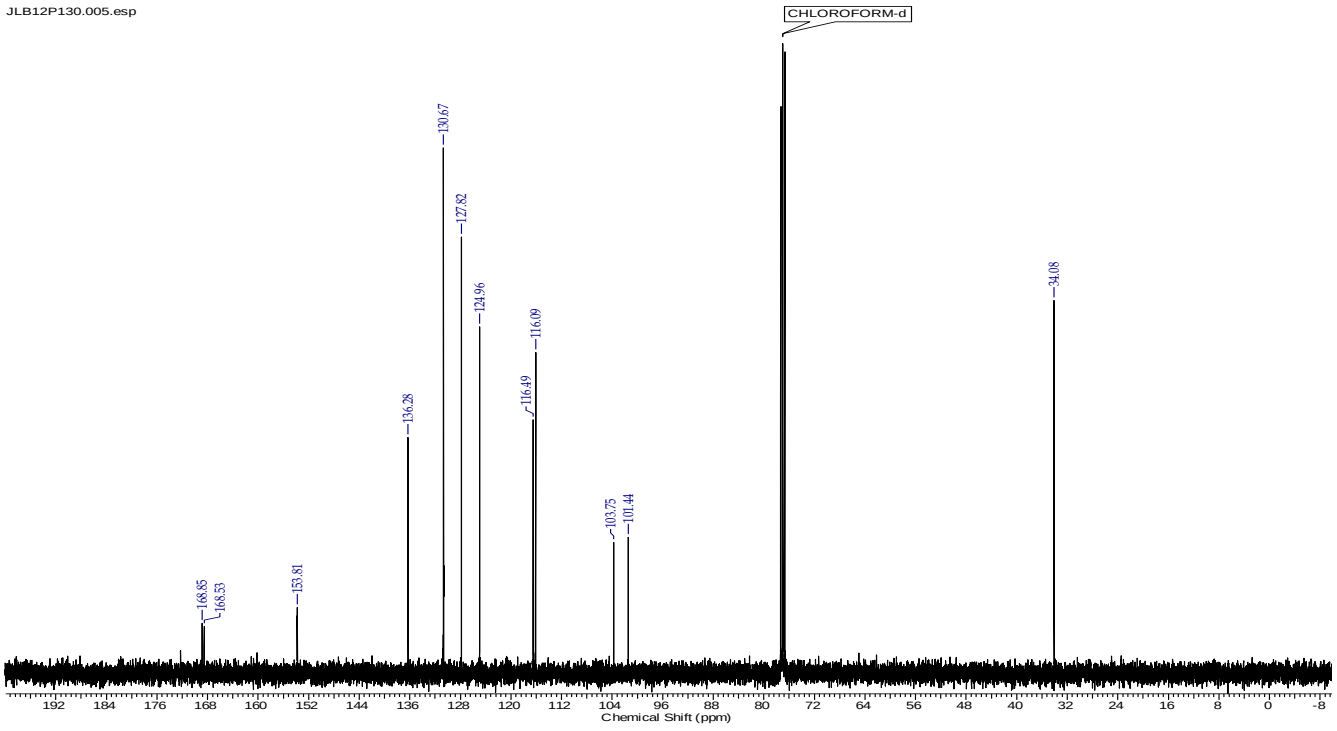
JLB12P130.005.esp
CHLOROFORM-d
130.67
127.82
124.96
116.09
116.49
136.28
103.75
101.44
34.08
168.85
168.53
153.81
Chemical Shift (ppm)

3.125a

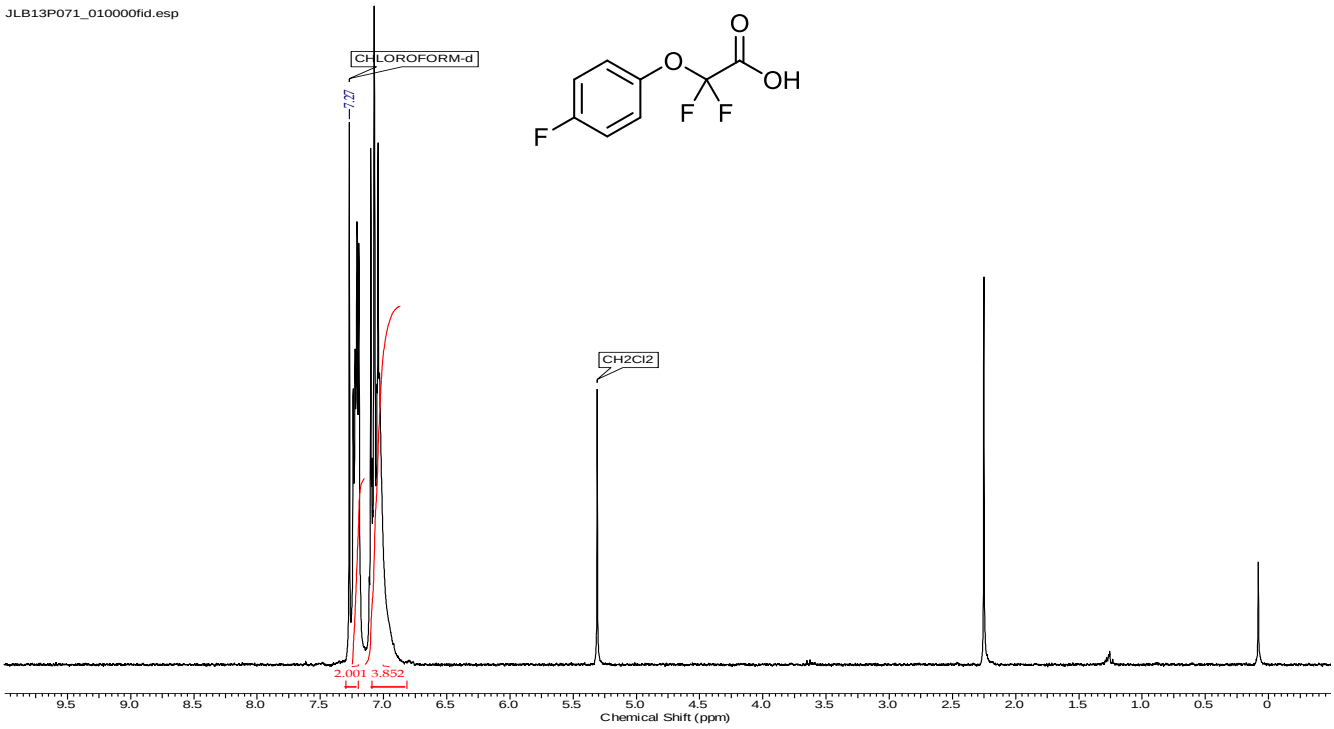
JLB13P071_010000fid.esp
CHLOROFORM-d
7.27
CH2Cl2
2.001
3.852
Chemical Shift (ppm)

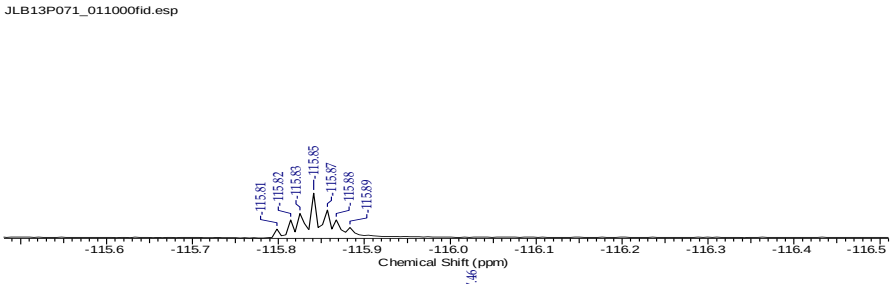
JLB13P071_011000fid.esp
115.81
115.82
115.83
115.85
115.87
115.88
115.89
Chemical Shift (ppm)

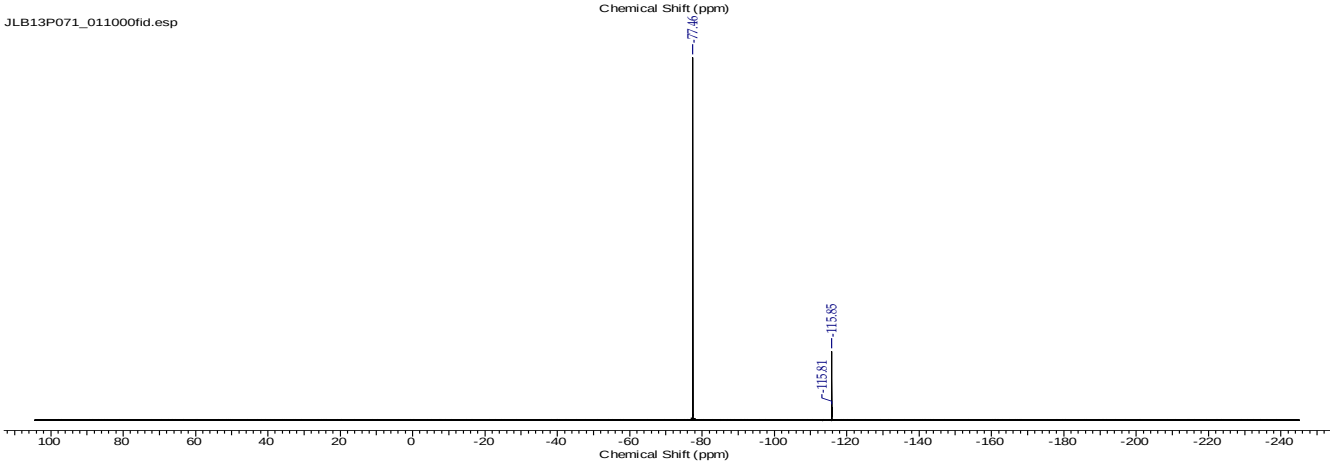
JLB13P071_011000fid.esp
-77.46
115.85
115.81
Chemical Shift (ppm)

3.125b

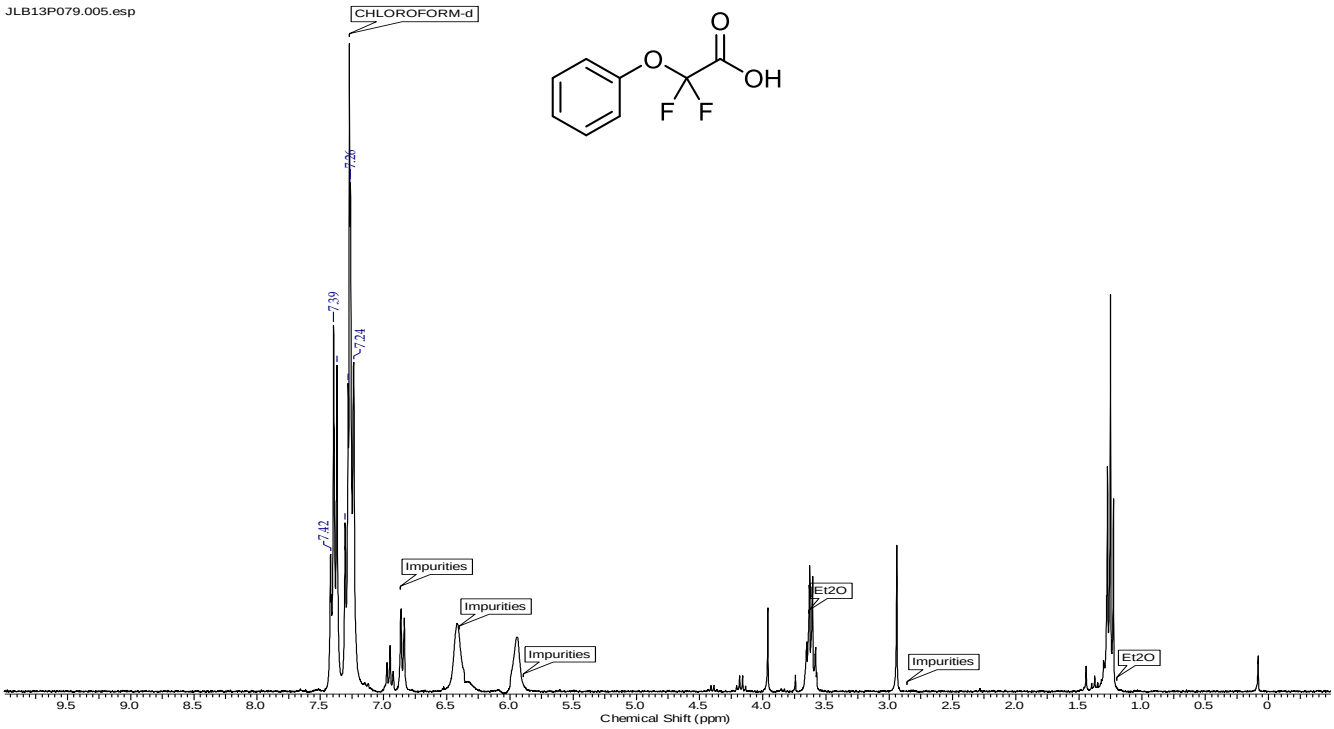
JLB13P079.005.esp
CHLOROFORM-d
O
O
OH
F F
7.26
7.39
7.24
7.42
Impurities
Impurities
Impurities
Et2O
Impurities
Et2O
9.5 9.0 8.5 8.0 7.5 7.0 6.5 6.0 5.5 5.0 4.5 4.0 3.5 3.0 2.5 2.0 1.5 1.0 0.5 0
Chemical Shift (ppm)

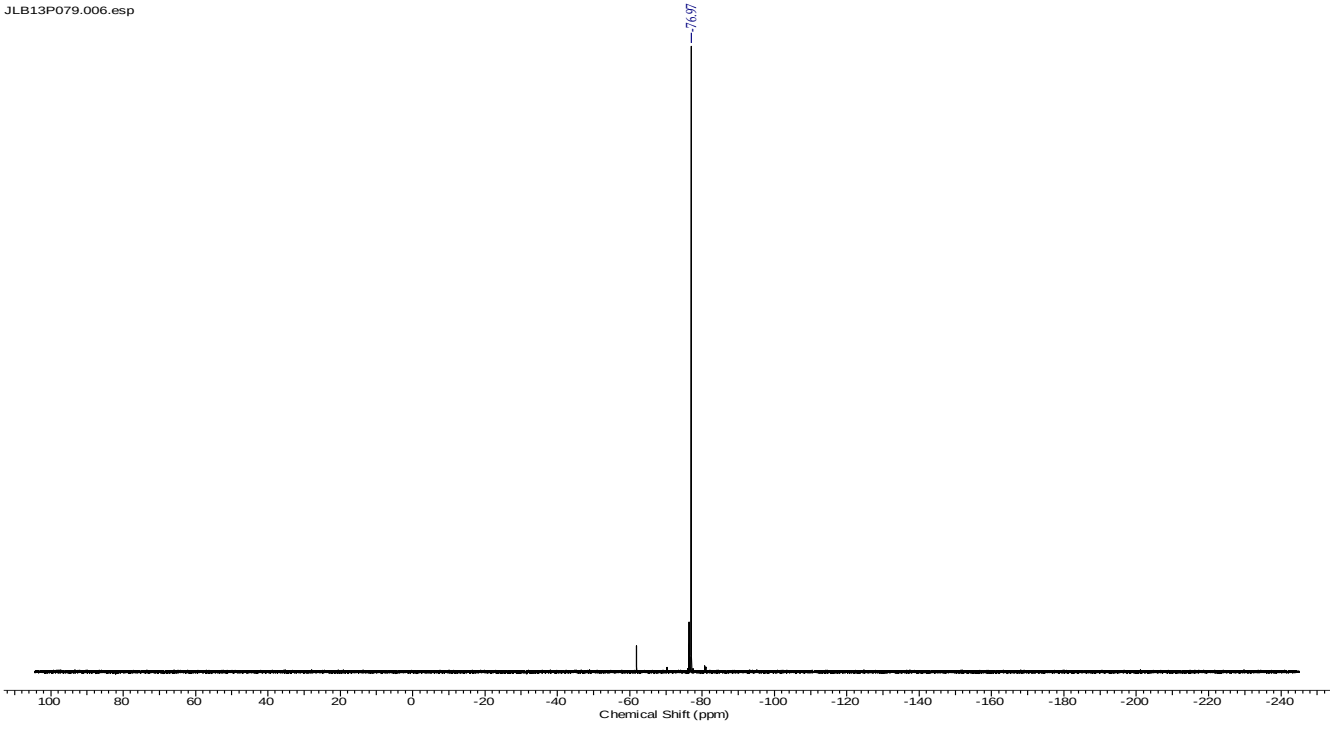
JLB13P079.006.esp
-76.97
100 80 60 40 20 0 -20 -40 -60 -80 -100 -120 -140 -160 -180 -200 -220 -240
Chemical Shift (ppm)

3.125c

JLB13P073.010.esp

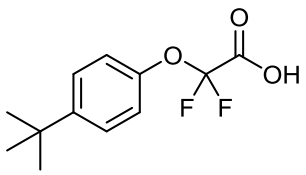

JLB13P073.011.esp

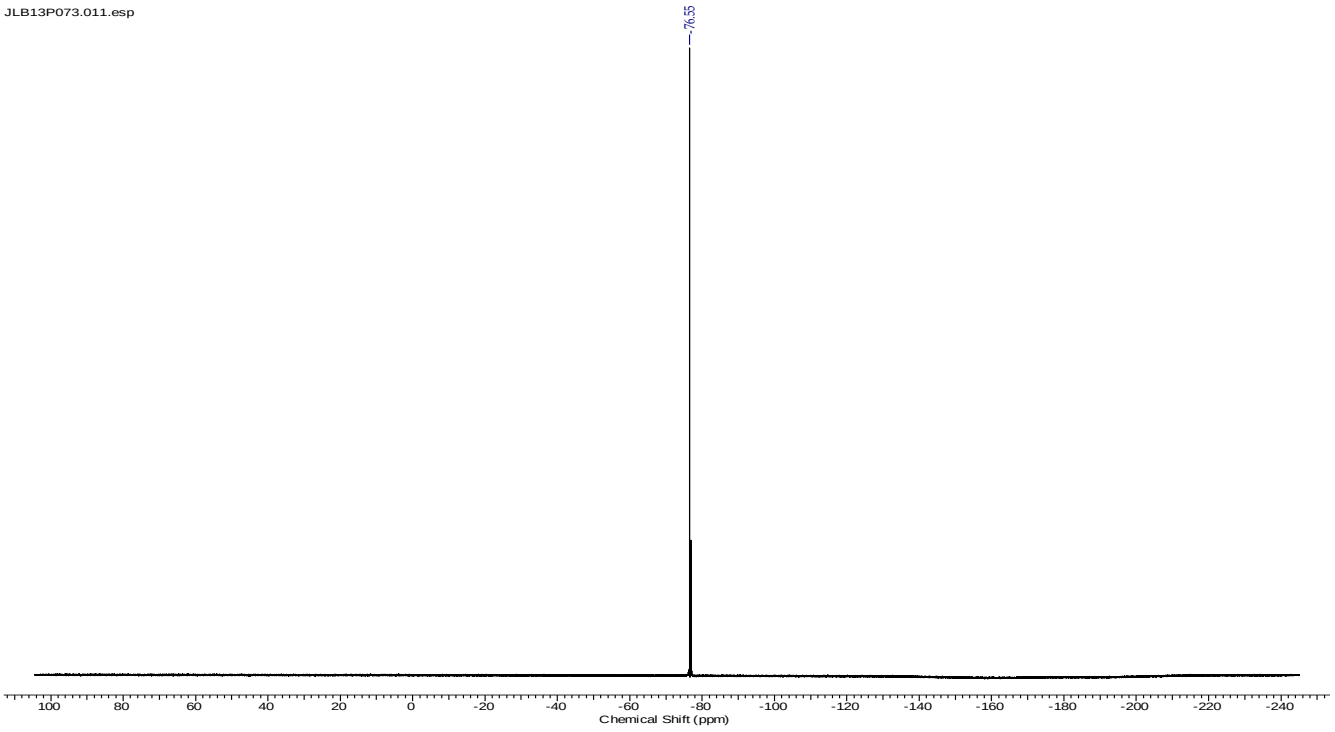

3.125d

JLB13P086.001.esp

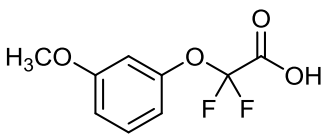

JLB13P086.002.esp

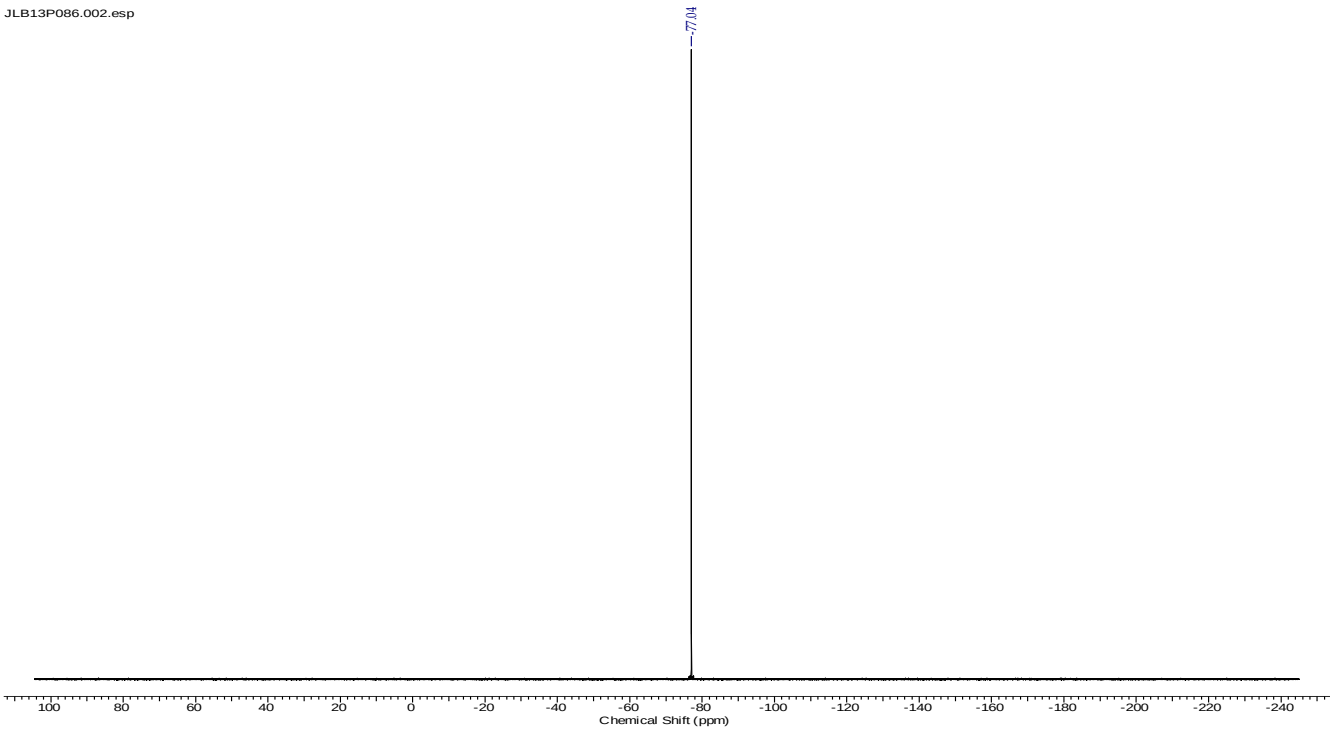

3.125e

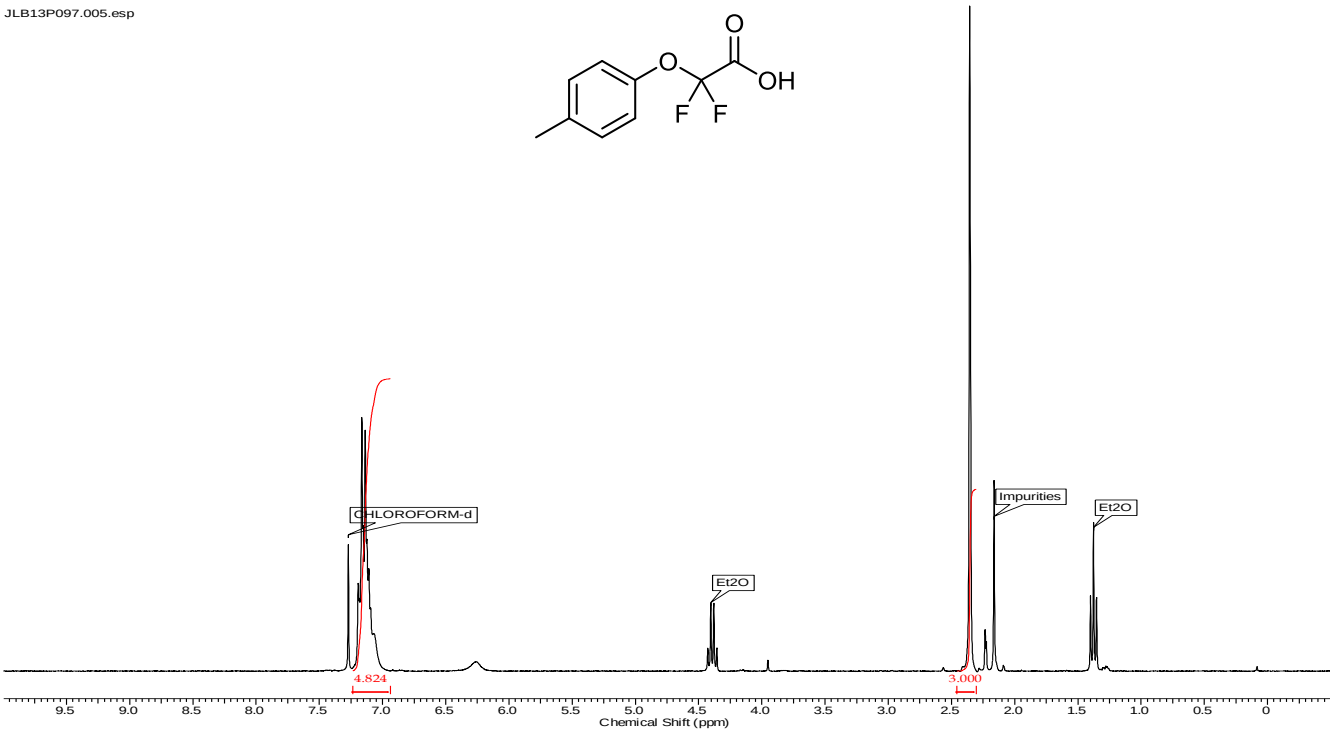
JLB13P097.005.esp
O
O
OH
F F
CHLOROFORM-d
Et2O
Impurities
Et2O
4.824
3.000
Chemical Shift (ppm)

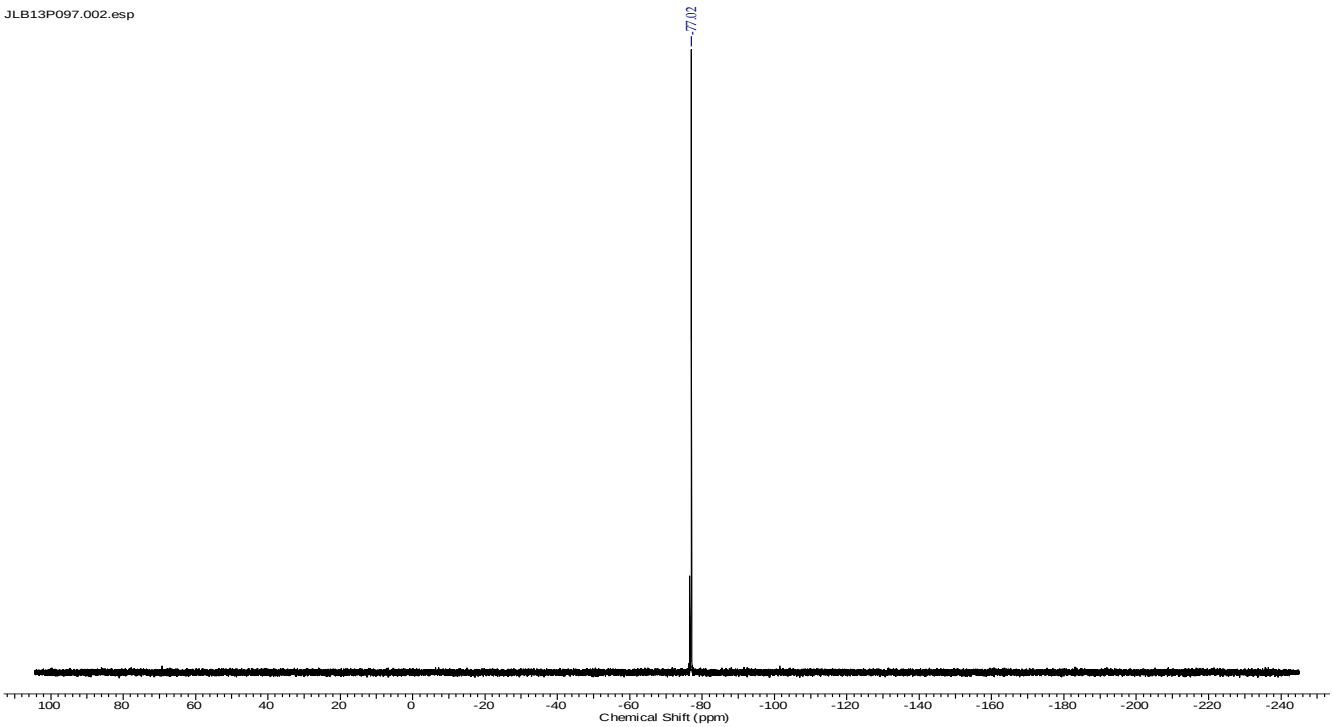
JLB13P097.002.esp
-77.02
Chemical Shift (ppm)

1.112

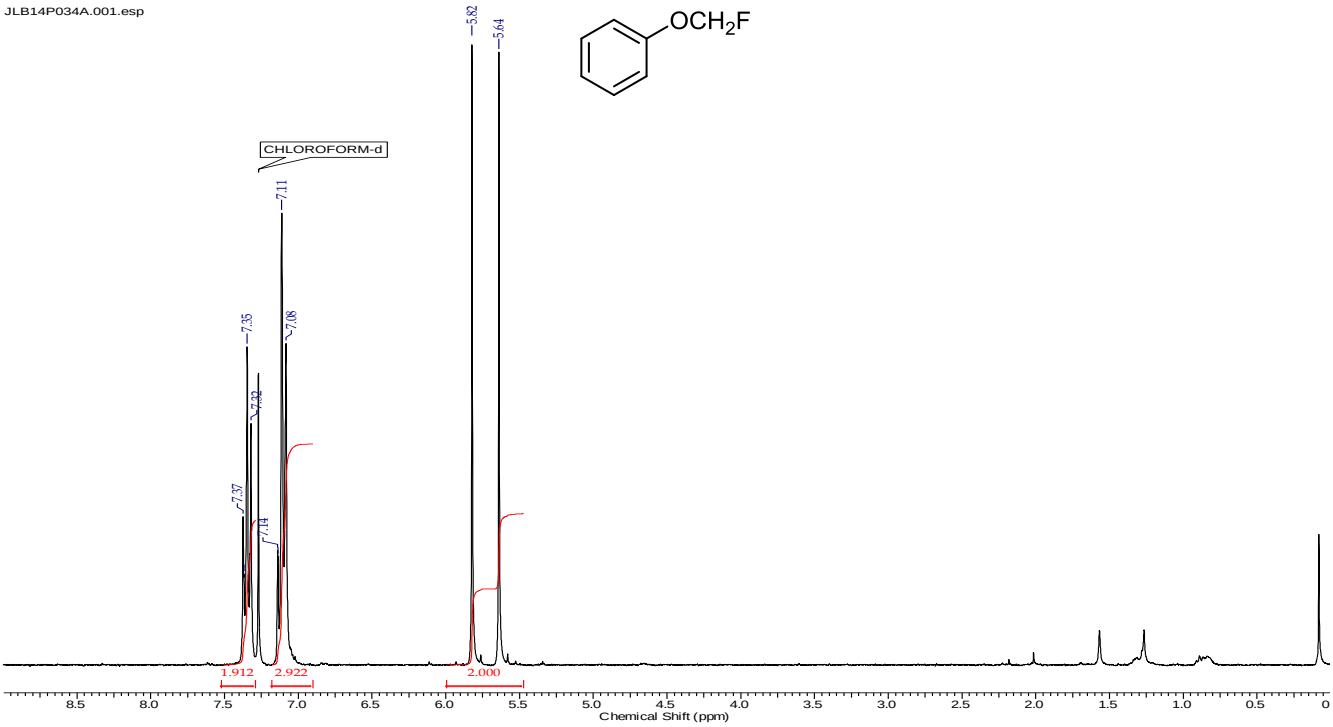
JLB14P034A.001.esp
OCH2F
CHLOROFORM-d
5.82
5.64
7.11
7.35
7.08
7.32
7.37
7.14
1.912
2.922
2.000
Chemical Shift (ppm)

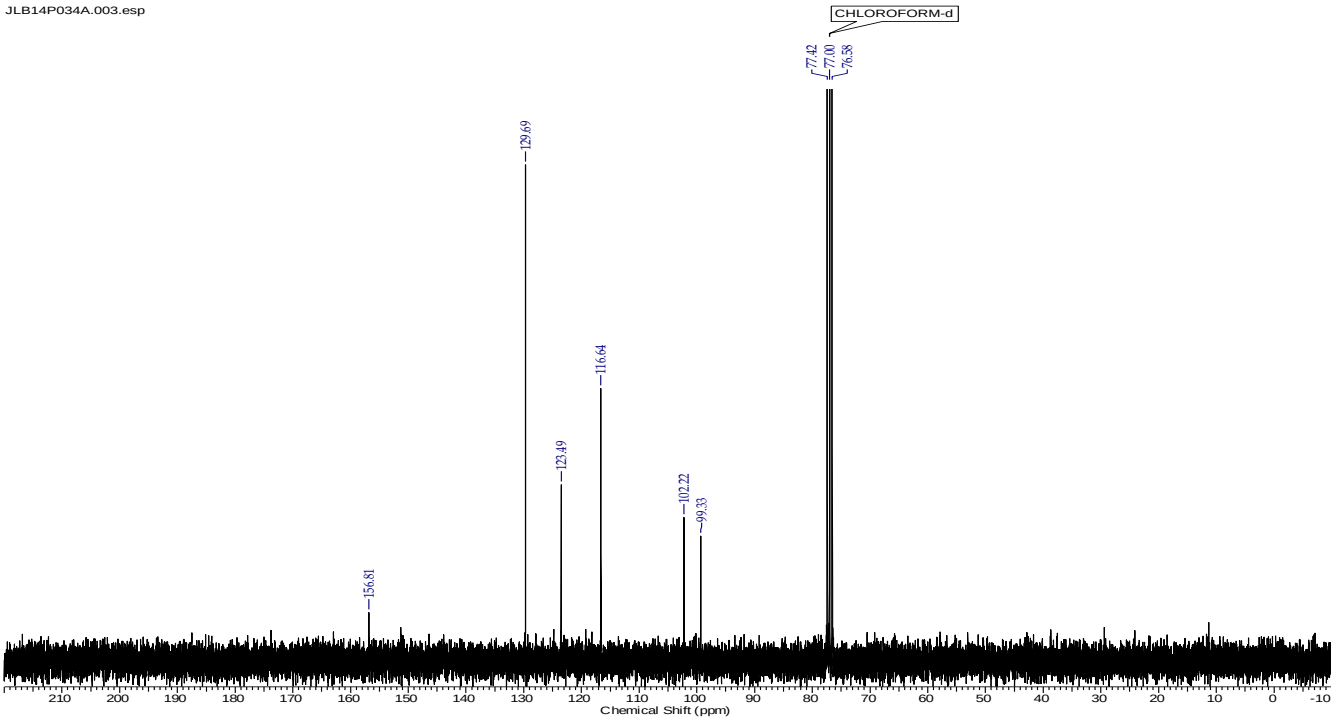
JLB14P034A.003.esp
CHLOROFORM-d
77.42
77.00
76.58
129.69
123.49
116.64
102.22
99.33
156.81
Chemical Shift (ppm)

3.100

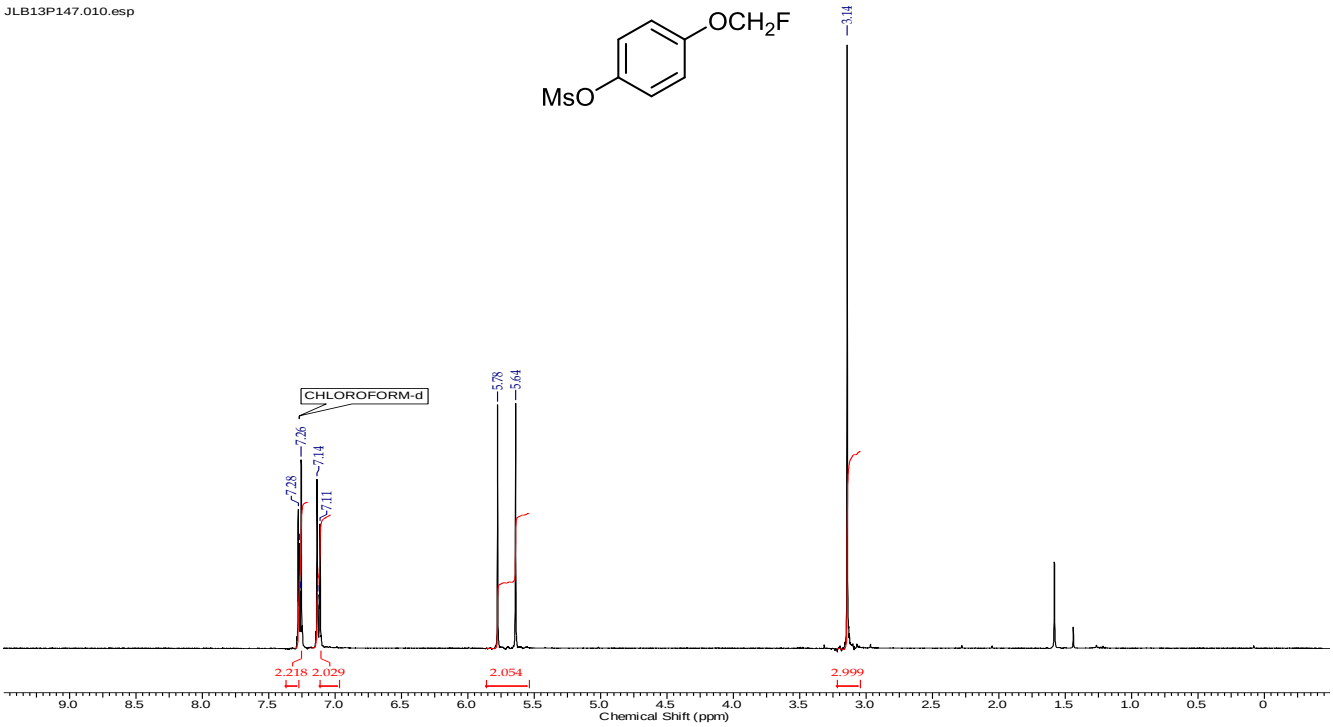
JLB13P147.010.esp
OCH2F
MsO
3.14
CHLOROFORM-d
5.78
5.64
7.26
7.14
7.28
7.11
2.218
2.029
2.054
2.999
Chemical Shift (ppm)

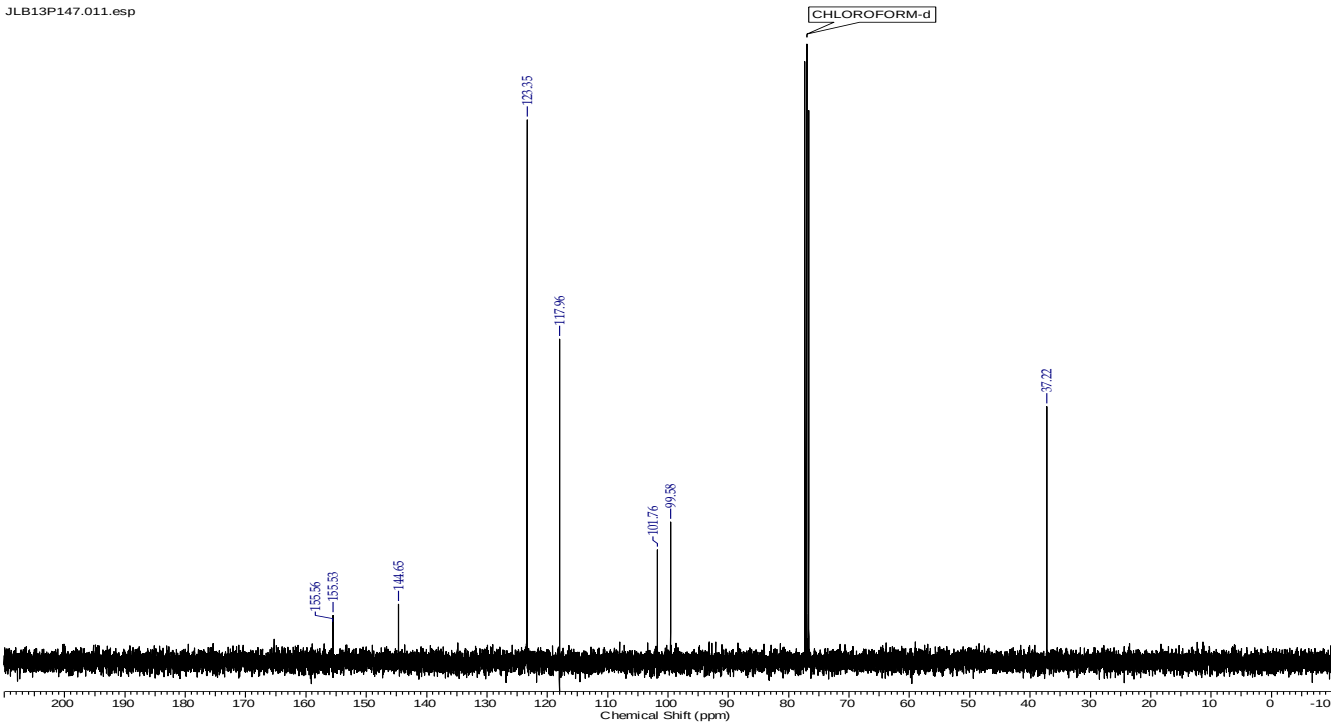
JLB13P147.011.esp
CHLOROFORM-d
123.35
117.96
37.22
101.76
99.58
155.56
155.33
144.65
Chemical Shift (ppm)

3.121

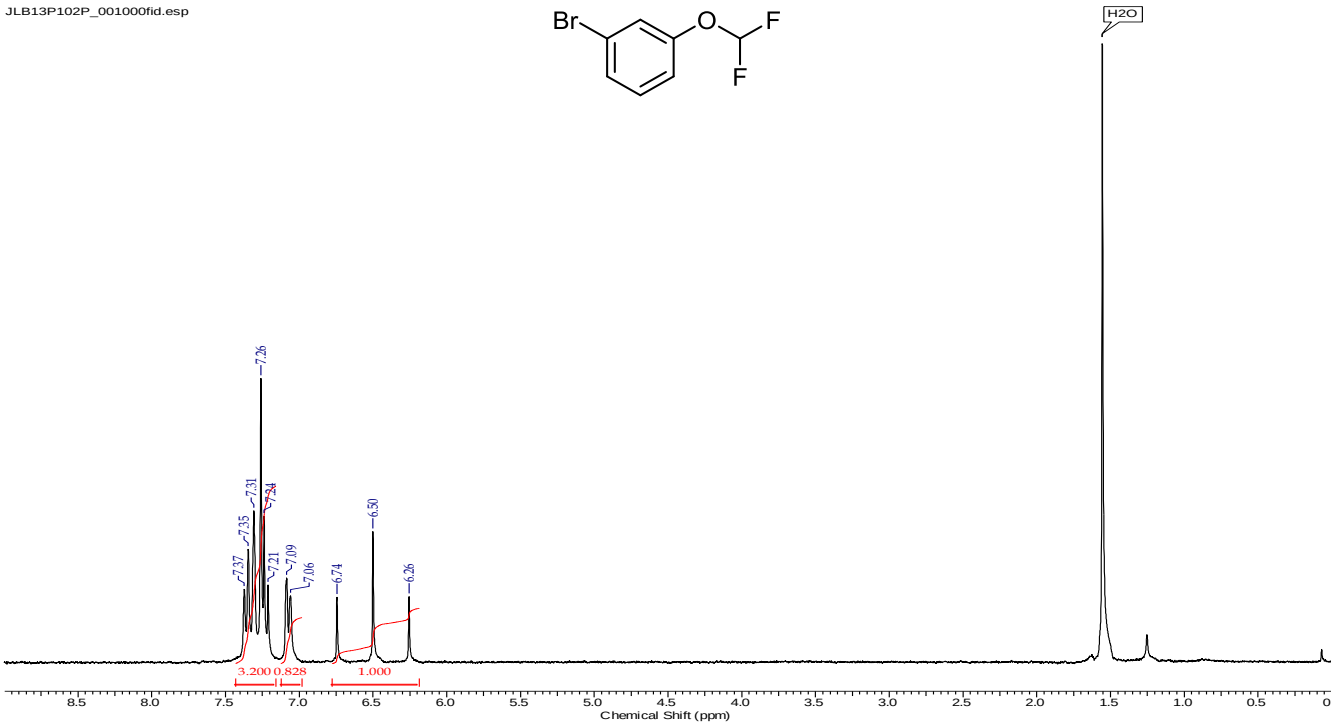
JLB13P102P_001000fid.esp
Br
O
F
F
H2O
7.26
7.37
7.35
7.31
7.24
7.21
7.09
7.06
6.74
6.50
6.26
3.200
0.828
1.000
Chemical Shift (ppm)

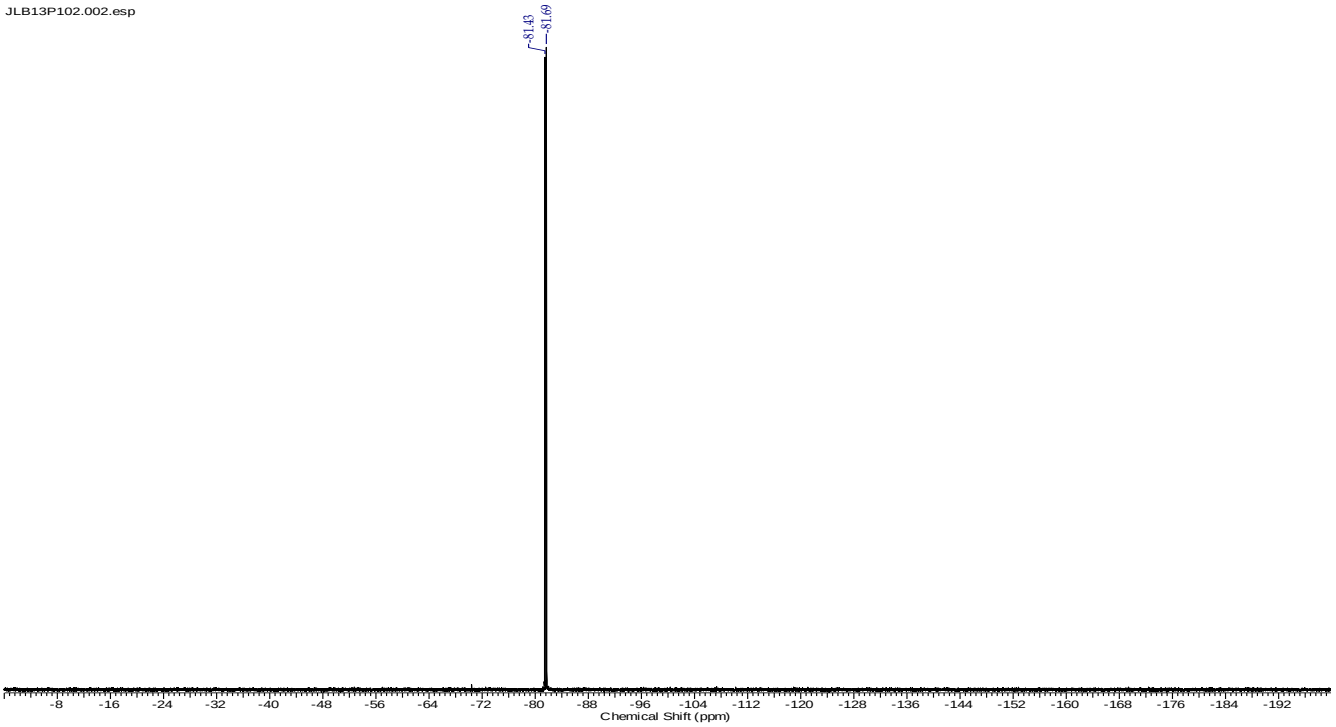
JLB13P102.002.esp
81.43
81.69
Chemical Shift (ppm)

3.153

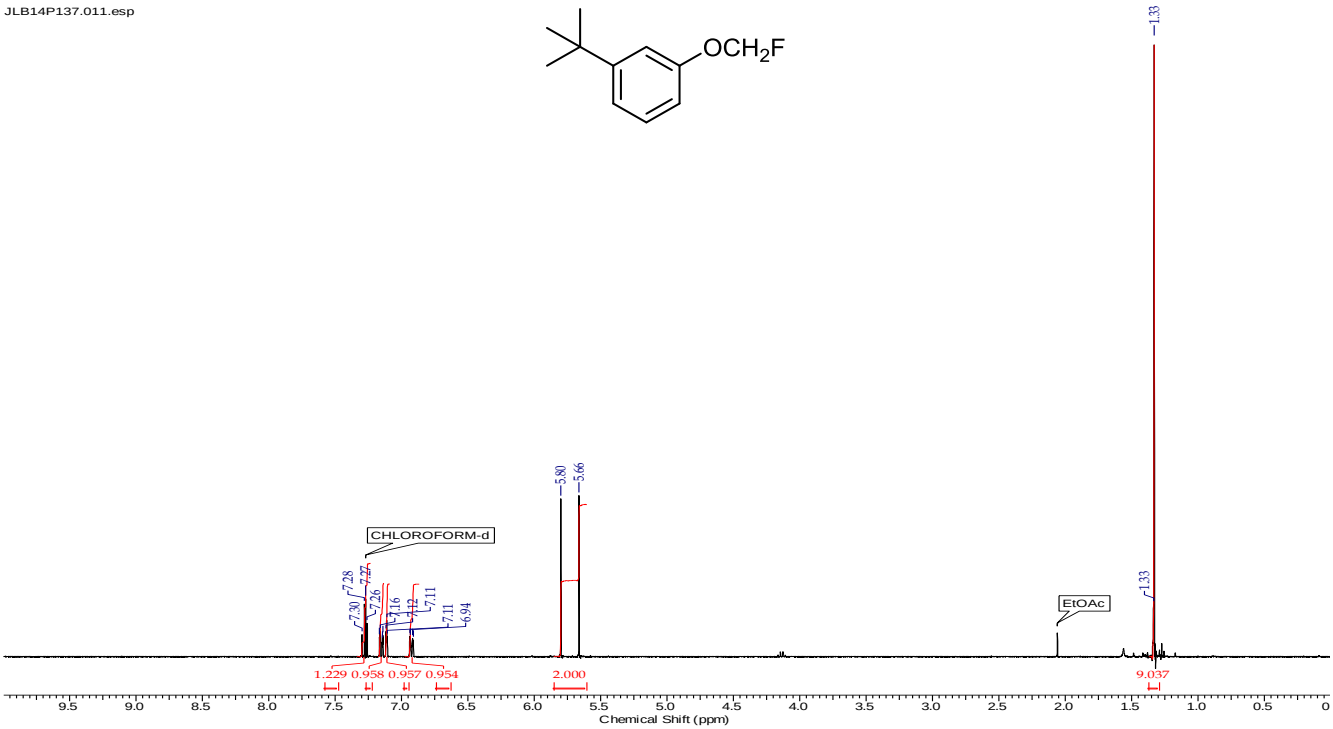
JLB14P137.011.esp
OCH2F
1.33
5.80
5.66
CHLOROFORM-d
7.28
7.27
7.26
7.16
7.12
7.11
7.11
6.94
EtOAc
1.33
1.229 0.958 0.957 0.954
2.000
9.037
Chemical Shift (ppm)

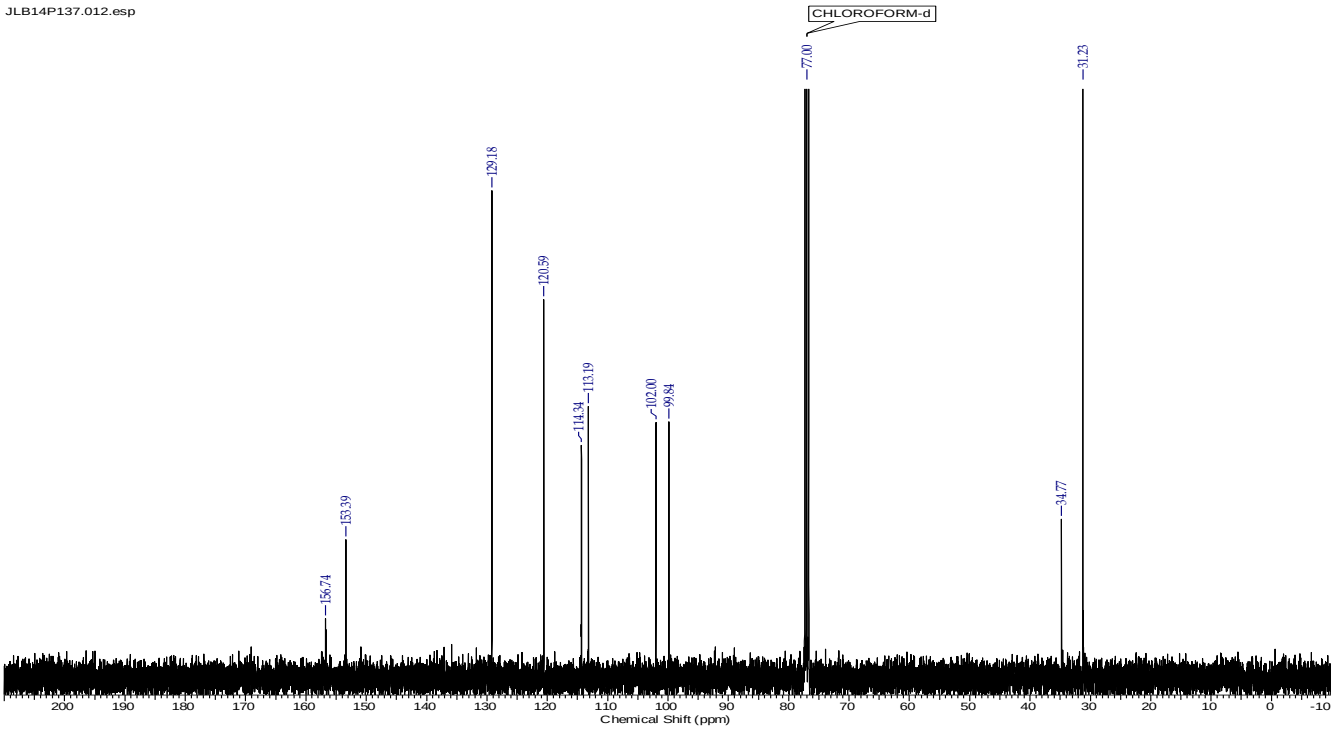
JLB14P137.012.esp
CHLOROFORM-d
77.00
31.23
129.18
120.59
114.34
113.19
102.00
99.84
153.39
156.74
34.77
Chemical Shift (ppm)

3.154

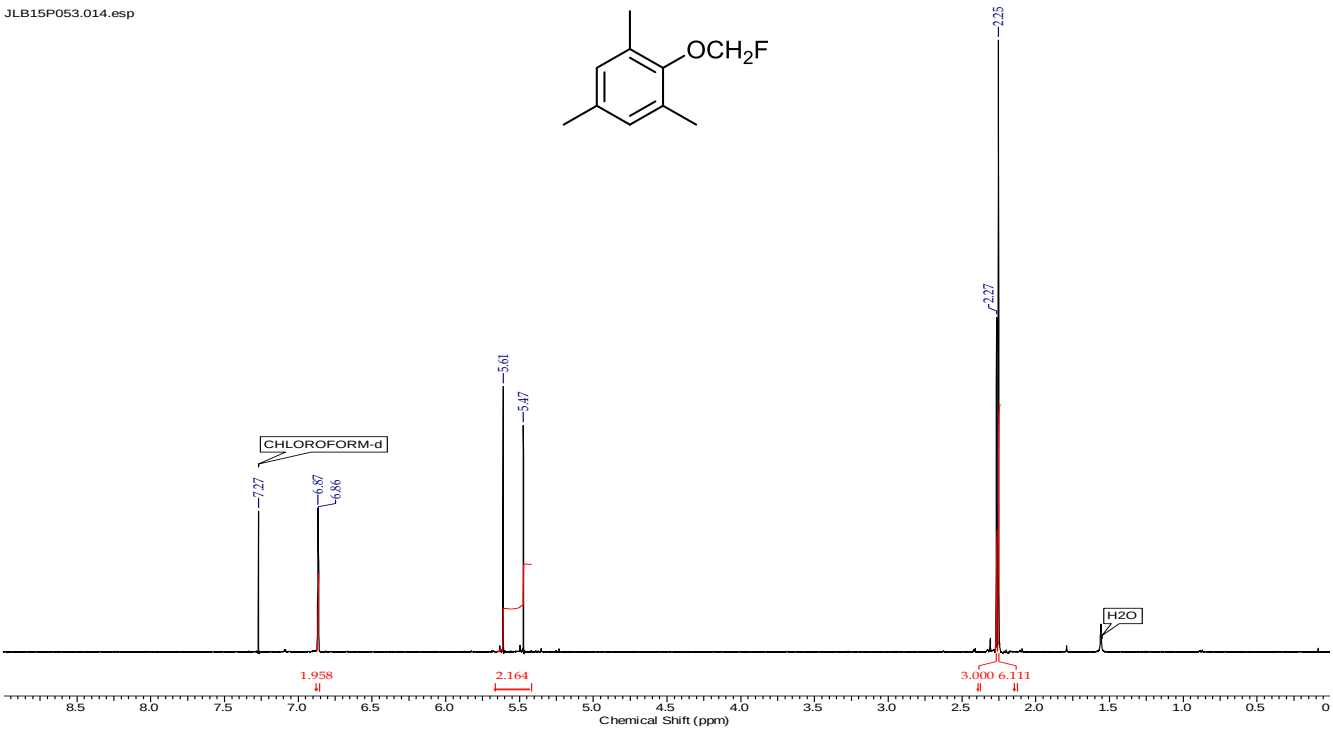
JLB15P053.014.esp
OCH2F
2.25
2.27
5.61
5.47
CHLOROFORM-d
7.27
6.87
6.86
H2O
1.958
2.164
3.000
6.111
Chemical Shift (ppm)

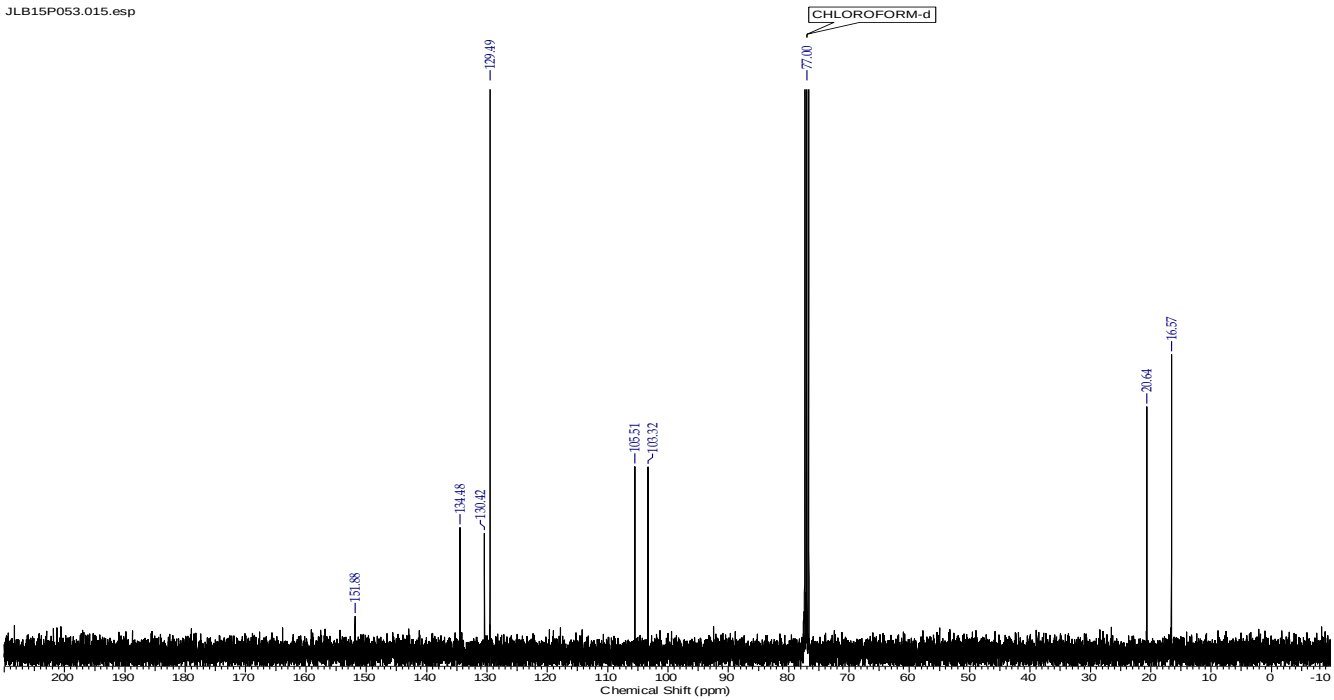
JLB15P053.015.esp
CHLOROFORM-d
129.49
77.00
16.57
20.64
105.51
103.32
134.48
130.42
151.88
Chemical Shift (ppm)

3.158

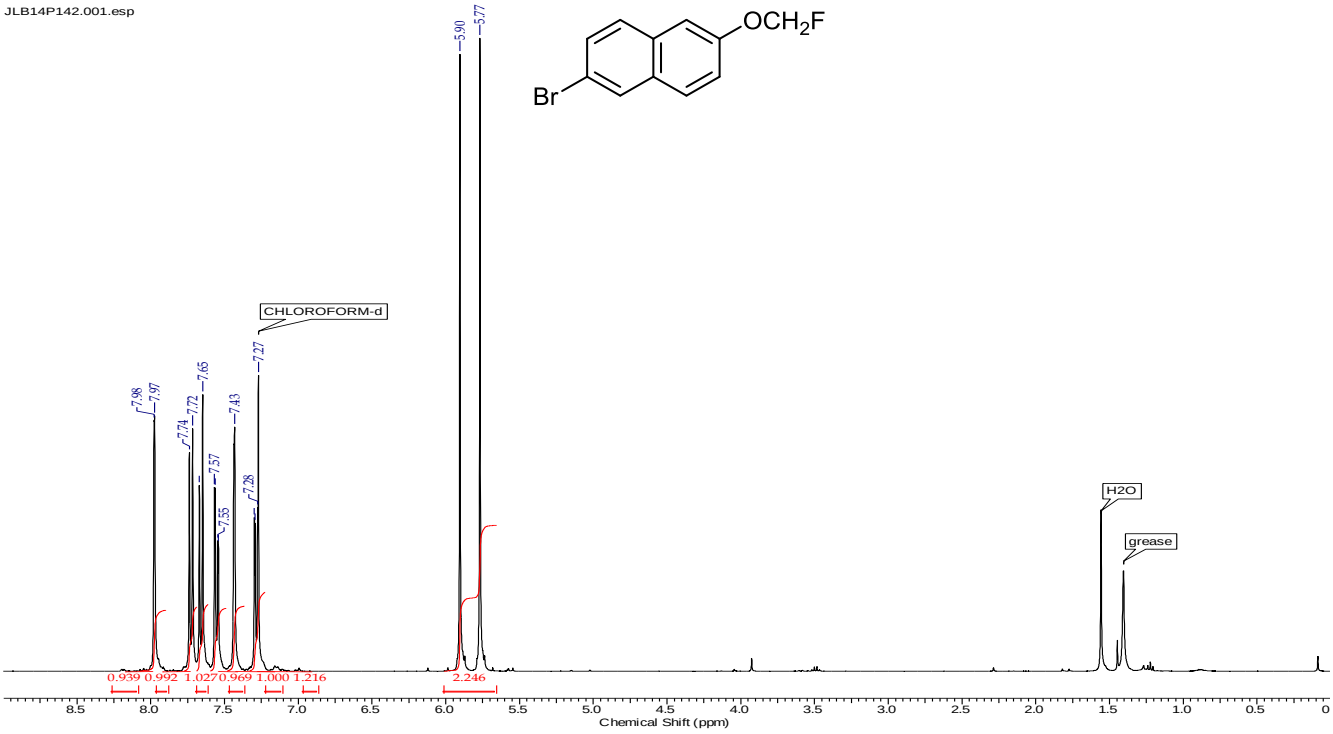
JLB14P142.001.esp
Br
OCH2F
5.90
5.77
CHLOROFORM-d
7.98
7.97
7.74
7.72
7.65
7.57
7.55
7.43
7.28
7.27
H2O
grease
0.939 0.992 1.027 0.969 1.000 1.216
2.246
Chemical Shift (ppm)

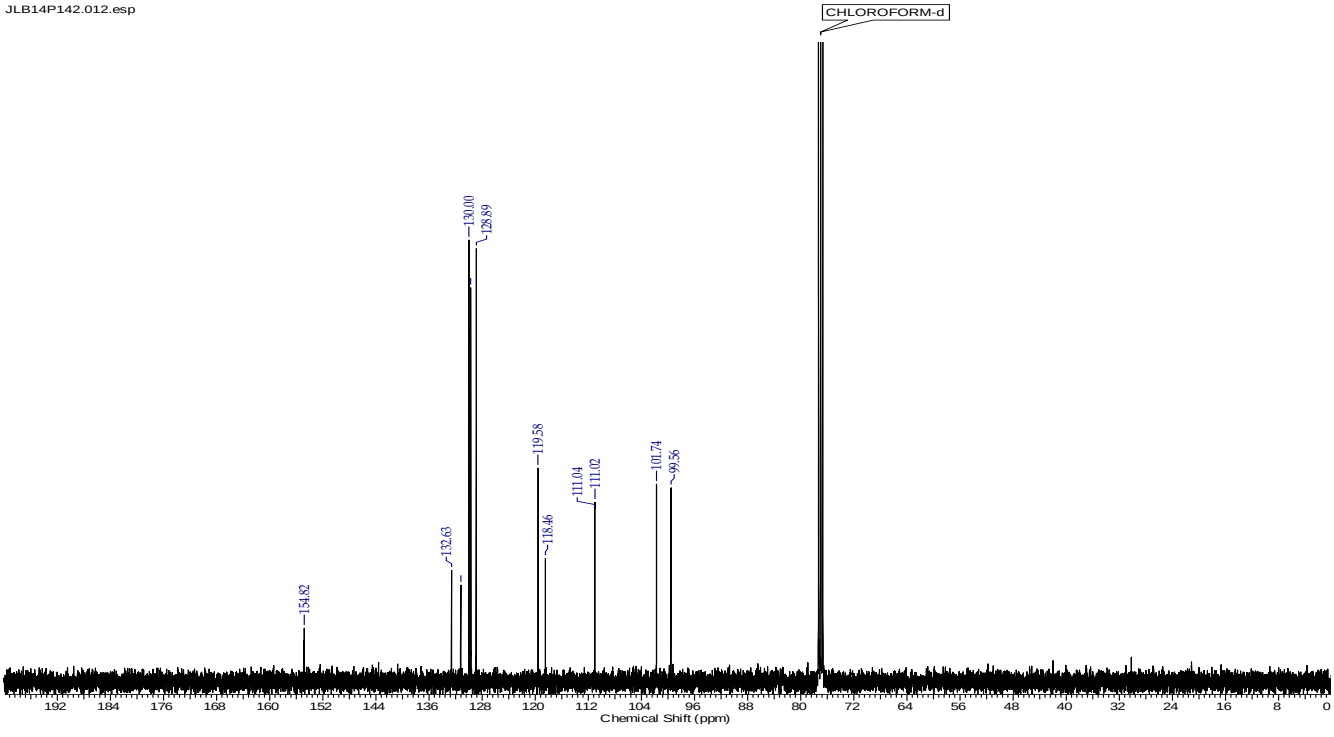
JLB14P142.012.esp
CHLOROFORM-d
130.00
128.89
119.58
118.46
111.04
111.02
101.74
99.56
132.63
154.82
Chemical Shift (ppm)

3.159

JLB14P133.011.esp

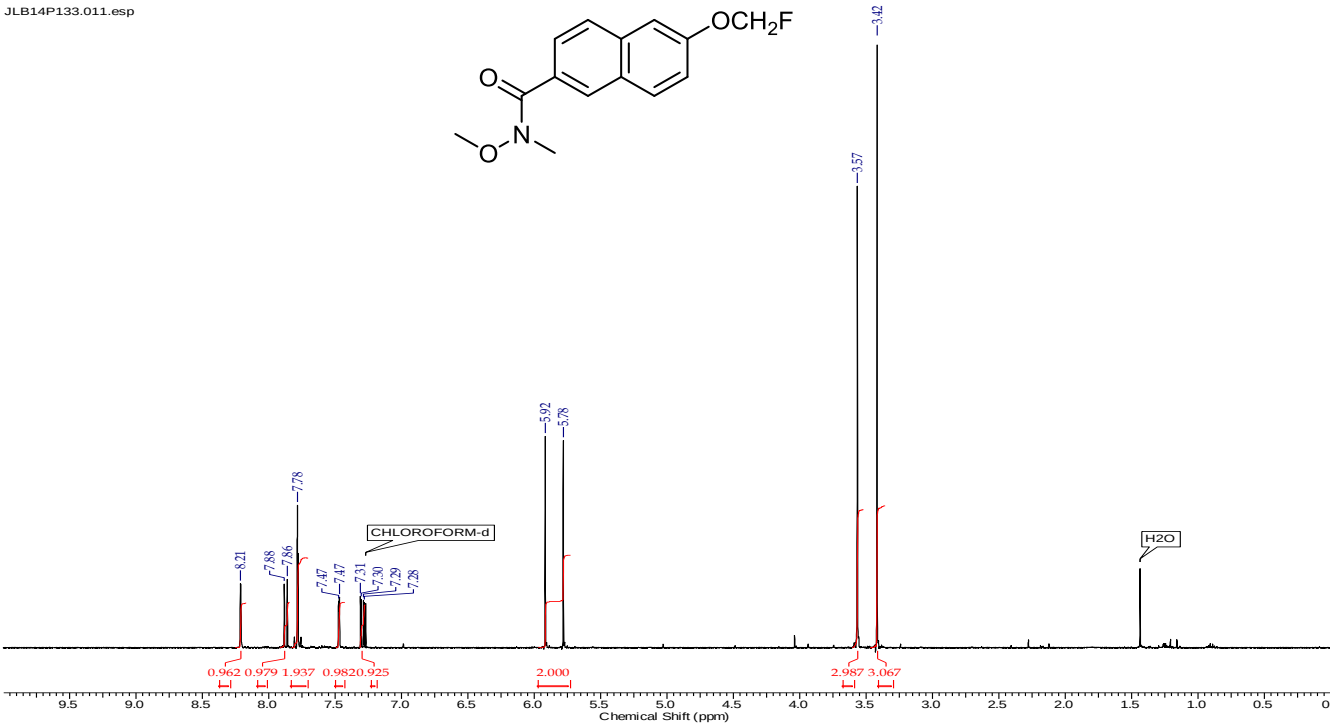

JLB14P133.012.esp

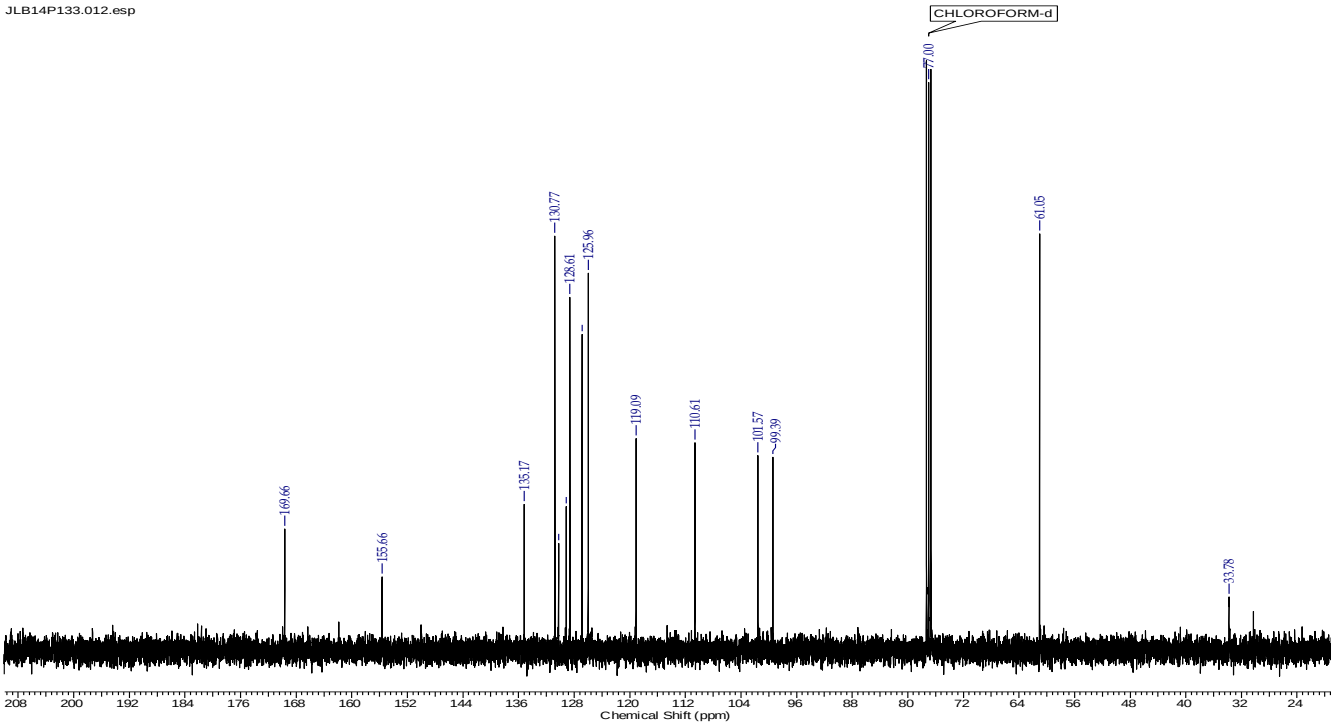

3.105

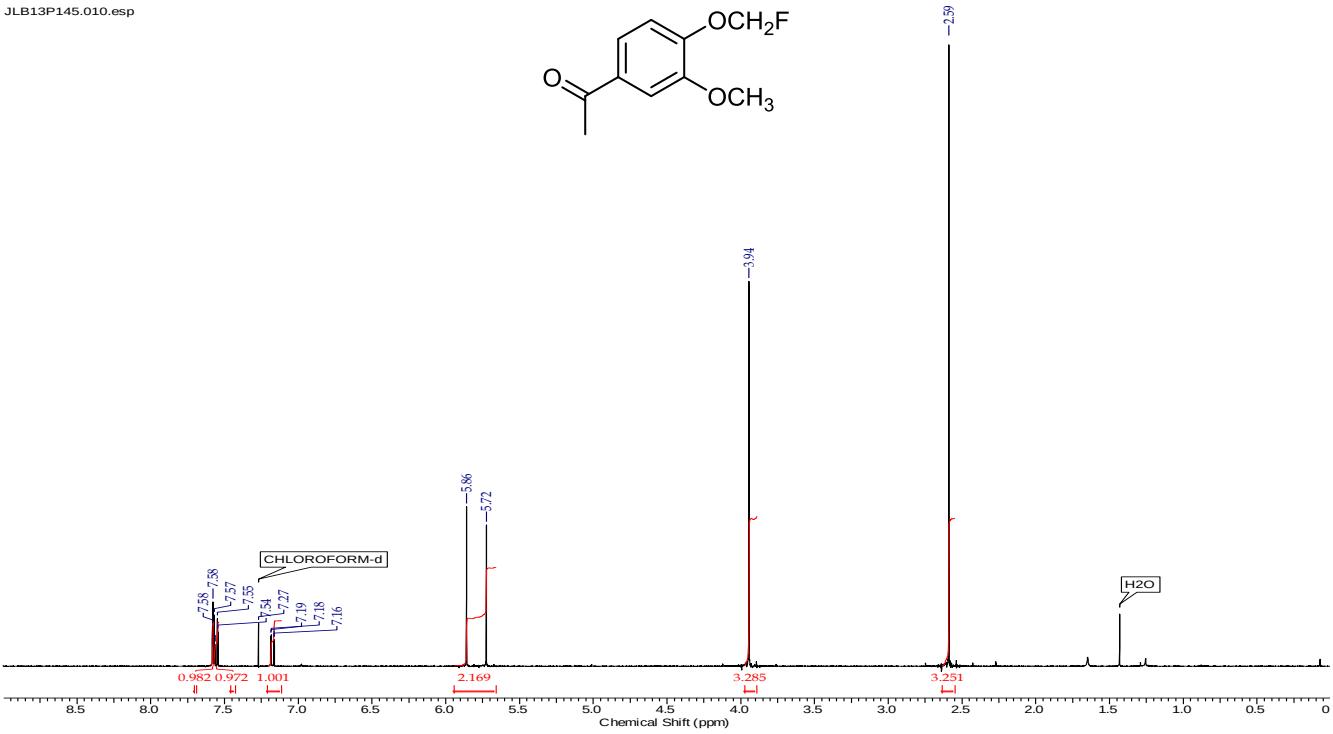
JLB13P145.010.esp
OCH2F
O
OCH3
2.59
3.94
5.86
5.72
CHLOROFORM-d
H2O
7.58
7.58
7.57
7.55
7.54
7.27
7.19
7.18
7.16
0.982
0.972
1.001
2.169
3.285
3.251
Chemical Shift (ppm)

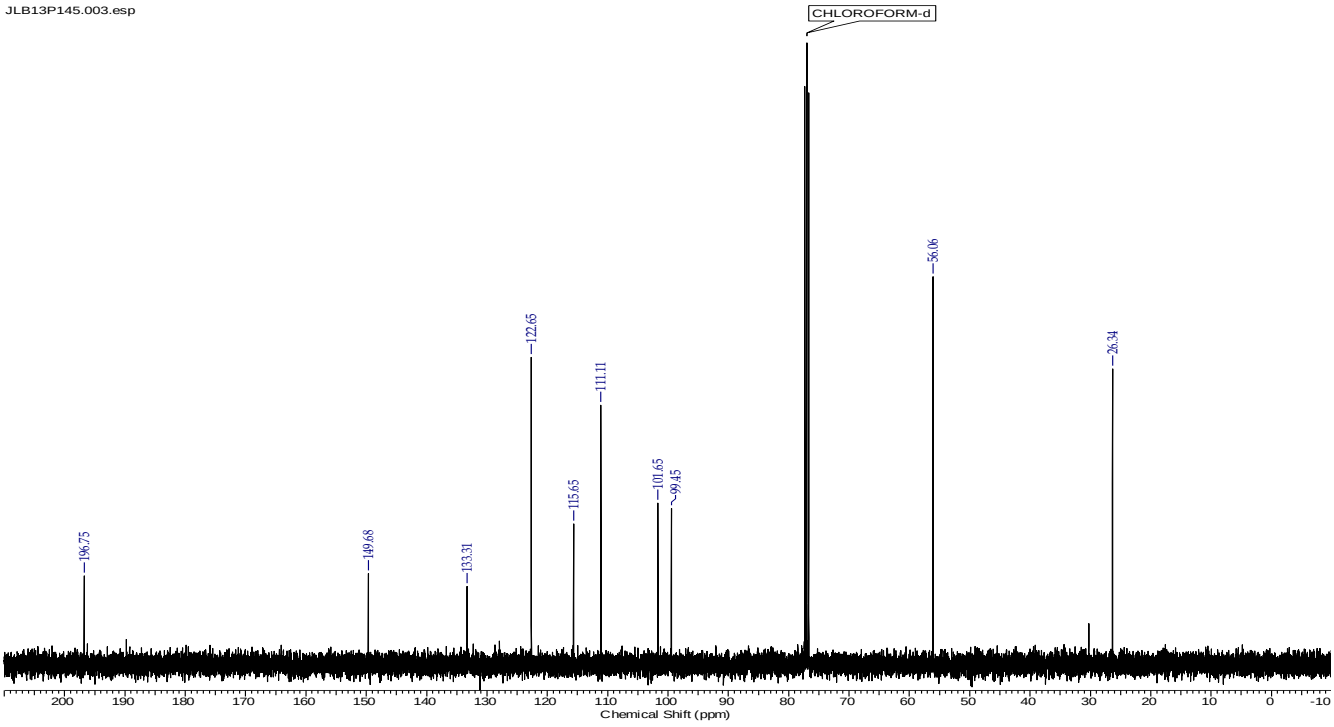
JLB13P145.003.esp
CHLOROFORM-d
196.75
149.68
133.31
122.65
115.65
111.11
101.65
99.45
56.06
26.34
Chemical Shift (ppm)

3.163

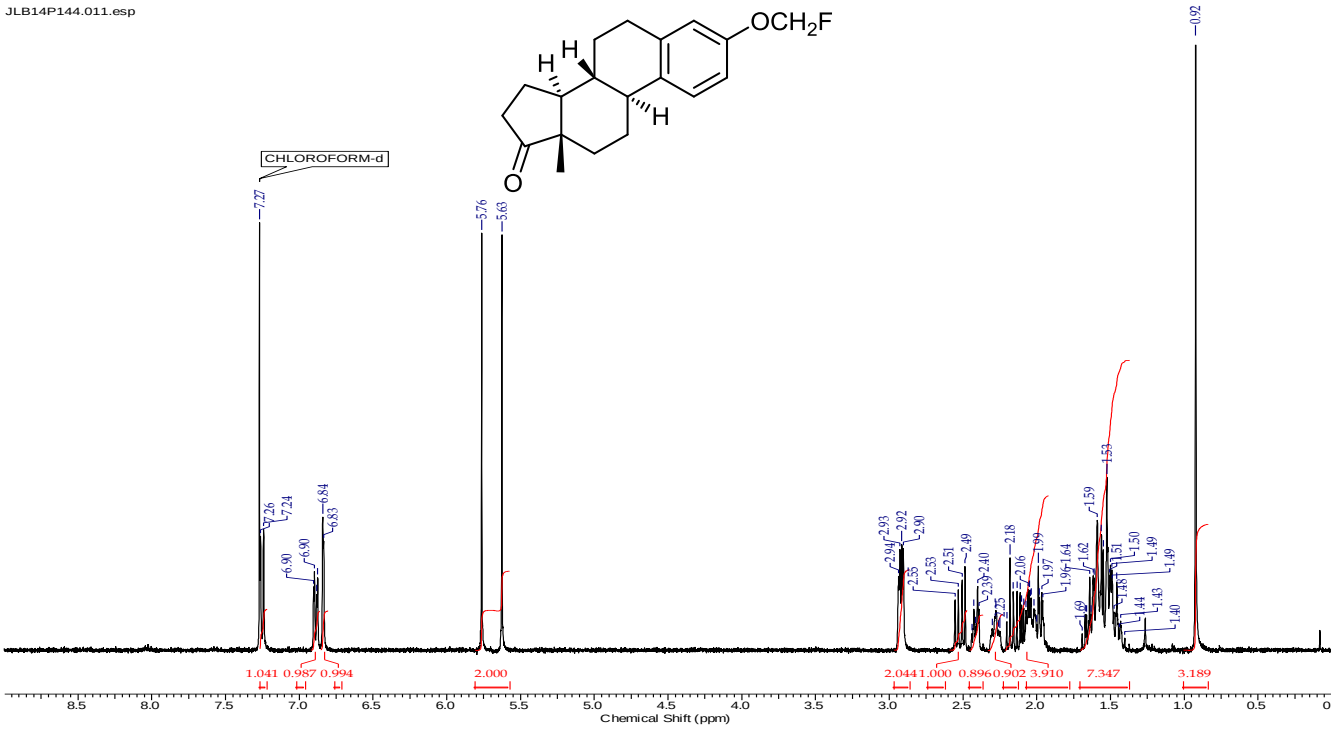
JLB14P144.011.esp
OCH2F
H
H
H
O
CHLOROFORM-d
7.27
7.26
7.24
6.90
6.90
6.84
6.83
5.76
5.63
2.93
2.92
2.90
2.51
2.49
2.40
2.18
1.99
1.97
1.64
1.62
1.59
1.53
1.50
1.49
1.49
1.44
1.43
1.40
0.92
1.041 0.987 0.994
2.000
2.044 1.000 0.896 0.902 3.910
7.347
3.189
Chemical Shift (ppm)

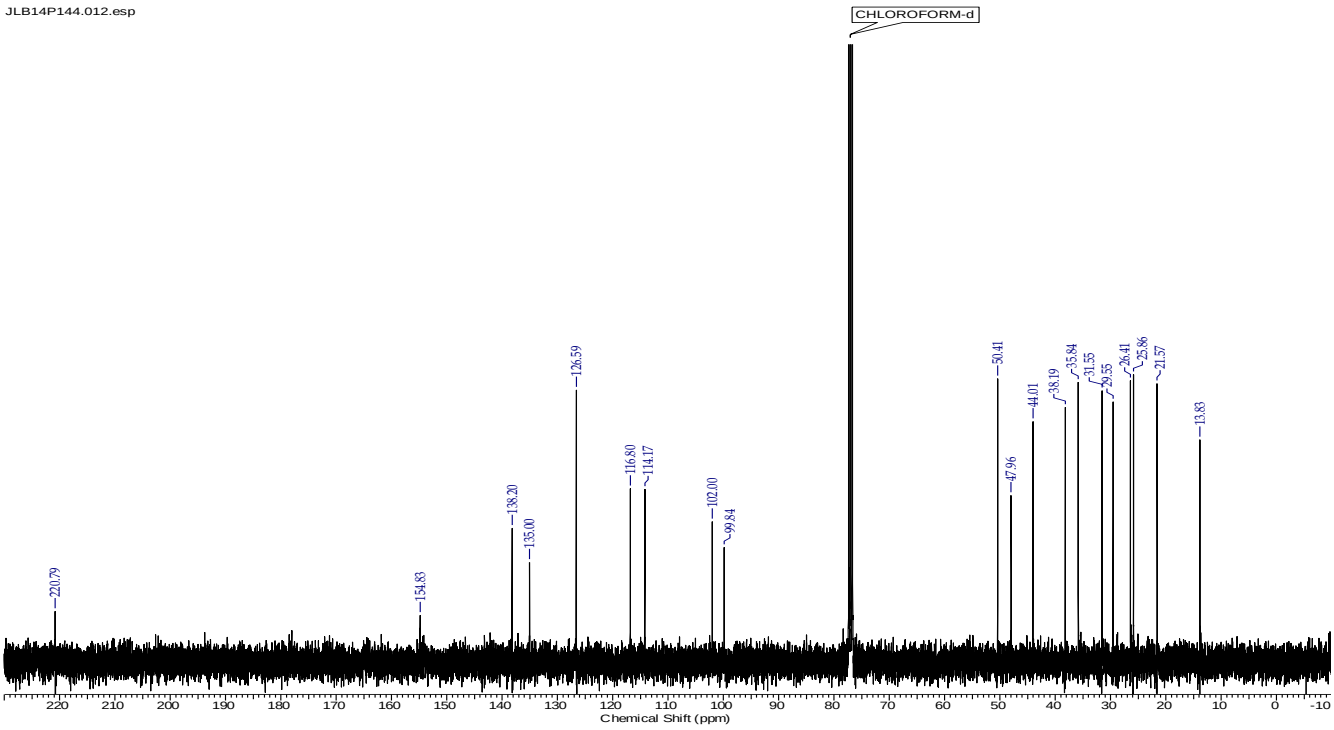
JLB14P144.012.esp
CHLOROFORM-d
220.79
154.83
138.20
135.00
126.59
116.80
114.17
102.00
99.84
50.41
47.96
44.01
38.19
35.84
31.55
29.55
26.41
25.86
21.57
13.83
Chemical Shift (ppm)

Appendix B Selected NMR spectra for Chapter 4

4.103

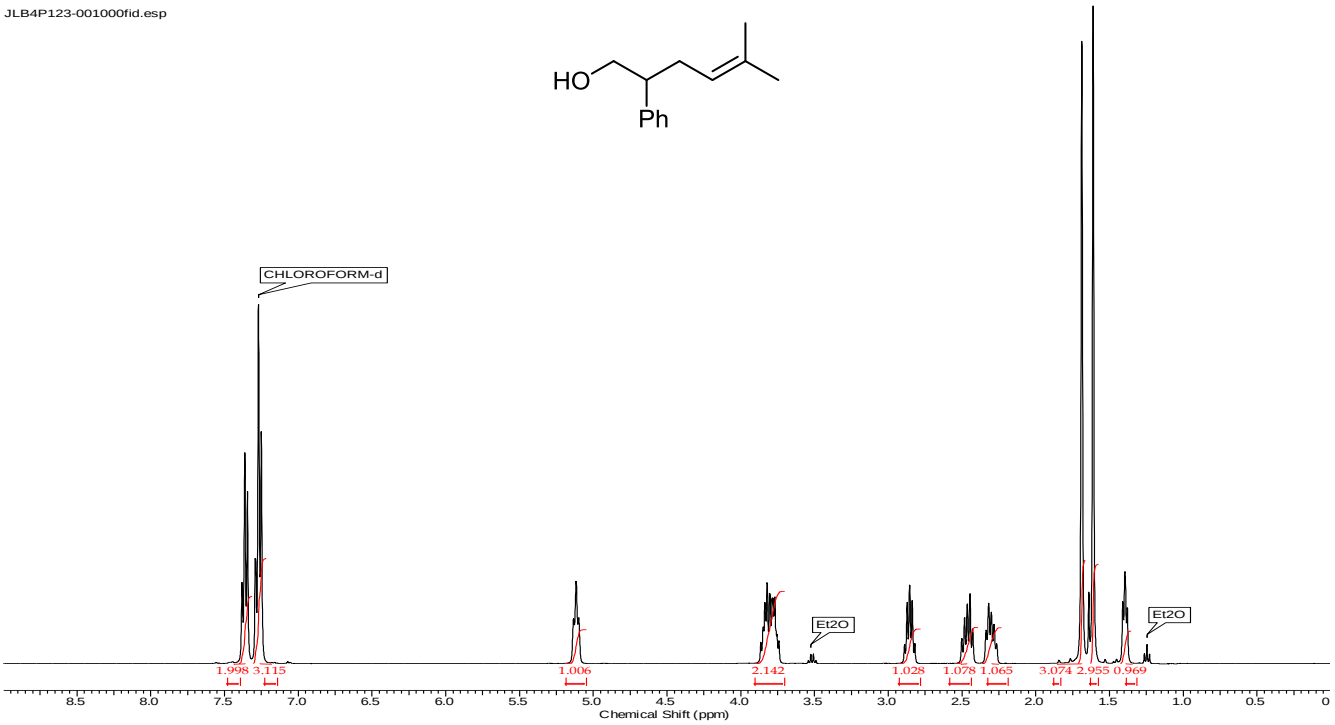
JLB4P123-001000fid.esp
HO
Ph
CHLOROFORM-d
Et2O
Et2O
1.998 3.115
1.006
2.142
1.028
1.078 1.065
3.074 2.955 0.969
Chemical Shift (ppm)

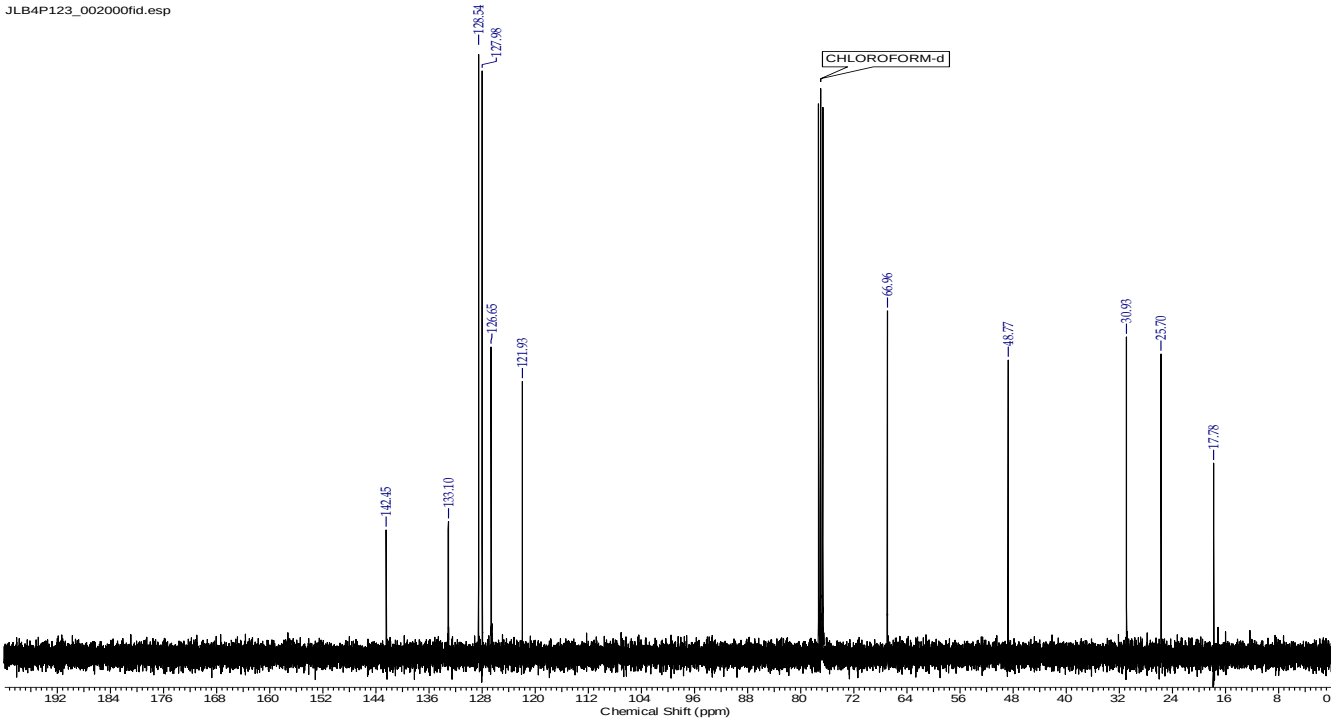
JLB4P123_002000fid.esp
128.54
127.98
126.65
121.93
142.45
133.10
CHLOROFORM-d
66.96
48.77
30.93
25.70
17.78
Chemical Shift (ppm)

4.98b

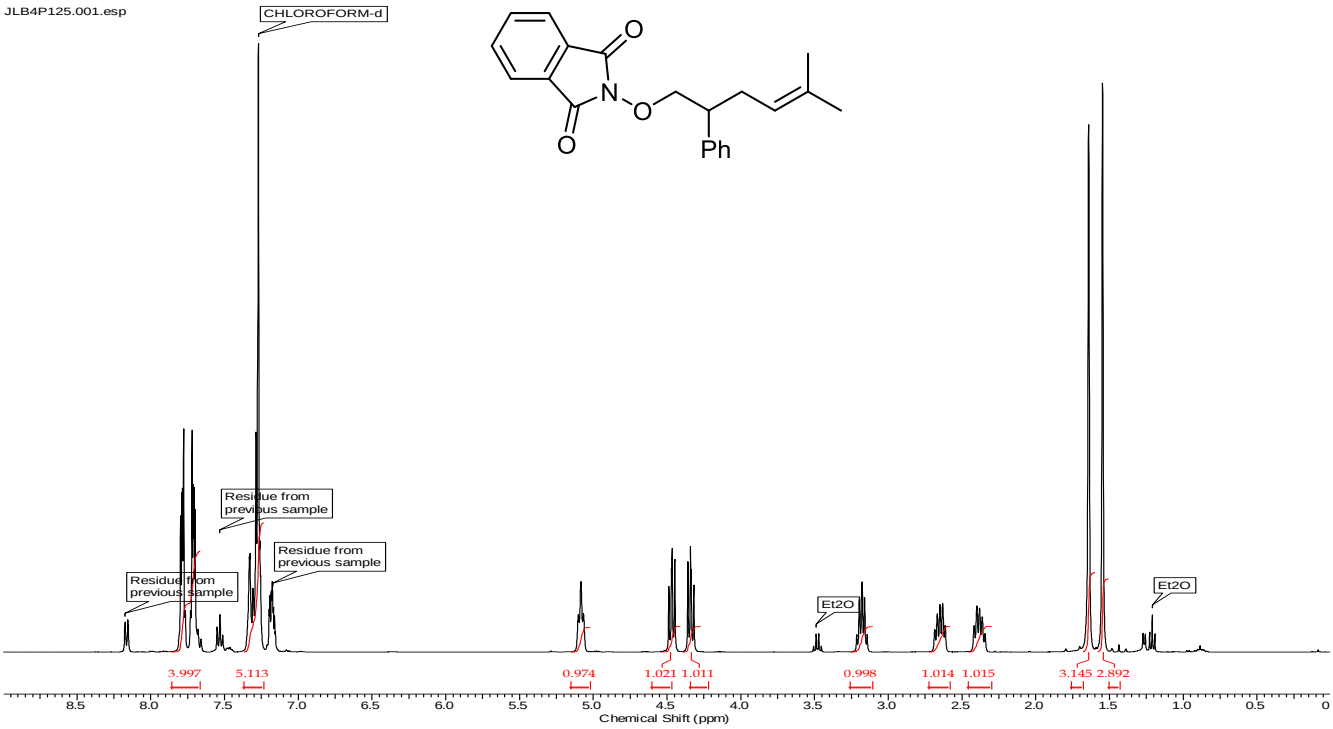
JLB4P125.001.esp
CHLOROFORM-d
Residue from previous sample
Residue from previous sample
Residue from previous sample
Et2O
Et2O
3.997
5.113
0.974
1.021
1.011
0.998
1.014
1.015
3.145
2.892
Chemical Shift (ppm)

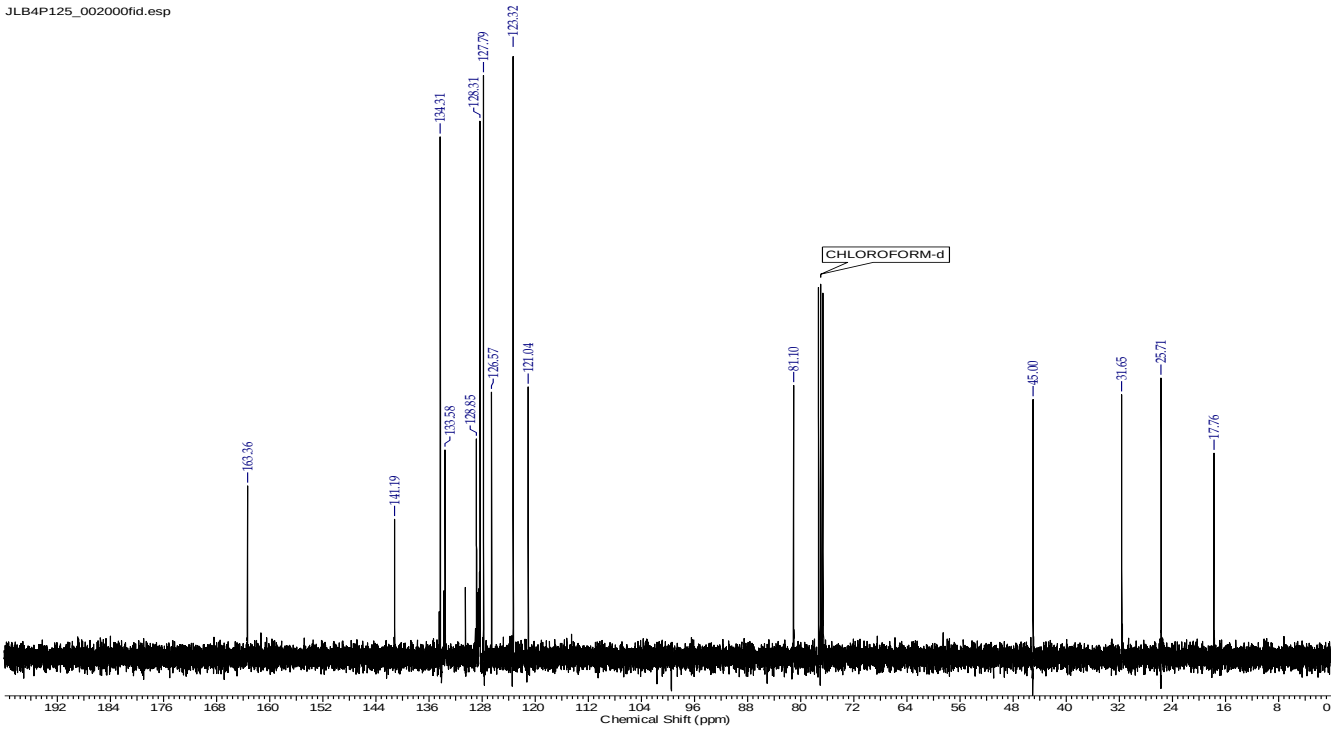
JLB4P125_002000fid.esp
163.36
141.19
134.31
133.58
128.85
128.31
127.79
126.57
123.32
121.04
81.10
CHLOROFORM-d
45.00
31.65
25.71
17.76
Chemical Shift (ppm)

4.110

JLB5P033.001.esp

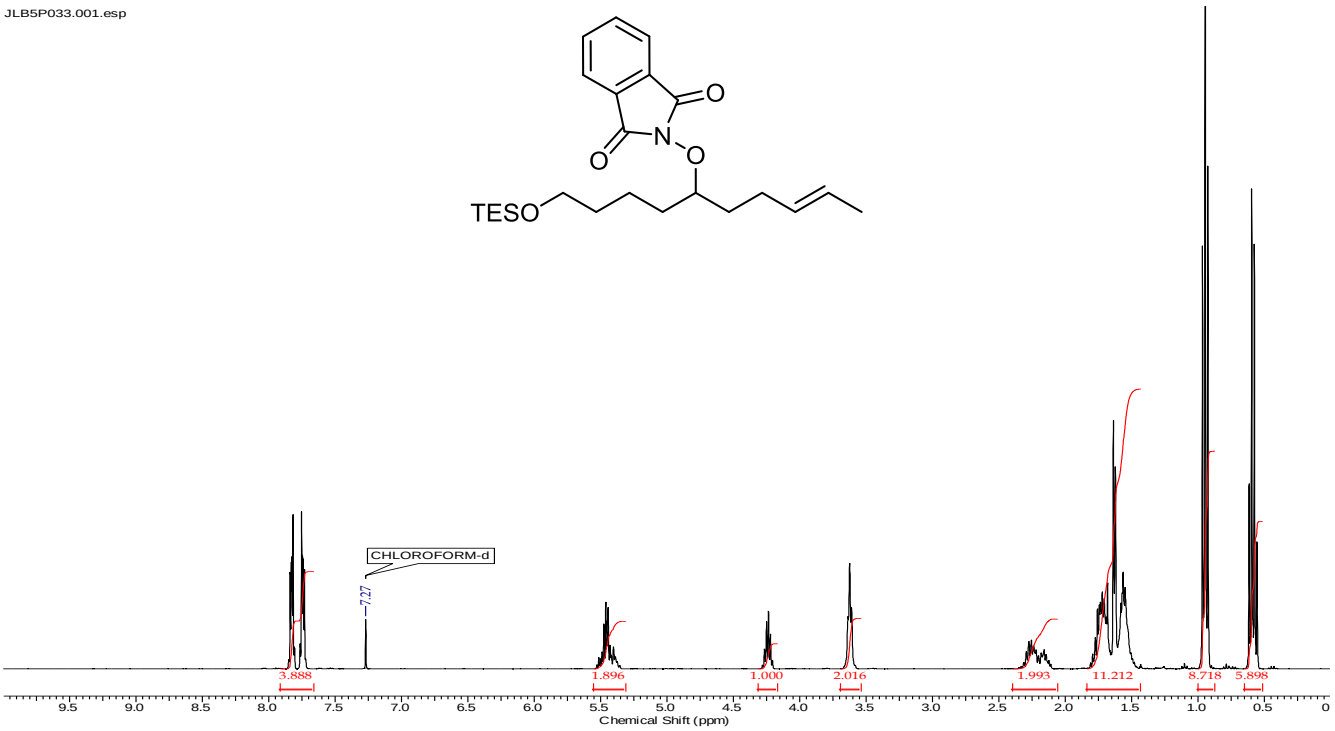

JLB5P033.002.esp

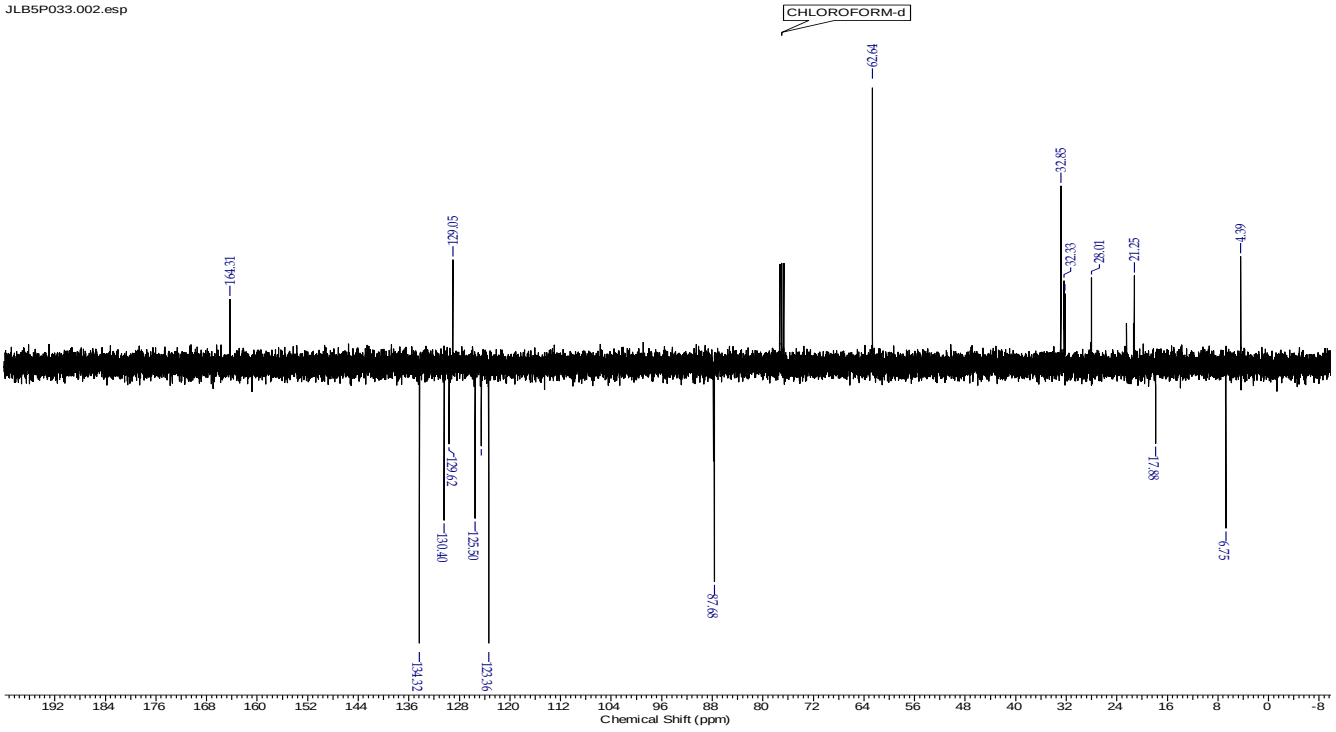

4.117

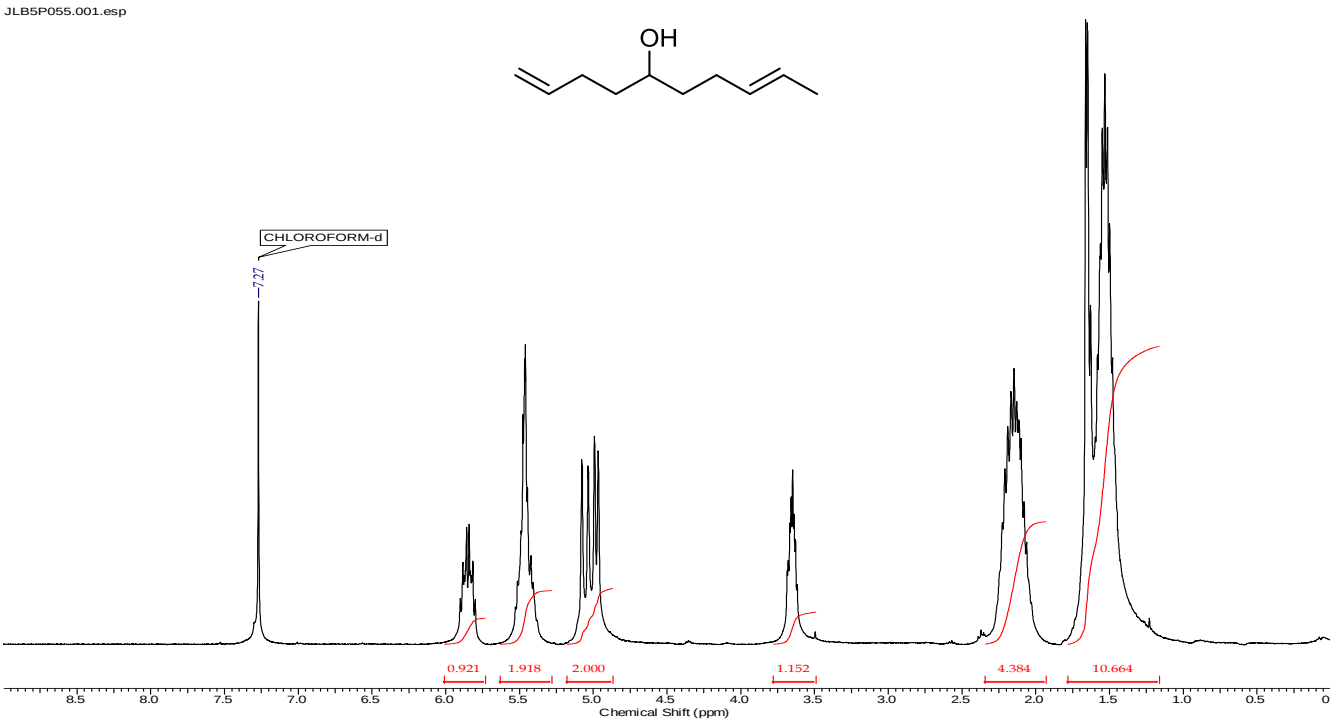
JLB5P055.001.esp
OH
CHLOROFORM-d
7.27
0.921
1.918
2.000
1.152
4.384
10.664
Chemical Shift (ppm)

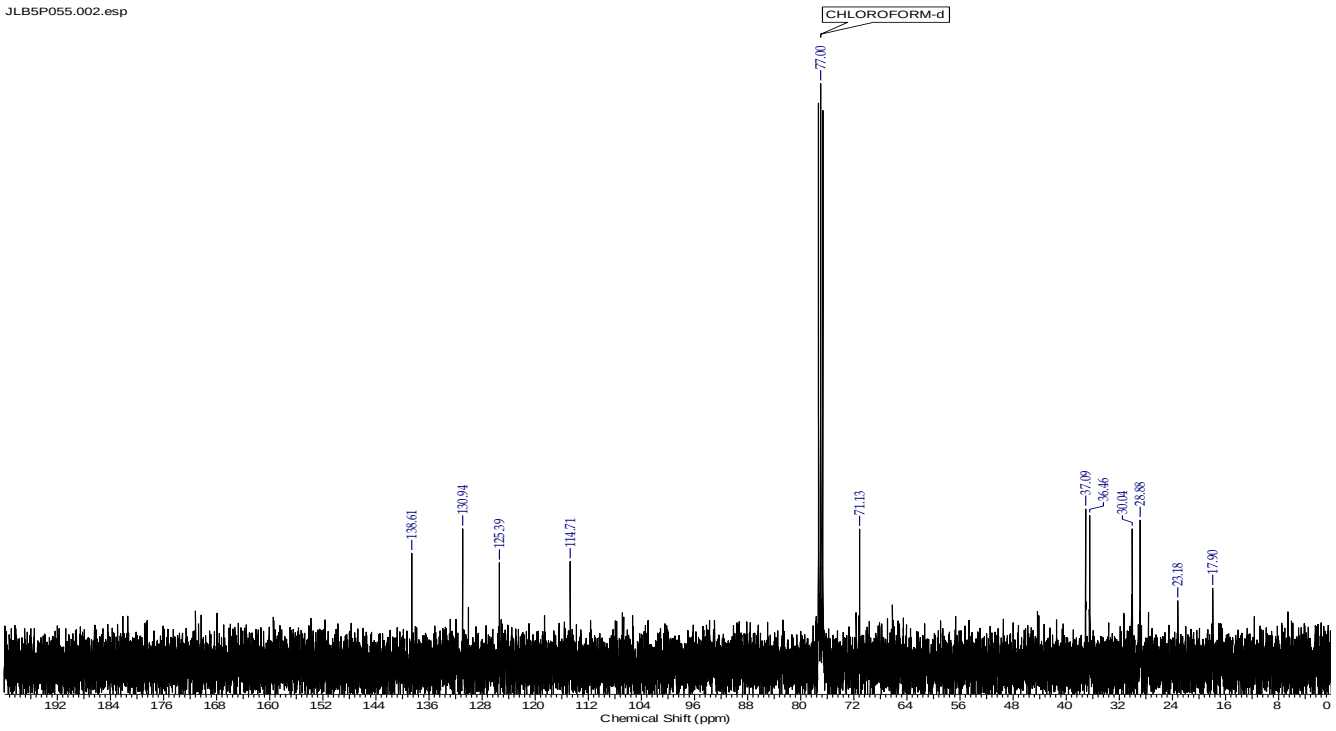
JLB5P055.002.esp
CHLOROFORM-d
77.00
138.61
130.94
125.39
114.71
71.13
37.09
36.46
30.04
28.88
23.18
17.90
Chemical Shift (ppm)

4.107

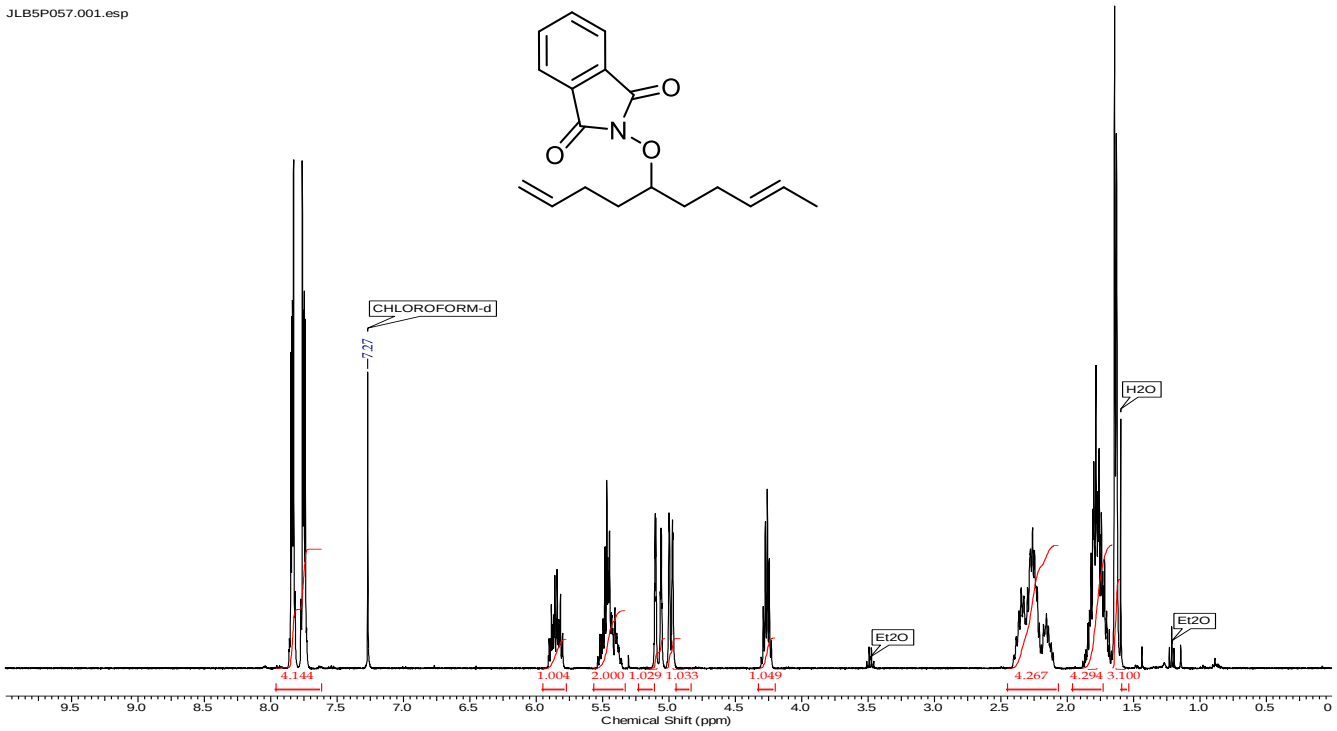
JLB5P057.001.esp
CHLOROFORM-d
7.27
H2O
Et2O
Et2O
4.144
1.004
2.000
1.029
1.033
1.049
4.267
4.294
3.100
Chemical Shift (ppm)

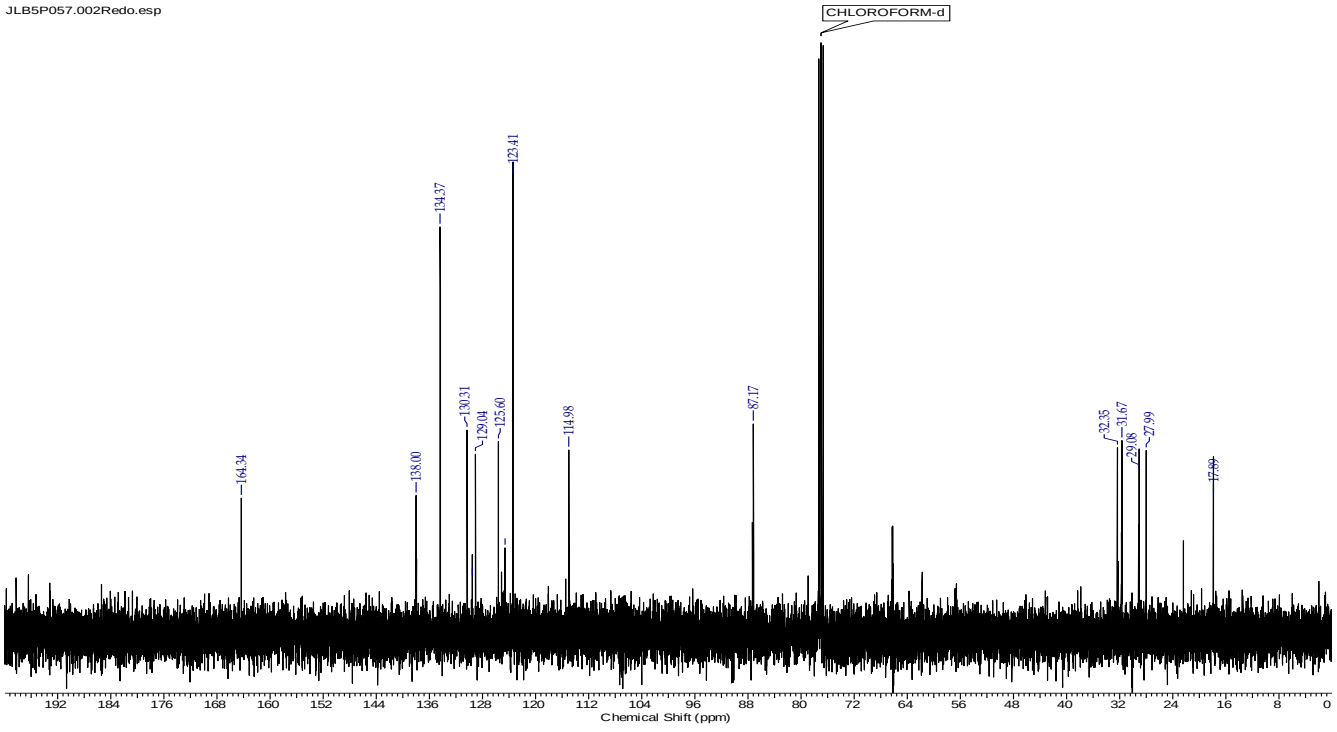
JLB5P057.002Redo.esp
CHLOROFORM-d
164.34
138.00
134.37
130.31
129.04
125.60
123.41
114.98
87.17
32.35
31.67
29.08
27.99
17.89
Chemical Shift (ppm)

4.125

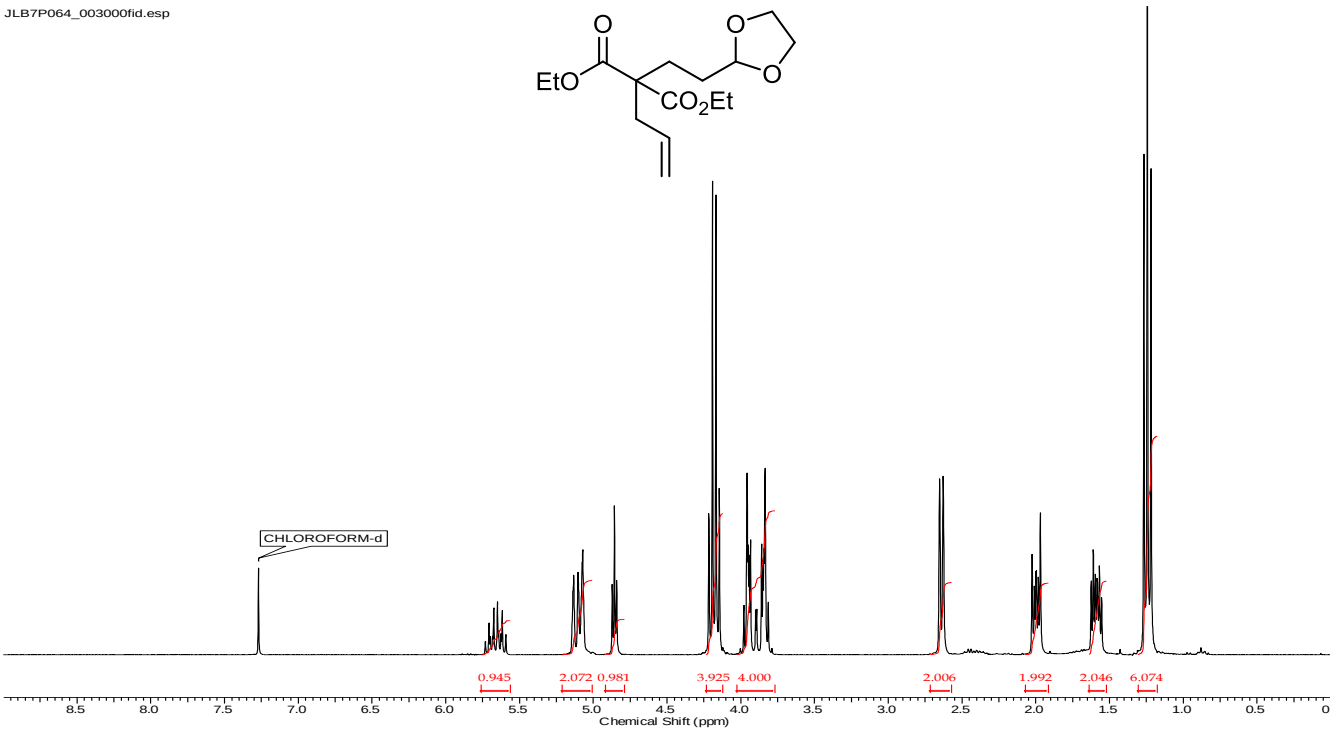
JLB7P064_003000fid.esp
EtO
O
O
O
O
CO2Et
CHLOROFORM-d
0.945
2.072
0.981
3.925
4.000
2.006
1.992
2.046
6.074
Chemical Shift (ppm)

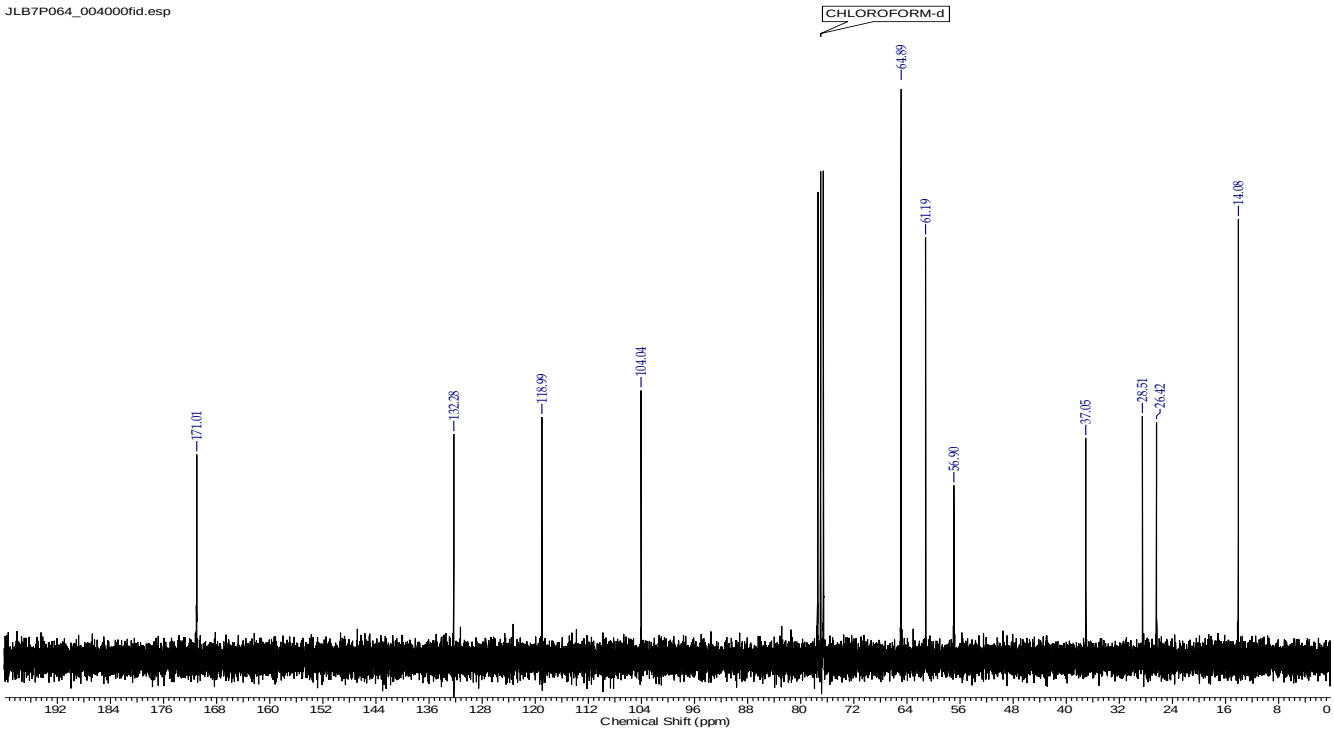
JLB7P064_004000fid.esp
CHLOROFORM-d
171.01
132.28
118.99
104.04
64.89
61.19
56.90
37.05
28.51
26.42
14.08
Chemical Shift (ppm)

4.126

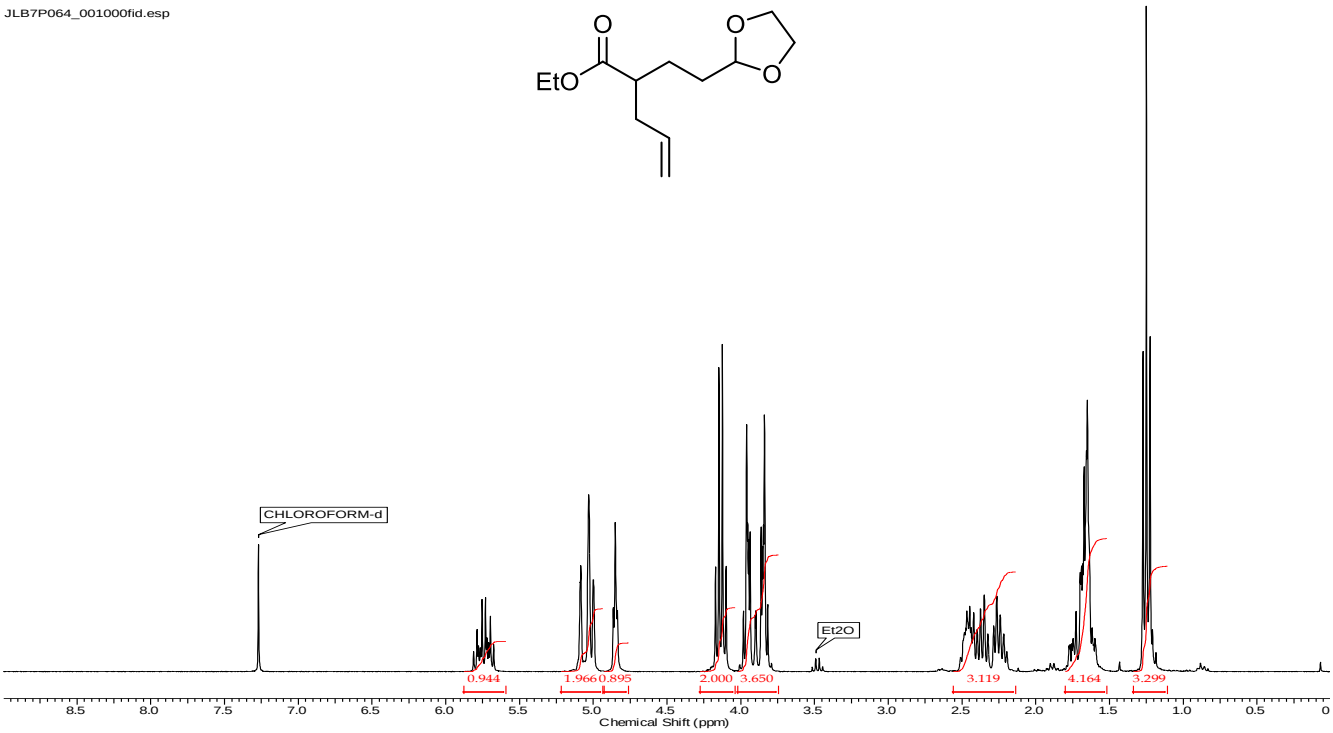
JLB7P064_001000fid.esp
O
O
O
O
EtO
CHLOROFORM-d
Et2O
0.944
1.966
0.895
2.000
3.650
3.119
4.164
3.299
Chemical Shift (ppm)

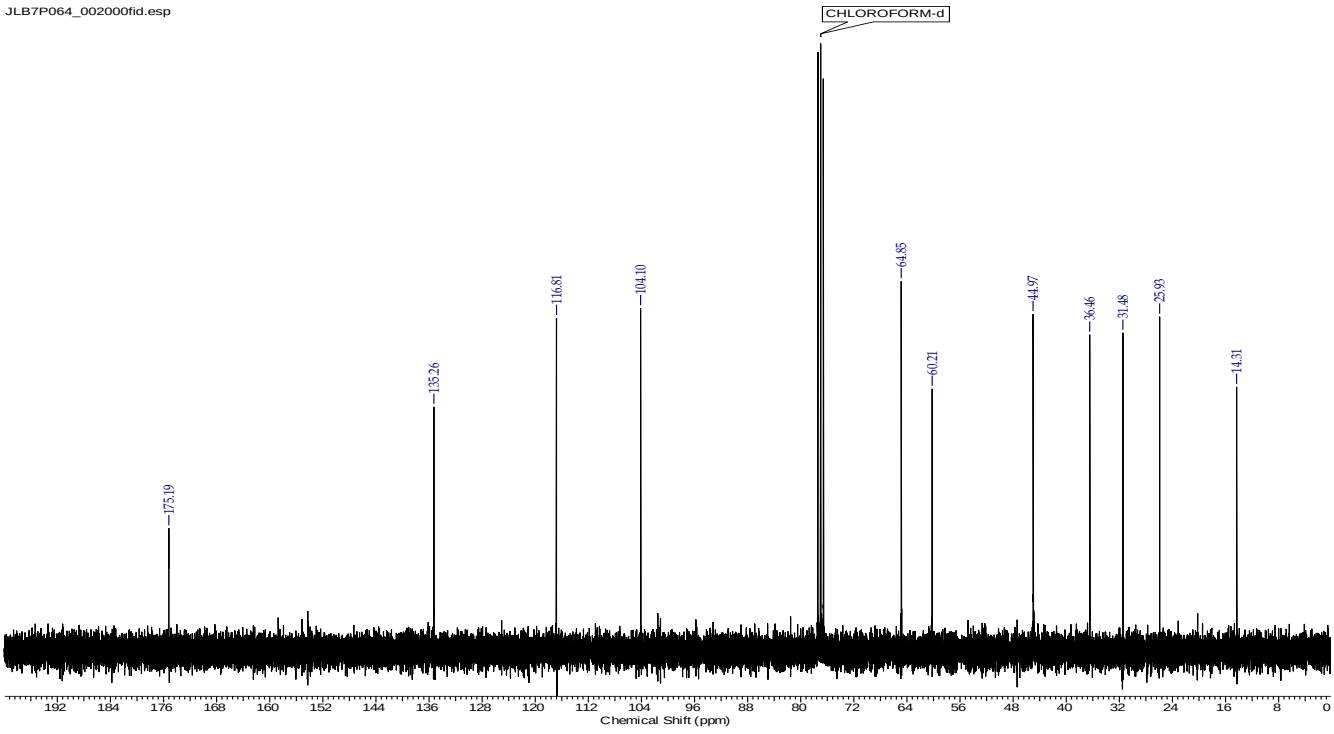
JLB7P064_002000fid.esp
CHLOROFORM-d
175.19
135.26
116.81
104.10
64.85
60.21
44.97
36.46
31.48
25.93
14.31
Chemical Shift (ppm)

4.122

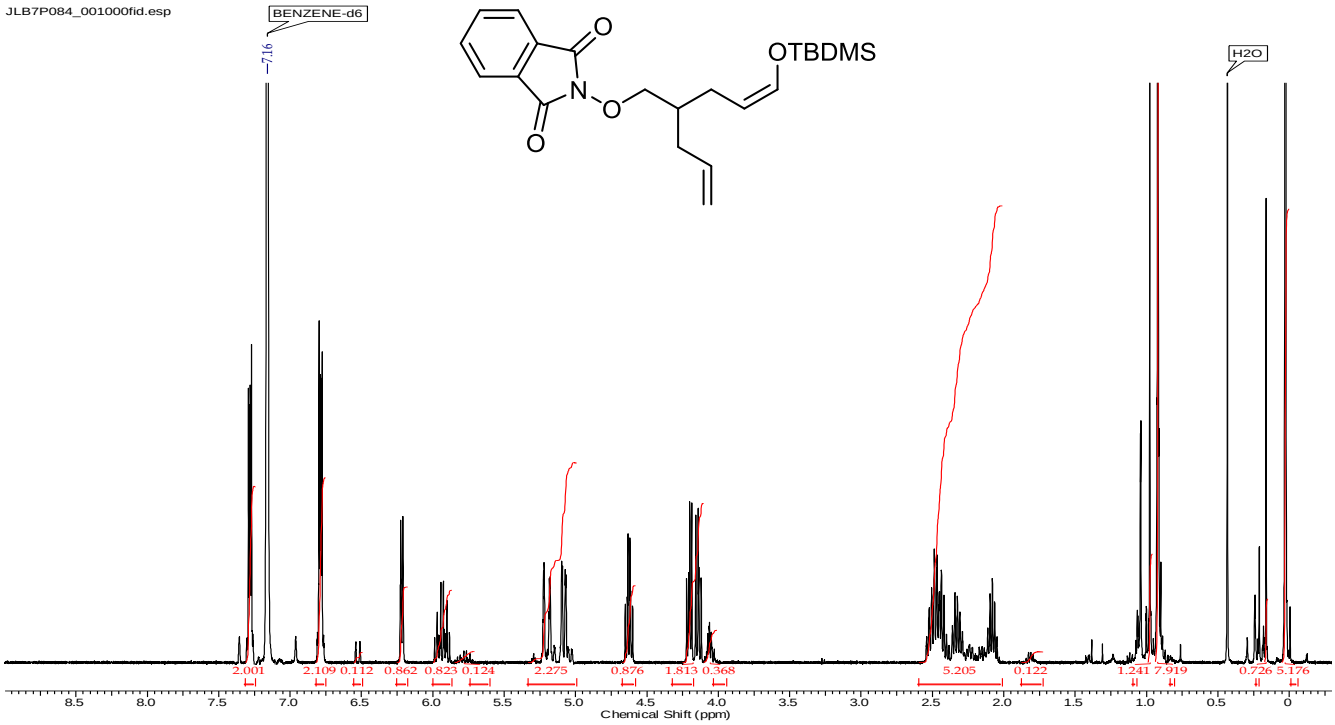
JLB7P084_001000fid.esp
BENZENE-d6
7.16
OTBDMS
H2O
2.001
2.109
0.112
0.862
0.823
0.124
2.275
0.876
1.813
0.368
5.205
0.122
1.241
7.919
0.726
3.176
Chemical Shift (ppm)

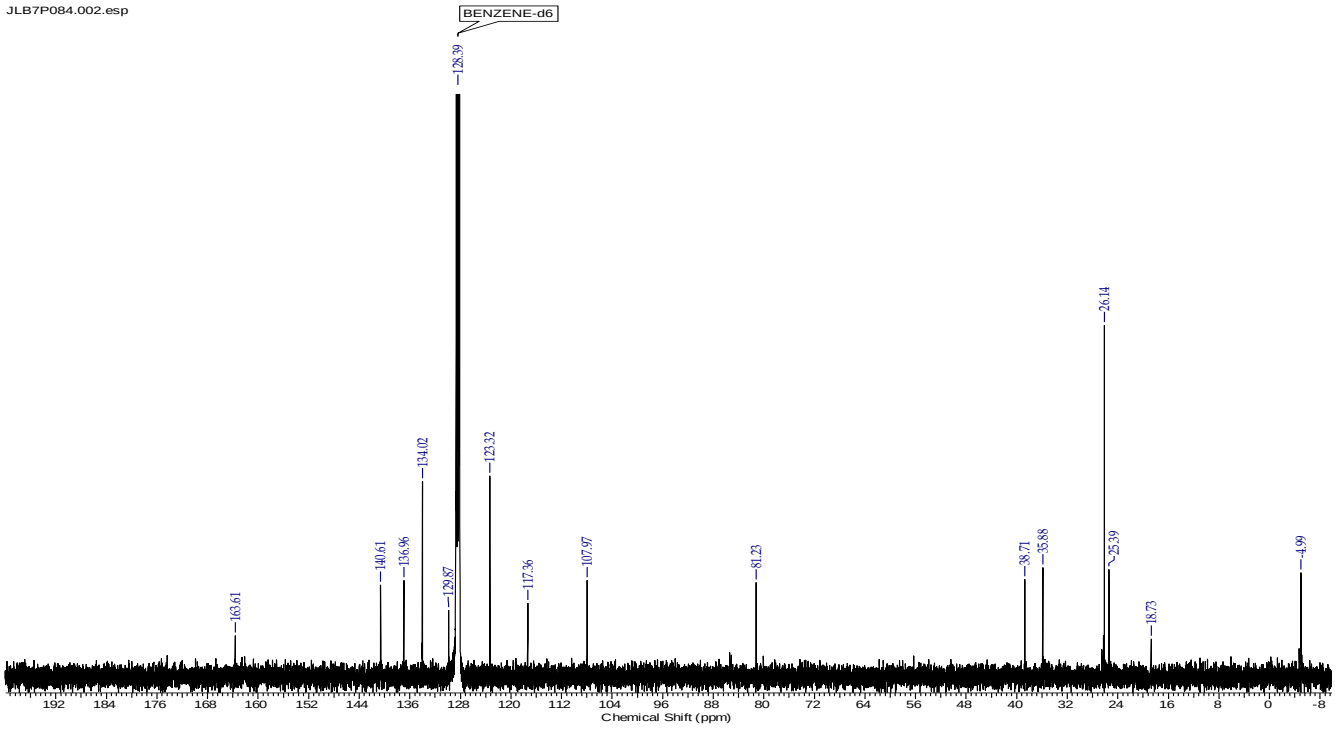
JLB7P084.002.esp
BENZENE-d6
126.39
134.02
123.32
140.61
136.96
129.87
117.36
107.97
81.23
163.61
38.71
35.88
26.14
25.39
18.73
4.99
Chemical Shift (ppm)

4.143

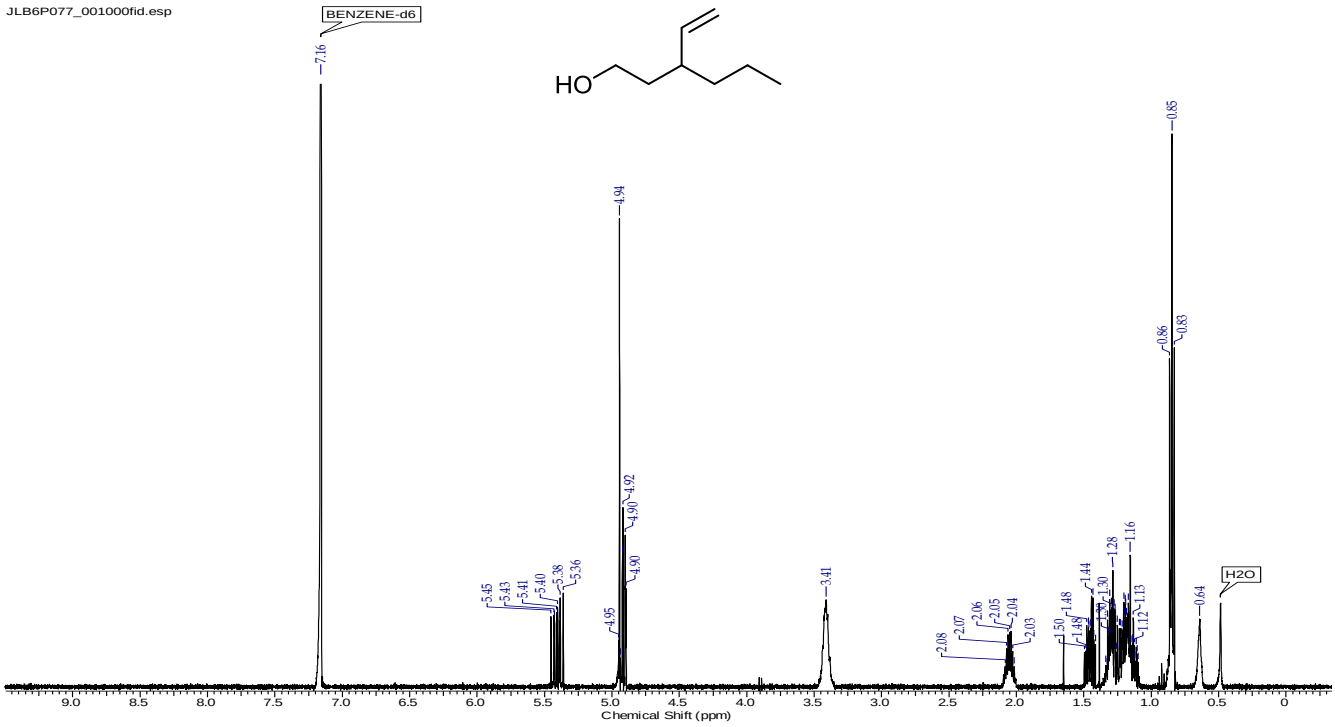
JLB6P077_001000fid.esp
BENZENE-d6
HO
7.16
4.94
0.85
0.86
0.83
4.92
4.90
4.90
5.45
5.43
5.41
5.40
5.38
5.36
4.95
3.41
2.08
2.07
2.06
2.05
2.04
2.03
1.50
1.48
1.48
1.44
1.30
1.28
1.16
1.13
1.12
0.64
H2O
Chemical Shift (ppm)

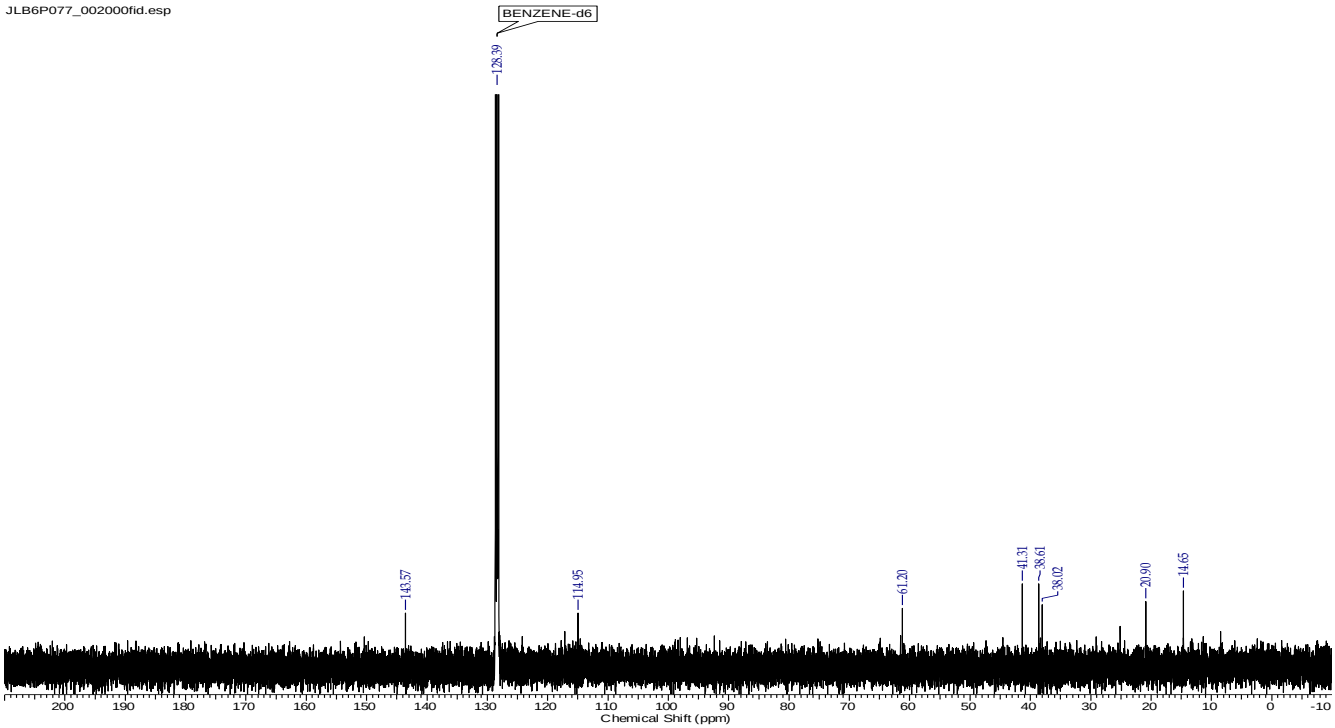
JLB6P077_002000fid.esp
BENZENE-d6
128.39
143.57
114.95
61.20
41.31
38.61
38.02
20.90
14.65
Chemical Shift (ppm)

4.144

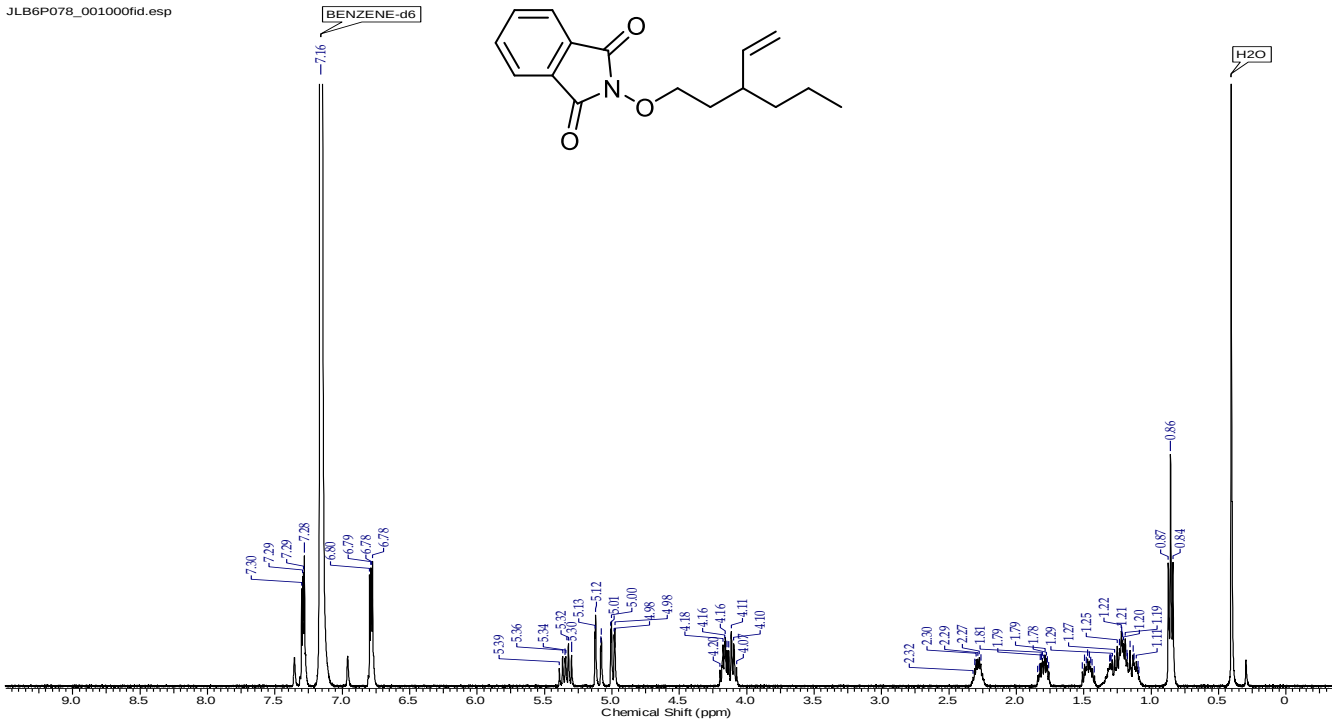
JLB6P078_001000fid.esp
BENZENE-d6
H2O
Chemical Shift (ppm)

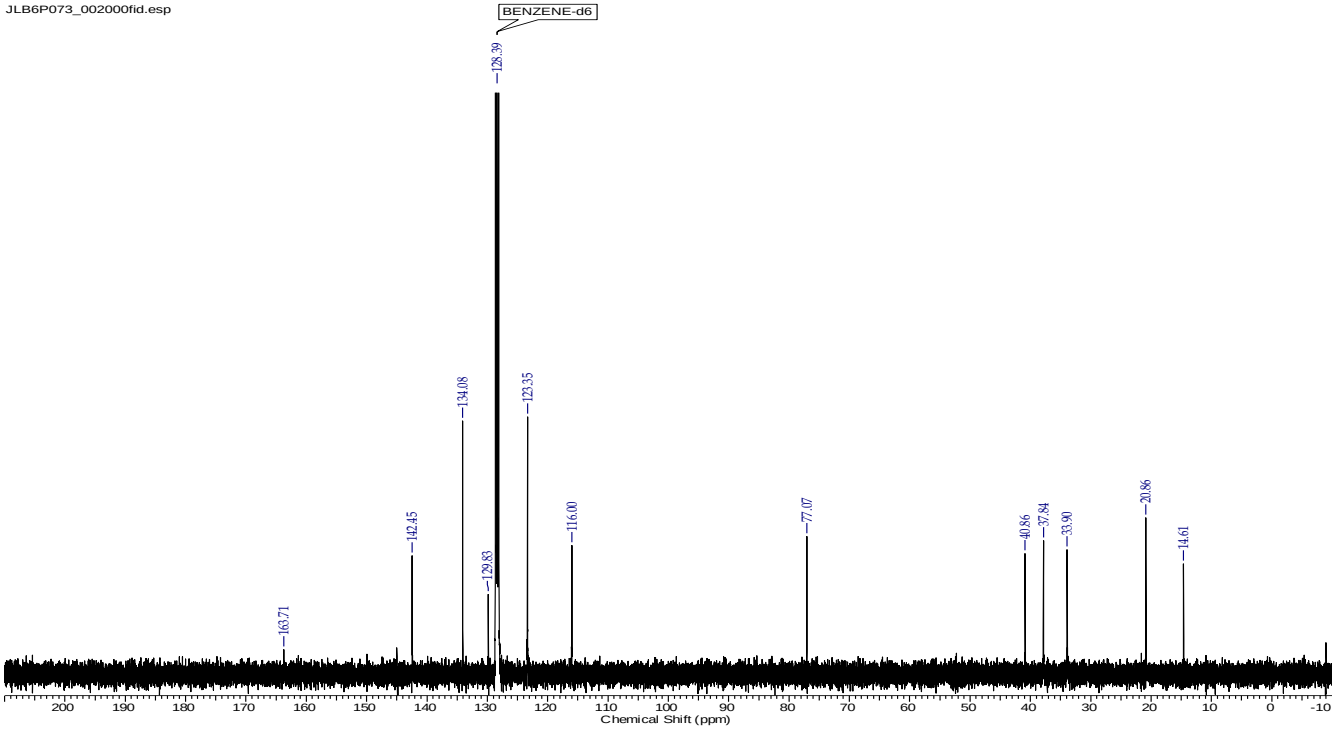
JLB6P073_002000fid.esp
BENZENE-d6
Chemical Shift (ppm)

4.146

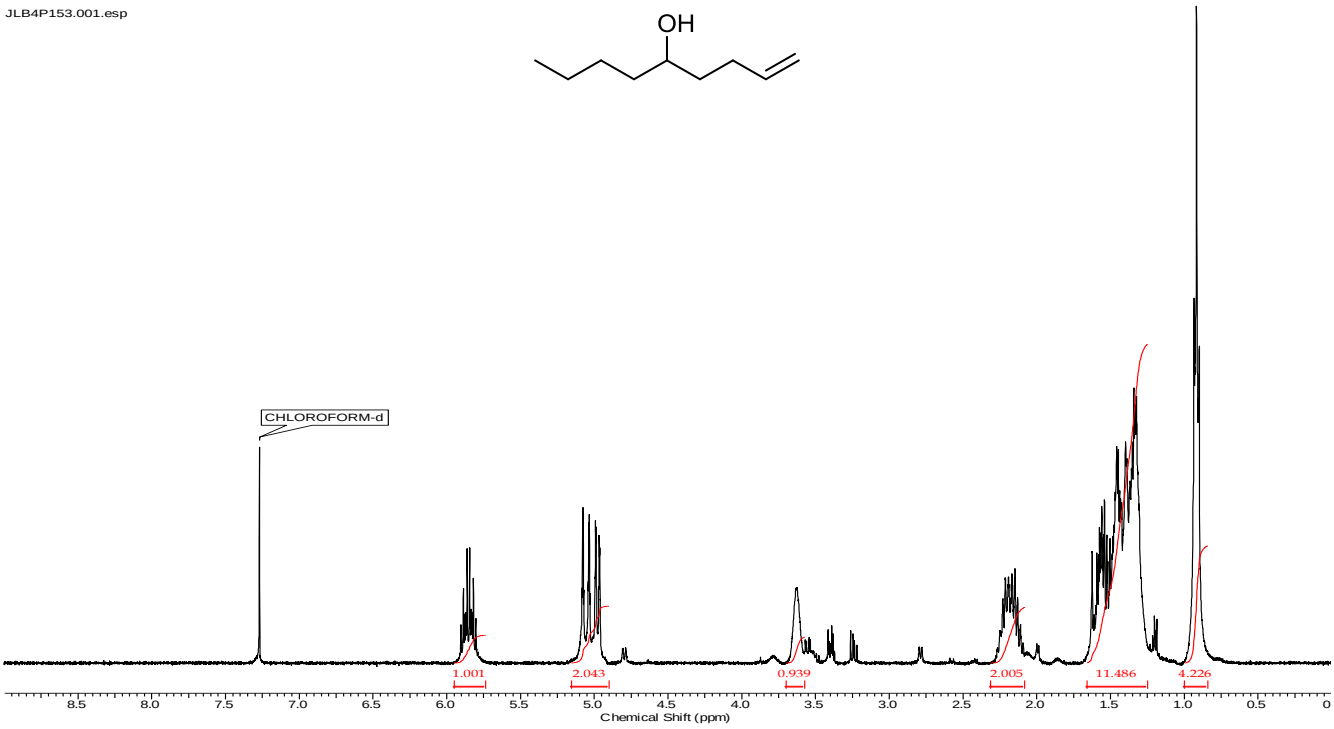
JLB4P153.001.esp
OH
CHLOROFORM-d
1.001
2.043
0.939
2.005
11.486
4.226
Chemical Shift (ppm)

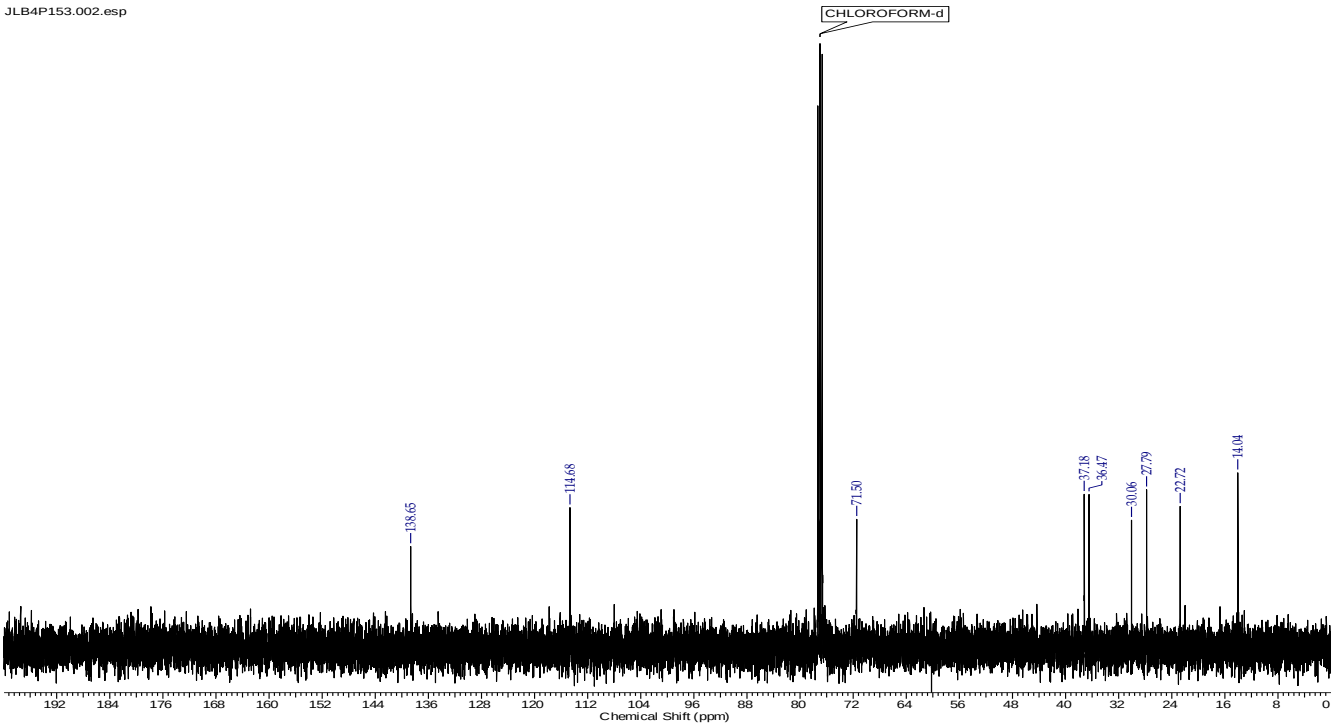
JLB4P153.002.esp
CHLOROFORM-d
138.65
114.68
77.50
37.18
36.47
30.06
27.79
22.72
14.04
Chemical Shift (ppm)

4.147

JLB5P011.001.esp

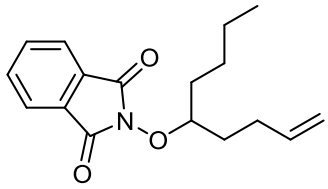

JLB5P011.002.esp

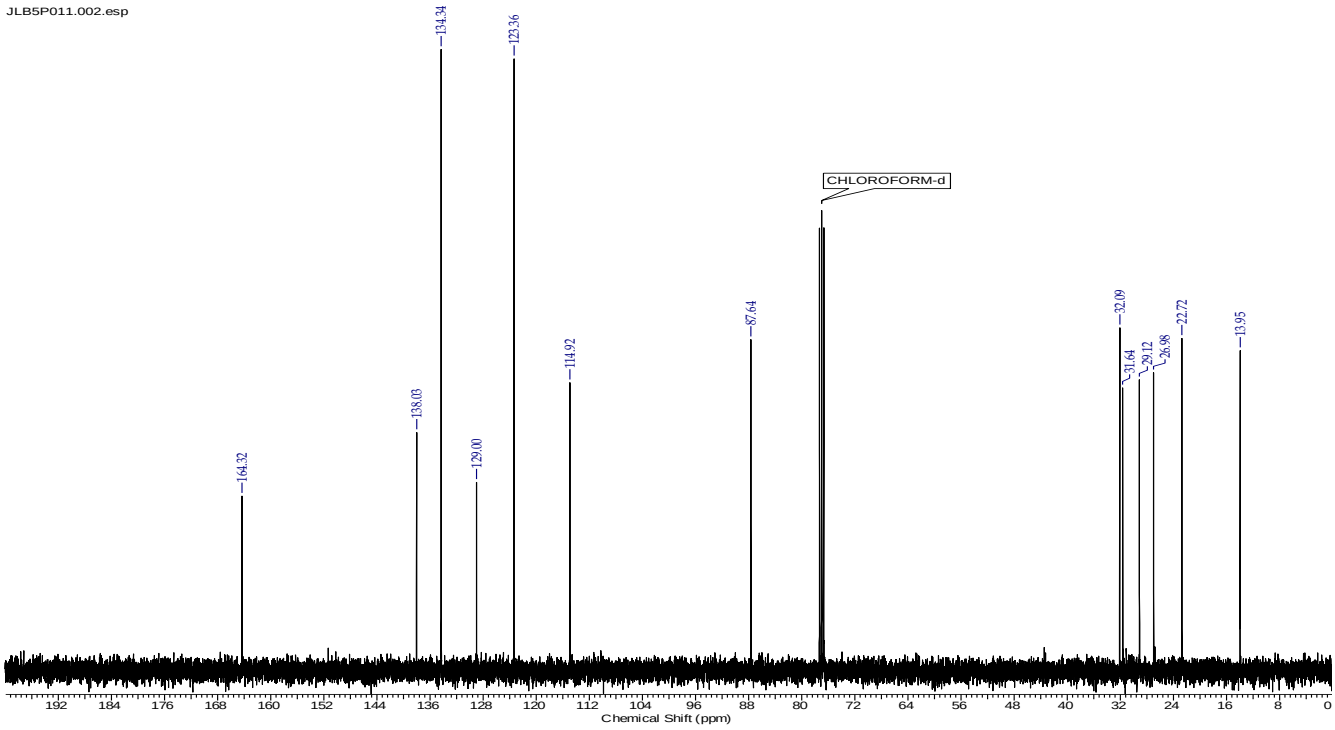

4.174

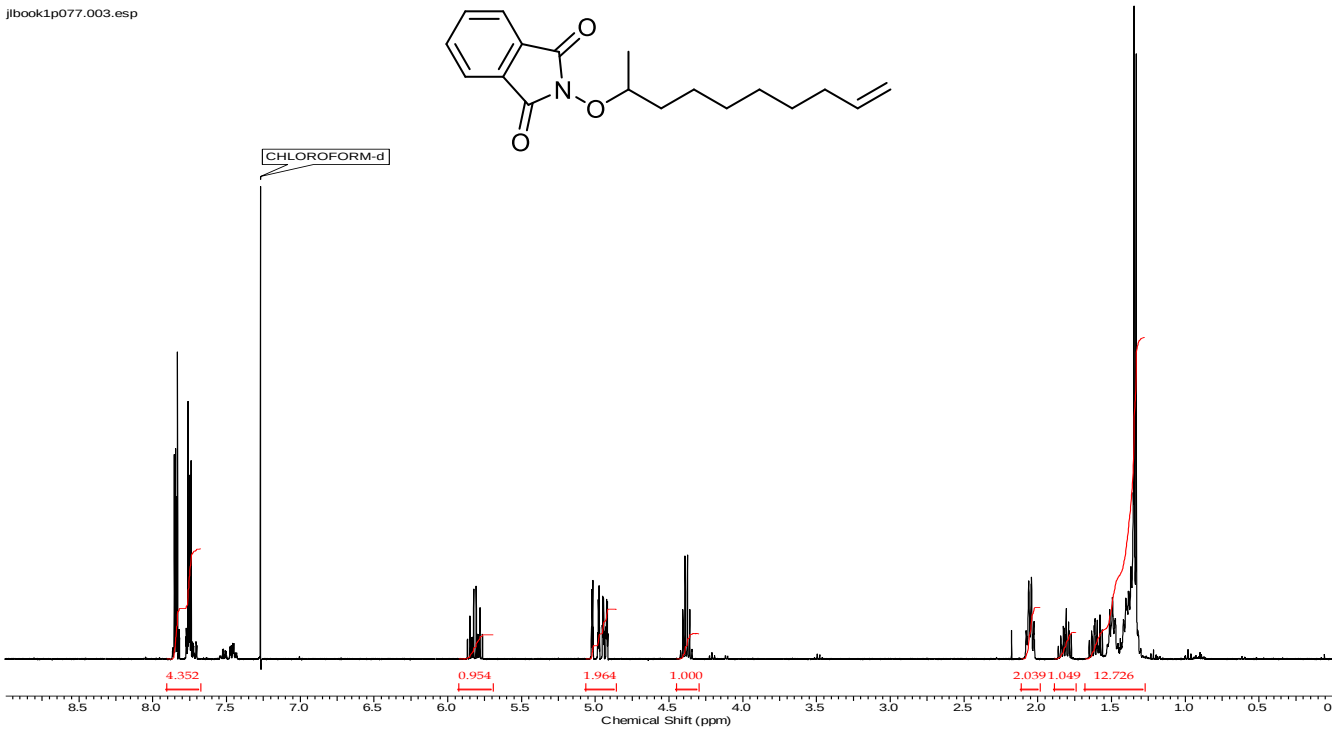
jlbook1p077.003.esp
CHLOROFORM-d
4.352
0.954
1.964
1.000
2.039
1.049
12.726
Chemical Shift (ppm)

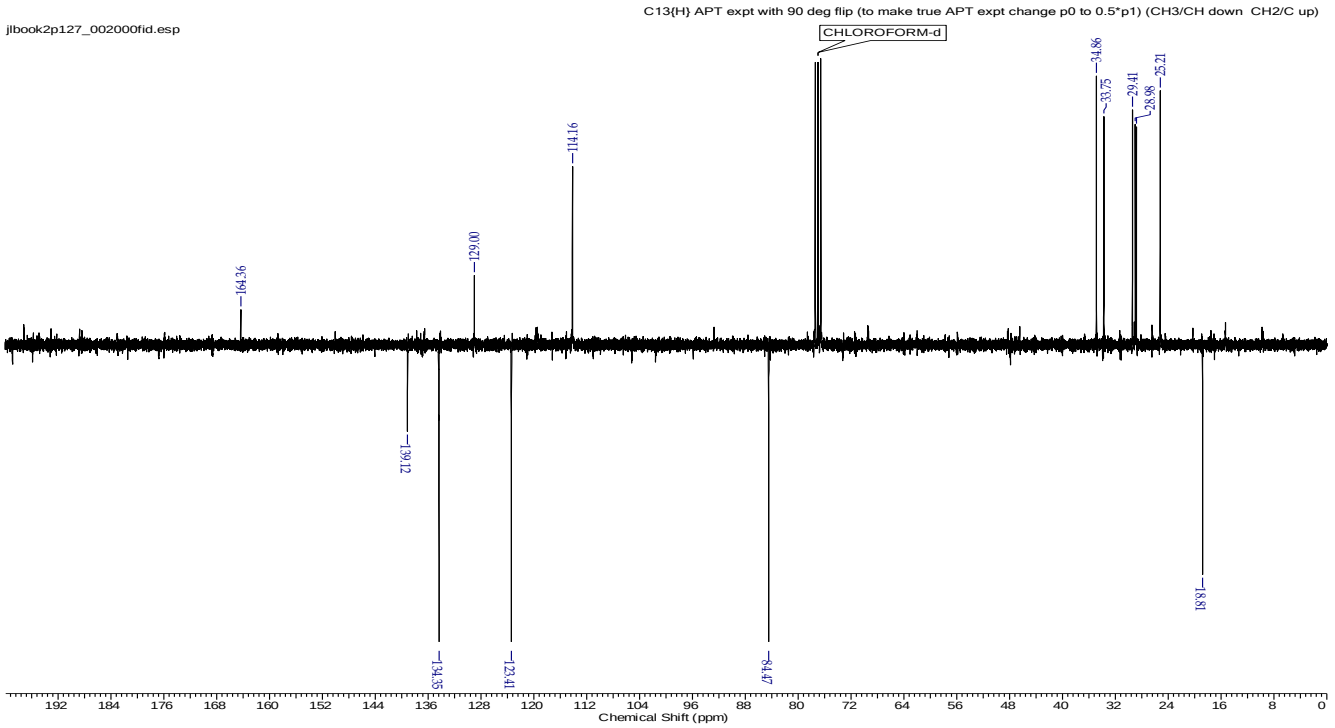
jlbook2p127_002000fid.esp
C13{H} APT expt with 90 deg flip (to make true APT expt change p0 to 0.5*p1) (CH3/CH down CH2/C up)
CHLOROFORM-d
164.36
136.12
134.38
129.00
123.41
114.16
84.47
34.86
33.75
29.41
28.98
25.21
18.81
Chemical Shift (ppm)

4.183

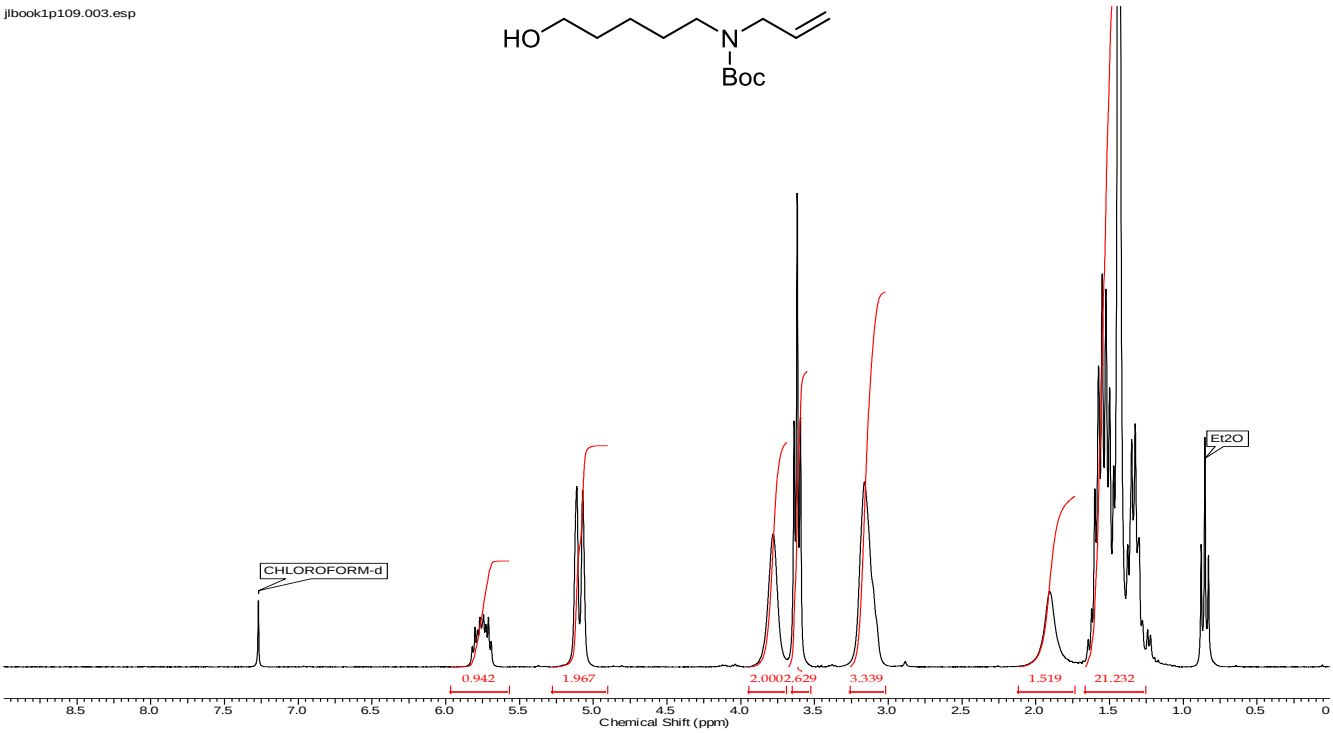
jlbook1p109.003.esp
HO
N
Boc
CHLOROFORM-d
Et2O
0.942
1.967
2.000
2.629
3.339
1.519
21.232
Chemical Shift (ppm)

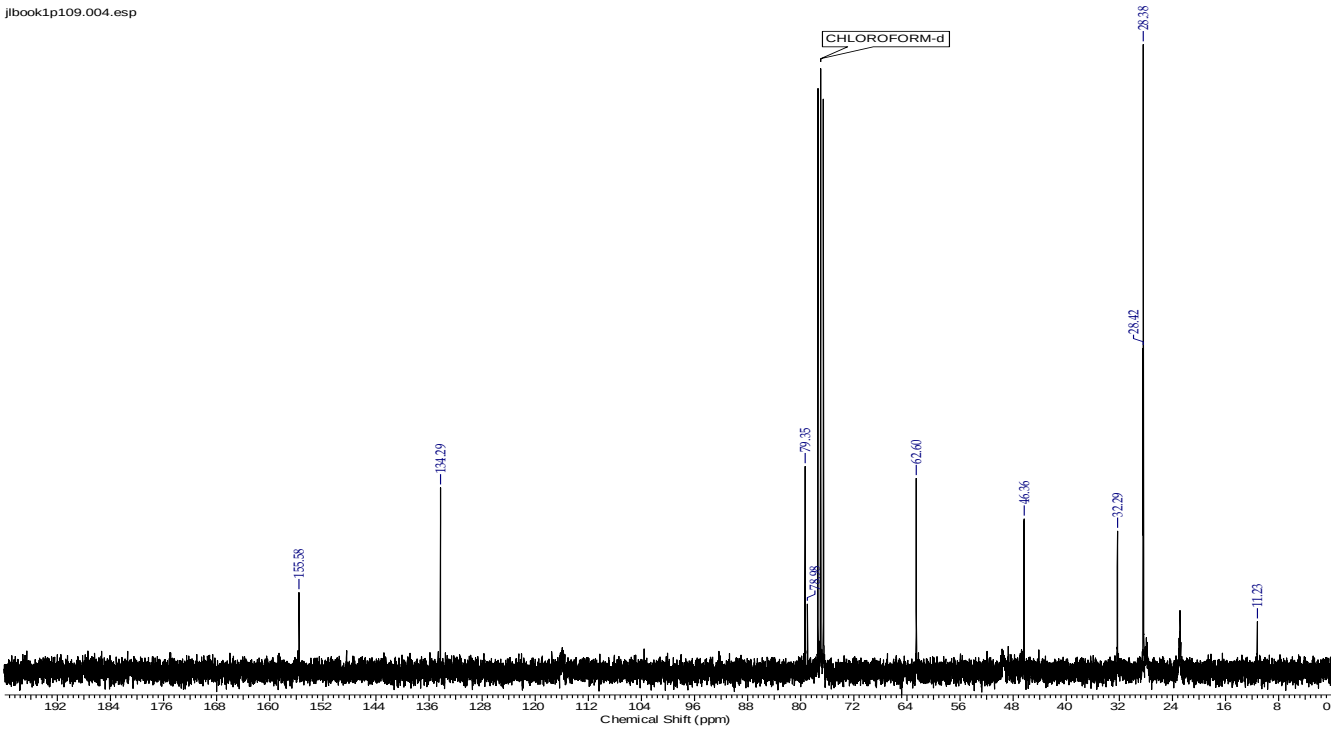
jlbook1p109.004.esp
CHLOROFORM-d
155.58
134.29
79.35
78.98
62.60
46.36
32.29
28.42
26.38
11.23
Chemical Shift (ppm)

4.184

Acquisition Time (sec)	2.1999	*Comment*	JOB NO: 1H spectrum ref. to CDCl3 at 7.27 ppm			*Date*	29 May 2008 16:49:04
Date Stamp	29 May 2008 16:49:04			*File Name*	D:\data\jlbook1p111\jlbook1p111_003000fid		
Frequency (MHz)	400.13	*Nucleus*	1H	*Number of Transients*	24	*Origin*	av400
Original Points Count	13189	*Owner*	root	*Points Count*	16384	*Pulse Sequence*	zg30
Receiver Gain	45.30	*SW(cyclical) (Hz)*	5995.20	*Solvent*	CHLOROFORM-d		
Spectrum Offset (Hz)	2595.9211	*Sweep Width (Hz)*	5994.84	*Temperature (degree C)*	25.060		

1H NMR (400 MHz, CHLOROFORM-*d*) δ ppm 1.36 - 1.67 (m, 45 H) 1.74 - 1.88 (m, 7 H) 3.19 (br. s., 8 H) 3.82 (br. s., 5 H) 4.19 (t, *J*=6.77 Hz, 7 H) 5.01 - 5.18 (m, 5 H) 5.77 (dddd, *J*=16.65, 10.79, 5.85, 5.49 Hz, 3 H) 7.67 - 7.89 (m, 13 H)

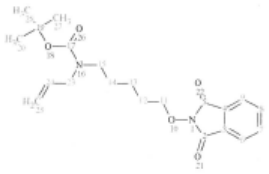

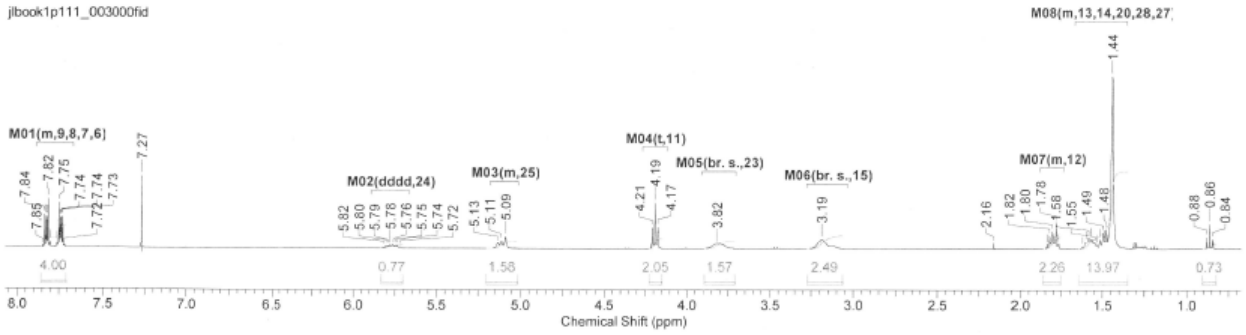

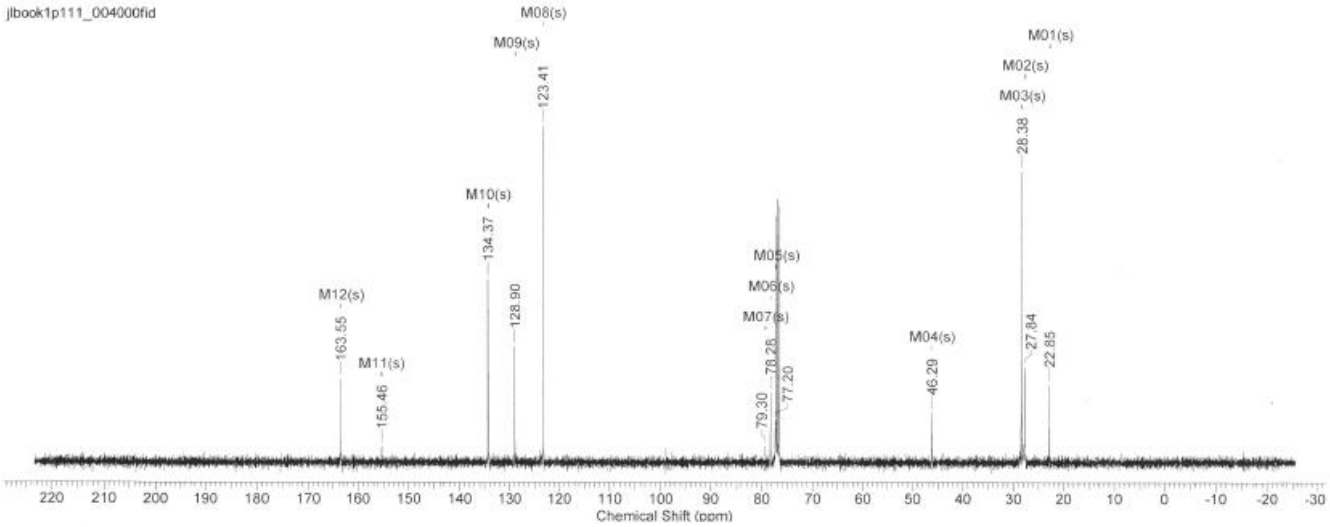

4.186

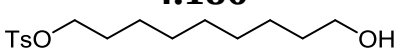

jlbook1p081_001fid.esp

jlbook1p081_002fid.esp

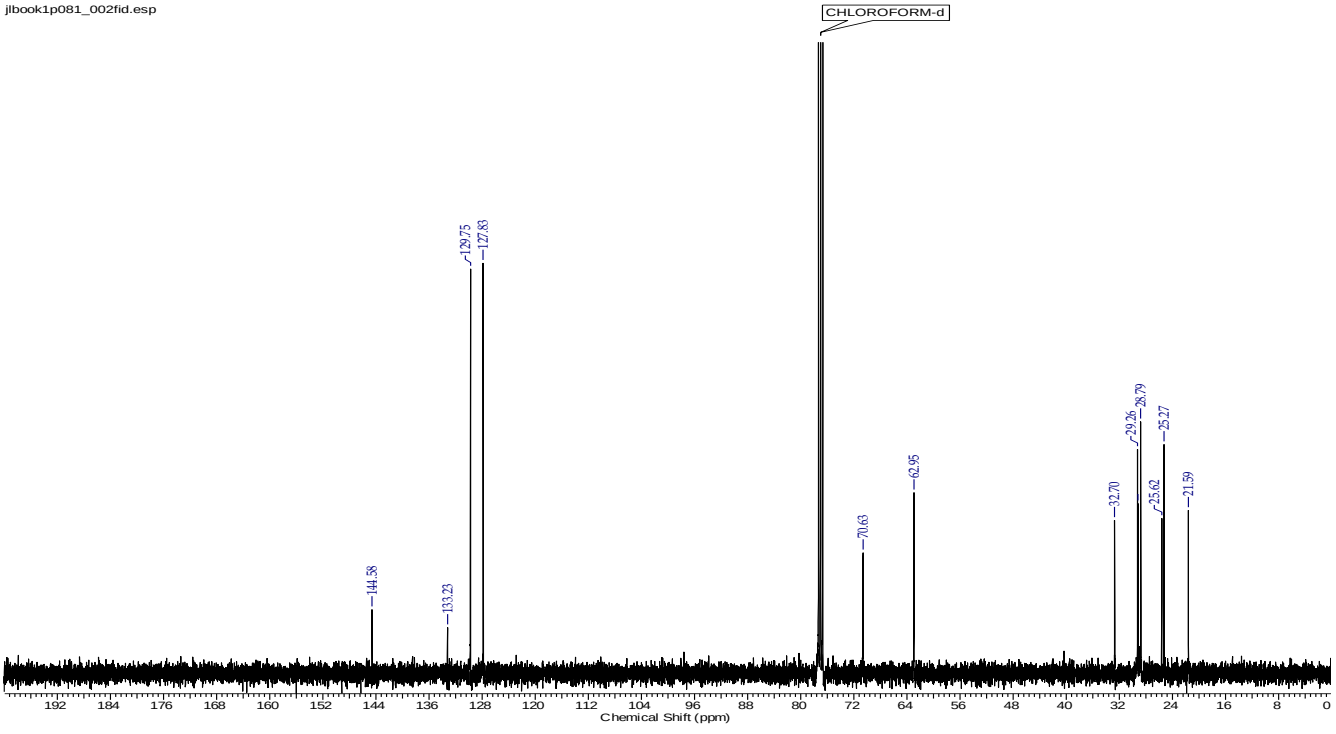

4.187

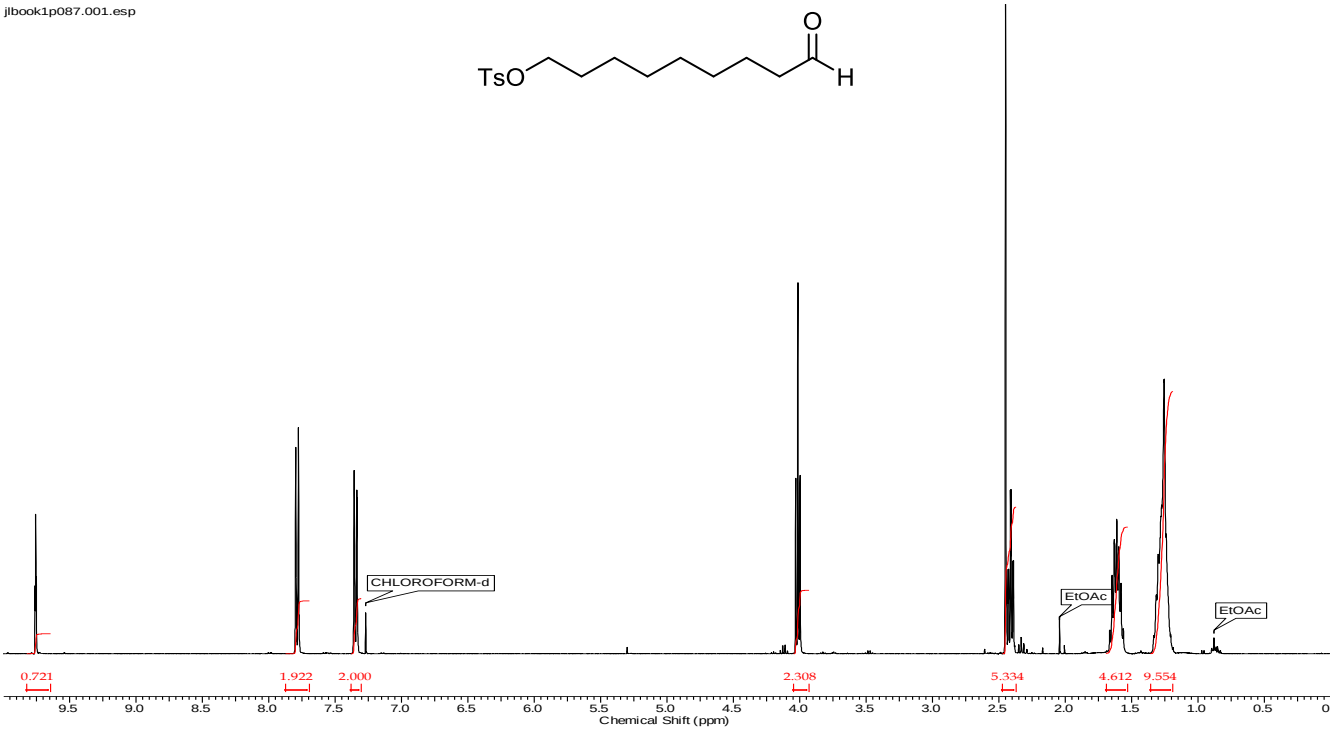
jlbook1p087.001.esp
TsO
O
H
CHLOROFORM-d
EtOAc
EtOAc
0.721
1.922
2.000
2.308
5.334
4.612
9.554
Chemical Shift (ppm)

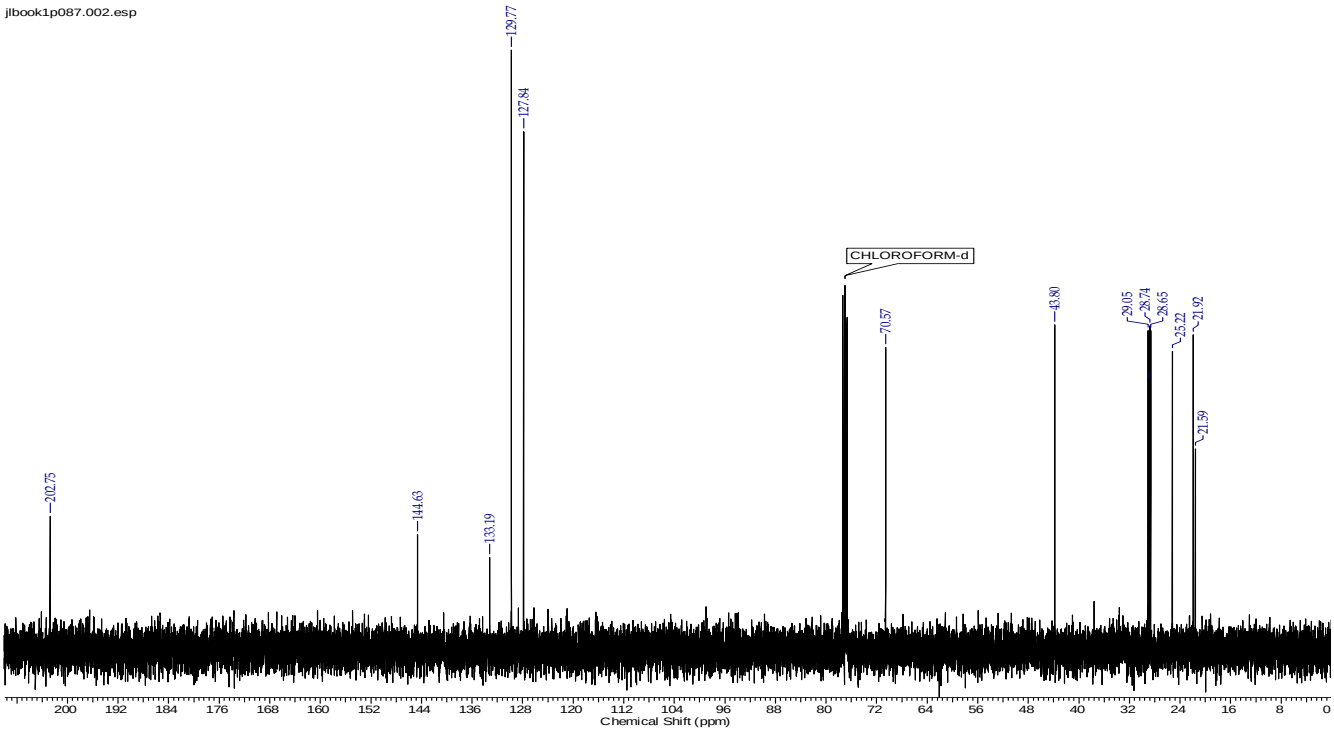
jlbook1p087.002.esp
129.77
127.84
CHLOROFORM-d
70.57
43.80
29.05
28.74
28.65
25.22
21.92
21.59
202.75
144.63
133.19
Chemical Shift (ppm)

4.189

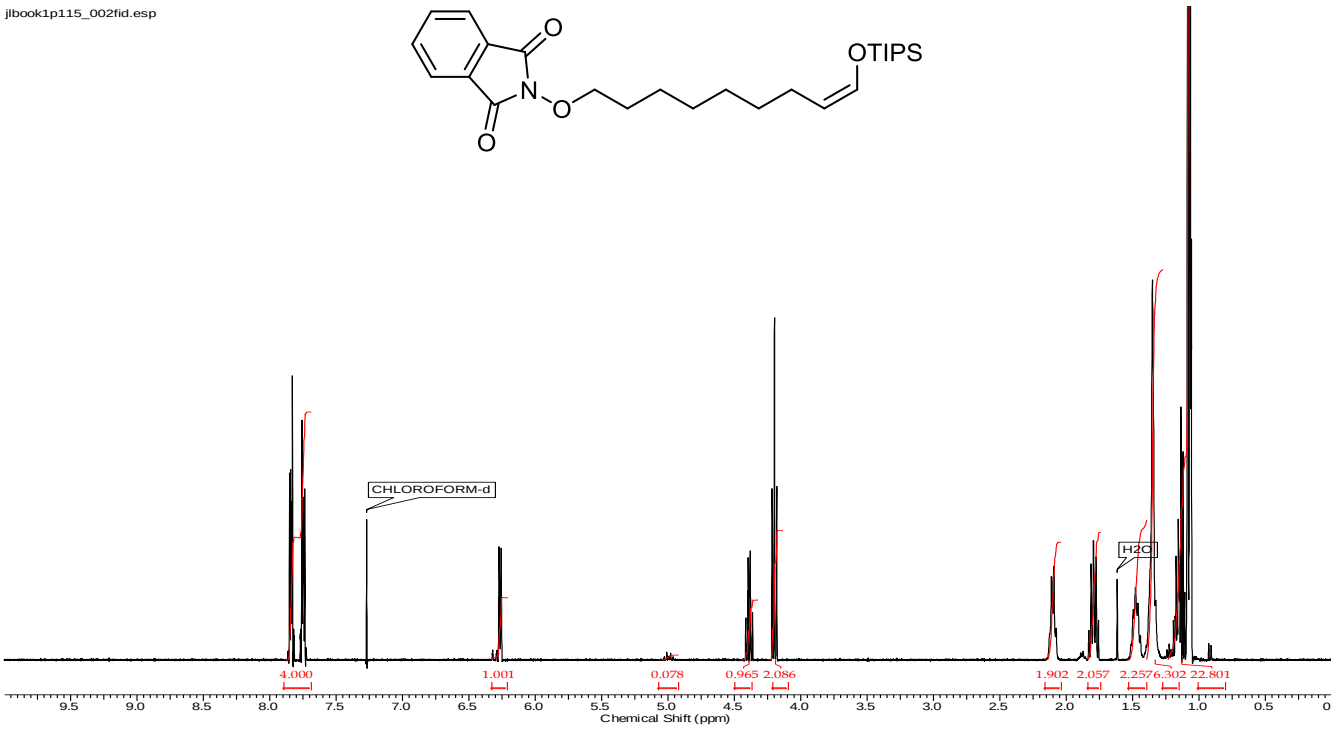
jlbook1p115_002fid.esp
O
N
O
O
OTIPS
CHLOROFORM-d
H2O
4.000
1.001
0.078
0.965
2.086
1.902
2.057
2.257
6.302
22.801
Chemical Shift (ppm)

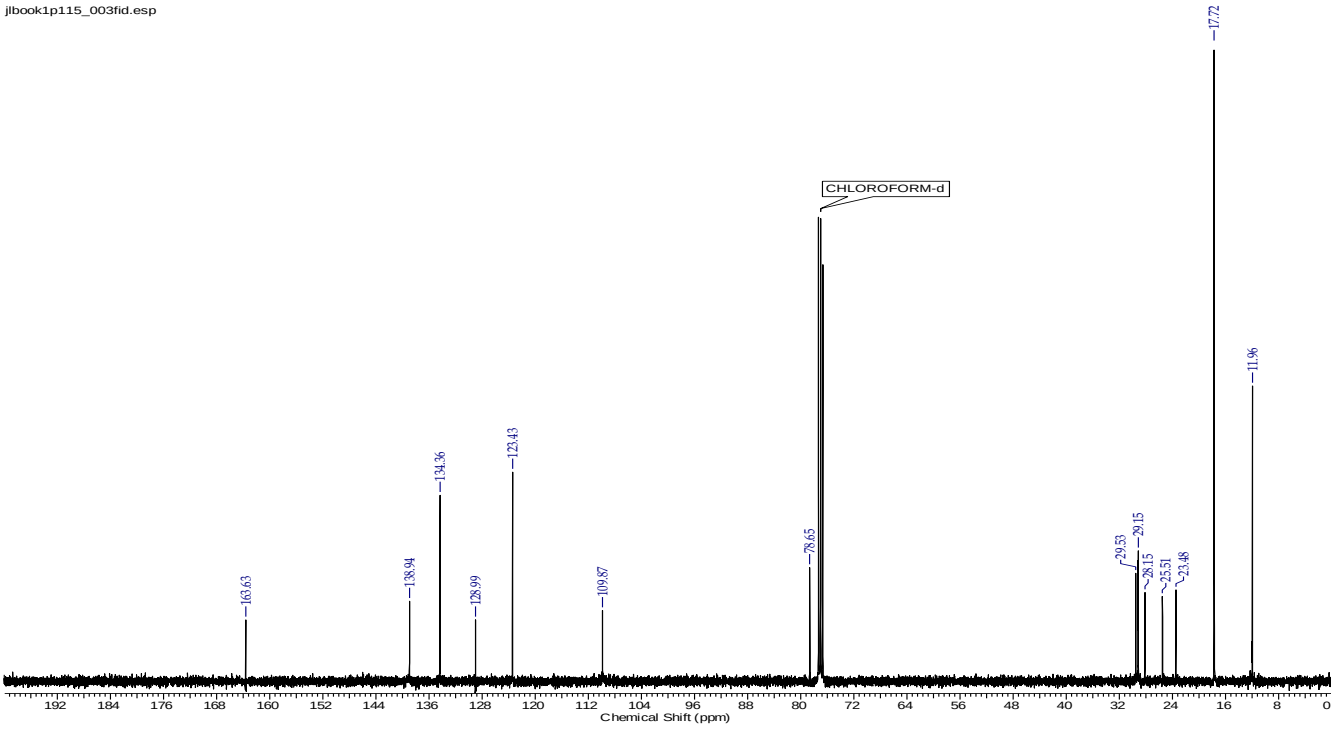
jlbook1p115_003fid.esp
17.72
CHLOROFORM-d
11.96
163.63
138.94
134.36
128.99
123.43
109.87
78.65
29.53
29.15
28.15
25.51
23.48
Chemical Shift (ppm)

4.177

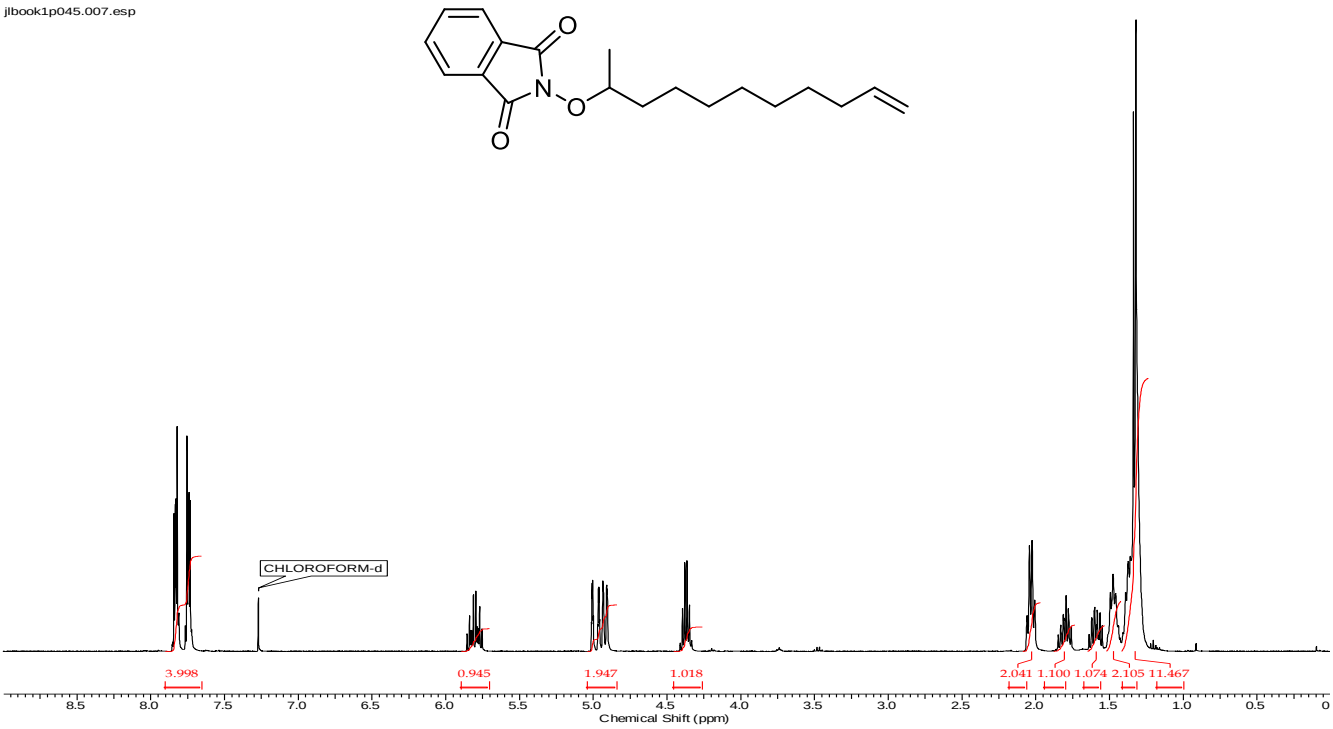
jlbook1p045.007.esp
O
N
O
O
CHLOROFORM-d
3.998
0.945
1.947
1.018
2.041
1.100
1.074
2.105
11.467
Chemical Shift (ppm)

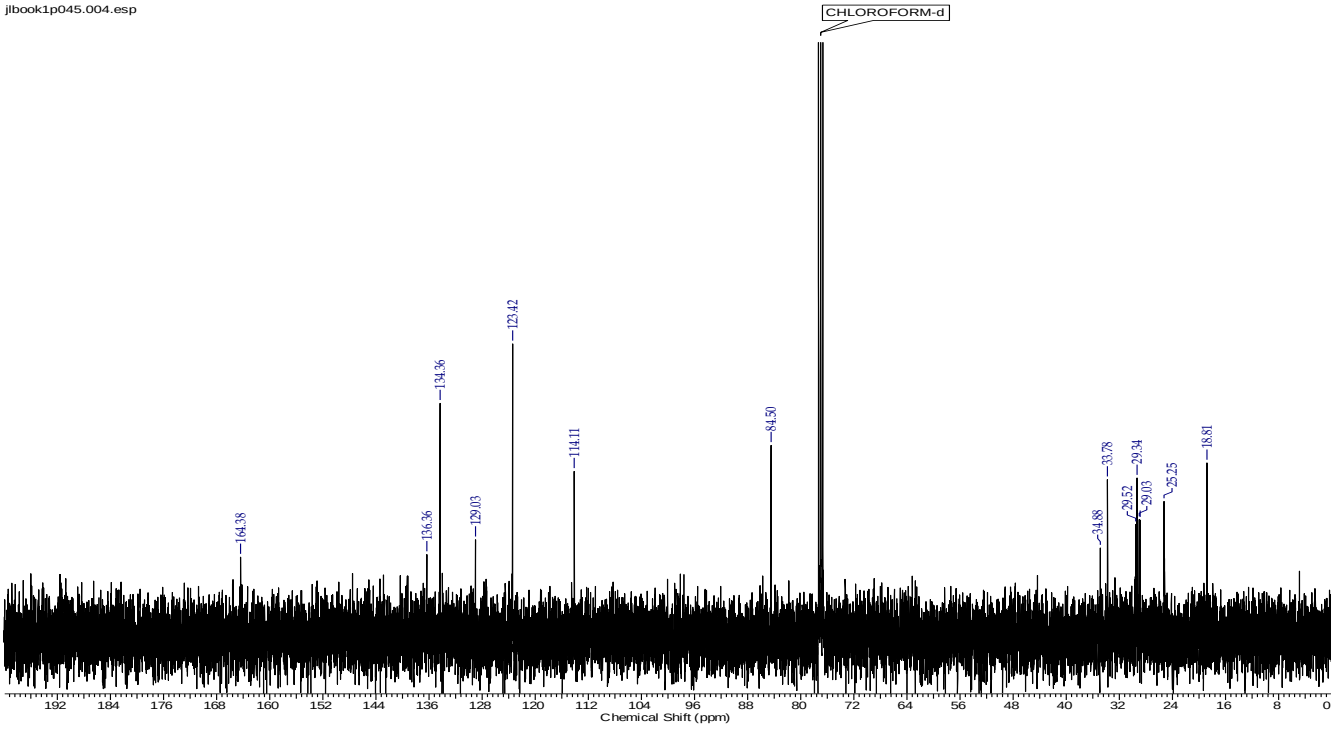
jlbook1p045.004.esp
CHLOROFORM-d
164.38
136.36
134.36
129.03
123.42
114.11
84.50
34.88
33.76
29.52
29.34
29.03
25.25
18.81
Chemical Shift (ppm)

4.167b

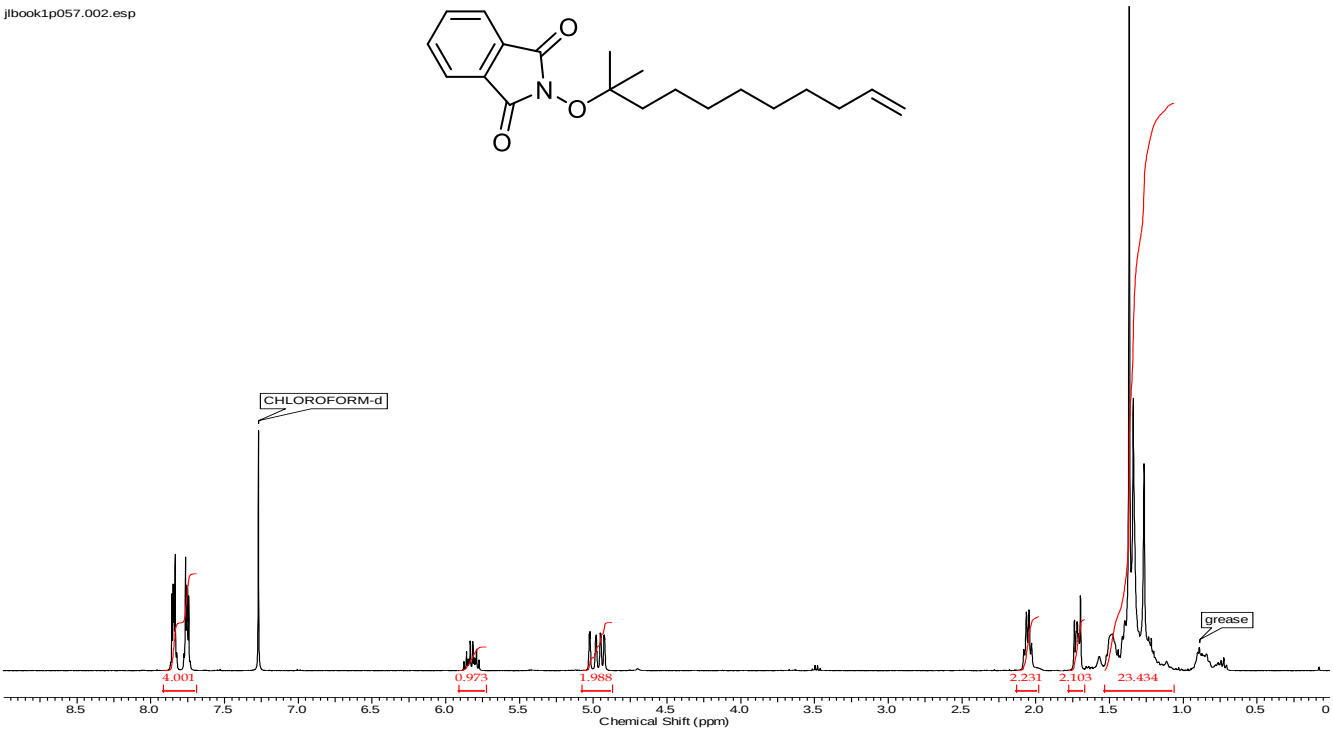
jlbook1p057.002.esp
O
N
O
O
CHLOROFORM-d
grease
4.001
0.973
1.988
2.231
2.103
23.434
Chemical Shift (ppm)

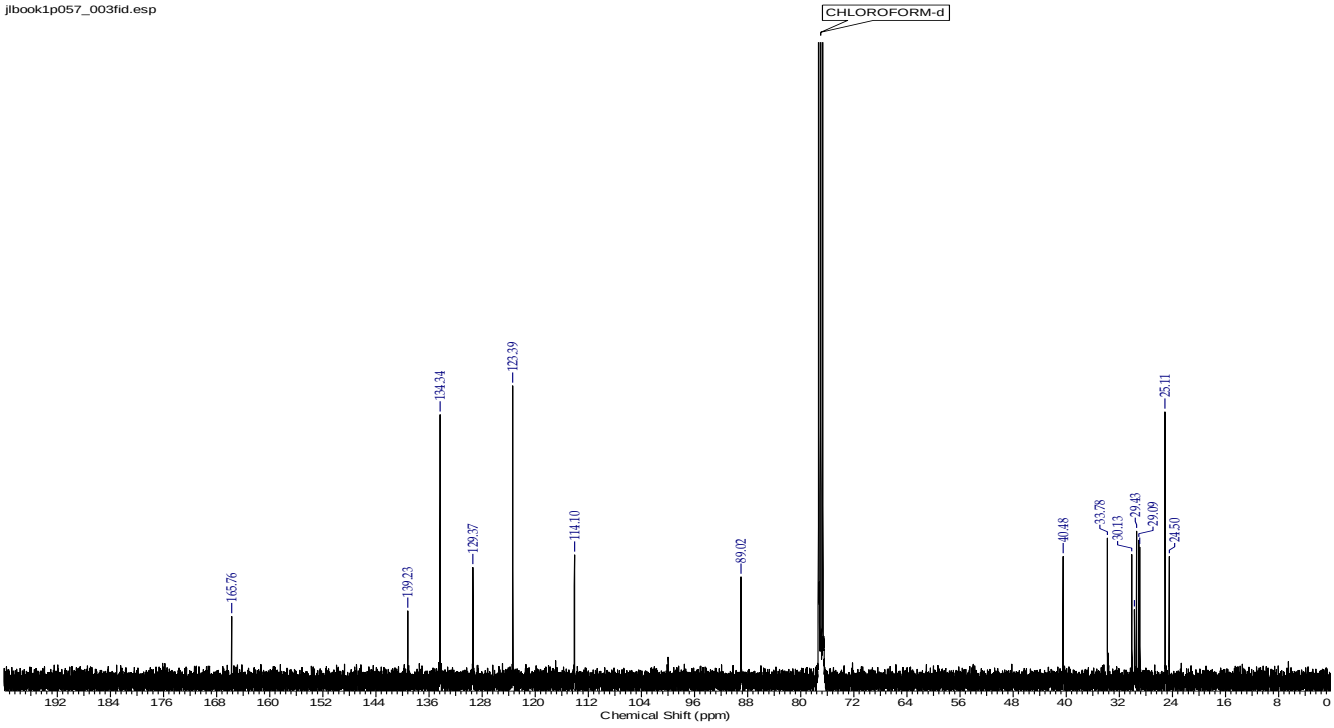
jlbook1p057_003fid.esp
CHLOROFORM-d
165.76
139.23
134.34
129.37
123.39
114.10
89.02
40.48
33.78
30.13
29.43
29.09
25.11
24.50
Chemical Shift (ppm)

4.179

jlbook1p033.001.esp

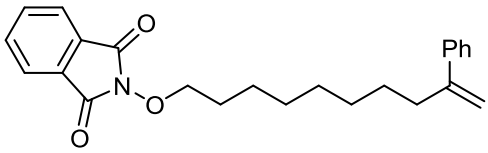

jlbook1p033.002.esp

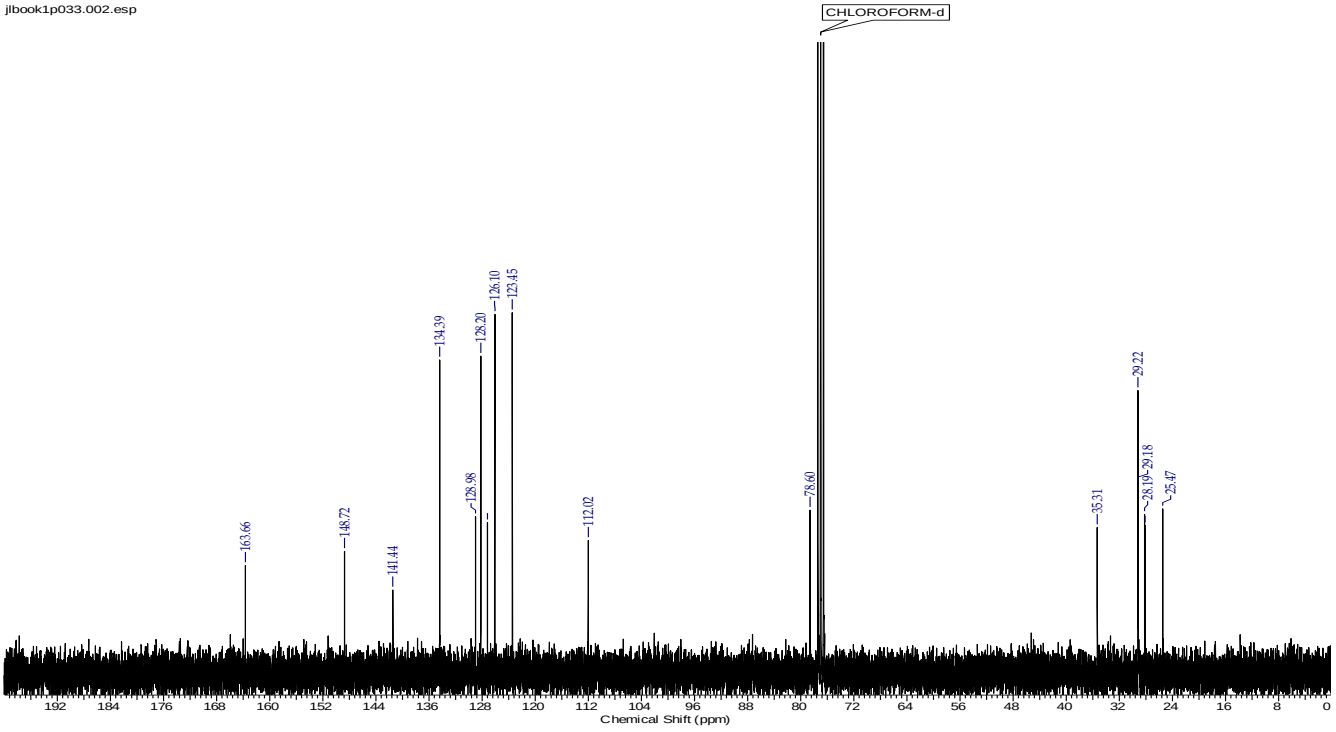

4.194

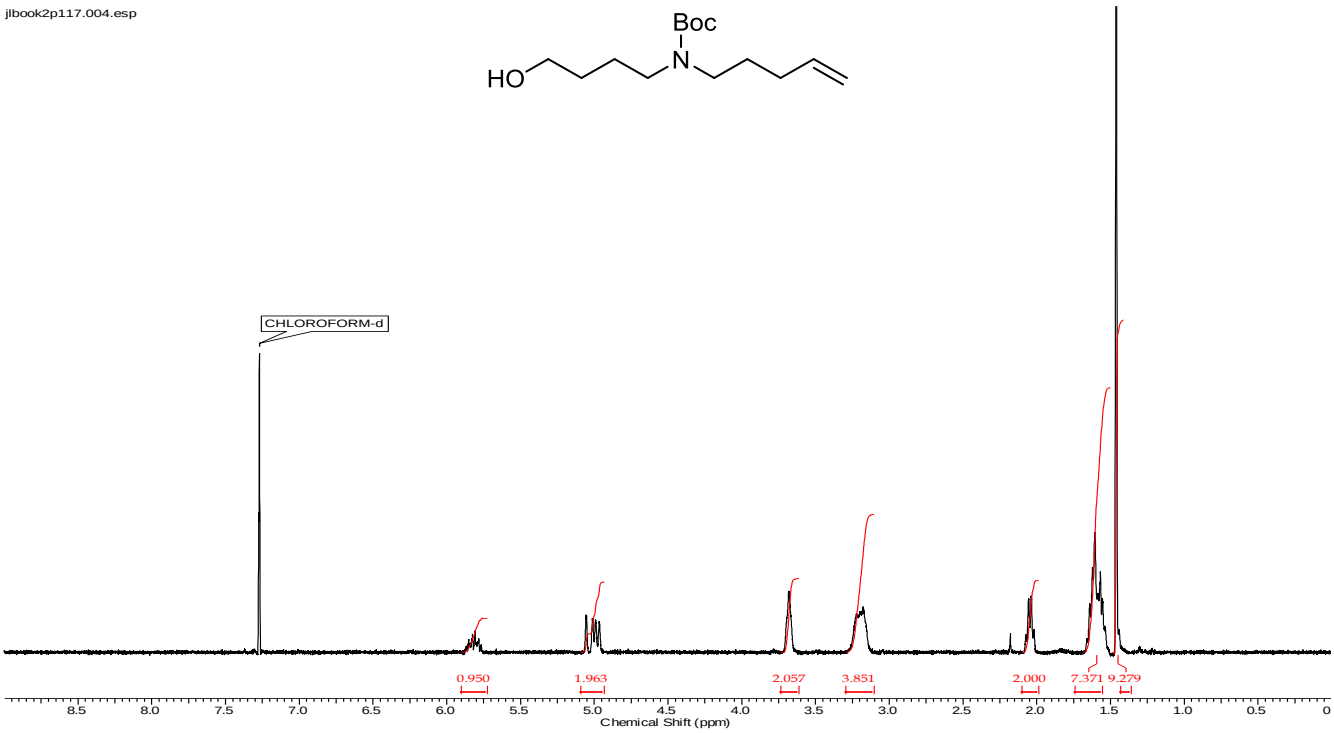
jlbook2p117.004.esp
Boc
N
HO
CHLOROFORM-d
0.950
1.963
2.057
3.851
2.000
7.371
9.279
Chemical Shift (ppm)

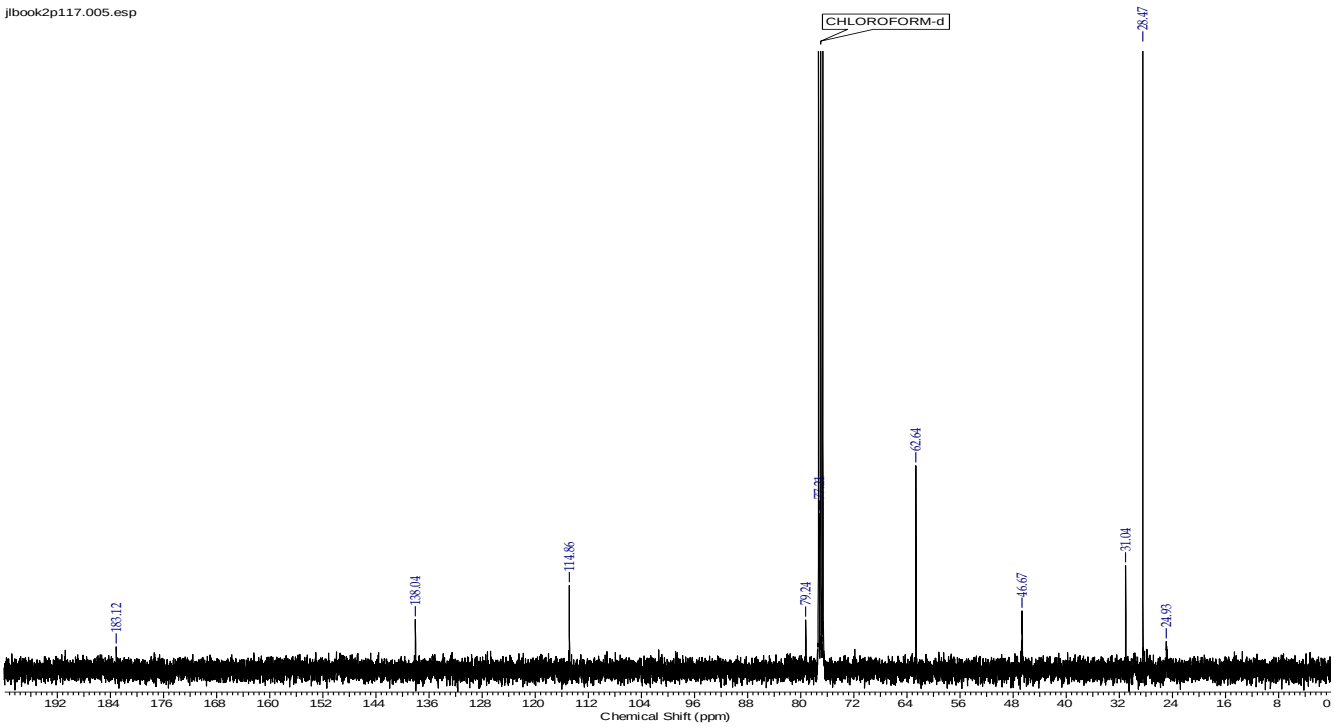
jlbook2p117.005.esp
CHLOROFORM-d
183.12
138.04
114.86
79.24
62.64
46.67
31.04
28.47
24.93
Chemical Shift (ppm)

4.195

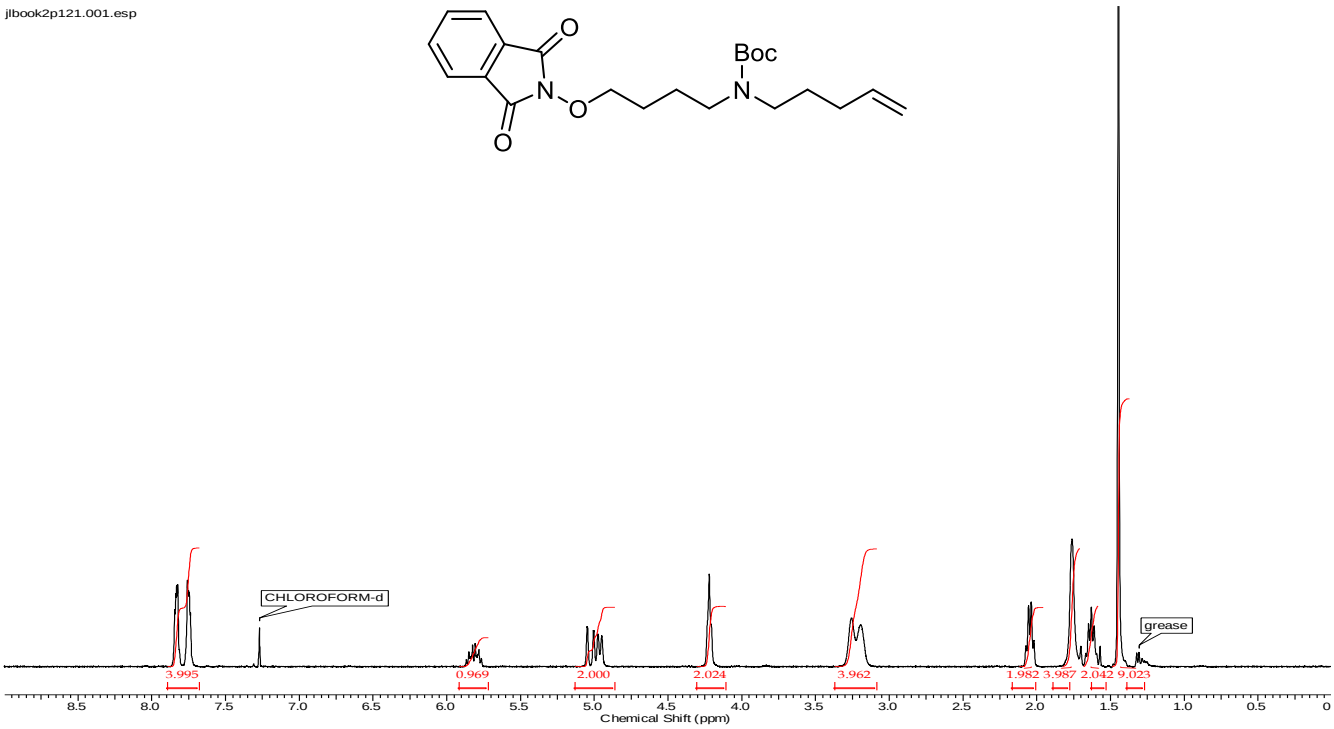
jlbook2p121.001.esp
O
O
N
O
Boc
N
CHLOROFORM-d
grease
3.995
0.969
2.000
2.024
3.962
1.982
3.987
2.042
9.023
Chemical Shift (ppm)

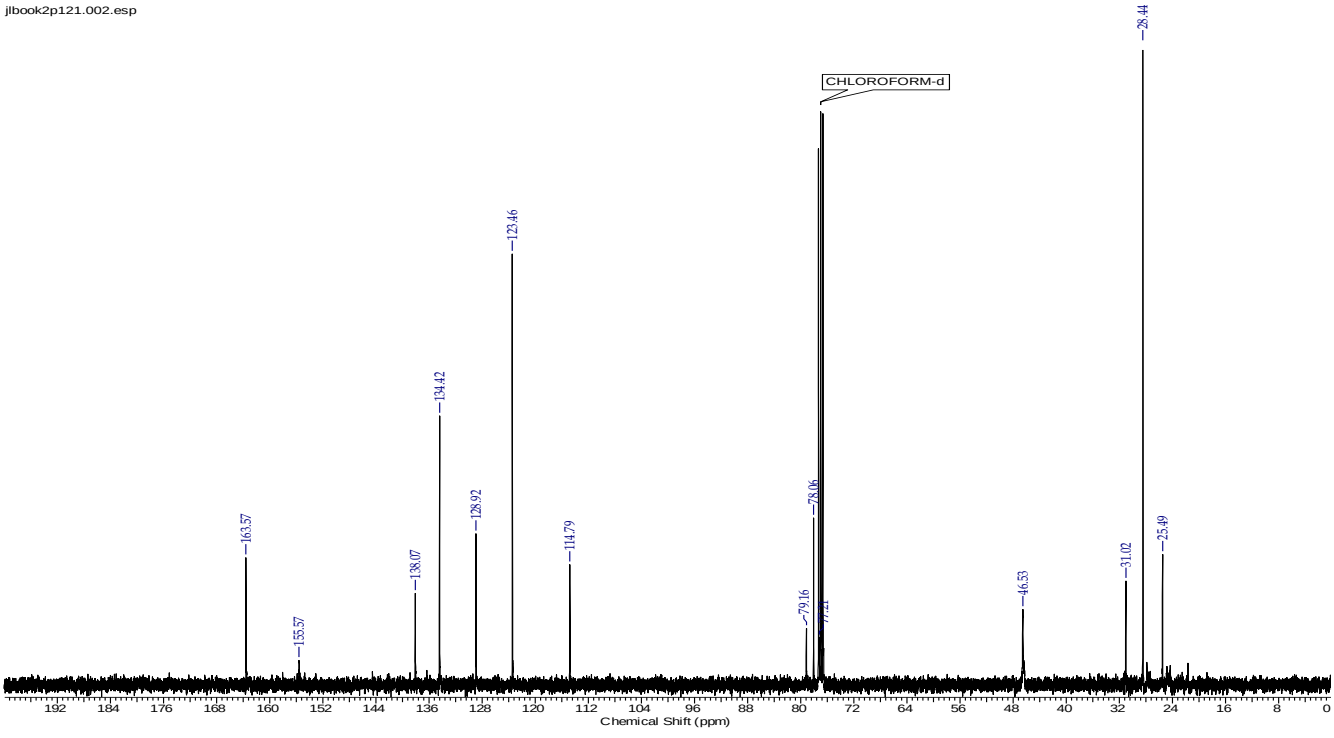
jlbook2p121.002.esp
28.44
CHLOROFORM-d
123.46
134.42
128.92
163.57
138.07
114.79
78.06
155.57
79.16
77.41
46.53
31.02
25.49
Chemical Shift (ppm)

4.162

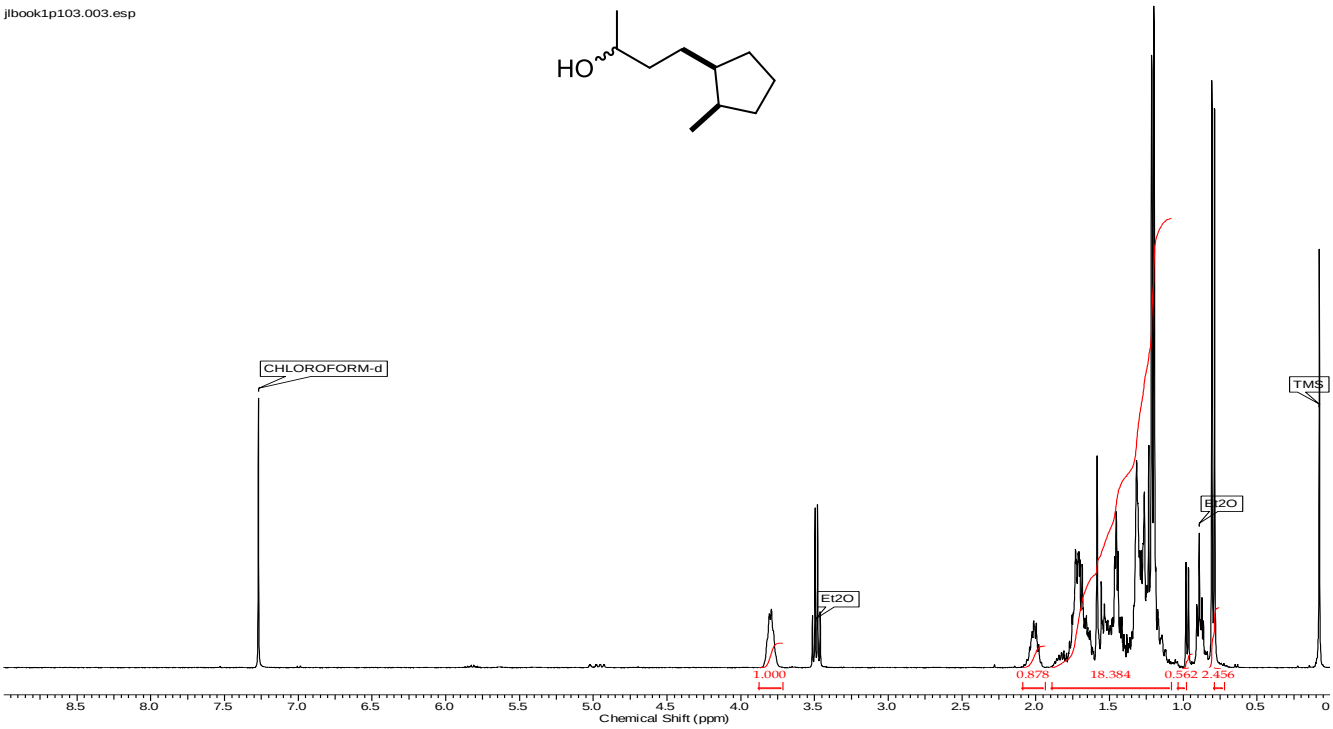
jlbook1p103.003.esp
HO
CHLOROFORM-d
Et2O
Et2O
TMS
1.000
0.878
18.384
0.562
2.456
Chemical Shift (ppm)

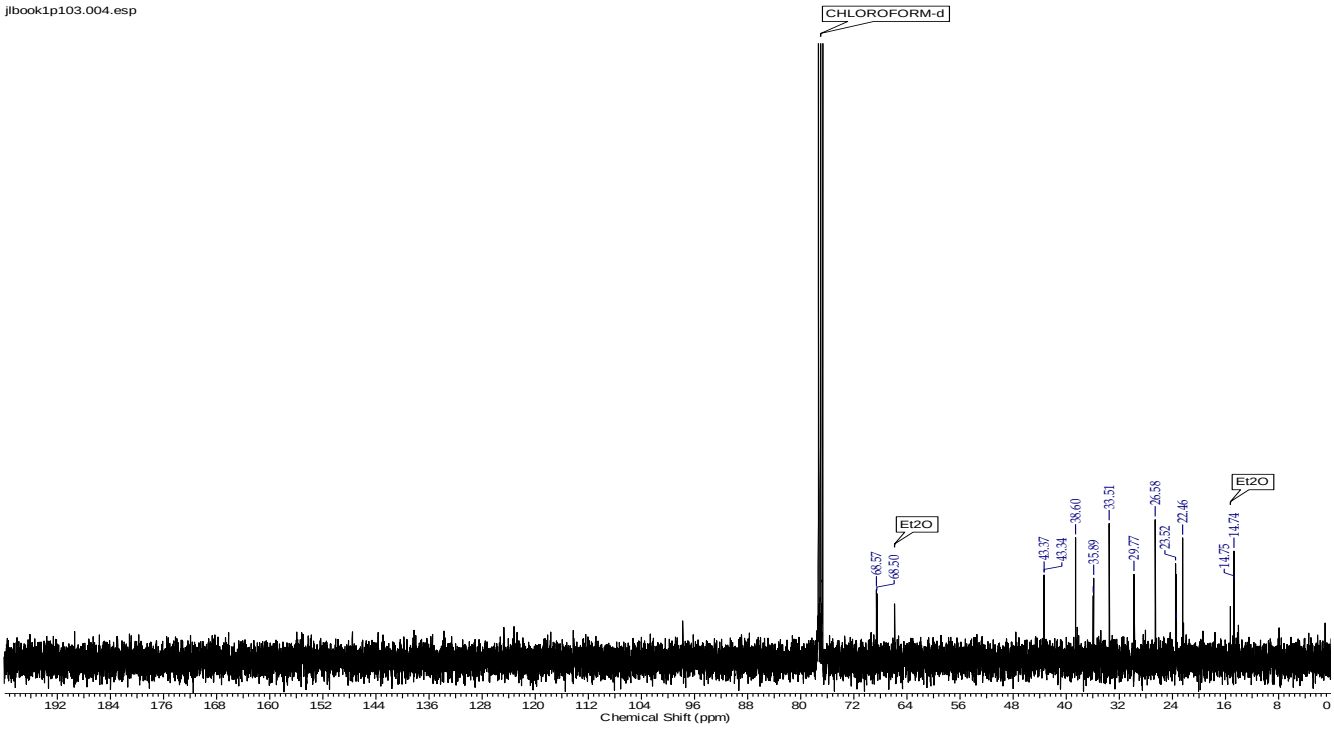
jlbook1p103.004.esp
CHLOROFORM-d
Et2O
Et2O
68.57
68.50
43.37
43.34
38.60
35.89
33.51
29.77
26.58
23.52
22.46
14.75
14.74
Chemical Shift (ppm)

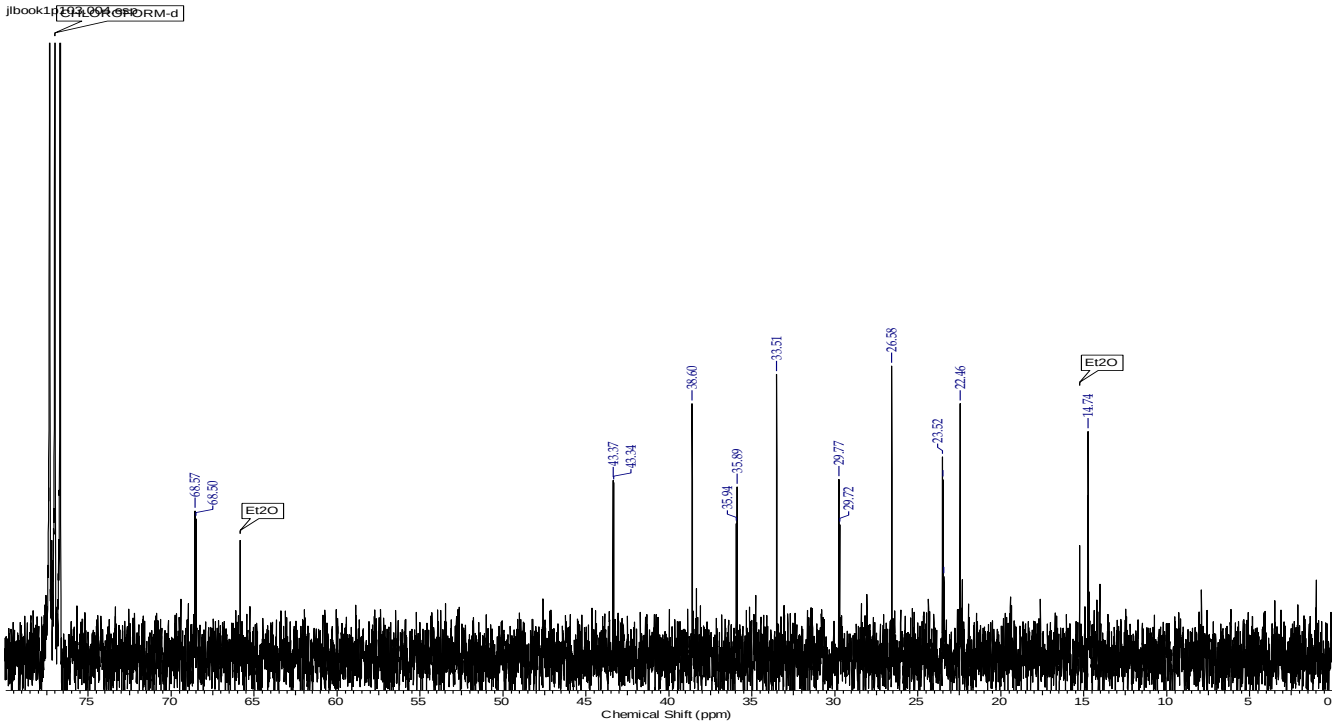
CHLOROFORM-d
68.57
68.50
Et2O
43.37
43.34
38.60
35.89
35.94
33.51
29.77
29.72
26.58
23.52
22.46
Et2O
14.74
Chemical Shift (ppm)

4.185

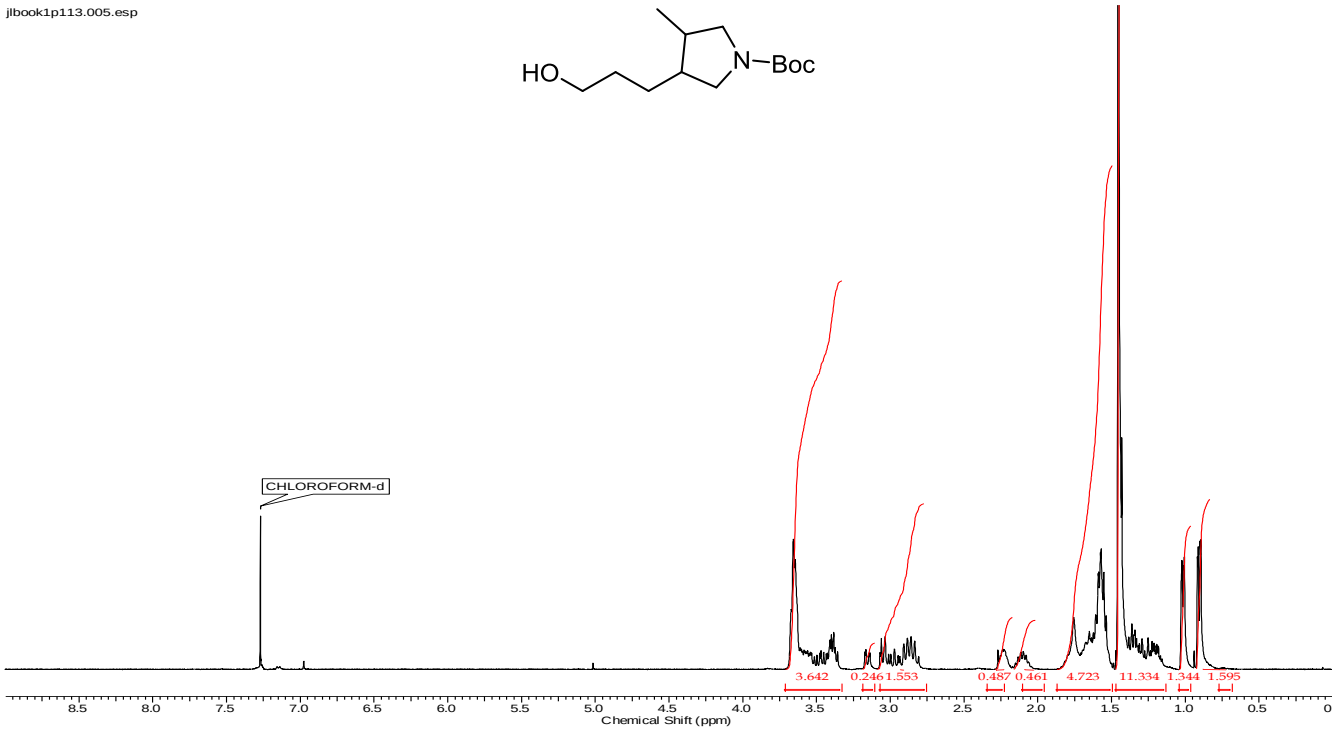
jlbook1p113.005.esp
HO
N–Boc
CHLOROFORM-d
3.642
0.246
1.553
0.487
0.461
4.723
11.334
1.344
1.595
Chemical Shift (ppm)

4.165

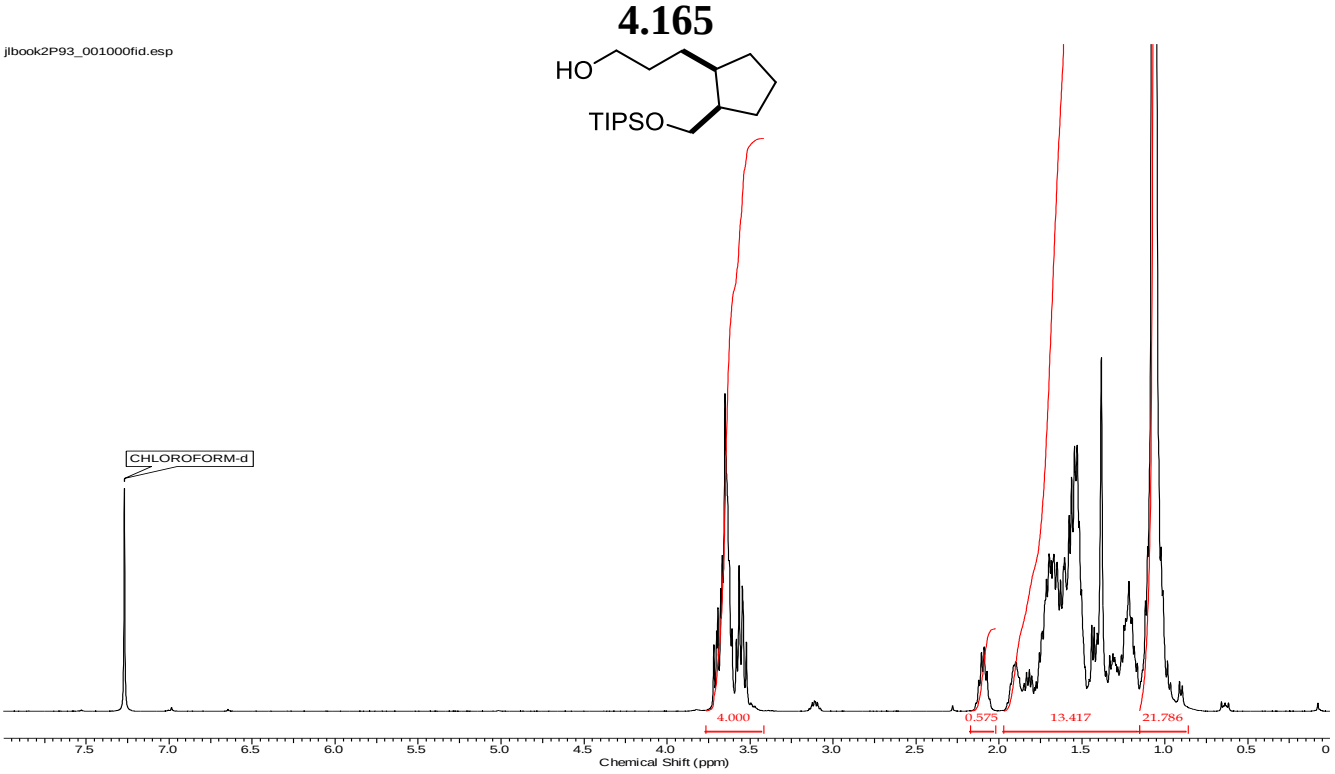
jlbook2P93_001000fid.esp
HO
TIPSO
CHLOROFORM-d
4.000
0.575
13.417
21.786
Chemical Shift (ppm)

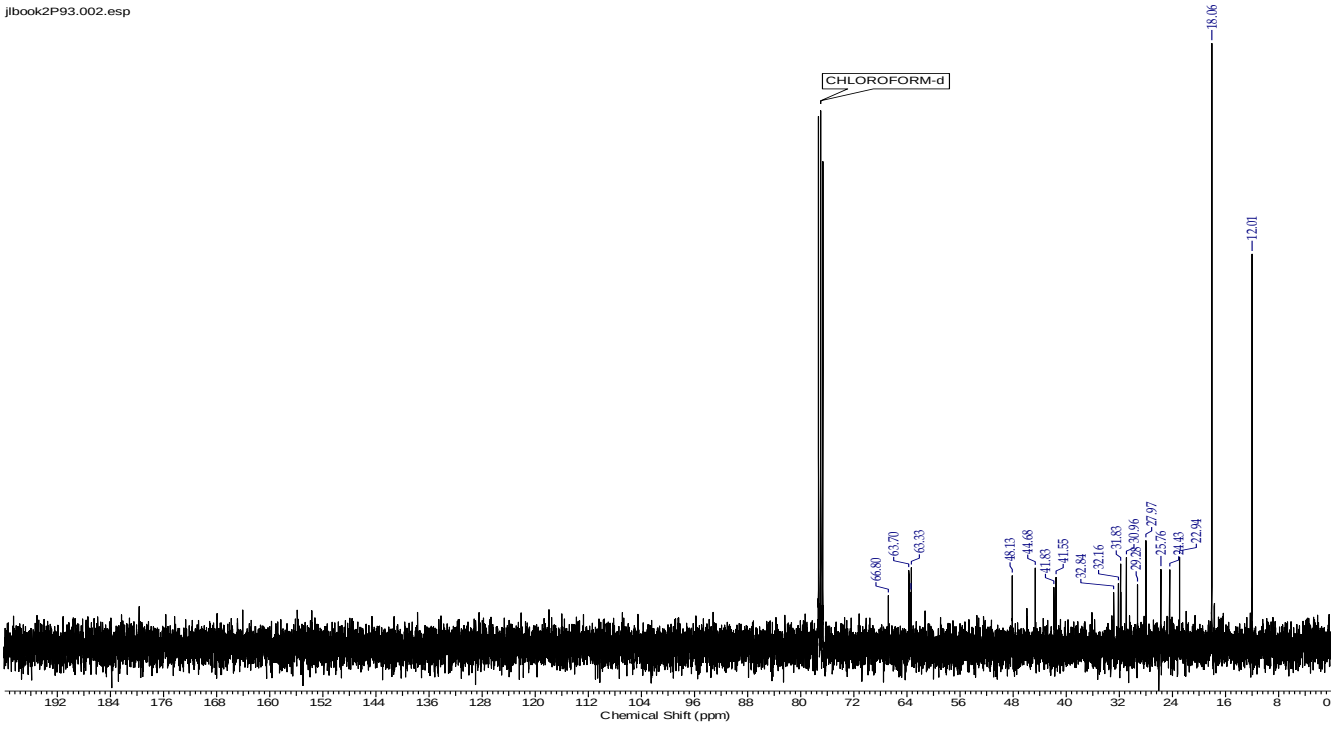
jlbook2P93.002.esp
CHLOROFORM-d
18.06
12.01
66.80
63.70
63.33
48.13
44.68
41.83
41.55
32.84
32.16
31.83
30.96
29.28
27.97
25.76
24.43
22.94
Chemical Shift (ppm)

4.191

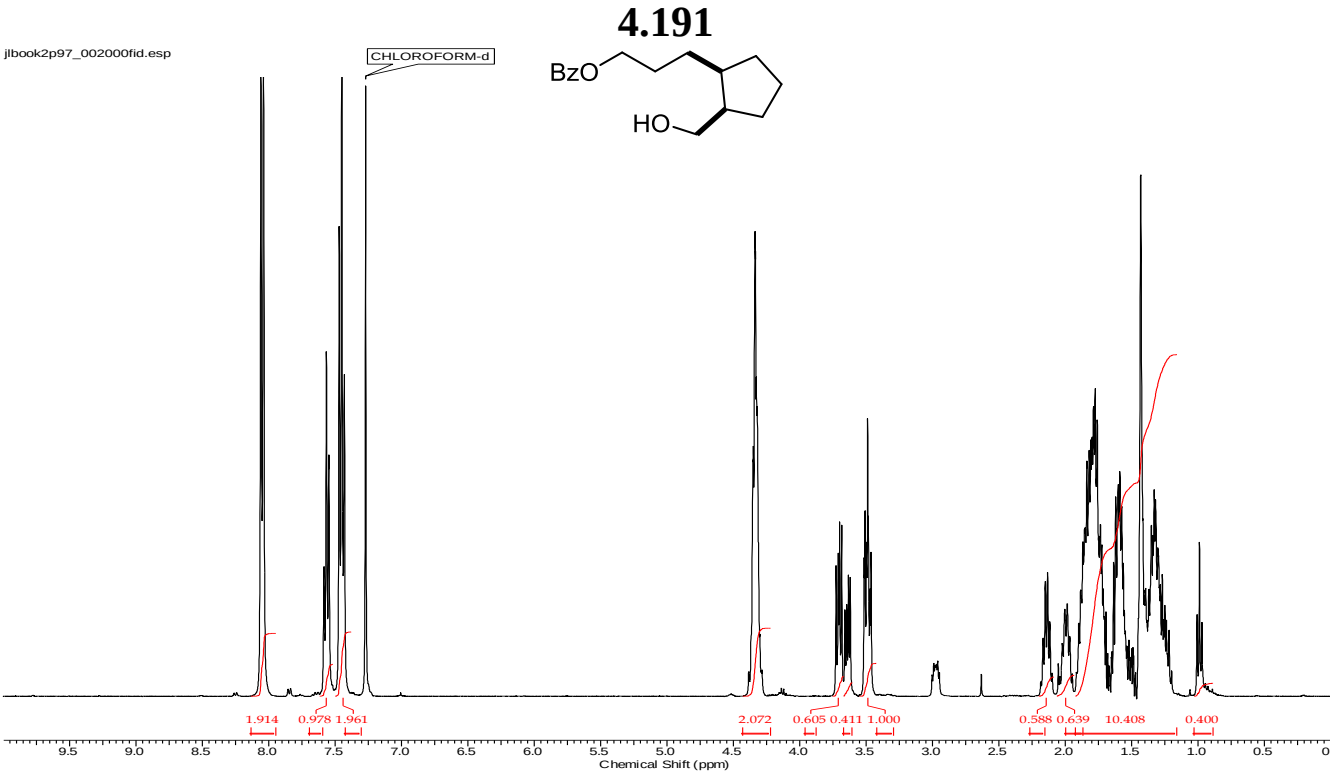
jlbook2p97_002000fid.esp
CHLOROFORM-d
BzO
HO
1.914
0.978
1.961
2.072
0.605
0.411
1.000
0.588
0.639
10.408
0.400
Chemical Shift (ppm)

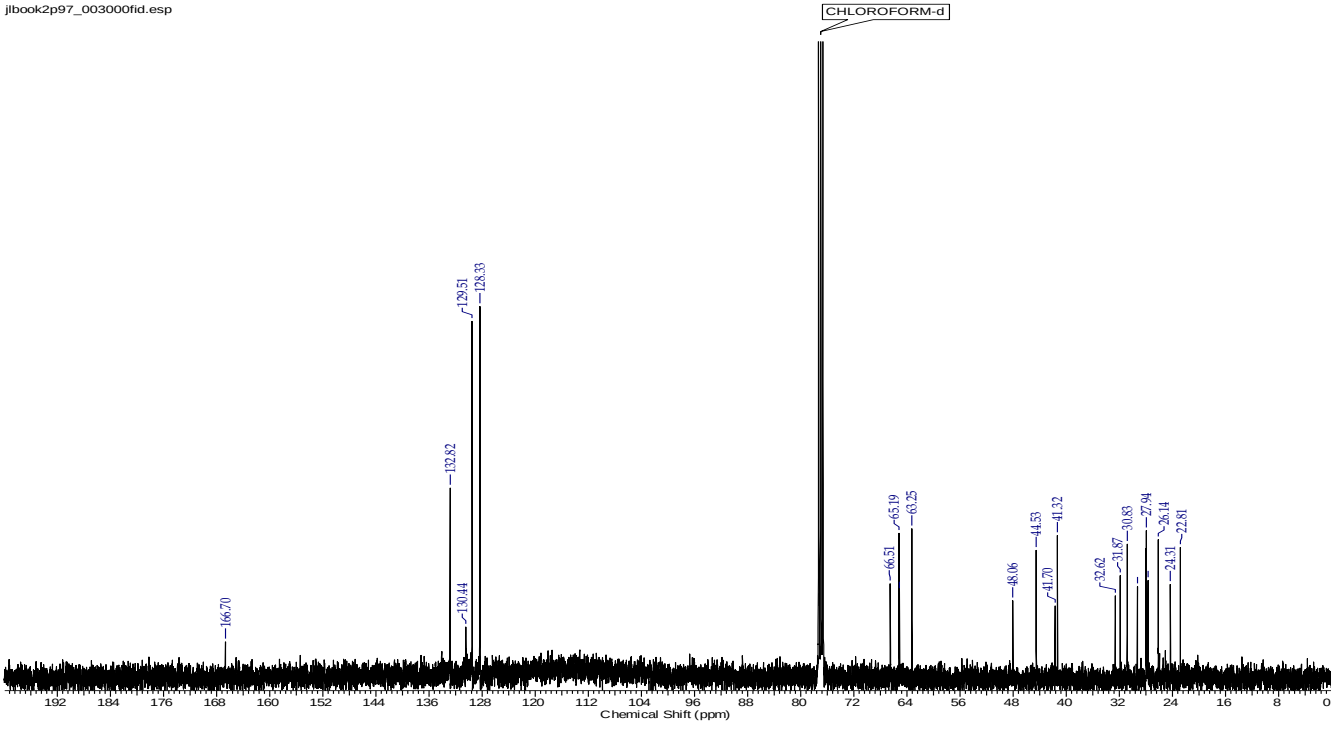
jlbook2p97_003000fid.esp
CHLOROFORM-d
166.70
132.82
130.44
129.51
128.33
65.19
66.51
63.25
48.06
44.53
41.70
41.32
32.62
31.87
30.83
27.94
26.14
24.31
22.81
Chemical Shift (ppm)

4.197

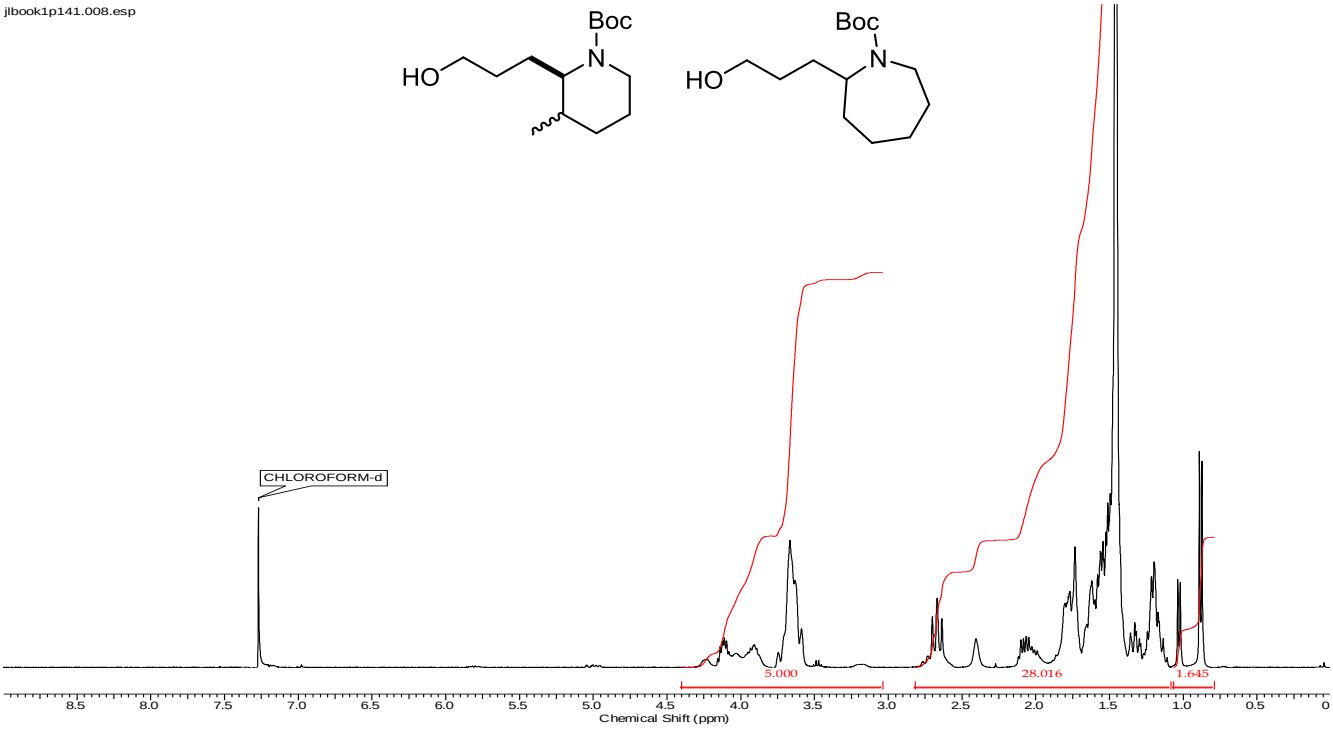
jlbook1p141.008.esp
Boc
N
HO
Boc
N
HO
CHLOROFORM-d
5.000
28.016
1.645
Chemical Shift (ppm)

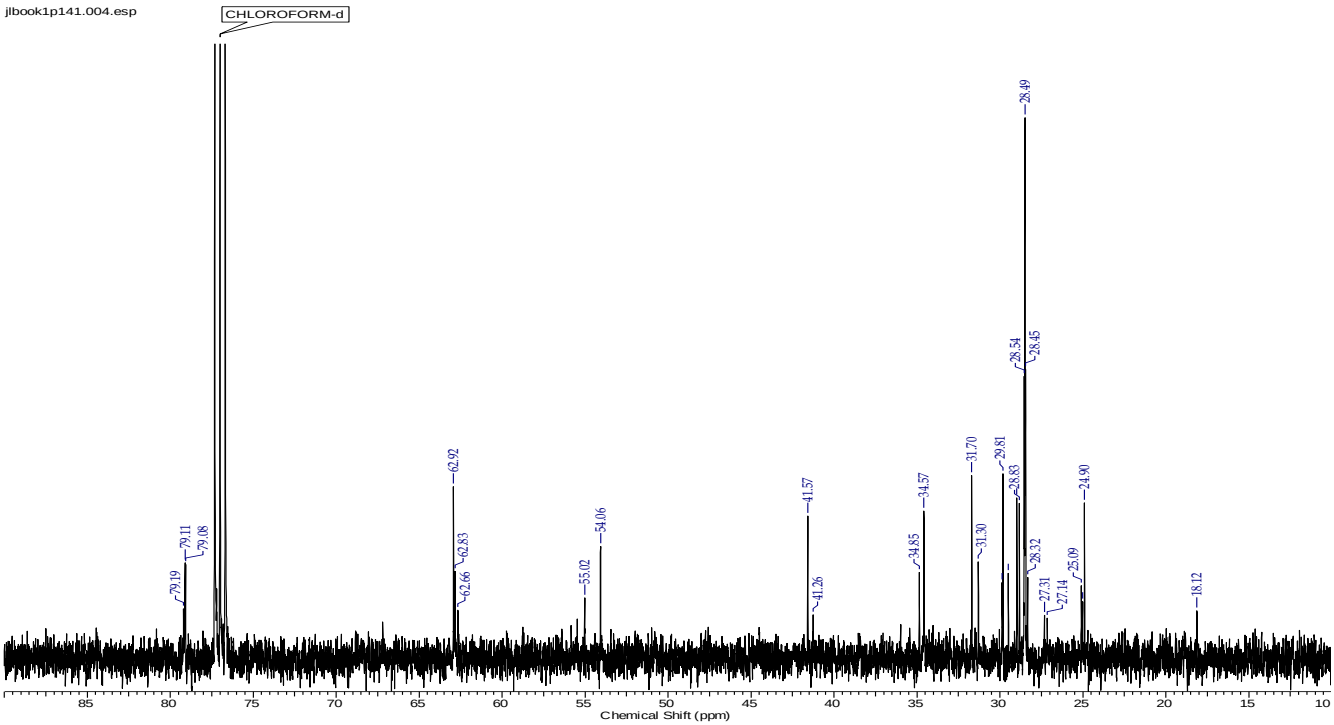
jlbook1p141.004.esp
CHLOROFORM-d
79.19
79.11
79.08
62.92
62.83
62.66
55.02
54.06
41.57
41.26
34.85
34.57
31.70
31.30
29.81
28.83
28.54
28.49
28.45
28.32
27.31
27.14
25.09
24.90
18.12
Chemical Shift (ppm)

4.199

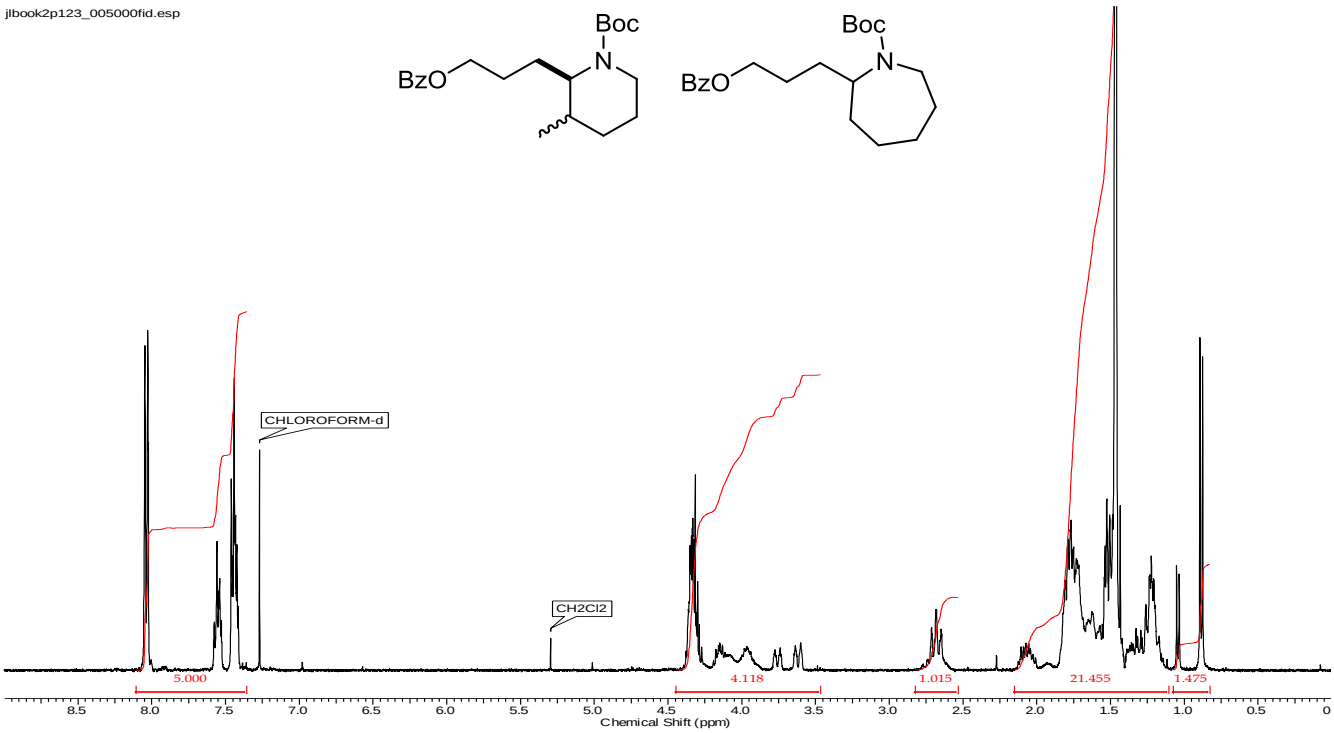
jlbook2p123_005000fid.esp
Boc
N
BzO
Boc
N
BzO
CHLOROFORM-d
CH2Cl2
5.000
4.118
1.015
21.455
1.475
Chemical Shift (ppm)

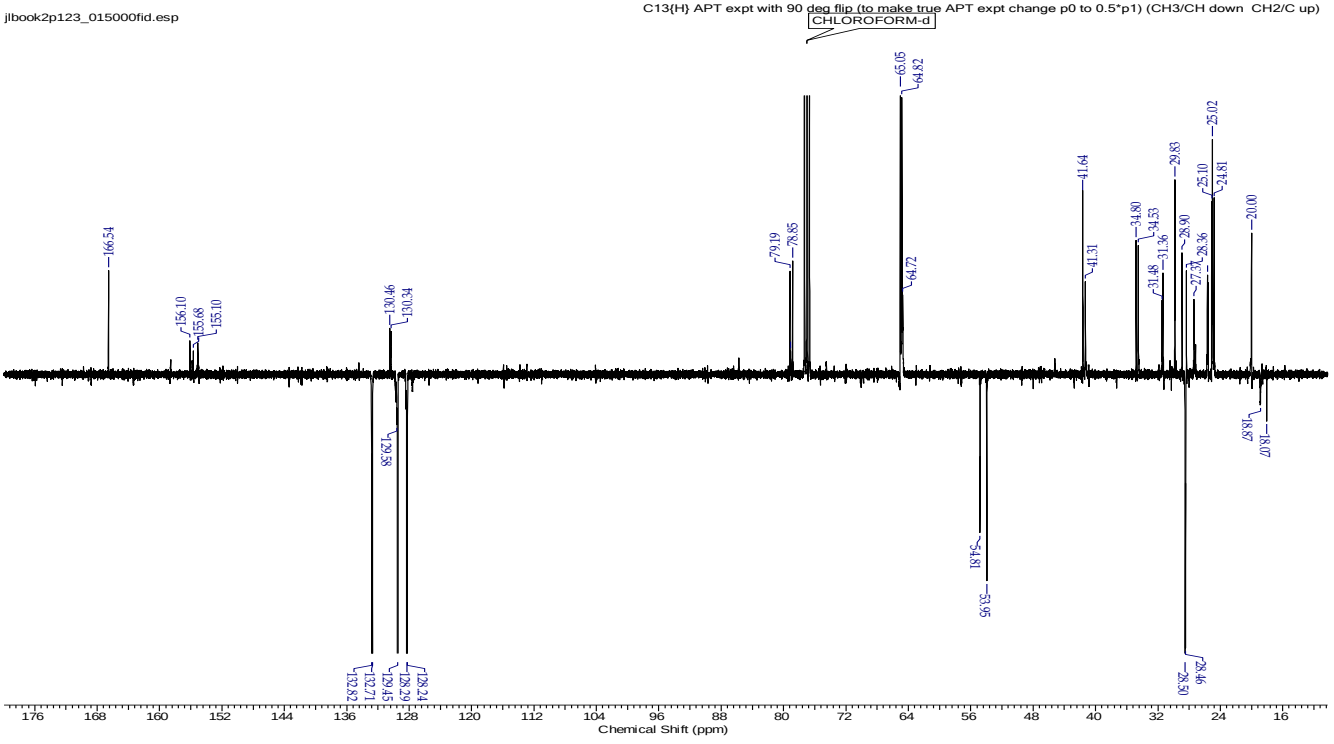
jlbook2p123_015000fid.esp
C13{H} APT expt with 90 deg flip (to make true APT expt change p0 to 0.5*p1) (CH3/CH down CH2/C up)
CHLOROFORM-d
166.54
156.10
155.68
155.10
130.46
130.34
129.58
132.82
132.71
129.45
128.29
128.24
79.19
78.85
65.05
64.82
64.72
54.81
53.95
41.64
41.31
34.80
34.53
31.48
31.36
29.83
28.90
28.36
27.37
25.02
25.10
24.81
20.00
18.87
18.07
28.46
28.36
Chemical Shift (ppm)

4.167

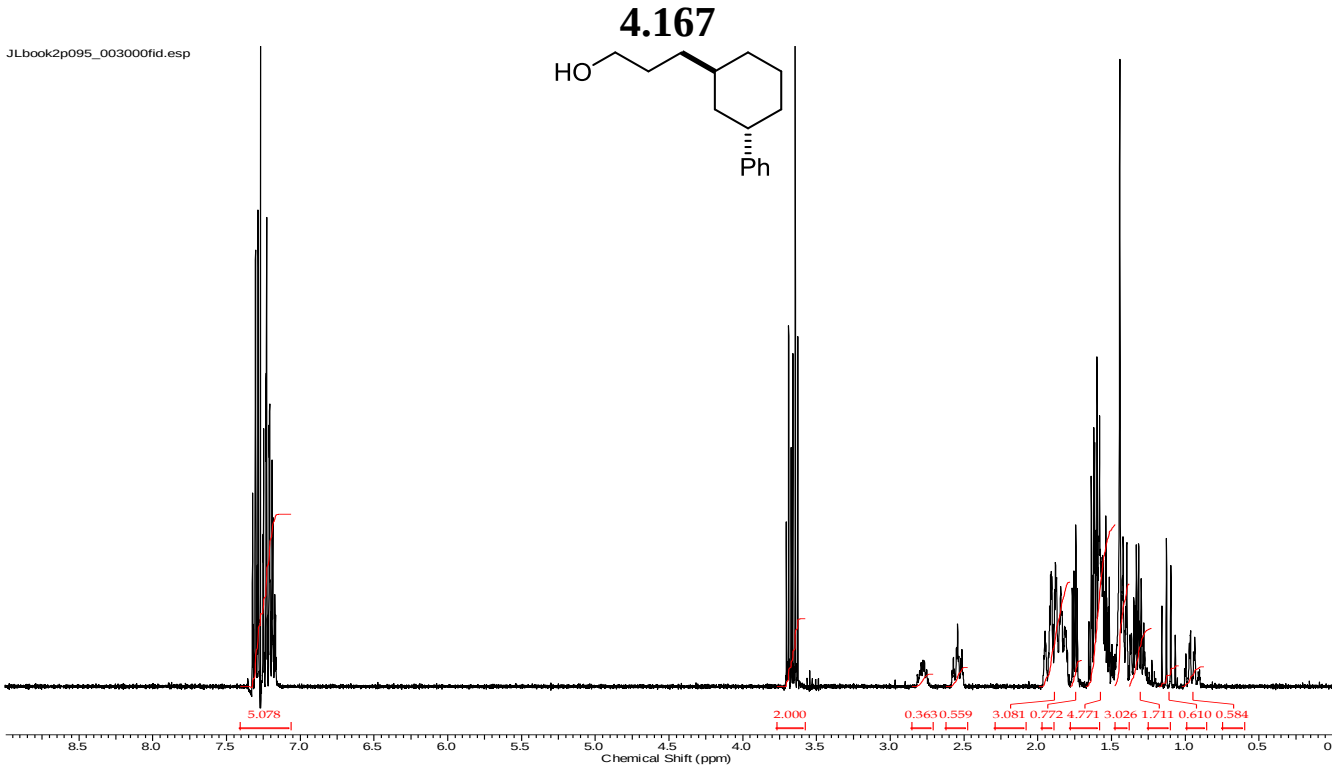
JLbook2p095_003000fid.esp
HO
Ph
5.078
2.000
0.363 0.559
3.081 0.772 4.771 3.026 1.711 0.610 0.584
Chemical Shift (ppm)

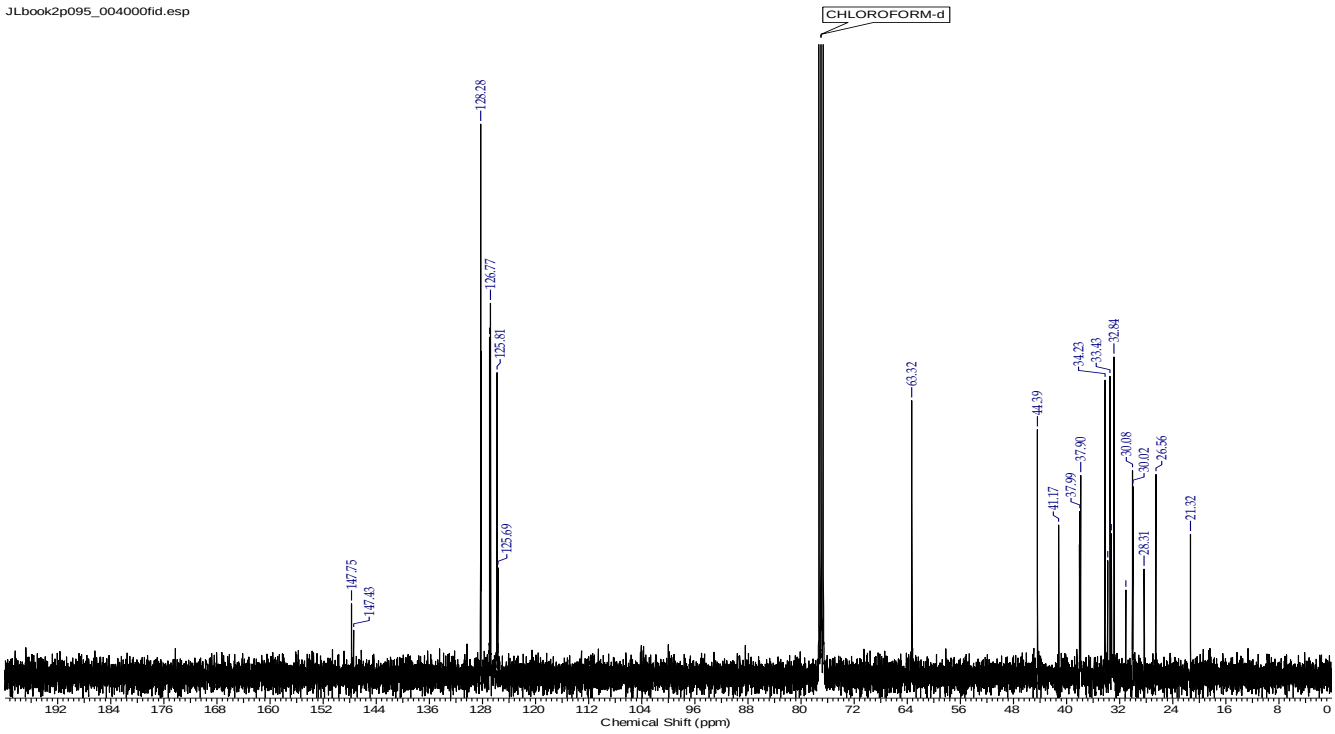
JLbook2p095_004000fid.esp
CHLOROFORM-d
128.28
126.77
125.81
125.69
147.75
147.43
63.32
44.39
41.17
37.99
37.90
34.23
33.43
32.84
30.08
30.02
28.31
26.56
21.32
Chemical Shift (ppm)